

# Geological Classification of Uranium Deposits and Description of Selected Examples



GEOLOGICAL CLASSIFICATION  
OF URANIUM DEPOSITS AND  
DESCRIPTION OF SELECTED EXAMPLES

The following States are Members of the International Atomic Energy Agency:

AFGHANISTAN	GERMANY	PALAU
ALBANIA	GHANA	PANAMA
ALGERIA	GREECE	PAPUA NEW GUINEA
ANGOLA	GUATEMALA	PARAGUAY
ANTIGUA AND BARBUDA	GUYANA	PERU
ARGENTINA	HAITI	PHILIPPINES
ARMENIA	HOLY SEE	POLAND
AUSTRALIA	HONDURAS	PORTUGAL
AUSTRIA	HUNGARY	QATAR
AZERBAIJAN	ICELAND	REPUBLIC OF MOLDOVA
BAHAMAS	INDIA	ROMANIA
BAHRAIN	INDONESIA	RUSSIAN FEDERATION
BANGLADESH	IRAN, ISLAMIC REPUBLIC OF	RWANDA
BARBADOS	IRAQ	SAINT VINCENT AND THE GRENADINES
BELARUS	IRELAND	SAN MARINO
BELGIUM	ISRAEL	SAUDI ARABIA
BELIZE	ITALY	SENEGAL
BENIN	JAMAICA	SERBIA
BOLIVIA, PLURINATIONAL STATE OF	JAPAN	SEYCHELLES
BOSNIA AND HERZEGOVINA	JORDAN	SIERRA LEONE
BOTSWANA	KAZAKHSTAN	SINGAPORE
BRAZIL	KENYA	SLOVAKIA
BRUNEI DARUSSALAM	KOREA, REPUBLIC OF	SLOVENIA
BULGARIA	KUWAIT	SOUTH AFRICA
BURKINA FASO	KYRGYZSTAN	SPAIN
BURUNDI	LAO PEOPLE'S DEMOCRATIC REPUBLIC	SRI LANKA
CAMBODIA	LATVIA	SUDAN
CAMEROON	LEBANON	SWAZILAND
CANADA	LESOTHO	SWEDEN
CENTRAL AFRICAN REPUBLIC	LIBERIA	SWITZERLAND
CHAD	LIBYA	SYRIAN ARAB REPUBLIC
CHILE	LIECHTENSTEIN	TAJIKISTAN
CHINA	LITHUANIA	THAILAND
COLOMBIA	LUXEMBOURG	THE FORMER YUGOSLAV REPUBLIC OF MACEDONIA
CONGO	MADAGASCAR	TOGO
COSTA RICA	MALAWI	TRINIDAD AND TOBAGO
CÔTE D'IVOIRE	MALAYSIA	TUNISIA
CROATIA	MALI	TURKEY
CUBA	MALTA	TURKMENISTAN
CYPRUS	MARSHALL ISLANDS	UGANDA
CZECH REPUBLIC	MAURITANIA	UKRAINE
DEMOCRATIC REPUBLIC OF THE CONGO	MAURITIUS	UNITED ARAB EMIRATES
DENMARK	MEXICO	UNITED KINGDOM OF GREAT BRITAIN AND NORTHERN IRELAND
DJIBOUTI	MONACO	UNITED REPUBLIC OF TANZANIA
DOMINICA	MONGOLIA	UNITED STATES OF AMERICA
DOMINICAN REPUBLIC	MONTENEGRO	URUGUAY
ECUADOR	MOROCCO	UZBEKISTAN
EGYPT	MOZAMBIQUE	VANUATU
EL SALVADOR	MYANMAR	VENEZUELA, BOLIVARIAN REPUBLIC OF
ERITREA	NAMIBIA	VIET NAM
ESTONIA	NEPAL	YEMEN
ETHIOPIA	NETHERLANDS	ZAMBIA
FIJI	NEW ZEALAND	ZIMBABWE
FINLAND	NICARAGUA	
FRANCE	NIGER	
GABON	NIGERIA	
GEORGIA	NORWAY	
	OMAN	
	PAKISTAN	

The Agency's Statute was approved on 23 October 1956 by the Conference on the Statute of the IAEA held at United Nations Headquarters, New York; it entered into force on 29 July 1957. The Headquarters of the Agency are situated in Vienna. Its principal objective is "to accelerate and enlarge the contribution of atomic energy to peace, health and prosperity throughout the world".

IAEA-TECDOC-1842

GEOLOGICAL CLASSIFICATION  
OF URANIUM DEPOSITS AND  
DESCRIPTION OF SELECTED EXAMPLES

INTERNATIONAL ATOMIC ENERGY AGENCY  
VIENNA, 2018

## COPYRIGHT NOTICE

All IAEA scientific and technical publications are protected by the terms of the Universal Copyright Convention as adopted in 1952 (Berne) and as revised in 1972 (Paris). The copyright has since been extended by the World Intellectual Property Organization (Geneva) to include electronic and virtual intellectual property. Permission to use whole or parts of texts contained in IAEA publications in printed or electronic form must be obtained and is usually subject to royalty agreements. Proposals for non-commercial reproductions and translations are welcomed and considered on a case-by-case basis. Enquiries should be addressed to the IAEA Publishing Section at:

Marketing and Sales Unit, Publishing Section  
International Atomic Energy Agency  
Vienna International Centre  
PO Box 100  
1400 Vienna, Austria  
fax: +43 1 2600 29302  
tel.: +43 1 2600 22417  
email: [sales.publications@iaea.org](mailto:sales.publications@iaea.org)  
<http://www.iaea.org/books>

For further information on this publication, please contact:

Nuclear Fuel Cycle and Materials Section  
International Atomic Energy Agency  
Vienna International Centre  
PO Box 100  
1400 Vienna, Austria  
Email: [Official.Mail@iaea.org](mailto:Official.Mail@iaea.org)

© IAEA, 2018  
Printed by the IAEA in Austria  
April 2018

### IAEA Library Cataloguing in Publication Data

Names: International Atomic Energy Agency.  
Title: Geological classification of uranium deposits and description of selected examples / International Atomic Energy Agency.  
Description: Vienna : International Atomic Energy Agency, 2018. | Series: IAEA TECDOC series, ISSN 1011-4289 ; no. 1842 | Includes bibliographical references.  
Identifiers: IAEAL 18-01150 | ISBN 978-92-0-101618-8 (paperback : alk. paper)  
Subjects: LCSH: Uranium ores — Geology. | Petrology. | Ore deposits.

## FOREWORD

During the 1970s and 1980s, attempts were made to classify uranium deposits under a simple descriptive system. However, many challenges still remain in classifying some deposits, such as those associated with carbonate rocks which have yet to be described or included in any classification. A sharp increase in the price of uranium at the beginning of 2005 led to greatly increased exploration, which resulted in the discovery of new deposits. In response, the IAEA created a working group to review the various existing classifications and to propose a new, or modified, classification to be used internationally. The many publications and company data made available since the revival of uranium exploration in 2005 provide a wealth of information on uranium deposit geology, which has been used to revise the classification, which appears in publications such as the Red Book, a joint IAEA and OECD Nuclear Energy Agency publication series on uranium resources, production and demand.

Compared to other metallic mineral deposits, uranium has a very short history of scientific study, and current understanding of its mineralization and origin is incomplete. There are a number of uranium deposit types with a unique genesis that are not well understood. The increased exploration for uranium has resulted in a wealth of new information, which has made it possible to investigate some of the least understood aspects of uranium metallogeny.

This publication defines a new classification scheme that is simple and descriptive but flexible enough to encompass the recent advances in the understanding of uranium geology and deposit genesis. Improved definitions of the deposit types, supported by examples for which good data are available, but which are not well described in previous literature, are also presented. Together with the descriptive information, new data on uranium resources available for each deposit type are also provided.

The IAEA expresses its gratitude to all who have contributed to this publication, either by directly providing suggestions for new types and subtypes or by providing new data to improve deposit descriptions. The classification was largely inspired by the work of the late F.J. Dahlkamp (Germany), fondly remembered as the uranium guru and who guided this work with an intense level of participation. He will be greatly missed by the uranium community. The IAEA officers responsible for this publication were M. Fairclough and H. Tulsidas of the Division of Nuclear Fuel Cycle and Waste Technology.

#### *EDITORIAL NOTE*

*This publication has been prepared from the original material as submitted by the contributors and has not been edited by the editorial staff of the IAEA. The views expressed remain the responsibility of the contributors and do not necessarily represent the views of the IAEA or its Member States.*

*Neither the IAEA nor its Member States assume any responsibility for consequences which may arise from the use of this publication. This publication does not address questions of responsibility, legal or otherwise, for acts or omissions on the part of any person.*

*The use of particular designations of countries or territories does not imply any judgement by the publisher, the IAEA, as to the legal status of such countries or territories, of their authorities and institutions or of the delimitation of their boundaries.*

*The mention of names of specific companies or products (whether or not indicated as registered) does not imply any intention to infringe proprietary rights, nor should it be construed as an endorsement or recommendation on the part of the IAEA.*

*The authors are responsible for having obtained the necessary permission for the IAEA to reproduce, translate or use material from sources already protected by copyrights.*

*The IAEA has no responsibility for the persistence or accuracy of URLs for external or third party Internet web sites referred to in this publication and does not guarantee that any content on such web sites is, or will remain, accurate or appropriate.*

# CONTENTS

1.	INTRODUCTION .....	1
2.	URANIUM DEPOSITS CLASSIFICATIONS .....	2
2.1.	The various classifications.....	2
2.1.1.	Lithological/geotectonic classifications .....	2
2.1.2.	Genetic classifications.....	5
2.2.	The 2013 IAEA classification of uranium deposits.....	11
2.2.1.	Detailed classification of deposit types, subtypes and classes .....	11
2.2.2.	Geological description of uranium deposits types and subtypes.....	14
3.	DESCRIPTION OF SELECTED URANIUM DEPOSITS.....	32
3.1	Intrusive deposits.....	32
3.1.1.	Definition.....	32
3.1.2.	Geological setting.....	32
3.1.3.	Metallogenesis.....	37
3.1.4.	Description of selected deposits .....	37
3.2.	Granite-related deposits.....	68
3.2.1.	Definition.....	68
3.2.2.	Geological setting.....	70
3.2.3.	Metallogenesis.....	71
3.2.4.	Description of selected deposits .....	72
3.3.	Polymetallic iron oxide breccia complex deposits.....	95
3.3.1.	Definition.....	95
3.3.2.	Geological setting.....	96
3.3.3.	Metallogenesis.....	96
3.3.4.	Description of a selected deposit: Olympic Dam deposit (Australia) .....	97
3.4.	Volcanic-related deposits .....	102
3.4.1.	Definition.....	102
3.4.2.	Geological setting.....	103
3.4.3.	Metallogenesis.....	105
3.4.4.	Description of selected deposits .....	105
3.5.	Metasomatite deposits.....	130
3.5.1.	Definition.....	130
3.5.2.	Geological setting.....	131
3.5.3.	Metallogenesis.....	133
3.5.4.	Description of selected deposits .....	134
3.6.	Metamorphite deposits .....	171
3.6.1.	Definition.....	171
3.6.2.	Geological setting.....	172
3.6.3.	Metallogenesis.....	173
3.6.4.	Description of selected deposits .....	174
3.7.	Proterozoic unconformity deposits.....	203
3.7.1.	Definition.....	203
3.7.2.	Geological setting.....	206
3.7.3.	Metallogenesis.....	207
3.7.4.	Description of selected deposits .....	208
3.8.	Collapse breccia pipe deposits .....	237
3.8.1.	Definition.....	237
3.8.2.	Geological setting.....	238
3.8.3.	Metallogenic aspects .....	239
3.8.4.	Description of a selected deposit: The Canyon deposit (USA) .....	241

3.9.	Sandstone deposits .....	244
	3.9.1. Definition.....	244
	3.9.2. Geological setting.....	245
	3.9.3. Basal channel sandstone deposits.....	246
	3.9.4. Tabular sandstone deposits.....	250
	3.9.5. Roll-front deposits.....	262
	Sandstone-hosted roll-front deposits in the USA .....	264
	3.9.6. Tectonic-lithologic sandstone deposits.....	280
	3.9.7. Mafic dykes/sills in Proterozoic sandstone .....	287
3.10.	PalAeo quartz-pebble conglomerate deposits .....	300
	3.10.1. Definition.....	300
	3.10.2. Geological setting.....	301
	3.10.3. Metallogensis.....	304
	3.10.4. Description of a selected deposit: The Denison mine deposit (Canada) .....	304
3.11.	Surficial deposits .....	307
	3.11.1. Definition.....	307
	3.11.2. Geological setting.....	308
	3.11.3. Metallogensis.....	310
	3.11.4. Description of selected deposits .....	311
3.12.	Lignite–coal deposits.....	327
	3.12.1. Definition.....	327
	3.12.2. Geological setting.....	328
	3.12.3. Metallogensis.....	329
	3.12.4. Description of selected deposits .....	329
3.13.	Carbonate deposits .....	343
	3.12.5. Definition.....	343
	3.12.6. Geological setting.....	344
	3.12.7. Metallogensis.....	344
	3.12.8. Description of selected deposits .....	345
3.14.	Phosphate deposits .....	357
	3.12.9. Definition.....	357
	3.12.10. Geological setting.....	358
	3.12.11. Metallogensis.....	360
	3.12.12. Description of selected deposits .....	360
3.15.	Black shale deposits .....	372
	3.12.13. Definition .....	372
	3.12.14. Geological setting.....	372
	3.12.15. Metallogensis.....	374
	3.12.16. Description of selected deposits .....	375
4.	CONCLUSIONS .....	389

# 1. INTRODUCTION

## Background

In 2009, a working group was created by the IAEA in order to review the various existing classification schemes for uranium deposits and to propose a new or a modified classification that would be used internationally. Numerous new publications have appeared and more company data have been made available since the rise of uranium prices that began in 2005 (Fig. 1) and the ‘flurry’ of exploration work that followed. This has provided a wealth of information on uranium deposit geology that has been used to revise the previous classification dating back to 1993.

## Objective

In 2009, when this TECDOC was initiated, 878 deposits were recorded in the IAEA uranium deposits database (UDEPO) [1]. By the end of 2015, the database had increased to 1807 deposits from which the data used in this report were supplied.

## Scope

The IAEA classification presented in this volume was officially accepted in 2013 [2, 3]. It has since been adopted in the 2014 and 2016 Red Books [4, 5]. This publication, after a review of the past and current classifications, presents the new classification.



FIG. 1. Uranium prices for the past 15 years (source: The Ux Consulting Company, LLC, 2016) (reproduced courtesy of Ux Consulting Company).

## Structure

The main characteristics of the types, subtypes and classes and about 50 selected uranium deposits/districts representing all types and subtypes are described.

## 2. URANIUM DEPOSITS CLASSIFICATIONS

### 2.1. THE VARIOUS CLASSIFICATIONS

#### 2.1.1. Lithological/geotectonic classifications

In 1955, three major types of uranium deposits were recognized [6]:

- (i) Deposits originating from ‘warm fluids’ with three subtypes:
  - (a) Deposits derived from partial melting, such as pegmatites (Bancroft district and Charlebois Lake, Canada);
  - (b) Disseminations in migmatitic rocks (Nipissing Lake, Canada);
  - (c) Veins in various rock types (Radium Hill (Australia); Port Radium, Ace–Fay–Verna, Gunnar (Canada); Shinkolobwe (former Zaire); Jachymov (former Czechoslovakia); Limousin district (France));
- (ii) Deposits associated with ‘old’ sediments (Proterozoic quartz-pebble conglomerates) (Blind River district (Canada); Witwatersrand Basin (South Africa));
- (iii) Deposits located within ‘normal’ sediments: sandstones (Wyoming and Colorado Plateau (USA)), black shale, coal and lignite, and phosphorites.

Various global and regional classifications of uranium deposits have been published in the past 50 years including those of Roubault [7], Heinrich [8], Maucher [9], Ruzicka [10], Ziegler [11], Mickle and Mathews [12], Mathews et al. [13], Nash et al. [14], Barthel et al. [15], Dahlkamp [16–19], Plant et al. [20] and McKay and Miezitis [21], mainly for deposits in the Western World, and by Kazansky and Laverov [22], Boitsov [23, 24], Stoikov and Bojkov [25], Petrov et al. [26, 27], Mashkovtsev et al. [28] and others for deposits in the Commonwealth of Independent States and associated countries. These classifications follow two alternative approaches, focusing either on descriptive features of the mineralization, such as host rock type and orebody morphology or on aspects of ore genesis.

After the 1965–1970 uranium exploration ‘boom’, much new data on uranium deposits became available and several new types of deposits were discovered, such as the vein, intra-intrusive and calcrete types. Thus, up-to-date reviews and reclassifications of those deposits of economic significance were proposed by Ziegler [11] and Dahlkamp [16]. However, the studies had to be restricted to deposits in the West, since information on uranium deposits in the Eastern Block countries was not only too sparse and incomplete but restricted at the time.

In 1974, Ziegler [11] suggested that the primary distribution of uranium and thorium is closely associated with the structural history of the sialic crust and hence with sialic magmatism. Accordingly, far from being distributed homogeneously, uranium should be associated preferentially with certain structural elements of the continental crust. Economic to sub-economic concentrations of uranium are derived for the most part from the primary distribution through hypogene or supergene remobilization and should therefore also be distributed in fairly close association with these structural elements. The author proposes a metallotectonic classification with 15 types of deposits, grouped according to both the metallogenic class and to the main structural elements with which they are associated.

In 1978, Dahlkamp’s classification [16], based on the stratigraphic (temporal) relationship of host rock to ore emplacement, distinguished 19 types of deposit, of which six had economic significance:

- (i) Oligomictic quartz-pebble conglomerate;
- (ii) Sandstone types;
- (iii) Calcrete;
- (iv) Intra-intrusive type;

- (v) Hydrothermal vein;
- (vi) Vein-like types.

The author proposes that the different types can be genetically related to the prevailing geological environment: (a) the primary uranium occurrences formed by endogenic processes, (b) the secondary occurrences derived from the primary by subsequent exogenic processes and (c) the tertiary occurrences assumed to be formed by endogenic, metamorphic processes. This classification was used for the OECD Nuclear Energy Agency's Red Book.

In 1989, Tarkhanov and Poluarshinov [29] suggested a new classification for uranium-bearing geotectonic elements and presented the results of a study of the characteristics of the geotectonic position, age and formation conditions of the Precambrian deposits within the Shields of ancient platforms. Summarized by Boitsov [30], the Russian classification of deposits based on geotectonic location includes deposits in: (a) cratons (Precambrian Shields and platforms, (b) geosynclinal fold belts and median massifs (orogenic belts) and (c) platform cover. Other classifications that take account of the geotectonic situation of deposits have been published by McMillan [31], Wilpolt and Simov [32], Sullivan [33] and others for various regions of the world.

In 1989, the IAEA prepared a uranium deposit classification which was descriptive in nature. It was similar to the classification used in the Red Book. At that time, 582 uranium deposits were recorded in the IAEA database with 15 types and 17 subtypes [34]. They were conventionally listed, in order of economic ranking:

- (1) Unconformity-related;
- (2) Sandstone;
- (3) Quartz-pebble conglomerate;
- (4) Veins;
- (5) Breccia complex;
- (6) Intrusive;
- (7) Phosphorite;
- (8) Collapse breccia pipe;
- (9) Volcanic;
- (10) Surficial;
- (11) Metasomatite;
- (12) Metamorphite;
- (13) Lignite;
- (14) Black shale;
- (15) Others (limestone, bony detritus, dolomite).

In 1993, Dahlkamp [18], in his book, *Uranium Ore Deposits*, recognizes 16 principal types of uranium deposit and occurrence based on host environment and/or geometry. More than 40 subtypes and classes were defined. The principal types are:

- (1) Unconformity-contact;
- (2) Subconformity epimetamorphic;
- (3) Vein;
- (4) Sandstone;
- (5) Collapse breccia pipe;
- (6) Surficial;
- (7) Quartz-pebble conglomerate;
- (8) Breccia complex;
- (9) Intrusive;
- (10) Phosphorite;
- (11) Volcanic;
- (12) Metasomatite;

- (13) Synmetamorphic;
- (14) Lignite;
- (15) Black shale;
- (16) Strata controlled, structure-bound.

In 1999, Plant et al. [20] regrouped the types listed by the IAEA into three associations in recognition of the shared geological settings among groups of uranium deposits: (i) igneous (plutonic and volcanic); (ii) metamorphic and (iii) sediment/sedimentary basin associations. In 2009, Dahlkamp [19], in his book *Uranium Deposits of the World: Asia*, indicates that recent information on uranium deposits, particularly from the former Eastern Block countries, and new research data on earlier established and defined types of uranium deposit justify a rearrangement and refinement of the classification scheme proposed by the author in 1993. The terminology selected for types and subtypes refers primarily to the host environment or to geotectonic settings of the types. On this basis, Dahlkamp distinguished 20 principal types of uranium deposit, including about forty subtypes and classes:

- (1) Unconformity-contact deposits;
- (2) Proterozoic subunconformity–epimetamorphic deposits;
- (3) Sandstone deposits;
- (4) Granite-related deposits (in veins, stockworks and episyenites);
- (5) Volcanic deposits (in veins, stockworks and stratiform lodes);
- (6) Metasomatite-related deposits (in veins and stockworks);
- (7) Undifferentiated (meta)sediment hosted deposits (in veins and shear zones);
- (8) Collapse breccia pipe deposits (Arizona Strip type);
- (9) Polymetallic haematite breccia complex deposits (Olympic Dam type);
- (10) Palaeoproterozoic quartz-pebble conglomerate deposits;
- (11) Surficial deposits;
- (12) Intrusive deposits;
- (13) Uraniferous carbonaceous shale-related stockwork deposits (Ronneburg type);
- (14) Uraniferous bituminous cataclastic limestone deposits (Mailuu-Suu type);
- (15) Uraniferous carbonaceous lutite (lacustrine) deposits;
- (16) Uraniferous organic phosphorous deposits (Mangyshlak type);
- (17) Uraniferous minerochemical phosphorite deposits (Idaho Phosphoria type);
- (18) Uraniferous lignite–coal deposits (Cave Hills and Freital type);
- (19) Uraniferous stratiform black shale deposits (Ranstad and Chattanooga types);
- (20) Uraniferous synmetamorphic and contact metamorphic deposits (Forstau and Mary Kathleen deposits).

The formerly used ‘vein type’ was abandoned by Dahlkamp as a principal deposit category since it causes confusion with other deposit types. Uraniferous veins are found in various rock types, including granite, volcanic, metasomatites, metasedimentary rocks, sandstone and others. In this revised classification, the term ‘vein’ is only used to describe the configuration of orebodies in any of the specific deposit types.

A paper by Kreuzer et al. [35] in 2010 describes the uranium potential of 90 geological regions in Australia. The authors use the 14 principal uranium deposit types recognized by the IAEA [36] and group them, on the basis of similarity of genetic processes, environments of ore formation and mappable criteria, into six uranium system models: (i) surficial; (ii) sedimentary; (iii) igneous related; (iv) metamorphic/metasomatic; (v) unconformity-related and (vi) vein type (Fig. 2). The proposed uranium system models are structured according to the mineral system approach and emphasize the critical mineralization processes that must occur for a uranium deposit to form in a particular region. The authors state that as such, this is not a purely scientific classification scheme, unlike the recent genetic classification proposed by Cuney [37], with deposit types grouped according to the main fractionation processes occurring within the geological cycle.

In some respects it differs from the classification proposed in 2009 by Skirrow et al. [38], where deposit types are grouped according to their fluid compositions. Rather, it is a practical scheme for exploration targeting on the broad, regional to continent scale. Kreuzer et al. [35] also indicate that their uranium system models are simplified, flexible and have internally consistent structures that not only emphasize depositional but also source and transport criteria, which are key parameters for area selection at the regional to continent scale (as reported in 2010 by McCuaig et al. [39]). If the five first system models are clearly related to major types of geological environment and not to a specific geological process, as with the sedimentary system (including syngenetic and epigenetic uranium concentrations), then the vein type category does not correspond to any specific geological environment.

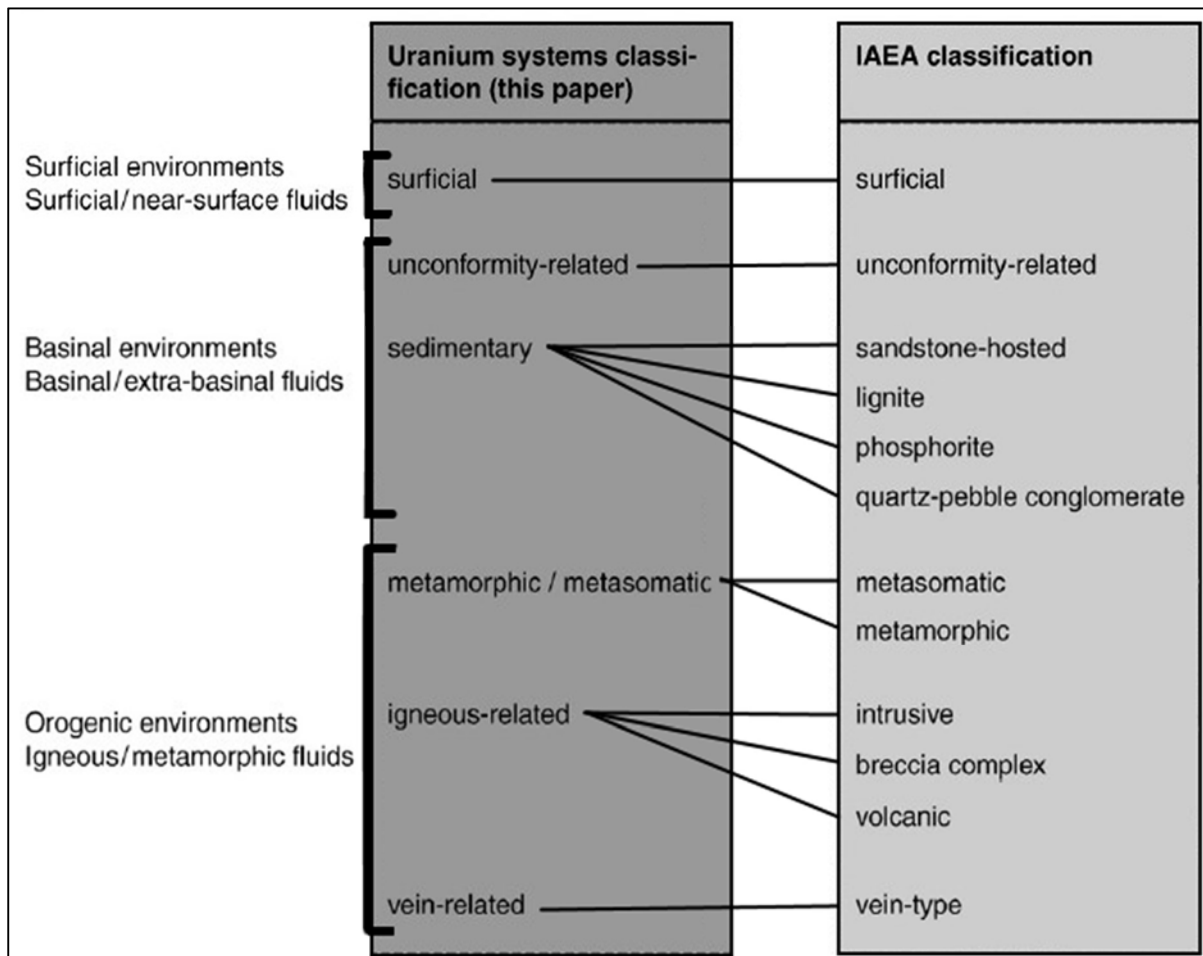


FIG 2. Comparison of the IAEA's uranium classification scheme [36] with the uranium system classification scheme proposed by Kreuzer et al. [35]. In this new scheme, uranium deposit types are grouped according to similar genetic processes, environments of ore formation and mappable features (adapted from Ref. [36]).

## 2.1.2. Genetic classifications

### 2.1.2.1. Geoscience Australia classification

For Skirrow et al. [38], the OECD Nuclear Energy Agency Red Book classification has served a useful purpose, particularly in assigning uranium resource data to deposit categories. The authors note, however, that there are limitations to the application of this and other empirically based

classification schemes where there is a need to predict the locations of undiscovered resources. They propose an alternative classification approach that emphasizes the similarities in the processes of formation of uranium deposits and which takes account of the crustal–deposit scales of the mineralizing processes; what the authors term a ‘mineral system’ approach. Underpinning the new classification scheme is the concept of redistribution of uranium from the mantle to the crust and its progressive concentration and subsequent recycling via igneous, metamorphic, sedimentary and fluid processes (Fig. 3). The authors suggest that the large number of known uranium deposit types listed in previous schemes may be simplified, as proposed by Plant et al. [20], to fit within three families of uranium mineralizing systems (Fig. 4): (i) magmatic-related; (ii) metamorphic-related and (iii) basin- and surface-related. In addition to accommodating known deposit types, the new scheme predicts a continuum of deposit types between the three end-member mineralizing systems.

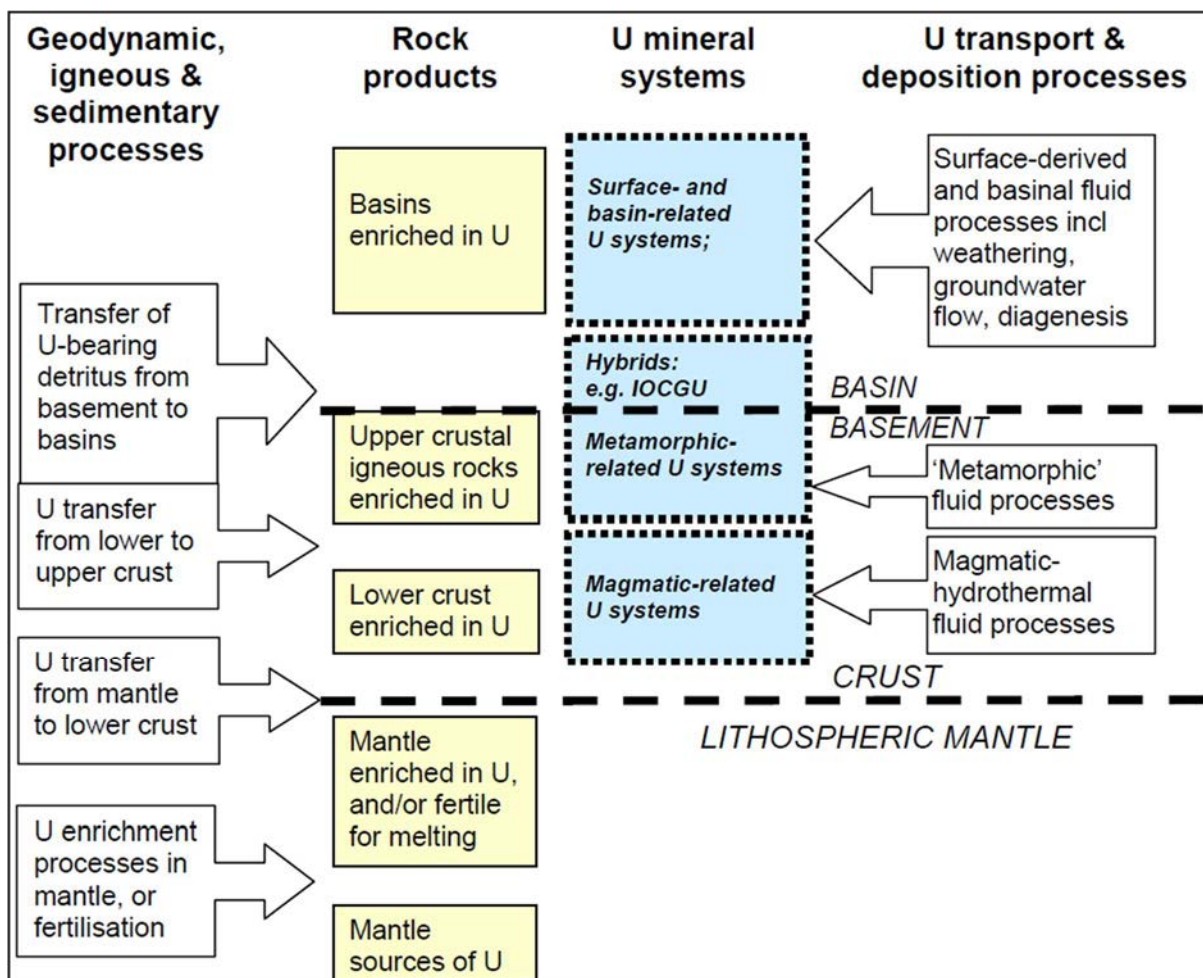


FIG. 3. Scheme relating uranium mineral systems to earth processes [38] (reproduced with permission.).

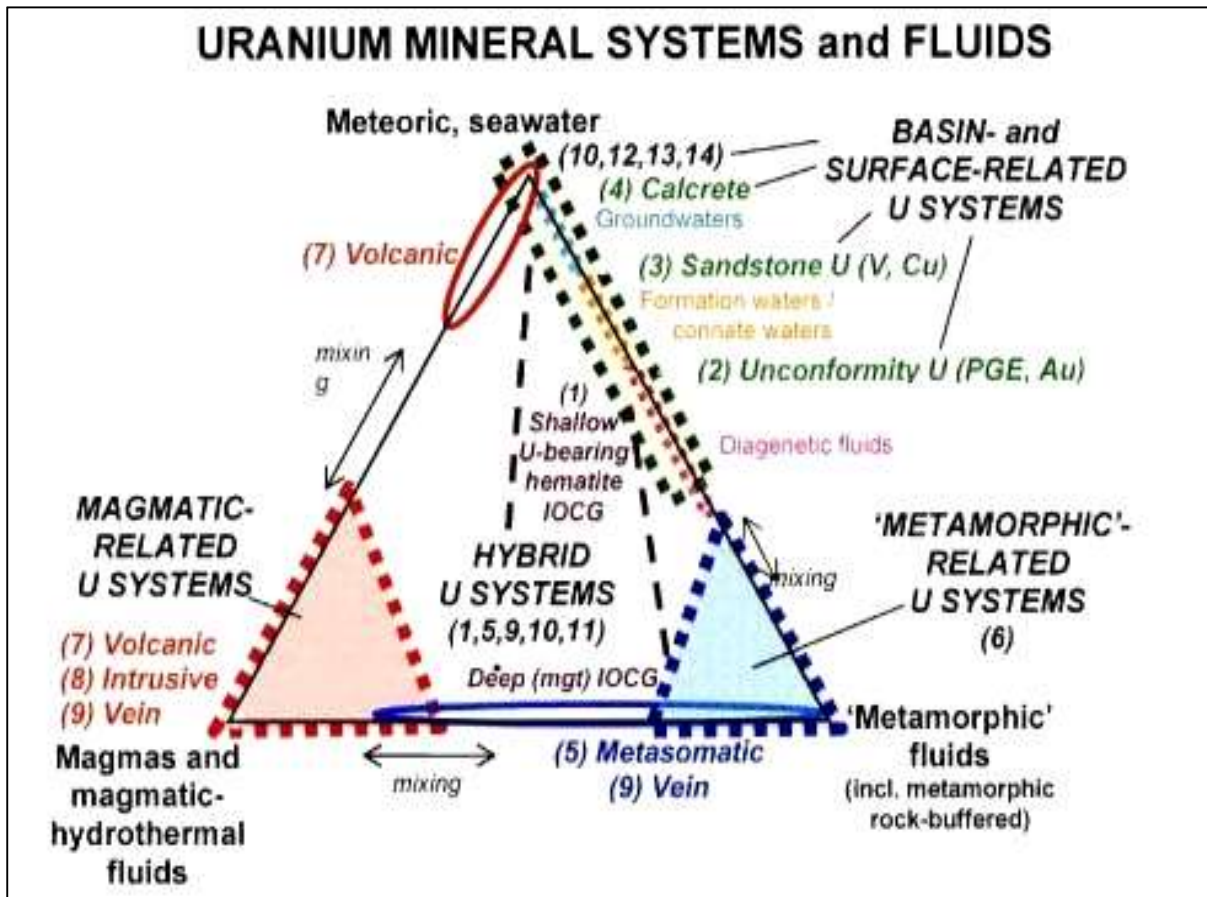


FIG. 4. Scheme of three families of uranium mineralizing systems and three end-member fluid types [38] (reproduced with permission).

#### 2.1.2.2. Russian genetic classification

As summarized by Boitsov [30], the genetic classification used by Russian geologists is primarily a subdivision into deposits related to endogenic (igneous and metamorphic) processes and those related to exogenic (sedimentary and near surface) processes. As outlined in Table 1, both of these main classes contain syngenetic and epigenetic (hydrothermal) types. The different deposit types within these groups are characterized according to specific tectonic settings, host rock, alteration style, mineralization, orebody geometry and age.

TABLE 1. RUSSIAN GENETIC CLASSIFICATION OF URANIUM DEPOSITS [30]

Deposit group	Tectonic setting	Deposit type
Endogenic deposits		
Syngenetic	Shield blocks affected by granitization	U, Th-U at final granitization (Rössing)
	Tectonic activation of Precambrian shields	U in long lived faults (Ukraine)
		Au-U in ancient faults reactivated in the Mesozoic (Elkon)
Proto-platform basins	U at tectonic and stratigraphic unconformities (McArthur River, Ranger)	
Epigenetic	Tectonism and magmatism in fold belts	U at contacts of orogenic granites (Příbram)
		U-Mo in volcanic calderas (Streltsovskoye)
		U in radioactive granite (Limousin)
		Mo-U in volcanics and subvolcanic intrusives (northern Kazakhstan)
Exogenic deposits		
Syngenetic (sedimentary-diagenetic)	Young sedimentary platforms	U, REE, P in shallow marine basins, with fish bone detritus (Melovoye)
	Precambrian platform basins	U, Au in Proterozoic conglomerates (Witwatersrand)
Epigenetic (infiltrational)	Marginal parts of platforms affected by orogenies	U controlled by regional redox zones in large synclines (Kazakhstan, Uzbekistan)
		U controlled by local redox zones in basins and grabens (Ambrosia Lake, Hamr)
	Sedimentary basins in uplifted Shields and fold belts	U in palaeochannels controlled by redox fronts or ground oxidation (Khiagda)
		U-V in evaporation areas in palaeochannels (Yeelirrie, Langer Heinrich)
	Post-platform orogenic belts	U in coal in intermontane grabens and synclines (Koldzhat)
U in intermontane grabens and synclines, redox or ground oxidation controlled (Karaat)		

### 2.1.2.3. *Cuney genetic classification*

For Cuney, the classification of the uranium deposits proposed by the IAEA is essentially based on the nature of the rocks enclosing the deposits and their morphology [37, 40, 41]. This leads to grouping in the same category those deposits formed by very different genetic processes and localized in contrasting geological environments. For example, uranium deposits hosted in metamorphic rocks group uranium mineralization resulting from low temperature, hydrothermal, epigenetic processes formed at relatively shallow crustal levels, such as Schwartzwalder (USA) and mineralization

resulting from synmetamorphic processes formed at relatively deep levels in the crust, such as at Shinkolobwe (Democratic Republic of Congo). Such a grouping may be misleading when defining exploration strategies. Therefore, the use of a genetic classification may provide complementary information to the IAEA classification.

There are three major difficulties in establishing an accurate genetic classification [37]:

- (i) Insufficient knowledge of the genesis of some deposits;
- (ii) Many deposits may result from a succession of concentration episodes, with very different mechanisms and occurring over a long period of time, making it difficult to identify the main mechanism involved in genesis;
- (iii) Secondary processes may obliterate the features characterizing the initial concentration processes involved in the primary phase of uranium mineralization, such as: (a) metamorphism of primary uranium mineralization (e.g. deposits of the Lagoa Real district, Brazil [42]) or (b) remobilization by supergene fluids (e.g. Poços de Caldas deposit, Brazil).

The genetic classification proposed by Cuney [37] is based on the dominant mechanism that is believed to have supplied the primary accumulation of uranium in the deposit. Uranium deposits can be formed at nearly each stage of the geological cycle (Fig. 5) and they have been grouped into five major types, the sixth type includes the deposits for which the mechanisms of uranium accumulation are insufficiently known:

- (1) **M: magmatic deposits:** The uranium concentration process is predominantly controlled by magmatic processes. There are two subtypes of magmatic uranium deposit:
  - (a) **MCf: magmatic crystal fractionation deposits** represented by the most extremely fractionated magmas of peralkaline plutonic complexes and which are located at their roof or margin (e.g. Ilimaussaq, Greenland; Bokan Mountain, USA);
  - (b) **MPm: magmatic partial melting deposits** represented by anatectic melts crystallizing commonly as coarse-grained felsic pegmatoids resulting from low degrees of partial melting of quartz-rich and feldspar-rich metasedimentary and/or metavolcanic rocks.
- (2) **H: hydrothermal deposits:** These result from the precipitation of uranium from hydrothermal fluids of various origins in various geological environments, resulting in a large number of hydrothermal deposit subtypes:
  - (a) **HV: hydrothermal–volcanic deposits** resulting from the remobilization of uranium from highly fractionated tuffaceous volcanic rocks of variable geochemistry (predominantly peralkaline, occasionally highly potassic calc-alkaline and rarely peraluminous (Streltsov, Russian Federation; Dornod, Mongolia);
  - (b) **HG: hydrothermal–granitic deposits** result from the remobilization of magmatic uranium mainly from (i) peraluminous, uraninite-bearing leucogranitoids (e.g. the European Variscan Belt) but also from (ii) high K calc-alkaline granites (HKCA) (Hotagen, Sweden), when the U silicates hosting most of the uranium in the HKCA granites become metamict;
  - (c) **HD: hydrothermal–diagenetic deposits** are formed by the circulation of hot, saline, diagenetic fluids derived from sedimentary basins during their burial. Three principal sub-subtypes are distinguished according to the location of the redox interface controlling the deposition of uranium:
    - (i) HDI: with intraformational redox control, the redox boundary is located within the mineralized host strata:
      - HDItb: tabular type: the ores form flat, elongated bodies parallel to the strata;
      - HDItl: tectonic-lithologic: the orebodies are controlled both by the lithological characteristics of the host rocks and structures;
      - HDIcb: dissolution collapse breccias pipes.

- (ii) HDBb: HD with redox control at the **basement/basin** interface that typically characterizes the unconformity-related deposits;
  - (iii) HDIf: **interformational**, with redox control between two formations within the basin (Oklo, Gabon).
- (d) *HMM: hydrothermal–metamorphic deposits* result from the mobilization of uranium by fluids produced by metamorphic reactions, during deformation;
- (e) *HMs: hydrothermal–metasomatic deposits* are associated with the percolation of large quantities of fluids along regional scale shear zones:
- HMs-Na: **Na**-metasomatic deposits are associated with dequartzification of the host rocks (either of plutonic, volcanic or sedimentary origin) associated with albitization;
  - HMs-K: **K**-metasomatic deposits are represented only by the Aldan ore district in the Russian Federation;
  - HMs-Sk: **skarn** deposits result from the alteration of marble to a calc-silicate mineralogy.
- (3) **E: evapotranspiration deposits** occur as calcretes, where the uranium is accumulated in poorly sorted, siliclastic sediments by evaporation–transpiration processes;
- (4) **S: symsedimentary deposits** contain three subtypes. In these deposits, uranium is accumulated during sedimentation (syngenetic origin):
- (a) SMS: **symsedimentary** deposits controlled by **mechanical sorting**, represented by quartz-pebble conglomerates, where uraninite is accumulated with other heavy;
  - (b) SRt: **symsedimentary** deposits controlled by **redox trapping** (black shale, coal, lignite);
  - (c) SRtc: **symsedimentary** deposits controlled by **redox trapping** and **crystal–chemical** control of U substitution in phosphates.
- (5) **P: phreatic water infiltration deposits:**
- (a) *PB: phreatic basal* type (or palaeovalley) deposits are hosted in organic matter-bearing, poorly sorted, siliclastic sediments deposited in elongate palaeovalleys;
  - (b) *PRf: phreatic roll-front* deposits result from the infiltration of oxidized phreatic waters into reduced sandstone.
- (6) **O: other deposit** types is reserved for those deposits which cannot be attributed to any of the preceding types or which may belong to several of these types, such as Olympic Dam in Australia, or the Itataia deposit in Brazil.

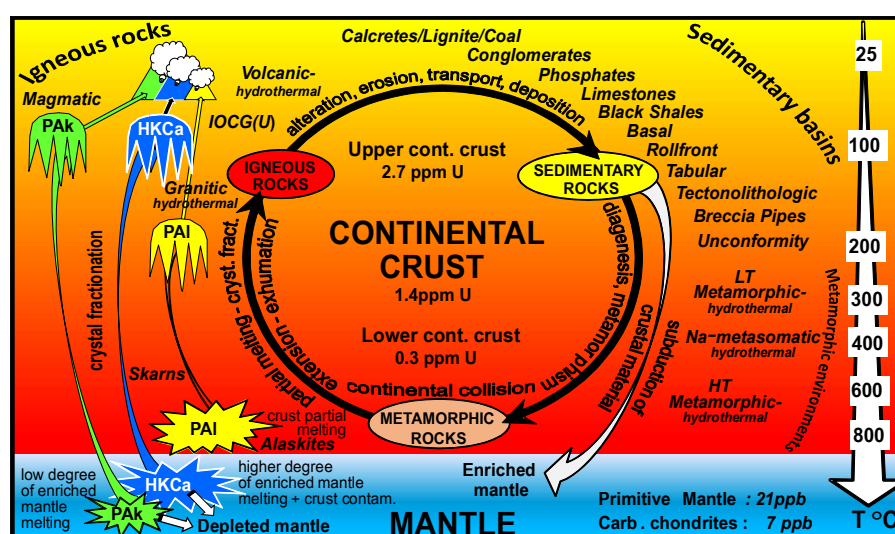


FIG. 5. Position of uranium deposit types with respect to the main fractionation processes along the geological cycle. The different types of uranium-rich magmas are indicated (PAk: peralkaline, HKCa: high K calc-alkaline, PAI: peraluminous) [37] (reproduced with permission).

## 2.2. THE 2013 IAEA CLASSIFICATION OF URANIUM DEPOSITS

For the OECD Nuclear Energy Agency Red Book, a uranium deposit is a mass of naturally occurring mineral assemblages from which uranium has been or could be exploited at present or in the future [4, 5]. For this publication and for the UDEPO database, this definition has been expanded to include any calculated or identified geological concentration of uranium resource regardless of the tonnage or the grade [43].

Fifteen types of deposit have been retained in the new IAEA classification scheme [2, 3, 44]. In contrast to the ordering of previous IAEA classifications, the economics parameter has not been taken into account. Instead, the deposits are listed in a geologically meaningful order, ranging from deep, primary magmatic deposits to sedimentary and surficial deposits. The classes are as follows:

- (1) Intrusive;
- (2) Granite-related;
- (3) Polymetallic iron oxide breccia complex;
- (4) Volcanic-related;
- (5) Metasomatite;
- (6) Metamorphite;
- (7) Proterozoic unconformity;
- (8) Collapse breccia pipe;
- (9) Sandstone;
- (10) Palaeo quartz-pebble conglomerate;
- (11) Surficial;
- (12) Lignite–coal;
- (13) Carbonate;
- (14) Phosphate;
- (15) Black shale.

In comparison to the 1993 IAEA classification, and following the recommendation of Dahlkamp [19], the ‘vein type’ class has been abandoned. As explained by Dahlkamp, veins are associated with various rock types, including granite, volcanic, metasomatite, metasedimentary, sandstone and others. Therefore, the term ‘vein’ is only used to describe the configuration of an orebody in any respective geological environment. ‘Vein type’ deposits have been assigned to two types: (i) granite-related deposits (a new category) and (ii) metamorphite deposits. The category ‘breccia complex’ has been renamed as ‘polymetallic iron oxide breccia complex’, ‘unconformity-related’ are referred to as ‘proterozoic unconformity’, ‘quartz-pebble conglomerate’ has become ‘palaeo quartz-pebble conglomerate’ and ‘phosphorite’ deposits have been renamed ‘phosphate’ to allow inclusion of continental phosphate deposits. Lignite–coal, carbonate and black shale are now recognized as separate types.

Within the 15 types, 36 subtypes and 14 classes have been retained. Most subtypes and classes are those defined by Dahlkamp [19], with minor modifications. Deposit type, subtype and class are listed in the following section.

### 2.2.1. Detailed classification of deposit types, subtypes and classes

Type 1. Intrusive:

Subtype 1.1. Anatectic: pegmatite–alaskite (Rössing, Namibia; Bancroft district, Canada);

Subtype 1.2. Plutonic:

*Class 1.2.1. Quartz monzonite* (Bingham Canyon, USA; Chuquicamata, Chile);

*Class 1.2.2. Peralkaline complex* (Kvanefjeld, Greenland; Poços de Caldas, Brazil);

*Class 1.2.3. Carbonatite* (Phalabora, South Africa; Catalão, Brazil).

- Type 2. Granite-related:  
 Subtype 2.1. Endogranitic (La Crouzille district, France; Xiazhuang district, China);  
 Subtype 2.2. Perigranitic (Příbram region, Czech Republic; Niederschlema Germany).
- Type 3. Polymetallic iron oxide breccia complex (Olympic Dam, Carrapateena, Australia).
- Type 4. Volcanic-related:  
 Subtype 4.1. Stratabound (Dornod No. 7 ore zone, Mongolia; Maureen, Australia);  
 Subtype 4.2. Structure-bound (Streltsov–Antei, Russian Federation; Kurišková, Slovakia);  
 Subtype 4.3. Volcano-sedimentary (Anderson Mine, USA; Sierra Pintada district, Argentina).
- Type 5. Metasomatite:  
 Subtype 5.1. Na- metasomatite:  
   Class 5.1.1. *Granite derived* (Kirovograd district, Ukraine; Lagoa Real, Brazil);  
   Class 5.1.2. *Metasediment–metavolcanic derived* (Krivoy Rog district, Ukraine).  
 Subtype 5.2. K-metasomatite (Elkon district, Russian Federation);  
 Subtype 5.3. Skarn (Mary Kathleen, Australia; Tranomaro, Madagascar).
- Type 6. Metamorphite:  
 Subtype 6.1. Stratabound (Forstau, Austria; Nuottijarvi, Finland);  
 Subtype 6.2. Structure-bound:  
   Class 6.2.1. *Monometallic veins* (Schwartzwalder, USA; Ace–Fay–Verna, Canada);  
   Class 6.2.2. *Polymetallic veins* (Shinkolobwe, Democratic Republic of Congo);  
   Class 6.2.3. *Marble-hosted phosphate* (Itataia, Brazil; Zaozernoje, Kazhakstan).
- Type 7. Proterozoic unconformity:  
 Subtype 7.1. Unconformity-contact (Cigar Lake, Key Lake, McArthur River, Canada);  
 Subtype 7.2. Basement-hosted (Jabiluka, Ranger, Australia; Eagle Point, Canada);  
 Subtype 7.3. Stratiform fracture-controlled (Lambapur, Chitrial, India).
- Type 8. Collapse breccia pipe (Arizona Strip, USA);
- Type 9. Sandstone:  
 Subtype 9.1. Basal channel (Dalmatovskoye, Russian Federation; Beverley, Australia);  
 Subtype 9.2. Tabular (Arlit District, Niger; Ambrosia Lake District, USA):  
   Class 9.2.1. *Continental fluvial, U associated with intrinsic reductant* (Arlit type, Niger);  
   Class 9.2.2. *Continental fluvial, U associated with extrinsic bitumen* (Grants type, USA);  
   Class 9.2.3. *Continental fluvial vanadium–uranium* (Salt Wash type, USA).  
 Subtype 9.3. Roll-front (Wyoming Province, USA; Chu-Sarysu Basin, Kazakhstan):  
   Class 9.3.1. *Continental basin, U associated with intrinsic reductant* (Wyoming type, USA);  
   Class 9.3.2. *Continental to marginal marine, U associated with intrinsic reductant* (Chu-Sarysu type, Kazakhstan);  
   Class 9.3.3. *Marginal marine, U associated with extrinsic reductant* (South Texas type, USA).  
 Subtype 9.4. Tectonic-lithologic (Lodève Basin, France; Franceville Basin, Gabon);  
 Subtype 9.5. Mafic dykes/sills in Proterozoic sandstone (Westmoreland district, Australia; Matoush, Canada).
- Type 10. Palaeo quartz-pebble conglomerate:  
 Subtype 10.1. U dominant (Elliot Lake district, Canada);  
 Subtype 10.2. Au dominant (Witwatersrand Basin, South Africa).
- Type 11. Surficial:  
 Subtype 11.1. Peat bog (Kamushanovskoye, Kyrgyzstan; Flodelle Creek, USA) ;

- Subtype 11.2. Fluvial valley (Yeelirrie, Australia; Langer Heinrich, Namibia);
- Subtype 11.3. Lacustrine–playa (Lake Maitland, Lake Way, Australia);
- Subtype 11.4. Pedogenic and fracture fill (Beslet, Bulgaria).

Type 12. Lignite–coal:

- Subtype 12.1. Stratiform (Koldzhat, Kazakhstan; Williston Basin, USA);
- Subtype 12.2. Fracture-controlled (Freital, Germany; Turakavak, Kyrgyzstan).

Type 13. Carbonate:

- Subtype 13.1. Stratabound (Tumalappalle, India);
- Subtype 13.2. Cataclastic (Mailuu-Suu, Kyrgyzstan; Todilto district, USA);
- Subtype 13.3. Palaeokarst (Sanbaqi, China; Tyuya-Muyun, Kyrgyzstan).

Type 14. Phosphate:

- Subtype 14.1. Organic phosphorite (Mangyshlak Peninsula, Kazakhstan; Ergeninsky region, Russian Federation);
- Subtype 14.2. Minerochemical phosphorite (Phosphoria Formation, USA);
- Subtype 14.3. Continental phosphate (Bakouma district, Central African Republic).

Type 15. Black shale:

- Subtype 15.1. Stratiform (Ranstad, Sweden; Chattanooga Shale Formation, USA);
- Subtype 15.2. Stockwork (Ronneburg district, Germany; Dzhantuar, Uzbekistan).

The names of most deposit types are related to host rock type except for types 3, 7 and 8 which are related to structures, type 5 which is related to metasomatic transformations and type 11 which is associated with surficial processes (Table 2). The deposit types can be grouped into the three major classes of rock, as shown in Table 3 or grouped by geodynamic setting, as in the Russian classification system (Table 4). These groupings show several important factors. Uranium deposits can be found in a wide variety of rock types and can be formed in a wide range of geological environments, from high temperatures at deep crustal levels in orogenic belts to low temperature surficial environments. Most importantly, however, it should be recognized that these classes have far greater significance than the simple names. As outlined in the following descriptions, these deposit types have fundamental characteristics and recognition criteria. In that respect, while mainly named by host rock, the types are essentially empirical models, based on observable characteristics.

TABLE 2. GENERAL CLASSIFICATION CRITERIA FOR URANIUM DEPOSIT TYPES

Classification criteria	Deposit type
Host rock	1. Intrusive 9. Sandstone 10. Palaeo quartz-pebble conglomerate 12. Lignite–coal 13. Carbonate 14. Phosphate 15. Black shale
Structure	3. Polymetallic iron oxide breccia complex 7. Proterozoic unconformity 8. Collapse breccia pipe
Host rock and structure	2. Granite-related 4. Volcanic-related 6. Metamorphite
Metasomatic alteration	5. Metasomatite
Surficial processes	11. Surficial

TABLE 3. DEPOSIT TYPES CLASSIFIED ACCORDING TO MAJOR LITHOLOGICAL GROUPS

Sediments/sedimentary basins	Igneous (plutonic and volcanic)	Metamorphic
7. Proterozoic unconformity	1.2. Intrusive plutonic	1.1. Intrusive anatectic
8. Collapse breccia pipe	2. Granite-related	5. Metasomatite
9. Sandstone	3. Iron oxide breccia complex	6. Metamorphite
10. Palaeo quartz-pebble conglomerate	4. Volcanic-related	
11. Surficial		
12. Lignite–coal		
13. Carbonate		
14. Phosphate		
15. Black shale		

TABLE 4. URANIUM DEPOSIT TYPES ACCORDING TO TECTONIC SETTING (RUSSIAN CLASSIFICATION [30])

Cratons (ancient shields and platforms)	Orogenic belts and median massifs	Platform cover
1. Intrusive		9. Sandstone
3. Iron oxide breccia complex	2. Granite-related	8. Collapse breccia pipe
5. Metasomatite	4. Volcanic-related	11. Surficial
7. Proterozoic unconformity	6. Metamorphite	12. Lignite–coal
10. Palaeo quartz-pebble conglomerate	15. Black shale	13. Carbonate
		14. Phosphate

### 2.2.2. Geological description of uranium deposits types and subtypes

#### Type 1: Intrusive deposits

Deposits included in this type are contained in intrusive rocks of many different petrochemical compositions (granite, pegmatite, monzonite, peralkaline syenite and carbonatite). Two main subtypes are recognized: (i) intrusive anatectic deposits associated with partial melting processes (Rössing and Rössing South, Namibia, and deposits in the Bancroft area, Canada), and (ii) intrusive plutonic deposits related to magmatic differentiation. Examples of this latter type include the uranium occurrences in the porphyry copper deposits of Bingham Canyon and Twin Buttes (USA), the Kvanefjeld deposit (Greenland) and the Phalabora carbonatite complex (South Africa).

#### *Subtype 1.1: Anatectic pegmatite–alaskite deposits*

Deposits related to partial melting in anatectic environments are those corresponding to enrichment of uraninite in the form of disseminations in pegmatitic and/or granitic dykes/sills which were injected into high grade migmatitic gneiss. The term ‘alaskite’ corresponds to quartz-rich, leucocratic granites that often exhibit a pegmatitic texture. Alaskite in relation to uranium deposits was first described at the Rössing deposit in Namibia. Pegmatites prospective for uranium deposits are of the anatectic type and are related to low degrees of partial melting during metamorphism. These contrast with the less prospective pegmatites formed as the final crystallization fractions of large igneous intrusions.

In anatectic pegmatites, uraninite and other uranium–thorium minerals occur in non-zoned granitic and syenitic pegmatite dykes (siliceous as well as syenites of mafic tendency with aegirine and augite) in sedimentary and igneous rocks, which have been metamorphosed to amphibolite facies grade. Haematite is a characteristic alteration product (Bancroft district, Canada). Other examples are the deposits of the North Shore District in Quebec and the Charlebois Lake area in Saskatchewan (Canada). Deposits are small to medium in size (300–5000 tU) and generally of low grade (0.01–0.10% U).

In Namibia, disseminated uranium minerals occur in medium- to coarse-grained alaskite bodies (leucocratic, quartz and alkali feldspar-rich granite/pegmatite) that are either discordant or concordant with surrounding folded and highly metamorphosed and migmatized sedimentary rocks. The alaskite bodies range in size from small lenses and tabular dykes to large stocks and domes that are several hundreds of metres in diameter. No alteration is associated with the uranium mineralization. The main example is Rössing, Namibia. Other examples include Rössing South (Husab), Anomaly A and Valencia, all located in Namibia. Deposits are medium to large/very large in size (5000–250 000 tU) and of low grade (0.01–0.04% U).

#### *Subtype 1.2: Plutonic deposits*

Deposits related to magmatic differentiation correspond to low to very low grade uranium and thorium disseminated in various intrusive magmatic rocks. These deposits are classified as ‘unconventional resources’ by the IAEA. Uranium can only be extracted as a by-product of Cu–Au–Mo in porphyry copper deposits or as a by-product of Cu–REE–Zr–Ta–Nb–P–Th–Fe–Ti in peralkaline carbonatite complexes.

***Class 1.2.1: Quartz monzonite:*** Very low grade concentrations of disseminated uranium occur in highly differentiated granitic to quartz monzonitic complexes (copper porphyry). Owing to their very low uranium content (20–50 ppm), uranium has been and can only be recovered as a by-product of Cu–Au–Mo heap leaching. Examples are Bingham Canyon, Twin Buttes and Yerington (USA), Chuquicamata and Rodomiro Tomic (Chile).

***Class 1.2.2: Peralkaline complex:*** Low grade uranium disseminations occur in peralkaline granite or syenite domes or stocks that are enriched in REE, Ta, Nb, Zr and Th. Uranium phases are commonly of a refractory nature (e.g. streenstrupine, eudyalite, monazite), such as those found in the large Kvanefjeld deposit (Greenland). Other examples are Gurayah (Saudi Arabia), Lolodorf (Cameroon) and Poços de Caldas (Brazil). Resources are medium to large in size (2000–100 000 tU) and low to very low grades (0.005–0.025% U).

***Class 1.2.3: Carbonatite:*** Disseminated uranium can occur in the form of uranothorianite, perovskite, pyrochlore and rare earth element-bearing minerals in carbonatite complexes. Up to 2002, uranium was recovered at Phalabora (South Africa) as a by-product of copper production. Other examples of uranium-bearing carbonatite intrusions are Araxa and Catalão (Brazil), and Sokli (Finland). Average grades are low to very low (0.005–0.020% U).

#### Type 2: Granite-related deposits

Deposits related to granite include: (i) true veins composed of ore and gangue minerals in granite or adjacent (meta-) sedimentary rocks and (ii) disseminated mineralization occurring in granite as episyenite bodies. Uranium mineralization occurs within, at the contact or peripheral to the intrusion. In the Hercynian Belt of Europe and other parts of the world, these deposits are generally associated with large, peraluminous two mica granite complexes (leucogranites). Resources range from small to large in size and grades vary from low to high. Two subtypes are distinguished on the basis of their spatial setting with respect to the granitic pluton and the host country rock.

### *Subtype 2.1: Endogranitic deposits*

Endogranitic deposits are commonly monometallic and consist of: (i) discontinuous, linear orebodies in veins and stockworks localized in fractured granite (La Crouzille district, France) or (ii) disseminations in pipes or columns of episyenite (Le Bernardan, France). Veins can extend from within the granite to beyond the granite contact into the enclosing rocks. Veins can extend to depths of 700 m while episyenite orebodies can reach 1000 m vertical extension. Deposits are small to medium in size (10–5000 tU) with medium grades (0.10–0.50% U).

### *Subtype 2.2: Perigranitic deposits*

Perigranitic deposits may consist of monometallic or polymetallic veins (Příbram district and Erzgebirge region, respectively, Czech Republic) surrounding granitic plutons. Uranium and other elements (most notably As, Bi, Ag, Co and Ni) are not genetically related. Veins persist to depths as great as 2000 m. Deposits vary from small to large (100–95 000 tU) and grades are low to high (0.05–1% U).

### Type 3: Polymetallic iron oxide breccia complex deposits

This type of deposit has been assigned to a broad category of iron oxide–copper–gold deposits occurring around the world, although Olympic Dam (Australia) is the only known representative of this type with significant by-product uranium resources. This deposit is the world's largest individual uranium resource and contains with more than 2 Mt of uranium at low grade (230 ppm). Deposits of this group occur in haematite-rich granite breccias (Olympic Dam, Gawler Craton) or in metasedimentary–metavolcanic breccias (Salobo, Carajas district, Brazil) and contain disseminated uranium in association with copper, gold, silver and rare earth elements. At Olympic Dam, this breccia is hosted within a Mesoproterozoic, highly potassic granitic intrusion that exhibits regional Fe–K metasomatism.

Other significant deposits and prospects of this type occur on the Gawler Craton, including Prominent Hill and Carrapeteena, as well as some younger breccia hosted deposits (Mount Gee and Radium Ridge) in the Mount Painter area.

The Carajas district is one of the most important mineral provinces of Brazil. Copper–gold deposits occur within a mixed metavolcanic–metasedimentary Late Archaean (2.85–2.70 Ga) sequence that has been intruded by alkaline and calc-alkaline granites (2.75–2.55 Ga) and by I to A type granites (1.9–1.8 Ga). Data on the uranium content of the deposits are sparse. The range of uranium concentrations varies from 30–50 ppm to 100–170 ppm.

### Type 4: Volcanic-related deposits

Uranium deposits of this type are located within and near volcanic calderas filled with mafic to felsic volcanic lavas or, more commonly, pyroclastic rocks and intercalated clastic sediments. Uranium mineralization is largely controlled by structures such as veins and stockworks with minor stratiform lodes. This mineralization occurs at several stratigraphic levels within the volcanic and sedimentary units and may extend deeply into the underlying basement where it is found in fractured granite and metamorphic rocks. Uranium minerals (pitchblende, coffinite, hexavalent uranium minerals and, less commonly, brannerite) are associated with molybdenum-bearing sulphides and pyrite. Other anomalous elements include As, Bi, Ag, Li, Pb, Sb, Sn and W. Associated gangue minerals consist of violet coloured fluorite, carbonates, baryte and quartz. The most significant deposits are located within the Streltsovskaya caldera in the Russian Federation. Other examples are known in China (Xiangshan district), Mongolia (Dornod) and Gurvanbulag districts), USA (McDermitt caldera) and Mexico (Peña Blanca district).

#### *Subtype 4.1: Stratabound deposits*

Stratabound deposits consist of disseminations and impregnations in permeable and/or chemically reactive flows, flow breccias, tuffs and intercalated pyroclastic and clastic sediments. Mineralization may be stratabound and structurally controlled (both stratabound and structure-bound) in the same deposit (Streltsovskaya and Dornod calderas, Russian Federation and Mongolia, respectively). Resources are small to medium in size (500–5000 tU) and the grades low to medium (0.03–0.10% U).

#### *Subtype 4.2: Structure-bound deposits*

Structure-bound deposits include veins or stockworks in sub-volcanic intrusions, diatremes, flows, bedded pyroclastic units and surficial fractures fillings in similar lithologies (Streltsovskaya and Dornod calderas, Russian Federation, and Mongolia, respectively). Intense fracture zones and breccias occur along both steep and shallow dipping faults and control the sites of mineralization and the dimensions of the orebodies. Some veins persist to depths of more than 1000 m and extend into the basement rocks. Mineralization is generally polymetallic and uranium is associated with molybdenum and, locally, fluorine. Deposits are medium to large in size (1000–40 000 tU) and grades are medium (0.10–0.40% U).

#### *Subtype 4.3: Volcano-sedimentary deposits*

Volcano-sedimentary deposits consist of carbonaceous lacustrine or fluvial/alluvial sediments with a tuffaceous component. Widespread, peneconcordant, low grade (50–200 ppmU) uranium accumulations associated with anomalous V, Mo, Li, F, B, Cu and Ni encompass irregularly shaped zones with higher grade mineralization (Anderson Mine, USA; Sierra Pintada district, Argentina). Resources range from a few tens of tonnes to over 5000 tU.

### Type 5: Metasomatite deposits

Deposits of this type are generally confined to Precambrian Shields (an exception being Coles Hill, USA) in orogenic belts affected by intense Na- or K-metasomatism, which produced albitized or illitized rocks along deeply rooted fault systems. In Ukraine, these deposits are developed within a variety of basement rocks, including granite, migmatite, gneiss and ferruginous quartzite which produced albitite, aegirinite, alkali amphibolite, as well as carbonate and ferruginous rocks. The principal uranium phases are uraninite, brannerite and other titaniferous and uraniferous minerals, pitchblende, coffinite and hexavalent uranium minerals. The resources range in size from medium to very large. Examples include the Michurinskoye, Vatutinskoye, Severinskoye, Zheltorechenskoye, Novokonstantinovskoye deposits (Ukraine), deposits of the Elkon district (Russian Federation), Espinharas and Lagoa Real (Brazil), Valhalla (Australia), Kurupung (Guyana), Coles Hill (USA), Lianshangan (China), Michelin (Canada) and several small deposits in the Arjeplog region of northern Sweden. Three subtypes of metasomatite deposits are distinguished on the basis of precursor rock lithology and type of metasomatism: Na-metasomatite, K-metasomatite and skarn deposits.

#### *Subtype 5.1: Na-metasomatite deposits*

Na-metasomatite deposits are of two classes:

*Class 5.1.1: Granite-derived:* Uranium minerals occur as disseminations and veinlets within the interstices of closely spaced joints, shears and breccias in albitized dequartzified granite along pre-metasomatic fault zones in uraniferous granites. Deposits in the Kirovograd district (Ukraine) have large resources (10 000–100 000 tU) at low to medium grades (0.07–0.15% U) hosted in discontinuous orebodies extending to depths in excess of 2000 m. In contrast, most deposits of this subtype elsewhere in the world are much smaller (Aricheng, Guyana), with the exception of Lagoa Real (Brazil) and Coles Hill (USA).

*Class 5.1.2: Metasediment–metavolcanic-derived:* In the Krivoy Rog Basin (Ukraine), Proterozoic metasediments (carbonate, quartzite, schist and banded iron formations) and late intrusive microcline-bearing granites are intensely altered along structural zones by Na-metasomatism, carbonate metasomatism and, finally, silicification. Deposits in the Krivoy Rog Basin persist to depths of about 2000 m. In the Central Mineral Belt of Labrador (Canada), several deposits (Michelin, Jacques Lake) are located within Proterozoic felsic metavolcanic rocks. Resources are small to large in size (500–40 000 t) and of low to medium grade (0.07–0.15% U).

*Subtype 5.2: K-metasomatite deposits*

K-metasomatite deposits have only been found in the Elkon district (Russian Federation), where gneiss and migmatite of the Archaean–Palaeoproterozoic crystalline basement were affected by Palaeoproterozoic faults reactivated during the Mesozoic. Several stages of alteration are documented in the district. Early K–Si metasomatism is developed in the granitoids, followed by multistage, superimposed Mesozoic alteration types consisting of albite, sericite, K-feldspar, chlorite, haematite, pyrite and carbonate. Mineralization persists to depths greater than 2000 m. The main uranium mineral is brannerite and occurs associated with gold, although uraninite occurs in some ore lenses. Deposits are medium to large (2000–100 000 tU) and of low to medium grade (0.05–0.15% U).

*Subtype 5.3: Skarn deposits*

In skarn deposits, the uranium mineralization (generally thorium-bearing uraninite) is disseminated in calc-silicate rocks which may have resulted from contact or regional metamorphism of sedimentary or volcanic rocks. Rare earth elements, thorium and other metals may also be associated (Mary Kathleen, Australia; Tranomaro, Madagascar; Inca, Namibia). Grades are highly variable. These deposits are not common.

Type 6: Metamorphite deposits

Metamorphite deposits consist of disseminations, impregnations, veins and shear zones within metamorphic rocks of various ages with no relation to granitic intrusions. These deposits are highly variable in size, resources and grades. Two subtypes are recognized:

*Subtype 6.1: Stratabound deposits*

The mineralization in stratabound deposits has resulted from regional metamorphism of uraniferous sediments. Such deposits consist of small lenses of disseminated uranium mineralization that are erratically distributed but concordant with the strata in metasedimentary rocks (Forstau, Austria). Pitchblende is the main uranium mineral occurring in low grade (greenschist facies) metamorphism. Resources are small (500–1000 tU) and grades are low (0.05–0.10% U).

Other examples include stratabound deposits hosted within metamorphosed phosphorites (Nuottijarvi and Lampinsaari, Finland). These deposits are not common.

*Subtype 6.2: Structure-bound deposits*

Structure-bound deposits consist of uranium mineralization occurring as lenses, sheets and disseminations filling joints, fissures, breccias and stockworks in deformed and fractured rocks. The size and complexity of vein sets are variable, and the distribution and intensity of mineralization is very irregular. Veins and stockworks may persist to depths of more than 1000 m. The principal uranium phases are pitchblende, uraninite and coffinite. Deposits are small to large (200–20 000 t) and of low to medium grade (0.05–0.50% U). Three classes of structure-bound deposit are identified:

*Class 6.2.1: Monometallic veins:* Uranium and gangue minerals with only traces of other metallic minerals form stringers, veins and veinlets within larger dilational structures. Mineralization is relatively continuous and grades are highly variable (Schwartzwalder, USA; Ace-Fay-Verna, Canada; Kamyshevoye, Kazakhstan).

*Class 6.2.2: Polymetallic veins:* Uranium associated with Co, Cu, Fe, Mo, Ni, Pb, Zn, Ag, As and gangue minerals occur in veins, stockworks and breccia matrix as well as replacement masses and disseminated particles and aggregates in fractured host rocks. Mineralization is fairly continuous but highly variable in grade and extent (Shinkolobwe, Democratic Republic of the Congo; Port Radium, Canada; Jaduguda, India).

*Class 6.2.3: Marble-hosted phosphate deposits:* The Itataia (Brazil) deposit is a hydrothermal metasomatic Cambrian–Ordovician uraniumiferous collophane (apatite) deposit, which is hosted by Precambrian metamorphic rocks. Two major ore types have been identified: (i) black ore in Nametasomatized episyenites and marbles with coffinite, hydrothermal zircon and organic matter and (ii) the pink ore represented by massive uranium-rich collophane (cryptocrystalline hydroxyapatite) coloured pink by the presence of haematite veins and stockworks in marble, gneiss and episyenite. Similar deposits are also found in Kazakhstan (Zaozernoye).

#### Type 7: Proterozoic unconformity deposits

Unconformity-related deposits are associated with and occur immediately below, above, or spanning an unconformable contact that separates Archaean–Palaeoproterozoic crystalline basement from overlying, red bed clastic sediments of Proterozoic age. In most cases, the basement rocks immediately below the unconformity are strongly haematized and clay altered, possibly as a result of palaeoweathering and/or diagenetic/hydrothermal alteration. Deposits consist of pods, veins and semi-massive replacements comprising mainly pitchblende. Strong quartz dissolution is generally associated with them. They are preferentially located in two major districts, the Athabasca Basin (Canada) and the Pine Creek Orogen (Australia). The Proterozoic unconformity deposits include three subtypes of variable importance: unconformity-contact, basement-hosted and stratiform structure-controlled deposits.

##### *Subtype 7.1: Unconformity-contact deposits*

With the exception of the low grade Karku deposit (Russian Federation), unconformity-contact deposits all occur within the Athabasca Basin (Canada). Deposits are situated at the base of the sedimentary cover, directly overlying the unconformity. The deposit form varies from elongate pods to flattened linear orebodies typically characterized by a high grade core surrounded by a lower grade ‘halo’ of mineralization. Most of the orebodies have root-like extensions into the basement rock. While some mineralization is open space infill, much of it is replacement style. Mineralization also often extends up to several tens of metres into the overlying sandstone cover and along breccias and fault zones forming so-called ‘perched mineralization’. Deposits can be monometallic (McArthur River) or polymetallic (Cigar Lake). Deposits are medium to large or very large (1000–200 000 tU) and are characterized by their high grades (1–20% U).

##### *Subtype 7.2: Basement-hosted deposits*

Basement-hosted deposits are both stratabound and structure-bound in metasedimentary rocks (except for Nabarlek (Australia) which is partly hosted by amphibolite) below the unconformity on which the basal clastic sediments rest. The basement ore typically occupies moderate to steep dipping brittle shears, fractures and breccia zones extending for hundreds of metres along strike and extending down-dip for several tens of metres to more than 1000 m below the unconformity, as with the Jabiluka deposit (Australia). Disseminated and vein uraninite/pitchblende occupies fractures and breccia matrix but may also replace the host rock. High grade ore is commonly associated with brecciated graphitic schist (exceptions include Nabarlek, some zones of Eagle Point and Centennial). These deposits

comprise small to very large resources (300–200 000 tU) of medium grade (0.10–0.50% U), but some deposits (Millennium and Nabarlek) may have grades of several per cent. Examples are Kintyre, Jabiluka and Ranger (Australia), Millennium and Eagle Point in the Athabasca Basin and Kiggavik and Andrew Lake in the Thelon Basin (Canada). Except for some mineralization of the recently discovered Angularli deposit in Arnhem Land, all of the Australian unconformity deposits are basement-hosted.

#### *Subtype 7.3: Stratiform structure-controlled deposits*

Stratiform structure-controlled deposits are typically low grade (0.05–0.10% U), stratabound, narrow (1–5 m) zones of mineralization which are located along the unconformity between Archaean, uranium- and thorium-rich granites and Proterozoic metasedimentary rocks with minor enrichments occurring along fractures. This type of deposit (Chitrial and Lambapur) has only been observed in the Cuddapah Basin (India). Resources of individual deposits are in the range 1000–8000 tU.

#### Type 8: Collapse breccia pipe deposits

Deposits in this group occur in sedimentary basins within cylindrical, vertical pipes filled with fragments from overlying lithological units filling karst solution cavities excavated in the thick, underlying carbonate strata. The uranium is concentrated as primary, tetravalent uranium minerals, mainly pitchblende, in the permeable breccia matrix and in the arcuate, ring fracture zone surrounding the pipe. The pitchblende is associated with numerous sulphide and oxide minerals containing Cu, Fe, V, Zn, Pb, Ag, Mo, Ni, Co, As and Se. Type examples are the deposits of the Arizona Strip north of the Grand Canyon and those immediately south of the Grand Canyon (USA). Resources are small to medium (300–2500 tU) and of relatively high grade (0.20–0.80% U).

#### Type 9: Sandstone deposits

Sandstone-hosted uranium deposits occur in medium- to coarse-grained sandstones deposited in continental fluvial or marginal marine sedimentary environments. Volcanic ash may represent a major uranium source within the sandstone (Arlit district, Niger; Lodève Basin, France; Wyoming, USA). Uranium is precipitated by reduction processes caused by the presence of a variety of possible reducing agents within the sandstone. These include carbonaceous material (mainly detrital plant debris), sulphides (pyrite), ferro-magnesian minerals (chlorite), bacterial activity, migrated fluids from underlying hydrocarbon reservoirs and others. Sandstone uranium deposits can be divided into five main subtypes with frequent transitional types between them.

#### *Subtype 9.1: Basal channel deposits*

Palaeodrainage systems consist of wide channels filled with thick, permeable alluvial–fluvial sediments. The uranium is predominantly associated with detrital plant debris forming orebodies that display, in a plan view, an elongated lens or ribbon-like configuration and, in a section view, a lenticular or, more rarely, a roll shape. Individual deposits may range from several hundred tonnes to 20 000 tU, at grades of 0.01–3% U. Examples include the deposits of Dalmatovskoye (Transural region), Malinovskoye (western Siberia), Khiagdinskoye (Vitim district) in the Russian Federation, as well as deposits of the Tono district (Japan), Blizzard (Canada) and Beverley (Australia).

#### *Subtype 9.2: Tabular deposits*

Tabular deposits consist of uranium matrix impregnations that form irregularly shaped lenticular masses within reduced sediments. The mineralized zones are mostly oriented parallel to the depositional trend. The size of individual deposits may range from several hundred tonnes to 150 000 tU at average grades of 0.05–0.5% U and occasionally up to 1% U. Examples of tabular deposits include Hamr-Stráz (Czech Republic), Akouta, Arlit and Imouraren (Niger) and those of the Colorado Plateau (USA).

*Class 9.2.1: Continental fluvial uranium associated with intrinsic reductant (Arlit district, Niger):* Tabular or lenticular uranium orebodies are hosted in sediment-rich in detrital carbonaceous matter in a continental fluvial system consisting of sandstone interbedded with claystone–shale beds. Uranium with V, Mo, Zn and Zr occurs as pitchblende and coffinite disseminated in reduced, pyritic sandstone and as finely disseminated argillaceous–organic uranium complexes in shale. Uranyl vanadates are dominant in oxidized zones. Resources range in size from small to large (<100–100 000 tU) and are of low to medium grade (0.10–0.50% U). Type examples are deposits from the Arlit district (Niger), which has resources exceeding 600 000 tU.

*Class 9.2.2: Continental fluvial uranium associated with extrinsic humate/bitumen (Grants region, USA):* Uranium is associated with humate/bitumen derived from redistributed carbonaceous matter. Mineralization is of a disseminated nature and occurs as lenses within continental sandstone which is intercalated with shale. Sandstone represents 60–80% of the stratigraphic thickness but some pyroclastics may be present. The host sandstone was deposited in a mid-fan environment within an extensive fluviolacustrine sedimentary system. Resources are medium to large (500–5000 tU) and the grades medium (0.10–0.40% U). Deposits of the Ambrosia Lake district (USA) such as the Jackpile deposit, with resources on the order of 130 000 tU, are typical examples.

*Class 9.2.3: Continental fluvial U–V (Salt Wash Member, USA):* Uranium associated with vanadium occurs in reduced fluvial sandstone within a sequence of continental red bed sediments. The suite comprises thin, widespread units of selectively reduced sandstone with intercalated layers of grey clay and carbonaceous debris. Deposits are small to medium (1–2000 tU) and of low to medium grade (0.05–0.50% U), but the high vanadium content often makes these deposits viable targets.

#### *Subtype 9.3: Roll-front deposits*

The mineralized zones of roll-front deposits are convex in shape, oriented down the hydrological gradient. They display diffuse boundaries with reduced sandstone on the down-gradient side and sharp contacts with oxidized sandstone on the up-gradient side. The mineralized zones are elongate and sinuous along strike and perpendicular to the direction of deposition and groundwater flow. Resources range in size from a few hundred tonnes to several thousand tonnes of uranium, at grades averaging 0.05–0.25% U. Examples include Budenovskoye, Tortkuduk, Moynkum, Inkai and Mynkuduk (Kazakhstan), Crow Butte and Smith Ranch (USA) and Bukinay, Sugraly and Uchkuduk (Uzbekistan).

*Class 9.3.1: Continental basin uranium associated with intrinsic reductant (Wyoming, USA):* Uranium occurs in disseminations at the redox boundary at the contact with pyrite-bearing sandstone and detrital carbonaceous debris on the down-gradient side in arkosic and subarkosic sandstones deposited in intracratonic or intermontane basins. These basins are proximal to rocks such as granites and felsic tuffs containing anomalous uranium concentrations. Most deposits occur within interbedded sequences of fluvial sandstone and volcanic-rich sediments. The shapes of deposits are strongly controlled by the hydrology of the host rocks. Resources are small to large (100–1000 tU) at medium grades (0.05–0.20% U). Typical examples are deposits from the Wyoming basins which host resources of the order of 250 000 tU.

*Class 9.3.2: Continental to marginal marine uranium associated with intrinsic reductant (Chu-Sarysu Basin, Kazakhstan):* Deposits are similar to roll-front deposits in continental basins but host lithologies belong to a sequence of mixed continental and marginal marine origin. Resources are medium to large (1000–100 000 tU) with grades generally low (0.04–0.08% U). The world's largest resources of this type (800 000 t) are located in the Chu-Sarysu and Syr-Darya Basins (Kazakhstan).

*Class 9.3.3: Marginal marine uranium associated with extrinsic reductant (south Texas, USA):* Uranium is concentrated in roll type deposits near faults and in contact with pyrite/marcasite-bearing sandstone on their down-gradient side. Host environments include point bars, lateral bars and crevasse splays deposited in a fluvial environment and barrier bars and offshore bars deposited in a marine environment. Deposits are small to medium (50–5000 tU) and grades are low to medium (<0.05–0.25% U). The south Texas uranium region contains about 100 000 tU of resources.

#### *Subtype 9.4: Tectonic-lithologic deposits*

Tectonic-lithologic deposits are discordant to the host strata. They occur in permeable fault zones and adjacent sandstone beds in reduced environments created by the presence of hydrocarbons and/or detrital organic matter. Uranium is precipitated in fracture or fault zones related to tectonic extension. Individual deposits contain a few hundred tonnes up to 5000 tU at grades of 0.1–0.5% U. Examples include the deposits of the Lodève district (France) and those of the Franceville Basin (Gabon).

#### *Subtype 9.5: Mafic dykes/sills in Proterozoic sandstones*

Uranium mineralization is associated with mafic dykes and sills which are concordant with, or cross-cut, Proterozoic sandstone formations. Deposits may be subvertically oriented along the dyke's margins (Matoush, Otish Basin, Canada), hosted within the dykes, or stratabound within the sandstones along lithological contacts with mafic sills (Redtree, Westmoreland district, Australia). Deposits are small to medium (300–10 000 tU) and have low to medium grades (0.05–0.40% U).

#### Type 10: Palaeo quartz-pebble conglomerate deposits

Detrital uranium oxide ores are found in quartz-pebble conglomerates deposited as basal units (Elliot Lake district, Canada or intraformational conglomerates (Witwatersrand Basin, South Africa) in fluvio-lacustrine braided stream systems older than 2400–2300 Ma. The conglomerate matrix is pyritic, and gold, as well as other accessory oxide and sulphide detrital minerals, are often present in minor quantities. Examples include deposits of the Witwatersrand Basin, South Africa, where uranium is mined as a by-product of gold, as well as deposits in the Blind River/Elliot Lake area of Canada. Two economic subtypes are distinguished.

#### *Subtype 10.1: U-dominant deposits*

In uranium dominant deposits, the uranium is accompanied by rare earth elements and thorium (Elliot Lake district, Canada). Uraninite, uranothorite, zircon, monazite, xenotime and Ti–Fe oxides are the prevailing detrital minerals. Resources are medium to large (2000–150 000 tU) and of low grade (0.03–0.10% U).

#### *Subtype 10.2: Au-dominant deposits*

In gold dominant deposits, the gold occurs in combination with uranium (Witwatersrand Basin, South Africa) and is sometimes accompanied by rare earth elements and thorium. Detrital ore minerals include uraninite, uranothorite, native gold and platinoids. These deposits are the oldest known. Resources are medium to large (5000–100 000 tU) and of low grade (0.01–0.05% U).

#### Type 11: Surficial deposits

Surficial uranium deposits are broadly defined as young (Tertiary–Recent), near surface uranium concentrations hosted in sediments and soils. The largest of the surficial uranium deposits are found in calcrete (calcium and magnesium carbonates) and they are mainly located in Australia (Yeelirrie) and Namibia (Langer Heinrich). These calcrete hosted deposits mainly occur in valley fill sediments along Tertiary drainage channels and in playa lake sediments in areas of deeply weathered, uraniferous

granites. Carnotite is the main uranium mineral. Surficial deposits also occur less commonly in peat bogs, karst caverns and soils.

#### *Subtype 11.1: Peat bog deposits*

In humid climatic regions in uranium-rich source areas, uranium can accumulate in organic and clay-rich shallow depressions (swamps, bogs, muskegs) predominantly composed of vegetal organic matter, often peats, within alluvial pelitic–psammitic sediments. No discrete uranium minerals occur. Resources are small (100–500 tU) and grades low (0.03–0.08% U). Typical examples are Kamushanovskoye (Kyrgyzstan) and Flodelle Creek (USA). This type of deposit is uncommon.

#### *Subtype 11.2: Fluvial valley deposits*

The mineralization comprising fluvial valley deposits forms flat lying lenses up to a few metres thick in duricrust sediments, with most of the mineralization deposited below the current water table. Uranium mineralization occurs as carnotite and rarely as other uranyl minerals, which are disseminated as fracture coatings and vug linings in earthy or porcellaneous calcrete. Resources are small to large (500–50 000 tU) and are, with the exception of Yeelirrie (Australia) which has grades above 0.10% U, generally of low grade (0.02–0.06% U). Vanadium can in some deposits be economically recovered. An example of a fluvial valley deposit is the Langer Heinrich deposit (Namibia).

#### *Subtype 11.3: Lacustrine–playa deposits*

In lacustrine–playa deposits, mineralization is similar to the fluvial valley type but is hosted in duricrust layers in shallow lakes or playa sediments. Resources are small to medium (500–5000 tU) and of low grade (0.01–0.03% U). Typical examples include Australian deposits from the Yilgarn Craton (Lake Way, Lake Maitland and Centipede).

#### *Subtype 11.4: Pedogenic and fracture fill deposits*

Pedogenic and fracture fill deposits comprise surface bound uranium concentrations in soils and pedogenic encrustations, as well as disseminations, coatings and fillings of near surface cataclastic zones (shears, fissures, joints) (Beslet, Bulgaria). Deposits are small (100–500 tU) and of low grade (0.05–0.10% U).

### Type 12: Lignite–coal deposits

Elevated uranium contents occur in lignite or coal mixed with mineral detritus (silt, clay) and in immediately adjacent carbonaceous mud and siltstone–sandstone horizons. Pyrite and ash contents are high. Lignite–coal seams are often interbedded or overlain by felsic pyroclastic rocks. Examples include deposits in the southwestern Williston Basin (USA), Koldjat and Nizhne Iliskoye (Kazakhstan), Freital (Germany), Ambassador (Australia) and the Serres Basin (Greece). Two subtypes are recognized: stratiform lignite–coal deposits and fracture-controlled lignite–coal deposits.

#### *Subtype 12.1: Stratiform lignite–coal deposits*

Stratiform, syngenetic lignite–coal deposits possess uniformly disseminated mineralization throughout the carbonaceous/lignite–coal horizons. Uranium grades are very low and average less than 50 ppm U (Northern Great Plains, USA), but tonnages are very large. Mineralization can also be present in lignite seams intercalated with sandstones and located within palaeochannels such as the Ambassador polymetallic deposit (Western Australia), which has an average uranium grade of 0.04% U.

### *Subtype 12.2: Fractured-controlled lignite–coal deposits*

Mixed stratiform and fracture-controlled, epigenetic lignite–coal deposits contain ‘spotty’ and irregularly distributed mineralization along joints and cataclastic zones with strong variation in the grade. Resources are low to medium and grades are also low to medium (0.01–0.10% U). Examples include Cave Hills and Slim Buttes (USA) and Freital (Germany).

### Type 13: Carbonate deposits

Deposits are hosted in carbonate rocks (limestone, dolostone). Mineralization can be syngenetic and stratabound or, more commonly, structure related within karsts, fractures, faults and folds. Three types of carbonate hosted uranium deposits are recognized: stratabound, cataclastic and karst.

#### *Subtype 13.1: Stratabound carbonate deposits*

The deposit at Tumulappalle (India) is the only example of a stratabound carbonate deposit known. The deposit is hosted in phosphatic dolostone and although the uranium grades are low (0.03% U), the size of the deposit (>72 000 tU) combined with almost isotropic mineralization and considerable lateral and down-dip extensions indicate that this area is likely to emerge as a major uranium province.

#### *Subtype 13.2: Cataclastic carbonate deposits*

In cataclastic carbonate deposits, the mineralization is structure-bound in organic-rich, (bituminous/petroliferous) calcareous sediments. Ore zones are controlled by fractured intervals in intraformational folds and flexures (Mailuu-Suu (Kyrgyzstan); Todilto district (USA)). Resources are small to medium (300–2000 tU) and grades are low to medium (0.05–0.20% U).

#### *Subtype 13.3: Palaeokarst deposits*

Palaeokarst deposits are developed in solution collapse breccias occurring in limestone. Mineralization may be preferentially concentrated along annular faults (Bentou-Sanbaqi, China) or may coat and fill fractures and solution voids and impregnate the matrix of the cavern fill (Tyuya-Myuyun (Kyrgyzstan) and Pryor–Little Mountains district (USA)). Resources are small to medium (100–2500 tU), although grades are medium to high (0.10% U to >1% U).

### Type 14: Phosphate deposits

Phosphate deposits are principally represented by marine phosphorite of continental shelf origin containing synsedimentary, stratiform, disseminated uranium in fine-grained apatite. Phosphorite deposits constitute very large uranium resources (millions of tonnes) but of very low grade (0.005–0.015% U). Uranium can be recovered as a by-product of phosphate production. Examples include the Land Pebble district, Florida (USA), Gantour (Morocco) and Al-Abiad (Jordan). Another type of phosphorite deposit consists of organic phosphate, including argillaceous marine sediments enriched in fish remains that are uraniferous (Melovoe, Kazakhstan). Deposits in continental phosphates are not common. Three types of uranium-bearing phosphate deposits are identified: organic, mineral-chemical and continental.

#### *Subtype 14.1: Organic phosphorite deposits*

In organic phosphorite deposits, U–Sc–REE mineralization is bound to detritus of phosphatized fish remains in clay beds enriched in fish bones, fish scales, pyrite and melnicovite concretions. Uranium resources are medium to large (4000–40 000 tU) and grades are low (0.02–0.08% U). These deposits have only been identified in Kazakhstan (Melovoe, Mangyshlak district) and in the Russian Federation (Ergeninsky region) near the Caspian Sea.

#### *Subtype 14.2: Minerochemical phosphorite deposits*

Minerochemical uraniferous phosphorite deposits consist of synsedimentary, stratiform disseminated uranium in marine phosphorite of continental shelf origin. Uranium is bound in cryptocrystalline fluor-carbonate apatite. Phosphorite deposits constitute very large uranium resources (several millions of tonnes) but of very low grade (0.005–0.015% U) (Land Pebble district and Phosphoria Formation, USA).

#### *Subtype 14.3: Continental phosphate deposits*

Continental phosphate deposits are only known in the Bakouma district (Central African Republic). The deposits correspond to newly formed continental lacustrine uraniferous phosphate lenses hosted in fine-grained sediments and deposited within a karst environment. Uraniferous phosphate minerals consist of fine-grained disseminations of uraniferous apatite as well as fracture coatings of autunite and torbernite. Resources of the district are around 50 000 tU of medium grade (0.10–0.30% U).

#### Type 15: Black shale deposits

Black shale related uranium mineralization includes marine, organic-rich shale and coal-rich pyritic shale, containing synsedimentary, disseminated uranium adsorbed onto organic material and clay minerals, and fracture-controlled mineralization hosted within or adjacent to black shale horizons. Examples include the uraniferous alum shale in Sweden and Estonia, the Chattanooga Shale (USA), the Chanziping deposit (China) and the Gera-Ronneburg deposit (Germany).

#### *Subtype 15.1: Stratiform black shale deposits*

Stratiform uranium mineralization consists of synsedimentary, uniformly disseminated uranium adsorbed onto organic and clay particles in marine, organic-rich, pyritic shale with thin coalified, phosphatic and/or silty intercalations. Discrete primary uranium minerals are absent. Resources are large (100 000 tU to >1 000 000 tU) and of low grade (0.005–0.02% U) (Randstad, MMS Vicken, (Sweden) and Chattanooga Shale (USA))

#### *Subtype 15.2: Stockwork black shale deposits*

Carbonaceous shale related stockwork uranium deposits consist of strata controlled, structure-bound uranium mineralization concentrated in stockworks of microfractures within or immediately adjacent to carbonaceous, pyritic black shale/pelitic horizons. High organic carbon (up to 9% C), sulphur (up to 3.5% S) and anomalous trace element (U, Mo, Ni, V, As, Sb) contents are typical of carbonaceous shales (Ronneburg district, Germany). Deposits are small to large (300–50 000 tU) and of low to medium grade (0.05–0.20% U).

As noted in Ref. [43], all the data presented in Tables 5–9 are taken from the UDEPO database:

- (a) Table 5 presents the number of deposits recorded for each type and subtype. Sandstone deposits represent 35% of the total, followed by the granite-related deposits (15%);
- (b) Table 6 lists the largest uranium deposits with resources >50 000 tU. This list includes examples from twelve of the deposit types, indicating that large deposits may originate from a wide variety of geological processes;
- (c) Table 7 presents the uranium resources contained in the various types and subtypes. Total uranium resources for the 1807 deposits/resources listed in the UDEPO database in amount to 58 159 800 tU;
- (d) Table 8 indicates that the largest uranium resources are unconventional resources associated with phosphate, black shale and lignite–coal. These three types represent more than 42.6 Mt (73%) of the world's uranium geological resources.
- (e) Table 9 lists the uranium resources within each of the subtypes.

TABLE 5. NUMBER OF DEPOSITS FOR EACH TYPE AND SUBTYPE (as of 31 December 2015)

Type of deposit	Number of deposits	Subtype	Number of deposits
1 Intrusive	89	1.1. Anatectic	55
		1.2. Plutonic	34
2 Granite-related	277	2.1. Endogranitic	206
		2.2. Perigranitic	59
3 Polymetallic iron oxide breccia complex	15		15
4 Volcanic-related	138	4.1. Stratabound	18
		4.2. Structure-bound	88
		4.3. Volcano-sedimentary	16
5 Metasomatite	78	5.1. Na-metasomatite	54
		5.2. K-metasomatite	17
		5.3. Skarn	5
6 Metamorphite	111	6.1. Stratabound	6
		6.2. Structure-bound	95
		6.3. Marble-hosted	9
7 Proterozoic unconformity	103	7.1. Unconformity-contact	39
		7.2. Basement-hosted	59
		7.3. Stratiform fracture-controlled	4
8 Collapse breccia pipe	17		17
9 Sandstone	662	9.1. Basal channel	78
		9.2. Tabular	306
		9.3. Roll-front	243
		9.4. Tectonic-lithologic	24
		9.5. Mafic dykes/sills	8
10 Palaeo quartz-pebble conglomerate	88	10.1. U-dominant	26
		10.2. Au-dominant	62
11 Surficial	77	11.1. Peat bog	5
		11.2. Fluvial valley	33
		11.3. Lacustrine-playa	24
		11.4. Pedogenic/fracture fill	3
12 Lignite-coal	35	12.1. Stratiform	28
		12.2. Fracture-controlled	1
13 Carbonate	10	13.1. Stratabound	1
		13.2. Cataclastic	8
		13.3. Palaeokarst	1
14 Phosphate	57	14.1. Organic phosphorite	7
		14.2. Phosphorite	45
		14.3. Continental phosphate	5
15 Black shale	50	15.1. Stratiform	31
		15.2. Fracture-controlled	19
		Unknown	53
	1807		1807

TABLE 6. LARGEST (&gt;50 000 tU) URANIUM DEPOSITS (as of 31 December 2015)

Country	Deposit name	Deposit status	Deposit type	Total resource (tU)	Grade (% U)
USA	Northern Great Plains	Dormant	Lignite-coal	7 000 000	<0.01
Morocco	Tarfaya Basin	Dormant	Black shale	6 400 000	0.0080
Estonia	Baltoscandia district	Dormant	Black shale	5 667 000	0.0085
USA	Phosphoria Formation	Dormant	Phosphate	5 000 000	<0.01
USA	Chattanooga Shale Formation	Dormant	Black shale	5 000 000	<0.01
Morocco	Oulad Abdoun Basin	Dormant	Phosphate	3 220 000	0.0120
Australia	Olympic Dam	Operating	Polymetallic breccia complex	2 111 316	0.0220
Morocco	Timahdit Basin	Dormant	Black shale	2 100 000	0.0050
Morocco	Meskala Basin	Dormant	Phosphate	2 043 000	0.0100
Morocco	Gantour Basin	Dormant	Phosphate	1 206 000	0.0150
Sweden	MMS Vicken	Exploration	Black shale	447 755	0.0147
Sweden	Haggan	Exploration	Black shale	308 000	0.0133
South Africa	Free State Geduld	Dormant	Palaeo quartz-pebble conglomerate	277 450	0.0390
Niger	Imouraren	Care and maintenance	Sandstone	276 200	0.0700
USA	East Florida district	Closed	Phosphate	270 000	0.0090
Canada	McArthur River	Operating	Proterozoic unconformity	261 000	19.5000
Sweden	Narke	Exploration	Black shale	257 000	0.0175
Sweden	Ranstad	Dormant	Black shale	254 000	0.0340
Namibia	Rössing	Operating	Intrusive	246 500	0.0300
Iraq	Swab	Dormant	Phosphate	245 000	0.0070
USA	Central Florida district	Closed	Phosphate	225 000	0.0090
South Africa	Vaal Reefs mine	Dormant	Palaeo quartz-pebble conglomerate	195 645	0.0272
Iraq	Dwaima	Dormant	Phosphate	193 000	0.0070
Canada	Denison mine	Closed	Palaeo quartz-pebble conglomerate	185 000	0.1000
Australia	Carrapateena	Exploration	Polymetallic breccia complex	184 000	0.0155
USA	North-east Florida district	Dormant	Phosphate	180 000	0.0090
Australia	Ranger 1 (No. 3)	Operating	Proterozoic unconformity	179 792	0.0840
Kazakhstan	Inkai 1-2-3	Development	Sandstone	152 500	0.0460
Brazil	Pitinga	Operating	Intrusive	150 000	< 0.01
Iraq	Marbat	Dormant	Phosphate	148 000	0.0070
Poland	Lubin-Sieroszowice	Dormant	Black shale	144 000	0.0060
Denmark	Kvanefjeld	Exploration	Intrusive	141 611	0.0220
Canada	Cigar Lake	Development	Proterozoic unconformity	135 038	16.5900
Kazakhstan	Mynkuduk East	Operating	Sandstone	127 000	0.0360
Brazil	Itataia-Santa Quitéria district	Development	Metamorphite	121 800	0.0800
USA	South Florida district	Dormant	Phosphate	120 000	0.0090
Algeria	Tebessa district	Dormant	Phosphate	120 000	0.0060
Australia	Jabiluka 2	Dormant	Proterozoic unconformity	119 884	0.4120

(cont.)

Country	Deposit name	Deposit status	Deposit type	Total resource (tU)	Grade (% U)
Morocco	Twihinate	Exploration	Intrusive	118 500	0.0212
Egypt	Nile Valley district	Dormant	Phosphate	118 500	0.0070
Saudi Arabia	Umm Wu'al	Exploration	Phosphate	112 500	0.0100
Spain	East Ebro Valley	Dormant	Lignite-coal	102 000	0.0170
Brazil	Lagoa Real-Caetite district	Operating	Metasomatite	100 770	0.1200
South Africa	Dominion Reefs	Dormant	Palaeo quartz-pebble conglomerate	96 525	0.0410
Russian Federation	Druzhnoye	Development	Metasomatite	95 840	0.1340
South Africa	Ezulwini	Operating	Palaeo quartz-pebble conglomerate	94 200	0.0238
Ukraine	Novokostyantynivske	Development	Metasomatite	93 630	0.1390
South Africa	Freddies		Palaeo quartz-pebble conglomerate	93 330	0.0115
India	Tummalapalle-Rachakuntapalle	Operating	Carbonate	90 962	0.0400
USA	North Florida district	Dormant	Phosphate	90 000	0.0090
Germany	Niederschlema-Alberoda	Depleted	Granite-related	84 658	0.2500
Jordan	Al Shedeye-Eshidia	Dormant	Phosphate	83 000	0.0070
South Africa	Hartebeestfontein	Operating	Palaeo quartz-pebble conglomerate	82 570	0.0330
South Africa	Springbok Flats	Dormant	Lignite-coal	81 920	0.0420
Namibia	Rössing South (Zone 2)	Exploration	Intrusive	81 620	0.0441
Namibia	Rössing South (Zone 1)	Exploration	Intrusive	80 426	0.0380
Saudi Arabia	Al Jalamid	Operating	Phosphate	80 000	0.0150
Canada	Arrow	Exploration	Proterozoic unconformity	77 456	2.2290
Germany	Schmirchau-Reust	Closed	Black shale	73 410	0.0850
Brazil	Catalao	Dormant	Intrusive	72 125	0.0133
Namibia	Langer Heinrich	Operating	Surficial	66 605	0.0510
USA	Ambrosia Lake district (Dysart)	Closed	Sandstone	64 967	0.1440
Niger	Dasa 1-2-3	Exploration	Sandstone	64 680	0.0490
South Africa	Potchefstroom goldfield	Dormant	Palaeo quartz-pebble conglomerate	62 810	0.0250
Russian Federation	Elkonskoye Plateau	Development	Metasomatite	62 400	0.1570
Greenland	Sørensen	Exploration	Intrusive	62 370	0.0260
Russian Federation	Strel'tsovskoye	Operating	Volcanic-related	62 166	0.1810
Ukraine	Tsentralne	Operating	Metasomatite	61 800	0.1000
Russian Federation	Severnoye	Development	Metasomatite	61 526	0.1490
Kazakhstan	Budennovskoye 2	Operating	Sandstone	60 269	0.0630
Kazakhstan	Nizhne Iliskoye	Dormant	Lignite-coal	60 000	0.0980
Morocco	Oued Eddahab Basin	Dormant	Phosphate	57 000	0.0060
Kazakhstan	Inkai South-4	Operating	Sandstone	56 840	0.0360
Kazakhstan	Budennovskoye 1-3-4	Operating	Sandstone	56 800	0.0700
South Africa	Phalabora	Operating	Intrusive	56 000	0.0061

(cont.)

Country	Deposit name	Deposit status	Deposit type	Total resource (tU)	Grade (% U)
Australia	Yeelirrie	Dormant	Surficial	55 600	0.1110
United Republic of Tanzania	Nyota	Exploration	Sandstone	55 135	0.0250
Russian Federation	Kurung	Dormant	Metasomatite	54 850	0.1450
Mongolia	Zoovch Ovoo	Exploration	Sandstone	54 640	0.0230
Namibia	Marenica	Exploration	Surficial	53 130	0.0080
Australia	Ranger 1 (No. 1)	Depleted	Proterozoic unconformity	51 861	0.2880
South Africa	Rietkuil–Dominion	Exploration	Palaeo quartz-pebble conglomerate	51 711	0.0390
Botswana	Gorgon Main	Exploration	Sandstone	51 667	0.0178
Canada	Banana Lake	Dormant	Palaeo quartz-pebble conglomerate	51 436	0.0300
Kazakhstan	Mynkuduk Central	Operating	Sandstone	50 400	

TABLE 7. GEOLOGICAL URANIUM RESOURCES ACCORDING TO DEPOSIT TYPE  
(as of 31 December 2015)

Type of deposit		Number of deposits	UDEPO resources (tU)
Type 1	Intrusive	89	1 894 496
Type 2	Granite-related	277	478 482
Type 3	Polymetallic iron oxide breccia complex	15	2 432 923
Type 4	Volcanic-related	138	663 512
Type 5	Metasomatite	78	1 023 986
Type 6	Metamorphite	111	509 847
Type 7	Proterozoic unconformity	103	1 522 720
Type 8	Collapse breccia pipe	17	16 217
Type 9	Sandstone	662	4 365 515
Type 10	Palaeo quartz-pebble conglomerate	88	2 136 950
Type 11	Surficial	77	436 470
Type 12	Lignite–coal	35	7 404 309
Type 13	Carbonate	10	112 057
Type 14	Phosphate	57	14 198 525
Type 15	Black shale	50	20 963 792
		1807	58 008 294

TABLE 8. GEOLOGICAL URANIUM RESOURCES FOR DEPOSIT TYPES IN ORDER OF IMPORTANCE  
(as of 31 December 2015)

Type of deposit		Number of deposits	UDEPO resources (tU)
Type 15	Black shale	50	20 963 792
Type 14	Phosphate	57	14 198 525
Type 12	Lignite-coal	35	7 404 309
Type 9	Sandstone	662	4 365 515
Type 3	Polymetallic iron oxide breccia complex	15	2 432 923
Type 10	Palaeo quartz-pebble conglomerate	88	2 136 950
Type 1	Intrusive	89	1 894 496
Type 7	Proterozoic unconformity	103	1 522 720
Type 5	Metasomatite	78	1 023 986
Type 4	Volcanic-related	138	663 512
Type 6	Metamorphite	111	509 847
Type 2	Granite-related	277	478 482
Type 11	Surficial	77	436 470
Type 13	Carbonate	10	112 057
Type 8	Collapse breccia pipe	17	16 217
		1807	58 008 294

TABLE 9. GEOLOGICAL URANIUM RESOURCES ACCORDING TO DEPOSIT SUBTYPES  
(as of 31 December 2015)

Type of deposit	Deposit subtype	Number of deposits	UDEPO resources (tU)	
1	Intrusive	1.1. Anatectic	54	802 647
		1.2. Plutonic	34	1 091 849
2	Granite-related	2.1. Endogranitic	201	205 104
		2.2. Perigranitic	57	251 249
3	Polymetallic iron oxide breccia complex	15	2 432 920	
4	Volcanic-related	4.1. Structure-bound	86	552 161
		4.2. Stratabound	18	35 462
		4.3. Volcano-sedimentary	16	40 919
5	Metasomatite	5.1. Na-metasomatite	54	622 028
		5.2. K-metasomatite	17	380 592
		5.3. Skarn	5	17 816
6	Metamorphite	6.1. Stratabound	6	20 763
		6.2. Structure-bound	95	341 396
		6.3. Marble-hosted	9	146 944
7	Proterozoic unconformity	7.1. Unconformity-contact	39	681 701
		7.2. Basement-hosted	59	822 947
		7.3. Stratiform fracture-controlled	4	18 072
8	Collapse breccia pipe	17	16 217	
9	Sandstone	9.1. Basal channel	78	336 634
		9.2. Tabular	300	2 042 321
		9.3. Roll-front	241	1 869 844
		9.4. Tectonic-lithologic	24	78 768
		9.5. Mafic dykes/sills	8	37 897
10	Palaeo quartz-pebble conglomerate	10.1. U-dominant	26	467 872
		10.2. Au-dominant	62	1 669 082
11	Surficial	11.1. Peat bog	5	3 295
		11.2. Fluvial valley	33	303 754
		11.3. Lacustrine-playa	24	67 897
		11.4. Pedogenic/fracture fill	3	1 650
12	Lignite-coal	12.1. Stratiform	28	7 368 672
		12.2. Fracture-controlled	1	5 430
13	Carbonate	13.1. Stratabound	1	90 962
		13.2. Cataclastic	7	20 445
		13.3. Palaeokarst	1	650
14	Phosphate	14.1. Organic phosphorite	6	73 900
		14.2. Minerochemical phosphorite	45	14 088 225
		14.3. Continental phosphate	5	36 400
15	Black shale	15.1. Stratiform	30	20 737 940
		15.2. Stockwork	18	225 852
		1807	58 008 294	

### 3. DESCRIPTION OF SELECTED URANIUM DEPOSITS

More than 50 uranium deposits/districts have been selected for description, representing the various types and subtypes. For each type, the largest deposits have been tabulated in order of importance. Tabulated resources include all resource categories plus past production. All data in the text and tables are reported in metric tonnes (tU) and grade as a percentage (% U). As noted in Ref. [43], these data were extracted from the UDEPO database at the end of 2015.

#### 3.1 INTRUSIVE DEPOSITS

##### 3.1.1. Definition

Uranium deposits associated with intrusive rocks consist of disseminated primary uranium minerals, dominantly uraninite, uranothorianite and/or uranothorite hosted in rocks of intrusive magmatic or anatectic origin. These deposits are generally low grade (20–500 ppm U), but may contain substantial resources (Table 10). Only deposits associated with pegmatites have higher grades, some as high as 0.10% U.

In 2015, 89 deposits associated with intrusive rocks were recorded in the UDEPO database. The only producing deposit is the Rössing mine (Namibia), which is hosted in alaskite. In the period 1957–1982, about 5750 tU were produced from the Bancroft district (Canada) from deposits hosted in pegmatite. In addition, uranium was extracted as a by-product from porphyry copper (Bingham Canyon and Twin Buttes, USA) hosted in quartz monzonite intrusions and from the Phalabora carbonatite (South Africa).

##### 3.1.2. Geological setting

The intrusive class is divided into two subtypes: (i) deposits associated with partial melting (anatectic deposits) and (ii) deposits related to magmatic differentiation (plutonic deposits) (Fig. 6). Major deposits for each subtype are listed in Tables 10 and 11.

###### 3.1.2.1. Anatectic deposits

Deposits related to partial melting in anatectic environments are those consisting of uraninite disseminated in pegmatitic/granitic dykes and injections or segregations in migmatitic gneiss of high metamorphic grade. These are termed ‘pegmatoids’ because the zonation that is commonly observed in pegmatite bodies derived from the fractionation of large plutonic bodies is generally absent. These deposits represent the most extreme temperature and pressure conditions for economic uranium mineralization [45]. Classically, two categories have been distinguished: deposits associated with pegmatites and deposits associated with alaskites. Alaskites, which were originally defined in Namibia, are leucocratic, quartz-rich and alkali feldspar-rich granitic–pegmatitic rocks and are considered in this report as pegmatites.

In the Bancroft/Madawaska district (Canada), where several deposits were mined in the past, uraninite and other uranium–thorium minerals occur in unzoned granitic and syenitic pegmatitic dykes (of siliceous but also of mafic tendency with the presence of aegirine and augite) and in sedimentary and igneous rocks, metamorphosed to amphibolite facies [46]. Pegmatites are emplaced as en-echelon dykes of tabular to flat, lenticular shapes with swells, offshoots and apophyses both cross-cutting or paralleling the compositional banding of the surrounding host rocks. Deformation and metasomatism commonly post-date metamorphism. Haematite is a characteristic alteration product. Randomly distributed orebodies are usually small, typically only a few hundred tonnes. Pegmatite deposits may average up to 0.10% U. Uranium is irregularly distributed in pods, shoots and bands, often controlled by mafic minerals and particularly by the presence of haematite and magnetite. Some mineralization is associated with late fracturing.

The North Shore district (Canada), where exploration is focused on several deposits (Doran, Drucourt Zone, North Shore Double S, Middle and TJ), contained, in 2011, geological resources estimated at 22 600 tU at grades of 100–200 ppm U. Resources of the Charlebois Lake district (Canada) are estimated at 17 500 tU with an average grade of 0.06% U. Other important deposits are situated in China (Chenjiashuang and Guangshigou) and in Ukraine where the three known deposits (Kalinovskoye, Lozovatskoye and Yuzhnoye) are located in metasomatic potassic pegmatites.

In the alaskites of Namibia, disseminated uranium occurs in medium- to very coarse-grained bodies that are discordant with the surrounding folded, highly metamorphosed and migmatized sedimentary rocks. The alaskite bodies range in size from small lenses and tabular dykes to large stocks and domes several hundreds of metres in width. No alteration is associated with the uranium mineralization. The main examples are the Rössing and Rössing South (Husab project) deposits.

Other examples include Anomaly A (Goanikontes), Z 20, Ongolo, Valencia and Garnet Valley, all situated in Namibia, and the Crocker Well district in Australia. In 2015, total geological uranium resources associated with Namibian alaskites are estimated at 720 000 tU hosted in 24 deposits. The Rössing mine in Namibia produced 1308 tU in 2014, 1057 tU in 2015 and more than 100 000 tU since 1976.

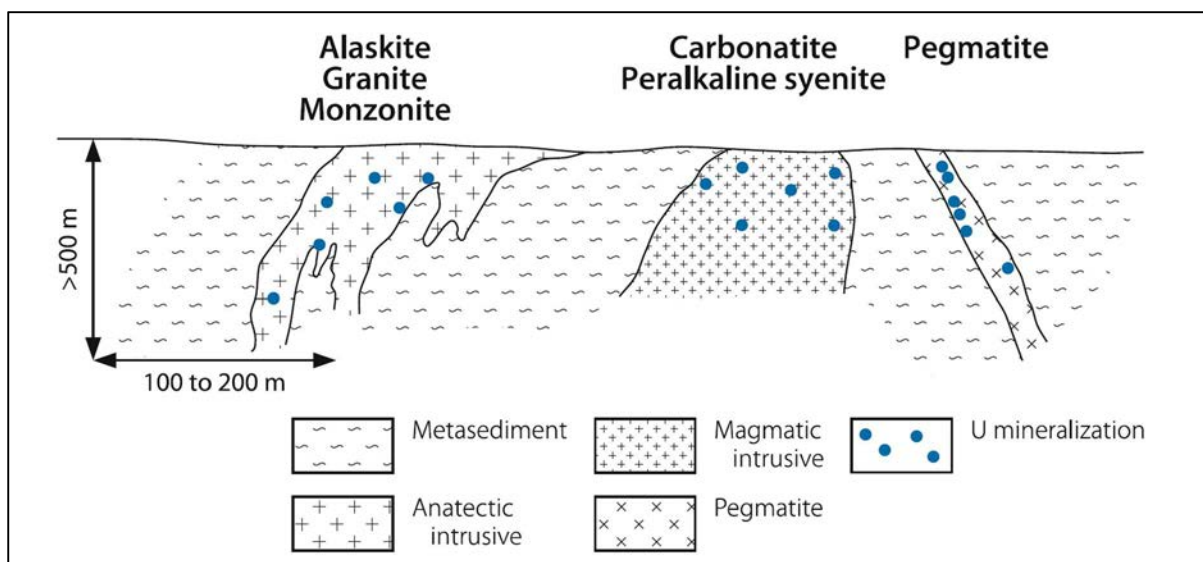


FIG. 6. Intrusive uranium deposit [19] (reproduced with permission).

TABLE 10. PRINCIPAL INTRUSIVE (ANATECTIC) DEPOSITS  
(as of 31 December 2015)

Deposit	Country	Resources (tU)	Grade (% U)	Class	Status
Anatectic					
Rössing	Namibia	246 500	0.030	Alaskite	Operating
Rössing South deposits	Namibia	188 000	0.041	Alaskite	Development
Anomaly A	Namibia	48 740	0.0175	Alaskite	Exploration
Z 20	Namibia	46 274	0.030	Alaskite	Dormant
Valencia	Namibia	41 580	0.0108	Alaskite	Dormant
Anomaly 18	Namibia	40 570	0.025	Alaskite	Dormant
Namibplass	Namibia	30 415	0.013	Alaskite	Dormant
Garnet Valley	Namibia	18 280	0.019	Alaskite	Dormant
Charlebois Lake	Canada	17 500	0.060	Pegmatite	Dormant
Ondjamba	Namibia	12 045	0.0141	Alaskite	Dormant
Anomaly 2-15	Namibia	11 540	0.025	Alaskite	Dormant
North Shore Double S	Canada	8 925	0.011	Pegmatite	Dormant
Ongolo	Namibia	8 778	0.037	Alaskite	Dormant
Oshively	Namibia	7 970	0.0166	Alaskite	Dormant
Onkelo	Namibia	7 780	0.0165	Alaskite	Dormant
Kalinovskoye	Ukraine	7 550	0.050	Pegmatite	Dormant
North Shore Middle Zone	Canada	5 275	0.010	Pegmatite	Dormant

TABLE 11. PRINCIPAL INTRUSIVE (PLUTONIC) DEPOSITS (as of 31 December 2015)

Deposit	Country	Resources (tU)	Grade (% U)	Class	Status
Quartz monzonite					
Chuquicamata	Chile	50–100 000	0.0015	Monzonite	Operating
Bingham Canyon	USA	25–50 000	0.002	Monzonite	Operating
Twin Buttes	USA	25–50 000	0.002	Monzonite	Depleted
Yerington	USA	25–50 000	0.002	Monzonite	Dormant
Peralkaline complex					
Pitinga	Brazil	150 000	<0.010	Peralkaline complex	Dormant
Kvanefjeld	Greenland	141 610	0.022	Peralkaline syenite	Exploration
Twihinate	Morocco	118 500	0.0212	Peralkaline complex	Dormant
Sørensen	Greenland	62 370	0.0258	Peralkaline granite	Exploration
Ghurayyah	Saudi Arabia	45 700	0.012	Peralkaline granite	Exploration
Round Top	USA	43 775	0.0045	Peralkaline complex	Development
Poços de Caldas	Brazil	22 700	0.29	Peralkaline syenite	Reclamation
Nolans Bore	Australia	5 160	0.018	Peralkaline complex	Exploration
Carbonatite					
Catalão	Brazil	72 175	0.0133	Carbonatite	Dormant
Phalabora	South Africa	56 000	0.0061	Carbonatite	Operating
Glibat Lafhouda	Morocco	43 000	0.0425	Carbonatite	Dormant
Araxa	Brazil	13 000	0.080	Carbonatite	Dormant
Drag al Farnane	Morocco	9 400	0.0203	Carbonatite	Dormant
Toongi	Australia	8 690	0.012	Carbonatite	Exploration
Saima	China	5 000	0.05–0.10	Carbonatite	Dormant

### 3.1.2.2. Plutonic deposits

Deposits related to magmatic differentiation correspond to low to very low grade uranium and thorium mineralization disseminated in magmatic rocks of varying composition. They are classified as ‘unconventional resources’ by the IAEA. Uranium can only be extracted economically as a by-product of Cu–Au–Mo in porphyry copper or as a by-product of REE–Zr–Ta–Nb–P–Fe–Ti–Th in peralkaline–carbonatite complexes.

(a) Quartz monzonite

Very low grade uranium disseminations occur in highly differentiated granitic–quartz monzonitic (copper porphyry) complexes. At very low levels, uranium has been recovered as a by-product of copper heap leaching, such as at Bingham Canyon (USA), which has levels of 20–50 ppm U in the Cu–Au–Mo ore. Annual uranium production as a by-product in 1978–1989 amounted to about 40 t and a total production of 416 tU was recorded from dump leach. The mineralogy of the uranium has not been reported but it may be present as uraninite or uranothorianite [47]. Uranium is almost universally present in the solutions resulting from the leaching of the waste dumps to recover copper. The uranium content varies in the range 2–15 ppm. At Bingham Canyon, the uranium was recovered by ion exchange techniques.

Other examples include Twin Buttes (Arizona) where uranium was recovered (397 tU in total production) from copper ore and Yerington (Nevada), both in the USA. In Chile, Codelco indicated in 2010 that uranium would be extracted as a by-product of copper from the Chuquicamata and Radomiro Tomic porphyry copper mines. Production is expected to total 85 tU/year but the uranium content of these porphyry copper deposits has not been reported. Although only seven of these deposits appear in the UDEPO database, 646 porphyry copper deposits are listed in the US Geological Survey database [48]. Production of uranium from these polymetallic mines may become significant in the future.

(b) Peralkaline complex

Low grade uranium disseminations occur in peralkaline granitic–syenitic domes and stocks. At Kvanefjeld (Greenland), uranium phases in the syenitic complex are commonly of a refractory nature (streenstrupine, eudialyte, monazite). Associated elements include F, Li, Be, Zn, Zr, Y, Nb, Th and REE. Orris and Grauch [49], in their compilation, list 125 peralkaline complexes around the world, of which only 15 are listed in the UDEPO database.

Other examples of peralkaline complexes are Twihinate (Morocco), Poços de Caldas (Brazil) and Bokan Mountain (USA). The Toongi deposit (Australia), which is being developed to recover Zr, Hf, Nb, Ta, Y and REE, is located in a Jurassic trachyte plug with an average uranium content of 120 ppm. Two peralkaline granitic complexes, Ghurayyah and Jabal Sayad (Saudi Arabia) were being evaluated for their high Ta–Nb–Zr resources.

(c) Carbonatite

At Phalabora (South Africa), disseminated uranothorianite occurs in a cuprififerous carbonatite complex. From 1971 to 2001, uranium was recovered as a by-product of copper extraction, with a cumulative production of 9154 tU. The average uranium content of the ore mined was only 30–40 ppm, whereas the Th content was twice this value. Thorium resources are estimated at 10 500 t for every 100 m of depth [50].

Other typical examples of carbonatite type deposits are Araxa and Catalão (Brazil), Glibat Lafhouda (Morocco), Sokli (Finland) and Saima (China). Such carbonatite complexes are actively explored around the world owing to their high Ta–Nb–REE–F–P contents. The main projects are Mount Weld (Australia), Bear Lodge and Mountain Pass (USA) and Sarfartoq (Greenland). They frequently contain relatively high U and Th (20–200 ppm) values, with Th always higher than the U value, although precise figures have not been published for most of these projects. A total of 527 carbonatite bodies are recorded around the world [51] of which only 12 are listed in the UDEPO database.

### 3.1.3. Metallogenesis

Intrusive uranium deposits can be divided into two classes: deposits related to partial melting (pegmatite–alaskite) and deposits related to magmatic differentiation (granite–monzonite, peralkaline complexes and carbonatites) [37].

Partial melting of uraniumiferous sedimentary rocks is considered to be the main primary genetic process for the the creation of alaskite deposits, although mineralization may, in part, be related to the percolation of late stage magmatic fluids and supergene enrichment as hexavalent uranium minerals. Deposits related to partial melting are found as uraninite disseminated in pegmatitic dykes and injected into high grade migmatitic gneiss. It has been proposed that these deposits result either from extreme fractionation of a deeper body, as suggested for the mineralized pegmatites of the Grenville Province in Quebec [52], or from partial melting of uranium-rich metasedimentary or metavolcanic rocks, as proposed for Rössing and the Mont Laurier (Canada) pegmatoids [53].

The genetic link between porphyry copper deposits and magmatic–hydrothermal processes is well established. Formation of such deposits involves the separation of melt and hydrothermal fluids from a magma chamber situated well below the deposit and precipitation of sulphides in structurally focused zones as a consequence of cooling, interaction with wall rocks, boiling and/or mixing with meteoric waters [54].

Extreme fractional crystallization of peralkaline magmas may lead to the formation of large, low grade uranium and thorium resources, such as at Kvanefjeld in Greenland. Such an association can also be extended to the ultimate fractionation products of peralkaline complexes, namely carbonatite intrusions such as Phalabora, South Africa. Peralkaline granite and syenite bodies are always enriched in U–Th and other elements such as Zr, Nb, Ta and REE. Uranium mineralization is associated with the most fractionated part of the peralkaline complexes and is therefore located in the apical parts of the complexes or at their margins [45]. Peralkaline intrusions are emplaced in post-orogenic to anorogenic settings. Forming by cauldron subsidence in consolidated basement, they are generally found as cylindrical to concentric intrusions associated with ring dykes. The plutonic complexes may range from small to very large.

### 3.1.4. Description of selected deposits

#### 3.1.4.1. *Alaskite: The Rössing South deposits (Namibia)*

##### Introduction

The Rössing South deposits are located within the Husab project, 5 km south of the Rössing mine and 25 km west of the Langer Heinrich mine (Fig. 7). On February 2008, Extract Resources Ltd, the operator, released results from the first holes ever drilled into the Rössing South zone which included intersections of 40 m at 205 ppm U and 69 m at 272 ppm U hosted in alaskite.

As of the end of 2012, the Rössing South deposits comprise five mineralized zones (Fig. 8) with total resources of 188 000 tU at an average grade of 410 ppm U [55]. In addition, several anomalous zones (Garnet Valley, Salem and Ida Dome) are being explored south of the property and are estimated to contain geological resources of 20 000 tU. Surface coatings of carnotite in calcretes have also been identified in the area, indicating the potential for additional, secondary hosted uranium mineralization.

On the basis of a preliminary feasibility study, Extract Resources planned to develop a large scale, open pit mining operation and an acid leach process plant that would produce up to 5800 tU/year. In April 2012, following a successful takeover of Extract Resources, Taurus Minerals Ltd, owned by China Guandong Nuclear Power Company (CGNPC) and the China–Africa Development Fund, became the new owner of the Husab project. The project is being developed by Extract Resources' subsidiary, Swakop Uranium, in which Namibian State-owned mining company Epangelo acquired a

10% stake. A mining licence was granted for the project at the end of 2012 and construction was completed in 2016. Production is planned to be 5800 tU/year by 2018–2019. The expected life of the mine is estimated at more than 20 years, according to CGNPC.

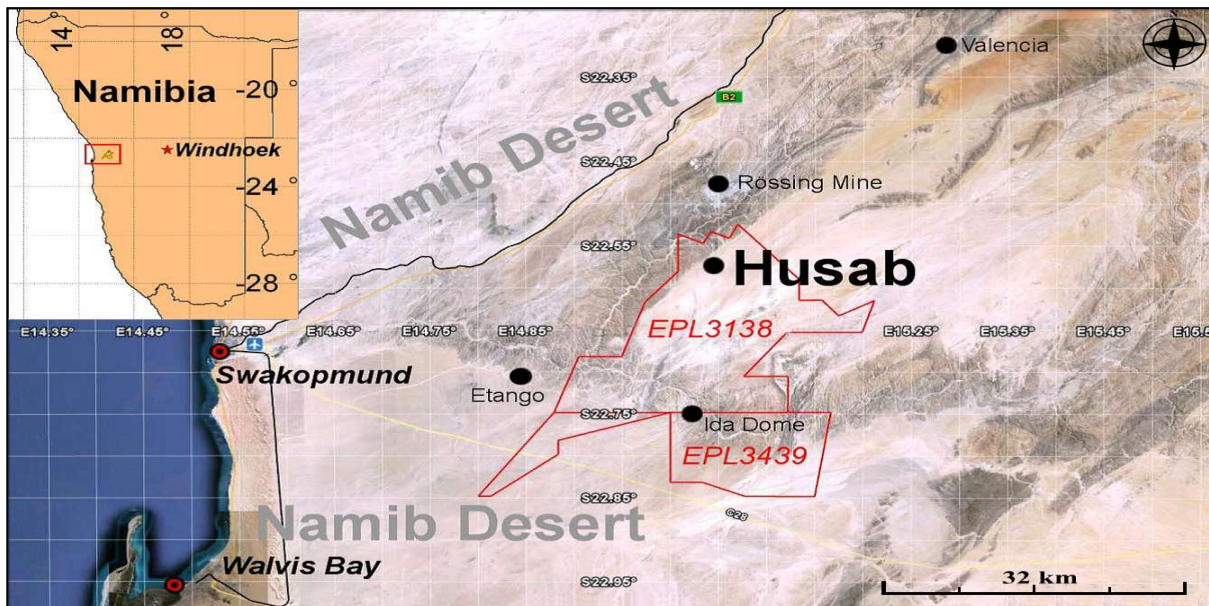


FIG. 7. Location of the Husab project contains the Rössing South deposits [55] (reproduced with permission).

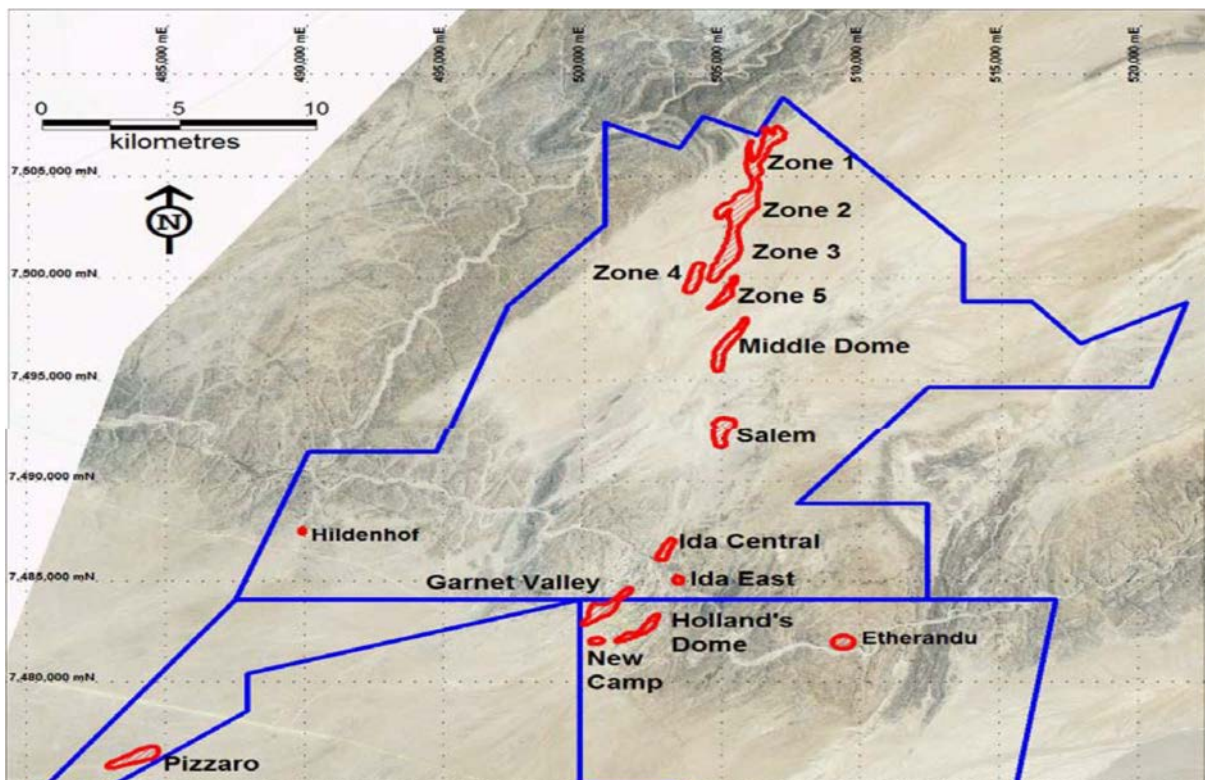


FIG. 8. Location of the various deposits of the Husab project [55] (reproduced with permission).

## Geological setting

The mineralization at Rössing South is covered by approximately 30 m of sandy overburden, which completely eliminates any radiometric signature. Initial drilling was aimed at testing a magnetic low anomaly interpreted as representing the unconformity between the Khan and Rössing formations. It has been established that the Rössing South area contains the folded extensions of the stratigraphy hosting the Rössing deposit [56].

## Regional geology

The Rössing deposit lies within the 400–500 km wide Neoproterozoic Damara Orogenic Belt, which extends from the Atlantic Ocean in a north-eastern direction across south-western Africa where it is covered by the post-Palaeozoic Kalahari Basin. Further north, it connects with the Lufilian Belt of similar age in Zambia and the Democratic Republic of the Congo. The Husab project is located in the central Swakop Zone of the Damara Orogen. Mineralization is controlled by structural and intrusion associated settings formed during major thrust deformation events in the orogeny.

Rössing is located on the south-western flank of a regional scale, oval shaped, NE–SW trending dome, about 2 km from the contact with Proterozoic gneissic basement and metasedimentary rocks consisting of schist and graphite- and sulphide-rich marble that originated as 1000–800 Ma continental platform sediments of the Damara Supergroup. There are many alaskite bodies in the Rössing area and many others are found in the middle and western parts of the Damara Hills which formed when the northern Congo Craton merged with the southern Kalahari Craton, during the Pan-African period.

The Central Swakop Zone is interpreted as a palaeo-arch, where Damaran and pre-Damaran rocks exhibit complex deformation in a dome and basin pattern following the collision of the Congo and Kalahari Cratons. The Central Swakop Zone is bounded by two NE trending structures: the Omaruru Lineament on the northern margin and the Okahandja Lineament to the south [57].

The regional setting features a NE trending anticlinal hinge zone with extensive inliers of Palaeoproterozoic rocks of the Abbabis Metamorphic Complex, commonly present as elongate, domes surrounded by younger, folded Damara Sequence lithologies. The Abbabis Metamorphic Complex consists of paragneiss, orthogneiss and ortho-amphibolite metamorphosed at amphibolite to granulite facies and extensively intruded by pegmatite.

The Damara Orogenic Belt is a major Pan-African mobile belt of sedimentary and volcanic rocks that extends from the Namibian coast north-east into Botswana and Zambia. The supracrustal sequence records rifting between the Kaapvaal and Congo Cratons at 1000–900 Ma with collision at 500 Ma and major thrust faulting and granitoid intrusion. Structures developed during initial rifting continued to influence the tectonic development of the Namibian region up until the Jurassic period, when the African and South American continents moved apart to produce the southern Atlantic Ocean.

The Damara Orogenic Belt is broadly divided into three successions:

- (i) The Nosib Group comprises metamorphosed sandstone, quartzite and minor conglomerate, and records sedimentation due to erosion of uplifted basement during the initial rifting of the orogen. The Nosib is further subdivided into the Etusis Formation (quartzite, arenite and arkose) and the Khan Formation, which consist mainly of calc-silicate rocks with lesser clastic components;
- (ii) The Lower Swakop Group, which overlies the Nosib Group, comprises an alternating succession of dolomite, marble, schist and schistose diamictite. The succession includes, from bottom to top, the Rössing Formation (mainly carbonate, wacke, quartzite and mica schist), the Chuos Formation (mica schist, calc-silicate rocks and carbonate), and the Arandis and Karibib Formations (mica schist, calc-silicate rocks and marble);

- (iii) The Kuiseb Formation, which comprises the upper part of the Swakop Group, is developed predominantly within the southern portion of the Damara Orogen. The Kuiseb Formation, comprising mainly flysch type sediments, is represented by a thick succession of mainly biotite schist with subordinate calc-silicate rocks and carbonaceous schist. A unit of metamorphosed mafic volcanic rocks, referred to as the Matchless Amphibolite Member, has a composition consistent with mid-ocean ridge basalts.

All the above rock types have been intruded by a wide variety of syntectonic and post-tectonic intrusive rocks, including the Goas Diorite Suite, which includes a series of small, disconnected plutons in the area south of Karibib. Other late to post-tectonic intrusives include the Salem Granite, commonly represented by a grey biotite granite–granodiorite locally intruding Damara rocks.

The so-called ‘red’ granites, which are a heterogeneous group of intrusives composed of foliated and massive varieties, often occur as small bodies intruding the marble and schist of the Swakop Group. Other, mainly post-tectonic intrusive types include leucogranite and alaskite, some of which are uraniferous. These typically appear below and around the lowest Damara marble and are characterized by their vein or dyke-like appearance or anastomosing forms, although massive or plug-like occurrences are known. A body of grey granite has itself been intruded by a uranium-bearing alaskite and the Rössing mine exploits low grade uranium mineralization within one such intrusive system.

The Damara Orogen underwent major, southerly directed thrusting, resulting in a pervasive NNW–NW dipping foliation. Thrusts are interpreted to have transported portions of the sequence up to 200 km to the south over basement rocks. Rocks of the Damara Orogenic Belt are covered by the Kalahari Sands in north-eastern Namibia and are continuous through Botswana and into Zambia, where the orogen is represented by the Muva and Katanga Groups of the Lufilian Arc.

#### Local geology

The Husab project area is dominated by a series of NNE–NE trending, regional scale antiforms and synforms that make up the main structural architecture of the entire Central Zone of the Damara Belt. The folds are cored by gneissic and metasedimentary rocks of the Abbabis Formation. The basement rocks are overlain in the north-east and south by flat lying cover sequences consisting of calcrete and alluvial deposits in a broad NE trending valley marginal to the Khan River [56].

The basement gneiss crops out as a series of semi-ovoid features within the Central Zone of the Damara Belt. These generally form poorly exposed extensions of the basement rocks exposed in the Swakop River gorge on either side of the Ida Dome and in the Khan River valley, immediately south of the Khan copper mine, to the junction of the Khan and Swakop Rivers. Flanking Damara sequence sediments show a complex pattern of folding and faulting, and the entire sequence is extensively intruded by syntectonic and post-tectonic granitoids and pegmatite swarms. Cross-cutting Mesozoic dolerite dykes are also locally present.

Basement domes to the east and west of the Husab project area, the latter along the Khan River, are predominantly composed of metasedimentary rocks, although the domes in the Ida and Husab areas have gneiss cores. Regional magnetic data indicate that the regional structural history is complex.

The main constituents of the Rössing host rocks are quartz, microcline, microcline–perthite (sometimes with more than 20% plagioclase), biotite (locally enriched) and fluorite (as an accessory mineral). Textures are mainly pegmatitic, with occurrences of aplite, granite and graphic fabrics. Syntectonic medium- to very coarse-grained alaskites corresponds to potassic alkali feldspar granites as defined by Tröger [58].

## Mineralization

Individual ore shoots in the Rössing South area may range from several tens of metres to several hundreds of metres (~700 m) in length (trending NE–SW) and several tens of metres to 600 m in width (Fig. 9). Mineable ore has been proven to a depth of approximately 300 m (the lowest level of the planned open pit) but drilling has intersected ore grades to a depth of at least 700 m. Reports of some high grade uranium mineralized intersections have been published by Extract Resources during the exploration drilling phases: 6 m at 1.45% U, 14 m at 0.31%, 21 m at 0.217%, 63 m at 0.112% and 67 m at 0.10%.

Primary uranium mineralization is observed only in the felsic rocks. Some alaskite bodies are barren or only weakly mineralized, whereas a few restricted sections are sufficiently rich to support mining. The mineralized alaskites are mainly located in the lower part of the Rössing Formation, near to or at the contact with the Khan Formation.

The ore minerals include euhedral primary, thorium-rich uraninite (grain sizes ranging from a few microns to 0.3 mm sized inclusions in quartz, feldspar and biotite, in intergranular spaces and in veinlets), uranothorianite, uranothorite, betafite and hexavalent uranium minerals, predominantly yellowish beta uranophane. The mineralogical distribution of the uranium in the ore is approximately 55% in uraninite, 5% in betafite and 40% in hexavalent uranium minerals. Associated minerals include monazite, zircon, apatite, titanite, occasionally pyrite, chalcopyrite, bornite, molybdenite, arsenopyrite, magnetite, haematite, ilmenite and fluorite. The Th/U ratios in the ore are generally <1 and up to 3.

The yttrium and REE contents are elevated in uraninite as, is commonly observed when the mineral is formed at high temperatures. More surprising is the high and variable Ca content (0.3–9.5 wt% CaO) for uraninite formed in leucocratic granite, which generally has a low Ca content. This high Ca content is interpreted as reflecting the interaction of the alaskite melts with the calcium-rich host lithologies comprising the Khan and Rössing formations [45].

Hexavalent uranium minerals are common in the alaskite orebodies and contribute to their grade enrichment, particularly in the upper parts of the deposits. Oxidizing meteoric fluids have dissolved uraninite in the eroded parts of the orebodies and redeposited the uranium in small fractures, mainly as uranophane, but also as metatorbernite, metahaweeite and carnotite.

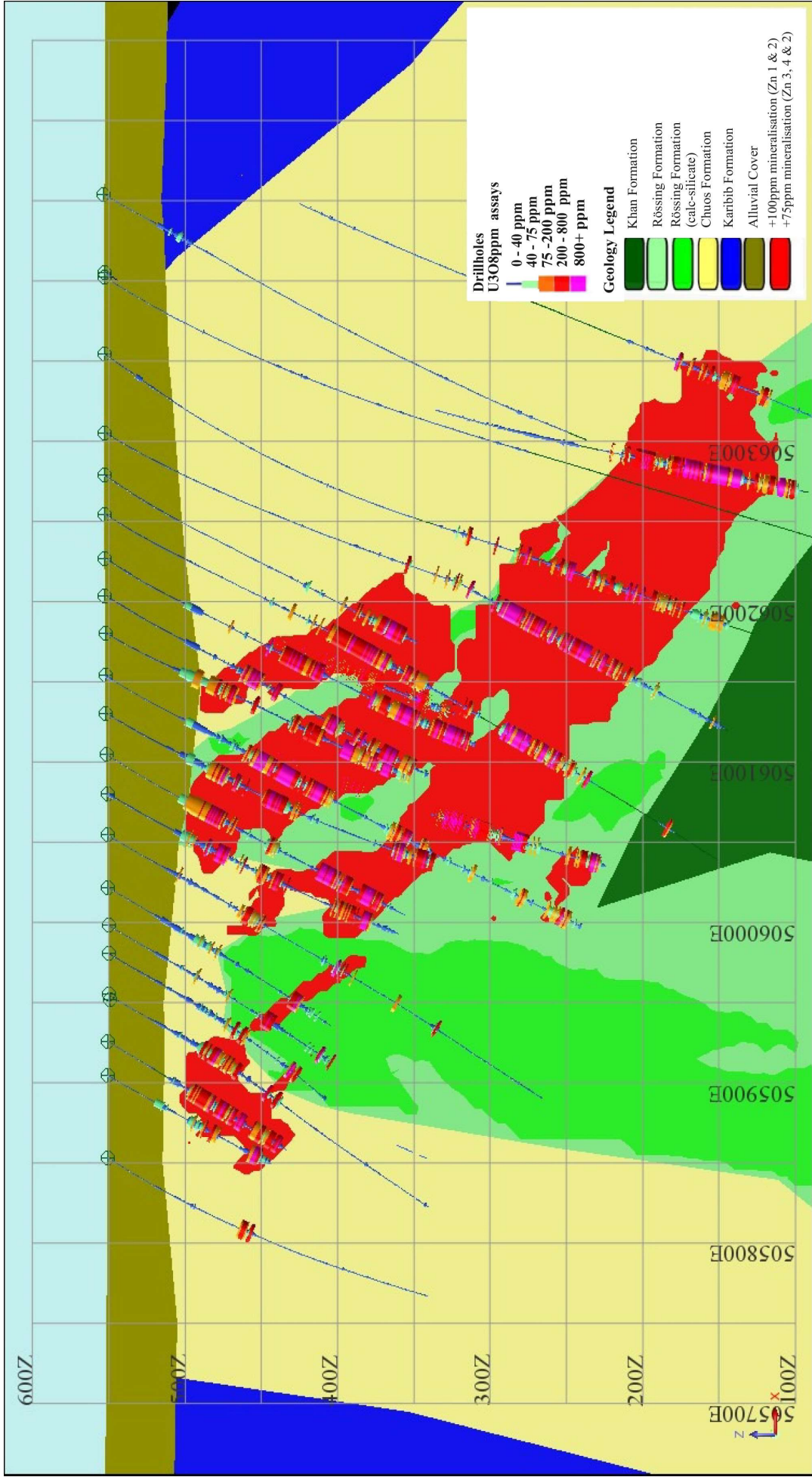


FIG. 9. Section through the Rössing South 1 uranium deposit [59] (reproduced with permission).

## Metallogenic aspects

According to Spivey and Penkhetman [57], alaskite mineralization is associated with a zone of abnormally high heat flow which has produced leucogranite melts from pre-Damara basement and preferentially enriched uranium over thorium with respect to the source rock. Magmas appear to be passively emplaced as sheeted bodies and more infrequently as stocks. They occur in an area of high metamorphic grade. Mineralization is thought to be related to dilatational zones which have formed as the result of regional deformation. The age of both the mineralization and the host alaskite is Cambrian (510 Ma, which corresponds to the Damara Orogeny and the end of Pan-African Orogeny).

Two models have been proposed for the origin and evolution of the uraniumiferous alaskites: (i) extreme fractionation of a larger granitic body located at depth as proposed for Rössing [60] and mineralized pegmatoid bodies from the Grenville Belt in Quebec, Canada, or (ii) as the result of partial melting of uranium-rich metasedimentary or metavolcanic rocks as proposed for Rössing [53, 61] and for the Mount Laurier alaskite and pegmatoid in Quebec, Canada [53]. As the position, size and uranium content of the alaskitic intrusions are similar to the lower marble unit in the Swakop Group, several authors believe that the marble played a major role as an ore control. The change from a terrigenous to carbonate sedimentary setting may have acted to change local conditions and/or to trap and focus mineralized fluids beneath marble caps [57].

The partial melting model for the origin of the mineralized alaskite dykes is preferred by Cuney and Kyser [45] for the following reasons:

- (i) The larger granitic bodies that exist in the central part of the Damara Belt are either older or younger than the alaskite dykes;
- (ii) This type of alaskitic dyke, generally trending parallel to the regional metamorphic foliation, always occurs in high grade migmatitic domains where partial melting remains limited. The foliation of the original metamorphic rocks is always well preserved, except where meta-arkoses and meta-felsic volcanic rocks allowed a high degree of melting, as observed in the Etusis Formation of the Rössing area;
- (iii) No correlation between the uranium enrichment of the alaskite dykes and other major and trace elements is evident, but would be expected if fractionation were important;
- (iv) Mineralogy and major elements define three main compositions: (i) a plagioclase-rich group with a more restite-rich composition; (ii) a granitic group with near eutectic composition and (iii) a K-feldspar-rich group generally poorer in quartz and pegmatite;
- (v) There is evidence for restite material such as biotite schlieren, but also garnet in some occurrences;
- (vi) Internal zonation of the pegmatitic, granitic dykes is generally absent;
- (vii) Rather than diverging from a deeper granitic body, the alaskite dykes tend to merge to form small (10–100 m thick) granitic lenticular bodies;
- (viii) The high and variable initial  $^{87}\text{Sr}/^{86}\text{Sr}$  ratios (0.724–0.759) obtained from Rössing alaskite implies an old crustal source for the magmas.

Large felsic magma volumes such as those typical of the leucogranites of the Limousin district (France) result from a higher grade of partial melting than the alaskites and are only moderately enriched in uranium (15–30 ppm). Further hydrothermal and structural processes are necessary in order to create economic concentrations of mineralization. Where a low grade of partial melting occurs, higher uranium concentrations are obtained in the melts. This condition, though necessary, is not sufficient in itself to generate economically viable disseminated orebodies in alaskites owing to the typically small size of individual alaskite occurrences. A series of alaskite dykes have to ‘merge’ to form a significant uranium resource. For example, large mineralized alaskite bodies in metamorphic domains such those of Mont Laurier or the North Shore district (Grenville Province, Canada) or those at Charlebois Lake (Wollaston Domain north of the Athabasca Basin, Canada) have never been mined because the mineralized dykes are too disseminated within metamorphic host rocks and the average grade remains low (50–200 ppm U) [45].

### 3.1.4.2. *Pegmatite: The North Shore district deposits (Canada)*

#### Introduction

The North Shore deposits are located in the Havre Saint Pierre, Aguanish and Natashquan corridor along the north shore of the Gulf of Saint Lawrence, Quebec, Canada (Fig. 10). Radioactive minerals were first discovered in 1955 in the Baie Johann Beetz area and intermittent exploration activity took place during the 1960s and 1970s. Since 2004, resources have been delineated by several projects that have evaluated the potential of the district:

- (a) *North Shore project*: Uracon Resources outlined in 2010 a resource of 16 890 tU at an average grade of 100 ppm U within three mineralized zones; Double S (8925 tU), Middle Zone (5275 tU) and TJ (2690 tU);
- (b) *Baie Johann Beetz project*: The Drucourt Zone, explored by Jourdan Resources, contains resources of 3370 tU at a grade of 212 ppm U;
- (c) *Doran project*: Entourage Mining has defined resources of 2355 tU at a grade of 210 ppm U in the Doran deposit;
- (d) *Lake Kachiwiss project*: Terra Ventures has announced resources of 2180 tU at a grade of 130 ppm U in the Kachiwiss deposit.

In 2011, total resources in the district were estimated at 24 800 tU at a grade of about 125 ppm U. In addition, several new mineralized zones have since been discovered on the four projects. The companies are targeting near surface, bulk tonnage deposits that could be mined by open pit.

#### Geological setting

The North Shore project is located in the Grenville Province of the Canadian Shield. The Grenville Province extends for more than 2000 km along the north shore of the St Lawrence River and its width varies around 300–600 km (Fig. 10). It forms the south-eastern part of the Canadian Shield from Labrador in the north-east to the Great Lakes area of Ontario in the south-west. The Grenville Orogeny (1090–990 Ma) is the last Proterozoic event that affected this part of Canada and is associated with extensive reworking and high grade regional metamorphism.

Archaean rocks of the Superior Province and Palaeoproterozoic rocks of the Otish Basin and New Quebec Orogen are separated from the para-autochthonous belt by the Grenville Front, a major and complex NE–SW oriented structural zone. The Grenville Front is characterized by a NW trending thrust and by late strike-slip displacement with a sharp, well delineated metamorphic boundary with the Superior Province. The main crustal build up of the Grenville Province occurred through prolonged (1800–1240 Ma) Andean type continental arc and intracontinental, back-arc magmatism with some lateral accretion of magmatic arcs.

The Grenville Province is subdivided into two main, semi-continuous, parallel stacked belts known as the para-autochthonous belt and the structurally overlying allochthonous polycyclic belt. In addition, there is a series of supracrustal dominated belts termed the allochthonous monocyclic belt. The Grenville Domain features complex, irregular folded structures, numerous gneiss domes and basins, and variable intrusive rocks ranging from gabbro to alkali-rich rocks.

The North Shore district contains various rock types but is dominantly comprised of migmatite, gneiss and gneissic textured S-type granite. Other facies include strongly metamorphosed sandstone and arkose, transformed into quartzite and feldspathic gneiss, mafic volcanic rocks (now amphibolite), aplitic to coarse-grained granite and granitic gneiss with pegmatitic dykes. The quartzite and quartzo-feldspathic gneiss are found in the Wakeham Basin, which is surrounded by metamorphic complexes. The Wakeham Group is a thick, moderately metamorphosed siliciclastic supracrustal sequence deposited between 1630 and 1500 Ma. Regional structures trend N–NW and granites are exposed in the cores of large scale curvilinear folds. Gneisses are ‘draped’ around these cores and have been

partially melted by the granite plutons. Locally, the granitic gneisses are very weakly to strongly foliated and the distinction between metamorphic and plutonic phases is difficult to make [62].

Granitic rocks in the region are ‘true’ granites, varying in colour from white to pink and with granularity varying from very fine- to medium-grained uniform granite to extremely coarse-grained very heterogeneous pegmatitic granites. This latter type also contains pegmatite exhibiting internal quartz veins and individual feldspar crystals in the centimetre to metre size range, large bronze to black coloured biotite euhedra and magnetite and/or ilmenite grains. The pegmatitic granites and true pegmatites tend to show higher and more uniform levels of radioactivity [62].

Migmatites were likely formed by recrystallization of, and introduction of, pegmatitic and granitic melts into metasedimentary rocks and, to a lesser extent, amphibolite. There is evidence of at least two phases of pegmatite development. An older group, probably related to the gneissic granite, generally forms narrow sills and dykes that cut the metasedimentary rocks and migmatites and ‘feather out’ along the foliation and schistosity of the metasedimentary host rocks. The younger group of pegmatites cuts indiscriminately across the older pegmatites and has well-defined, sharp contacts with the enclosing rocks [62].

In the Doran project (Fig. 11), the granitic pegmatites form white to pinkish white, medium- to coarse-grained dykes consisting of quartz, plagioclase and K-feldspar. They typically display irregular contacts with the country rocks. Some pegmatite dykes are poorly zoned, with a coarse-grained core attaining 0.5–1 m in width and fine-grained, aplitic margins. Some pegmatite occurrences contain small biotite flakes while in other cases pegmatite can contain up to 10–15% of biotite porphyroblasts forming sheets, 10–15 cm in size. Traces of muscovite have also been noted. Locally, pegmatites can contain 2–5% of opaque minerals, comprising coarse magnetite grains or aggregates, but these occurrences are irregularly distributed [63].

The granitic rocks consist of quartz, plagioclase, K-feldspar and local biotite flakes together with very fine disseminations of magnetite. A ferruginous alteration product associated with chlorite is present in fractures and as impregnations in plagioclase. Accessory minerals include magnetite, titanite, altered allanite, metamict zircon and uraninite.

One of the largest mineralized zones, the Double S deposit (Figs 12 and 13), is associated with the Turgeon Lake intrusion, a late to post-Grenvillian granitoid intrusive complex. Age determinations using U–Pb in monazite give an age of 962–961 Ma for the granite and the pegmatites. The emplacement of the intrusive complex was the last significant geological episode in the area [64].

#### Mineralization

The uranium mineralization of the North Shore project is hosted by felsic intrusive bodies, predominantly granite and pegmatite, but also tonalite, syenite and monzonite (Figs 12 and 13). The proportion of granitic pegmatite and pegmatitic granite in the main granite intrusive phase seems to correlate directly with the number of lenses and the grade of uranium mineralization. Pegmatite is generally more abundant, more voluminous and more closely spaced in the central part of the ovoid intrusion, where the shallow dipping pegmatite dykes and sills occurring in variably altered granite and syenite form resistant topographic highs. Uranium mineralization tends to be strongest in zones around the pegmatitic cores where the abundant pegmatite and altered granitic rocks grade into the main granite body. Uranium mineralization generally weakens towards the intrusion margins in the granite. Airborne radiometric anomaly patterns also suggest that uranium mineralization occurs around the core of ovoid intrusive bodies [65].

The amount of uranium mineralization appears to be dependent or correlative with the amount of characteristic ‘smokey’ grey quartz occurring along the pegmatite–granite interface. Together with 20–60% of grey quartz, coarse-grained aggregates of biotite and/or magnetite occur in the uranium mineralized zones and may be, in addition to grey quartz, useful minerals indicative of uranium

mineralization. Alteration of beige–white granite and pink to brick red syenite is commonly more intense in uranium-bearing areas and in areas of abundant pegmatite [65].

Mineralization is essentially composed of two mineral phases, uraninite and uranothorite. Uraninite is finely crystallized as cubes or irregular grains disseminated around biotite and in clear albite overgrowths along with muscovite and chlorite. Pure uraninite grains are surrounded by zircon and apatite, locally intergrown with monazite. In other occurrences, it is present as exsolutions a few micrometres in size. Most granitic pegmatite dykes/bodies from the Doran project are poorly zoned and the U–Th mineralization is heterogeneously distributed throughout the pegmatite. There is no evidence of supergene uranium redistribution [63].

**Metallogenic aspect**

Two models have been proposed for the origin and evolution of the uraniumiferous pegmatites: (i) extreme fractionation of a larger granitic body located at depth as proposed for the Rössing alaskites [60] and mineralized pegmatoid bodies from the Grenville Belt in Canada, or (ii) partial melting of uranium-rich metasedimentary or metavolcanic rocks as proposed for Rössing [53, 61] and for the Mount Laurier alaskite and pegmatoid in Canada [53].

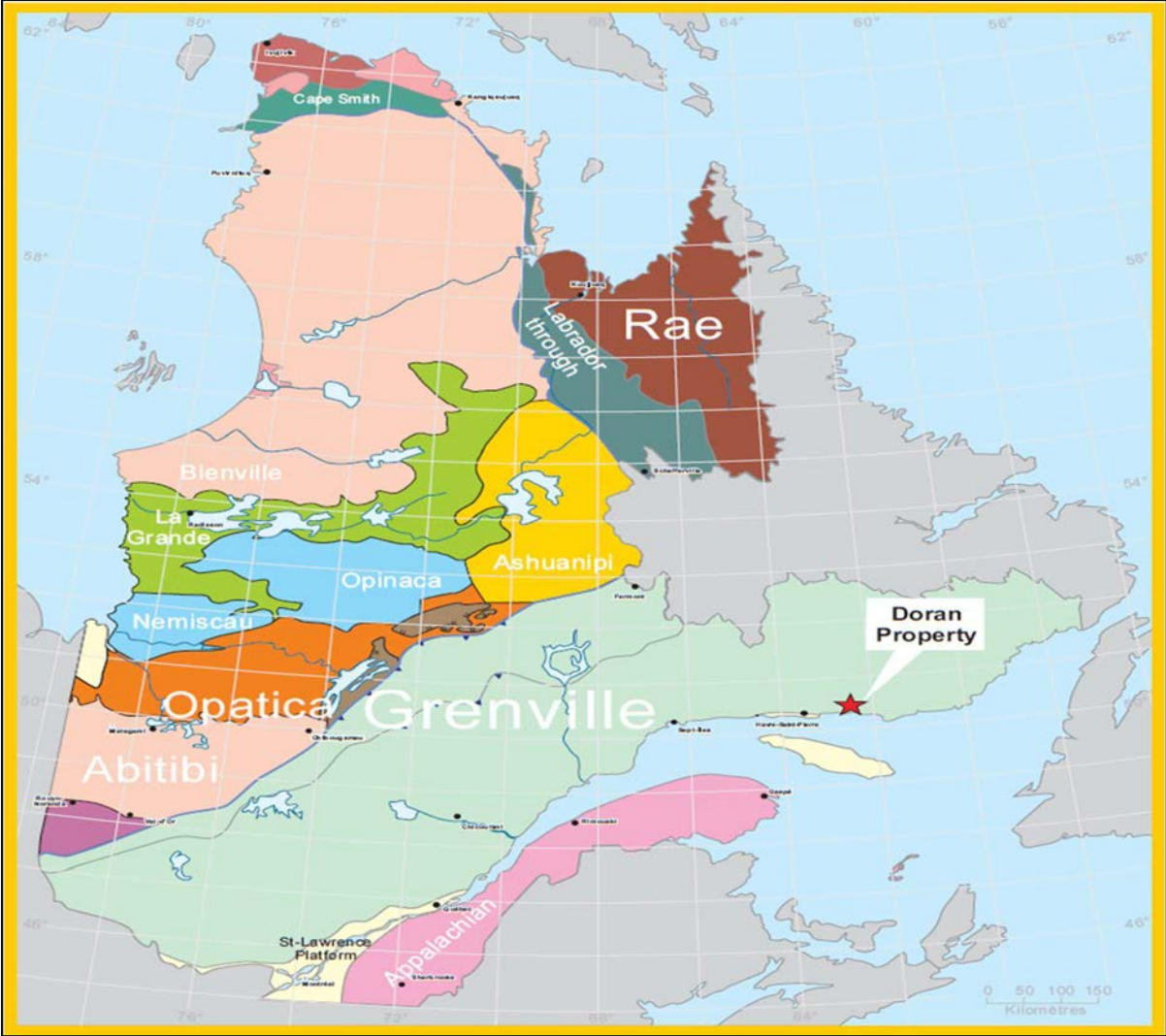


FIG. 10. Geological map of Quebec, Canada, with the geological provinces and subprovinces and the localization of Entourage Mining’s Doran project [63] (reproduced with permission).

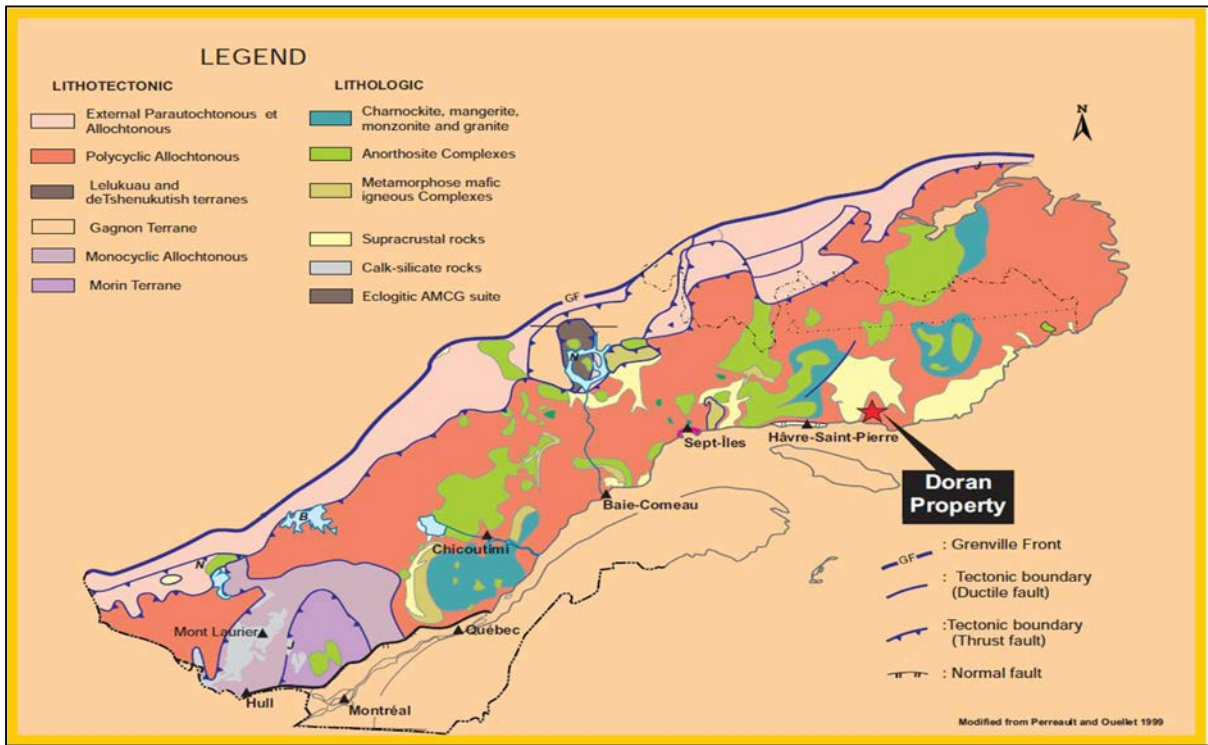


FIG. 11. Localization of the Doran property within the Grenville Belt [63] (reproduced with permission).

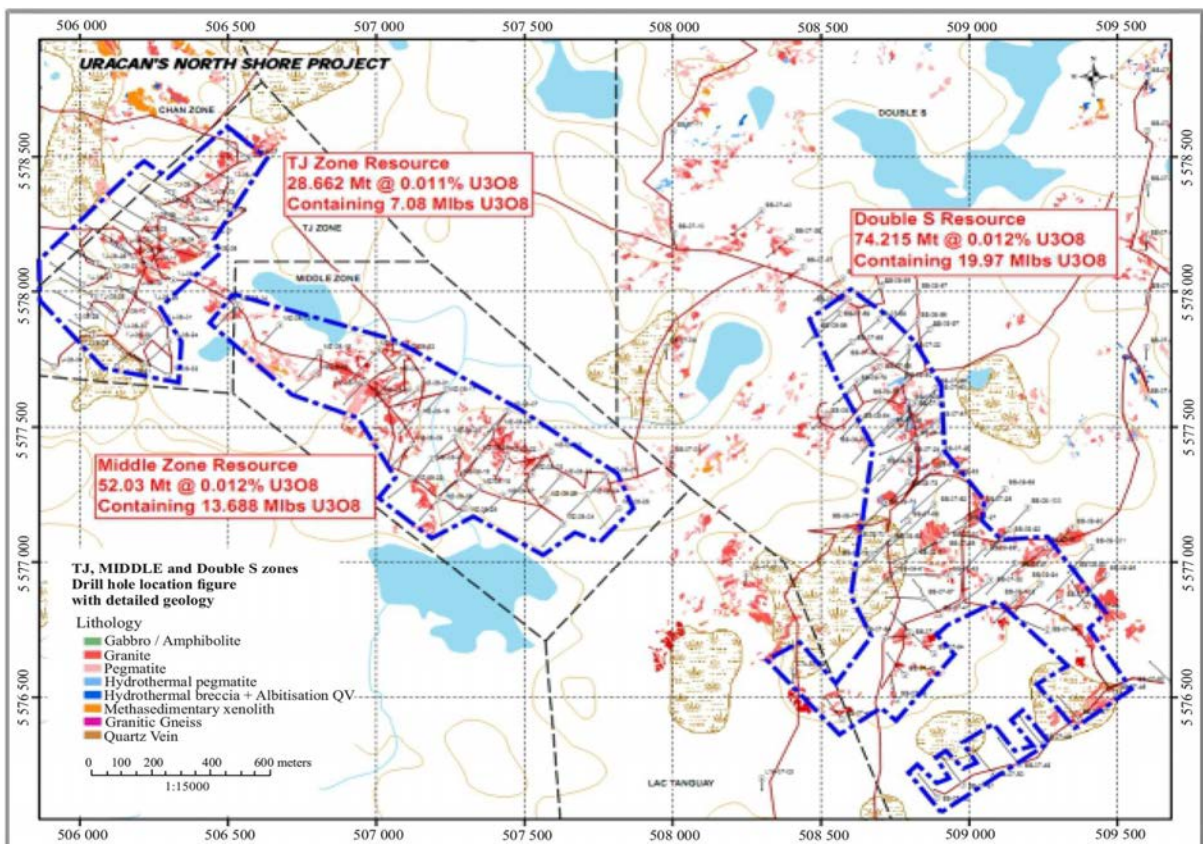


FIG. 12. North Shore project (Uracan Resources Ltd): local geology and location of the mineralized zones [65] (reproduced with permission).

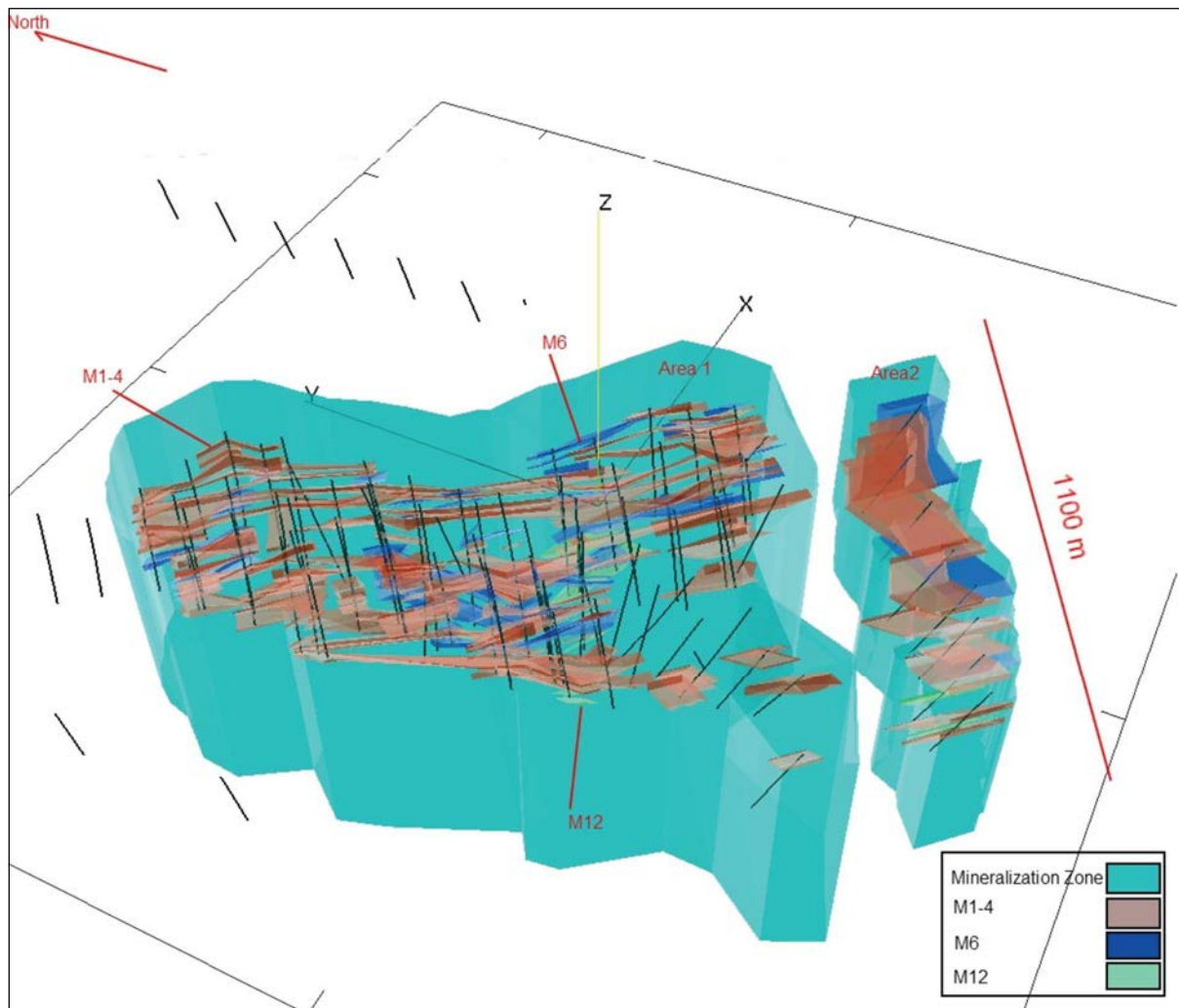


FIG. 13. The Double S deposit (Uracan Resources Ltd): isometric view of the mineralized envelopes for Areas 1 and 2 [65] (reproduced with permission.).

### 3.1.4.3. Quartz monzonite: The Bingham Canyon porphyry copper deposit (USA)

#### Introduction

The Bingham Canyon Cu–Au–Mo porphyry deposit is located in the Oquirrh Mountains of Utah, 35 km south-west of Salt Lake City (Fig. 14). It is one of the largest and highest grade porphyry orebodies in the world. The high grade zone (>1% Cu, >1 g/t Au) contains more than 500 Mt of ore. Of the world's porphyry copper deposits, Bingham ranks seventh based on contained Cu metal (28 Mt), second based on contained gold (1600 t) and fifth based on copper grade. Total current (2011) mineral resources are 1100 Mt at 0.44% Cu, 0.2 ppm Au, 0.063% MoS<sub>2</sub> and 2 ppm Ag. Mine production is expected to continue until 2028.

The open pit mine is owned by Kennecott Copper Corporation (Rio Tinto Group). The mine has been in production since 1906, which has resulted in the creation of a pit over 1200 m deep, 3.5 km wide and covering 10 km<sup>2</sup>, making it the world's second largest human excavation (after the Chuquicamata copper mine in Chile). Annual production is 300 000 t Cu, 18 t Au, 170 t Ag and 13 000 t Mo. Over its life, Bingham Canyon has proven to be one of the world's most productive mines, with production of about 17 Mt Cu, 790 t Au, 7000 t Ag and 440 000 t Mo. Uranium was temporarily extracted as a by-

product to Cu and other metals in 1978–1989 at a maximum rate of about 40 tU per year from a copper dump leach liquor containing 8–12 ppm U [47]. Total production was 416 tU.

### Geological setting

The Bingham Canyon porphyry deposit is centered on a Late Eocene composite pluton known as the Bingham stock that intruded a thick sequence of quartzite, calcareous quartzite and limestone of the Pennsylvanian Oquirrh Group. The Bingham stock is one of a series of ore related granitoid intrusions emplaced along the E–W trending Uinta Arch during the mid-Tertiary. The Oquirrh Mountains lie on the eastern edge of the Basin and Range Province and were tilted eastwards at about 11° during post-mineralization extensional faulting during the mid- to Late Tertiary [54].

The Bingham stock is made up of a pre-mineralization equigranular monzonite phase that was intruded by a series of ore related porphyry dykes. Five porphyry intrusions have been recognized (Fig. 15), which are, from oldest to youngest: (i) quartz monzonite porphyry (QMP), (ii) latite porphyry (LP), (iii) biotite porphyry (BP), (iv) quartz latite porphyry breccia (QLPbx) and (v) quartz latite porphyry [54].

Porphyry copper mineralization is associated with each of these essentially coaxial porphyry phases. Analysis of zircon has yielded U–Pb isotopic ages for the early monzonite of  $38.55 \pm 0.19$  Ma and  $^{40}\text{Ar}/^{39}\text{Ar}$  isotopic ages of hydrothermal biotite in porphyry dykes ranging from  $37.74 \pm 0.11$  to  $37.07 \pm 0.21$  Ma [66]. These data suggest that ore related hydrothermal alteration associated with emplacement of the porphyry dykes continued for a period of about 0.75 Ma after emplacement of the monzonite.

The quartz monzonite porphyry is the earliest and largest porphyry intrusion and contains the highest Cu and Au grades in porphyry hosted ore. This body dips 55–60° NW, has a strike length of 1500 m, a width of 350 m and persists to depths of over 2 km (Fig. 16). The QMP contains 50–60% phenocrysts of plagioclase, orthoclase, hornblende, biotite and rare quartz ‘eyes’. Unaltered groundmass is aplitic and composed primarily of quartz and orthoclase [54].

Ore related porphyry dykes in the Bingham Canyon pit were emplaced along steeply dipping, NE striking faults of probable extensional origin. This structural control is seen on the district scale. The NNE striking LP and QLP dykes have NW striking apophyses and thickened nodes at the intersections of NNE and NW striking faults. These intersections are also marked by abundant quartz veins which run parallel to these two fault sets and are sites of intense potassic alteration and high grade Cu–Au mineralization in both the LP and QLP. Redmond and Einaudi [54] suggest that the flow of magmatic–hydrothermal fluids within successive porphyries was focused at these structural intersections.

Hydrothermal alteration within and peripheral to the ore hosting QMP consists of Mg- and K-metasomatism, forming an inner zone of quartz–orthoclase–phlogopite, an outer zone of actinolite–chlorite–epidote, and a late sericitic and argillic (mainly montmorillonite) overprint.

### Mineralization

Ore minerals form overlapping sulphide mineral zones consisting of, from the interior low grade core outwards: molybdenite, chalcocite–bornite, chalcopyrite, chalcopyrite–pyrite, pyrite and galena–sphalerite. Gold and silver are present in significant amounts while Bi, Pt, Pd, Re, Se and U occur in recoverable, but trace amounts. The average uranium grade is less than 10 ppm and no uranium mineral has been identified. Molybdenite and Cu sulphides occur as disseminations and galena–sphalerite and part of the pyrite are present as veins. Mineralization is concentrated in and ‘drapes’ around and through the QMP facies. Distribution and zoning of mineralization and alteration is controlled by distance from the QMP within the intrusive complex, reactivity of the host rock, degree of fracturing and permeability [47].

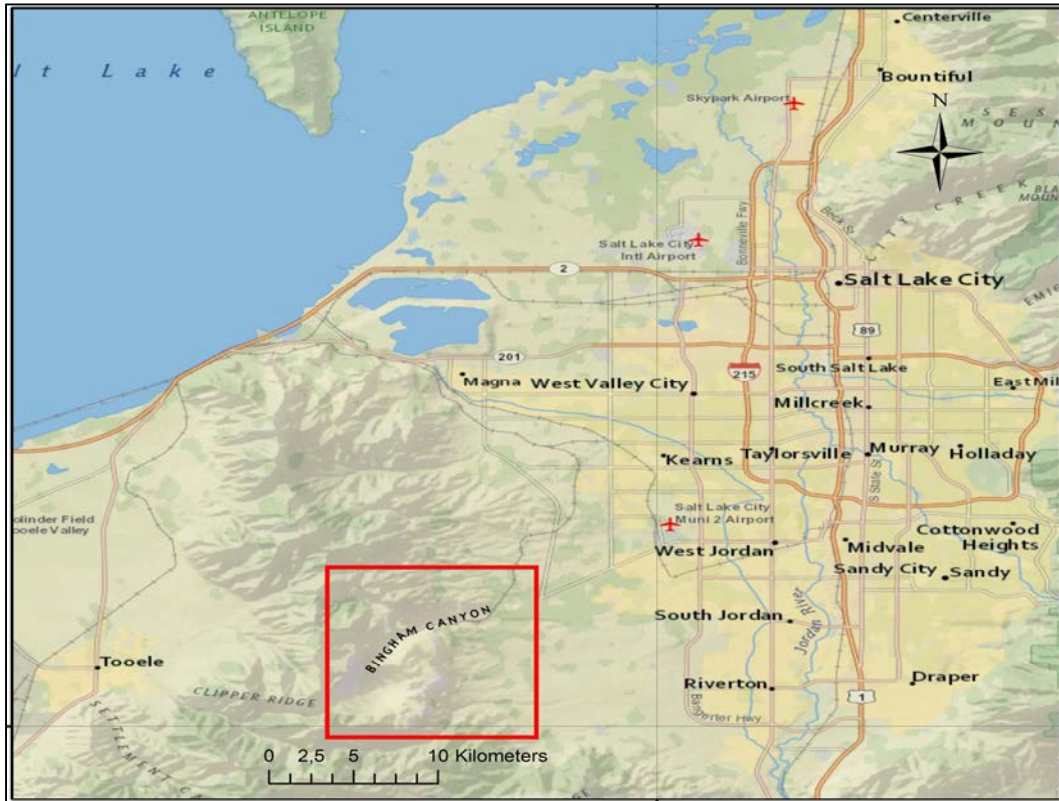


FIG. 14. Location of the Bingham Canyon mine, Utah, USA [67] (reproduced with permission).

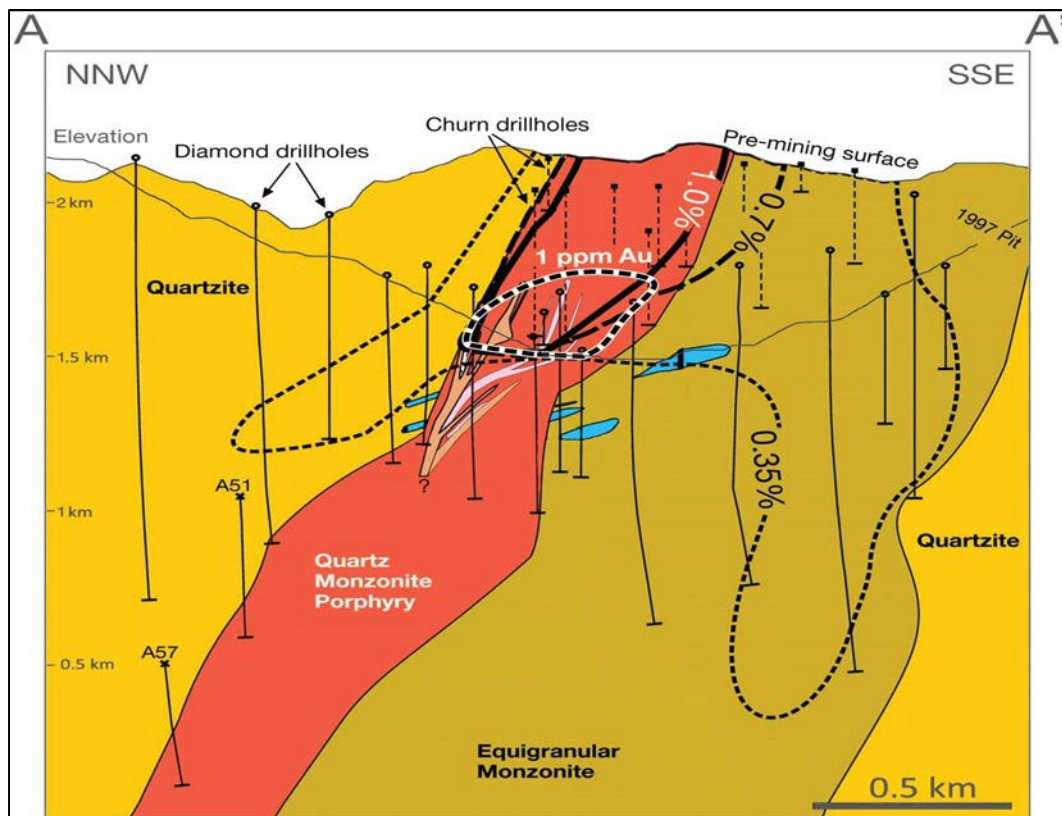


FIG. 15. Geological cross-section of the Bingham Canyon mine, showing rock type, copper grade contours and the location of the high grade gold zone (adapted from Ref. [54]).

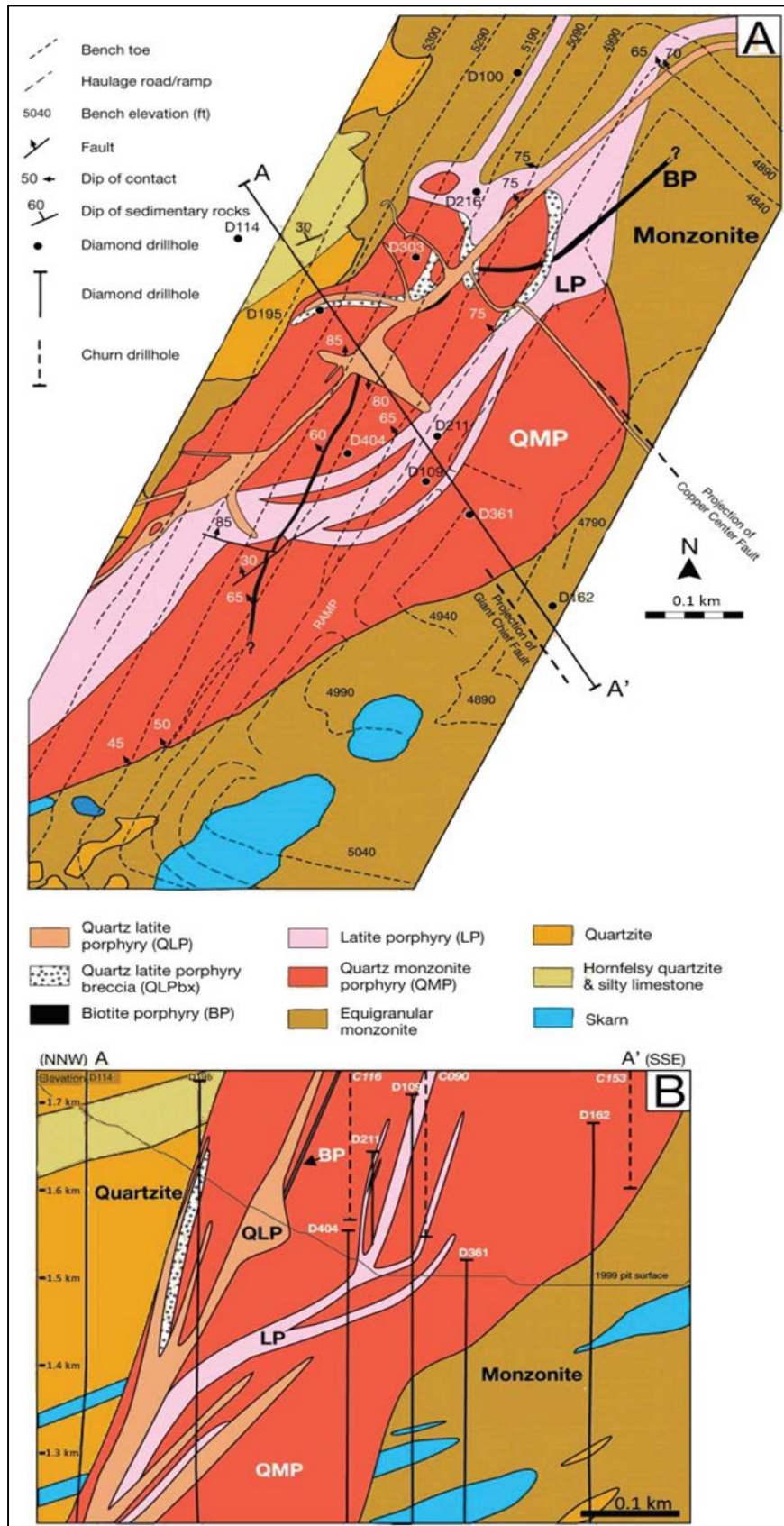


FIG. 16. Bingham Canyon mine. Detailed geological map (A) and cross-section (B) of the quartz monzonite porphyry (QMP) and latite porphyry (LP) zone, showing the disposition of the five porphyry intrusions (adapted from Ref. [54]).

#### 3.1.4.4. *Peralkaline complexes: Ghurayyah and Kvanefjeld*

The Ghurayyah deposit (Saudi Arabia)

##### Introduction

The Ghurayyah deposit is located in the north-western part of Saudi Arabia, 85 km south of the city of Tabouk and 55 km from the Dhuba harbour along the Red Sea (Fig. 17). The operator of the project is Tertiary Minerals plc in association with two local partners [68].

In 2006, mineral resources at Ghurayyah were estimated at 385 Mt grading 245 g/t Ta<sub>2</sub>O<sub>5</sub>, 2840 g/t Nb<sub>2</sub>O<sub>5</sub>, 8915 g/t ZrO<sub>2</sub>, 1270 g/t Y<sub>2</sub>O<sub>3</sub> and 140 g/t U<sub>3</sub>O<sub>8</sub> (45 700 tU at an average grade of 120 ppm U). Resources remain open below 250 m [70]. Rare earth element concentration is also high, but no grades have been reported, and the thorium content is reported at 399 ppm. The deposit contains the world's largest undeveloped tantalum resource [69].

A technical and economic scoping study for development of the deposit as an open pit was completed in 2006 with positive results. The fine-grained disseminated ore minerals would be processed by flotation and magnetic separation. Smelting of the ore concentrate will be required to remove the high concentrations of U and Th and to produce a low radioactivity Nb–Ta ferroalloy and/or tantalum salt [68]. A new exploration licence application was submitted in 2007 but the granting of this licence was still awaited in 2015. The production of uranium was excluded from the original licence.

##### Geological setting

The deposit is situated within the Arabian Nubian Shield, which constitutes the northern part of the Neoproterozoic–Early Palaeozoic East African Orogen. It consists of juvenile Neoproterozoic crust, now widely exposed in parts of Egypt, Saudi Arabia, Sudan, Eritrea, Ethiopia, Yemen and Somalia (Fig. 18). The Arabian Nubian Shield is considered an accretionary orogen that formed between 900 and 550 Ma, during the formation of the supercontinent of Gondwana. The Shield is comprised mainly of metamorphosed volcano-sedimentary sequences, disaggregated ophiotitic suites and various pre-, syn- and post-kinematic intrusives [69]. A major period of post-orogenic, granitic magmatism associated with crustal extension lasted from 620 to 530 Ma [70].

Rare metal mineralization associated with radioactive peralkaline microgranite intrusions in the north-western part of the Arabian Shield was discovered in 1964. The Ghurayyah stock is the largest and best mineralized intrusion among the peralkaline granites and was explored in detail in the 1970s and 1990s.

The Ghurayyah peralkaline granite is a subcircular stock about 800 m in diameter, cropping out with positive relief above the alluvial desert plain (Fig. 19). The stock was emplaced into greenschist facies metavolcanic and metasedimentary rocks of the Midyan terrane, has steeply dipping discordant contacts and the wall rocks of the intrusion show little sign of contact alteration [71]. The age of the Ghurayyah granite is not precisely known, but may be correlated with the 585–570 Ma phase of voluminous post-orogenic granitoid magmatism in the Arabian Nubian Shield. The large peralkaline granite complex of Jabal Dabbagh, 3 km east of Ghurayyah, has an age of  $577 \pm 4$  Ma and has been genetically linked to the mineralized stock [72].

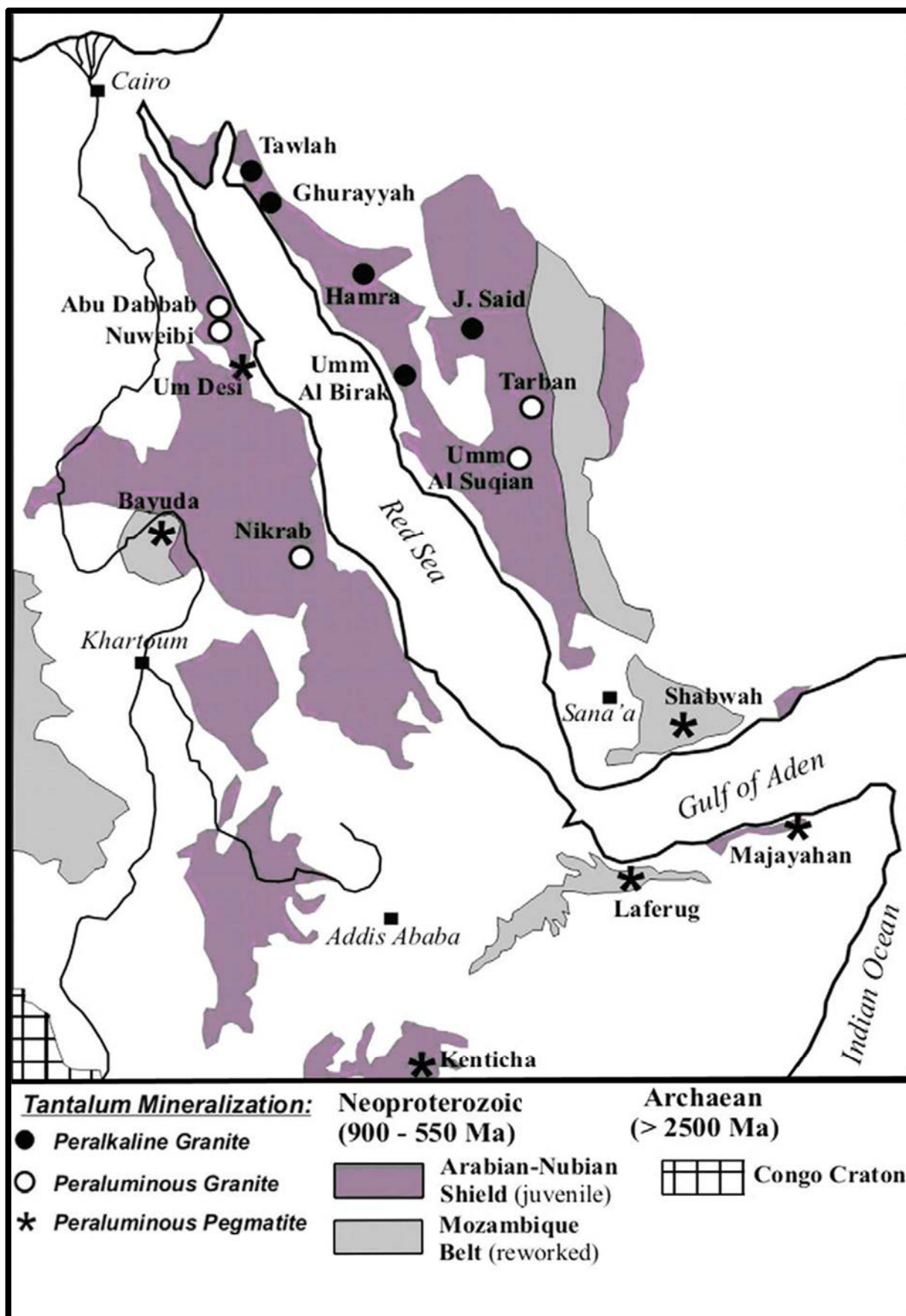


FIG. 17. Geological sketch map of north-eastern Africa and Arabia, showing major crustal segments and the location of tantalum mineralization (adapted from Ref. [69]).

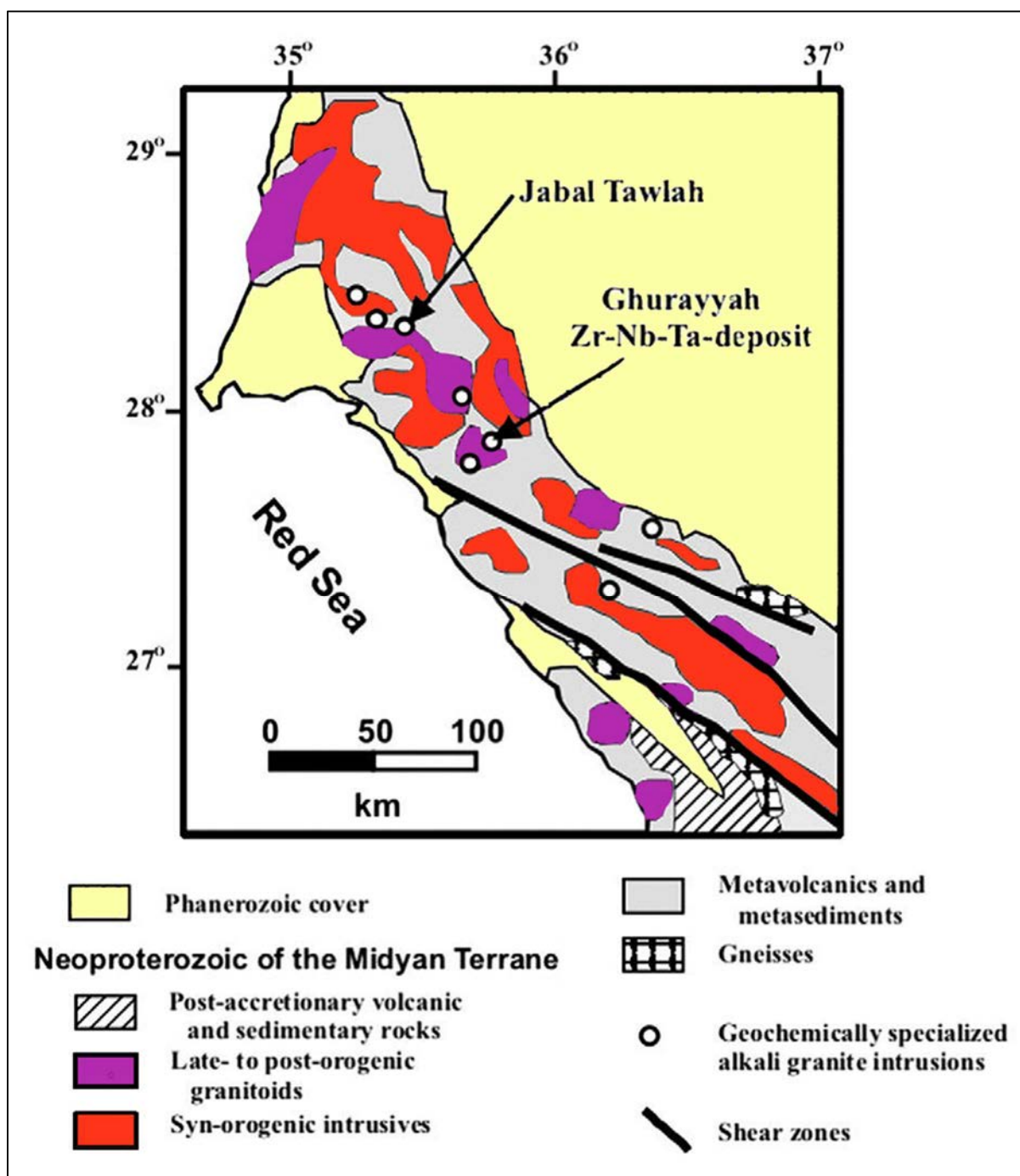


FIG. 18. Geological sketch map of the north-western Arabian Shield and the location of specialized peralkaline granites (adapted from Ref. [69]).

The Ghurayyah peralkaline granite is characterized by subsolvus feldspar mineralogy and the occurrence of sodic amphibole (arfvedsonite) and sodic pyroxene (aegirine). Texturally, it comprises a porphyritic microgranite with variable proportions of euhedral phenocrysts of quartz, microcline and arfvedsonite with chloritized remnants of aegirine. The phenocrysts are set in a chloritized matrix of albite laths, quartz and microcline with minor mica and fluorite [71]. Pegmatitic veins, lenses and pods as well as fluorite veinlets are also present.

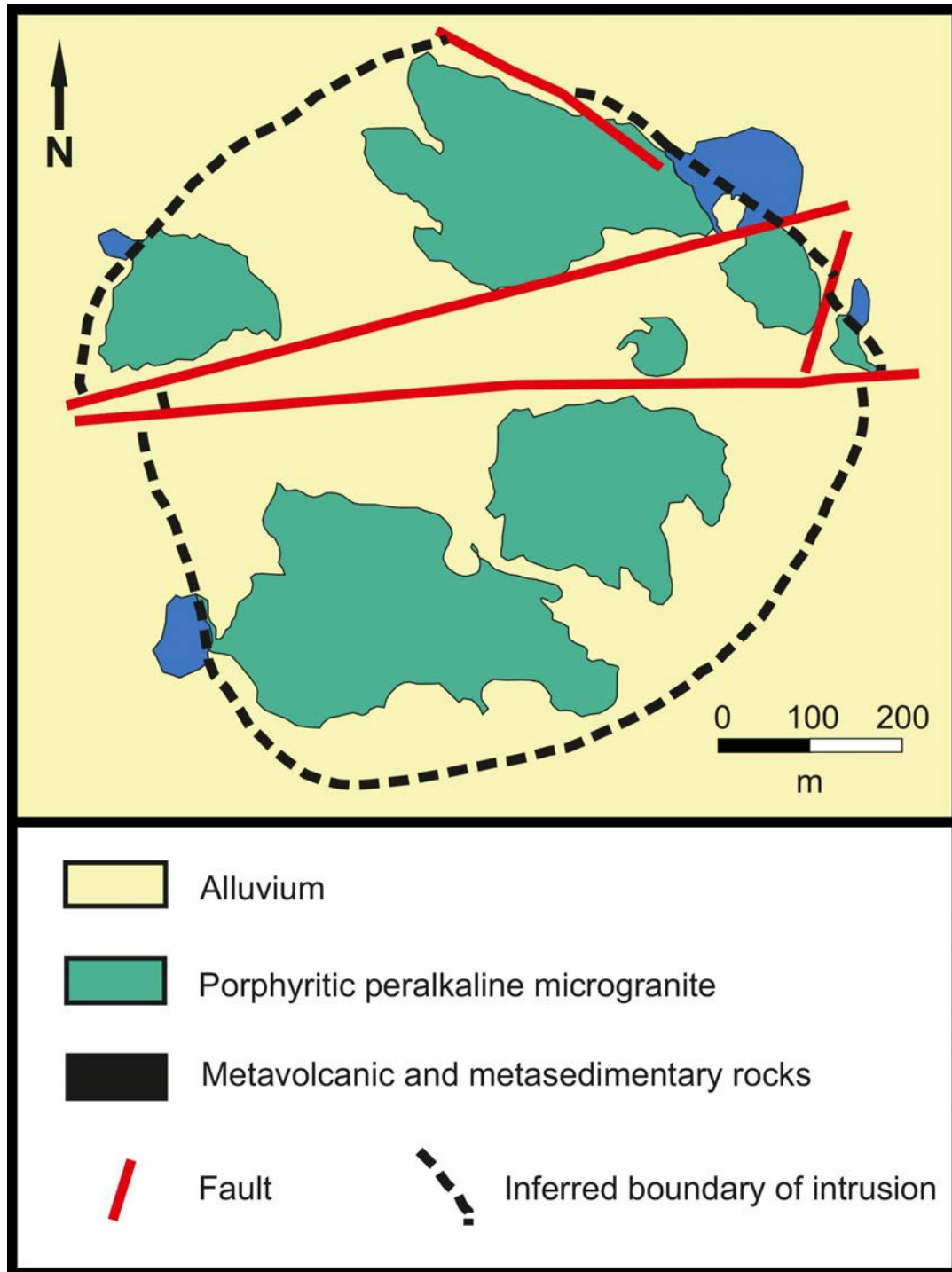


FIG. 19. Geological sketch map of the Ghurayyah peralkaline granite (adapted from Ref. [71]).

#### Mineralization

The accessory assemblage comprises a wide range of minerals, mainly zircon, pyrochlore, samarskite, aeschinite, columbite–tantalite, cassiterite, xenotime, monazite, uraninite, thorite, ilmene-rutile, galena, sphalerite and other sulphide minerals [73]. The fine-grained ore minerals are disseminated in the groundmass throughout the granite stock. The grade appears to vary inversely with the proportion of phenocrysts [71]. However, a remarkable consistency in grade distribution has been observed in drill core [68]. The major tantalum ore minerals are columbite, tantalite and, potentially, pyrochlore.

## Metallogenic aspect

Enrichment in tantalum and other rare metals is thought to be due to magmatic fractionation of an A type granitic melt together with volatile complexing of the metals and delay of crystallization of the respective accessory minerals until the latest stage. The resulting highly rare metal enriched residual magma finally crystallized under high volatile pressure at a high level in the crust [66]. Tantalum mineralization in the Ghurayyah peralkaline granite was therefore due essentially to magmatic processes and involved little meteoric fluid overprinting [74].

## The Kvanefjeld deposit (Greenland)

### Introduction

The Kvanefjeld deposit, which crops out, is located at the southern end of Greenland, about 8 km inland from the port of Narsauaq. It was discovered in 1956, one year after the commencement of a regional exploration programme. In the early 1970s, aerial and ground prospecting were carried out, followed by a drilling programme in 1977. A resource of 43 000 tU at an average grade of 340 ppm U was estimated. Further exploration up to 1986 resulted in the identification of 60 000 tU of speculative resources. Until recently uranium exploration in Greenland was carried out exclusively by Danish Government organizations (Geological Survey of Denmark and Greenland and the Danish Atomic Energy Organization). To investigate the extraction of uranium, a 960 m long adit was driven in 1979–1980 and 4000 t of ore were excavated for test work, including preliminary studies on mining and milling. In the mid-1980s, it was determined that uranium recovery by mining and milling was not economic.

The project has been operated since 2006 by Greenland Minerals and Energy Ltd, an Australian based company. Exploration was mainly focused on non-radioactive minerals as exploration for, and exploitation of, both uranium and thorium are prohibited. In 2014, the company indicated resources of 141 610 tU at an average grade of 220 ppm U, 6.6 Mt REE and 3 Mt Zn for the Kvanefjeld deposit. In addition, Y, F and Zr are anomalous. A higher grade zone near the surface has also been defined which could improve mine scheduling: 49 300 tU at a grade of 345 ppm U and 1.7 Mt REE at a grade of 1.4%. The Kvanefjeld project is recognized as the world's largest undeveloped compliant resource of REO in a multielement deposit [75].

In 2012, two new mineralized zones were recognized in the lujavrite formation of the Ilimaussaq Complex which had resources of 62 370 tU at a grade of 258 ppm U for Zone 2 (now known as Sorensen) with 1.10% REE and 0.26% Zn and 24 250 tU at a grade of 254 ppm U for Zone 3 with 1.16% REE (Fig. 20). The project overall resource inventory stands at 228 240 tU, 10.33 Mt REE and 2.25 Mt Zn [76]. A feasibility study was completed with planned production, starting in 2016–2017, of 1100 tU/year with a projected mine life of at least 30 years.

In November 2012, the position of Greenland in regard to uranium policy was addressed in Greenland's Parliament. Unanimous support was given from all political parties to fast-track an independent review to finalize the Government driven, multi-year phase of information gathering on uranium production and associated issues. Importantly this review includes aspects that relate to Greenland's foreign policy, which is determined by Denmark.

### Geological setting

The Ilimaussaq peralkaline, silica undersaturated plutonic intrusive complex, in which Kvanefjeld is located, covers an area of about 156 km<sup>2</sup> (Fig. 21). The mineralized occurrences are connected in space and time to the alkaline igneous formations of the Gardar intracratonic rift province, which were emplaced in the Ketilidian Mobile Belt of south Greenland. Magmatism in the Gardar Province is related to two main rifting events dated at 1280 Ma and 1180–1140 Ma. A series of 10 major plutonic complexes of gabbroic and nepheline-bearing to quartz saturated granitoid rocks intrude a basement consisting of Palaeoproterozoic granite and gneiss which were unconformably overlain by

Mesoproterozoic Gardar basalts and sandstones of the Eriksfjord Formation. Surrounding the complex is a large area of fenitization (sodium metasomatism by magmatic sodic solutions).

Two of the intrusive complexes contain carbonatite and many alkali gabbro dykes throughout the Gardar Province contain anorthosite xenoliths. The association of alkali gabbro intrusions, anorthosite xenoliths and carbonatite with granitoid intrusions has been interpreted to reflect large scale melting of asthenospheric mantle.

According to scientific studies undertaken during the various phases of investigation, the area is considered to host one of the most unusual examples of magmatic differentiation. The magmatic suite represents several pulses of mainly silica undersaturated intrusions. The intrusion of Ilimaussaq is composed of an early stage augite syenite which is followed by a suite of peralkaline agpaite nepheline syenite which is highly alkaline, carrying sodic pyroxenes and sodic amphiboles.

The differential crystallization developed from pulaskite through foyaite, naujaite, kakortokite and, finally, to lujavrite as the latest differentiate phase. In the same order, the uranium and thorium content increases from 10 ppm U and 20 ppm Th in the pulaskites to more than 60 ppm U and 60 ppm Th in the lujavrite. In some lujavrite varieties, the uranium concentration may exceed 1000 ppm and the thorium up to 5000 ppm.

The lujavrite is typically a dark, fine-grained laminated rock composed of microcline, albite, nepheline, arfvedsonite and aegirine as rock forming minerals. A medium- to coarse-grained variety of similar mineralogy is found within the main mineralized area. Eudialyte, streenstrupine, sphalerite and lithium-rich mica are examples of the large number of minor constituents [77].

A significant portion of the radioelements in the lujavrite is contained in streenstrupine, monazite and pigmentary materials. Streenstrupine, the most widespread, occurs disseminated in the rock mainly as small interstitial crystals or as poikilitic grains. The uranium and thorium contents of the streenstrupine are 0.2–1.5% and 0.2–7.5%, respectively, and the whole rock radioelement contents vary in the range 0.01–0.30% U and 0.03–1.50% Th [77].

The general appearance of the Kvanefjeld area is that of a huge intrusive breccia. The lujavrites intruded and deformed the overlying, older intrusive rocks and a series of continental sandstones and lavas forming the roof of the intrusion. The mode of occurrence of the lujavrites ranges from tiny veins to continuous belts several hundreds of metres in width. The highest and most extensive concentrations of uranium (>300 ppm) are found close to, and within, contact zones between sheets of lujavrites and altered volcanic cover rocks [77].

#### Mineralization

The deposit is magmatic and formed during the latest emplacement stages of the intrusion. The uranium mineralization is associated with the youngest nepheline syenite and the medium- to coarse-grained lujavrite (Figs 22 and 23). At Kvanefjeld, under a roof composed of gabbro and mafic volcanic rocks, a megabreccia of volcanic and sedimentary rocks, together with the rocks of the intrusion, are cemented by lujavrite.

In the nepheline syenite, accessory silicate minerals of unusual composition such as eudialyte and rinkite are present. The suite of rocks is characterized by the abundance of volatile phases (fluorine and chlorine) as well as by a number of incompatible elements, such as rare earth elements, Nb, Be, Li, Zn, Zr and Sn together with the radioactive elements uranium and thorium.

The high concentration of these rare elements is explained as the result of magmatic differentiation and crystallization. The latest stages of the intrusive phase are represented by unusual rocks, such as kakortokite and lujavrite, which are the economically most important types. In some areas, uranium may be enriched to more than 0.1% and thorium to about 0.5%. Late stage veins which locally extend

into the country rocks are enriched in uranium and thorium to about the same concentrations as those in the late stage intrusive phases.

According to Bohse et al. [78], the highest concentrations of radioactive elements are found in the minerals rinkite (fluor-silicate with Ca, Na, Ce, Ti, Zr), which has 0.3–1.2% U and 0.3–0.4% Th, and streenstrupine (phosphato-silicate with Na, Ce, Mn, Nb, Fe), which has 0.2–1.5% U and 0.2–7.4% Th. Other important minerals are britholite, eudialyte, monazite, pyrochlore and thorite.

Streenstrupine is the main uranium mineral in the medium- to coarse-grained lujavrite, where it occurs instead of eudialyte, the main uranium–thorium mineral in the other rocks of the complex. It is also common in sodic pegmatite bodies, hydrothermal mineralization and in the fenitized volcanic rocks forming the roof of the Kvanefjeld plateau.

Two uranium enrichment trends can be observed in the Kvanefjeld mineralization: (i) a magmatic trend with an average Th/U ratio of about 3.5, similar to the main fractionation trend defined by the less fractionated units of the complex and (ii) a fluid fractionation trend with a uranium enrichment at constant Th content and a Th/U ratio decreasing to less than 2. These two trends and the large variations in U and Th contents observed in the different types of lujavrite reflect the effects of magmatic and late stage to post-magmatic processes related to the exsolution of a fluid phase [45]. Numerous mineralized veins, up to several kilometres long, striking NE–SW and predominantly vertical, transect all rock types to the east of the Ilimaussaq Complex [79]. Three main types of mineralized vein are present:

- (i) Brown albitic veins, composed of albite, haematite, quartz and small amounts of chlorite, calcite, apatite, monazite, eudialyte and thorite;
- (ii) Green veins composed of albite and aegirine, with occasional microcline, haematite and minor accessory minerals, such as mica, apatite, chlorite, quartz, sphalerite, monazite, bastnaesite, neptunite and thorite;
- (iii) Composite veins with the components of the two above types, together with accessory eudialyte and thorite.

Nearly all veins have elevated and highly variable Th/U ratios (1–57), Th (60–4500 ppm) and U (17–1500 ppm) contents, indicating that Th has been mobilized by a fluid and deposited in the veins over a distance of several kilometres. Uranium has migrated further, as reflected by low Th/U ratios of the veins, because of the highly oxidizing conditions recorded by the presence of haematite in the veins. The Ilimaussaq Complex is the obvious source of these veins because they have been traced to the contact with the complex and similar veins have been observed within the complex [45].

#### Metallogenic aspects

The origin of the deposit is clearly connected to the origin of the lujavrites. According to Steenfelt and Bohse [80] volatiles, uranium and rare earth elements were retained in the melt during the crystallization of the upper syenite units. Uranium likely formed stable complexes with allogenens or hydrocarbons. In addition, fractionation of uranium depleted rock forming minerals led to a considerable enrichment in uranium in the last liquid in the magma chamber. An impermeable roof prevented the escape of the volatiles, favouring the formation of minerals rich in uranium, rare earth elements, alkalis and volatiles, such as streenstrupine and monazite [81].

In addition to this type of mineralization, which is clearly syngenetic, epigenetic enrichment of uranium is seen in favourable positions, such as in the arched structures in the volcanic roof rocks. The uranium and thorium were contained in fluids expelled from the remaining lujavritic melt and then trapped below the roof. Large numbers of pegmatite and hydrothermal analcite–albite veins are located within the areas of epigenetic enrichment. The veins are frequently rich in streenstrupine [81].

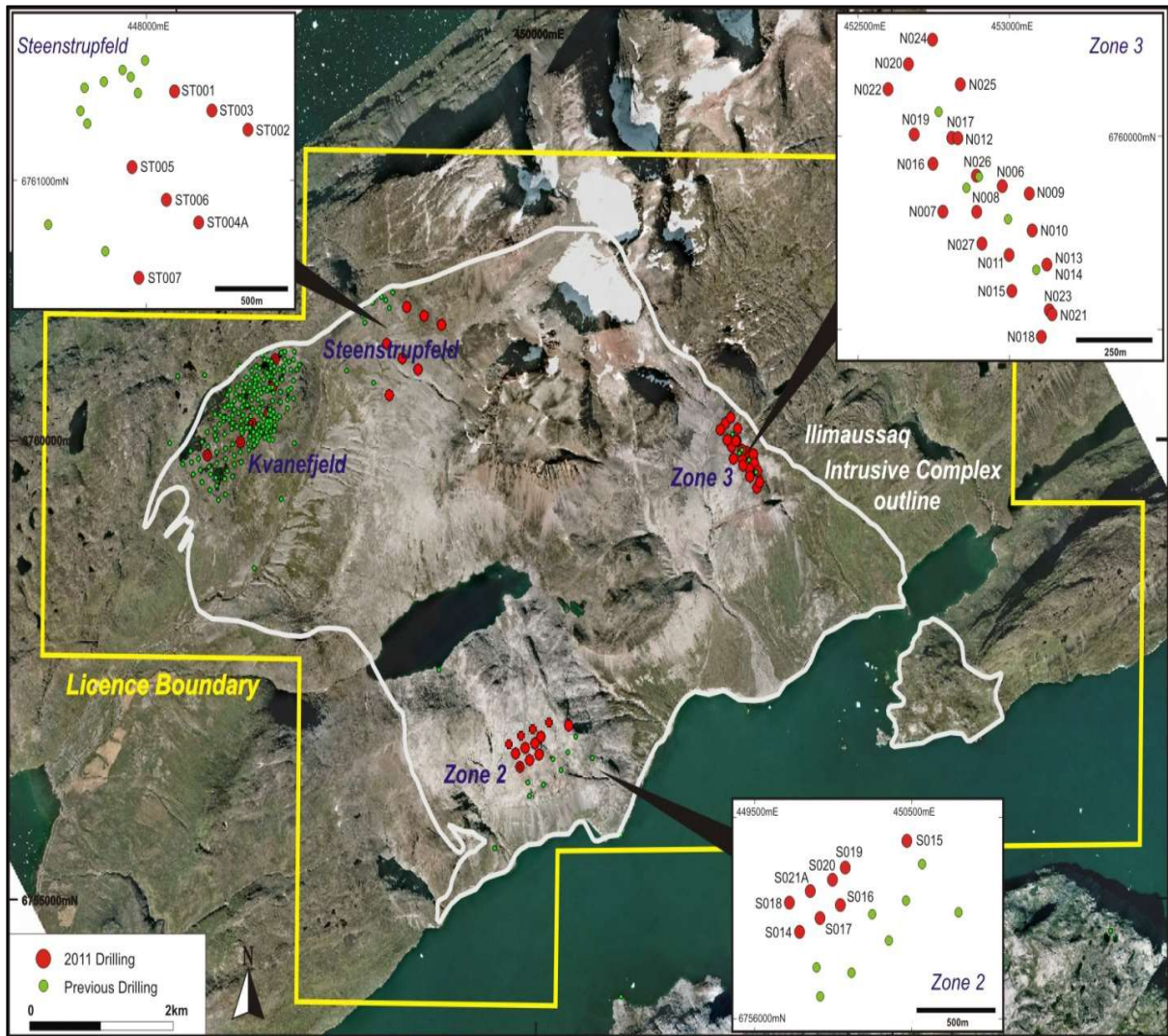


FIG. 20. Aerial view of the northern part of the Ilimaussaq Complex showing the location of the three deposits [82] (reproduced with permission).

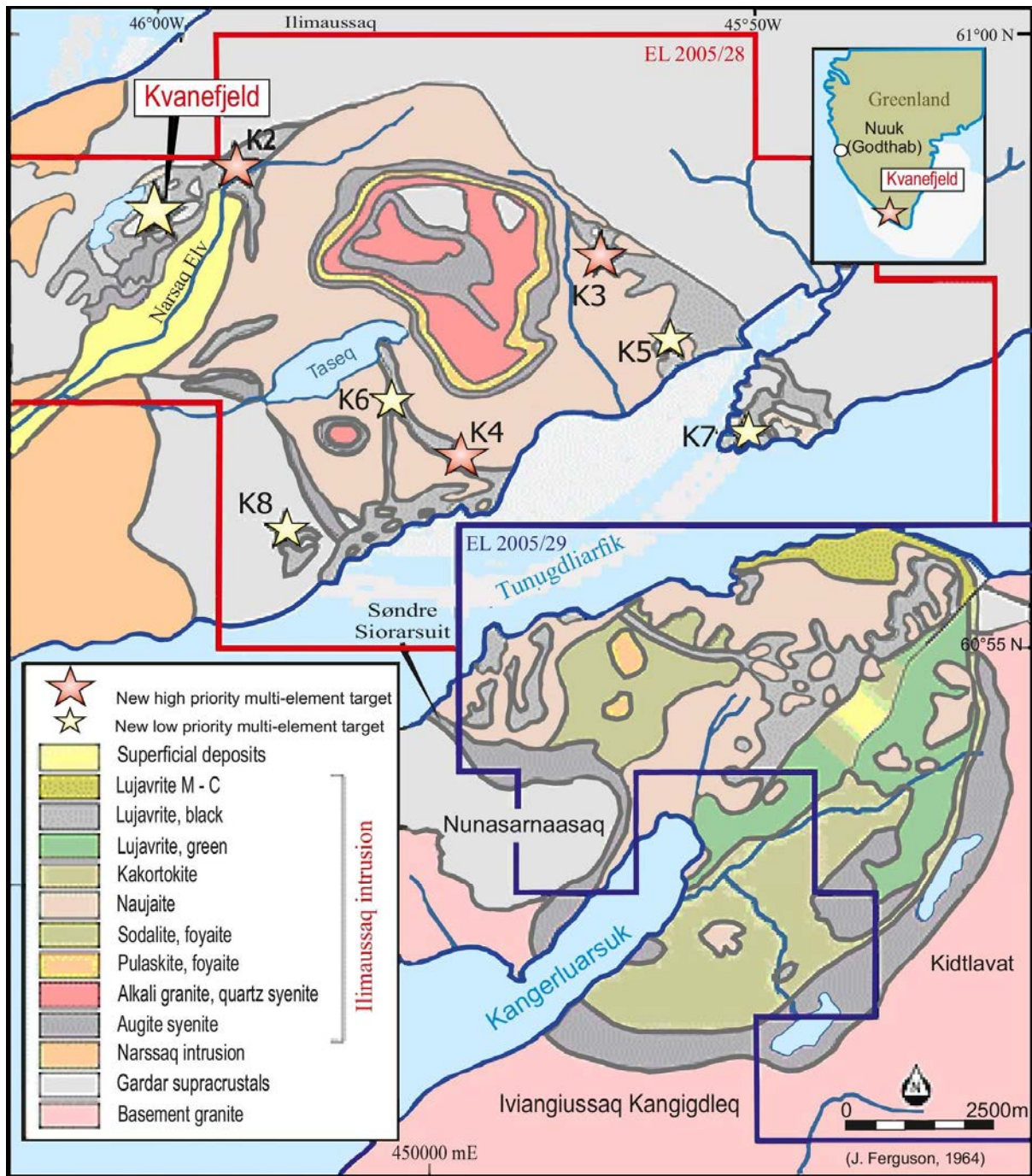


FIG. 21. Geological map of the Ilimaussaq peralkaline complex with the location of the Kvanefjeld deposit, as well as a series of new multi-element exploration targets (K2–K8) [83] (reproduced with permission).

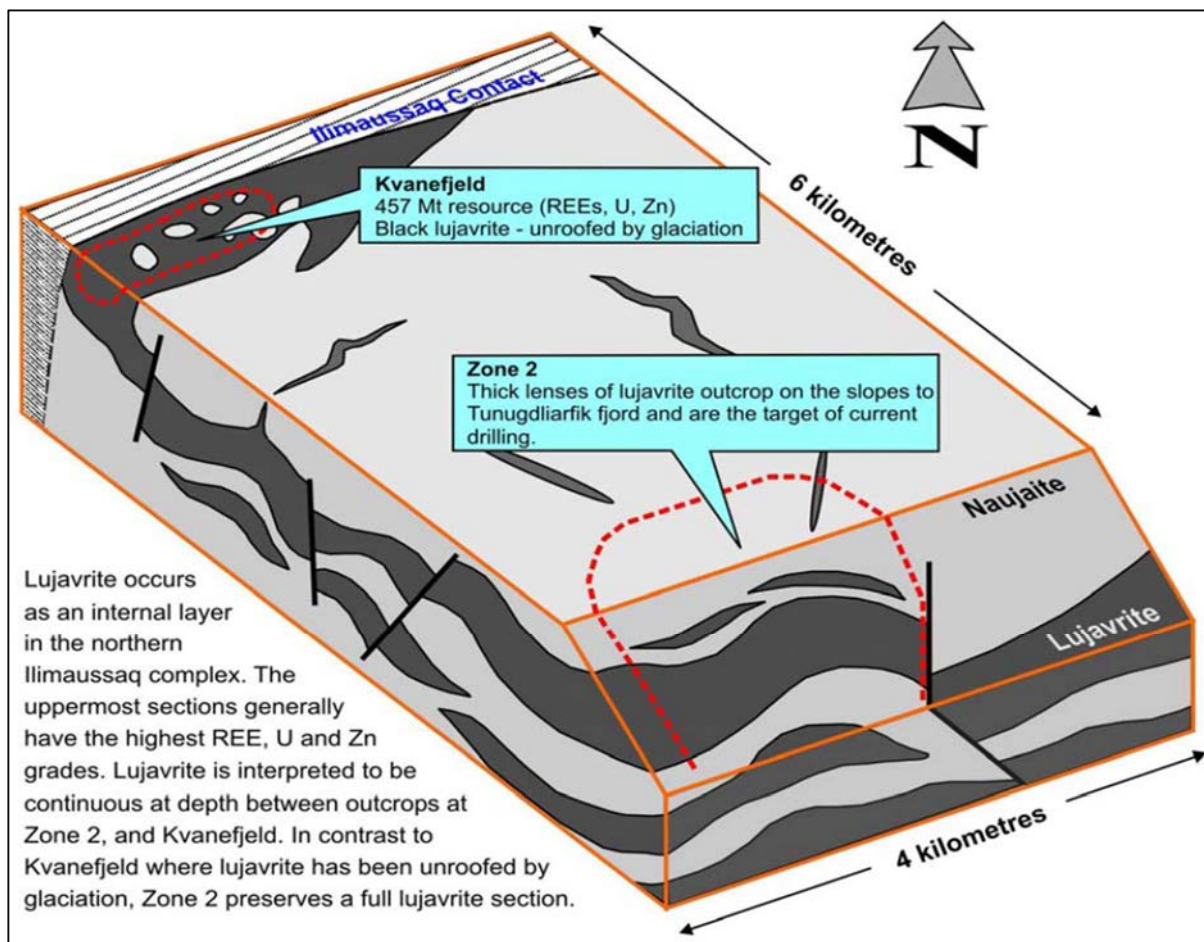


FIG. 22. Position of the lujavrite layers in the northern part of the Ilimaussaq Complex [84] (reproduced with permission.).

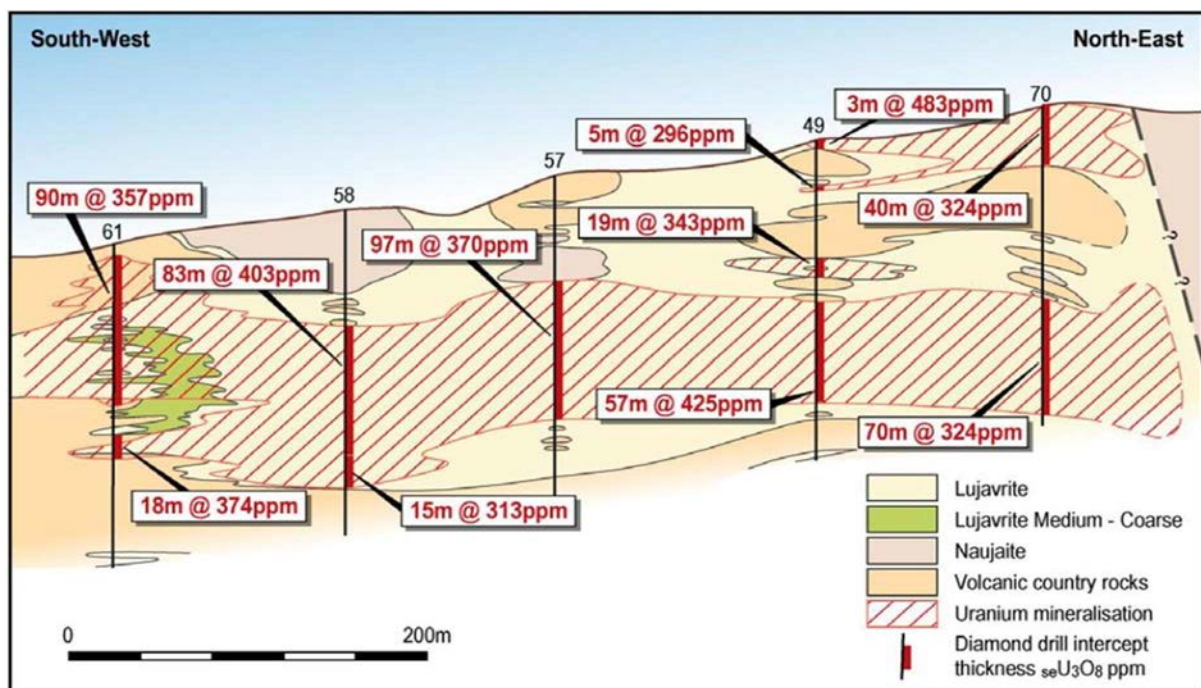


FIG. 23. A SW-NE cross-section of the Kvanefjeld deposit [85] (reproduced with permission).

### 3.1.4.5. Carbonatite: The Catalão deposit (Brazil)

#### Introduction

Catalão I, is a carbonatite complex located 15 km NE of the city of Catalão in south-eastern Goiás, 280 km south of the capital, Brasília. Apatite and pyrochlore ores are mined for phosphate and niobium, respectively. Data sourced from NUCLEBRAS from the late 1970s and the current (2007) indicate phosphate ore reserves totalling 191 Mt, which contain approximately 24 300 tU at an average grade of 135 ppm U.

The ultramafic alkaline complex of Catalão I exhibits a strong radiometric anomaly, with values 18–20 times the regional background. This is mainly due to Th but to a lesser extent U and K. In 1969, METAGO conducted a radiometric survey [86] showing that areas of stronger radioactivity coincide with areas of phosphate (fluorapatite) and niobium (pyrochlore) ores. Soil analysis in areas of high radioactivity indicated U values in the range 0.004–0.037% and ThO<sub>2</sub> values in the range 0.032–0.1%. One sample, containing goethite, magnetite and thorite, comprised 28.86% ThO<sub>2</sub>.

#### Geological setting

The Catalão I and Catalão II alkaline ultramafic complexes are part of an alkaline ultramafic intrusive province extending from the coast of the state of São Paulo to beyond Ipameri in Goiás. The segment between Tapira (Minas Gerais) and Catalão (Goiás) is characterized by the presence of large ultramafic alkaline complexes such as Tapira, Araxa, Salitre I, Salitre II, Serra Nagra, Catalão I and Catalão II. In this portion of the belt, the complexes are intruded into Proterozoic metasediments of the Araxa Group, composed predominantly of schist and quartzite.

Catalão I is an ultramafic–carbonatite complex of Upper Cretaceous age (83 Ma) and forms a subcircular plateau with a diameter of 6 km (Fig. 24). The current relief is the result of the greater resistance to weathering of the fenites which form the ring of the dome, supporting the plateau and protecting the thick blanket of weathered material in the central part of the dome [87].

The Catalão I complex (Fig. 25) is formed by an ultramafic phase consisting of dunite and subordinate pyroxenite that were intensely altered to phlogopite-rich rock as a result of intense K-metasomatism accompanying the multiple intrusions of carbonatite. Only remnant relict portions of the ultramafic rocks can be recognized among the dominant carbonatites and phlogopitites. Following the phlogopitization process, nelsonite and carbonatite intrusions were emplaced successively.

Nelsonite is a phoscorite group rock containing pyrochlore, consisting mainly of magnetite, phlogopite, calcite and/or dolomite. It is usually massive, but may also be banded and medium- to coarse-grained. It occurs as dykes and veins ranging from centimetres to metres in thickness and often cut by carbonatite veins and dykes. Pyrochlore, apatite and sulphides are accessory minerals but may locally be present as essential minerals. Pyrrhotite is the main sulphide mineral and calcite is the main carbonate phase. The pyrochlore is dominantly Na–Ca-rich but a Pb-rich pyrochlore is also present [88, 89].

Ribeiro [88] detailed the evolution of the Catalão complex, identifying three petrogenetic series:

- (i) The bebedourite series, which was crystallized from an immiscible silicate liquid derived from a primitive silica–carbonate magma yielding, by differentiation, dunite, pyroxenite and veins of carbonatite residuals;
- (ii) In a second immiscibility event, the initial carbonatite liquid differentiated into a phoscorite component and other carbonatites. The phoscorite was initially olivine-rich and evolved to form apatite cumulates;
- (iii) The carbonatite crystallized in the third and final episode of immiscibility, generating a new phoscorite phase and carbonatite components. This second phoscorite generation does not contain olivine, but is rich in magnetite and pyrochlore.

Both hydrothermal and weathering related alterations (Fig. 26) were strongly developed, forming lateritic soils and thick limonitic crusts. Thick sequences (150 m) of clay-rich sediments are present in the central depression of the structure (Lagoa Seca). The presence of pebbles at the base and below the limonitic crust suggests that, during the Tertiary, the depression consisted of a large cavity at least 150 m deep, possibly related to a slowly subsiding sinkhole. Two potential rare earth element mineralization types have been distinguished: lateritic and silicite [89].

A lateritic cover overlies the mineralization as a ferruginous and intensely weathered zone where no relict primary texture is recognizable. Its thickness is variable, but does not exceed 25 m. The dominant mineral is goethite. Goethite, typical of laterites, predominates in the interval around 17–20 m. Pyrochlore, which is always present, is fine-grained. The saprolite below, which contains the economic niobium mineralization, is comprised of weathered rocks in which relict primary igneous textures are still recognizable. The saprolite is rich in apatite and anatase. The niobium mineralization, present as dykes and fracture filling veins, occurs in variable form, both horizontally and vertically, reflecting the distribution of pyrochlore in the host rocks. Large blocks and masses of supergene silicite are abundant in the saprolite with a varied suite of minerals, including magnetite, baryte, apatite and secondary phosphates [87].

### Mineralization

At least five mineral commodities are identified in the Catalão I carbonatite complex: (i) phosphate (two operating mines); (ii) niobium (one active mine producing niobium–iron); (iii) rare earth elements; (iv) anatase and (v) vermiculite (Figs 27 and 28). Uranium is present in two ore types.

#### (a) Uranium in phosphate ores

Only one systematic evaluation of uranium associated with phosphatic ores has been performed for Catalão I. In 1979, NUCLEBRAS conducted a sampling campaign at the active mine wall and at the semi-industrial processing plant at the local METAGO operation [90].

The values listed in Table 12 were obtained from chemical analyses of 5 m channel samples from the mine, samples from the the plant feed, fines, flotation and magnetic separation tailings and the final concentrate [90–92].

TABLE 12. AVERAGE  $U_3O_8$  GRADE OF THE PHOSPHATE ORE AND OF THE SEMI-INDUSTRIAL PLANT STREAMS

Sample	Number of samples	$U_3O_8$ (ppm)	$ThO_2$ (ppm)
Mine (ore)	50	168	
Plant feed	15	157	520
Magnetic tailings	4	57	
Fines	16	248	799
Flotation tailings	16	186	459
Final concentrate	16	80	145

Preliminary sulphuric acid extraction tests by Benedetto [91] on the fines and on the flotation tailings yielded  $U_3O_8$  recoveries of 52.5% and 25%, respectively, and acid consumption of 200 and 250 kg/t, respectively.

The official 2007 proven ore reserves of phosphate in Catalão I, combining both the ULTRAFÉRTIL and COPEBRAS mines, totalled 191 Mt (10.26%  $P_2O_5$ ), as well as 233 Mt of indicated and 118 Mt of inferred resources. A total of 382 Mt was considered as mineable reserves, with 39.6 Mt of contained  $P_2O_5$  [93]. If the 157 ppm  $U_3O_8$  value measured in 1979 is considered representative, a total reserve of 59 974 t of contained  $U_3O_8$  (51 000 tU at 133 ppm U) could be expected for the prospect. Total geological resources of uranium are estimated at 72 000 tU. The ore also contains high concentrations of REEs, with 2.58% REE (the average of 743 samples analysed by Ribeiro [88]), potentially adding 9.9 Mt total REEs as a by-product.

*(b) Uranium in pyrochlore, in the slag of Fe–Nb production and in anatase*

There are no published data regarding the content of uranium in the Nb (pyrochlore) and Ti (anatase) ores of Catalão I. A hydrometallurgical test plant was built by CETEM at another mine to assess the recovery of valuable elements (mainly REE and Al) from the Fe–Nb aluminothermy. The recovery of 1.5 kg of  $U_3O_8$ /t of slag, with a solubilization rate of 82% for uranium and 79% for Th was considered very encouraging. The slag contained 0.14%  $U_3O_8$  and 2.71%  $ThO_2$  [94], and the average production of slag was 40 000 t/year.

#### Metallogenic aspects

Cordeiro [95] suggested that the igneous protoliths at Catalão I were responsible for the genesis of metallic mineral deposits, namely:

- (a) Deposits of apatite (phosphorus): residual enrichment from late pyroxenites of the bebedourite series and olivine phoscorites;
- (b) Deposits of pyrochlore (niobium): residual enrichment from phoscorites generated in the third event of immiscibility;
- (c) Deposits of monazite (rare earth elements): residual enrichment from metasomatic phlogopitites, phoscorites with niobium and carbonatitic dolomite metasomatized by hydrothermal carbonate-rich fluids;
- (d) Deposits of anatase (titanium): residual enrichment from initial pyroxenite from the bebedourite series.

The origin of the Catalão I niobium deposit is related to carbonatite magmatism but the process generating such Nb-rich rocks is still undetermined. It could possibly be a result of crystal accumulation and/or emplacement of iron–phosphate oxide magma [96].

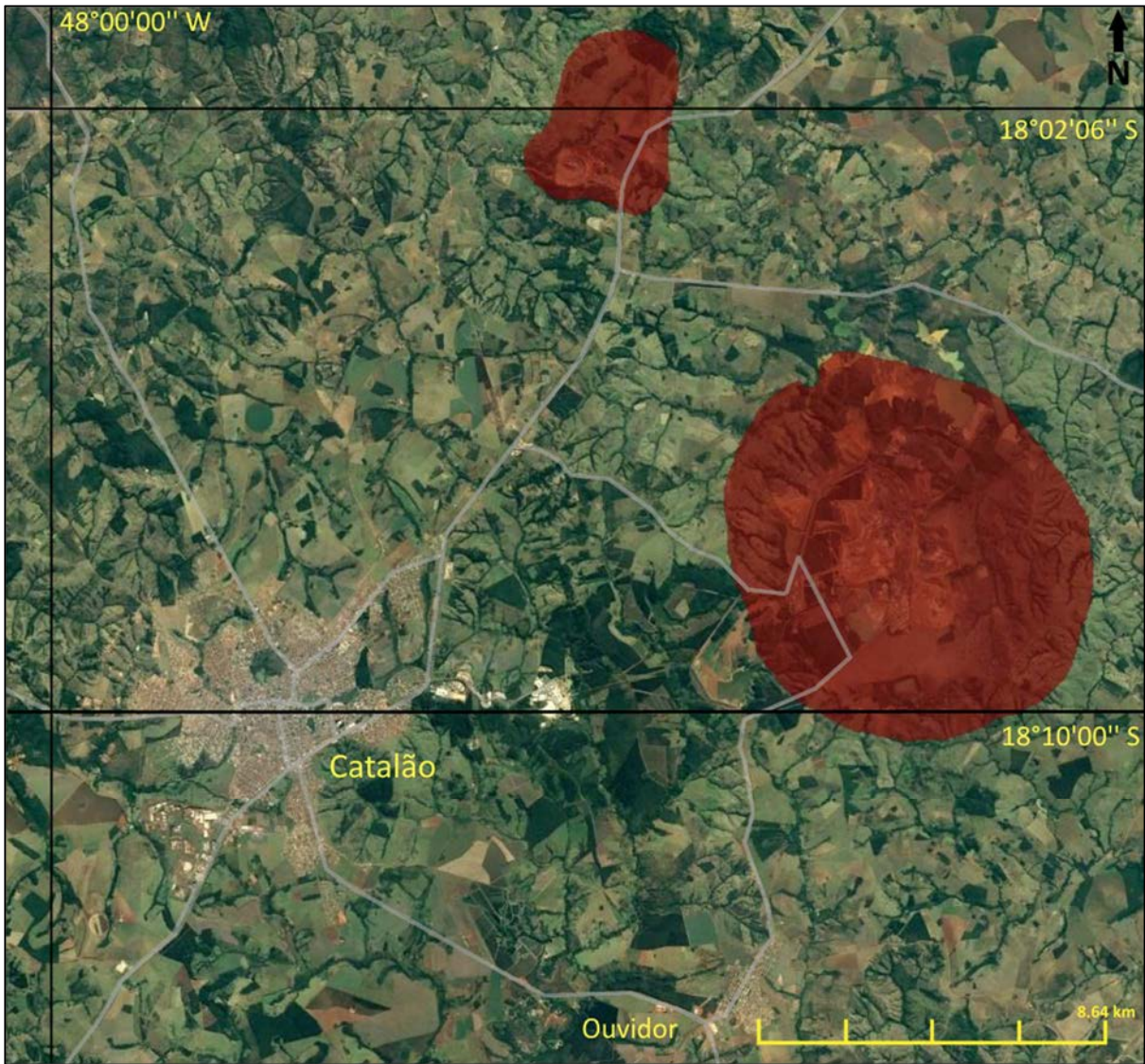


FIG. 24. Location of the Catalão I and Catalão II intrusions (adapted from Ref. [87]).

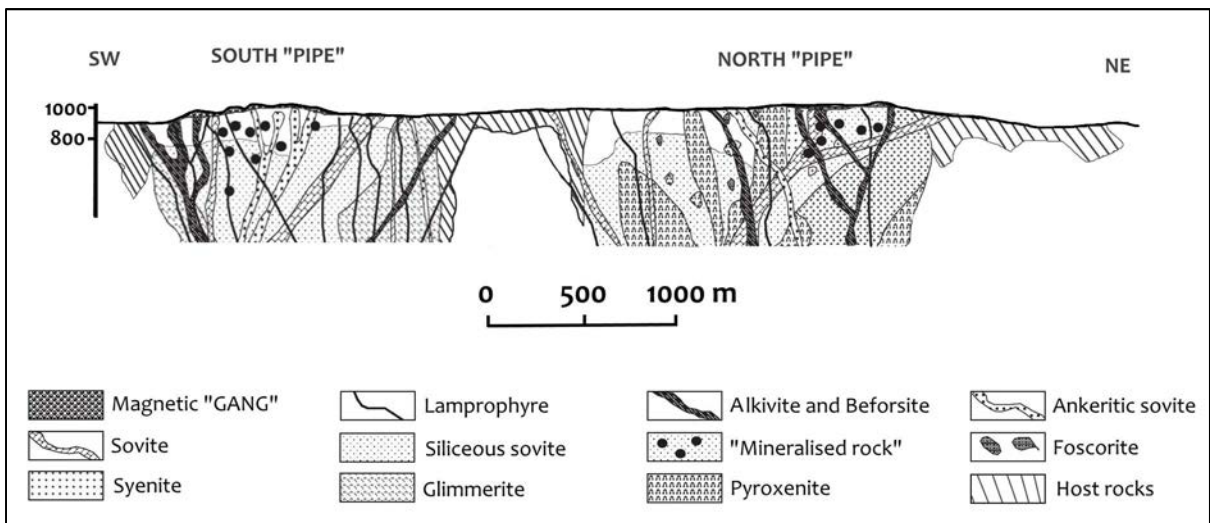


FIG. 25. Schematic cross-section showing the relationships between the Catalão I lithologies (adapted from Ref. [87]).

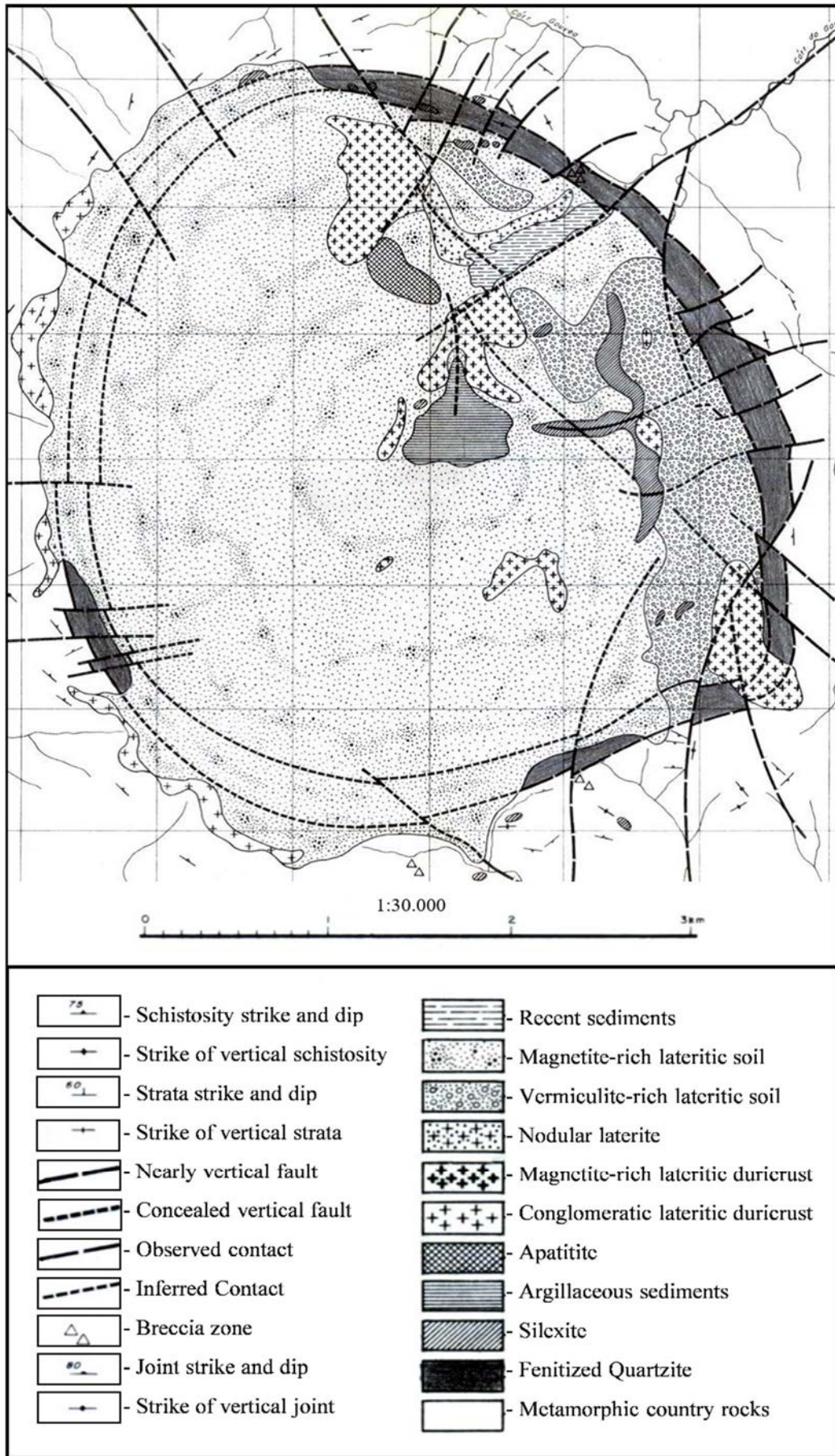


FIG. 26. Geological map of the Catalão I intrusion (adapted from Ref. [88]).

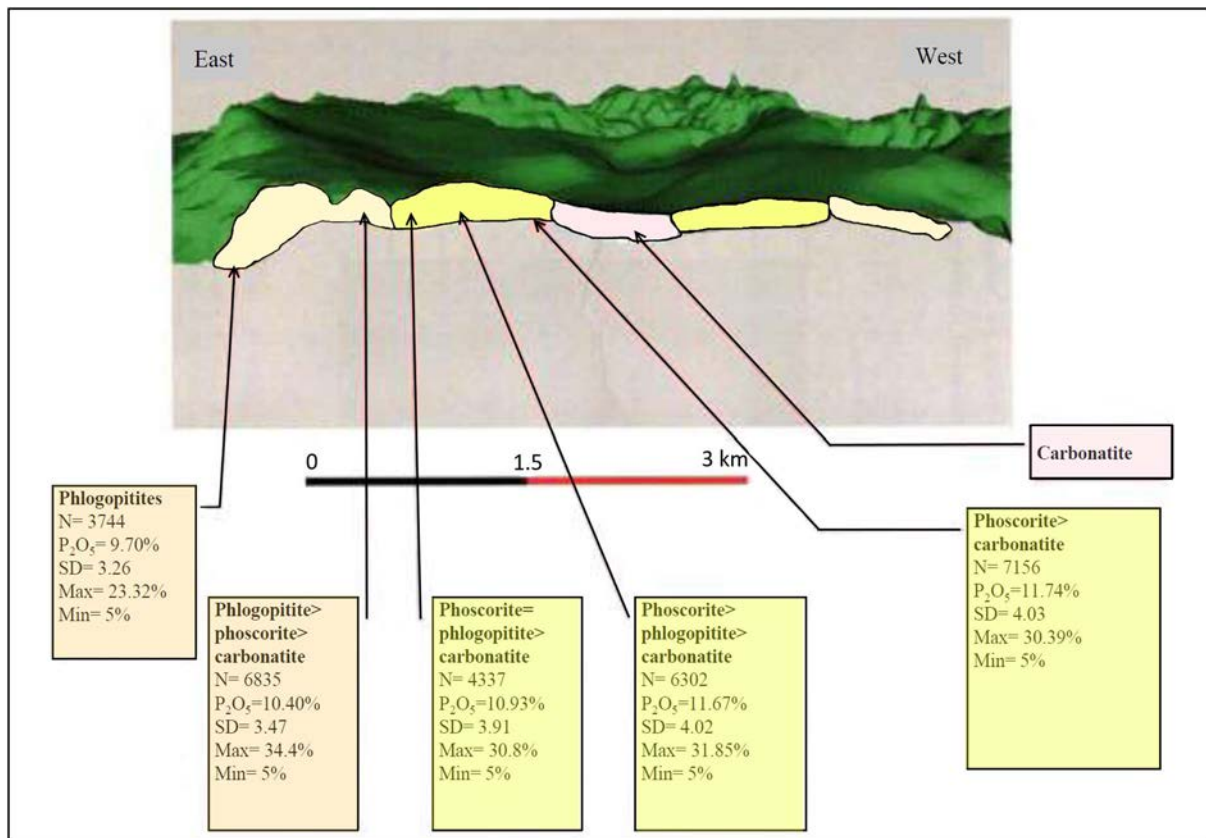


FIG. 27. 3-D image of the main lithological series of the Catalão I intrusion and phosphate distribution by lithology (number of samples, average P<sub>2</sub>O<sub>5</sub> grade, standard deviation, maximum and minimum grade). Phosphates are the main hosts of uranium (adapted from Ref. [88]).

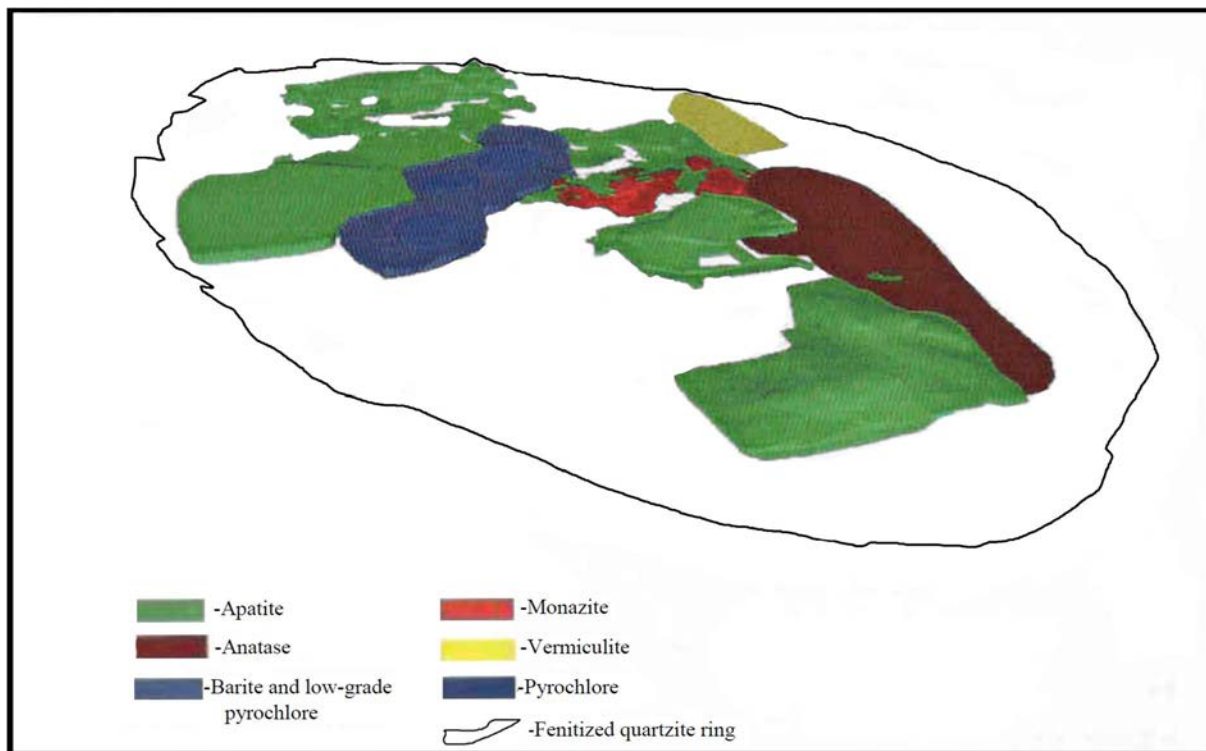


FIG. 28. 3-D image of the mineral deposits at Catalão I (adapted from Ref. [88]).

## 3.2. GRANITE-RELATED DEPOSITS

### 3.2.1. Definition

Granite-related uranium deposits include: (i) veins composed of ore and gangue minerals in granite or adjacent (meta)sediments and (ii) disseminated mineralization in episyenite bodies internal to the granite that are often gradational to veins. In Europe's Hercynian Orogenic Belt, these deposits are associated with large batholiths of peraluminous leucogranite (two mica granites) modified by late magmatic and/or autometamorphic processes [19].

There are 277 granite-related deposits recorded in the UDEPO database (Table 13), most of which are located in Europe, within the Variscan chain. Between 1950 and 2000, more than 95 000 tU were produced in the former German Democratic Republic, 60 000 tU in France, 58 000 tU in the Czech Republic, about 5000 tU in Spain and 3700 tU in Portugal. Large resources exist in Spain, where exploration is ongoing, and also in Algeria. China is the only country currently producing minor amounts of uranium (100–200 tU) from this type of deposit.

TABLE 13. PRINCIPAL GRANITE-RELATED DEPOSITS (as of 31 December 2015)

Deposit	Country	Resources (tU)	Grade (% U)	Status
Niederschlema–Alberoda	Germany	84 660	0.25	Depleted
Příbram district	Czech Republic	49 225	0.18	Depleted
Timgaouine	Algeria	12 270	0.21	Dormant
Xiazhuang district	China	12 000	0.20	Depleted
Tinef	Algeria	11 750	0.075	Dormant
Taoshan	China	10 500	0.10–0.20	Operating
Bukhovo district	Bulgaria	10 000	0.10	Depleted
Copper Mountain district	USA	9 470	0.023	Dormant
Margnac-Pény	France	9 320	0.147	Depleted
Abankor	Algeria	9 130	0.32	Dormant
Lujing	China	9 000	0.10–0.20	?
Alameda	Spain	8 855	0.039	Exploration
Midnite	USA	8 700	0.12	Depleted
Oberschlema	Germany	7 945	0.20–0.50	Depleted
Jachymov district	Czech Republic	7 540	0.50	Depleted
Mina Fe	Spain	7 200	0.055	Depleted
Lantian	China	7 160	0.171	Depleted
Bois Noirs	France	6 920	0.27	Depleted
Bernardan	France	6 610	0.56	Depleted
Gornoye	Russian Federation	6 200	0.245	Development
Agashskoye	Kazakhstan	6 170	0.146	Dormant
NW Flanke-Pohla	Germany	6 050	?	Dormant
Dzhusandalinskoye	Kazakhstan	5 300	0.16	Dormant
Retortillo	Spain	5 159	0.032	Exploration

### 3.2.2. Geological setting

Two subtypes of granite-related deposits are recognized, on the basis of their spatial relationship with granitic plutons and the surrounding (intruded) host rocks (Fig. 29):

- (i) **Endogranitic** deposits (Limousin–Vendée type (France)). These are usually monometallic and consist of: (a) discontinuous linear orebodies within distinct veins or stockworks localized in fractured granites or (b) disseminations in pipes or columns of episyenite. Contact granitic veins persist from inside the granite across and beyond the granite contact but in some examples are found only in the country rocks near the contact. Depths of granitic deposits can attain 700 m whereas episyenite orebodies can reach 1000 m (Le Bernardan (France));
- (ii) **Perigranitic** deposits in metasediments can be monometallic (pitchblende and gangue minerals), such as in the Příbram district (Czech Republic) or polymetallic (U, Cu, Ni, Bi, Ag and other metals in economic quantities), for example the Erzgebirge types (Czech Republic). Uranium and other elements are not genetically related. Deposits can persist to depths of 2000 m. Perigranitic deposits in the contact metamorphosed rocks of granitic intrusions (Iberian type) have monometallic mineralization in the form of veinlets and disseminations in intensely fractured, hornfels schists up to 2 km from the granite. Host rocks are intensely altered.

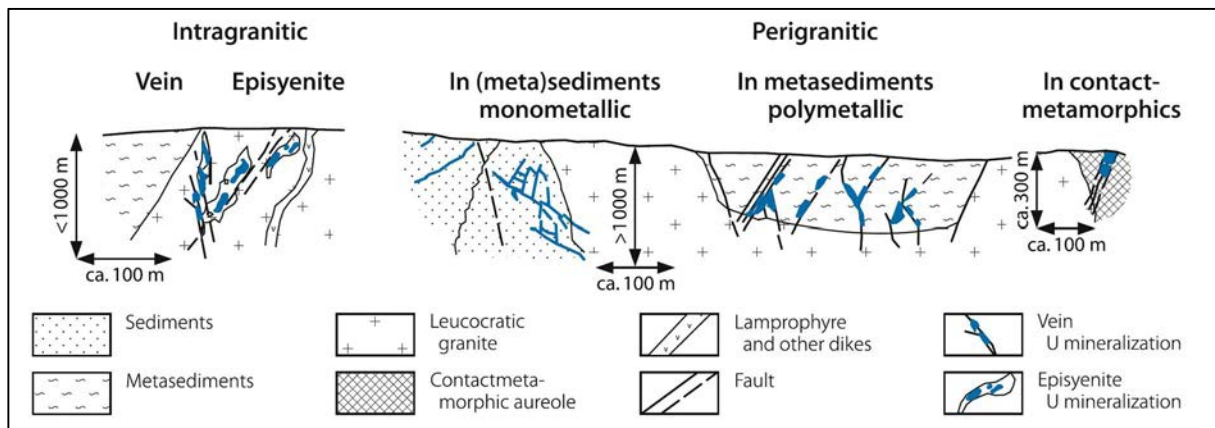


FIG. 29. Schematic representation of the various granite-related uranium deposits [19] (reproduced with permission).

The mid-European Variscan Uranium Province, which extends for more than 2000 km from Spain to the Erzgebirge (Czech Republic), through Cornwall (United Kingdom), Brittany, Vendée, Massif Central, Vosges (France) and the Black Forest (Germany), (Fig. 30) represents a major U–Sn–W–Au province in which known granite-related uranium deposits are related to Late Carboniferous peraluminous two mica leucogranites emplaced in 335–310 Ma. Granites were derived from the partial melting of the continental crust during the collision between the Eurasian and African Plates at about 400 Ma. The deposits are located either in the granite, such as in the Massif Central and Brittany (France), or in their enclosing metamorphic rocks, such as in the Erzgebirge district (Czech Republic) and are predominantly of Permian age [45].

In France, orebodies occur as veins or stockworks in granites or the enclosing rocks, or disseminated in episyenites. Episyenitic alteration is generally developed at the expense of the host granite, but also occasionally at the expense of the enclosing gneiss. The vein and stockwork systems that characterize granite-related deposits vary widely in terms of configuration, size and complexity. The mineralized

veins range from a few metres to several hundred metres in length. The thickness of the mineralized veins is commonly 1–2 m but ranges from a few centimetres to 15 m and their vertical extent varies between 10 m and several hundred metres. Grades are typically in the range 0.10–0.30% U, but are highly variable, ranging from a few parts per million of uranium to several tenths of one per cent. Uranium enrichment also occurs at the intersection of the veins with lamprophyre dykes [45].

### 3.2.3. Metallogenesis

Uranium mineralization in granite-related deposits generally occurs as pitchblende and/or coffinite, accompanied by minor gangue and alteration minerals. Deposits with a simple paragenesis contain pitchblende in association with varying amounts of pyrite/marcasite, quartz, haematite, carbonate and minor base metal minerals. Complex deposits contain a significant base metal sulphide stage (often with Co–Ni–As). In most cases, pitchblende is a paragenetically early phase.

The last event recorded in the veins is the oxidation of primary uranium minerals and formation of roll-front type mineralization in the episyenite and development of clay alteration (mainly montmorillonite), fluorite and secondary uraninite [97]. Uranium was redeposited in variable amounts by infiltration of meteoric fluids. Sooty pitchblende occurs in the reduced zones and hexavalent uranium minerals, mainly uranophane, autunite and chalcocite, in the oxidized zones. This remobilization can be important economically. In the Bois Noirs–Limouzat deposit (7170 tU at 0.26% U), for example, it has been estimated that more than half of the production came from remobilized ore [98].

A number of metallogenic models have been proposed for the formation of Hercynian uraninite veins within peraluminous leucogranites. An epithermal origin was first proposed, then several authors favoured a supergene origin (the ‘per descensum’ theory) for many uranium deposit types, wherein leaching of uranium took place under tropical climatic conditions at the time of formation of the deposits. More recently, Poty et al. [99] and others have demonstrated from fluid inclusion studies that the fluids involved in the genesis of the Variscan granite-related uranium deposits are of hydrothermal origin. These fluids were of relatively low salinity with temperatures of 100–200°C in the French deposits. The CO<sub>2</sub> enriched fluids are related to early fluids responsible for arsenopyrite deposition. Stable isotope studies suggest that uranium deposition resulted from the mixing of two fluids, an oxidized meteoric water that leached uraninite from the enclosing granite and a connate fluid with high  $\delta^{18}\text{O}$ . These latter fluids infiltrated from overlying Permian formations and provided hydrocarbons or H<sub>2</sub>S that reduced the uranium and also resulted in low  $\delta^{13}\text{C}$  values of the associated carbonates. Later formed fluorite, baryte and calcite were deposited from more saline fluids at temperatures of 100–150°C [100].

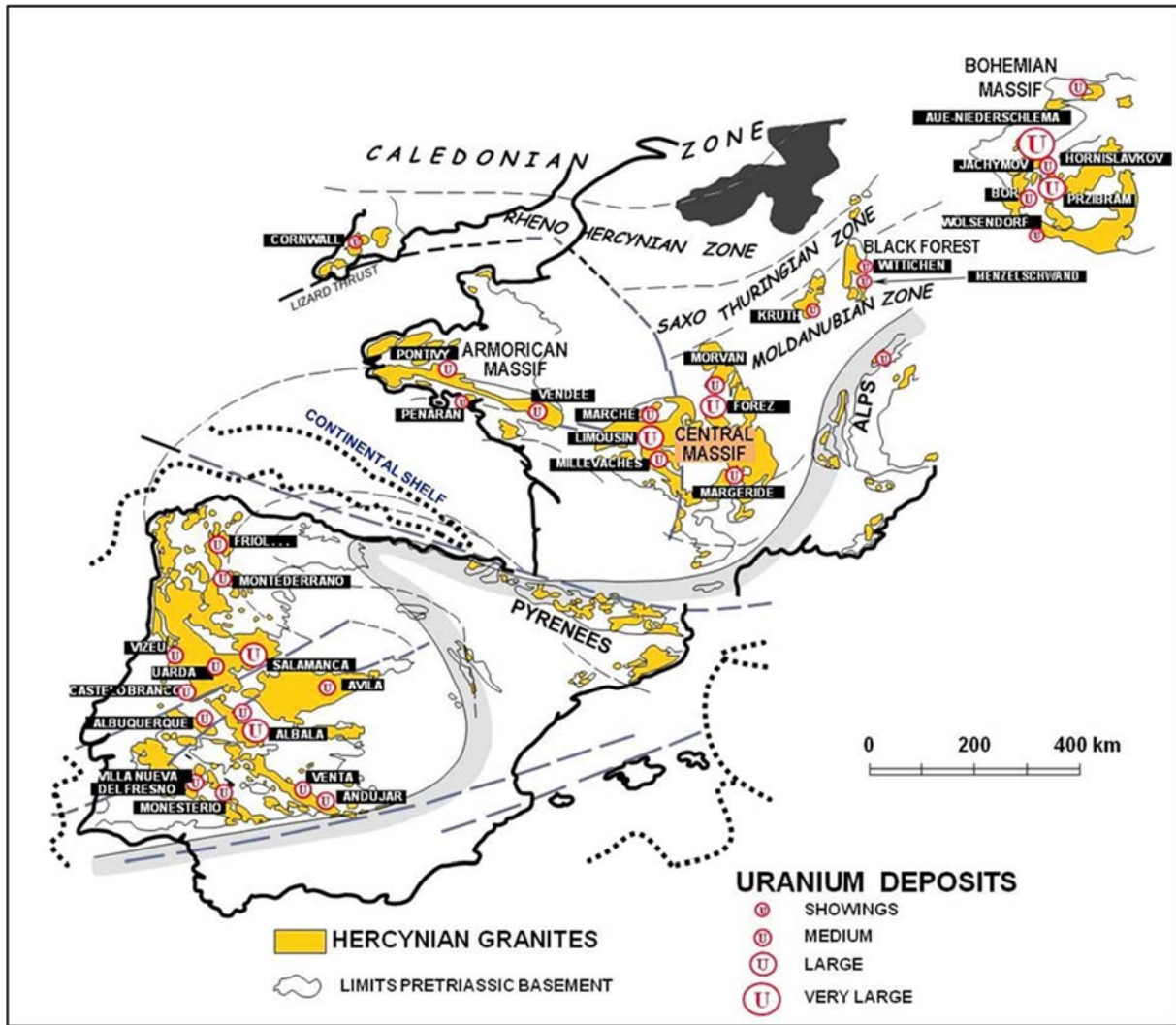


FIG. 30. Location of the uranium deposits within the European Variscan chain (adapted from Ref. [98]).

### 3.2.4. Description of selected deposits

#### 3.2.4.1. Intragranitic deposits

#### The Gornoye deposit (Russian Federation)

##### Introduction

The Gornoye deposit is located in the Krasnochikoisky district (Transbaikalia region (Russian Federation)), 110 km SSE of the Hilock Trans-Siberian railway station and to the north-west spur of the Chersky Ridge. The deposit area is characterized by a sharply dissected topography, with elevations ranging between 1000 and 1943 m. The relief is intense, with deeply incised gullies and stream valleys often with V-shaped profiles.

The uranium resources of the Gornoye deposit amount to 11 000 tU (comprising C1 resources of 1087 tU, C2 resources of 4226 tU, probable P1 resources of 4800 tU and off-balance sheet ore categories (C1 and C2) of about 874 tU). The uranium grade varies in the range 0.05–8.7% U, with an average grade of 0.239% U. In 2012, the deposit was at the development stage.

## Geological setting

The Gornoye uranium deposit is located in the Jurassic Zhergokonsky granitic intrusion (Fig. 31). Regionally, the central Transbaikalia region is part of the Mongol–Okhotsk Lineament and is confined to the axial part of the Chikoy–Ingodinsky structural zone, which is characterized by extensive development of leucocratic granites during a Mesozoic tectono-magmatic phase. The Zhergokonsky Massif is situated within the Khentei–Daursky structural metallogenic zone containing rare metals and gold mineralization in the north-eastern closure of the tin–tungsten Transbaikalia Ore Belt.

The oval shaped granitic Zhergokonsky Massif covers an area of 150 km<sup>2</sup>. It is elongated in a northeasterly direction, corresponding to a network of approximately N–S trending faults (Fig. 31) and is composed of light grey and pinkish grey medium-grained granites intruded into Triassic and early Palaeozoic granitoids containing xenoliths of metamorphosed, Proterozoic strata. The age of the granite is 180–150 Ma. Rocks of the massif are clearly distinguishable from the surrounding formations by their high radioactivity and high background concentrations of uranium and thorium in the unaltered medium-grained granite (12 ppm U and 18–24 ppm Th).

Two major fault zones cross-cut the massif, the Meridional and Zhergokonsky (Main zone) fault zones. The Meridional fault zone passes through the central part of the massif and can be traced beyond it for more than 40 km. It divides the massif into eastern and western zones with a displacement of 3 km. The fault zone has a subvertical dip, is 0.2–8.0 km wide and consists of an array of fractures and breccias that are hydrothermally altered. The Main fault zone is structurally similar to the Meridional fault and passes along the western boundary of the massif. The north-east trending fault zones exhibit major control on the location of mineralization, best developed in a 3 km long portion in the central part of the massif. The largest structure of this system is the main area, which can be traced for over 25 km.

The Main fault zone consists of a number of subparallel structures, developed as zones 20–150 m wide, sometimes containing breccia and clay. In the central part of the massif, at the intersection with the Meridional fault, the Main zone bends sharply and splits into a series of higher order faults of predominantly north-eastern trend forming a wedge shaped block about 12 km<sup>2</sup> in extent. The Gornoye uranium deposit is located between the Meridional and the Main faults of the Zhergokonsky Massif.

Most of the deposit is covered with turf pits and alluvial–diluvial sediments with a thickness typically of 0.5–1.0 m but increases to 10 m in river and stream valleys. Intermittent outcrops of bedrock are present on ridges. At the top of the steep slopes, piles of large blocks and screes can be observed.

The deposit is located in medium-grained, light grey, leucocratic granite of the mid-upper Jurassic Haralginsky Complex, which contains xenoliths of fine-grained porphyritic biotite granite of Triassic age, aplite dykes and sediments. Large xenoliths of the Bichursky fine-grained granite complex are present on the south-western flank of the Gornoye deposit as a plate shaped body of more than 300 m in width plunging gently to the south-east. Aplite dykes are common in the south-western and central parts of the deposit, controlled by a system of flat lying latitudinal (20–50°) fractures, and less frequently by shallow and steep fractures in other areas. The dykes extend for a few hundred metres along strike and dip and although usually only a few centimetres wide, they may attain widths of 5–20 m. Contacts are usually sharp.

Structurally, the Gornoye deposit is situated near the intersection of the Meridian and the Main fault zones. In the deposit area, repeated displacement along these faults resulted in the development of areas of subparallel zones of higher order structures, mainly with north-east strikes.

The deposit is controlled mainly by north-east faults related to the first order Main fault zone structure. The Main fault zone features numerous bends in which smaller, subsidiary faults are developed. The Main fault zone dips steeply to the south-east (70–80°) except for the north-east margin, where dips

are shallower (40–55°). The mineralization is controlled by a series of faults in brecciated granite, with some structures becoming mylonitic at depth. The metasomatic veins feature clay–zeolite alteration

The Main fault zone one intersects the Meridional fault at a sharp bend in both strike and dip, where it splits into a number of subparallel faults (approximately twelve) over a 3 km width. While the faults strike 020–030° they may range from 350–055° in bends. This zone varies in length from 1.5–2 km to 3–6 km and the faults have been traced to a depth of 600–700 m, with no signs of thinning, although alteration decreases below 600–900 m. Individual zones dip steeply to subvertically to the south-east and in thickness typically vary in the range 1–30 m. The fault zones are sharp, with variably fractured rock and from one to three subparallel, steeply dipping strands containing quartz–clay–zeolite cemented breccia.

Five fracture systems are present in the granite of the Gornoye deposit, the most prominent of which are steeply dipping NE and E–W trends. Steep planar fractures are filled mainly by zeolites but rarely by carbonates, whereas flat lying fractures are dry, often with gouge zones with hydromica, chlorite and brown iron hydroxide. In general, the deposit shows considerable structural complexity, with high degrees of deformation of host rocks but small (<10–40 m) total vertical and horizontal displacements in the largest areas.

### Mineralization

Uranium mineralization at the Gornoye deposit is hosted in the structurally weakened block between the Main zone and zone 6, covering a total area of about 3.5 km<sup>2</sup>. The majority of the uranium resources are located in the steep to moderately dipping, NE trending faults (Fig. 32). Where these intersect the N–S faults, mineralization is sometimes locally developed along the latter. The vertical extent of mineralization at the deposit (which often crops out), is about 700 m. In general, the orebodies are typically steep (75–90°) but with some moderate (50–70°) veins, controlled by major fault zones. The orebodies have no distinct geological boundaries and are identified by gamma ray logging. It should be noted that owing to the bright colour of uranium mineralization, the orebodies, particularly the higher grade ores, are clearly visible in mines. Orebodies usually consist of at least two or three contiguous ore intervals separated by barren areas or sequences of subeconomic mineralization.

Uranium mineralization is found in open cavities, caverns and fractures and has high contrast. The highest grade ores are found in quartz–clay–zeolite breccias. The thickness of ore breccias in minor sutures is usually only a few centimetres, whereas in the main sutures, thickness ranges from tens of centimetres to 1–2 m. The dimensions of the orebodies are on the order of 20–50 m × 150–200 m. The average thickness of lenses is 1–3 m, and more rarely up to 5–8 m. The zones typically range from 3–5 m up to 30–50 m, averaging 18 m. The vertical extent of mineralization is about 700 m. Uranium is present in easily processed ores, mainly as beta-uranotile and uranophane.

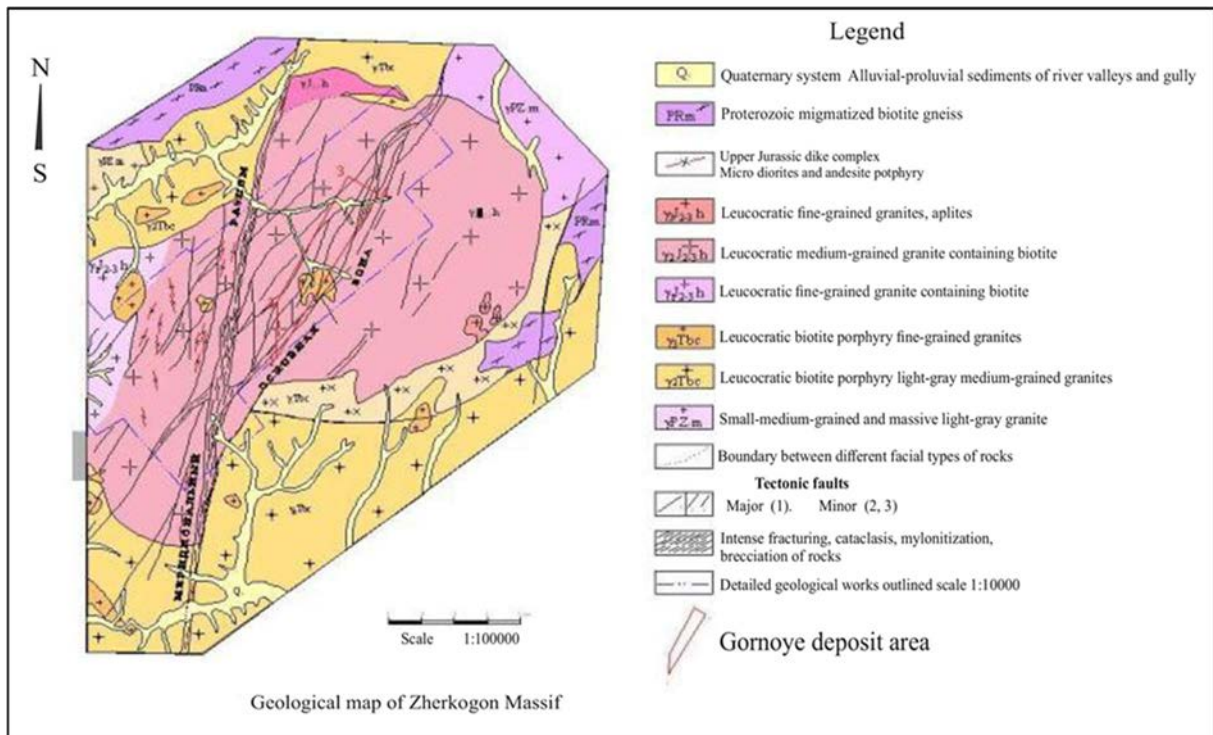


FIG. 31. Map of the Zherkogon Massif (reproduced courtesy of A. Boitsov, ARMZ/Uranium 1).

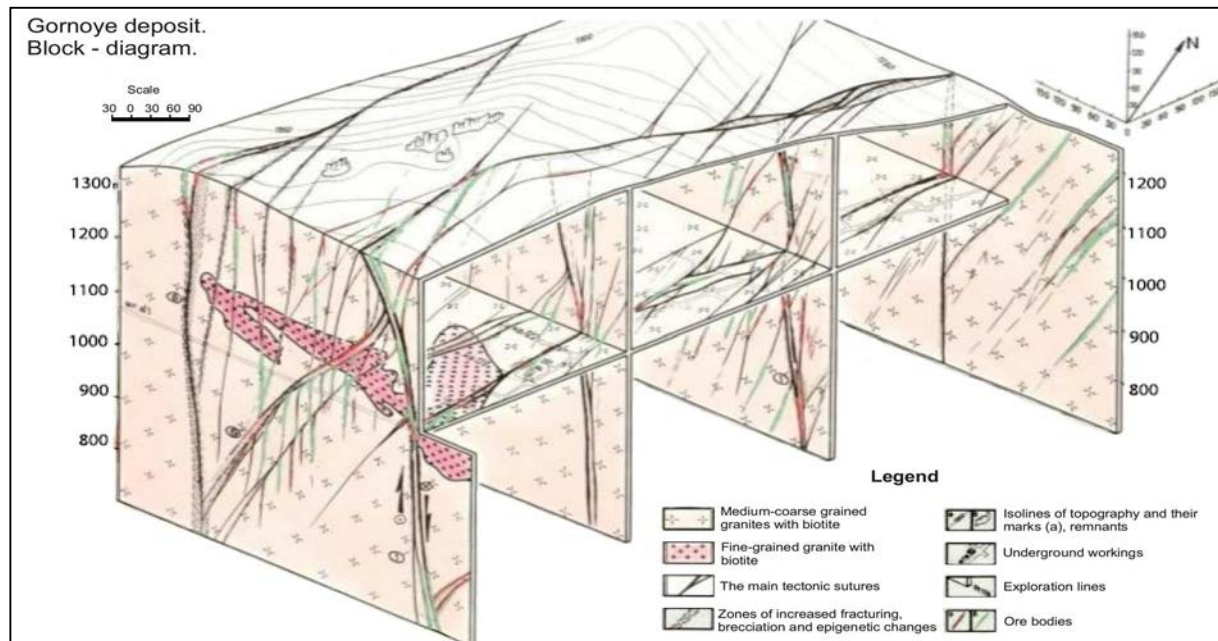


FIG. 32. Block diagram of Gornoye deposit (reproduced courtesy of A. Boitsov, ARMZ/Uranium 1).

### Deposits of the Xiazhuang orefield (China)

#### Introduction

The Xiazhuang orefield is situated in the eastern part of the Guidong granite massif, north of Guangdong Province (Fig. 33) About 15 intragranitic uranium deposits have been identified in the orefield, including Damaofeng, Shijiaowei, Shituling, Xinqiao, Xianrenzhang, Xiwang, Zhaixia, Zhushanxia and Zhutongjian [19]. Original in situ resources were reported to be 12 000 tU [101].

Mining operations commenced in 1960 and the Xiwang deposit (1500–5000 tU, grading 0.10–0.30% U) became one of the first uranium mines in China. Additional to these intragranitic deposits, the orefield also includes perigranitic deposits hosted in surrounding metasediments.

#### Geological setting

The polyphase Guidong Massif covers an area of about 1000 km<sup>2</sup>. Cambrian and Ordovician formations prevail to the east and north of the massif and Devonian–Carboniferous strata are dominant to the south and south-west. Several granitic intrusions dominate the eastern part of the Guidong Massif, which hosts the Xiazhuang orefield (Fig. 34):

- (a) Medium-grained two mica Xiazhuang granite (196 Ma) in the eastern section;
- (b) Coarse-grained porphyritic biotite Luxi granite (185 Ma) in the south-eastern section;
- (c) Medium- to coarse-grained hornblende–biotite Aizi granite (157 Ma) in the western section;
- (d) Medium- to fine-grained Siquan granite (151 Ma), which is the last of the pre-volcanic Jurassic intrusions.

A belt of subvolcanic dacite porphyry intrusions (143–119 Ma) is present along the northern margin of the massif. Later felsic intrusions include small stocks of fine-grained two mica or muscovite granite (143–125 Ma) and pegmatite and aplite dykes. Several generations of mafic and intermediate dykes (140–90 Ma) are comprised mainly of diabase with minor lamprophyre/spessartite and microdiorite. These dykes, as well as later quartz veins, silicified structures and faults are almost exclusively confined to the Xiazhuang and Luxi plutons [19].

The easterly granite segment was uplifted in response to block faulting and eroded during the Late Cretaceous before subsidence and local down-faulting resulted in the deposition of red bed basins. The internal structural pattern of the subsided block is marked by three fault and fracture systems. Structures range from several hundreds of metres to kilometres in length and consist of brittle fault and breccia zones, silicified mylonite, silicified cataclasite with hydromica, coarse- to fine-grained quartz and variably coloured microquartz and fluorite [19].

The Xiazhuang orefield is located within this subsided block in which the uranium deposits preferentially occur in the Xiazhuang granite (Fig. 35). The orefield is about 320 km<sup>2</sup> in size and is hosted mainly in granites that intrude Palaeozoic formations. Prominent lithostructural elements in the orefield include:

- (a) Five diabase dyke swarms approximately equidistant from each other, some 3.5 km apart and trending WNW. Individual dykes range in width from 2–10 m but locally may be up to 100 m and persist downdip in excess of 500 m;
- (b) Five swarms of silicified fracture zones composed of microquartz and oriented NNE;
- (c) ESE and ENE striking silicified fracture zones;
- (d) Two regional ENE trending giant quartz veins.

Li Tiangang and Huang Zhizhang [102] indicate that the medium-grained, porphyritic two mica granite of the Xiazhang intrusion and lamprophyre–spessartite dykes are the most important host rocks. The two mica granite is described as a siliceous, potassium-rich and aluminium oversaturated felsic rock composed of quartz (34%), microcline (33%), plagioclase (25%), biotite (5%) and muscovite (3.5%). Accessory minerals include apatite, zircon, pyrite, tourmaline, ilmenite and uraninite. Uraninite occurs as intergranular growths between and within the rock forming minerals. The uraninite content varies in the range 6–10 ppm.

The Xiazhuang two mica granite and to some extent the Luxi porphyritic biotite granite complexes have been affected by large scale metasomatism described as autometamorphism by Li Tiangang and Huang Zhizhang [102] and less commonly by allometamorphism (allometamorphism is defined as the recrystallization of minerals by younger intrusions within older igneous rocks. It is often associated

with pegmatitization). The metasomatized facies were later overprinted by syn-ore hydrothermal processes. The authors describe the characteristic features of the alteration as:

- (a) Autometamorphism/metasomatism includes potassic feldspathization, albitization and muscovitization. Tourmalinization and chloritization of biotite is also common;
- (b) Potassic feldspathization is an intense and widespread phenomenon characterized by an increase of pink K-feldspar associated with chloritization of biotite and quartz dissolution (locally complete removal);
- (c) Albitization is manifested as fine-grained albite that crystallized later and more locally than K-feldspar. Locally, albitization forms relatively large metasomatic bodies as exemplified by the Zhushanxia uranium deposit;
- (d) Muscovitization is a feature in the main granite body as well as in later, small intrusive bodies. Muscovite may be autometamorphic, allometamorphic or hydrothermal and the three types can be superimposed on each other. Muscovitization caused by hydrothermal activity occurs with silicification along faults and veins.

Autometamorphism and allometamorphism not only recrystallized the main rock constituents of the granites but also decreased the quantity of uranium accessory minerals such as zircon, allanite, apatite and xenotime. Syn-ore hydrothermal alteration of wall rocks adjacent to quartz veins is superimposed on autometamorphosed and allometamorphosed facies. The composition of these precursor facies had an impact on the intensity of alteration, mineral assemblage and localization of uranium mineralization [19].

Veins in medium-grained porphyritic two mica granite are fringed by wall rocks altered by silicification and haematization but more extensively by argillization and pyritization. These alteration assemblages exhibit a lateral zonation that extends for a few metres from a central, ore hosting breccia zone cemented by fine to microcrystalline, dark and pink quartz, into silicified, haematized, hydromica altered and pyritized cataclastic wall rocks. Silicification and haematization become more prominent with proximity to the orebodies and the amount of hydromica and associated pyrite decreases with distance from the ore veins [19].

#### Mineralization

Orebodies are of vein-like, lenticular or columnar in shape and with a stockwork structure. They vary considerably in size and commonly persist to depths of 300–500 m. Grades typically vary in the range 0.10–0.50% U. Most orebodies are ‘blind’. Intragranitic deposits are controlled by the following parameters [19]:

- (a) Primary control is by silicified fracture zones (Fig. 35) cutting silicified granite, episyenite, diabase and Palaeozoic carbonaceous sandstone;
- (b) Zones of intense muscovitization and potassic feldspathization within the two mica granite;
- (c) Contacts between two mica granite and late muscovite granite;
- (d) Attitude of structures along the intrusive contacts;
- (e) Intersections of microquartz veins with mafic dykes that cut alkali metasomatized rocks;
- (f) En echelon silicified zones, changes in strike and dip of silicified zones and intersections of silicified zones.

In general, the size of the deposit is a function of the number of structural intersections, the size, attitude and type of silicified and contact zones, and the size of the dykes.

Three principal hydrothermal mineral stages have been described [102]:

- (i) *Pre-ore stage*: white, fine-grained quartz occurring in the form of breccia and fragmented relicts in silicified zones, and containing 1–10 ppm U;

- (ii) *Syn-ore stage*: microcrystalline quartz and pitchblende. The uranium content is highly variable, ranging from several tens to several thousands of parts per million. Three mineral assemblages have been identified:
  - (a) Red microcrystalline quartz, pitchblende and coffinite represent the principal generation of mineralization;
  - (b) Black microcrystalline quartz, pitchblende, coffinite and sulphides are common, but less well developed than the previous assemblage;
  - (c) Late, dark purple fluorite, pitchblende and, locally, minor calcite have a more limited distribution and lower intensity than the previous two assemblages.
- (iii) *Post-ore stage*: white comb quartz, banded microquartz, white calcite and fluorite. This stage may contain minor low grade uranium.

Pitchblende occurs as either disseminations or as massive aggregates commonly exhibiting colloidal textures. Massive pitchblende is usually broken, veined or occurs as 'blebs' and disseminated pitchblende exhibits spheroidal textures. Coffinite is minor but widespread. It is younger than pitchblende and is associated with marcasite. All microcrystalline quartz veins contain Au (up to 295 ppb) and sulphides. Mineralization is preferentially hosted in granite except for a few veins that extend into Palaeozoic metasedimentary wall rocks [19].

#### Metallogenic aspects

To explain the uranium mineralization of the Xiazhuang orefield, Li Tiangang and Huang Zhizhang [102] suggest the following tectono-hydrothermal model:

- (a) Specific granites with elevated uranium contents underwent autometamorphic modification prior to regional scale tectonic subsidence;
- (b) The tectonic regime generated faults extending to great depth, allowing the development of a deep circulating hydrothermal system in which groundwater percolated downwards and then ascended after heating;
- (c) Hot solutions leached uranium and other components from the granite during circulation;
- (d) Uranium was transported mainly as uranyl-carbonate and uranyl-fluorine-carbonate complexes;
- (e) A second, highly saline fluid derived from the magmatic water and gases from the granite rose and mixed with the meteoric water convection system;
- (f) The hydrostatic pressure of the hydrothermal system decreased abruptly, inducing boiling of the mineralizing solutions and release of large amounts of CO<sub>2</sub> and dissociation of uranyl-carbonate complexes. Silica was precipitated and uranium was reduced by various reductants, crystallizing as pitchblende in quartz veins.

Shen Feng et al. [103] identified an extended period elapsing between the intrusion of the granite (135 Ma) and diabase dykes (110–100 Ma) and the formation of the ore mineralization (86–60 Ma). These authors, therefore, assume the provenance of the ore mineralization to be crystallized uraniferous granite and not derived from magmatic differentiation. The high average uranium content (20.2 ppm) of the two mica granite with a major proportion of this uranium bound to uraninite indicates that the Xiazhuang granite is a viable uranium source. The authors also postulate that the intrusion of the diabase dykes provided the heat source for the deep circulating solutions that are thought to have leached uranium from the granite and precipitated it at upper levels.

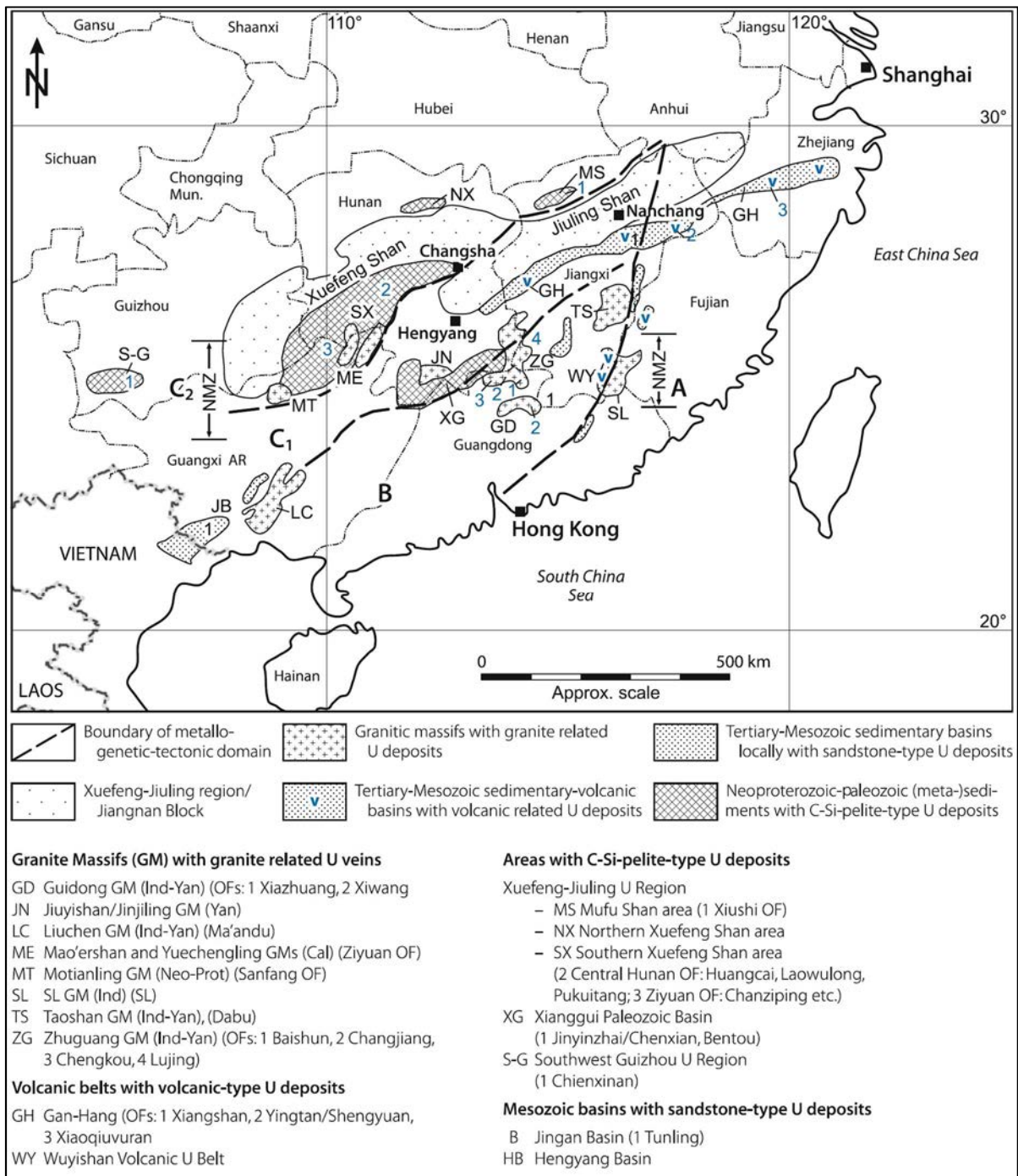


FIG. 33. Southern China: location of uranium domains, belts, districts, orefields and deposits [19] (reproduced with permission).

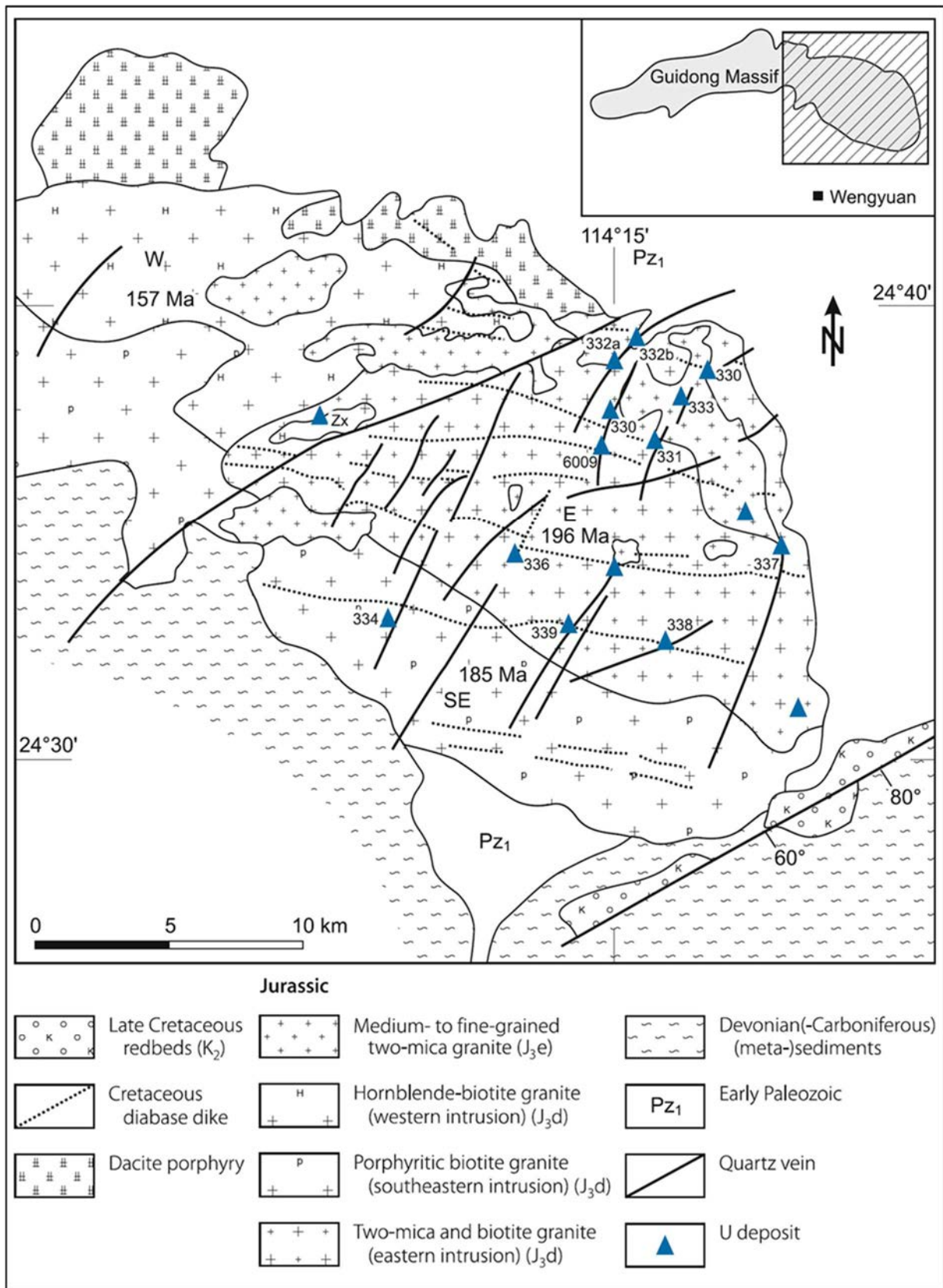


FIG. 34. Geological map of the eastern part of the Guidong granite massif showing the location of intragranitic uranium deposits [19, 102, 103] (reproduced with permission).

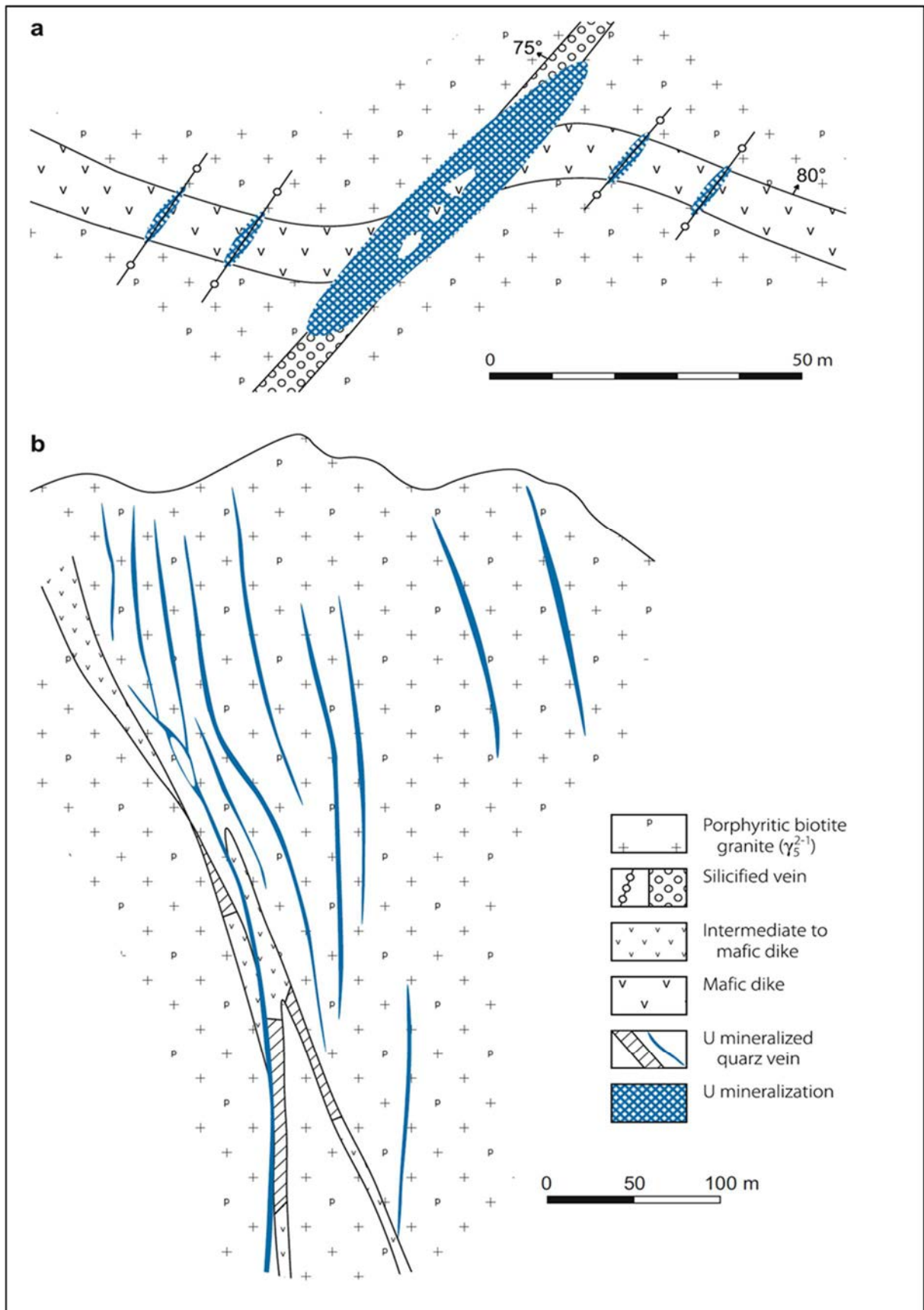


FIG. 35. (a) Sketch map of the Shijiaowei deposit depicting the affinity of uranium in quartz veins to a mafic dyke; (b) Cross-section of the Zhushanxia deposit showing the position of uraniumiferous quartz veins in the hanging wall of mafic dykes [19, 102] (reproduced with permission).

## **Intracranitic episyenites: The Bernardan deposit (France)**

### Introduction

The Bernardan deposit is located in the Western Marche district of the north-western margin of the Massif Central. Radiometric anomalies were first discovered in 1955. Five deposits, Bernardan, Côte Moreau, Les Loges, Mas Grimaud and Piégut were found in the district between 1958 and 1966.

The Bernardan deposit was discovered in 1964, approximately 10 km west of the town of St. Sulpice-les-Feuilles and 75 km NNW of Limoges. Uranium ore occurs in ten episyenite bodies (referred to as 'amas') down to depths in excess of 800 m, which makes Bernardan the deepest uranium deposit in France.

Minable deposits are of granite-related vein and episyenite types. Original in situ reserves of the district totalled approximately 10 000 tU at grades of about 0.5% U. Bernardan, with original reserves in excess of 8000 tU at a grade averaging about 0.5% U, was the largest deposit while the other four deposits had original reserves of several hundred tonnes of uranium, all at grades of between 0.2 and 1.6% U.

The district produced 9260 tU between 1978 and 2001 when the last mine, Bernardan, was closed. The Bernardan deposit itself produced 6870 tU at an average grade of 0.58% U from an open pit sunk to a depth of 110 m and from underground mining to 500 m depth. The mineralized episyenites have been recognized by drilling to depths greater than 800 m where the orebody is still open. Geological resources probably exceed 10 000 t U.

Ore was treated in the Cherbois mill near Bernardan, which operated from 1979 to September 2001 and also milled ore from the La Crouzille district further south, after the closure of the mill at Bessines sur Gartempe in 1993. The last owner and operator was Société des Mines de Jouac, a subsidiary of COGEMA (now AREVA), which had acquired the property from TOTAL Compagnie Minière in 1993. The site has since been remediated.

### Geological setting

#### *(a) Regional geology*

The Bernardan deposit is located in Hercynian leucogranite of the western La Marche Granitic Complex (Fig. 36). Granites were intruded along the WNW–ESE oriented La Marche left-lateral shear zone into metamorphosed Proterozoic–Early Palaeozoic formations. The La Marche Shear Zone is an eastwards trending structural extension of the South Armorican Shear Zone, which is a prominent late Hercynian ductile shear zone that is traced from southern Brittany into the eastern Massif Central (Fig. 37). Additionally, three successive stages of tectonic compression generated NE–NNE, NW–NNW and WNW oriented structures [104]. The NE–SW system includes the St. Hilaire Shear Zone, which forms the south-eastern boundary of the western La Marche district.

Two main generations of granite types have been identified in the western La Marche district: (i) an older tonalite–granodiorite facies of Late Devonian age ( $356 \pm 10$  Ma) referred to as Guéret or G-type granite and (ii) a younger suite of peraluminous two mica leucogranites of Viséan–Westphalian age ( $320 \pm 5$  Ma) referred to as Limousin or L type granite. The latter belongs to a group of synkinematic granite intrusions that were emplaced during the Hercynian Orogeny in France. Numerous pegmatite and microgranite dykes occur throughout the district while lamprophyre dykes are rare. Gravimetric surveys indicate that this western La Marche Granitic Complex occurs as a laccolith with a thickness averaging 2 km but with deeper roots where the leucogranite intrusions are located.

Petrochemically, the western Marche L type leucogranites are strongly peraluminous with aluminopotassic tendencies [105] and typically show a distinct increase in the peraluminous index with an

increase in incompatible elements (Sn, Li, Rb, F, etc.) and a decrease in Zr, Th and LREE, the latter largely hosted in monazite.

Several almost synchronous intrusive stages have been recognized within L type granites. In the Les Loges and Le Bernardan open pits, the latest granite facies is richer in biotite than the earlier one and all prominent aplo-pegmatitic networks are related to the emplacement of the latest intrusions.

The leucogranites were subjected to various hydrothermal processes reflected in pervasive alteration of plagioclase, chloritization of biotite, development of perthite and, most notably, selective episyenitization. The latter produced highly irregular, porous bodies, some of which became the host of uranium ore lodes in the western La Marche district. Most of these mineralized episyenite bodies are located on either side of the irregular contacts between Lm (biotite-rich) and Ll (biotite poor) leucogranites, which suggests that structural and petrographic discontinuities between the two granite facies provided favourable conditions for the formation of episyenite bodies.

#### *(b) Geological setting of the Bernardan deposit*

Bernardan lies along the northern margin of the western La Marche leucogranite batholith, 2 km south of the La Marche Shear Zone (Fig. 38). Two main types of medium- to coarse-grained, peraluminous two mica leucogranites occur in the deposit:

- (i) Biotite-rich leucogranite (Lm), locally porphyritic, is the predominant type. G-type granite inclusions with very sharp rims are common in this granite. The biotite content is about 10vol.%, whereas muscovite accounts for less than 5vol.%. Inclusions of accessory minerals (zircon, monazite, apatite, anatase) are abundant in the biotite crystals;
- (ii) Biotite poor leucogranite (Ll) with generally less than 5vol.% biotite, a muscovite content as high as 10vol.% and scarce accessory minerals occurs as enclaves of variable size (up to 50 m) in the mesocratic (Lm) granite. Contacts between the two granites are generally magmatic and enclaves of Ll granite within the Lm granite are commonly, but not exclusively, rounded, which indicates that the Ll leucocratic granite was not completely solidified during emplacement. The contact between the two granites is locally mylonitic. These mylonites do not exceed 20 cm in thickness.

Three subfacies of the Ll granite are identified: (i) coarse-grained granite with large quartz crystals (Ll-1), (ii) coarse-grained granite with rare garnet (<1 mm in diameter, partly accumulated in layers) and scarce biotite (Ll-2) and (iii) fine-grained granite (Ll-3) poor in micas but with abundant mica schlieren and pegmatitic segregations. This heterogeneous facies commonly occurs in contact zones between Lm and Ll-1 granites. Aplite and pegmatite with muscovite  $\pm$  biotite  $\pm$  tourmaline  $\pm$  garnet are also common but with minimal thickness, ranging from several centimetres to tens of centimetres.

Several fault systems cut the Bernardan area. The ESE–WNW trending La Marche Fault, located 2 km north of the deposit, is the most prominent structure. It includes several associated subparallel mylonitic zones over a width of several hundred metres. This structure is thought to be a reverse fault [101]. Other fault and fracture systems trend E–ENE, N–NNW and NNE.

Granite at Bernardan exhibits variably intense deformation. The major one is related to ENE–WSW structures that were active prior to complete magma crystallization (syntectonic). Major deformational effects are reflected by undulatory extinction in quartz grains, kink bands in muscovite, microclinization of feldspar and the formation of anisotropic planes in the rocks [106].

#### *(c) Host rock alteration*

Selective episyenitization (mica episyenitization) is the most prominent alteration feature in the leucogranite. It is found as highly irregular pipes, lenses, or steep to vertical dipping, elongated pods commonly with sharp contacts to the host granite, with selvages a few millimetres to a few centimetres wide. Sites of episyenitization are controlled by a dense network of superimposed fractures trending

N–NNE, E–W and ESE–WNW. Episyenite resulted from quartz dissolution and recrystallization of phengitic mica, essentially at the expense of plagioclase, but also to a minor degree K-feldspar and biotite. These mineral transformations are reflected chemically by a loss of SiO<sub>2</sub> and Na<sub>2</sub>O and an increase in K<sub>2</sub>O and Rb. Chloritization is rare. Silicification occurs peripherally to some episyenite bodies. As a result of these processes, a more or less vuggy, cataclastic, sponge-like rock with significant porosity (20–30%) and permeability evolved and as such provided favourable space for later uranium deposition. It should be noted, however, that although episyenites are commonly the host of uranium mineralization, there are also barren episyenites that may or may not be connected with uraniumiferous zones.

Episyenitic processes were not restricted to the actual episyenite body but extended for several tens of metres into the surrounding host granite, suggesting that the extension and intensity of the episyenitization process was a function of the degree of fracturing and microfracturing [107]. Alteration associated with uranium mineralization includes argillization and potassic feldspathization, reflected by potassium- and calcium-bearing montmorillonite and adularia, respectively, within the episyenite and the mineralized bodies, whereas smectite and kaolinite are typically found in the aureoles surrounding episyenites.

### Mineralization

Pitchblende, coffinite and black products (mainly sooty pitchblende) are the principal uranium minerals at Bernardan and most other episyenite hosted uranium deposits in the western La Marche district. Pitchblende is interpreted as the only primary uranium mineral but is scarce since much of the original pitchblende has been transformed into coffinite. Coffinite associated with minor dark purple fluorite (antozonite) and baryte are typical for deeper levels, whereas uranium hexavalent minerals, mainly autunite and, locally, ningyoite associated with locally abundant carbonates, extend from the surface to depths of approximately 30 m. The majority of ore minerals occur uniformly disseminated in the episyenite host rock, while stringers with small pitchblende spherules and sulphides were only rarely intersected by drilling at depth.

Michel [108] identified four major mineral parageneses in the central ore lode (Amas Central) that was mined by an open pit:

- (i) A reduced, uranium-rich paragenesis of pitchblende in association with pyrite and marcasite that completely impregnates the host episyenite by filling voids and episyenite controlling fractures at deeper levels (this paragenesis can also be locally oxidized to an assemblage rich in gummite, oxides and carbonates);
- (ii) A reduced, spatially extensive, uranium-poor paragenesis of coffinite with or without pyrite and marcasite or adsorbed onto interstratified illite–smectite, black uranium products adsorbed onto clay minerals, rare pitchblende enclosed in secondary pyrite, as well as (radiogenic) galena, sphalerite and barite;
- (iii) An oxidized, pink, weakly mineralized paragenesis rich in carbonate (dolomite) and iron oxyhydroxides (haematite and goethite) succeeded by a second carbonate generation (calcite) that fills the majority of voids. Fluorite (antozonite) may be intercalated between iron oxyhydroxides and calcite;
- (iv) An oxidized paragenesis of autunite, meta-autunite and iron oxide nodules with uranium adsorbed onto goethite, located in the first 15–20 m below the surface.

These parageneses show marked interrelationships, which indicate significant variations in the redox conditions over the course of evolution of the deposit. Coffinite is interpreted as having been formed by Late Jurassic (hydrothermal processes that altered the original pitchblende and also caused the earlier argillization and potassic feldspathization (adularia) [94]. Recent remobilization of earlier formed uranium mineralization has resulted in sooty pitchblende and uranium adsorbed onto clay minerals and iron oxides. These ‘black’ products constitute the cementation zone of the present day deposit [109, 110].

## Deposit morphology

Uranium mineralization is present mainly as disseminations in episyenite bodies locally termed 'amas'. Ore-bearing episyenite bodies are highly variable in size, ranging from about 100 m<sup>2</sup> to more than 1500 m<sup>2</sup> in horizontal section, and from a few tens of metres to more than 700 m in vertical extent and hosting from 50 tU to more than 3000 tU (Amas Profond Sud). Grades range from 100 ppm U to several tens of per cent.

Ten main ore-bearing episyenite lenses with grades averaging between 0.4 and 4% U have been identified in the Bernardan deposit (Figs 37 and 38). Most of these lodes are interconnected by low grade zones or 'fumées' ('smokes') along structural discontinuities.

Peinador-Fernandes et al. [111] provide the following geometric parameters for four of these bodies:

- (i) Amas Central (~2000 tU) mineralization occurs in an episyenite body of rather irregular shape. The body has a vertical extension of about 120 m, a NNE–SSW length of as much as 100 m and a width of 5–20 m at the 240 m level (above sea level) (ground level is 255 m above mean sea level). The orebody width expands to as much as 70 m at the 175 m level, narrows to less than 10 m below the 150 m level and ends at the 145 m level. Uranium minerals are irregularly disseminated within this episyenite body from surface to a depth of about 100 m. The orebody measures between 20 and 50 m across at a depth of 25 m and widens to 60–100 m at 75 m depth. Lower grade ore envelopes some high grade ore lenses that trend NNE–NE and generally dip moderately eastwards;
- (ii) Amas Sud Est and Sud Ouest (~500 tU) consist of moderately south dipping orebodies to depths of about 110 m;
- (iii) Amas Est (~100 tU) is hosted in an episyenite body which persists to a depth of about 150 m and contains mineralization from the surface to a depth of 50 m;
- (iv) Amas Profond Sud occurs between Amas Est and Amas Sud at depths of 230–270 m. It ranges from 20–50 m wide and contains almost 1000 tU at grades as high as 10% U and averaging 0.5% U.

Other ore lodes in the Bernardan deposit include: Amas Profond Nord with resources in excess of 3000 tU is the largest and deepest ore lode and still open at depth (a drill hole intersected 100 m of episyenite hosted ore at 0.4% U to a depth of 750 m); Amas Noël (375–700 m depth, joins Amas Profond Nord at depth; drill core has 0.78% U at 630–690 m depth in episyenite); Amas Intermediaire (100–350 m depth); Amas P14 (80–130 m depth) and Amas N27 (includes four ore lodes below Amas Sud Est at depths of 120–230 m) [112].

## Metallogenic aspects

Bernardan, as well as the other deposits of the district with the exception of Piégut, which is a vein deposit, contain disseminated epigenetic uranium mineralization in structurally controlled, vuggy episyenitic pipes in Hercynian leucogranite. They are therefore classified as episyenite subtype uranium deposits of the granite-related type [47]. Ore controls and recognition criteria are similar to episyenite hosted deposits in the La Crouzille–Limousin district. Episyenite mineralogy and related alteration processes provide key insights for understanding the metallogenesis of the uranium mineralization.

Patrier et al. [106] distinguish three varieties of episyenite pipes: (i) mineralized pipes, i.e. pipes with economic uranium mineralization; (ii) barren connected pipes, i.e. pipes barren of economic uranium mineralization but connected to mineralized pipes and (iii) barren unconnected pipes, i.e. pipes barren of economic uranium mineralization and unconnected to known mineralized pipes. The authors elaborate on the physicochemical conditions by which the various alteration stages developed in both mineralized (U) and unmineralized episyenite pipes and identified three successive crystallization stages:

- (i) Subsequent to the formation of episyenite at 315–308 Ma ( $305 \pm 1.5$  Ma), geodic crystallization of secondary K-feldspar, quartz, dolomite and fluorite occurred in all three types of pipe. These minerals formed from saline and  $^{18}\text{O}$  enriched fluids at high temperatures of up to  $360^\circ\text{C}$ . The  $^{87}\text{Sr}/^{86}\text{Sr}$  ratios in carbonates are consistent with those in aluminopotassic granite in western La Marche;
- (ii) The second event, around 170–140 Ma, is reflected by argillization of some episyenite pipes caused by  $^{18}\text{O}$  enriched, hot ( $100^\circ\text{C}$ ) fluids that originated in sedimentary basins. In view of the close association of uranium silicates (coffinite) with clay minerals, it is believed that the uranium was transported by these fluids, but the uranium source remains unidentified;
- (iii) Recent modification of mineralization by supergene processes resulted in oxidation and formation of high grade ore near the top of the deposit and adjacent to major permeable faults and fractures.

As in many uranium deposits of the Massif Central, uranium mineralization occurs as impregnations in rocks in subvertical columns of episyenite, as much as 700 m or more in vertical extent, several tens of metres in length, with a roughly elliptical horizontal section. These columns resulted from internal mineral alteration of the granite, mainly dissolution of quartz by hot, low salinity hydrothermal aqueous solutions that percolated through the abundant fractures, at all scales controlled by NNE–SSW structures and, less clearly, by NNW–SSE structures [109, 110].

Some of the percolating fluids have been preserved in numerous, healed microfractures which now appear as thin trails of fluid inclusions in the quartz. These are most commonly found in mesoscopic fractures but are also present in closely spaced microfractures in quartz crystals of the bulk granite surrounding episyenite bodies. Thermometric studies of these fluid inclusions [104] yield ice melting temperatures between  $-7^\circ$  and  $0^\circ\text{C}$  (corresponding to 10–0wt% NaCl equivalent) and homogenization temperatures for the liquid phase ranging from  $180^\circ\text{C}$  to more than  $350^\circ\text{C}$ .

With respect to potential uranium sources, no specific granite variety possessing elevated uranium background concentrations and accessory uraninite has yet been identified in the western La Marche pluton unlike those in the St. Sylvestre massif hosting the deposits of the La Crouzille district. However, this could be due to the paucity of fresh granite in outcrops and in mine workings rather than a lack of fertile granite facies. Circumstantial evidence provided by uraniferous monazite that has survived all alteration processes hints to increased uranium background values in the La Marche leucogranites, as is the case for the Limousin district.

The sequence of metallogenic events and processes suggested for the Bernardan and other deposits in western La Marche [113] are given in Table 14.

TABLE 14. METALLOGENIC EVENTS OF THE WESTERN MARCHE DISTRICT [113]

Approximate age	Event
Quaternary–Recent	Supergene ore remobilization at near surface levels Iron oxides and hydroxides associated with kaolinite and silica
Late Eocene	Local remobilization of U reflected by coffinitization of pitchblende remnants  Formation of richest ore shoots composed of microcrystalline U oxides and coffinite, haematite and goethite, followed by deposition of significant amounts of carbonate in voids
Jurassic (Late Liassic) (190–150 Ma)	Alteration of episyenite reflected by corrosion of primary micas and plagioclase, argillization (illite–smectite) Remobilization of Permian? pitchblende Formation of coffinite + black U products
Permian (280–260? Ma)	Assumed primary mineralization (pitchblende + pyrite) in episyenite (deduced by comparison with vein type U mineralization in Limousin district)
Carboniferous (315–305 Ma) (305 ± 1.5 Ma)	Selective episyenitization controlled by distinct fracture systems within leucogranite
325–315Ma	Intrusion of two mica leucogranite (latest stage Rouaret granite 314 ± 1.5 Ma)
Late Devonian (360–340 Ma)	Intrusion of G-type granites (Tersannes and Oradour St. Genest granites, western La Marche unit)

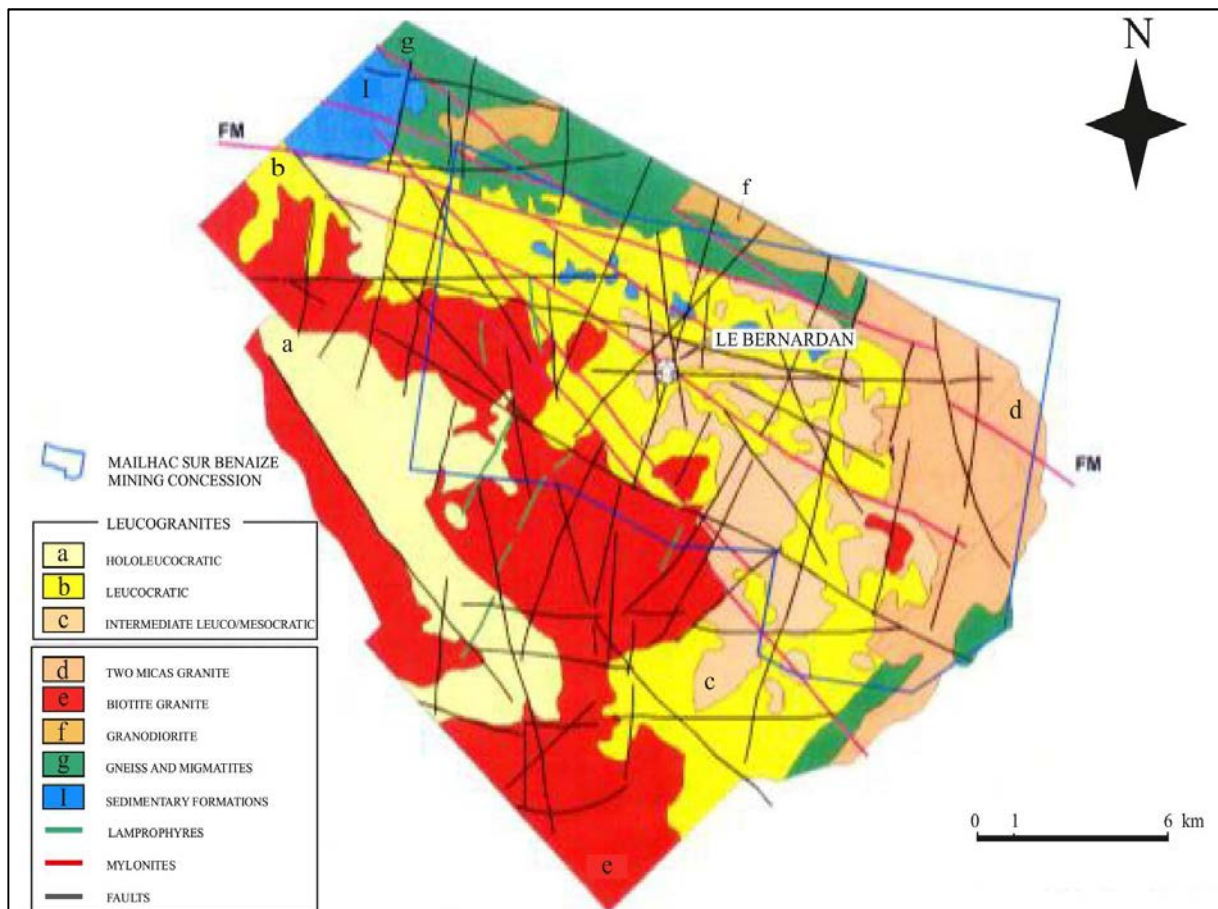


FIG. 36. Geology of the La Marche district (source: AREVA (reproduced with permission)).

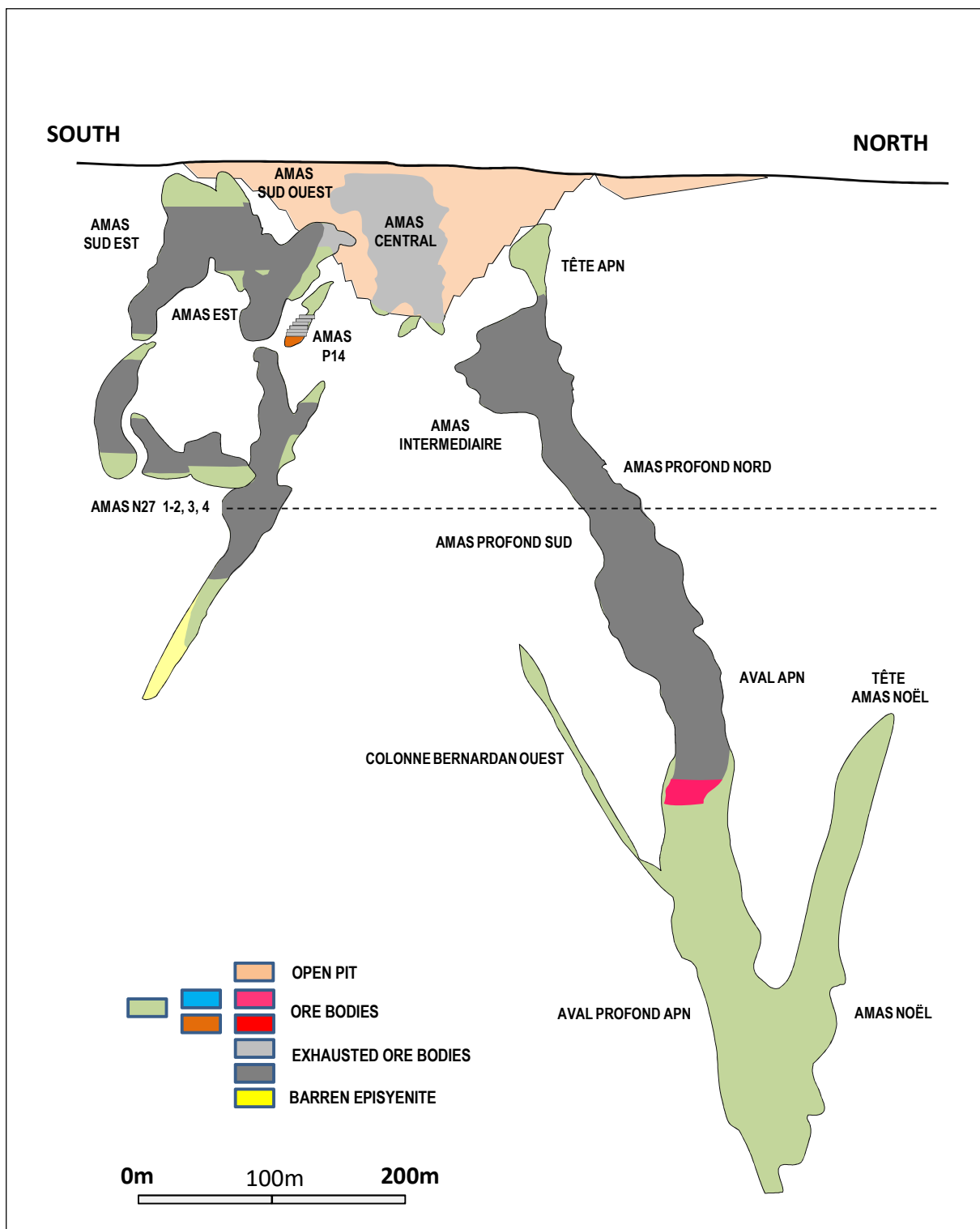


FIG. 37. Geological cross-section of the Bernardan deposit (source: AREVA (reproduced with permission)).

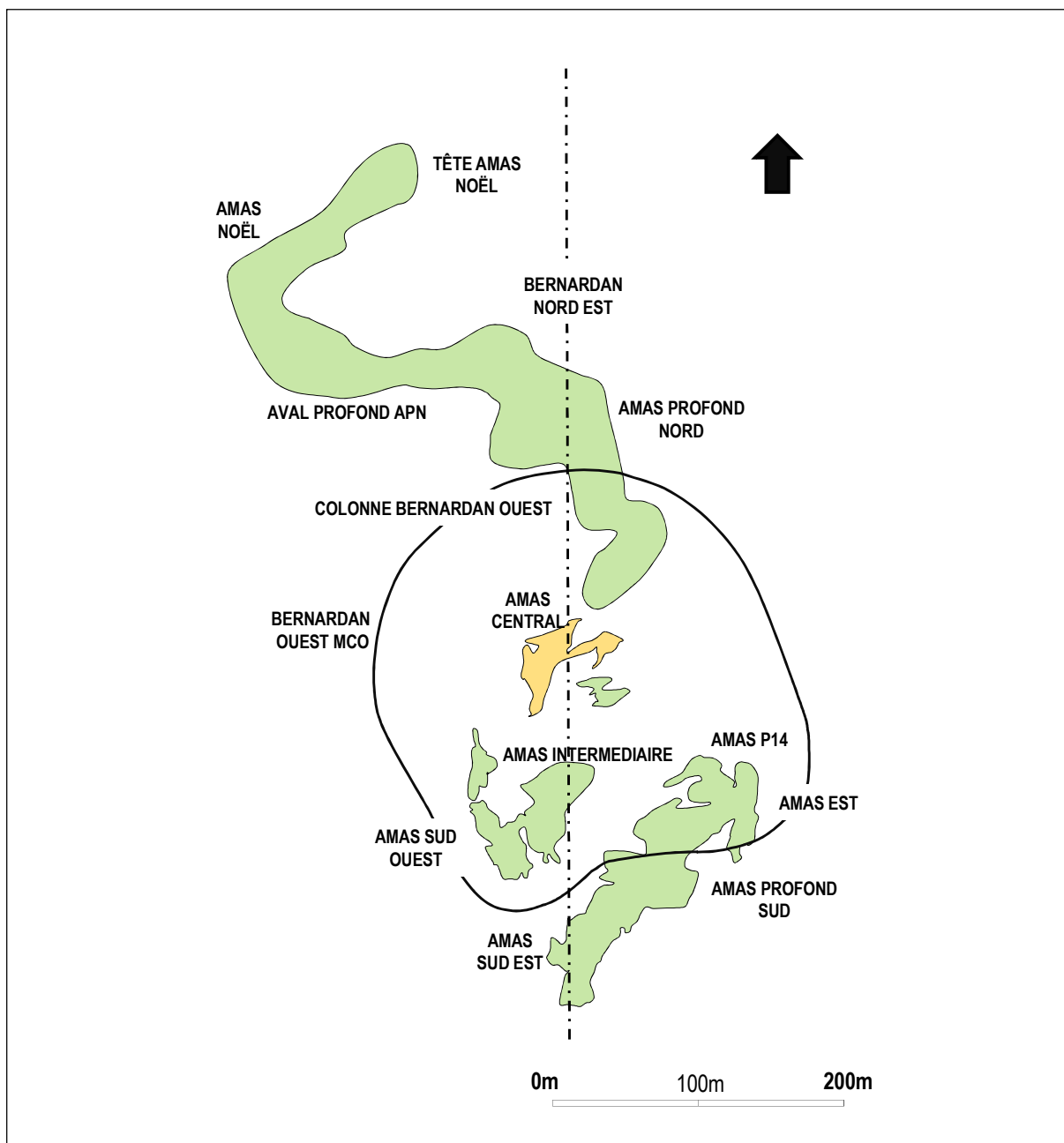


FIG. 38. Plan view of the Bernardan deposit showing the location of the mineralized lenses (source: AREVA (reproduced with permission)).

#### 3.2.4.2. Perigranitic deposits

##### Niederschlema–Alberola deposit (Germany)

###### Introduction

The Niederschlema–Alberoda deposit is a hydrothermal vein type uranium deposit located in the western part of the Erzgebirge (south-eastern Germany), 28 km south-west of the city of Chemnitz (Fig. 39). The exploration programme undertaken over about 45 years in this area by WISMUT, a company established jointly by the former Soviet Union and the German Democratic Republic, is probably one of the most intensive ever undertaken which specifically targeted the discovery of

hydrothermal vein type uranium deposits. The deepest exploration drill hole reached 2300 m in the Niederschlema–Alberoda area.

About 230 000 tU were mined from different deposit types along the NW border of the Bohemian Massif. Most of the uranium resources are present as hydrothermal veins in the Erzgebirge and hydrothermal stockwork/disseminated uranium mineralization in the Ronneburg district. The total production from Niederschlema–Alberoda deposits has been about 72 000 tU. Together with the production from the Schneeberg and Oberschlema deposits and taking account of production losses and unmined resources, a total uranium resource is estimated at 85 000 tU. This represents by far the world's largest hydrothermal uranium vein type deposit.

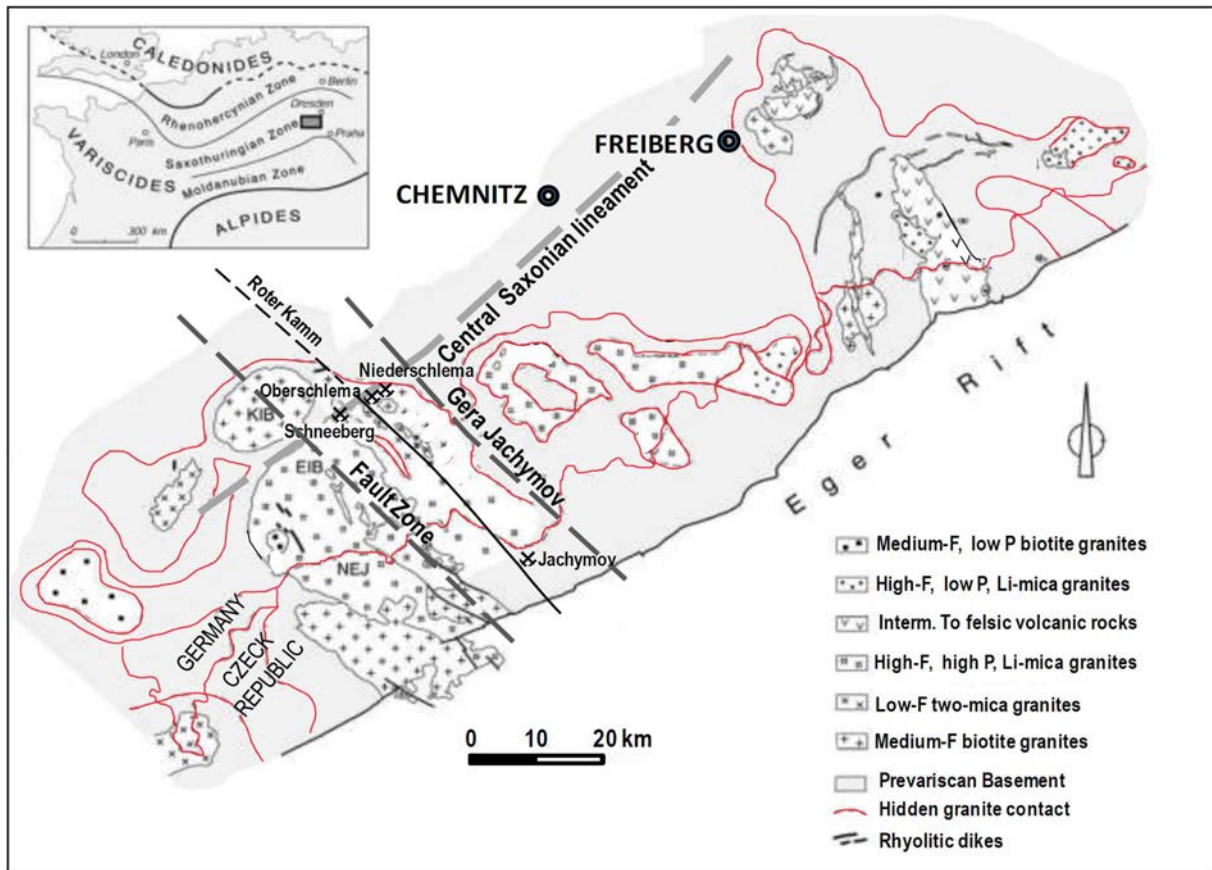


FIG. 39. Distribution of the Variscan granites in the Erzgebirge and location of the Niederschlema and some other uranium deposits. KIB: Kirchberg granite, EIB: Eibenstock granite, NEJ: Nejdek granite. The extension of the granites at depth is shown as a hatched line (adapted from Ref. [114]).

#### Geological setting

The veins are almost entirely hosted within the contact metamorphic aureole affecting weakly metamorphosed metasediments around peraluminous leucogranitic intrusions (Fig. 40).

The Erzgebirge granites were generated during the late collisional stage of the Variscan Orogeny. Overthickening of the crust of the Bohemian Massif during the continental collision, in combination with the presence of uraniumiferous lithologies, favoured intracrustal melting. The granites were emplaced at shallow crustal levels and intruded low grade metamorphic rocks (quartzite, phyllite, black shale, amphibolite and skarn) during a large scale extensional event between approximately 325 and 318 Ma. Recent dating by Tichomirowa and Leonhardt [115] using the single zircon Pb evaporation

methodology produced the following ages on the granites situated in the vicinity of the Schlema deposits: Aue ( $328.6 \pm 2.0$  Ma), Schwarzenberg ( $329.1 \pm 1.7$  Ma) and the Eibenstock pluton ( $319.8 \pm 1.0$  Ma).

Two major types of granite have been distinguished by Förster et al. [114]: mildly peraluminous transitional I–S types and strongly peraluminous S-type rocks. These can be further subdivided into three major groups: (i) low F biotite granite; (ii) medium F biotite granite; (iii) low F, two mica granite; (iv) high F, high P, lithium mica granite. and (v) high F, low  $P_2O_5$  lithium mica granite [114, 116]. The lithium mica granites have the highest concentrations of U as well as P, F, Li, Rb, Cs, Ta, Sn and W and the lowest Ti, Mg, Co, Ni, Sr, Ba, Y, Zr, Hf, Th and rare earth elements. Most of the vein type uranium deposits are associated with the peraluminous types (ii) and (iii).

This compositional classification supercedes the earlier classification of older versus younger granites with a large age range (330–290 Ma) that have not been confirmed by the new geochronology results [117]. The recent age data demonstrate that all large Variscan granite bodies were emplaced within less than 10 Ma regardless of their chemistry. The Th–U–Pb dating of uraninite in granite from the Ehrenfriedersdorf mining district provides ages of  $323.9 \pm 3.5$  (Greifenstein granite),  $320.6 \pm 1.9$  and  $319.7 \pm 3.4$  Ma (both from the Sauberg mine), which are in agreement with U–Pb apatite ages of  $323.9 \pm 2.9$  and  $317.3 \pm 1.6$  Ma (both from the Sauberg mine). Some small tin-bearing bodies may have slightly younger ages, such as the Seiffen granite with a Th–U–Pb chemical age of  $301 \pm 5$  Ma from monazite [118]. Dating of two molybdenite samples from Altenberg using Re–Os also provides ages of  $323.9 \pm 2.5$  and  $317.9 \pm 2.4$  Ma [113].

## Mineralization

### (a) *Regional structural controls*

The Niederschlema–Alberoda uranium deposit is spatially related to deeply rooted, NW trending tectonic structures several hundred kilometres long, running from the central Bohemian Massif in the Czech Republic to the central part of Germany. The most important is the Gera–Jachymov Fault Zone (Fig. 40), which contains the largest deposits of the area, including Jachymov on the Czech side of the Erzgebirge, Johanngeorgenstadt, Pöhla–Tellerhäuser, Schneeberg–Schlema–Alberoda in the German part of the Erzgebirge, and up to the Ronneburg black shale breccia type deposit in Thuringia. The Schneeberg–Oberschlema–Niederschlema–Alberoda uranium–silver district is also controlled by the NE–SW Central Saxonian Lineament where it cross-cuts the Gera–Jachymov Fault Zone (Fig. 40). The Rotter Kamm Fault is the most important one in the vicinity of the Schneeberg–Oberschlema–Niederschlema–Alberoda deposits. The crustal block located east of the Roter Kamm Fault has been down-dropped about 500 m with respect to the western crustal block [113].

### (b) *Structural/lithological controls of the orebodies*

The mineralized veins formed a ramifying network which occur within the exocontact of mostly concealed Variscan peraluminous two mica leucogranite bodies (the eastern flank of the Eibenstock high F, high P, lithium mica leucogranite) (Figs 40–42). The metamorphic rocks hosting the veins are termed the ‘productive series’, which consists of Upper Ordovician to Mid-Devonian phyllite with intercalations of metamorphosed black shales and metacarbonates and Mid-Devonian diabase intrusions. About 1800 mineralized veins have been mined.

The uranium ore veins in the Erzgebirge typically have a thickness of 0.1–0.3 m with a maximum of 1 m. In the Niederschlema deposit, the widths of the mineralized veins range from a few centimetres to several metres and have an average grade of 0.1% U, although locally massive pitchblende lenses may attain a width of up to 2 m. The highest concentrations of uranium are observed where the veins cross-cut black shales and skarns. Some of the veins were mined to a depth of nearly 1800 m [113].

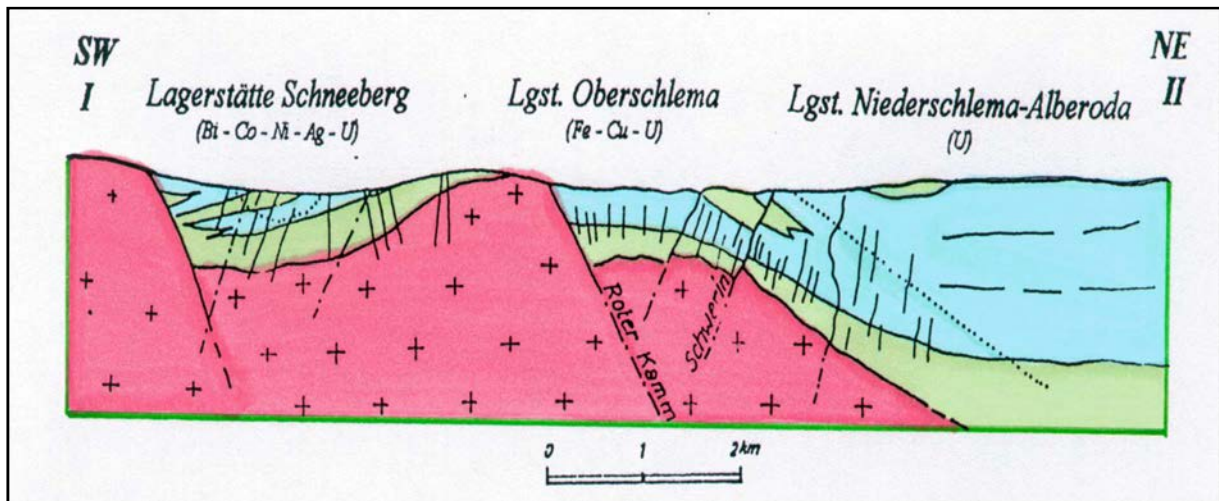


FIG. 40. A SW-NE schematic cross-section through the major uranium district: Schneeberg-Oberschlema-Niederschlema-Alberoda orefield in the German Erzgebirge. The dotted line represents the extension of the contact metamorphism in the metamorphic rocks (mica schists (green) and carbon-bearing mica schist (blue) enclosing the granites (pink)). The black continuous lines indicate the uranium veins and the hatched lines, the faults [119] (reproduced with permission).

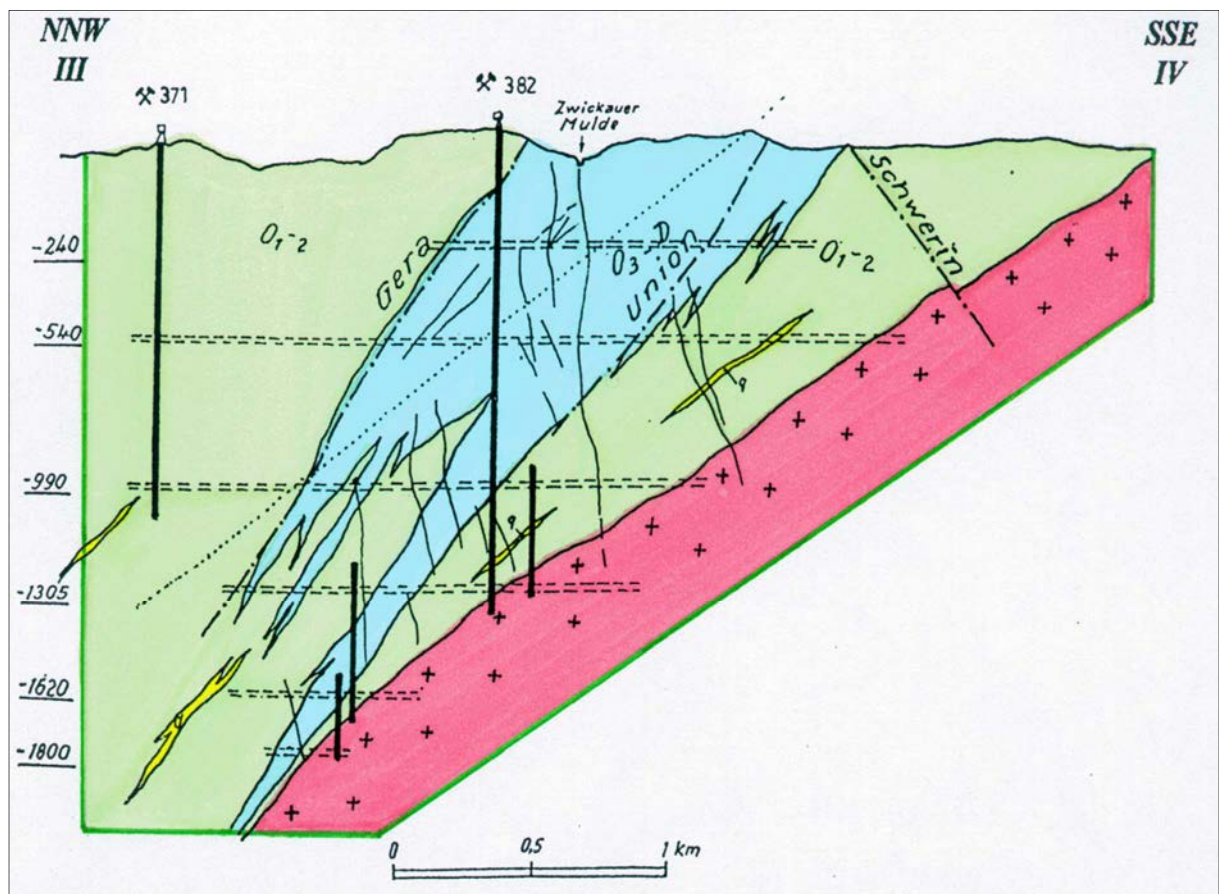


FIG. 41. A NNE-SSE schematic cross-section through the major Niederschlema-Alberoda uranium deposit showing the location of shafts 371 and 382. The legend is the same as that in Fig. 40, except for the quartzite layers (yellow) [119] (reproduced with permission).

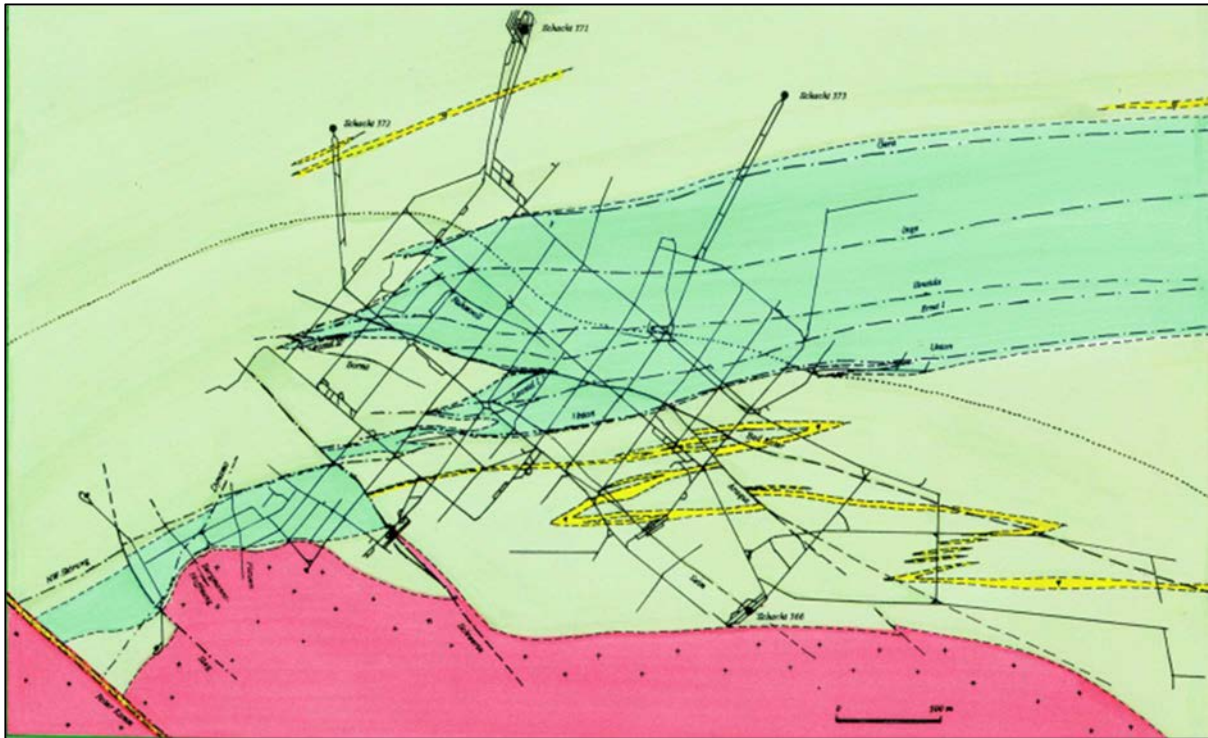


FIG. 42. Geological map of the Niederschlema–Alberoda uranium deposit at level -520 m. See Figs 40 and 41 for legend [119] (reproduced with permission).

(c) *Paragenetic succession in the veins*

The first detailed mineralogical and paragenetic studies in the Niederschlema–Alberoda uranium deposit were undertaken in the 1960s and 1970s [120] and more recently by Schuppan et al. [121].

Before the uranium ore depositional stages, two other types of mineralization are known: (i) a quartz–fluorite–wolframite–scheelite–cassiterite stage and (ii) a quartz–sulphide stage with either Cu sulphides only or with an association of Cu–Pb–Zn sulphides.

Following these, three major stages (kku, mgu and biconi) of uranium mineralization have been recognized in the Niederschlema–Alberoda uranium deposit, as in the other vein type deposits of the Erzgebirge [113]:

- (i) Comb quartz, calcite veins, colloform, reniform and botryoidal pitchblende (kku), with minor fluorite and sulphides deposited during the Early Permian, around 270 Ma [122]. This stage is the most widespread in the district and dominates at Oberschlema;
- (ii) Dolomite–pitchblende veins (MgU) of Jurassic age (about 190 Ma) developed as veins and stockworks. During this event, Permian pitchblende was dissolved and U was redeposited as a second generation of spherical aggregates of pitchblende associated with dolomite, ankerite, fluorite, haematite and diverse sulphides (chalcopyrite, galena, bornite, tennantite) and selenides (especially clausthalite). This association is very prominent in the Niederschlema–Alberoda deposit but minor in Schneeberg;
- (iii) Veins containing Bi–Co–Ni–As–Ag–U (biconi) together with quartz, calcite, Co–Ni arsenides, native bismuth, bismuthinite, galena, chalcopyrite, pyrite, native silver and pitchblende of Cretaceous age. Hydrothermal activity in response to tectonic processes at these times again gave rise to partial dissolution of earlier deposited pitchblende, coffinite and selenides and their replacement by the Bi–Co–Ni assemblage comprising native minerals (Ag, Bi, As), Co–Ni–Fe arsenides (skutterudite, safflorite, rammelsbergite, löllingite,

nickeline), acanthite, tennantite–tetrahedrite solid solutions, wittichenite, matildite and Bi-sulphides. Quartz, fluorite, baryte, siderite and dolomite form the gangue of the Bi–Co–Ni association and the remobilized uranium- and selenium-bearing minerals. This stage also occurs everywhere in the district, but dominates in the Schneeberg district.

Three other mineralization stages follow with: (i) silver and sulphides; (ii) calcite with minor sulphides, and (iii) iron–manganese oxides with chalcedony and jasper.

Pitchblende is the most important uranium ore mineral in all veins types but coffinite locally occurs and a wide range of secondary uranium minerals are found in the oxidation zones. The two last stages often caused cataclasis and remobilization of the (kku) pitchblende generation in association with the precipitation of selenides and/or Bi–Co–Ni arsenides and native Ag. Of the three uranium deposits in the Schneeberg–Oberschlema–Niederschlema–Alberoda ore district (Fig. 40), the Niederschlema–Alberoda deposit was the richest in terms of both uranium and selenium [113].

### Metallogenesis

*Source:* the uranium from the deposits was most likely derived from the adjacent peraluminous L two mica leucogranites, in which most of the uranium is hosted in easily leachable uraninite [116, 123]. According to Förster [123], the total amount of uranium that was leached from the Aue–Schwarzenberg Granite Zone, which corresponds to a part of the Roter Kamm structure in the vicinity of the Schlema deposits, must have been very large. Calculations made for the F–P enriched lithium mica granites of Eibenstock, Ehrenfriedersdorf, Satzung, Pobershau and others have shown that between 50% and 80% of the initial uranium concentrations were lost. The vertical extension of uranium depletion aureoles may approach a maximum depth of 2–3 km [124, 125].

*Transport:* the first studies of the fluid inclusions in vein type uranium deposits of the Erzgebirge were undertaken by Naumov and Mironova [126] and Naumov et al. [127]. They have shown the presence of CO<sub>2</sub> in the hydrothermal mineralizing fluid which supports the concept of transportation of uranium as uranyl carbonates at temperatures of 80–175°C. They also proposed a gradual decrease in CO<sub>2</sub> content of the fluid from 4 to 0.2mol% during the quartz–pitchblende–calcite stage which led to the dissociation of the aqueous uranyl carbonate species and, finally, the precipitation of uranium.

The most recent studies have been performed by Krylova et al. [128]. The fluid inclusions present in the comb quartz immediately prior to pitchblende deposition have homogenization temperatures in the range 190–240°C with salinities of 19.4–23.8wt% NaCl–CaCl<sub>2</sub> equivalent and with traces of N<sub>2</sub>. In post-pitchblende growth zones, homogenization temperatures vary in the range 82–178°C with salinities from 2.0–20.0wt% NaCl–CaCl<sub>2</sub> equivalent. Repeated boiling is indicated but CO<sub>2</sub> has not been detected in the solutions. Only post-pitchblende calcite contains fluid inclusions with the presence of carbonates, and hydrocarbons associated with haematite have been detected in fluorite.

The intrusion of lamprophyres is considered by Seifert [129] as a source of the CO<sub>2</sub> for the formation of the uranyl carbonate complexes in the mineralizing fluids that leached the uraninite from the adjacent late Variscan, uraniferous granites.

During the MgU stage, oxidizing hydrothermal solutions were introduced, overprinting and altering the early formed pitchblende veins and introducing new elements (Mg, Se, Bi, Pb, Ag, Cu) leached from the metamorphic wall rocks of the veins [118]. Fluid inclusions in dolomite and ankerite are rich in Mg and Ca chlorides, with salinities of 21.0–26.8wt% CaCl<sub>2</sub> equivalent, and homogenization temperatures vary in the range 110–137°C, but CO<sub>2</sub> was not detected [128, 130]. The association of bohdanowiczite with Cu selenides (umangite, berzelianite, eucairite) and the intergrowth of umangite and tiemannite confirm the temperature conditions of formation of this paragenesis. Umangite decomposes into berzelianite and klockmannite at ≈110°C [131]. During the Bi–Co–Ni stage, fluid inclusion studies indicate temperatures of 90–110°C [130].

*Deposition:* all the deposits have been found in the contact aureole of the granites. Uranium deposition seems to have been largely controlled by the reducing lithologies hosting the veins, mainly the carbonaceous schists (mainly in the Lössnitz–Zwönitzer Zwischenmulde Formation) of the so-called ‘productive series’ and, locally, the lamprophyres [113].

### 3.3. POLYMETALLIC IRON OXIDE BRECCIA COMPLEX DEPOSITS

#### 3.3.1. Definition

Deposits of this group occur in haematite-rich breccias and contain uranium in association with copper, gold, silver and rare earth elements. They are classically termed iron oxide–copper–gold systems (IOCG). The main representative of this deposit type, Olympic Dam, has been assigned to a broad suite of loosely related IOCG deposits that include Prominent Hill, Carrapateena, Ernest Henry, Starra, Osborne, Selwyn and Mt Elliot in Australia; Candelaria, Salobo, Monte Verde and Sossego in South America; Sue–Dianne in Canada; Khetri in India and Dahongshan in China [132]. Some of these iron-rich deposits contain uranium in trace to minor amounts, whereas Olympic Dam is the only known large, Proterozoic iron-rich deposit that contains uranium in sufficient concentrations to be extracted as a by-product.

In 2015, 15 iron oxide–copper–gold–uranium deposits were recorded in the UDEPO database, all located in Australia, Brazil and Canada (Table 15). Olympic Dam is the largest uranium deposit in the world, with resources exceeding 2 000 000 tU at an average grade of 0.023% U. Uranium is extracted as a by-product of copper, along with gold and silver. Production in 2015 totalled 3161 tU.

Another important district is the Serra dos Carajas Province in Brazil, which lies in the eastern part of the Archaean Amazon Craton. Major copper–gold deposits such as Igarape Bahia, Salobo and Sossego contain anomalous uranium, with 99–170 ppm U, 32–57 ppm U and 60 ppm U, respectively [133]. Geological resources for each of these three deposits are on the order of 25 000–35 000 tU.

TABLE 15. IRON OXIDE–COPPER–GOLD–URANIUM DEPOSITS (as of 31 December 2015)

Deposit	Country	Resources (tU)	Grade (% U)	Status
Olympic Dam	Australia	2 125 230	0.023	Operating
Carrapateena	Australia	184 000	0.0155	Development
Salobo	Brazil	36 000	0.0045	
Igarape Bahia	Brazil	30 000	0.0135	
Mount Gee	Australia	26 380	0.052	Dormant
Sossego	Brazil	21 000	0.006	
Prominent Hill	Australia	10 280	0.010	Operating
Moran Lake C-Zone	Canada	3 680	0.030	Exploration
E1 North and South	Australia	3 460	0.012	Exploration
Anna Lake	Canada	1 890	0.059	Exploration
Radium Ridge	Australia	1 845	0.050	Exploration
Armchair–Streiberg	Australia	1 540	0.085	Exploration
Queens Gift	Australia	910	0.024	Exploration
Thanksgiving	Australia	790	0.032	Exploration
Hodgkinson	Australia	480	0.0212	Exploration

### 3.3.2. Geological setting

IOCG deposits are a relatively recently recognized class of deposit [134]. They range in age from Late Archaean to Pliocene and are found in a number of different tectonic settings (rift, subduction zones and basin collapse) [135]. They display a wide variety of morphologies, but generally show a spatial relationship to major, crustal scale fault zones. The metal content of the deposits is highly variable but iron oxide is present as the dominant gangue mineral. The deposits are sought for Cu and Au but may also contain significant amounts of light rare earth elements, Ag, Mo, Zn, Co, Pb, W, Bi and U, as well as F, B and Cl [133].

IOCG deposits can occur in mafic to felsic igneous, metamorphic or sedimentary rocks. They are generally spatially and temporally associated with batholithic complexes of intermediate to felsic composition, although there is debate about whether they are directly genetically related to these magmas [136] or whether these intrusive bodies simply provide the thermal energy to drive large scale hydrothermal systems which scavenge the metals from the surrounding host rocks [137]. IOCG deposits are always associated with very large volumes of hydrothermally altered rocks (10–100+ km<sup>3</sup>) [135].

The deposits share a characteristic suite of alteration types. Magnetite-bearing sodic–calcic alteration, characterized by the development of replaced albite +/- scapolite in more felsic host rocks and albite–actinolite–diopside +/- scapolite in more mafic rocks, is the dominant alteration type in most IOCG systems. Potassic alteration generally post-dates sodic–calcic alteration. This style of alteration is also commonly by replacement, unlike the vein controlled alteration in porphyry systems, and is characterized by the formation of orthoclase–magnetite in more felsic rocks and biotite–magnetite in more mafic rocks. Some IOCG deposits contain hydrolytic alteration forming at a late stage or in high structural level zones characterized by the replacement of earlier alteration assemblages by haematite after magnetite, sericite, carbonate minerals and quartz [132, 134]. A Cu–Au assemblage and other metals may be precipitated during any of the alteration stages, but significant mineralization is most commonly formed during potassic alteration, although the Olympic Dam deposit is associated with hydrolytic alteration [138].

### 3.3.3. Metallogenesis

In IOCG deposits, uranium generally occurs as uraninite (euhedral and collomorph varieties), but brannerite and coffinite have also been described in some deposits and prospects. Uranium minerals are generally associated with Cu–Fe sulphides and occur within Cu enriched zones, commonly with potassic alteration. The main Cu-bearing phases are chalcopyrite, bornite and chalcocite. Rare earth elements are found in bastnaesite, florencite, monazite and xenotime.

Anomalous uranium is also commonly associated with late hydrolytic alteration in many systems, occurring with Cu sulphides or in late quartz veins cutting earlier sulphide assemblages. In many deposits and prospects, anomalous uranium also occurs outside zones of Cu mineralization, forming broad halos of weak uranium enrichment. It is suspected that the dispersal of minor uranium beyond the core of the hydrothermal alteration system is common in many IOCG systems [133].

The uranium grade of IOCG deposits is highly variable. Elevated uranium values could be related to uranium-rich magmatic fluids from causative intrusions, particularly oxidized granites. Uranium could also be contributed by a second fluid mixing with hydrothermal fluids at the site of mineralization. Oxygen and hydrogen isotope studies are consistent with a magmatic source for the fluids.

Data suggest that the uranium content of some IOCG deposits may be directly related to the amount of uranium in the unaltered host rock sequence. Hitzman and Valenta [133] suggest that the host rocks for the IOCG hydrothermal system must be enriched in uranium, as is the case for the Hiltaba Granite Suite in the Gawler Craton, in order to form a uranium-rich IOCG deposit.

### 3.3.4. Description of a selected deposit: Olympic Dam deposit (Australia)

#### Introduction

The Olympic Dam polymetallic deposit is located in South Australia, about 550 km NNW of Adelaide (Fig. 43). The deposit was discovered by Western Mining Corporation in 1975 near the Roxby Downs Station and started production in 1988. It is owned by BHP Billiton Ltd, which acquired WMC Resources in 2005. The deposit is situated beneath 350 m of cover rock. It covers an area of 6 km × 3.5 km and is up to 2 km deep.

The operation is a major producer of copper, gold, silver and uranium. Total resources are estimated at 30 Mt Cu, 1200 t Au and 6700 t Ag [139]. In addition, the deposit has significant amounts of rare earth elements (principally light rare earth elements) and has an iron content of about 26% Fe.

The Olympic Dam deposit contains the world's largest known resource of low cost uranium. Initial resources were estimated at more than 1 552 000 tU at an average grade of 0.034% U. Exploration drilling has discovered major extensions of the deposit to the south-east, which increased the size of the resources. As of June 2010, total resources at Olympic Dam were estimated to be 2 370 000 tU at a grade of 0.025% U. In 2015, production of uranium as a by-product totalled 3161 t and cumulative production to 2015 totals about 62 000 tU.

In October 2011, following State and Government approval, BHP Billiton announced that it would develop the deposit as an open pit mine. The plan is to develop a very large open pit with associated infrastructure over 11 years and increase uranium production to 16 000 t/year. The open pit will allow mining of up to 98% of the ore rather than the 25% mineable from underground. Most of the uranium will be separated at the mine, but up to 2000 t/year will be exported in copper concentrates, requiring a smelter to be constructed to treat these, possibly in China or Japan. The present underground mining will continue in the narrow, northern part of the orebody. The project has been suspended for the time being.

#### Geological setting

The Olympic Dam deposit occurs in a haematite-rich granitic breccia complex in the Gawler Craton, South Australia (Fig. 43). It is overlain by approximately 350 m of flat lying sedimentary rocks of the Pandurra Formation. The breccia complex is associated with a Mesoproterozoic plutonic intrusion and co-magmatic continental felsic volcanic rocks (Figs 44 and 45). The intrusion, volcanic rocks and breccia complex developed in a post-orogenic tectonic setting.

The Olympic Dam Breccia Complex (ODBC) occurs entirely within the Mesoproterozoic Roxby Downs Granite and includes a complete gradation from granite breccias through haematite–granite breccia to haematite-rich breccia:

- (a) *Granite-rich breccias* vary from fractured granite through breccias with altered granite derived matrix, to highly altered, matrix enriched breccias with relict granite fragments. The matrix of these granite-rich breccias consists of fine-grained granitic material combined with sericite, chlorite, haematite and variable amounts of baryte, fluorite, sulphides and uranium minerals;
- (b) *Haematite-rich breccias* have been subdivided into three general groups: (i) haematite–quartz breccias; (ii) haematite breccias and (iii) heterolithic haematitic breccias [138]:
  - (i) Haematite–quartz breccias consist of fragments of haematite and quartz in a matrix of microgranular haematite and quartz. This breccia type is essentially devoid of copper and uranium mineralization. Locally, this type of breccia contains abundant baryte veins and vein fragments;
  - (ii) Haematite breccias contain clasts and matrix composed mainly of haematite. Haematite breccias are the least abundant of the three main types of haematite-rich

- breccia, but they host a significant proportion of the ore mineralization. These breccias are typically steely grey to black in colour. Minor components include quartz, fluorite, baryte and altered granite derived mineral fragments;
- (iii) Heterolithic haematitic breccias include intermediate members of the range from granite to haematite breccias. This category is the most abundant of the haematite-rich breccias and it hosts most of the copper–uranium–gold–silver ore. Haematite clasts range from dark reddish brown through steel grey to jet black in colour. Other clasts include altered granite fragments, highly altered ultramafic, mafic and felsic intrusives, finely laminated haematitic siltstone and sandstone, and massive to poorly layered arkose-like rocks. These breccias also include variable proportions of sericite, chlorite, quartz, baryte, siderite and fluorite.

Within the ODBC there is a broad zonal distribution of the major rock types. The central core of the complex consists of barren haematite–quartz breccias, with several localized diatreme structures. The haematite–quartz core is flanked to the east and west by zones of intermingled haematite-rich breccia and altered granitic breccia. These zones are approximately 1 km wide and extend almost 5 km in a NW–SE direction. Virtually all the economic copper–uranium mineralization is hosted by haematite-rich breccias (heterolithic haematitic breccias and haematite breccias) within this broad zone. Heterolithic haematitic breccias form a large number of discrete, irregular, elongate or lenticular bodies within the zone. Haematite breccias form relatively small, irregular bodies either within or on the margins of larger heterolithic haematitic breccia bodies.

The zone of haematite-rich breccias is surrounded by granitic breccias which extend up to 3 km beyond the outer limits of the haematite-rich breccias. The outer limits of the ODBC are gradational with the Roxby Downs Granite.

Dykes and intrusive tuffs of ultramafic, mafic and felsic rock types intrude into the ODBC, particularly in the eastern and southern parts of the complex. These intrusive rocks are closely associated with volcanic diatreme structures. The diatremes contain subsided sub-aerial tuffs and conglomerates which pass laterally and downwards into phreatomagmatic breccias [138, 140].

Localized zones of volcanoclastic rocks broaden upwards and near the unconformity they include: surficial volcanoclastic rocks, mainly laminated ash and conglomerate (containing fragments of Gawler Range Volcanics) and reworked hydrothermal breccias. These volcanoclastic rocks appear to have accumulated in maar craters produced by phreatomagmatic eruption [138, 141].

Three key hydrothermal alteration and ore mineral assemblages are recognized in the Olympic Dam metallogenic province: (i) CAM: calc-silicate–alkali feldspar  $\pm$  magnetite  $\pm$  Fe–Cu sulphides (generally minor); (ii) MB: magnetite–biotite  $\pm$  Fe–Cu sulphides, and (iii) HSCC: haematite–sericite–chlorite–carbonate  $\pm$  Fe–Cu sulphides  $\pm$  U and REE minerals. Ore grade Cu–U–Au mineralization is generally associated with the HSCC assemblage, which is paragenetically later than the CAM and MB assemblages in most deposits and prospects [141].

## Mineralization

The Olympic Dam deposit contains iron, copper, uranium, gold, silver and rare earth elements (mainly light rare earth elements). Ore grade copper–uranium–gold–silver mineralization forms a large number of ore zones, mostly within heterolithic breccias and haematite breccias. The central core and mineralized breccias are approximately 3 km  $\times$  3.5 km (in plan view) with a north-west trending arm 3 km long and 300–500 m wide.

Uranium mineralization at Olympic Dam occurs within heterolithic haematitic breccias and in haematite breccias as disseminations, microveinlets and aggregates of fine-grained pitchblende intergrown with copper sulphides. Pitchblende also forms small aggregates that are intergrown with or replace breccia material. Small amounts of coffinite and brannerite are closely associated with pitchblende. Narrow, higher grade uranium zones often occur in the bornite–chalcocite zones,

especially with haematite breccias [141]. Some high grade zones of uranium mineralization cross the bornite–chalcopyrite interface.

The principal copper sulphide minerals are chalcopyrite, bornite and chalcocite. Throughout the deposit there is a well developed zonal distribution of the principal copper sulphide minerals. Chalcopyrite (and pyrite) occurs in the deeper and outer parts of the orebody whereas bornite and chalcocite occur in the upper and more central parts. The boundary between bornite–chalcocite mineralization and chalcopyrite mineralization (the bornite–chalcopyrite interface) is usually sharp. This boundary forms a convoluted surface that generally dips downwards towards the boundary of the central haematite–quartz breccia. Grades of 4–6% Cu are common in the bornite–chalcocite zones, whereas the chalcopyrite zones have usually less than 3% Cu. Ore textures show that much of the copper sulphide mineralization either post-dates or is coeval with the haematite [138, 141].

Gold and silver mineralization occurs mostly as fine-grained disseminations either within or closely associated with copper sulphide minerals. The mineralized haematite breccias commonly contain approximately 0.2% La and 0.3% Ce. The most abundant rare earth element minerals are bastnaesite and florencite, which are fine-grained and commonly intergrown with haematite and sericite [142].

#### Metallogenesis

The breccias and mineralization at Olympic Dam were formed by hydrothermal processes. Much of the brecciation occurred in the near surface eruptive environment of a crater complex during eruptions caused by boiling and explosive interaction of water (lacustrine, marine, groundwater) with magma [138].

On the basis of geological evidence, Reeve et al. [138] argue that the hydrothermal activity which formed the breccia complex occurred in the period elapsing between intrusion of the Roxby Downs Granite (~1590 Ma) and cessation of Gawler Range volcanic activity (1575 Ma). The results of U–Pb isotopic dating [143, 144], combined with geological evidence, suggest that introduction and deposition of ore metals occurred at the same time as the formation of the haematite breccias. For rocks within the breccia complex and the diatreme, U–Pb dates from zircon indicate that the breccia complex formed at 1596 Ma and that brecciation closely followed emplacement and cooling of the Roxby Downs Granite [144, 145].

Uranium mineralization was formed from relatively low temperature, saline and highly oxidized fluids. These fluids either mixed with hot, saline and reduced fluids carrying copper and gold [132, 142] or reacted with magnetite-bearing calc-silicate altered rocks enriched in copper and gold [146].

Compared with the other deposits, Olympic Dam has some unique characteristics that include [45]:

- (a) Most U-enriched;
- (b) Entirely hosted within a highly potassic, Fe-rich, calc-alkaline granite and associated with felsic volcanic rocks of the same nature;
- (c) Formed at shallow depth;
- (d) Meteoric water played a very important part in its genesis and therefore the main Fe-oxide component is haematite, not magnetite.

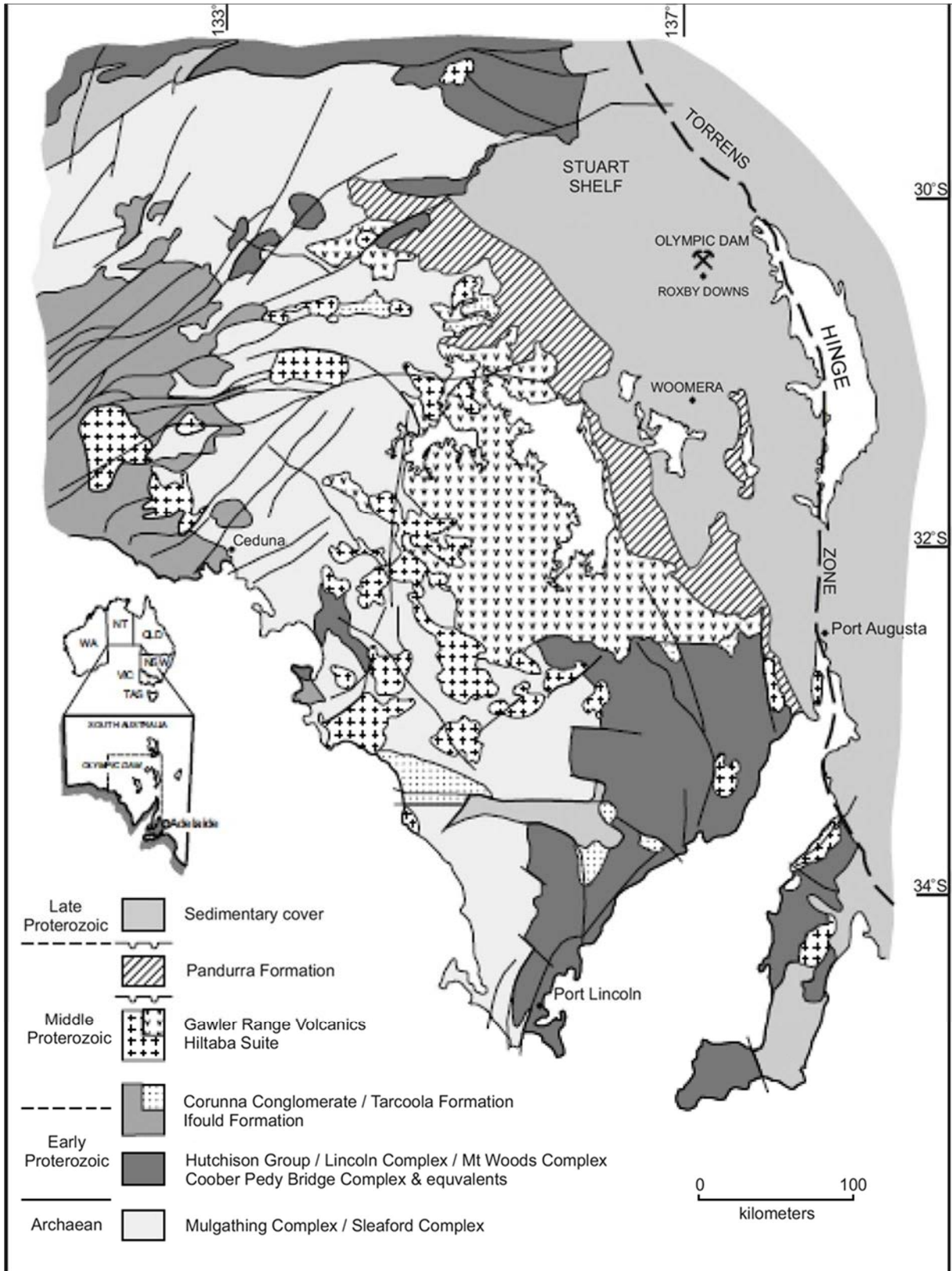


FIG. 43. Interpreted geology of the Gawler Craton, South Australia [139] (reproduced with permission).

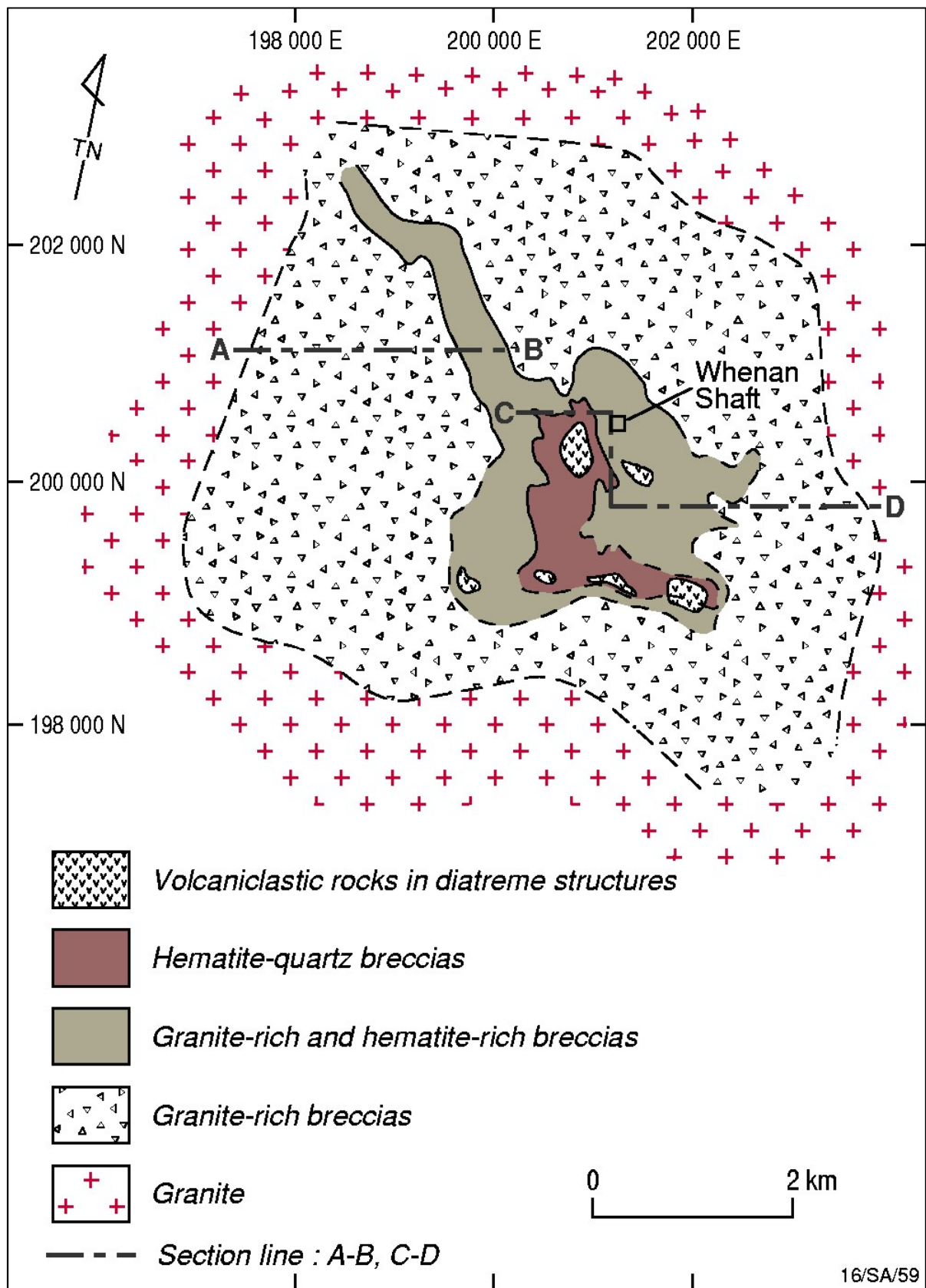


FIG. 44. Simplified geological map of the ODBC [138] (reproduced with permission).

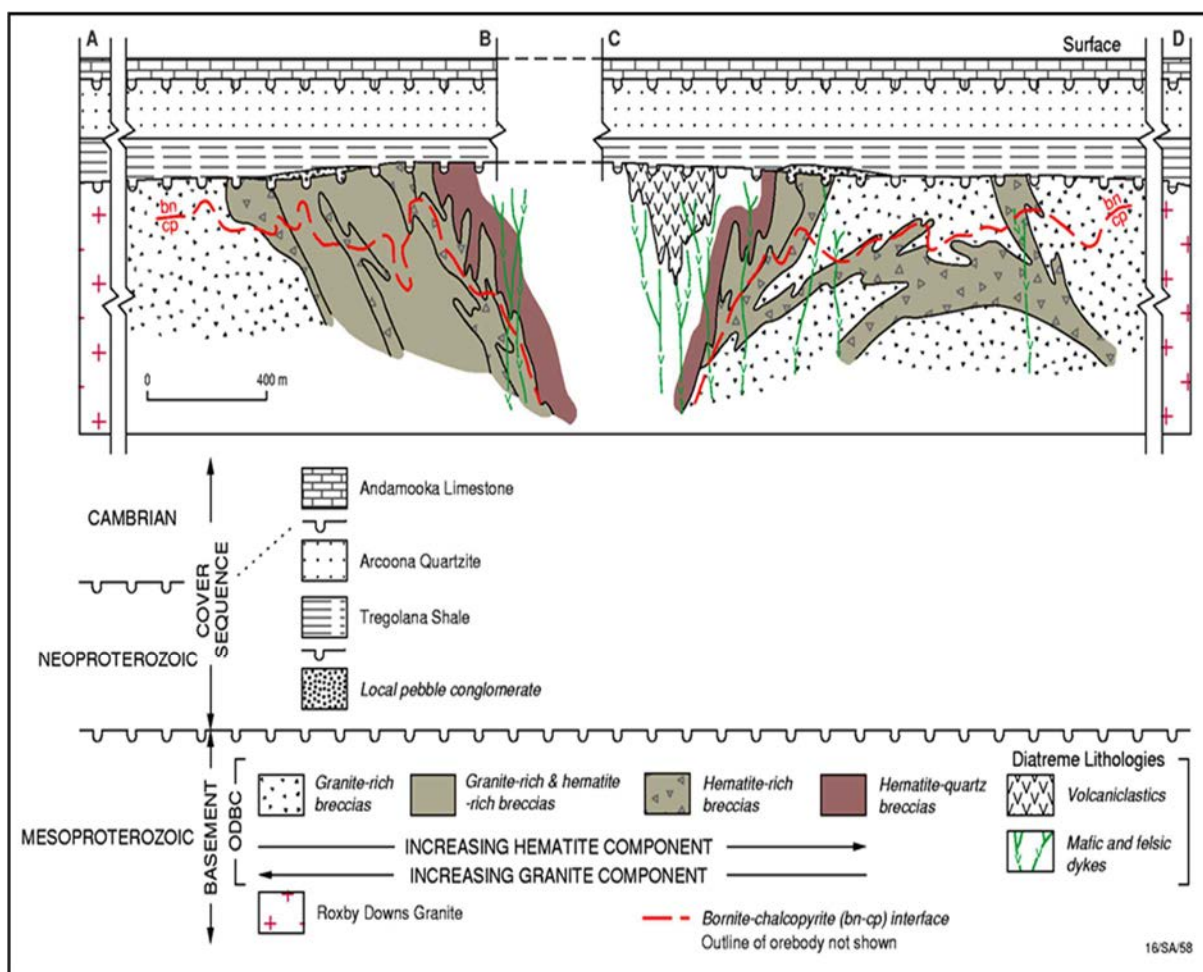


FIG. 45. Simplified geological cross-section of the ODBC [138]. Refer to Fig. 44 for location of section A–B (reproduced with permission).

### 3.4. VOLCANIC-RELATED DEPOSITS

#### 3.4.1. Definition

Volcanic-related uranium deposits occur mainly within or close to caldera complexes in the form of predominantly structure-bound with minor stratabound mineralization in extrusive and subvolcanic rocks. The uranium deposits of the Streltsovsk district (Russian Federation) and of the Dornod district (Mongolia) are the most important examples of caldera related volcanic deposits. Other examples include the Xiangshan district (China), the Macusani district (Peru), the Kurišková and Novoveská Huta deposits (Slovakia) and the deposits of the McDermitt caldera (USA) (Table 16).

As of 2015, 138 volcanic deposits/districts were listed in the UDEPO database. The world's largest district is the Streltsovsk district (Russian Federation), which hosts 20 deposits and resources totalling 270 000 tU. Since the discovery of the district in 1963, 144 000 tU have been produced from 10 deposits, with 1977 tU produced in 2015. Limited production is recorded from volcanic deposits in China.

TABLE 16. PRINCIPAL VOLCANIC-RELATED DEPOSITS/DISTRICTS (as of 31 December 2015)

Deposit/district	Country	Resources (tU)	Grade (% U)	Status
Streltsovskoye	Russian Federation	62 166	0.181	Production
Dornod district (12 deposits)	Mongolia	46 000	0.10	Dormant
Argunskoye	Russian Federation	37 438	0.178	Operating
Antei	Russian Federation	30 754	0.293	Operating
Xiangshan district (20 deposits)	China	29 000	0.10	Operating
Manybaiskoye	Kazakhstan	21 400	0.086	Depleted
Oktyabrskoye	Russian Federation	19 180	0.264	Operating
Chilcuno–Chico	Peru	16 229	0.026	Exploration
Kurišková	Slovakia	15 860	0.36	Dormant
Gurvanbulag district (12 deposits)	Mongolia	14 620	0.16	Exploration
Aurora district (5 deposits)	USA	14 580	0.021	Exploration
Olovskoye	Russian Federation	13 300	0.083	Development
Malo–Tulukuevskoye	Russian Federation	12 789	0.183	Development
Yubilenoye	Russian Federation	9 217	0.183	Operating
Shirondukuevskoye	Russian Federation	8 690	0.181	Dormant
Tantamaco	Peru	8 331	0.0186	Exploration
Colibri	Peru	7 915	0.019	Exploration
Daba	Kazakhstan	7 000	0.060	Dormant
Anderson Mine	USA	6 460	0.046	Dormant
Novoveská Huta	Slovakia	6 355	0.099	Dormant

### 3.4.2. Geological setting

Caldera related volcanic deposits are located within or in close proximity to calderas that are filled with complex assemblages of mafic to felsic volcanic rocks and intercalated clastic sediments. Mineralization in volcanic deposits is largely structure-bound, occurring as veins and stockworks in volcanic intrusions, diatremes and flows or bedded pyroclastic units. Smaller ore accumulations occur in stratabound mineralized zones as disseminations and impregnations in permeable and/or reactive flows, flow breccias, tuffs and intercalated pyroclastic and clastic sediments. Uranium mineralization may also extend into underlying and adjacent basement rocks, where it is concentrated in fractured granite and metamorphic rocks [19].

Three main subtypes of volcanic deposits are distinguished:

- (i) Structure-bound deposits include: (a) infill veins or stockworks in volcanic intrusions, diatremes, flows or bedded pyroclastic units and (b) surficial fracture fills in similar lithologies (Fig. 46). Deposits are hosted by mafic to felsic volcanic rocks in calderas

underlain by granite. They consist of structurally controlled orebodies consisting of veins found intermittently at several levels in stratified mafic to felsic volcanic sheets intercalated with terrestrial sediments. Intense fracturing and brecciation along steeply and shallowly dipping faults control the location and the dimensions of the orebodies. Rocks along these structures exhibit polystage alteration and mineralization is polymetallic. Uranium is associated with Mo–Fe–Pb-sulphides, quartz, carbonates, phyllosilicates, albite and fluorite. Mineralization may be disseminated, banded, streaky, massive and occur in irregularly shaped veins, stockworks and tabular, stratiform ore lodes of highly variable dimensions. Type examples correspond to the deposits of the Streltsovka caldera (Russian Federation);

- (ii) Stratabound deposits consist of disseminations and impregnations hosted in permeable and/or reactive flows, flow breccias, tuffs and intercalated pyroclastic and clastic sediments. Stratabound mineralization may be present in intracaldera (Aurora deposit, McDermitt caldera (USA); Yubilenoye, Streltsovka caldera, (Russian Federation) or exocaldera (Novazza (Italy), Margaritas (Mexico)) host environments. In the latter type, the volcanic rocks are mixed with non-volcanic clastic sediments;
- (iii) Volcano-sedimentary deposits are found in exocaldera settings and consist of carbonaceous sediments with a tuffaceous component. Widespread, peneconcordant low grade (50–200 ppm U) uranium accumulations associated with anomalous V, Mo, Li, F, B, Cu and Ni encompass irregular shaped zones of higher grade mineralization (Anderson Mine (USA)).

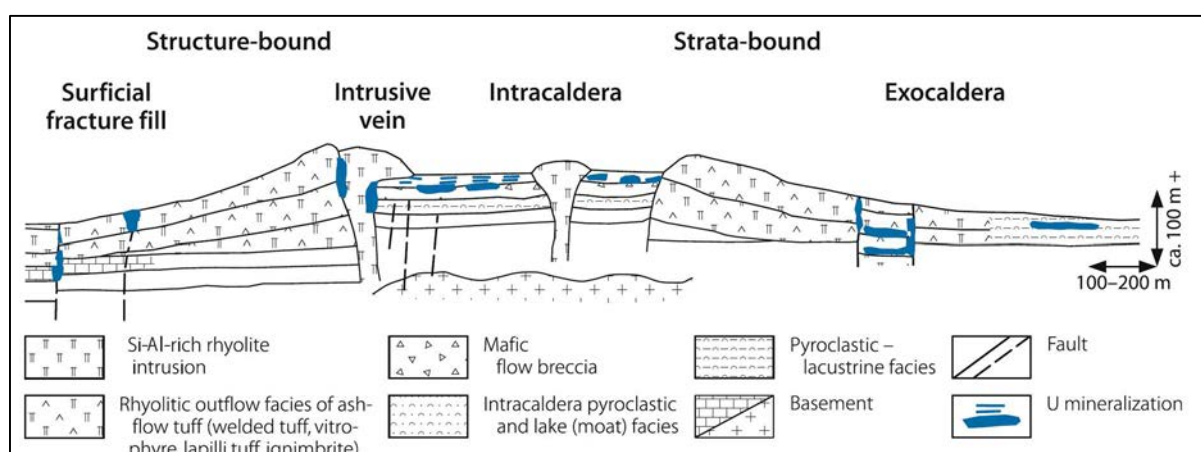


FIG. 46. Schematic representation of different volcanic-related uranium deposits [19] (reproduced with permission).

The Streltsovka caldera is the largest volcanic-related uranium orefield. It has a diameter of 20 km and was filled during the Late Jurassic with a succession of volcanic and interlayered sedimentary horizons more than 1 km thick. Similar uraniumiferous volcanic districts are known in eastern and central Asia. They all occur in caldera-like features filled by alternating basaltic–andesitic–rhyolitic lava flows with clastic and pyroclastic intercalations. These units may be cut by hypabyssal intrusions. The volcanic centres are found within cratonic regions, frequently of granitic nature. The mineralization is controlled by deep structures and characterized by a U–Mo–F association. The main districts in Asia are the Chatkalo–Kumarinski district (Uzbekistan) within Permian–Jurassic formations, the Betpak Dala area (Kazakhstan) within Silurian–Devonian rocks, the Mardai–Dornod district in Upper Jurassic–Lower Cretaceous formations and the Late Jurassic Xiangshan caldera (China).

In other parts of the world, important uraniumiferous volcanic districts are represented by the McDermitt caldera (USA), which hosts the Aurora deposit, the Macusani district in Peru and the Kurišková–Novoveská Huta deposits in Slovakia.

Volcanic rocks occur mainly in four types of geotectonic environment: (i) mid-ocean ridges where two oceanic plates diverge; (ii) subduction zones at convergent margins of two plates either in oceanic arc or continental arc settings; (iii) intra-plate 'hot spots', usually beneath oceanic crust but may also be present under continental plates, and (iv) intracontinental rift settings.

Deposits show no age restrictions. They range from the Palaeoproterozoic (Duobblon (Sweden)) to recent (Latium (Italy)).

### 3.4.3. Metallogenesis

The main uranium minerals, pitchblende and coffinite, are commonly associated with molybdenum sulphides and pyrite. Uranium may also be adsorbed onto or incorporated into various other host minerals (such as uranium-bearing clay minerals or uraniferous opal). Geochemical enrichments include minor As, Bi, Hg, Li, Pb, Sb, Sn and W. Associated gangue minerals include fluorite, quartz, carbonates, tourmaline and topaz (reflecting enrichment of volatiles such as F and B), as well as baryte and jarosite.

In many cases, the host rocks are interpreted to be the source of the uranium. Glassy and unwelded volcanic rocks are better sources than crystalline or welded rocks. Matrix bound uranium is easily liberated by devitrification in reaction to both volcanic hydrothermal (hot spring and fumarole) and supergene meteoric waters, which then transported the uranium to sites of deposition either in porous volcanic beds or fractures. Uranium may also be introduced by volcanic hypogene fluids. Uranium transporting solutions are believed to be oxidized and slightly acidic, containing F, CO<sub>2</sub> or other complexes which facilitate transport of uranium. Suggested processes for precipitating uranium include reduction and adsorption, associated with neutralization by wall rock interaction and boiling or evaporation of fluids. In near surface deposits, uranium precipitation often occurs at the water table [19].

Volcanic occurrences may also be important as potential uranium sources for other types of deposit, particularly those of the sandstone type. Rhyolite is the main rock type, occurring as layers of ash fall tuff or flows (ignimbrites), often extending over thousands of square kilometres. If such rocks are highly enriched in uranium they may represent a very important uranium source for hydrothermal deposits associated with the caldera system or for sandstone-hosted deposits in continental basins. As the pyroclastic material may be dispersed by the atmosphere over several tens to hundreds of kilometres, this type of volcanism may represent a significant uranium source in sedimentary basins located distant from the volcanoes. Caldera complexes, containing large amounts of highly fractionated rhyolitic pyroclastic material, represent the best setting for the genesis of volcanic-related uranium deposits [45].

### 3.4.4. Description of selected deposits

#### 3.4.4.1. *The Kurišková deposit (Slovakia)*

##### Introduction

The Kurišková deposit was discovered in 1985. It is located in eastern Slovakia, approximately 10 km north-west of Košice (Fig. 47). Kurišková (also known as Jahudná) is classified as a volcanic type deposit of structure-bound, polymetallic U–Mo mineralization [113].



FIG. 47. Location map of the Kurišková uranium project (adapted from Ref. [147].)

Since 2005, the Kurišková project has been operated by Tournigan Energy Ltd. Using a cut-off grade of 0.05% U, Rozelle [147] reports in situ resources of 7900 tU at 0.48% U and 1250 t Mo at 0.032% Mo in the indicated category, and of 6740 tU at 0.19% U and 1100 t Mo at 0.03% Mo in the inferred category. In 2011, total resources were estimated at 15 843 tU at an average grade of 0.37% U. Exploration is still ongoing.

At the beginning of 2012, Tournigan Energy changed its name to European Uranium Resources Ltd. The company was planning to complete a feasibility study on the Kurišková project, but in 2015, a proposed extension to the exploration licence was not granted by the Government of Slovakia.

Multiple exploration targets are present on the Kurišková licence area, which have the potential to increase the resources. In addition, European Uranium also owns the nearby Novoveská Huta deposit (6355 tU at 0.01% U).

#### Geological setting

The Kurišková deposit area is located in the south-eastern North Gemer Tectonic Zone and is underlain by the Permian Kropachy Group. Quaternary fluvial sediments and soil, 1–5 m thick, cover the Permian suite [147–153].

The Kropachy Group includes the following three formations, each of which is up to several hundred metres thick:

- (i) *Novoveská Huta Formation*: Lagoonal sediments containing evaporites constitute the upper portion and continental clastic sediments the lower portion of this formation;
- (ii) *Petrova Hora Formation*: The upper section consists of a 40–100 m thick unit of fine-grained, dark green meta-andesite and metadacite, and fine-grained metatuff with dispersed

pyrite. A 3–20 m thick layer of green pyritiferous slate grading downwards into violet slate with carbonate concretions is intercalated in the upper section of the metavolcanic rocks. Basal rocks of the meta-andesite unit are silicified along the contact with the underlying metatuff. The meta-andesite unit contains some uranium mineralization close to the violet slate horizon, while an andesitic metatuff horizon, 1–10 m thick, situated at the base of the Petrova Hora Formation forms the main uranium host;

- (iii) *Knola (Knolske) Formation*: Sandstone/quartzite and slate of the Markusovce Member form the uppermost horizon of this formation and constitute the footwall of the Kurišková deposit. An apparent fault contact marks the interface between the Petrova Hora Formation and the subjacent Knola (Knolske) Formation.

The Permian rocks are folded, strike south-east and dip variably to the south-west. Both high angle and low angle faults cut and segment the area and deposit into blocks. Wall rocks of fine-grained andesite and andesitic tuff are variably altered by argillization, carbonatization, chloritization, haematitization, sericitization, silicification and decomposition of ilmenite and magnetite. Alteration is manifested as both pervasive and moderate to strong with development of veinlets [148, 153].

Coarse-grained quartz occurs as irregularly distributed clusters in wall rocks and as selvages along carbonate veins. Pyrite and chalcopyrite are ubiquitous in intervals of quartz veining and silicification. Carbonates (calcite, ferroan dolomite and siderite) are pervasively distributed as foliation oriented veinlets and disseminated in the adjacent wall rocks. Carbonate veins are frequent along major faults. Selvages of carbonate veinlets often consist of quartz and, locally, tourmaline. Haematite impregnates the ubiquitously mylonitized wall rocks and is typically pervasively distributed throughout the matrix of mineralized intervals. Additional alteration minerals include apatite, Fe–Ti oxides, leucoxene, rutile and zircon [113].

#### Mineralization

As delineated in 2009–2010, the lateral extents of ore grade mineralization define a zone 550 m wide and over 650 m long. The zone is bounded to the south-east by ENE–WSW trending faults and to the north-east by a thrust fault. The deposit remains open at depth. Faults segment the deposit into blocks.

Four mineralized zones have been identified at the Kurišková deposit as shown in Table 17:

- (i) Main Zone;
- (ii) Stockwork Hanging Wall Zone;
- (iii) Metatuff–tuffaceous Zone;
- (iv) Zone 45.

TABLE 17. KURIŠKOVÁ DEPOSIT ORE ZONES AND IN SITU URANIUM AND MOLYBDENUM RESOURCES  
(status as of May 2010, based on a cut-off grade of 0.05% U) [147])

Ore zones	Resources							
	Indicated				Inferred			
	tU	% U	t Mo	% Mo	tU	% U	t Mo	% Mo
Main Zone	7708	0.482	1056	0.069	4740	0.205	353	0.015
Stockwork Hanging Wall Zone					1899	0.167	504	0.049
Zone 45	192	0.574	200	0.607	103	0.332	242	0.756

The Main Zone is the largest, hosting approximately 85% of the estimated total uranium resources of the deposit. The Stockwork Hanging Wall Zone and Zone 45 account for the remainder. No resource estimate has been prepared for the Metatuff-tuffaceous Zone (Figs 48–50).

The Main Zone consists of structure controlled, tabular U–Mo mineralized lenses hosted in andesitic metatuff at the base of the Permian Petrova Hora Formation. Mineralization extends locally into hanging wall andesite. The Main Zone strikes NW–SE and dips 70° SW in the upper section and decreases to 45° SW in the lower section. Transverse and thrust faults displace the ore zone by up to several tens of metres. Mineralization occurs in the form of veins, stringers and disseminations. Uraninite is the principal uranium mineral, along with minor coffinite. Molybdenite is abundant. Carbon (inorganic) contents may be as high as 6%. Uranium minerals occur as disseminations along fractures and to a lesser degree in quartz–carbonate–haematite–phyllosilicate assemblages. Mineralization is generally continuous and of high grade. It extends over a thickness of 2–8 m for a strike length of more than 650 m, and from about 200 m below the surface to an explored depth of 550 m. Where transected by thrust faults, uranium has been redistributed and upgraded [113].

The Hanging Wall Zone is hosted by meta-andesite of the Petrova Hora Formation. These lenses occur about 10–50 m stratigraphically above the tabular Main Zone. The ore hosting interval is 1–10 m, locally up to 20 m thick and peneconcordant with stratigraphy. Orebodies are lenticular in shape, as much as 4.5 m thick, and have an internal stockwork structure composed of irregular clusters of veinlets and stringers ranging from several millimetres up to 15 cm in thickness [148]. As shown in Table 17, grades are generally lower than in the Main Zone. A halo of weaker mineralization surrounds the orebodies. Uranium minerals, mainly coffinite and lesser quantities of uraninite, are concentrated along the edges of irregular quartz–carbonate stringers with a width of 1–5 mm and locally up to 5 cm. Molybdenite is less abundant than in the Main Zone. Zone 45 contains high grade uranium and molybdenum mineralization (averaging 0.33–0.57% U and 0.6–0.75% Mo) in an upper layer of the Petrova Hora Formation composed of psammite intercalated with tuffaceous metavolcanic rocks. The currently (2010) defined ore zone is 1–1.5 m thick, extends 100 m down-dip and 140 m along strike, although it remains open along strike. Locally observed fault gouge may indicate a tectonic control on the ore emplacement. The host unit is locally rich in carbonate and commonly contains pyrite.

In the Kurišková deposit, uraninite (pitchblende?) and coffinite are the principal uranium minerals with minor U–Ti oxides (described as brannerite and orthobrannerite). Associated metallic minerals include haematite, molybdenite, pyrite and minor to trace amounts of Cu–Ni–Pb sulphides and sulpharsenides. Gangue minerals include apatite, baryte, carbonates and quartz [113, 151].

Uraninite is: (i) largely rimmed by pyrite; (ii) coats and replaces chalcopyrite and tennantite; (iii) shows a notable affinity to the margins of small apatite stringers and (iv) tends to replace haematite. Uraninite occurs: (i) most commonly in selvages of quartz–carbonate–sulphide veinlets; (ii) locally, together with sulphides in breccia cement; (iii) as micro-veinlets and (iv) as irregularly distributed aggregates distal from veins.

Coffinite occurs as: (i) disseminated grains and aggregates; (ii) small veinlets in pinkish altered rocks and, (iii) intergrowths with uraninite. Hair-like stringers of coffinite cut pyrite grains and cross-cut quartz–carbonate–sulphide veins.

Orthobrannerite (U–Ti oxide phase without Th and Ce) forms euhedral crystals and aggregates and occurs in higher grade ore with uraninite, coffinite and molybdenite. Chalcopyrite and molybdenite replace orthobrannerite.

Molybdenite is present as: (i) minute intergranular inclusions apparently affiliated with uraninite clots and stringers, and (ii) rare flakes disseminated in wall rocks.

Pyrite is commonly present as euhedral grains and as stringer veinlets which often contain disseminated U–Ti minerals. Pyrite occurs as: (i) a ubiquitous constituent of uranium mineralization,

in which it partially coats uraninite and base metal sulphides; (ii) stringers within quartz–carbonate veins; (iii) along vein selvages, and (iv) fine disseminations in the host rocks.

Quartz is present in two generations. Quartz I is coarse-grained and forms polycrystalline aggregates rimming carbonate veins. Quartz II is fine-grained, overgrows quartz I and occurs in pygmatic bends. Carbonate also occurs in two stages. Carbonate I is replaced by carbonate II and transected by quartz II stringers. Veins of iron-bearing dolomite and quartz with associated chalcopyrite and tennantite cut across U–Mo mineralization.

Apatite is a constituent of uranium ore and is usually associated with carbonate. Higher grade ore contains thin stringers and isolated grains of apatite. Sericite is found as selvages along some apatite veinlets and dissects apatite as hair-like stringers. Baryte commonly occurs in haematitic host rocks and is replaced by uraninite and coffinite. It is also found enclosing minute uraninite grains and is often overgrown by chalcopyrite and quartz.

Rozelle [147] reports uraninite ages in the range 200–25 Ma.

#### Metallogenic aspects

Uranium mineralization of the Kurišková deposit is of epigenetic origin and both structurally and lithologically controlled. However, the actual factors governing the metallogenesis are largely enigmatic [113].

The influences of host rock geochemistry and physical competency on ore precipitation and concentration remains unknown. As currently understood, the lithological control appears more mechanical than chemical. The favourable fracture systems required as pathways for ore forming fluids and for ore deposition are generally restricted to specific meta-andesitic flow and pyroclastic layers. These units reacted to tectonic stress by brittle deformation, with pervasive cataclasis and stockwork development, while phyllitic metasedimentary rocks reacted in a ductile fashion or remained unbroken.

Moran et al. [151] note that multiple tectonic and related hydrothermal processes caused repeated remobilization of uranium and other elements, resulting in several generations of mineralization.

The destruction of ilmenite and magnetite indicates that alteration fluids were reducing and possibly that ore forming processes involved reduction, as suggested by co-precipitation of pyrite and uraninite. The apparent coexistence of apatite and carbonate with uranium minerals, as described from Kurišková and other fracture hosted volcanic deposits in Slovakia by Rojkovič [153] may indicate that uranium was transported as carbonate and/or phosphate complexes.

Kurišková is in the same geological/geotectonic setting as the nearby Novoveská Huta deposits, and the mineralogy and alteration of these deposits are similar, except for the distinctly higher uranium grades at Kurišková. Therefore, the ore forming conditions and sequence of mineralizing events postulated by Rojkovič [153] for the Novoveská Huta deposits may also apply to Kurišková [113].

The geological setting of the Kurišková deposit resembles, to some extent, those of volcanic type uranium deposits described in Russian literature, such as the U–Mo deposits of the Streltsovsk caldera in the Russian Federation and in the Dornod district in Mongolia. Therefore, metallogenic concepts for these latter deposits may also apply to the genesis of Kurišková [113].

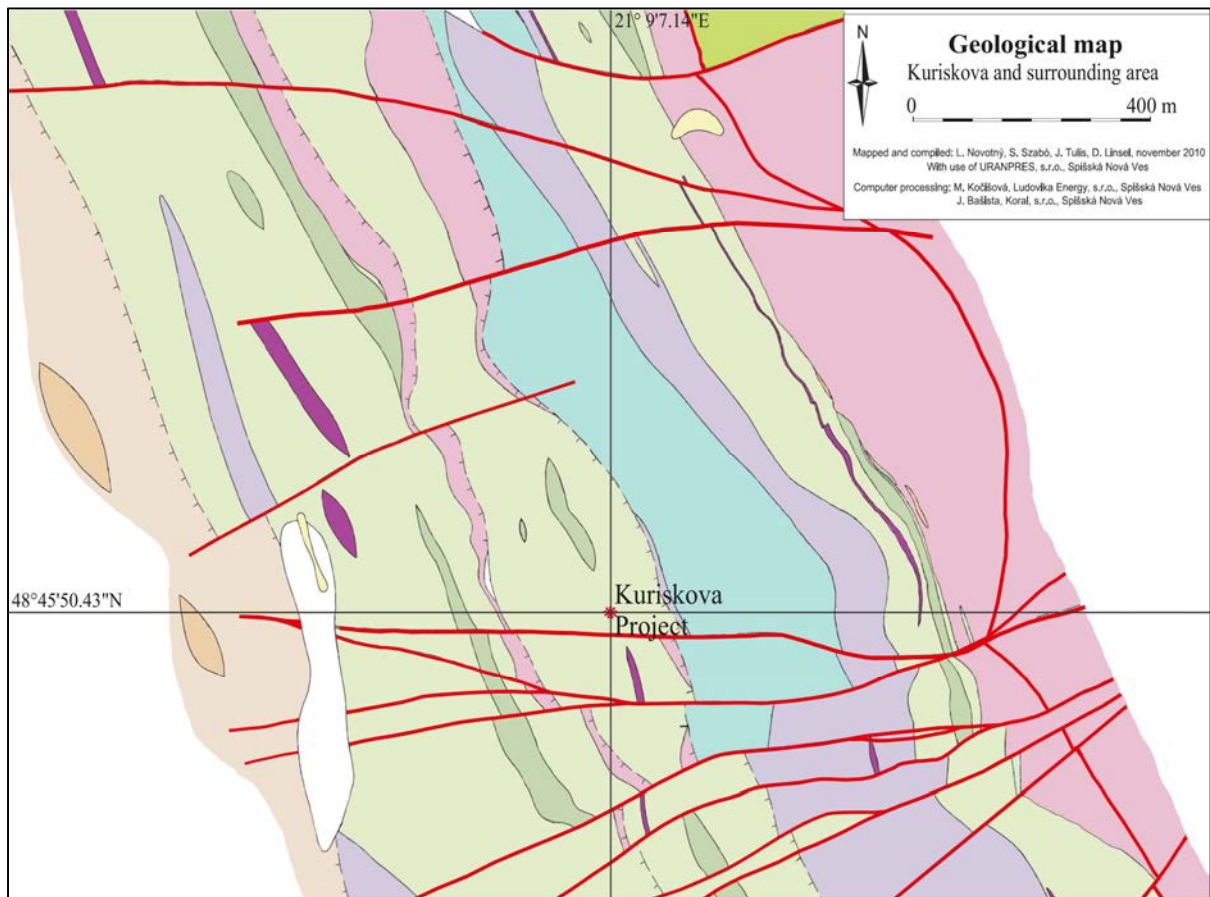


*FIG. 48. Kurišková deposit, surface geology showing the intricate structural setting and principal lithostratigraphic units of the deposit area (adapted from Ref. [147]).*

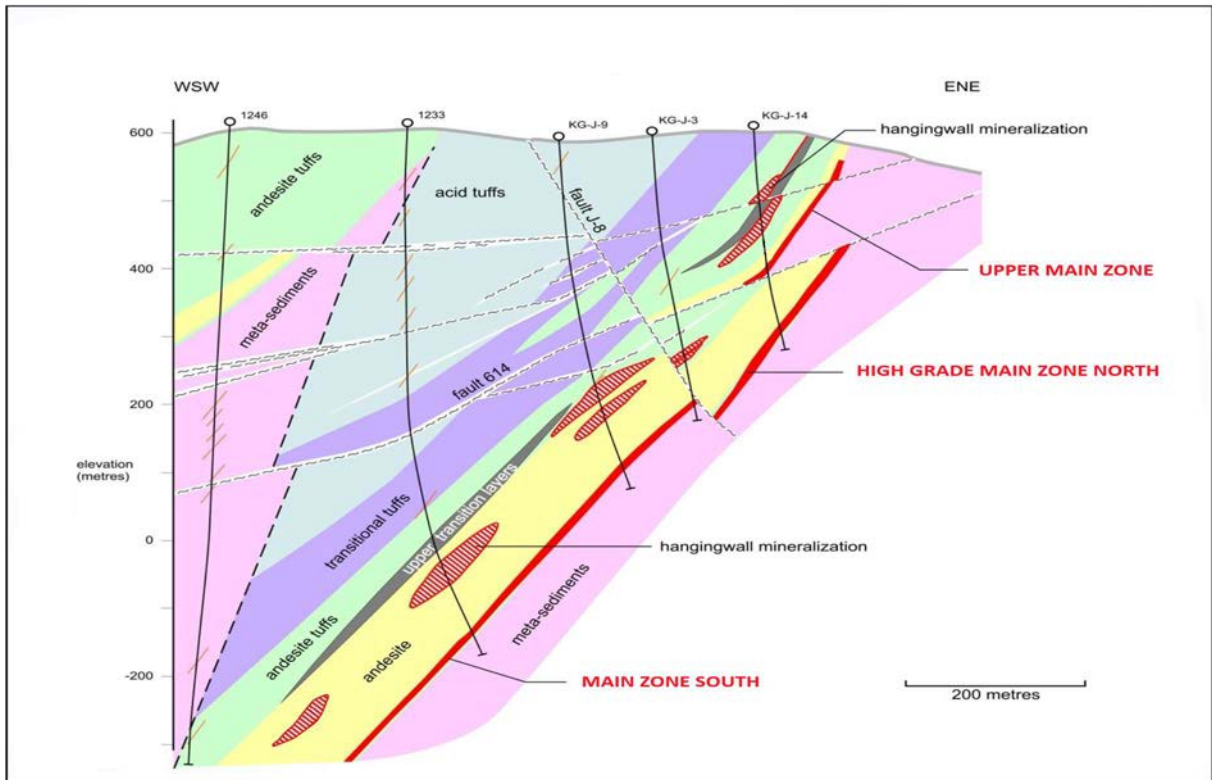


FIG. 49. Kurišková deposit: schematic cross-section (adapted from Ref. [154]).

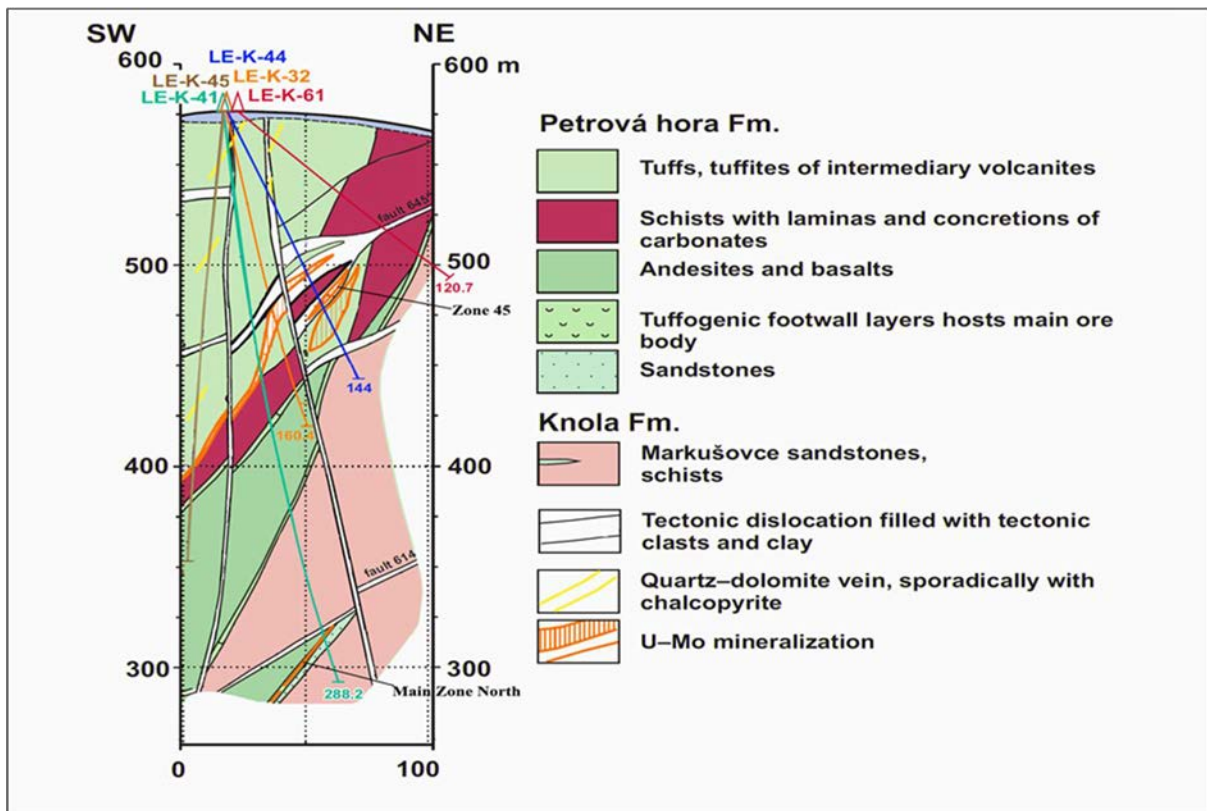


FIG. 50. Kurišková deposit, WSW-ENE section across the upper part of the deposit illustrating the perched position of Zone 45 (adapted from Ref. [149]).

#### 3.4.4.2. Deposits of the Xiangshan district (China)

##### Introduction

The Xiangshan uraniumiferous volcanic district is located within the Gan-Hang Volcanic Belt, which is the largest and most prominent volcanic-related uranium district in China [19]. The belt is 50–80 km wide and extends for about 600 km. The resources of the belt (30 000 tU) are situated within three districts: (i) Xiaoqiuvuran/Dazhou to the north-east; (ii) Shengyuan/Yingtang in the central part and (iii) Xiangshan to the south-west (Fig. 51).

The volcanic uranium deposits are situated in down-faulted or volcanic collapse basins with flows, pyroclastic rocks, fluviolacustrine sedimentary rocks and subvolcanic intrusions that have been affected by volcanic hydrothermal alteration. On the basis of their emplacement environment, they can be divided into four subtypes: (i) volcanic breccias pipes; (ii) subvolcanic; (iii) altered fracture zones, and (iv) interstratified cataclastic zones.

The Xiangshan caldera (Fuzhou orefield) covers an area of about 300 km<sup>2</sup> and contains 20 uranium deposits and major occurrences. Typical deposits include Hengjian, Zoujiashan, Baquan and Yunji (Fig. 52). Original reported resources are in the order of 26 000 tU at an average grade of 0.10–0.30% U.

##### Geological setting

The Xiangshan caldera is dome shaped as a result of volcanic eruptions, effusions and large scale, late extrusions. The basement to the caldera is composed of Precambrian schist and phyllite, Caledonian porphyritic granitoid and gneissic granite, Indosinian granodiorite, Lower Carboniferous siltstone and quartz arenite (Huashanling Formation) and Upper Triassic quartzo-feldspathic sandstone and shale with coal (Anyuan Formation). The upper strata consist of Upper Jurassic felsic to intermediate volcanic rocks with thin beds of intercalated sediments, with two volcanic cycles represented by the Daguding (volcanic cycle 1) and Ehuling (volcanic cycle 2) Formations. The north-western part of the basin is overlapped by Cretaceous down-faulted red bed basins with sandstone and conglomerate [19].

Lithologies of the first volcanic cycle comprise rhyolitic tuff, vitric tuff, ignimbrite, late stage rhyodacite lava (169–158 Ma), sandstone and tuffaceous sandstone. The second volcanic cycle followed after collapse and caldera development, with eruption of rhyolitic ignimbrite, rhyolitic crystal tuff, deposition of sediments and, finally, large scale extrusion of porphyritic rhyolite (150–140 Ma). The latter is prominent in the centre of the caldera and forms the main part of the dome shaped edifice of the volcanic complex. The latest magmatic activity (135–114 Ma) is of subvolcanic nature, consisting of stocks, veins and dykes occurring along peripheral faults.

The major faults affecting the basement trend E–W, NE and N–S, and are long lived active faults. Those developed in the cover strata trend mainly NE with subordinate NW orientations.

Mineralized areas exhibit a variety of alteration types. Pre-ore alteration is widespread and includes albitization and hydromica formation with lesser kaolinitization, dickitization, montmorillonitization and silicification. Both the albite and hydromica slightly predate uranium mineralization. Albitization is found near the surface at the northern and eastern margins of the caldera where it surrounds lodes with thorium free or thorium poor uranium mineral assemblages. Syn-ore alteration overprints the albitization and grades outwards from haematization at the ore lodes to carbonatization and chloritization. Hydromica alteration envelops lodes with U–Th ore near the surface in the western part of the caldera. Also at this locality, syn-ore alteration consists of fluoritization and linear zones of hydromica at the centre flanked by haematization. A vertical zonation of alteration is present along the western margin of the caldera, with an upper, planar zone of hydromica transitioning to albitization at depth [19].

## Mineralization

In the Xiangshan district deposits are structurally controlled and consist of many large, high grade ore zones persisting to significant depths (900 m). The orebodies consist mainly of disseminated uranium minerals concentrated within steeply dipping veins and stockworks (Fig. 53). Ore is mainly concentrated at the intersection of fracture zones with volcanic structures such as ring, collapse and crater structures and also in breccia pipes and diatremes. Host rocks are predominantly porphyries and lavas of rhyodacite composition. The uranium deposits exhibit a striking affinity to volcanic strata that immediately overlie the Proterozoic metamorphic basement [19].

Veins are distributed over vertical intervals exceeding 300 m. They range from a few centimetres to a few metres wide, persist laterally and vertically from a few metres to a hundred metres and contain a few tonnes to several hundreds of tonnes of uranium. Individual veins are of relatively small size, but they often group together in clusters to form sizable deposits. A large proportion of the resources of the Xiangshan orefield is hosted in veins.

Ore types have been subdivided into two groups based on thorium abundance [19]:

- (i) An early thorium free or thorium poor group with U–REE (Baquan deposit), U–Mo (deposits at the western edge of the caldera), U–Pb–Zn–Ag (Shazhou and Niutoushan deposits) and U–P (Yungi deposit) mineral assemblages;
- (ii) A later thorium- and uranium-rich group with a U–Th–Mo–P–REE mineral assemblage (Zoujiashan and Hengjian deposits). The latter assemblage forms the most significant ore lodes in the Xiangshan orefield. An age of  $115 \pm 0.5$  Ma was obtained by U–Pb dating of pitchblende for the thorium free group hosted in rocks altered by pre-ore albitization in contrast to  $98 \pm 0.8$  Ma for the U–Th group hosted in rocks showing hydromica alteration [19].

Deposits with the U–Th–Mo–P–REE assemblage occur preferentially in the western and northern parts of the Xiangshan caldera and are controlled by NE–SW basement faults that intersect annular structures of the caldera. Deposits of this group also contain small amounts of Be, Cd, Ni, Pb, Sn, Sr and Zn. The total REE content varies in the range 300–9000 ppm. Pitchblende, thorium-bearing pitchblende with up to 12% ThO<sub>2</sub> and brannerite are the principal uranium minerals. Other radioactive minerals include coffinite, thorium-rich brannerite, uraniferous titanite, wisaksonite, uraniferous thorite, uraniferous auerlite, uraniferous apatite, thorite and thorianite. Sulphide minerals are common and include pyrite, marcasite, molybdenite and ilsemannite. Host rocks are altered by hydromica and fluorite, often overprinted by collophane.

Deposits of the various early mineral assemblages are controlled by faults, fracture zones and often by intersections of major faults. Host rocks include rhyolite flows, rhyodacite, subvolcanic porphyry bodies, crypto-explosive breccias and, to a lesser degree, metasedimentary and sedimentary rocks adjacent to subvolcanic porphyry bodies. Deposits consist predominantly of steeply dipping veins, lenses and, locally, pods. They range from a few tens to a few hundred metres in length, 1–8 m in thickness and have vertical extents of 300–400 m, locally, to depths of 900 m [19].

## Metallogenic aspects

Zhou Weixun et al. (in Dahlkamp [19]) propose two possible models for the metallogenesis of uranium deposits in the Xiangshan caldera: a ‘porphyry model’ and a ‘down-faulted red bed basin model’. The porphyry model postulates a uranium origin from a fractionated fluid related to secondary boiling in a magma chamber after crystallization of the porphyries. In the down-faulted red bed basin model, subsequent processes mobilized uranium from consolidated volcanic rocks in the course of pre-ore alteration that formed planar hydromica altered zones, generating late stage uranium mineralization [19].

The porphyry model is suggested for deposits with thorium free or thorium poor uranium mineralization, where porphyry stocks or dykes occur nearby or at depth. Secondary boiling occurred in a transitional magma chamber after crystallization of minerals in the porphyries. As a result of boiling, a critical to supercritical fluid enriched in alkalis, volatile components, uranium and associated elements was fractionated. The critical state, closed system changed into an open system during fracturing and formation of shattered zones and crypto-explosive pipes above porphyry bodies and in adjacent country rocks. Albitization is a characteristic pre-ore alteration. Coeval, or immediately after, a uraniumiferous hydrothermal convection cell was formed by magmatic fluids and meteoric water, followed by ore stage haematization, carbonatization and chloritization with uranium precipitation. The down-faulted red bed basin model is applied to the formation of deposits with a U–Th mineral assemblage that occurs in well developed, planar shaped hydromica alteration zones and sometimes proximal to red bed basins. This model postulates the development of a convective hydrothermal system that formed as a result of the down-faulting of red bed basins and resultant fracturing and later intrusion of trachytic dykes. The dykes provided heat and reducing gaseous components. The planar hydromica alteration process is believed to have mobilized uranium and alkalis in the volcanic intrusive complex, particularly in porphyritic rhyolites. The mineralizing solution transported the elements to fracture zones favourable for ore deposition and concentration [19].

***Favourable criteria for the presence of uranium deposits in the Gan-Hang Volcanic Belt [19] are as follows:***

- (a) The volcanic type uranium deposits are hosted by relatively small volcanic basins, mainly less than 500–1000 km<sup>2</sup> in surface area;
- (b) The uranium mineralization is mainly hosted by four volcanic assemblages: (i) the dacite and rhyolite assemblage; (ii) the andesite–dacite–rhyolite assemblage; (iii) the basalt–rhyolite bimodal assemblage and (iv) the trachyte–basalt/trachyte–andesite/trachyte assemblage. The most favourable host rocks are rhyolite and trachyte;
- (c) The uranium mineralization is constrained by the crustal maturity of the basement below the volcanic complexes. Precambrian blocks constitute the basement, having undergone multiple cycles of tectonism and magmatism. This mature continental crust, which also contains organic matter, produced felsic melts enriched in uranium. The enrichment can reach up to 5–8 ppm U compared with the 2–3 ppm U background value, resulting in a significant increase in the uranium content of felsic volcanic rocks derived from mature continental crust;
- (d) The Precambrian blocks hosting the deposits contain rocks that form in transitional settings between island arcs and mature, continental margin arcs. The host rocks are mainly felsic differentiates of calc-alkaline series in continental arcs, especially late stage eruptions;
- (e) The host continental volcanic belts consist mainly of felsic and alkaline volcanic rocks with uranium contents of more than 6 ppm;
- (f) The main target areas in the volcanic belts are uplifted blocks;
- (g) The caldera and down-faulted basins are favourable areas whereas subsiding basins are relatively unfavourable;
- (h) The basement of the favourable volcanic basin consists of granite or slightly metamorphosed rocks (especially the metamorphic rocks of Sinian–Cambrian age);
- (i) Down-faulted basins or dyke swarms (especially intermediate to mafic ones) are developed adjacent to the volcanic basins;
- (j) Regional scale faults cut the volcanic basins;
- (k) Large scale hydrothermal alteration systems (especially hydromica) are developed;
- (l) Favourable sites for uranium mineralization include the intersection of regional faults and volcanic structures, the intersection of different fault trends, the contact zones between the volcanic rocks and subvolcanic intrusions, fracture or fissure zones in subvolcanic or volcanic terrains and crypto-explosive breccia pipes;
- (m) Owing to hydrothermal alteration, the ore forming solutions were further concentrated in fault, fracture and fissure zones and the pH increased. As the result, U and Th minerals crystallized and hydromica–fluorite veins were enriched in uranium and thorium;
- (n) Hydromica, fluorite, calcite and microcrystalline quartz veins without uranium mineralization were precipitated from residues of hydrothermal solutions.

## *Description of a selected example: The Zoujiashan deposit*

### Introduction

The Zoujiashan deposit is situated in the mid-western part of the Xiangshan caldera (Fig. 52). Resources are estimated to be in excess of 10 000 tU at an average grade of 0.10–0.30% U. Mining is by underground methods (2003 status) [19].

### Geological setting

Uranium deposits are hosted by a set of faults exhibiting a distinct rhombic-pattern. Uranium mineralization is associated with volcanic collapse structures, breccia pipes and volcanic pipes. The magmatic hydrothermal solutions ascended and migrated repeatedly along faults and uranium was precipitated at favourable sites. The wall rocks consist of rhyolitic porphyritic flows and rhyodacite with a highly potassic calc-alkaline composition. These have been dated at 140 Ma (Rb–Sr isochron) and 158 Ma by U–Pb geochronology.

The ore district is controlled by faults, volcanic collapse structures and fissures. The Zoujiashan–Shidong Fault is defined by a series of roughly parallel faults defining a 10 km strike length of north-easterly orientation (030–060°) and with a north-westerly dip. A large number of subsidiary volcanic structures and plume cracks are developed on both sides of the faults as the major ore hosting structures.

Alteration includes hydromica, albite, haematite, carbonate, chlorite, fluorite and apatite. These occurred as multistage activities, including pre-ore, syn-ore and post-ore phases, and exhibit a zonation along the host structures. Uranium–thorium mineralization is accompanied by strong fluorite and hydromica alteration in the central zone, with early stage haematization along the edges and a wide pre-ore hydromica outer alteration halo

### Mineralization

Uranium at the Zoujiashan deposit is present as veins and lenses as well as some more complexly shaped bodies. More than 1000 economic ore zones have been defined; most of them are of medium to small in size. In general, the orebodies are 50–150 m long, extend 20–100 m down-dip and are 3–4 m in thickness with grades of 0.1–0.6% U (Fig. 53) [19].

On the basis of mineral paragenesis and near ore wall rock alteration, the ore at the Zoujiashan deposit can be divided into two types: (i) uranium–haematite type, comprising typically low grade ores formed in the early stages of albitization; (ii) uranium–thorium–fluorite–hydromica type containing high grade uranium (0.10–14% U) associated with hydromica. This is the most important ore type at Zoujiashan. The uranium is present as distinct uranium- and thorium-bearing phases, including pitchblende, brannerite, uranotorite, coffinite and thorium-bearing coffinite [19].

The main associated elements in uranium ore at Zoujiashan are Th, Mo, P, Pb and Sn, of which Th and Mo are economically significant. The thorium reserves amount to 1569 t at an average grade of 0.046%, and the molybdenum reserves are 794 t. The ratio of Th/U is about 0.134–0.354. The main ore textures are amorphous–colloform and euhedral types. Mineralization is present as veinlets, disseminations, impregnations and spots, zoning, netted-zones, microveinlets and breccias. Two ages of mineralization are identified: 143–139 Ma and 105–88 Ma [19].

### Prospecting criteria

There are three principal prospecting criteria:

- (i) Ore controlling structure criteria: fault zones intersecting NW and NE trending faults controlling block margins;

- (ii) Early mineralization indication: presence of early albitization in deeper parts of the fault zones;
- (iii) Proximal hydrothermal alteration: the most visible prospecting criterion is the presence of 'grey zones', which are zones of strong hydromica alteration near the orebody. Uranium–thorium mineralization may be found at depth below the central cores of these grey zones.

**Metallogenic aspects**

- (i) The Zhoujiashan–Shidong Fault may extend at depth, reaching the top of the transitional magma chamber of the Late Jurassic volcanic centre, resulting in the ascending of acidic, mineralizing solutions rich in U, Th, P, Mo, CO<sub>2</sub>, F and Cl. These phases differentiated from the cooling magma and condensed in the chamber along the fault depressurized zone;
- (ii) The ascending ore forming fluids mixed with deeply circulated groundwater. The composition of hydrothermal ore forming solutions evolved as some minerals precipitated;
- (iii) The mixed hydrothermal ore forming solutions ascend along fault zones and infiltrate laterally at the fissure zone between the rhyodacite and the porphyritic rhyolite. The K-feldspar, plagioclase and the felsic matrix of the volcanic rocks may be hydrothermally altered, resulting in irregular widespread hydromica alteration.

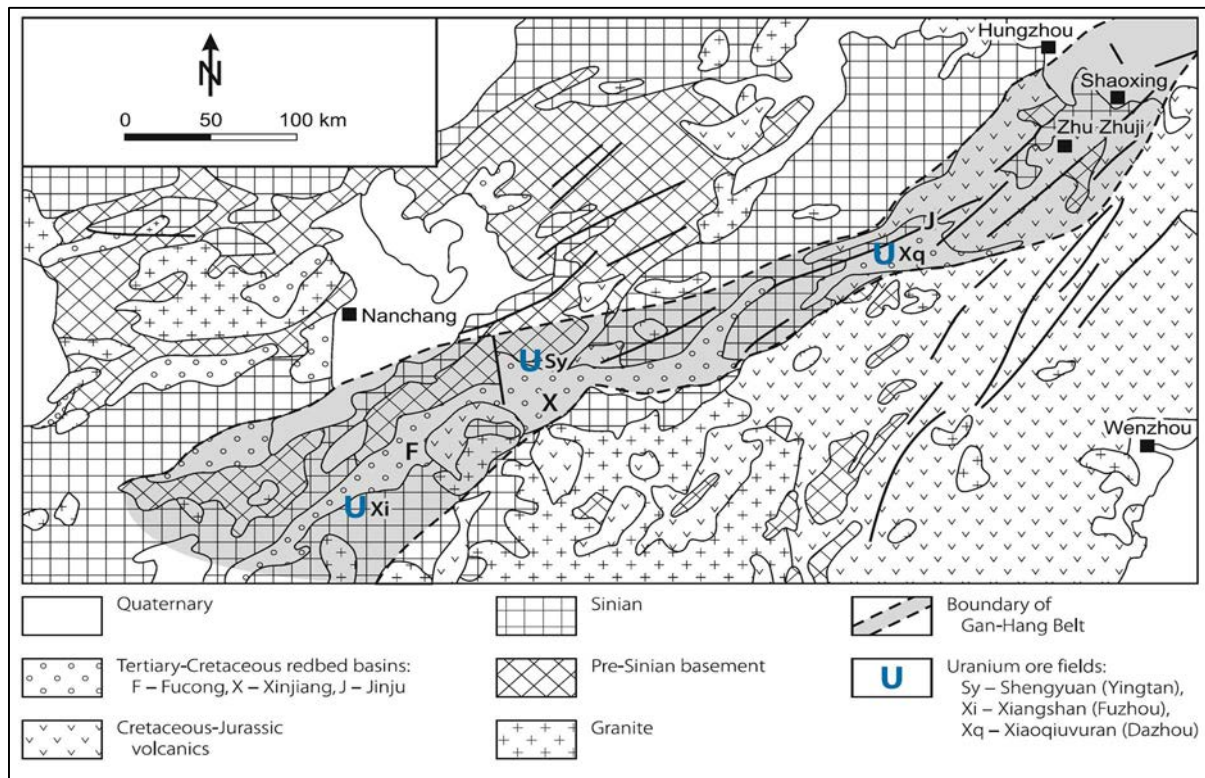


*FIG. 51. Schematic geological map of the Gan-Hang uraniumiferous volcanic belt showing the location of the major orefield (after Weixun et al. in Dahlkamp [19]) (reproduced with permission).*

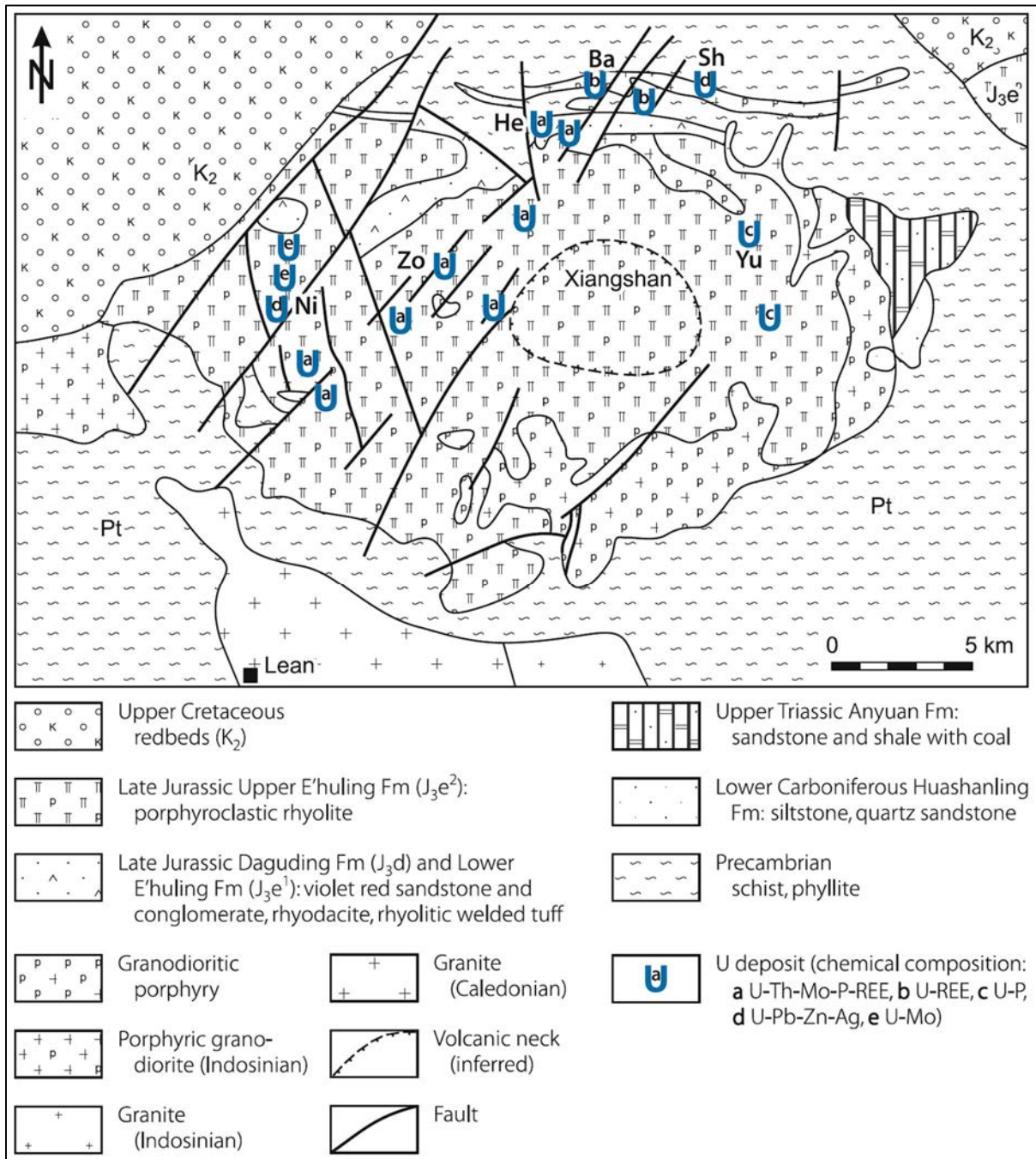


FIG. 52. Generalized geological map of the Xiangshan caldera showing the location of the uranium deposits (after Weixun et al. in Dahlkamp [19]) (reproduced with permission).

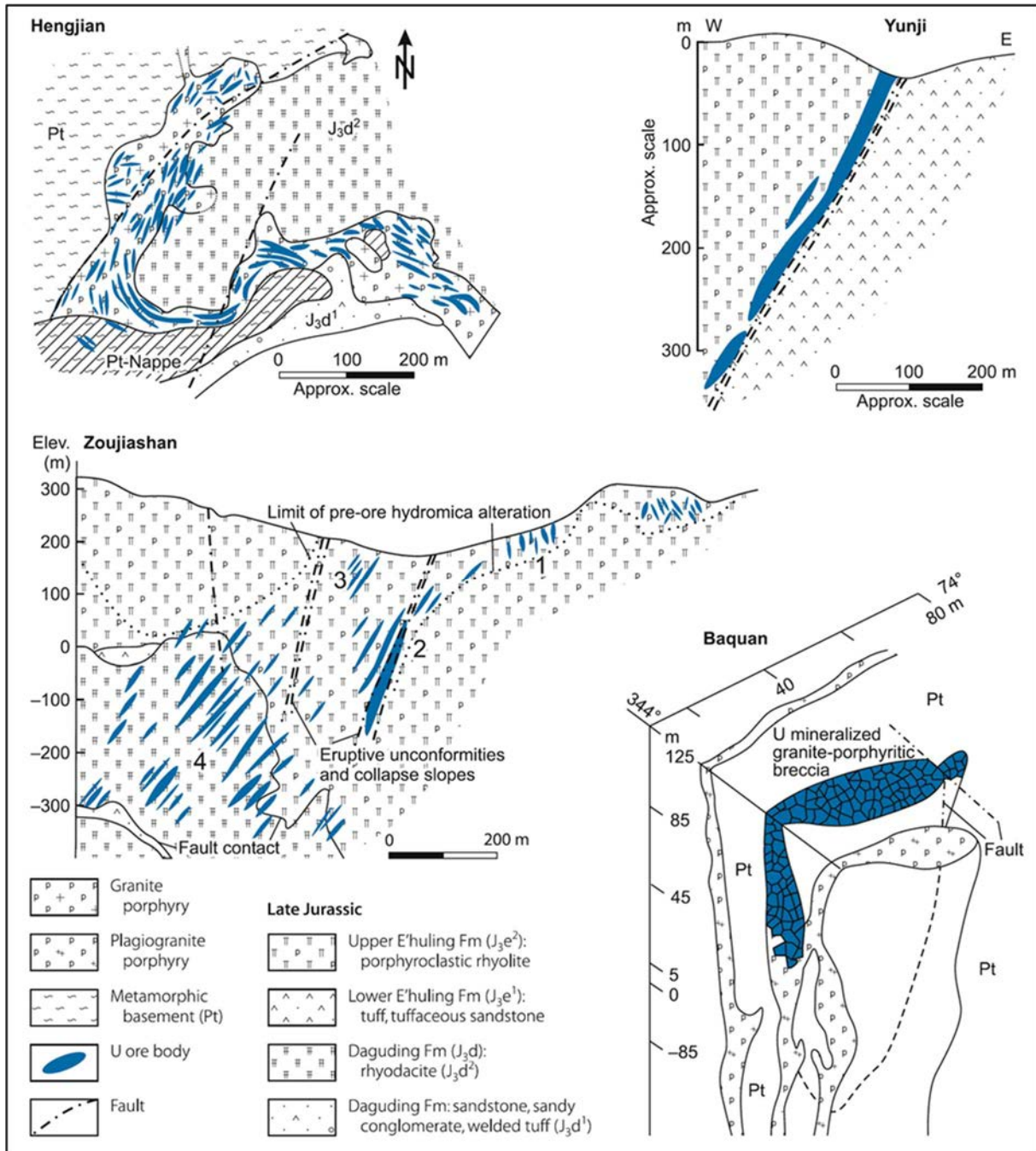


FIG. 53. Schematic geological maps and sections of typical uranium deposits from the Xiangshan caldera (after Weixun et al. in Dahlkamp [19]) (reproduced with permission).

### 3.4.4.3. Stratabound deposits of the Dornod district (Mongolia)

#### Introduction

The Mardai district, referred to as Dornod district in Russian literature, is located in north-eastern Mongolia, about 600 km east of Ulaanbaatar (Fig. 54). This district includes four uranium orefields, Dornod, Gurvanbulag, Mardaingol and Nemer, each containing several deposits or orebodies and a

number of occurrences. Resources of the four orefields total about 62 000 tU at a grade of 0.16% U. The district also contains deposits of Pb–Zn–Ag, fluorite, gold, molybdenum and tungsten. As of 1989, the Dornod, Gurvanbulag and Mardaingol orefields had been developed for underground mining and orebodies No.2a–2b of the Dornod deposit had been developed for open pit mining. Although underground mining ceased in 1992, open pit mining continued until 1995. A total of 627 tU were recovered during this period. All ore was transported 485 km by rail to the Krasnokamensk mill in Transbaikalia (Russian Federation).

The Dornod orefield is located about 90 km north of Choibalsan and contains twelve ore zones composed of one or more orebodies of monometallic, peneconcordant–tabular or vein-like to stockwork mineralization (Fig. 55). Initial resources totalled 33 000 tU at a grade of 0.17% U. Orebodies 2b and 2c were mined by open pit (130 m deep) in 1988–1995. The No. 7 orebody was mined underground (520–580 m deep) between 1989 and 1992, when exploitation ceased [17].

Khan Resources Inc, a Canadian company, owns 69% of the Dornod project. Priargunsky Mining & Chemical Enterprise (a subsidiary of ARMZ and Rosatom) and Monatom are the other partners. Khan Resources' definitive feasibility study (March 2009) demonstrated that the project was viable, on the basis of 24 780 tU in the indicated resource category, including 20 340 tU of probable reserves. Annual production of 1150 tU over 15 years was envisaged.

After suspending and then cancelling Khan's licences, the Nuclear Energy Authority announced in August 2009 that Monatom would develop Dornod in a joint venture with ARMZ and possibly Japanese or Chinese partners, and would hold at least 51% of the new entity, Dornod Uranium LLC. As of 2016, Khan and the Government of Mongolia reached a settlement of the dispute. Plans are unclear, but annual production of 1000–1200 tU is anticipated from Dornod.

#### Geological setting

The Mardai district is at the northern margin of the Dornod volcano-tectonic structure. This is one of the largest volcanic complexes within the Mongol–Argun intracontinental volcanic belt. It evolved during Late Mesozoic tectono-magmatic activity that affected the Precambrian Manzhur–Chinese Platform. The belt extends for 1200 km in a SW–NE direction from the edge of the Mongolian Altai Mountains in southern Mongolia to the Pri-Argun area in south-eastern Transbaikalia in the Russian Federation, where volcanic type uranium deposits are exploited in the Streltsovsk district [19].

The Mardai area is underlain by two geological units: Late Mesozoic continental sedimentary strata and a volcanic sequence that rests unconformably upon crystalline basement of Proterozoic–Early Mesozoic age.

The Late Mesozoic upper unit consists of the Zuunbayan Formation, which is composed of Lower Cretaceous lignite-bearing continental sediments and the underlying Dornod Formation of Upper Jurassic–Lower Cretaceous continental, subalkalic, volcanic and sedimentary facies which fill the grabens. The Dornod Formation, of 1000–1500 m thick, is subdivided into three members, each characterized by volcanogenic suites derived from subsequent volcanic cycles:

- (i) An upper member (>1000 m thick) of rhyolite–trachyrhyolite–trachyandesite;
- (ii) A middle member of rhyolite;
- (iii) A lower member (<400 m thick) of basalt–trachyandesite/dacite–rhyolite.

About 75% of the Dornod lithologies consist of stratified pyroclastic and outflow volcanic rocks composed of rhyolite, quartz feldspar porphyry, andesite–basalt and volatile enriched felsic volcanic rocks. Intercalated continental clastic and lacustrine sediments containing organic matter constitute the remainder. Conglomerates overlain by gritstone, sandstone and siltstone beds occur at the base of the Dornod Formation in palaeodepressions [19].

The crystalline basement includes:

- (a) Jurassic granite porphyry, granodiorite and diorite bodies, syenitic, dioritic, and diabase dykes, and subsequent subvolcanic bodies and dykes of felsic and andesitic porphyries;
- (b) Large bodies of Late Palaeozoic granite, diorite and gabbro–diorite (Tsenkher-gol Complex);
- (c) Widely distributed Early Palaeozoic K- and Na-metasomatized granodiorite and diorite (Modochudag Complex);
- (d) Proterozoic granitic gneiss and porphyroblastic granite;
- (e) An older complex of Proterozoic–Early Palaeozoic regionally metamorphosed (amphibolite facies) continental margin and continental sediments (schist, gneiss and marble) and volcanic rocks.

Structural elements of the region are characterized by arched uplifts and downfaulted grabens, largely controlled by NE–SW and NW–SE trending regional faults. Repeated reactivation of N–S and NW–SE structures generated high angle and shallowly dipping faults, shears and breccia zones. Shallowly dipping cataclastic zones with good permeability developed preferentially at or near the contacts of volcanic sheets with tuffaceous and sedimentary beds. Their development is most intense in tuffaceous sedimentary beds at the base of oligophyric rhyolite, which separate the Lower and Middle Members, and in andesitic–basaltic pillow lava of the Lower Member [19].

#### Mineralization

The Dornod deposit comprises 12 ore zones within an area of about 20 km<sup>2</sup> (Fig. 56). Individual zones contain one or more orebodies. The bulk of uranium resources is contained in ore zones 2–5 and 7–9, which are grouped in an area 3.7 km long and 2.5 km wide. These zones account for 29 000 tU at a grade of 0.175% U. About 4000 tU of sub-economic resources are delineated in ore zones 1, 6, 10–12 in the Khavar sector in the W–SW part of the deposit.

All orebodies are blind and occur over a depth interval of 30–600 m below surface. Distances between orebodies are 50–350 m. Zones 2, 3 and 7 contain the largest orebodies. Orebodies are of peneconcordant–tabular and vein-like to stockwork in configuration and exhibit the following characteristics [19]:

- (a) Tabular ore (ore zones 2, 3, 7 and 9) consists of heterogeneously distributed uranium forming strata peneconcordant tabular to lenticular, elongate to trapezoid shaped bodies controlled by cataclastic zones along flat to shallowly dipping faults. Orebodies may contain several laterally adjacent and/or superjacent ore lenses enveloped by weak mineralization;
- (b) Vein-like to stockwork orebodies (ore zones 1, 4, 5, 6, 8 and 10–12) are predominantly of irregular shape and may grade laterally into tabular ore. They consist of low grade mineralization enveloping unpredictably distributed, variably structured lodes composed of ore pods, pockets, and/or lenses interconnected by joint fillings, stringers and veinlets of ore grade material. Ore lodes are controlled by subparallel, steeply dipping NW–SE or N–S oriented faults cutting intraformational and flat to shallowly inclined fault and fracture zones positioned at stratigraphic contacts.

Ore zone 7 is the largest ore zone of the Dornod orefield. It is located in the central part of the deposit at a depth of about 500 m and accounts for about 14 000 tU at a grade of 0.23% U contained in nine ore lenses (zones 1–9). This peneconcordant, subhorizontal zone has a trapezoidal shape and is 800 m in length and 480 m in width. The upper edge of the zone dips from 540 m to 505 m above mean sea level. Ore is hosted in a brecciated section 20–40 m thick within the approximately 40 m thick third andesitic–basaltic pillow lava sheet of the Lower Member of the Dornod Formation. The cumulative thickness of superjacent ore shoots averages 11 m. Ore shoots are separated by barren intervals up to 3 m thick. The lava is interbedded with terrigenous, lacustrine sediments and fills a large palaeovalley incised into the basement. Ore is restricted to the marginal part of the brecciated lava sheet where the sheet gradually pinches out. Uranium is found mainly in the matrix material with highest grade intervals in fine-grained fractions in the brecciated lava. The highest grade ore, with a grade of 0.2–

0.45% U, is concentrated in the central part of ore zone 7, which averages 30–33 m in thickness and contains the bulk of the mineralization. The grade decreases laterally, forming a large, low grade uranium aureole around the ore zone [19].

Ore zones 2, 3 and 9 are located in the northern and eastern part of the Dornod orefield and account for about almost 10 000 tU, about 8000 tU of which are contained in ore zone 2 and about 1700 tU in zone 3. Grades vary between 0.06 and 0.6% U. The shallowly dipping, tabular orebodies are hosted in sandstone, siltstone and conglomerate in a palaeovalley immediately below a rhyolite sheet. Mineralization is found in several stacked levels near the contact of the Lower and Middle Members of the Dornod Formation, hosted in jointed intervals of lenses and interbeds of highly carbonaceous, fine- and coarse-grained sediments and tuff. Ore lenses may be up to 40 m apart and are surrounded by a wide aureole of low grade mineralization.

Argillization is the main alteration type associated with mineralization. Alteration products include hydromica, montmorillonite, kaolinite, chlorite, carbonate, fluorite, quartz and haematite. The most intense alteration products are hydromica and montmorillonite. Haematitization is typically present with mineralization and its intensity generally correlates with uranium grade. Weathering related alteration is very limited, essentially restricted to major fault zones along which it persists to depths of up to 300 m [19].

A distinct, primary geochemical dispersion halo of U, Pb, As, Ag and Mo envelops the orebodies. It is controlled by, and commonly confined to, the ore hosting permeable cataclastic lithologies and/or faults. Fault related halos are generally elongate in shape. Halo dimensions are one to three times larger than the ore zones. Uranium forms the most extensive aureole and may extend beyond the orebodies for a distance of up 500 m.

Coffinite and pitchblende are the principal uranium minerals. Uraniferous leucoxene and titanate, minor brannerite and uranophane are ubiquitous in orebody 7. Secondary uranium minerals include uranyl silicates (uranophane, beta-uranotile) and hydro-oxides (clarkeite, masuyite). Associated ore minerals include chalcopyrite, galena, marcasite, molybdenite, pyrite, sphalerite, haematite and minor arsenopyrite. Quartz, biotite, hydromica, montmorillonite, chamosite, minor ankerite, calcite, siderite, fluorite, baryte, leucoxene, K-feldspar, muscovite, tourmaline (rare) and anatase occur as gangue minerals [19].

Uranium minerals occur mainly as fine- to coarse-grained aggregates 0.001–2 mm in size. They are present as impregnations, including finely disseminated, globular, stringer and, rarely, banded and earthy textures. Higher grade mineralization may contain breccia and matrix cement textures.

Although uranium is found in almost all lithologies, larger ore grade accumulations are confined to sedimentary and volcanic horizons at the base of, and within, the Lower and Middle Members of the Dornod Formation and to faults cutting volcanic horizons at shallow angles.

Hexavalent uranium minerals occur in vein–stockwork orebodies to depths of 500 m. They constitute 35% of the mineralization in orebody 5.

Uranium–lead systematics of uranium minerals yield ages of 153–136 Ma. Golubev et al. [155] report an age of 138–136 Ma for uranium deposition in the Dornod volcano-tectonic structure. These Late Jurassic–Early Cretaceous ages are very similar to those recorded for the deposits in the Streltsovsk caldera in the Russian Federation (136–134 Ma). Sericite from propylitic alteration associated with polymetallic mineralization produced K–Ar ages of  $161 \pm 7$  Ma, while pre-uranium mineralization hydromica yielded 145–143 Ma dates (K–Ar). Rubidium–strontium ages of 170–140 Ma were obtained for rocks of the Lower Member of the Dornod Formation [19].

## Metallogenetic aspects

The metallogenesis of uranium deposits in the Mardai district is poorly understood. Uranium mineralization appears to be related to volcanic rocks, particularly of felsic composition, which may represent a source of uranium and other metals [156]. Chemillac et al. [156] investigated hydrothermally altered and brecciated samples of alkali rhyolite of the second volcanic cycle, and in addition, melt inclusions in quartz phenocrysts unaffected by alteration.

Relict primary minerals consist of quartz, rare K-feldspar, plagioclase, biotite and zircon embedded in an argillized matrix (mainly sericite). Late carbonate and fluorite occupy fractures and haematite occurs within sericite aggregates in extremely altered intervals. Devitrification features such as spherulites and perlites are common. Mineralized samples with up to 0.1% U contain hydrothermal uraniumiferous zircon, brannerite, coffinite and, as late phases, bastnaesite and strontianite.

Chemillac et al. [156] state that the initial rhyolitic magma (preserved as melt inclusions in quartz) had a highly evolved comenditic composition, was mildly peralkaline, and enriched in F, U, Th, REE and Zr. The U and Th contents are the same as those of rhyolites of the Streltsovsk caldera (Russian Federation) [157]. These comenditic rhyolites constitute substantial sources of uranium. They contain from 6 to more than 21 ppm U, with the highest concentrations occurring in vitric rocks. Chemillac et al. [156] report 14–25 ppm U contained in melt inclusions in comenditic rhyolite.

The initial uranium content of the melt combined with the volume of erupted rhyolite are largely sufficient to account for the ore resources. Mobilization of the ore forming elements was by hydrothermal activity, which is indicated by the largely aphyric nature of the rhyolite. The postulated hydrothermal solutions were of late volcanic, intraformational, or meteoric origin, or a combination thereof. Late volcanic events may have caused the mobilization of these fluids. Reducing conditions required for the precipitation of uranium existed particularly at sites where sediments contained abundant plant remains. An additional reductant may have been ferrous iron in mafic minerals in andesite and basalt. Physicochemical processes (effervescence, cooling, fluid mixing, etc.) may have also induced uranium precipitation, particularly in volcanic outflow facies [19].

Tectonic activity was an additional prerequisite for ore formation. Large, high angle and flat to shallowly dipping, peneconcordant faults and associated cataclastic zones in effusive volcanic and pyroclastic rocks and permeable continental clastic sediments provided favourable pathways for the migration of mineralizing fluids and voids for ore deposition [158]. Such sites host the majority of the tabular mineralization. Cataclasis of felsic volcanics may also have been a prerequisite for leaching of uranium if these facies are considered the source of uranium and other metals [19].

Isotope dating of uranium minerals indicates that the alteration and mineralization took place between 153 and 136 Ma, with ore formation most likely to have occurred between 138 and 136 Ma (i.e. Late Jurassic–Early Cretaceous). This latter time interval is essentially identical to U ore formation in the Streltsovsk caldera, in the same volcanic belt, just to the north in the Russian Federation. Hence, it may be assumed that the formation of the volcanic type U–Mo deposits in the Mardai district evolved by similar complex and perhaps multistage processes as deposits in the Streltsovsk caldera [19].

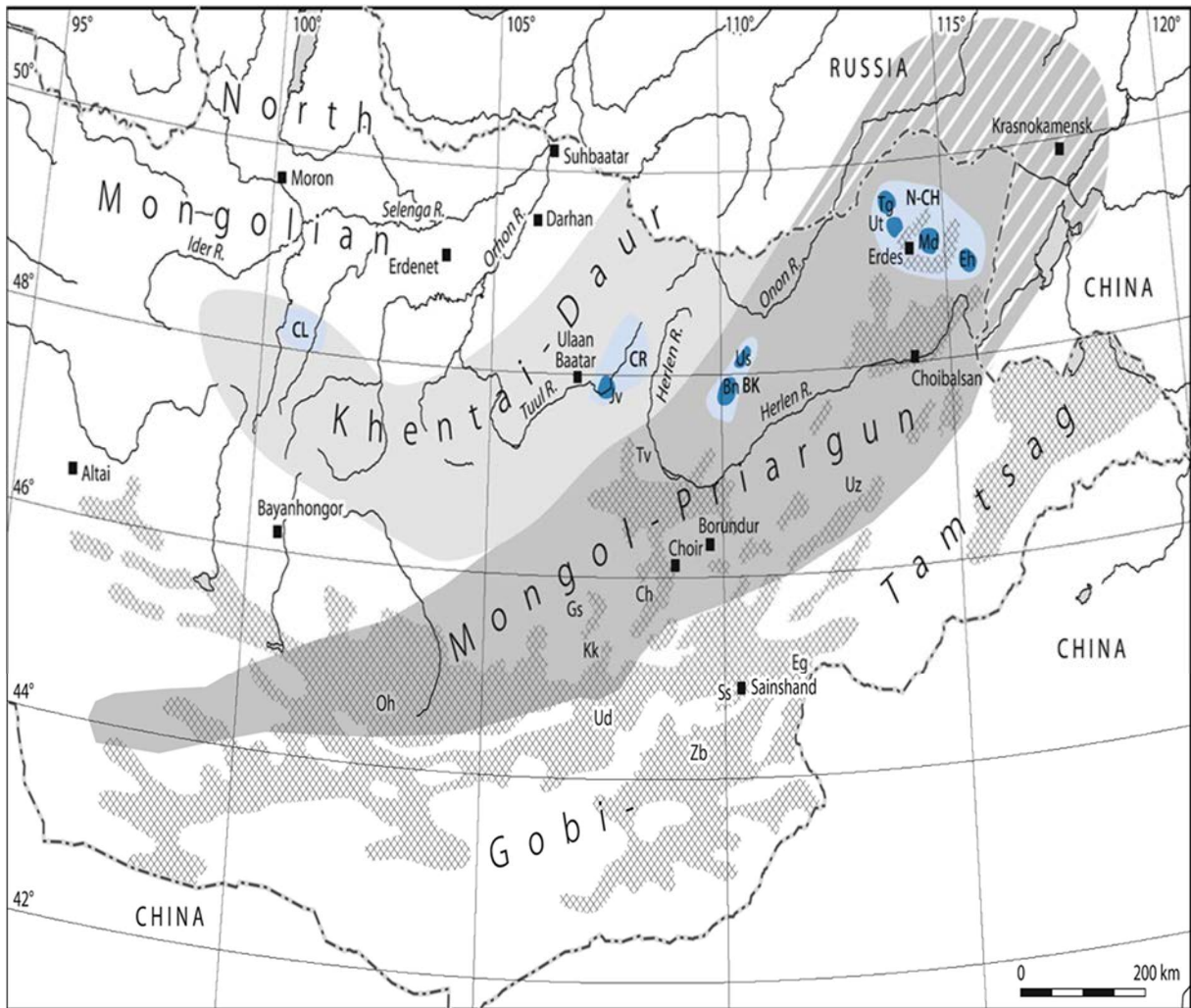


FIG. 54. Metallogenic provinces of Mongolia with principal uranium regions, basins and districts/areas. Uranium orefields of the North Choibalsan Region (N-CH). Eh: Engershand, Md: Mardai (or Dornod), Tg: Turgen, Ut: Ugtham [19] (reproduced with permission).

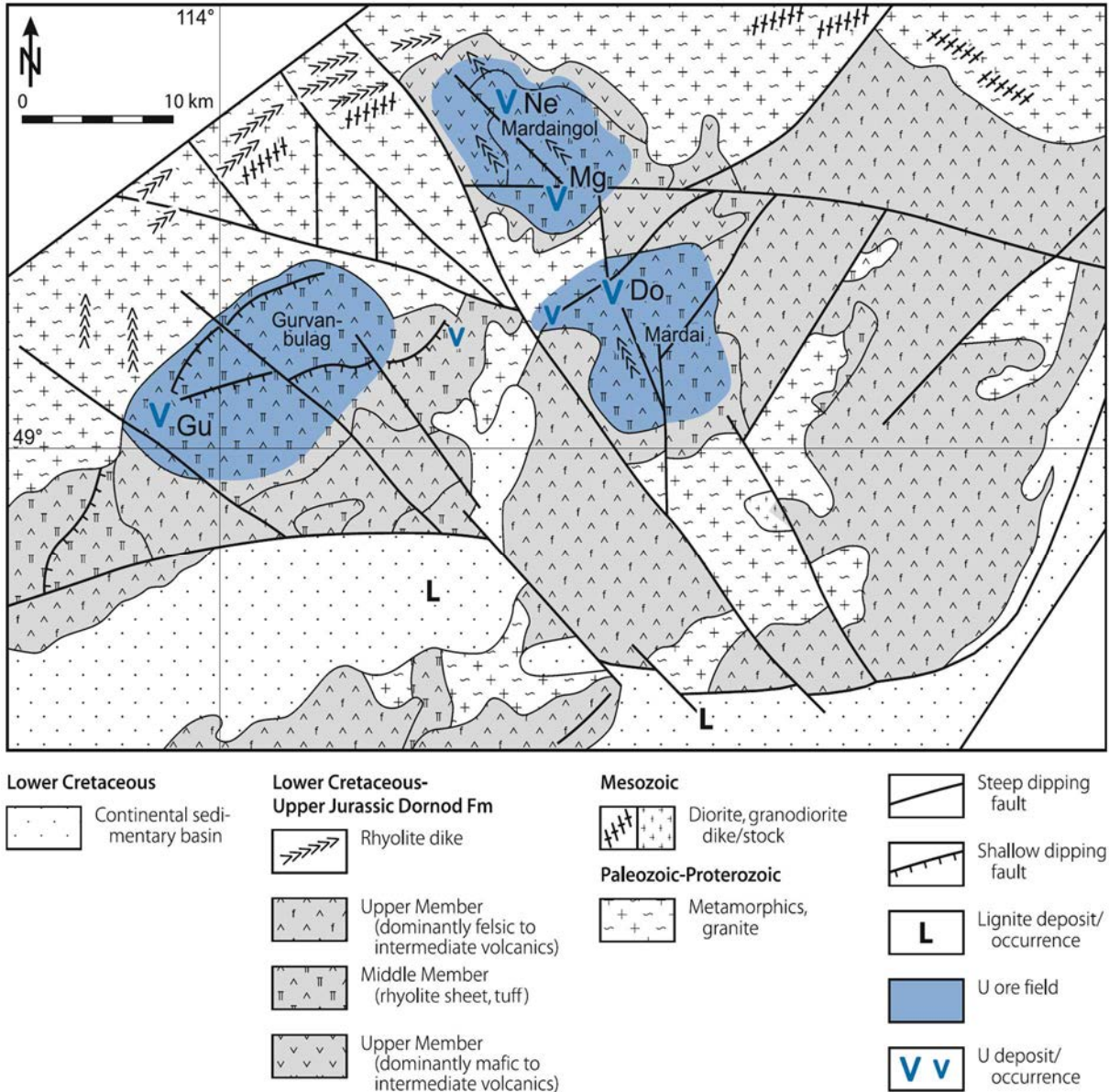


FIG. 55. The Mardai (Dornod) uranium district. Geological map showing the location of the ore fields and deposits (Do: Dornod, Gu: Gurvanbulag, Mg: Mardaingol, Ne: Nemer) [19] (reproduced with permission).

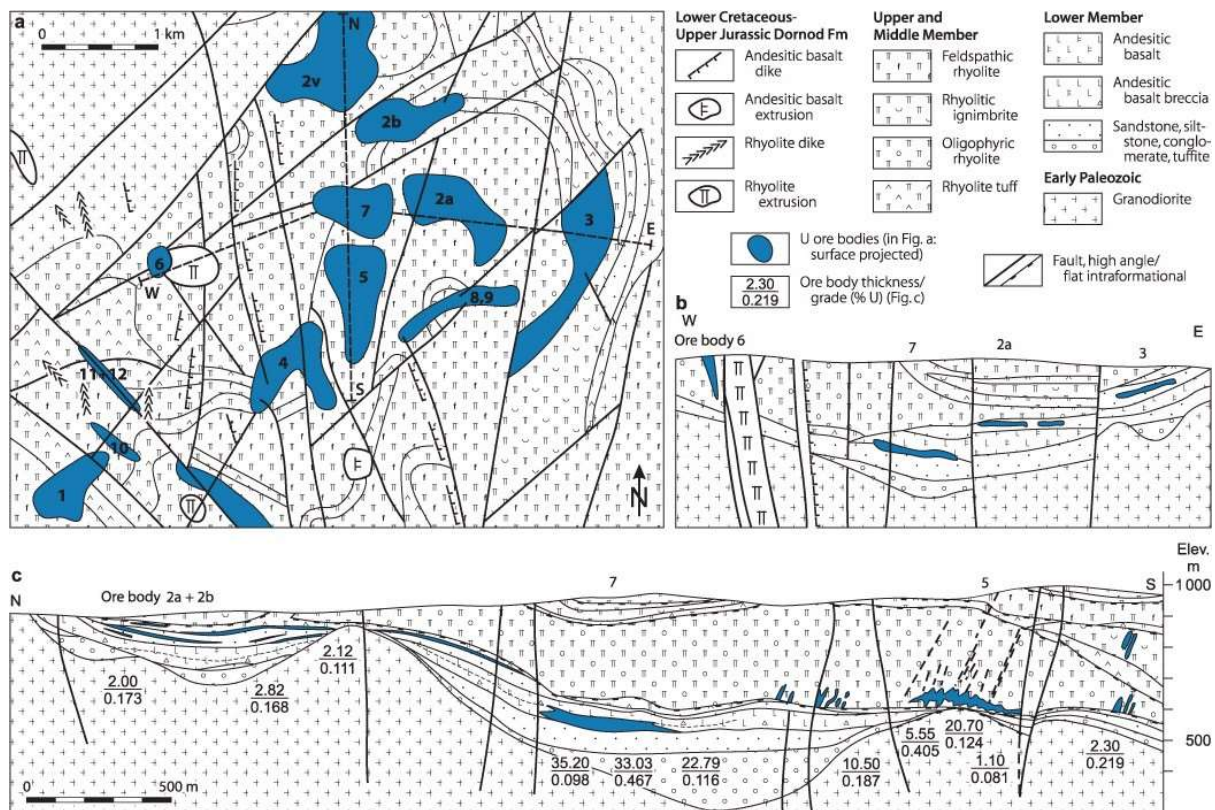


FIG. 56. The Mardai (Dornod) orefield: (a) geological map showing the location of the deposits; (b) E–W; and (c) N–S geological cross-sections illustrating the lithostratigraphic position of the orebodies in the Dornod Formation [19] (reproduced with permission).

#### 3.4.4.4. Volcano-sedimentary deposit: The Anderson Mine (USA)

##### Introduction

Located approximately 70 km NW of Wickenburg in central Arizona, the Anderson deposit, commonly referred to as the Anderson Mine, is a typical example of uranium mineralization of tabular configuration hosted by carbonaceous lacustrine sediments with felsic pyroclastic material [47].

Discovered in 1951, early mining by combined open pit and underground operation produced 12 tU at a grade of 0.12% U and 0.05%  $V_2O_5$ . Exploration was resumed in the 1970s and identified new resources of more than 12 000 tU at grades averaging 0.06% U. The mine was the property of Global Uranium Corporation, which reported in 2010 resources of 8740 tU at a grade of 290 ppm U (cut-off grade 85 ppm U) and 9540 t  $V_2O_5$ . In 2012, the new operator, Uranium Energy Corporation reported resources of 11 259 tU at a grade of 0.028% U.

##### Geological setting

The Anderson deposit is located in the north-eastern part of the Date Creek Basin (Fig. 57(a)). The basin is underlain by a basement of dominantly Precambrian gneissic and granitic rocks upon which a 1100 m thick sequence of Tertiary lacustrine sediments and volcanic rocks rest unconformably. Pliocene–Holocene alluvium covers this sequence. Block faulting along steeply dipping NW–SE trending faults in Late Miocene–Early Pliocene time caused moderate SW tilting of the Cenozoic strata (Fig. 57(b)) [47].

In the Anderson Mine area, Tertiary sediments thicken gradually to the south-west and thin to the north-east, where they onlap the Arrastra palaeohigh. The Tertiary sequence is divided into, from top to bottom [47]:

- (a) Pliocene–Middle Miocene comprises 0–30 m thick basalts and coarse clastic sediments. The 9–10 Ma basalt flows are undeformed while the 12–13 Ma Cobwebb basalt is faulted;
  - (b) Early–Middle Miocene Chapin Wash Formation is divided into Flat Top and Anderson Mine members:
    - Flat Top Member (<170 m thick) comprises arkosic siltstone, sandstone and conglomerate interbedded with minor bentonitic/tuffaceous siltstone;
    - Upper Anderson Mine Member, 80–150 m thick in the mine, 300 m thick about 2.5 km further south, comprises predominantly tuffaceous, in part paludal, lacustrine sediments in the northern part of the Date Creek Basin (Anderson Mine area) grading into sandy deltaic sediments about 2.5 km south of the mine;
- Lower Anderson Mine Member (or clastic unit) (0–120 m thick) comprises reddish to yellowish grey, coarse, poorly sorted arkosic and volcanic sandstone–conglomerate, reworked andesitic lapilli with ‘brick red’ clay matrix, bentonitic siltstone (distal part of a subaerial fan conglomerate, pinching out north of the Anderson Mine).
- (c) Eocene(?)–Oligocene(?) Arrastra Volcanics (>450 m thick) comprising basalt, andesite, andesitic tuff and interstratified conglomerate;
  - (d) Eocene(?) Artillery Formation or stratigraphic equivalent (up to 100 m thick) comprising reddish clastic sediments with ignimbrite and andesitic agglomerate.

Alteration phenomena related to diagenesis and ore related processes include argillization, carbonatization, silicification, zeolitization and pyritization, all of which affected, in varying intensity, the entire uranium hosting Anderson Mine Member [47]. Some alteration processes occurred in multiple phases:

- (a) Argillization and zeolitization of rhyolitic ash created light greenish–grey bentonitic clays, particularly smectite, illite, hectorite and other mixed layer clay minerals throughout the upper unit of the Anderson Mine Member. Some clays are significantly enriched in lithium (up to 0.4%). argillization and zeolitization occurred early during diagenesis but appear to post-date the initial stages of silicification and carbonatization;
- (b) Carbonatization of diagenetic origin generated magnesian calcite, which replaced feldspars and carbonaceous to tuffaceous mudstone. It also cements arkosic sandstone in the southern part of the area;
- (c) Silicification is common in almost all units except the Lower Anderson Mine Member. Some strata, including most carbonaceous beds, are partially to completely silicified. An early phase produced multicoloured chalcedony and tends to be associated with disseminated uranium in carbonaceous plant material. A later phase, active after Miocene faulting to probably Recent time, deposited jasper-like chalcedony and opal in voids and fractures. Opaline silica replaced carbonate–clay matrix in sediments and locally includes uranyl–silica complexes and colloform coffinite;
- (d) Pyritization is reflected by two modes, where fracture filling pyrite is considered to be of diagenetic origin, whereas an older generation of finely disseminated pyrite crystals is thought to be more likely a syngenetic product.

## Mineralization

The drilled out Anderson Mine area (1 km × 1.5 km) consists of peneconcordant, blanket-like uranium mineralization (Fig. 58). Individual mineralized beds are typically 1–3 m in thickness but the beds may accumulate in highly mineralized zones to more than 15 m in thickness. These beds are hosted by both the Upper and Lower carbonaceous units of the Anderson Mine Member, each 20–25 m thick at the Anderson Mine, but which thicken to about 35 m further south [47].

Extensive low grade uranium accumulations (<100–200 ppm U) occur peneconcordant with bedding within the two carbonaceous units of the Upper Anderson Mine Member. These low grade zones encompass irregularly shaped higher grade zones of 0.1–0.3% U, mainly in the upper unit. The mineralized area covers at least 5 km<sup>2</sup>. It is limited to the north and east by the pinching out of the two carbonaceous units, on the south by a complex of predominantly sandy deltaic sediments elongated in an E–W direction, and on the west by an alluvial fan and braided river system intertonguing with the lacustrine sediments [159].

Uranium mineralization is hosted by lacustrine, locally paludal sediments with tuffaceous material within both the upper and lower carbonaceous units of the Anderson Mine Member. Uranium hosting strata have general, although variable enrichments of B, Cu, F, Li, Mo, Ni, U and V. Otton [160] and Sherborne et al. [161] recognized two ore types, unoxidized and oxidized:

- (i) *Unoxidized ore*: The principal uranium mineral is colloform coffinite with highly variable uranium/silica ratios and a content of 4–20% U. It is generally associated with carbonaceous matter. Pitchblende is rare. Most mineralization is in thinly bedded, pyritic, carbonaceous mudstone and siltstone, lignitic mudstone and bioturbated marlstone that exhibit only minor silicification. Ore minerals occur either as fine disseminations in the matrix of the host rocks or as discontinuous microveinlets or patches. The highest concentrations of up to 2% U are found in individual seams of lignitic coal and as halos around root remains, often associated with framboidal pyrite. Sherborne et al. [161] note that uranium and organic carbon show a linear correlation coefficient of 0.55 and that the texture of the uranium–carbon mineralization is similar to Ambrosia Lake ore, suggesting that the organic matter is probably humate. Only very little uranium is associated with organic material that still retains its cellular structure. Elements enriched to various degrees in carbonaceous uranium ore are primarily As, Mo, S and V, and in lesser amounts Ag, B, Cu, Ga, Ge, Mn and Ti. Some of these elements correlate reasonably well with uranium, others more with carbon [161, 162];
- (ii) *Oxidized ore*: Very fine-grained carnotite is present as cement, thin fracture coatings and coarse, fibrous fillings in fractures, along bedding planes, or with haematite in jasper pods. Uraniferous silica occurs in the form of massive jasper and as small silica veinlets. Oxidized mineralization is confined to fractured, highly silicified, oxidized, light coloured mudstone, tuff, limestone and marlstone with abundant megascopic plant debris.

Sherborne et al. [161] list the following ore controls or recognition criteria of the mineralization and its geological setting at the Anderson Mine:

- (a) Emplacement in fine-grained sediments deposited in shallow lacustrine environments;
- (b) Close spatial relationship between carbonaceous beds and uranium mineralization;
- (c) Well mineralized zones coincide with the greatest thickness of carbonaceous matter accumulation (indicating the importance of a paludal environment in localizing uranium);
- (d) Extensive diagenetic alteration of sediments;
- (e) High uranium background (10–50 ppm) of Anderson Mine Member sediments;
- (f) Presence of uraniferous volcanic and granitic rocks providing potential uranium sources (felsic volcanic rock fragments comprising a major fraction of the Anderson Mine Member are favoured as the principal uranium source);
- (g) Presence of H<sub>2</sub>S as a reductant generated from gastropod-rich marlstone;
- (h) Regional geochemical zonation marked by increased contents of Li, V and possibly F, as well as a particularly anomalous concentration of Mo and As exclusively associated with zones of uranium mineralization.

Mueller and Halbach [159] note that uranium preferentially accumulated in thinly bedded carbonaceous siltstone, lignitic mudstone and bioturbated marlstone of lacustrine provenance, particularly in the upper part of the Upper carbonaceous unit of the Anderson Mine Member. Less favourable uranium traps include thickly bedded intervals of carbonaceous siltstone and sandstone and

dense limestone of the intermediate section of the upper unit, the limestone interval and the lower Carboniferous unit [47].

#### Metallogenetic aspects

The genesis of the Anderson deposit may be interpreted as the result of complex groundwater, sorption and precipitation processes within carbonaceous–humic lacustrine sediments. These processes probably occurred in an early diagenetic, low temperature environment, prior to the Late Miocene–Early Pliocene Basin and Range tectonism [47].

Sherborne et al. [161] present the model whereby uranium-bearing tuffaceous sediments were deposited in sheltered backwater areas marginal to an expanding Miocene freshwater lake. Reaction of tuffaceous sediments with lake water caused, in an early diagenetic stage, extensive alteration and development of alkaline carbonate pore water. Zeolites probably formed at this time.

Compaction and dewatering of uraniferous tuffaceous lake sediments released uranium and silica and led to migration of uranium–carbonate–silica enriched formational waters within the basin. Uranium was most likely transported in groundwater as a uranyl carbonate complex. It precipitated to form coffinite ore in, and adjacent to, carbonaceous strata and where H<sub>2</sub>S acted as a reductant. Hydrogen sulphide was generated to a large extent from intraformational marlstones.

Some remobilization of the original coffinite mineralization and deposition of carnotite ore in fractures has taken place in near surface oxidation zones in more recent geological time. However, this did not significantly affect uranium mineralization in either carbonaceous unit, as indicated by radiometric equilibrium.

Mueller and Halbach [159] propose that the alluvial fan braided river system, located west of the Miocene Anderson Mine Lake, collected uranyl-bearing groundwater from adjacent metamorphic and volcanic highlands. Volcanics of dacitic–rhyolitic composition are believed to have been the principal source of uranium as deduced from the widespread and most likely volcanic derived, lithium and fluorine enrichment throughout the lacustrine Anderson Mine Member. Hydrostatic pressure in river beds caused the uraniferous waters to migrate to the delta complex, when northwards flowing groundwater introduced it into lacustrine sediments of the Anderson Mine Member along numerous intercalated sandy layers.

Uranium was transported as uranyl carbonate complexes in solutions of slightly alkaline chemistry (pH7–9) produced by partial dissolution of high magnesian calcite during early diagenesis. This milieu was also favourable for argillization and zeolitization of interbedded rhyolitic glass fragments. Subsequent fixation of uranium began with a preconcentration phase during which considerable amounts of uranium were adsorbed onto humic material, perhaps similar to processes described from the Grants uranium region, as well as colloidal silica and zeolite. Most of the adsorption was in the uppermost 10 m of the sedimentary column where slightly acidic microenvironments developed in response to biochemical humification of plant relics. Local pH values of 6–7 destabilized incoming di- and tricarbonatate uranyl complexes.

Condensation of the sorbents to organic gels reduced most of the hexavalent uranium, which then precipitated as submicroscopic coffinite and pitchblende. Formation of coffinite was likewise accomplished by H<sub>2</sub>S, which developed as the result of sulphate reduction by bacteria continuously forming H<sub>2</sub>S halos around organic fragments. The influence of H<sub>2</sub>S as the main reductant is noted by the authors to have been important in the enrichment of uranium in permeable structures, especially in burrows. Although often associated and penecontemporaneous with uranium ore, framboidal pyrite spheres started to crystallize earlier than coffinite and resulted from processes at least not directly linked to uranium deposition. This is indicated by the lack of a statistical correlation between uranium and total sulphur [47].

Scarborough [162] and Otton [163] note several potential sources for uranium mineralization in the Date Creek Basin: (a) Miocene alkalic volcanic flows, tuff and ash, specifically highly potassic facies of which contain 10–20 ppm U, (b) Jurassic alkalic volcanics located in southern Arizona, which contain uranium occurrences and (c) Precambrian uraniferous granites in the nearby Artillery Peak region, which were presumably exposed and subjected to erosion during the Miocene period [47].

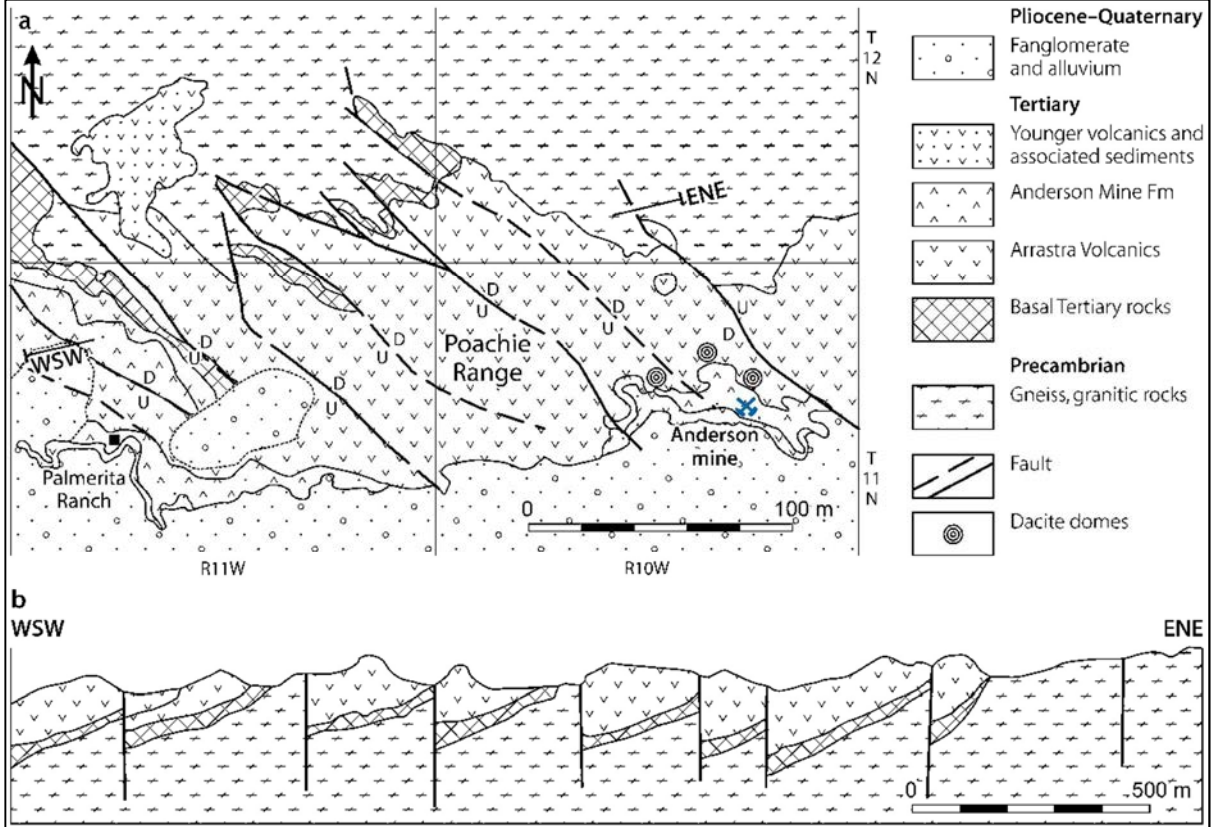


FIG. 57. North-eastern Date Creek Basin: (a) geological map showing the location of the Anderson Mine, (b) E–W geological cross-section showing the marked block faulting in this part of the Date Creek Basin [47] (reproduced with permission).

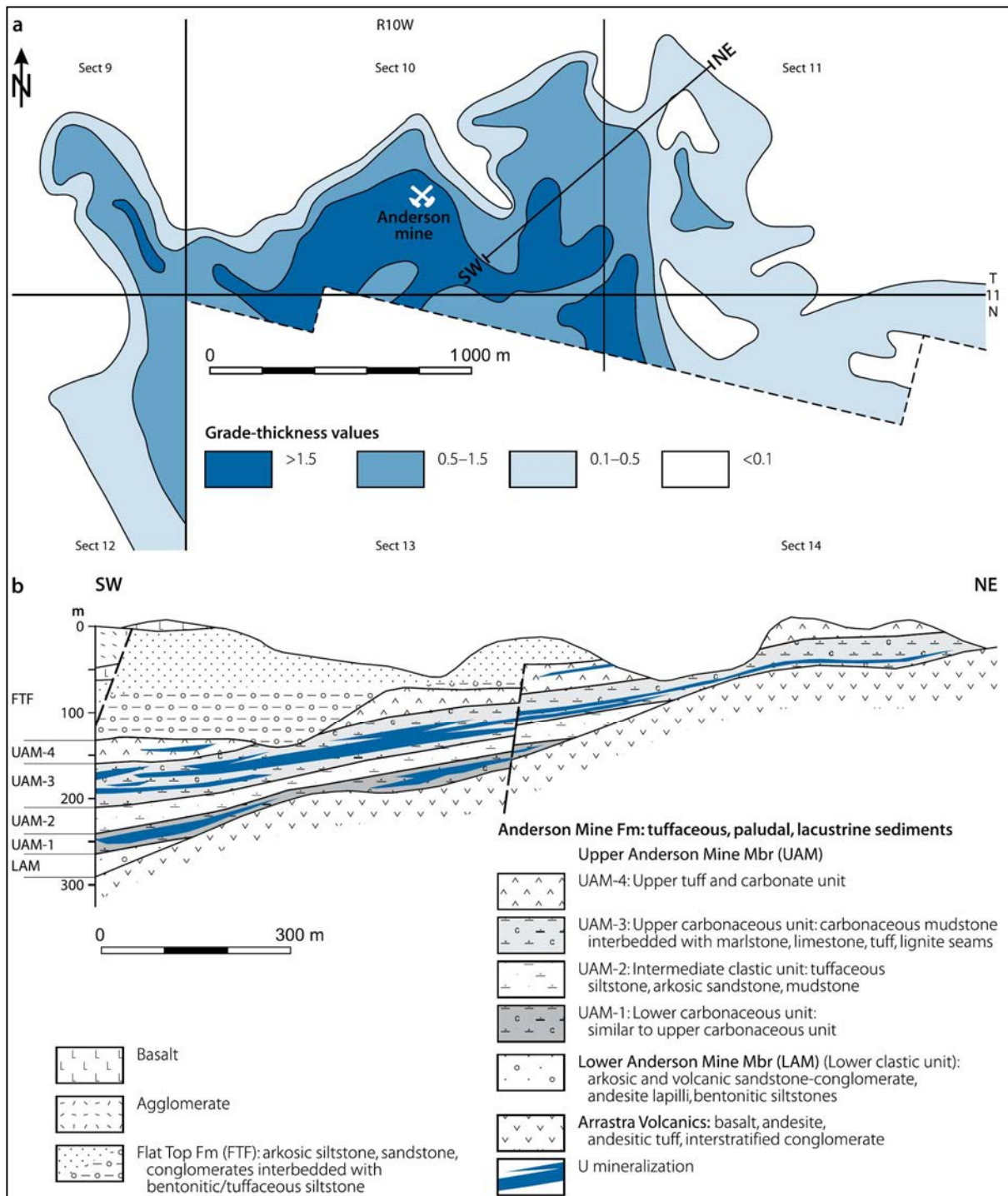


FIG. 58. Anderson Mine area: (a) contour map of uranium mineralization subdivided into grade-thickness areas based on a cut-off grade of 0.017% U, (b) SW-NE geological cross-section of the Anderson Mine deposit [47] (reproduced with permission).

### 3.5. METASOMATITE DEPOSITS

#### 3.5.1. Definition

Metasomatite uranium deposits are confined to areas of tectono-magmatic activity affected by intense Na- or Na-Ca metasomatism that has produced albitized facies including albitite, aegirinite, alkali

amphibole rocks and calcic–ferruginous facies along deeply rooted fault systems. Protoliths include granite, gneiss, migmatite, metasedimentary and metavolcanic rocks. Deposits are structurally controlled by intersections, bifurcations or abrupt bends of faults. Orebodies are of variable shape and size, composed of disseminated grains and thin veinlets of ore minerals. The main uranium phases are uraninite, U–Th oxides and U–Th silicates [19].

Table 18 lists the salient features of the principal metasomatite deposits taken from the 78 metasomatite deposits/districts recorded in the UDEPO database. The largest uranium deposits in Na-metasomatites occur in the Kirovograd district (Ukraine). Other regions with similar deposits are the Central Mineral Belt (Canada), the Coles Hill deposits (USA), the Lagoa Real and Itataia districts (Brazil), the Singhbhum Belt (India) and the Kokchetav Massif (Kazakhstan). Large uranium deposits associated with K-metasomatites are known in Elkon Horst district of southern Yakutia (Russian Federation). In 2015, all of the uranium production of Ukraine (1200 tU) and Brazil (40 tU), along with most of that of India (385 tU) originated from metasomatite deposits.

TABLE 18. PRINCIPAL METASOMATITE-RELATED URANIUM DEPOSITS/DISTRICTS  
(as of 31 December 2015)

Deposit	Country	Resources (tU)	Grade (% U)	Status
Lagoa Real district	Brazil	100 770	0.12	Operating
Druzhnoye	Russian Federation	95 840	0.134	Development
Novokonstantinovskoye	Ukraine	93 630	0.139	Development
Elkonskoye Plato	Russian Federation	62 400	0.157	Development
Tsentralne	Ukraine	61 800	0.10	Operating
Severnoye	Russian Federation	61 526	0.149	Development
Kurung	Russian Federation	54 850	0.145	Development
Coles Hill North and South	USA	45 850	0.054	Dormant
Neprokhodimoye	Russian Federation	42 760	0.119	Dormant
Michelin	Canada	41 195	0.102	Exploration
Elkon	Russian Federation	40 263	0.183	Dormant
Severinske	Ukraine	38 350	0.087	Dormant
Valhalla	Australia	29 340	0.069	Dormant
Prospecto Cerro Carmen	Chile	29 000	?	Dormant
Vatutinske	Ukraine	25 390	0.132	Operating
Zhovtorichenske	Ukraine	18 900	0.12	Dormant
Michurinske	Ukraine	18 490	0.082	Dormant
Pidhajtsivske	Ukraine	11 820	0.088	Development
Kitongo	Cameroon	11 130	0.090	Exploration

### 3.5.2. Geological setting

Alkali metasomatism is a widespread geological phenomenon that occurs in a wide variety of geological conditions, some of which are associated with uranium ore forming processes. Alkali metasomatism is commonly associated with albite enrichment and quartz dissolution, although potassic feldspathization may occur instead of albitization. Sodium metasomatic zones are normally

several metres wide and several hundred metres to several thousand metres long. Granitic rocks are commonly altered to albitites, but metasedimentary and metavolcanic rocks can be altered as well. One extreme example is the banded iron formations of the Krivoy Rog district (Ukraine), which are altered to aegirinite by addition of Na from fluid percolation [45].

In Na-metasomatite deposits, two subtypes have been defined on the basis of precursor rock facies: (i) granite derived and (ii) metasedimentary/metavolcanic derived [19] (Fig. 59).

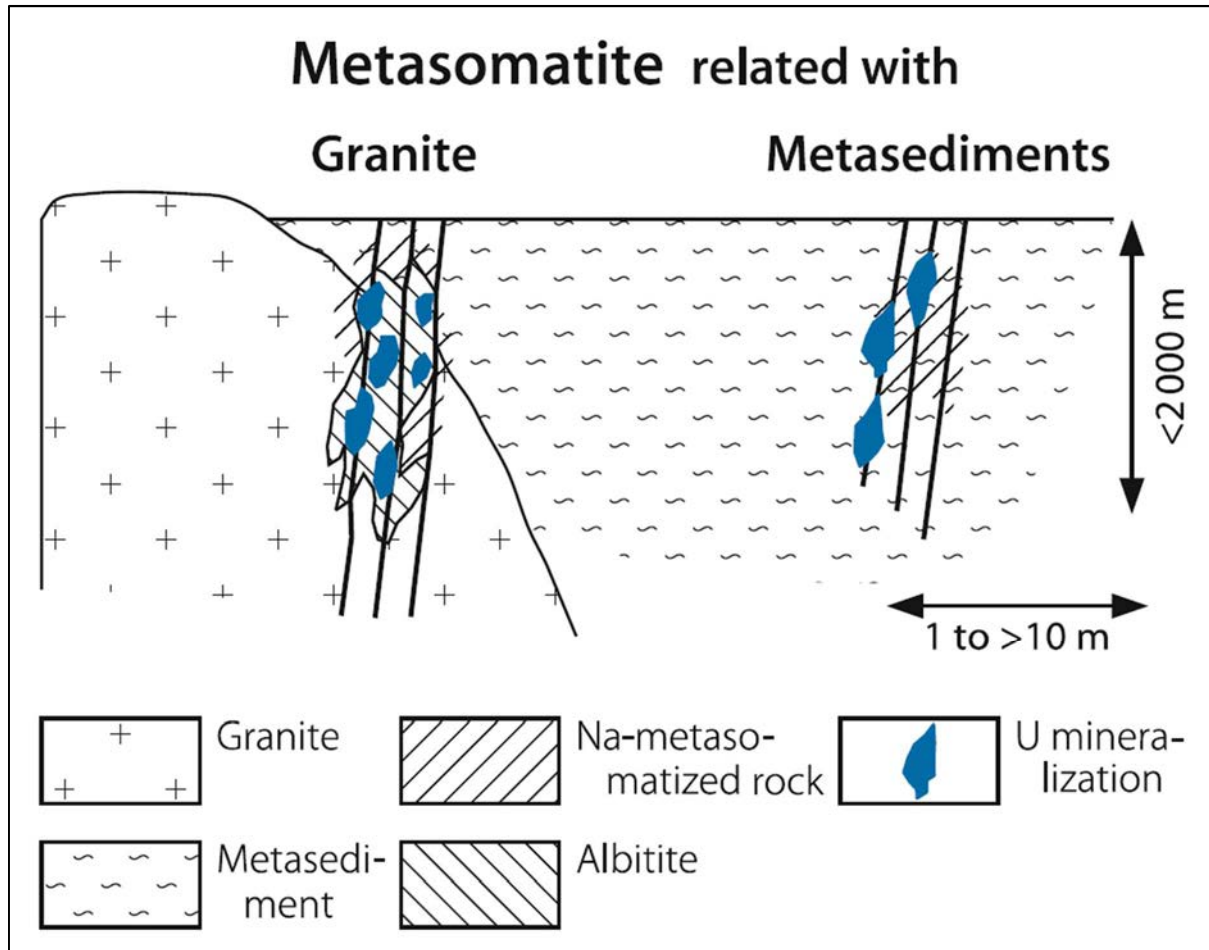


FIG. 59. Schematic representation of metasomatite uranium deposits [19] (reproduced with permission).

In granite derived deposits (Kirovograd type), uranium minerals occur as disseminations and in veinlets within intervals of closely spaced joints, shears and breccias in albitic aegirine granite, albitic arfvedsonite–aegirine granite and albitite that occupy pre-metasomatic fault zones in anomalously uraniumiferous granite. Ore minerals include uraninite ( $\pm\text{Th}$ ), uranothorianite, uranothorite, thorite, some brannerite and coffinite associated with accessory Fe and Pb sulphides, REE minerals, apatite and fluorite. Haematite and carbonates are locally abundant [19].

Metasedimentary/metavolcanic derived (Zhelte Vody type) deposits are exemplified by the Zhelte Vody district (Ukraine), which is situated in the Krivoy Rog Basin, a large synclinorium of Proterozoic carbonate, quartzite, schist and ferruginous metasedimentary rocks. These rocks are folded into large isoclinal folds with steep axes. Stocks and dykes of microcline granite have intruded along major lineaments. Repeated brittle tectonism caused deep faulting and strong fracturing. Metasedimentary rocks and granites are intensely altered along lineaments by early Fe–Mg

metasomatism resulting in stratiform iron ore, followed by Na-metasomatism and, finally, silicification with the development of secondary quartzites. Uranium mineralization is restricted to fractured sections in Na- and Ca-metasomatized zones. Uranium occurs in lenses, shoots and stratiform bodies with finely disseminated uranium minerals and also as veins. Uranium minerals include uraninite, pitchblende, coffinite, brannerite and nenadkevite associated with sulphides, apatite, malakon and carbonate [19].

Most of the known examples of uranium mineralization associated with Na-metasomatism formed during the Proterozoic. The major mineralizing event corresponds to the 1900–1700 Ma period and includes the highly mineralized Krivoy Rog district in Ukraine, the Singhbhum Belt in India, the Central Mineral Belt in Canada and smaller occurrences in Sweden. A second episode, around 1500–1400 Ma is represented by Valhalla (Australia) and Lagoa Real (Brazil). A more discrete event occurred around 600–500 Ma, associated with the Pan-African–Brazilian Orogeny, is represented by the Kitongo deposit (Cameroon), Inca (Namibia) and Espinharas (Brazil). Coles Hill (USA), probably of Mesozoic age, seems to be the most recent deposit of this type.

In K-metasomatite deposits, such as those of the Elkon district (Russian Federation), geochemical changes include desilicification and removal of Al, Ca, Mg, Mn, P and Ti. Potassium was introduced as K-feldspar, including adularia and illite, during a prominent, pre-uranium alteration assemblage consisting of pyrite–carbonate–K-feldspar and disseminated gold. Altered rocks show an addition of the order of 10–20% K<sub>2</sub>O and a loss of 80–90% Na<sub>2</sub>O [19].

A small group of deposits correspond to skarns in which uranium and uranium–thorium mineralization results from contact metamorphism of sediments or volcanic rocks and consists of disseminated U–Th in lenses and erratically scattered patches. Rare earth elements and/or other metals may also be present (e.g. Mary Kathleen (Australia), Tranomaro (Madagascar)).

### 3.5.3. Metallogensis

Sodium–calcium metasomatism and uranium mineralization are clearly controlled by structures at all scales. Regionally, the mineralized districts are located along prominent lineaments extending over several tens of kilometres. In Ukraine, lineaments are parallel to continental block boundaries. Lineaments were first active at high temperature with the formation of mylonites and granoblastic textures in albitites, the orientation of which is parallel to the regional foliation. The structural zones continued to be active at lower temperatures in the brittle structural regime with the formation of albite, pitchblende and carbonates in fractures and chlorite–epidote alteration of the wall rocks. At the scale of the deposits, alteration envelopes and the uranium mineralization are strictly controlled by vertical to moderately dipping structures, which tend to diverge upwards as flower-like structures [45].

Possible uranium sources for the Ukrainian deposits include protoliths with high initial uranium concentrations such as orthogneiss for the deposits hosted in granite and conglomerates, which can be the equivalent of Archaean or Proterozoic quartz-pebble conglomerates with detrital uraninite. The source of the fluids responsible for the Na-metasomatism and quartz dissolution is presumed to be metamorphic, derived from anatectic zones and ascending upwards along deeply seated, large structures [164] or from surficial origin [165]. However, there is a difference of 200 Ma between regional metamorphism and the mineralization processes, with Na-metasomatism and uranium mineralization related to Palaeoproterozoic tectono-magmatic activity along long lived, deeply seated structures, long after peak metamorphism [22].

Potassic metasomatism and U–Au–Ag deposits of the Elkon district (Russian Federation) are primarily controlled by reactivated, ancient, steeply dipping faults of Mesozoic age. Archaean–Palaeoproterozoic granitized rocks are considered the most likely source of uranium. A multistage metallogenic evolution has been deduced from various studies [19]. Uranium–lead isotope dating gives an age of 135–120 Ma for primary brannerite, which correlates with the emplacement of the Early Cretaceous intrusions.

### 3.5.4. Description of selected deposits

#### 3.5.4.1. Na-metasomatite: deposits of the Kirovograd district (Ukraine)

##### Geological setting

The Ukrainian Uranium Province is located within the Sarmatia Craton, which is composed of Archaean–Palaeoproterozoic units exposed on the Ukrainian Shield and in the Voronezh Massif in the Russian Federation. The Sarmatia Craton, along with the Fennoscandian and Volgo-Uralian Craton to the north, form the East European Craton.

In Ukraine, the Kirovograd district (Fig. 60) is underlain by migmatized and granitoid-rich Archaean and Palaeoproterozoic crystalline rocks of amphibolite facies. As a result of the intense Palaeoproterozoic orogenesis and metamorphism, gneisses alternate with migmatites and granites.

The uranium deposits occur in the central part of a N–S trending mobile zone between granite domes to the east and west. The mobile zone formed in the Palaeoproterozoic but has been repeatedly reactivated. Migmatites and blastomylonites formed first but were later overprinted by mylonitic and cataclastic sutures tens of metres wide.

Albitites are widespread in the tectonic zones and along splay faults. They form bodies tens to hundreds of metres in both lateral and vertical extent within structural zones that can be traced for tens of kilometres on the surface and to depths of 2.5–3 km. Uranium mineralization is hosted by these albitites.

Iron–uranium deposits are also found in the eastern part of the area (Krivoy Rog district). These ore deposits are genetically related to carbonate–alkaline metasomatism of ferruginous quartzites. The deposits are confined to deep faults that terminate the mobile zone to the east. Characteristics of these uranium ores are their development after magnetite ores and subconcordance of the bodies with host rocks that have been strongly altered by alkaline and carbonate metasomatism. For Cuney et al. [165], albitization and uranium mineralization are synchronous, occurring at about 1750–1800 Ma, as constrained by U–Pb geochronological data on the granite and on the uranium mineralization.

##### Ore geometry and metallogenesis

The orebodies have a convoluted shape and can be defined only by sampling. They consist mainly of flattened lenses and columnar stockworks arranged en echelon within mineralized albitites. The down-dip extent of separate bodies is 2–3 times greater than their strike lengths. Thickness varies from a few metres to 50 m, usually averaging about 10–15 m. Uranium content varies around 0.07–0.2% U, with the average of about 0.1% U. The ore mineralization consists of veinlets and disseminations.

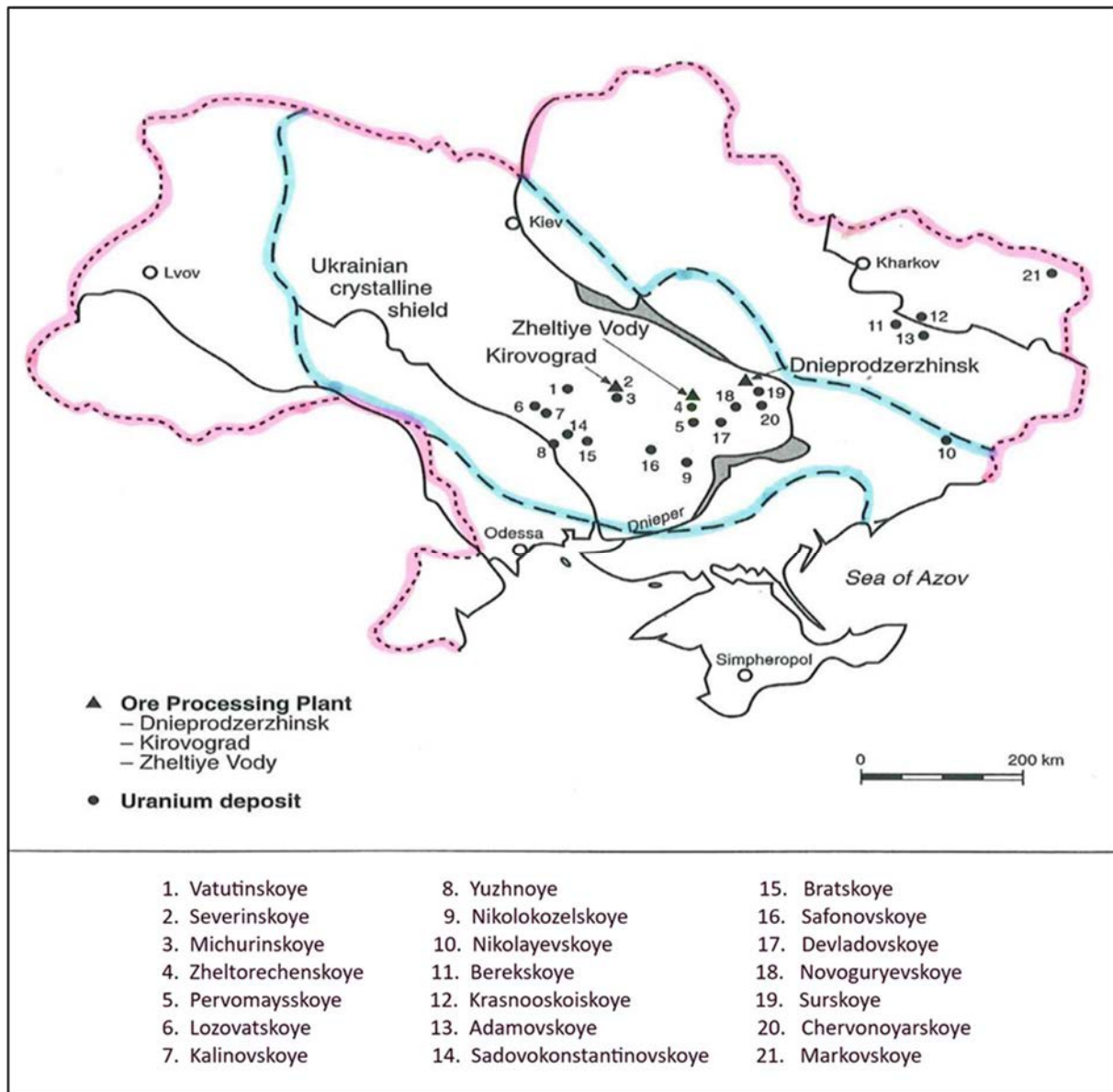


FIG. 60. Location of uranium deposits in Ukraine (adapted from Ref. [166]).

The ores have a rather complex composition, being dominated by uranium-bearing minerals. Predominant among them are davidite, nenadkevite, pitchblende and coffinite. These minerals are found as fine impregnations (tens of micrometres) within a gangue assemblage of chlorite, carbonate and haematite. In addition, uraninite and pitchblende form veinlets with carbonate and haematite.

Sodium metasomatites at the iron–uranium deposits are developed after quartz biotite, amphibole quartz and ferruginous hornfels. They consist of albite, riebeckite, rhodusite and carbonate, the proportions of which depend on the composition of the replaced rock. For example, aegirine is more abundant than albite in ferruginous hornfels and schists, cummingtonite schists are replaced by Mg–Fe carbonates and quartz interbeds in iron ores are replaced by dolomite. In addition, the mineralogical composition of uranium ores is a function of the type of metasomatism. Albitites are impregnated with uranium-bearing apatite, malacon and nenadkevite, whereas uraninite is predominant in essentially Ca-metasomatites.

The uranium deposits are believed to have been formed by fluids ascending from deep in the crust and related to Proterozoic tectono-magmatic reworking. This is supported by similar ages of the uranium-bearing albitites, cataclasites and mylonites (in fault zones) compared with the ages of

Palaeoproterozoic supracrustal belts, hypabyssal rapakivi, picritic dykes and gabbro–diabase intrusions, all of which are believed to be related to Proterozoic orogenesis.

Although all uranium deposits of this area are confined to albitite zones, not all albitites are uranium-bearing. Hence, the presence of these metasomatites is not the only prerequisite for uranium ore deposition. Other important ore controlling factors are large, permeable cataclastic zones, dilational parts of fold and fault systems (flexures and junctions) and mechanical heterogeneities (differences in permeability).

### **The Michurinskoye/Vatutinskoye deposits**

#### Introduction

Michurinskoye was the first large deposit found in the district in 1964, although mineralization had been identified at Pervomayskoye and Zheltorechenskoye in 1945 and 1946, respectively, and mined as early as 1959. Most of the deposits are exploited by underground workings to depths of up to 700 m below the surface (as at Michurinskoye), although some open pit mining was undertaken in deposits close to Zhovti Vody.

The largest deposit in the region is Novokonstantinovskoye (93 630 tU). Other large deposits are Tsentralne (61 800 tU), Severinskoye (38 350 tU), Vatutinskoye (25 390 tU) and Michurinskoye (18 490 tU) (Table 18). In addition to the albitite type deposits, several smaller ones have been discovered, associated with K-metasomatism and close to the age of the regional migmatization and intrusion (Yuzhnoye (5050 tU), Kalinovskoye (7550 tU), Lozovatskoye (2255 tU)). In addition, the Nikolo-Kozelskoye deposit (2090 t), hosted in sandstones and conglomerates that form the lower part of the Krivorozhian Series, is also located within the district.

#### Geological setting

The region containing the deposits is confined to the central portion of the crystalline Shield, an Archaean block deformed during the Palaeoproterozoic (Fig. 61). The regional geology is defined by a large granite–gneiss dome with a granitic core consisting of two granitoid suites of different age and nature. The southern part of the mass consists of anatectic and intrusive potassic granites (~2000 Ma) while the northern part is comprised of rapakivi granite and labradorite (1800–1700 Ma). The peripheral zone of the dome is made up of gneiss and migmatite, together with small granite bodies (2600 Ma) (Fig. 62).

The granite–gneiss dome is cut by a series of deep faults oriented approximately N–S and E–W, formed in the Archaean and reactivated in the Palaeoproterozoic. Numerous metasomatic albitite bodies formed in this latter event. The positions of these bodies are controlled by fault zones, both along the gneiss contacts, along the margins of the dome and along the granite bodies of the southern segment. However, these fault zones are absent in the rapakivi granites.

Uranium mineralization is observed only in a small portion of the albitite bodies, as large stockwork–metasomatic deposits of complex shape. The main uranium deposits (Novokonstantinovskoye, Severinskoye, Vatutinskoye and Michurinskoye) are localized along two N–S trending fault zones located east and west of the core portion of the dome (Fig. 62).

Intense alkali metasomatism represents both pre- and syn-ore alteration of the granitic and gneissic host rocks and forms large bodies of albitite. Fault systems controlled the formation of albitites, both during ductile deformation (blastomylonite seams) and the subsequent albitization that accompanied ore formation under brittle deformation conditions. Albitization and uranium mineralization were related to large scale cataclasis along reactivated and newly formed faults.

## Mineralization

The Michurinskoye deposit occurs along the Kirovograd Fault Zone in the Ingul–Ingulets gneiss and migmatite and adjacent to the Kirovograd granite. It is located in a wedge shaped tectonic block formed by convergent faults (Fig. 63). The major ore controlling structure is the main Eastern Fault, striking N–S and dipping 60–80° E. The Na-metasomatite bodies comprise aegirine–riebeckite or chlorite–albitite passing outwards to dequartzified chloritized gneiss, migmatite or granite and then to unaltered host rocks (Fig. 63). Uranium mineralization occurs in highly fractured and brecciated zones within albitite as lensoidal orebodies. The orebodies are oxidized near the surface and pinch-out at depths of 150–550 m [165].

The Vatutinskoye deposit is located near the western border of the Novoukrainska pluton. Orebodies develop along the footwall of the Main Western Fault Zone striking NW and dipping 60–80° SW. To the east, the deposit is bounded by the Eastern Fault (Fig. 64). These faults comprise extensive zones of mylonitized, brecciated and fractured rocks. Mineralized albitite extends over a distance of 3 km, with a width of up to 600 m and pinch-out at a depth of about 800 m. The major orebodies occur as lenses and stockworks in aegirine–riebeckite or chlorite–epidote albitite along the Main Western and the Eastern Faults. They are surrounded by zones of porous, pyritized episyenites (Fig. 64) [165].

Mineralization consists mainly of uraninite and brannerite. The metallurgical properties vary depending on the ratio of oxide and titanate forms of uranium and the amount of carbonate impurity. These characteristics determine whether the reserves are classified in either the <\$80/kgU or \$80–130/kgU production cost category.

The uranium ore deposits are related to albite–aegirine–riebeckite and albite–chlorite–epidote metasomatic alteration. The former represents altered cataclasites with disseminated uraninite, malacon, apatite and sphene. The chlorite–epidote–calcite type is less common than the amphibole–aegirine type, with ore minerals including pitchblende, uraniferous leucoxene, coffinite and a colloform/metacolloidal uranium–titanium silicate. The uranium minerals are located in zones of post-albitization cataclasis, within the inner parts of the metasomatic aureole.

The albitite bodies are zoned, as a consequence of sequential replacement of (metamorphic) plagioclase, quartz and biotite by albite. Riebeckite, aegirine, chlorite and epidote were formed in intermediate zones. The albitization is better developed in granite than in gneiss and schist, which is explained by the higher permeability of the former.

The Na-metasomatites also show a vertical zonation. Albite–aegirine–riebeckite metasomatites are followed up-dip by albite–chlorite–epidote metasomatites and silica is redeposited as veinlets and silicification zones in the upper part of metasomatic columns.

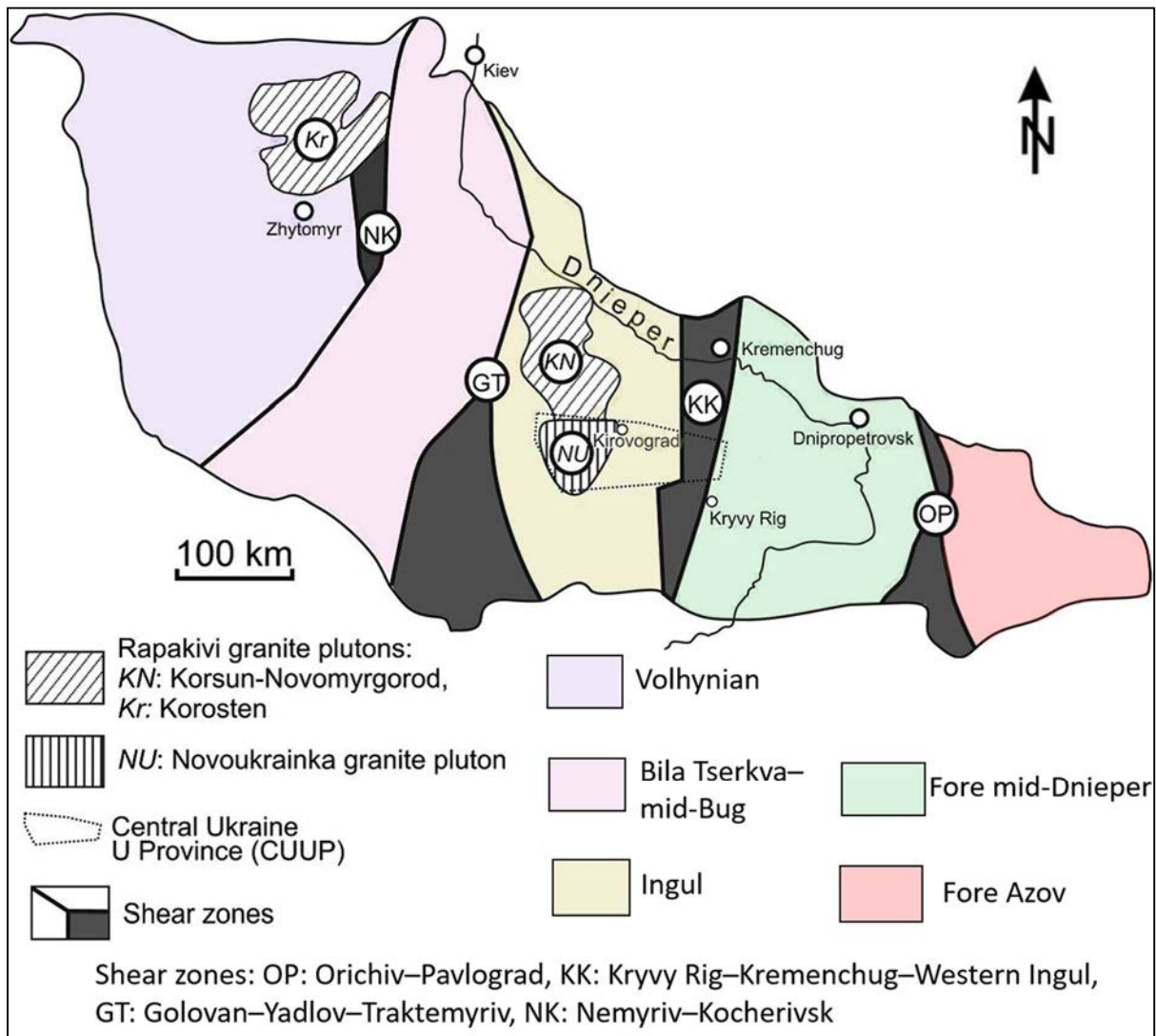


FIG. 61. Major geological structures of the Ukrainian Shield, with its subdivision into 'megablocks' (simplified after Glevasski and Kalayev) (adapted from Refs [165, 167]).

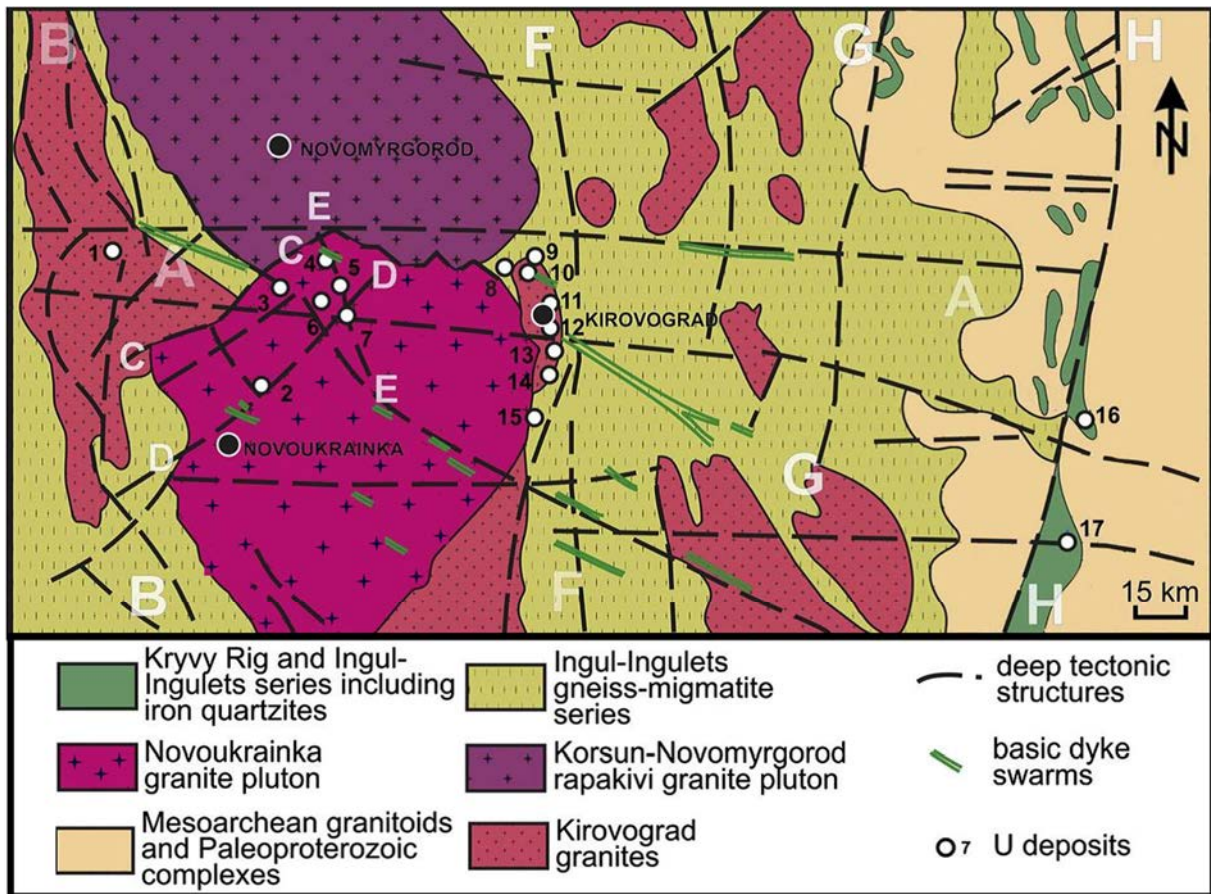


FIG. 62. Geological framework of the central Ukrainian Uranium Province related to Na-metasomatism in the Ukrainian Shield. Deep tectonic structures A–A: Subotin–Mashorin, B–B: Zvenygorod–Bratsk, C–C: Glodosk; D–D: Adabash; E–E: Novokonstantynivka, F–F: Kirovograd, G–G: Western Ingul, H–H: Krivoy Rog–Kremenchug. U deposits (1) Vatutinskoye, (2) Partyzanske, (3) April, (4) Novokonstantynovskoye, (5) Litne, (6) Lisne, (7) Dokuchayivka, (8) Schorsivka, (9) Pidgaytsi, (10) Severynskoye, (11) Central Tsentralne, (12) Michurinskoye, (13) Northern Konoplanka, (14) Western Konoplanka, (15) Kompaniyivka, (16) Zhovta Richka, (17) Pervomayske (adapted from Ref. [165]).

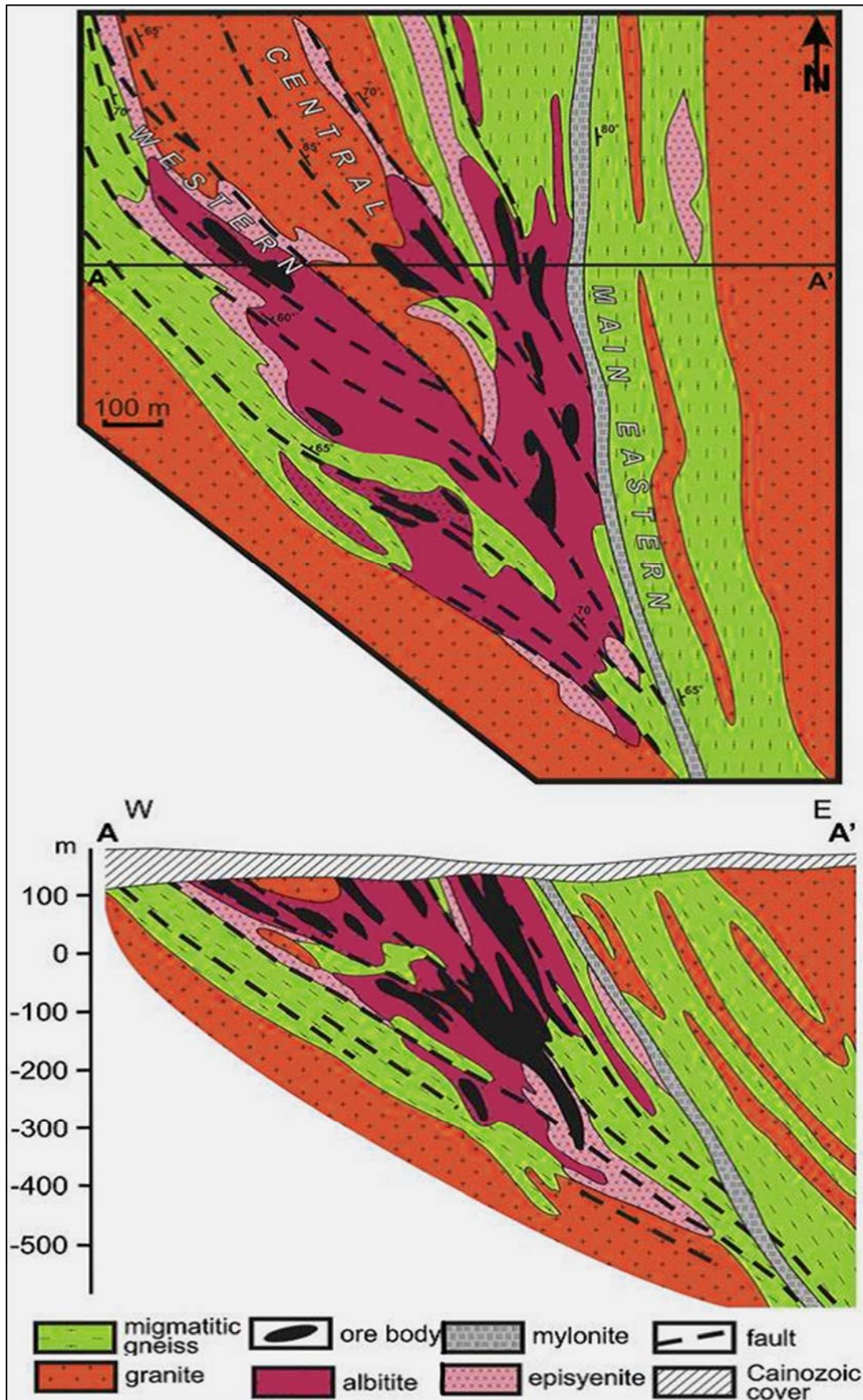


FIG. 63. Geological map: (a) and cross-section along line A-A'; (b) of the Michurinskoye deposit (adapted from Ref. [165]).

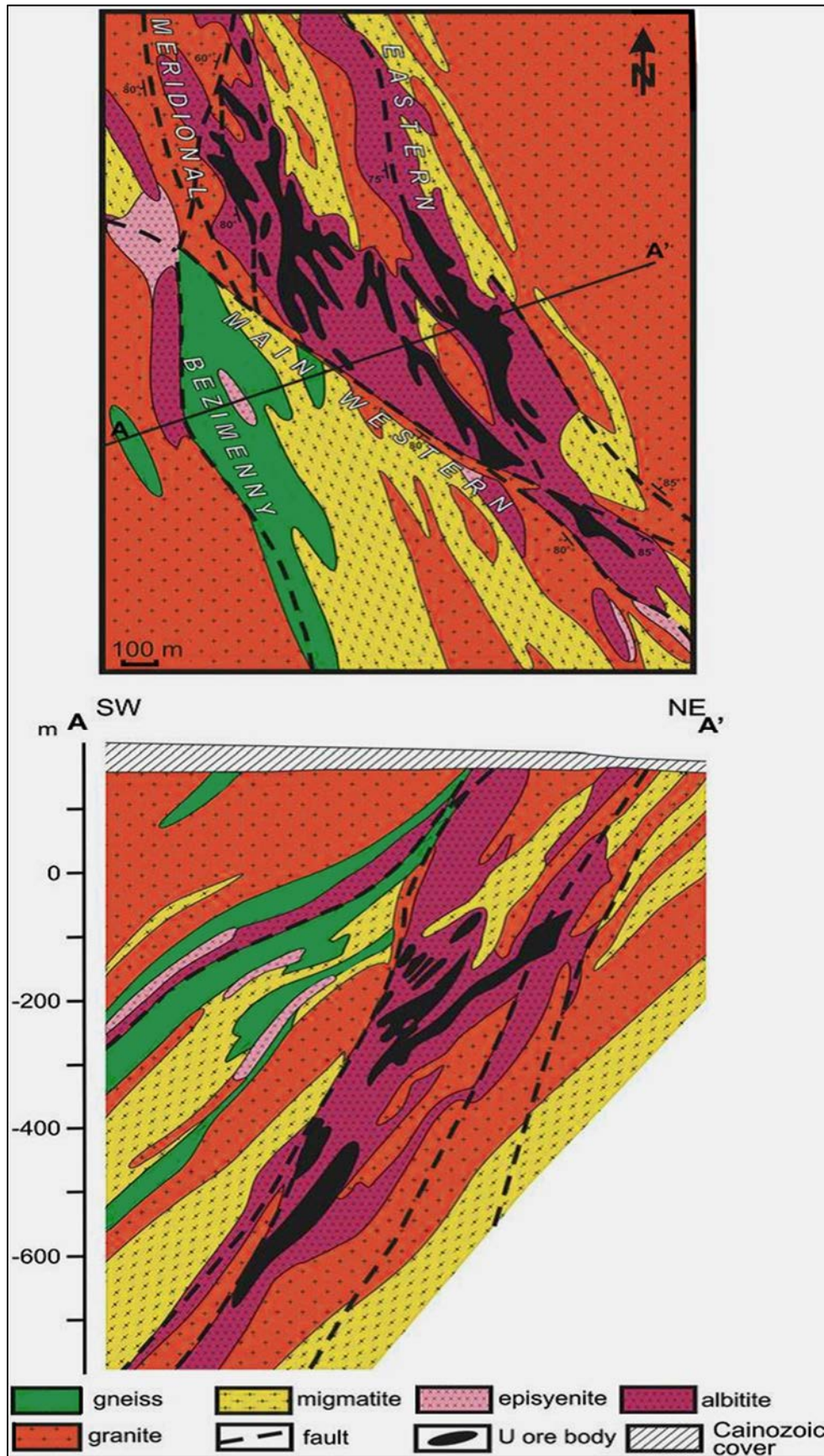


FIG. 64. Geological map and cross-section along line A-A' of the Vatutinskoye deposit (adapted from Ref. [165]).

## The Novokonstantinovskoye deposit

### Introduction

Located about 45 km west of Kirovograd, Novokonstantinovskoye, along with Lesnoye, Letneye and Dokuchaevskoye, form the Novokonstantinovsk orefield (Fig. 65). It is located within the northern Novoukrainska granitic massif, close to the boundary with the Korsun–Novomirgorod Massif in southern Ukraine. In earlier publications (e.g. Ref. [168]), Novokonstantinovskoye is referred to as “the northern sector of the far eastern flank of the Vatutinskoye deposit”. Novokonstantinovskoye is reportedly the largest metasomatite type uranium deposit in the Ukrainian Shield and hosts resources of 93 630 tU at a grade of 0.14% U [169].

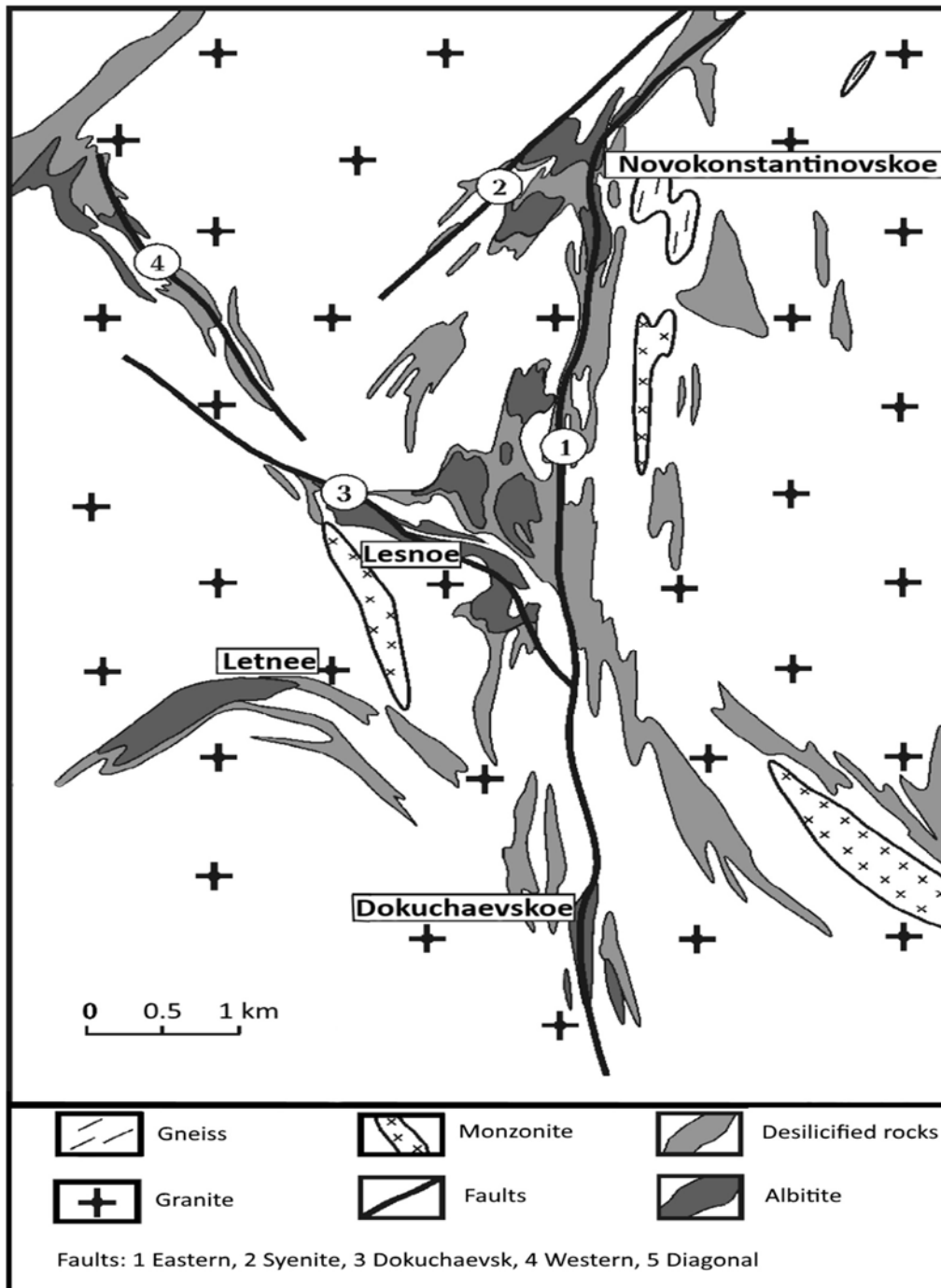


FIG. 65. Geological map of the Novokonstantinovskoye orefield showing the location of metasomatic zones and uranium deposits (adapted from Ref. [170]).

## Geological setting

Novokonstantinovskoye is hosted in the Palaeoproterozoic Novoukrainska Massif under up to 100 m of Tertiary–Recent cover. The Novoukrainska Massif is comprised of various granitic facies and minor gabbro and monzonite. Porphyritic garnet–biotite granite is the dominant lithology. Sills and leucocratic dykes of aplite–pegmatite, aplitic and gneissic granites as well as mafic dykes of diabase, lamprophyre and picrite cut the older rocks.

Granites are S-type and characterized by a negative Eu anomaly and regular chondrite normalized REE patterns. Petrological and geochemical data suggest an upper crustal melt, magmatic differentiation origin for the Novoukrainska intrusive rocks.

Uranium–lead isotope dating of zircons from pegmatitic, phaneritic and hypersthene–biotite granites indicate a date for these rocks of 2040–2025 Ma [171], whereas uraninite from the Novokonstantinovskoye deposit yields a U–Pb age of  $1808 \pm 27$  Ma [172].

The Novokonstantinovsk orefield is located at the junction of N–S, NW–SE, and NE–SW trending faults. This structural pattern is reflected in the distribution and morphology of large bodies of desilicified rocks and albitite, which reach maximum dimensions at intersections of these fault systems (Fig. 66). The structural pattern coincides with the orientation of plane parallel textures in porphyritic granite, monzonite bodies and gneiss xenoliths in granite.

A prominent structure in the orefield is the Novokonstantinovsk Fault Zone, which includes the Dokuchaevsk, Eastern and Syenite Faults. Novokonstantinovskoye is confined to the triple junction of the Eastern, Western and Intersecting Faults (Fig. 66). All three faults have similar deformation styles, comparable fault associated mineral assemblages, mylonite and cataclasite textures, concordant changes of fault orientation, smooth joining of these faults and related distribution of albitite and desilicified rocks [170].

The Eastern, Western and Intersecting Faults extend individually to depths of 300–450 m. At greater depth, the Intersecting Fault attains a steeper dip of 70–80°, joins the Western Fault and widens in a fan shaped manner. The expansion is accompanied by a marked volume increase in Na-metasomatite, predominantly of albitite, between mine levels -600 and -1200 m (Fig. 67).

Uraniferous Na-metasomatites preferentially occur within coarse-grained granite with variable amounts (10–60%) of feldspar porphyroblasts. Epidote–chlorite and chlorite–albitite are dominant to a depth of 300 m, intercalated with desilicified rocks. At a depth of 300–700 m, metasomatism consists of riebeckite and riebeckite–aegirine albitite assemblages that also contain phlogopite and carbonate. Aegirine–carbonate–phlogopite albitite occurs at the deepest levels, followed down-dip by desilicified rocks [19].

## Mineralization

Uraninite, brannerite, pitchblende and coffinite are the principal uranium minerals. Uranium silicates such as boltwoodite, kazdite(?) and sooty pitchblende occur in subordinate amounts. These minerals are present in all albitite facies.

Orebodies and albitite zones occur preferentially in granite and are controlled by a system of orthogonal and diagonal faults [173, 174]. Orebodies are clustered within two partially overlapping depth intervals: the upper interval (100–800 m) and the lower interval (750–1200 m). Orebodies in the upper interval are lens and tabular shaped and controlled by the Eastern Fault and a parallel trending, 35–40° eastwards dipping tectonic zone. Orebodies in the lower interval exhibit a more intricate shape and are surrounded by a large volume of barren albitite.

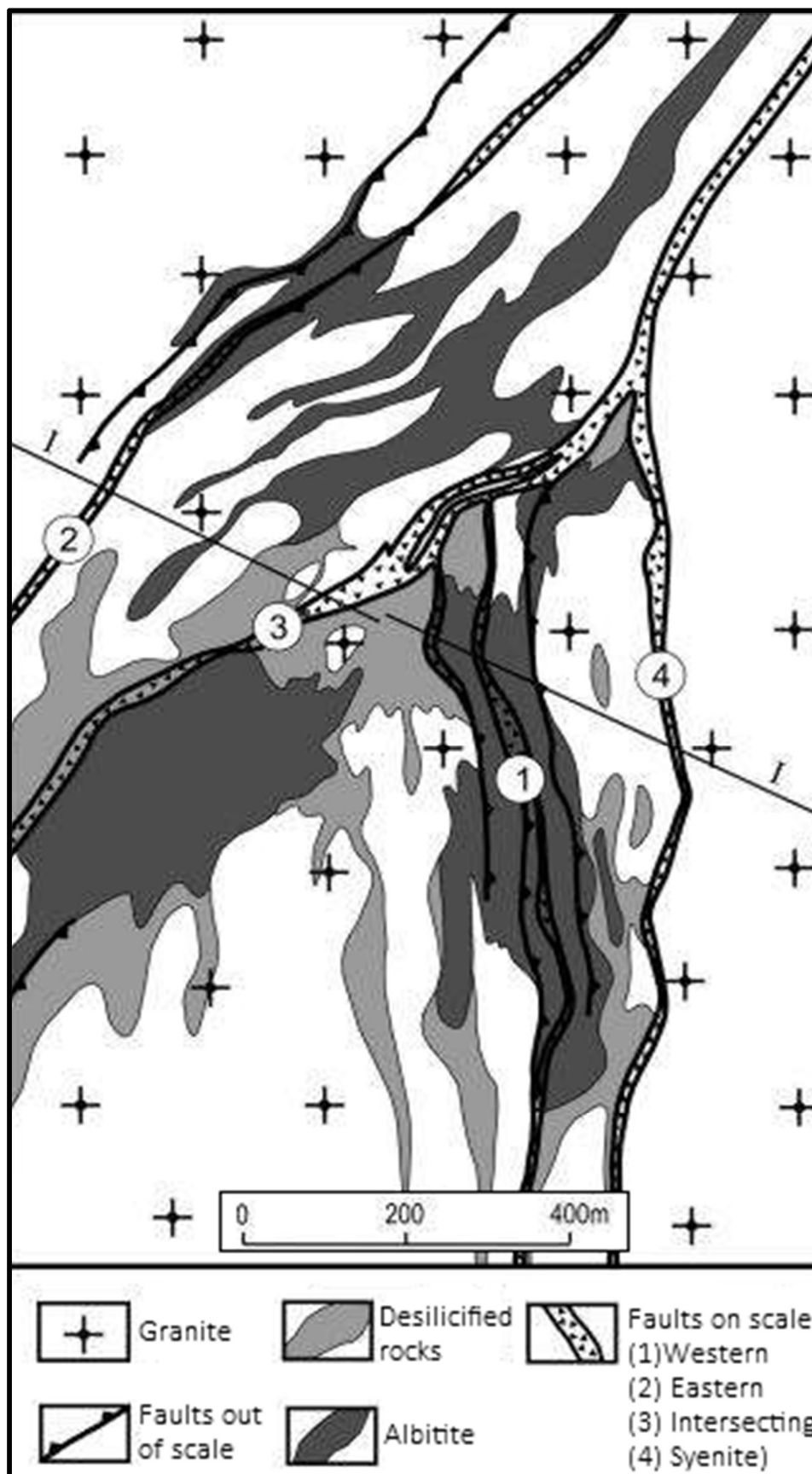


FIG. 66. Geological map of the Novokonstantinovskoye deposit showing distribution of ore hosting albitite and desilicified alteration zones in granitoids (I-I cross-section 36 shown in Fig. 67) (adapted from Ref. [170]).

## Metallogenic aspects

Uranium mineralization is of epigenetic, metasomatic–hydrothermal origin and primarily confined to structures cutting albitite bodies within granite. So-called ‘zones of volumetric cataclasis’ constitute the principal control on orebodies. These zones formed by repeated brittle deformation, which is assumed to have resulted from overpressurized hydrothermal fluids. As a result, distinctly fine-grained material was produced without obvious displacement of the affected lithologies. The deformation preceded and accompanied the formation of albitite, uranium ore and late stage mineralization [175]. In some places, these large cataclastic zones are associated with epidote–chlorite mylonite, but this association does not apply in every instance.

Circumstantial evidence provided by geophysical research, in particular by the seismically defined, E–W oriented depression of the Moho Discontinuity, suggests a similar hypogene origin for the fluids involved in metasomatism and uranium ore formation, which ascended along deeply rooted structures in the Novokonstantinovsk orefield, as postulated by Starostenko et al. [170] for the Kirovograd Fault Zone. The source of uranium and the nature of the ore forming fluids have not been determined.

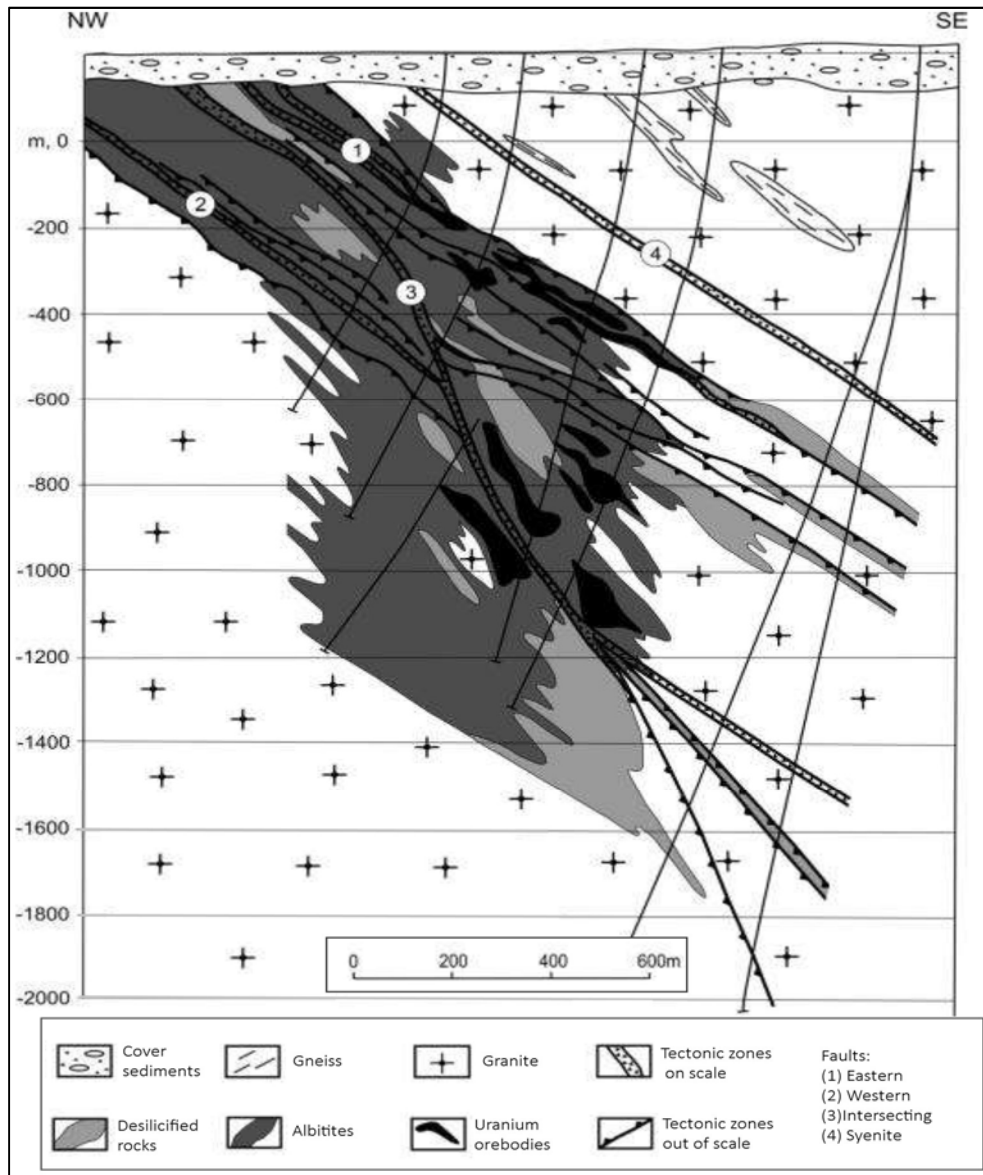


FIG. 67. Novokonstantinovskoye deposit. NW–SE cross-section along the exploration profile 36 showing the distribution of albitite bodies and associated uranium orebodies (adapted from Ref. [170]).

### 3.5.4.2. *The Michelin deposit (Canada)*

#### Introduction

The Michelin deposit is located in the Central Mineral Belt of Labrador, Canada (Fig. 68), approximately 50 km south-west of Postville and 130 km north-east of Happy Valley–Goose Bay. The region includes land where the subsurface resource rights are owned by the Provinces of Newfoundland and Labrador, as well as lands where the mineral rights are owned by the Labrador Inuit.

As outlined by Cunningham-Dunlop and Lee [176], Brinex (British Newfoundland Exploration Limited) began exploration in the area in 1955 following prospecting discoveries of copper, molybdenum and uranium. The surface showing of the Kitts deposit was discovered in 1956, with drilling and construction of an adit undertaken in 1957. No additional exploration was undertaken until 1966 when a Brinex–Metallgesellschaft AG joint venture resumed exploration. The Michelin deposit was discovered in 1968 and the Gear, Inda and Nash prospects were found in 1968–1969, all following up on airborne radiometric surveys.

During the 1970s, the Brinex–Urangesellschaft joint venture delineated the Kitts and Michelin deposits and conducted continued exploration follow-up on other radiometric anomalies in the Central Mineral Belt. Brinex plans for the mining of the Kitts and Michelin deposits were ended by the uranium price decline of the early 1980s, the properties were dropped and the sites were remediated by the Governments of Newfoundland and Labrador in 1992 [176].

A strategic alliance between Fronteer Development Group and Altius Resources Ltd obtained mineral licences to the area in 2003, which were operated as Aurora Energy Resources. From 2003 through 2007, the area was explored using airborne magnetic and radiometric surveys, ground mapping and prospecting, geochemical surveying and extensive diamond drilling. Environmental baseline work was also undertaken. Diamond drilling extended the strike length of the historic deposit and delineated resources to a vertical depth of 750 m [176], whereas previous drilling had only delineated resources to open pit depths. Additional resources have also been delineated for the Jacques Lake, Rainbow, Inda, Nash and Gear deposits.

In April 2008, the Nunatsiavut Government imposed a three year moratorium on uranium mining. In February 2011, Paladin Energy completed the acquisition of the uranium assets of Aurora Energy and published resources of 41 195 tU at a grade of 0.102% U. The moratorium on uranium mining was lifted in December 2011. As of 2015, the project remained dormant.

#### Geological setting

The Central Mineral Belt spans the junction of the Churchill, Makkovik, Nain and Grenville Provinces of the Canadian Shield (Fig. 68). The Michelin, Kitts and related deposits are found in the Makkovik Province, which is comprised of Palaeoproterozoic supracrustal rocks overlying Archaean age Nain Province basement, metamorphosed during the Makkovikian (Trans-Hudson) Orogeny. The Makkovik Province consists of three tectonic domains. The Kaipokok Domain in the north consists of reworked Archaean basement comprised mainly of granitoid gneiss with subordinate greenstone [177]. The Cape Harrison Domain represents a magmatic arc developed along the Makkovikian continental margin [176]. The Aillik Domain represents Palaeoproterozoic supracrustal rocks intruded by several Makkovikian and younger plutonic suites [176]. These strata host the uranium deposits.

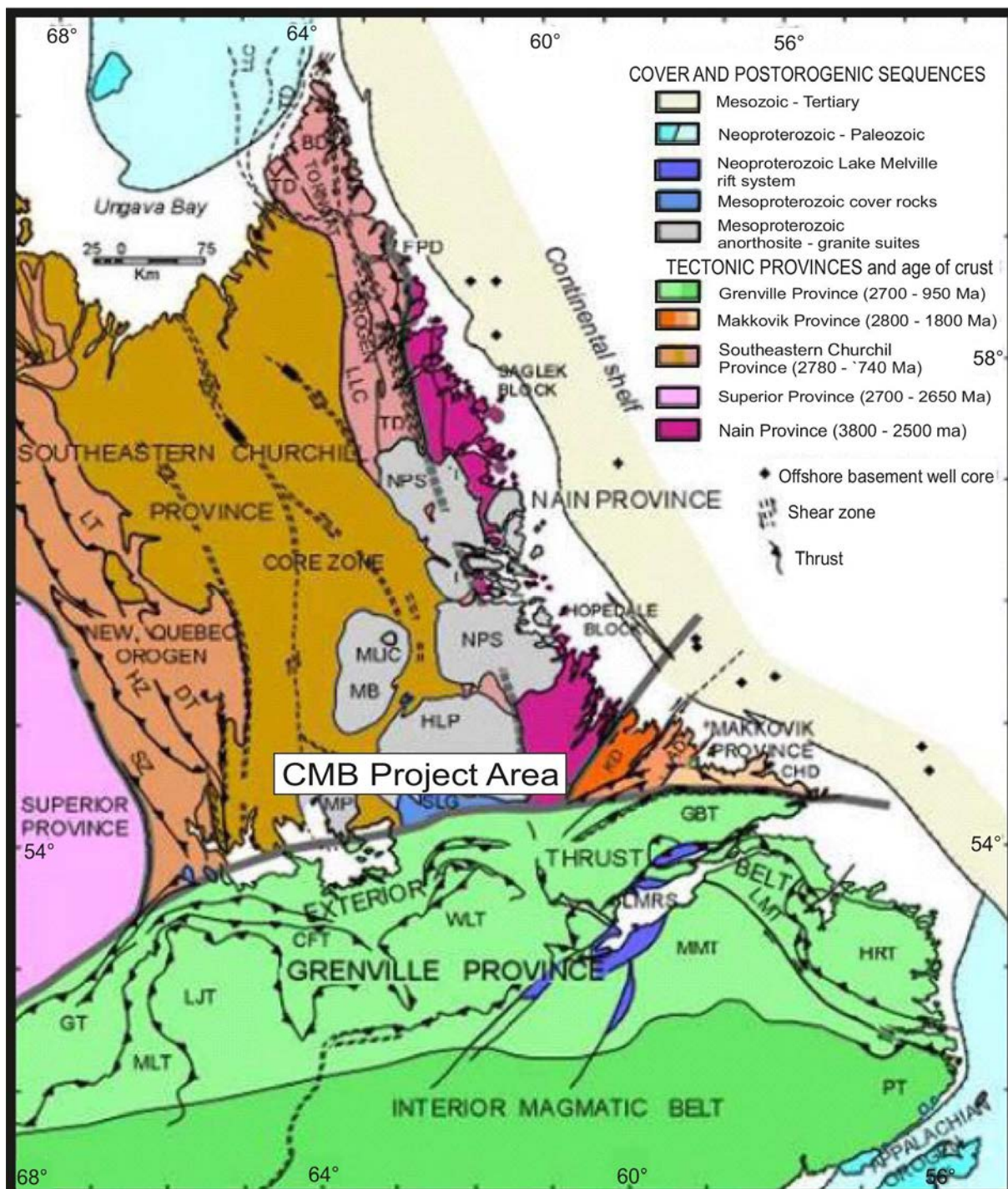
The geology of the eastern part of the Central Mineral Belt is shown in Fig. 69. The Post Hill group (~2000 Ma) consists of a shallow shelf sequence of pillow lavas, psammitic through pelitic sediments and iron formation deposited along the margin of the Nain Craton [178]. The Aillik group (~1850 Ma), which is dominated by felsic volcanic flows and fragmentals, also contains minor metasedimentary units, amphibolite and subvolcanic intrusives [178]. The Aillik group rocks in the

eastern Central Mineral Belt are represented by metavolcanic rocks comprising laminated quartz–feldspar–magnetite assemblages [176].

The Post Hill and Aillik groups were deformed during the 1810–1790 Ma Makkovikian Orogeny. The former was intensely folded and thrust, resulting in an interleaving of basement and cover rocks while the latter group was less deformed, with a single penetrative regional foliation and axial planar to isoclinal folds [177]. Overall, the metamorphic grade of the terrain is lower amphibolite, but in the Michelin area it is upper greenschist facies [178].

Deformation in the Aillik group is highly variable. Much of it is only mildly deformed and primary volcanic textures are often preserved. However, within regionally extensive but narrow high strain zones, the rocks exhibit a strong penetrative foliation and are strongly lineated and mylonitized. The uranium occurrences are localized in these strongly deformed zones [178].

The Michelin deposit is hosted in steeply dipping, highly strained felsic volcanic rocks. The host rock consists of alternating coarse- and medium-grained porphyritic and aphyric volcanic horizons, although these lithological variations do not control the distribution of mineralization in the deposit. The felsic volcanic rocks are cut by a swarm of narrow mafic dykes [176].



<p><b>Aurora Energy Inc.</b></p> <p>Regional Geology Map CMB Project Labrador Figure 3</p>	<p>SZ = Schefferville zone; HZ = Howse zone; DT = Doublet terrain; LT = Laporte terrane; LLC = Lac Lomier complex; TD = Tasiuyak domain; BD = Burwell domain; FPD = Four Peaks domain; KD = Kaipokok domain; AD = Albik domain; CHD = Cape Harrison domain; GBT = Groswater Bay terrane; LMT = xxxxxx; HRT = Hawke River terrane; MMT = Mealy Mountains terrane; WLT = Wilson Lake terrane; CFT = Churchill Falls terrane; MLT = Molson Lake terrane; LJT = Lac Joseph terrane; GT = Gagnon terrane; PT = Pinware terrane; LMRS = Lake Melville rift system; SLG = Seal Lake group; NPS = Nain Plutonic Suite; MB = Mistastin batholith; HLP = Harp Lake pluton; MP = Michikamau pluton; MLIC = Mistastin Lake Impact crater</p>
--	--

FIG. 68. Regional geology and location of the Michelin deposit and the Central Mineral Belt project [176] (reproduced with permission).

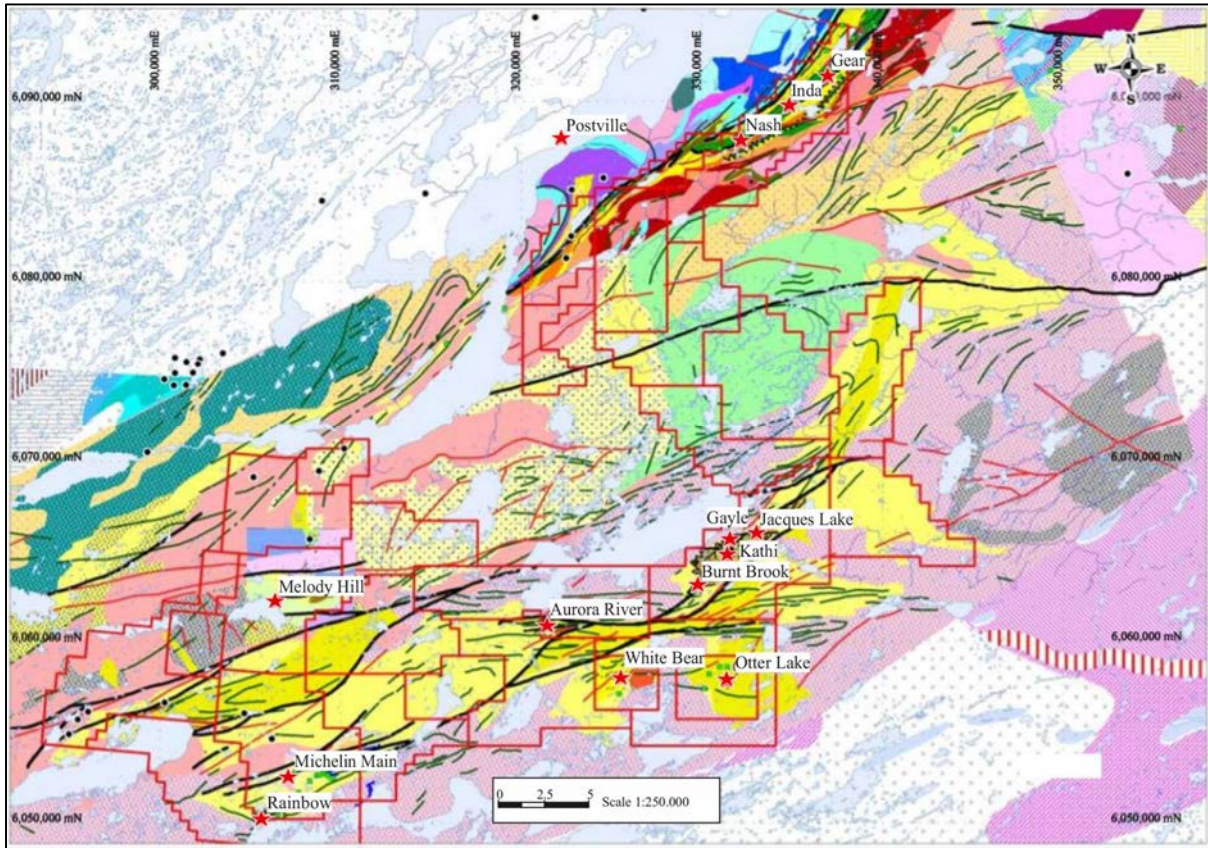


FIG. 69. Geology of the eastern part of the Central Mineral Belt, Labrador, showing the locations of the main uranium deposits. The Aillik group is shown in yellow and the Post Hill group is represented by the green and blue units in the north [176, 177] (reproduced with permission).

### Mineralization

As described by Cunningham-Dunlop and Lee [176], the Michelin orebody consists of a series of subparallel mineralized zones lying within a feldspar porphyroclastic quartz mylonite zone conformable to the composite  $S_0/S_1$  foliation (Fig. 70). The zones are oriented at  $060^\circ/55^\circ$  with a steep south-west plunge parallel to the regional lineation. The mineralized lenses span a 150–200 m thick zone but most of the mineralization is found within a 65 m thick interval in the upper part of the lower half of the alteration zone. Mineralization consists of microscopic disseminations of uraninite associated with visibly strong haematization. Alteration consists of the replacement of metamorphic biotite and chlorite by hornblende and, proximal to mineralization, by pyroxene and actinolite, as well as minor calcite and gypsum. This is consistent with the typical alteration assemblage of the other uranium deposits in the Aillik and Post Hill groups, which includes haematization and albitization of wall rocks, with uraninite found in thin black veins accompanied by hornblende, actinolite, clinopyroxene, magnetite, haematite, sphene, epidote, carbonate, quartz and sometimes sulphides [178, 179].

As described by Gandhi [179], pitchblende is by far the most abundant uranium-bearing phase, with only minor coffinite, soddyite and uranyl-bearing secondary minerals. The pitchblende is found as very small disseminations ( $<10\ \mu\text{m}$ ), often as inclusions in mafic silicates or in streaks with haematite and mafic minerals. At Michelin, the main host minerals are sphene and alkali pyroxene, which form aggregates with alkali amphiboles, Fe–Ti oxides, zircon, calcite and apatite in a quartz–albite host rock. Uranium–lead geochronology for Michelin indicates a near concordant date of 1806 Ma, reflecting Hudsonian metamorphism. Textures and petrographic relationships indicate that the

mineralization predates at least the latest deformation stage [179] and therefore could be either pre- or syn-deformational.

The Michelin deposit has a defined strike length of 1200 m and has been intersected to a depth of 700 m, but remains open in all directions [176]. At depth, the mineralized lenses coalesce, producing a higher grade core zone from about 330 m vertical depth to the lower extent of drilling. The Michelin resource is 41 195 tU at a grade of 0.102% U. Several other showings and deposits of similar mineralization are present in the region. Aurora Energy Resources (now Paladin Energy) also has NI 43-101 compliant resources for the nearby deposits of Jacques Lake, Rainbow, Nash, Inda and Gear.

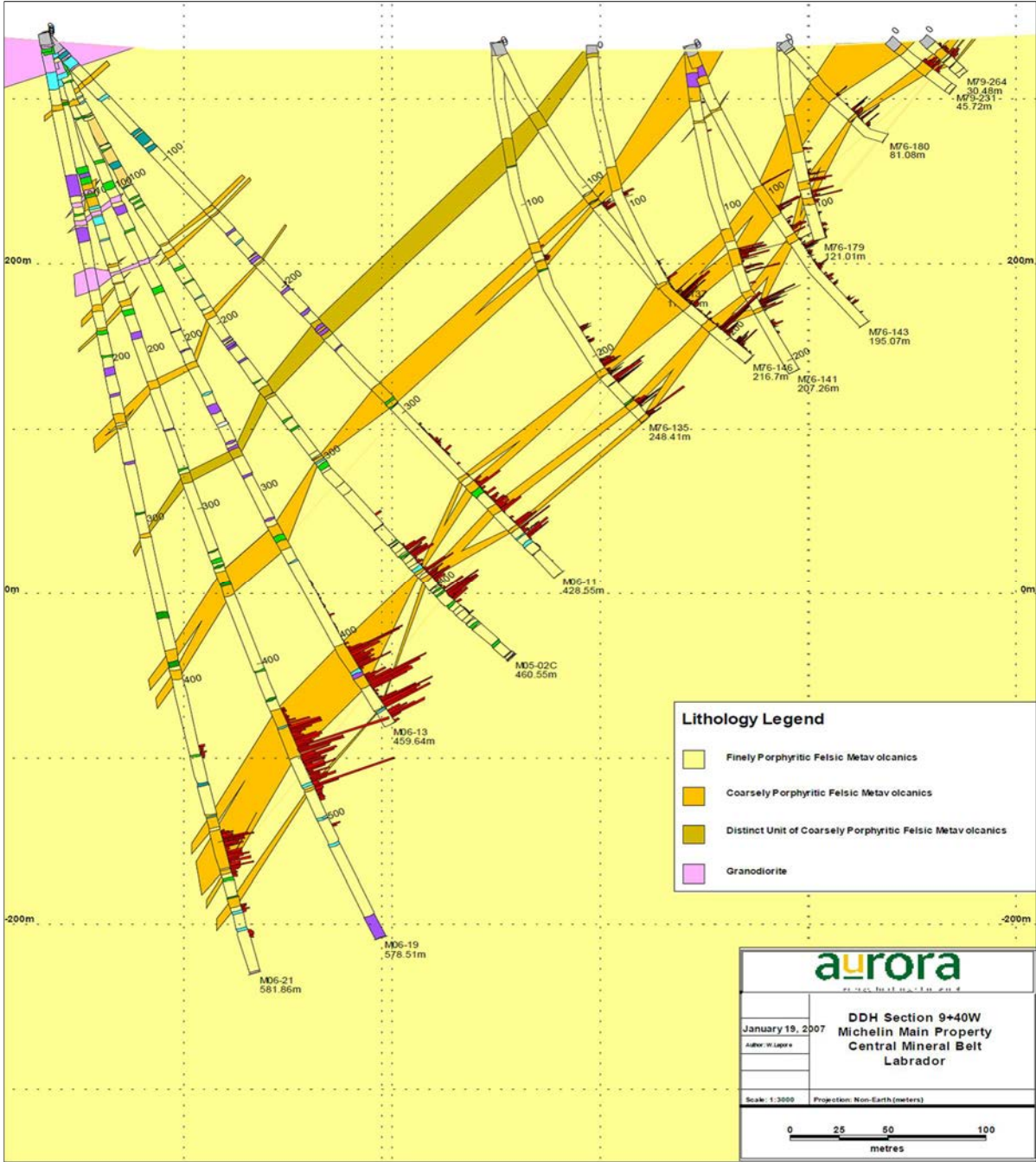


FIG. 70. Michelin deposit geological cross-section with assay histograms. Lithology legend: finely porphyritic felsic metavolcanics (yellow), coarsely porphyritic felsic metavolcanics (orange), granodiorite (pink) [176] (reproduced with permission).

## Metallogenic aspect

The Central Mineral Belt contains numerous U and U–Cu showings of different styles, ages and genesis. The most significant style is that found in the eastern part of the belt and typified by Michelin. While the local geological characteristics vary, as described by Cunningham-Dunlop and Lee [176], the common characteristics are: (a) deposits are hosted in Palaeoproterozoic supracrustal sequences of the Post Hill (metasedimentary) and Aillik (metavolcanic) groups; (b) host rocks were strongly foliated and sheared during the Makkovikian Orogeny, and (c) very fine-grained pitchblende is associated with magnetite, actinolite, hornblende, calcite, pyrite veins with pervasive haematite with or without magnetite and albite alteration.

Deposits in the Post Hill group rocks include Kitts, Gear, Inda and Nash, while those in the Aillik group include Michelin, Jacques Lake, Burnt Lake, Melody Hill, Otter Lake (Emben), Rainbow and Gayle. The relatively narrow time span elapsing between sedimentation/volcanism, metamorphism and mineralization, coupled with the stratiform/stratabound nature, led [179] to the interpretation of a syngenetic origin for the deposits. However, the Trans-Hudson isotopic dates of mineralization, approximately 200–300 Ma younger than the estimated age of the host rocks, coupled with the fracture filling and breccia style of mineralization led Wilton [178] and others to propose an epigenetic origin. The debate revolves around whether the mineralization is older than, but overprinted by, the Makkovikian Orogeny or whether it is genetically related to Makkovikian deformation.

Cunningham-Dunlop and Lee [176] note some similarities in alteration mineralogy of these deposits with IOCG deposits and speculate on a similar origin. However, this latter deposit class is interpreted so broadly in common usage that it essentially represents a style of alteration rather than a genetic model. The lack of a granitic relationship and a significantly different metal grade are only two factors that make comparison to Olympic Dam highly questionable.

The dominance of felsic volcanic host rocks has led to the deposits in the Aillik group being classified as volcanic-hosted (and in some cases volcanogenic) uranium deposits [179]. Those found in the Post Hill group have also been classified as volcanic-related and hosted solely in the country rocks adjacent to the volcanic flows and sub-volcanic intrusions. Support for this view derives from the observed U–Mo–F–W geochemical association and the presence of some alteration types (albite, haematite and carbonate) that are consistent with a volcanic model, although not exclusive to it. In this model, the deposits are interpreted as metamorphosed volcanic uranium deposits. If this were the case, it would be expected that siliceous and aluminous low temperature alteration phases such as opal and clays would, on undergoing metamorphism, produce diagnostic aluminous metamorphic mineral assemblages.

However, these deposits bear strong similarities to the metasomatites described in other parts of the world, including the Ukrainian Shield. Barthel [180] describes albitite related uranium occurrences as encompassing Na-metasomatism, uranium related to a high temperature calc-silicate alteration assemblage and controlled by regional scale structures in high grade metamorphic terrains. Considering the strong association of mineralization with Na–Ca–Mg metasomatism in highly strained volcanic rocks under ductile to brittle–ductile conditions, Michelin and the similar deposits of the Central Mineral Belt are best classified as Na-metasomatites related to the late stages of the Makkovikian Orogeny.

However, regardless of the genetic model, the empirical or exploration model, as outlined above, is diagnostic and features high strain zones affected by mylonitization, shearing and brecciation in Palaeoproterozoic supracrustal rocks, where pitchblende is found as veins, as fracture fillings and in breccias, with a mineral assemblage of actinolite, hornblende, magnetite, calcite and pyrite, within albitized and haematized wall rock.

### 3.5.4.3. Deposits of the Elkon district (Russian Federation)

#### Introduction

The Elkon district is located 100 km ENE of Aldan in the Sakha Republic. Uranium occurrences were first discovered here in the early 1960s. Since then, nine deposits have been delineated with total resources of 344 000 tU at an average grade of 0.146% U. In addition, the deposits also contain gold (177 t Au at a grade of 0.84 g/t Au), silver and molybdenum as by-products. The project is under development and is expected to begin production around 2017–2018. Planned production capacity is 5000 tU/year. Owing to the abundance of brannerite, the ore is classified as refractory. Recovery is in the range 85–89%.

#### Geological setting

The core of the Aldan Shield consists of Archaean–Palaeoproterozoic crystalline basement which is exposed in several uplifts, including the auriferous and uraniferous Elkon Horst. As much as 700 m of subhorizontally bedded Vendian–Lower Cambrian limestone and dolomite cover the basement to the north while Lower Jurassic coal-bearing continental deposits and pyroclastic rocks fill the grabens.

The Elkon Horst (Fig. 71) is a NW–SE trending, 60 km long and up to 40 km wide uplift in the southern part of the Aldan Shield. Principal lithologies are Archaean granulite, amphibolite, gneiss, schist, quartzite and marble. Intense Neoarchaean–Palaeoproterozoic orogenesis generated leucocratic biotite–microcline granite and migmatite. Only remnants of gneiss and schist are found in the granitized rocks.

Small laccoliths, stocks, sills and dykes of alkaline and calc-alkaline rocks of the Aldan volcanic–plutonic complex are intruded into the aforementioned units, particularly within the western part of the Elkon Horst. This took place during three phases in the Jurassic and Cretaceous.

The area was affected by several episodes of faulting, particularly during the Palaeoproterozoic and Mesozoic. The three prominent fault sets are: (i) ancient NW–SE trending faults formed during the Palaeoproterozoic; (ii) ancient faults reactivated during the Mesozoic and (iii) younger neotectonic NW–SE and N–S oriented faults of Mesozoic age. The latter caused block movements and resulted in horst and graben structures [19].

Several types of alteration have been described [177]. They include from oldest to youngest:

- (a) Post-granitization K–Si metasomatism developed in a zoned pattern in the palaeoproterozoic granitoids. These metasomatites often contain local concentrations of disseminated uraninite, cleveite, bröggerite, orthite, thorite, malacon and sphene;
- (b) Multistage Mesozoic, pre-uranium alteration processes generated various mineral assemblages that were superimposed on each other in the ore zones. All of these were controlled by Mesozoic and reactivated ancient fault zones. The oldest is an albite–sericite–chlorite facies that zonally overprints the wall rock and formed micro-veinlets extending up to a few tens of metres from the faults;
- (c) A younger and the most prominent pre-uranium alteration assemblage consists of pyrite–carbonate–potassium feldspar with disseminated gold. This alteration type is tan, greenish brown or dark grey and surrounds all ore-bearing structures. This facies overprints the albite–sericite–chlorite aureoles and forms micro-veinlets as much as several hundred metres along and down-dip of reactivated ancient faults and commonly persists for 6–10 m and locally up to 20 m into the wall rocks. In the outer zone, mafic minerals are completely replaced by dolomite, ankerite, pyrite and marcasite, while plagioclase is replaced by sericite and carbonate, magnetite by pyrite, and quartz by calcite. The proportions of carbonate and pyrite are highly variable. Carbonate can amount to 50%, as found in the Yuzhnaya Zone. Pyrite contains disseminated gold with values of up to 4.5 g/t Au in the pyrite concentrate. The inner halo is characterized, in addition to the above mentioned replacements, by a

markedly increased K-feldspar content. This results in a dense, dark grey, fine-grained alteration facies composed of 40–75% K-feldspar, 35–50% carbonate, 5–15% pyrite and minor sericite, sphene and apatite. Pyrite concentrates carry as much as 80 g/t Au;

- (d) Late and post-ore alteration includes carbonatization, silicification, fluoritization, sulphidization, and oxidation. The post-ore emplacement of Mesozoic alkaline intrusions caused fenitization of earlier facies.

## Mineralization

Location, shape, dimensions and internal structure of uranium–gold and uranium–gold–silver deposits are primarily controlled by reactivated Palaeoproterozoic NW–SE oriented and steeply SW dipping faults of Mesozoic age (Fig. 71). The principal structure, the Yuzhnaya Zone, contains, along its central section, five large, more or less continuous deposits spread over a distance of about 20 km.

Deposits consist of intermittently distributed orebodies separated by barren or erratically mineralized intervals. Mineralized zones consist of variably mineralized fractures, joints and disseminations, the distribution, intensity and dimensions of which are a function of the intensity of brecciation of the host rock (Fig. 72).

Ore lodes have a vein-like or columnar configuration and are usually 0.2–5 m wide in Mesozoic faults but may have widths of up to 10 m in reactivated Proterozoic faults (Figs 73 and 74). Lodes have an internal stockwork structure consisting of closely spaced brannerite stringers and impregnations that form an echelon, linear, 500–700 m long and 0.5 m to more than 10 m wide orebodies. Some deposits encompass several such orebodies. Ore shoots within these orebodies also carry gold and, locally, molybdenum.

Orebodies are rarely exposed at the surface. The upper limit of most orebodies is 200 m. Ore was intercepted by drilling to a depth of 2000 m, but there is no depth related change in ore mineralogy over the whole vertical interval, suggesting that mineralization probably continues to greater depths.

The only primary uranium mineral is a medium to low temperature U–Ti phase interpreted as brannerite. It commonly occurs in massive, colloform aggregates that enclose small fragments of the host rocks and, more rarely, as prismatic crystals up to 0.08 mm long. Associated minerals are pyrite and marcasite, which mainly predate the brannerite. Only a small fraction of the sulphides are contemporaneous with the brannerite.

Alteration products of brannerite include secondary brannerite, variably uraniferous TiO<sub>2</sub> phases, uranium oxides and, in oxidized intervals, hexavalent uranium minerals which formed after renewed cataclasis. Gold is a common constituent of most of the ores but it is not believed to be syngenetically related to the uranium. Gold mineralization both pre-dates and post-dates the brannerite formation.

Aggregates of subhedral to rounded uraninite and titanium oxide phases with or without brannerite occur in the vicinity of Mesozoic magmatic intrusions in the NW segment of the Elkon district. Their generation is attributed to the destruction of brannerite by thermal metamorphism. A final generation of endogenic mineralization consists of veinlets of dark quartz, dolomite, calcite, fluorite, pyrite, marcasite and minor baryte, chalcopyrite, sphalerite and galena.

Oxidation of primary ore persists to a depth of several tens of metres below the current surface in most deposits of the Elkon district but may extend to depths of 600 m along some ore-bearing structures. Characteristic minerals include iron and manganese hydroxides, carbonates, clay minerals, opal, chrysocolla, malachite, azurite, jarosite, various products of decomposed brannerite, uranyl-phosphates, and uranium adsorbed onto iron hydroxides and other minerals. The textures of uraniferous mineralization are dominated by fine to microclastic breccia and veinlet breccia. Veinlets and disseminations are less frequent [181].

Coffinite typically occurs in disseminated uranium mineralization as replacement of pyritized mafic minerals and as coatings on iron sulphides within fissures and voids.

Three uranium ore varieties have been distinguished [182]: (i) gold–brannerite; (ii) gold–uraninite, and (iii) brannerite–silver–gold mineralization and, additionally, three gold ore types that may contain minor uranium.

- (i) Gold–brannerite mineralization is typical for deposits occurring along the Yuzhnaya, Severnoye, Sokhsolookhsk, Pologaya, Vesennyyaya and Agdinsk zones. Ore control is by reactivated Palaeoproterozoic and younger NW–SE oriented and steeply SW dipping faults of Mesozoic age and by pyrite–carbonate–potassic feldspar altered rocks. Mineralized zones follow blastomylonites imposed on Palaeoproterozoic metadiorite dykes. Country rocks are Archaean–Palaeoproterozoic ultrametamorphic lithologies. Gold–brannerite mineralization is of veinlet–disseminated type and is commonly located within gold-bearing pyrite–carbonate–potassic feldspar altered zones. Brannerite is the only primary uranium mineral. Appreciable amounts of gold and silver are bound in pyrite of two pre-brannerite generations of the pyrite–carbonate–potassic feldspar alteration;
- (ii) Gold–uraninite mineralization is known from the Nadezhda and Interesnaya zones in the north-western sector of the Elkon district, where Mesozoic stocks and dykes are abundant. The ore control and geological setting are similar to those of the gold–brannerite deposits except that the uraninite is restricted to zones of thermal metamorphism. The gold–uraninite mineralization has higher uranium grades than the gold–brannerite mineralization. Early pyrite is the essential host of native gold, with contents of 9.1–24.5 g/t Au;
- (iii) Brannerite–silver–gold mineralization is reported from the Fedorov, Marsovaya, Mramornaya and Zvezdnaya zones in the south-western part of the Elkon district. Ore control and geological setting are similar to those of the gold–brannerite deposits. Ore lodes consist of gold-bearing metasomatic rocks intersected by thin brannerite stringers and a younger generation of small quartz and carbonate veinlets with pyrite, native gold, native silver and acanthite.

Brannerite–gold ore has uranium contents in the range 0.02–0.2% U or higher, but typically around 0.1–0.15% U. Gold grades average 1–2 g/t, silver 8–15 g/t and molybdenum grades vary around 0.01–0.1% Mo. Uraninite–gold ore averages 0.5–1 g/t Au, 10–20 g/t Ag and has uranium contents exceeding those of the brannerite–gold ore. Brannerite–gold–silver ore has average grades of 3–10 g/t Au and 15–200 g/t Ag, but locally the gold and silver grades can be substantially higher. Uranium grades are typically 0.02–0.2% U but can exceed 0.5% U. The carbonate content of ore varies from 1.5% CO<sub>2</sub> in silicified ore to 10% CO<sub>2</sub> in other ore types. The sulphur content is typically 1–4% S but can be higher than 20% S [19].

#### Metallogenic aspects

The ore forming process began with the gold-bearing pyrite–carbonate–orthoclase alteration event, with most of the gold contained in pyrite. Subsequently, uranium was introduced into the previously altered rocks by hydrothermal fluids. Both processes occurred during the Mesozoic tectono-magmatic event affecting the Aldan Shield. Uranium was deposited as brannerite under medium to low temperature conditions at medium to shallow depth and formed structurally controlled deposits in reactivated Palaeoproterozoic and younger Mesozoic fault zones. Owing to the association of deposits and intrusions in spatially and temporally, it is suggested that the hydrothermal process was initiated by Mesozoic magmatic activity. Uranium was likely derived from the Archaean granitized rocks, which have elevated uranium contents. Uranium leaching resulted from the interaction of ascending, medium temperature, sulphur- and carbonate-bearing solutions with granitized rocks. Later, the Au–Ag mineralization with native gold and silver minerals precipitated in some of the previously formed U–Au zones in areas with Mesozoic intrusions, as exemplified by the Fedorov zone [19].

It is noteworthy that there is no vertical zonation in the uranium-bearing zones of the Elkon district except for extensive silicification in the upper parts of the deposits ('quartz caps'). Mineralogical and chemical compositions of ores are quite uniform over the drill intercepted interval, which in the Yuzhnaya zone is down to about 2000 m, which indicates relatively stable conditions of ore deposition, presumably due to uniform conditions [19].

Thermobarometric studies indicate pronounced variations in temperature during the entire metallogenic evolution of the Elkon district and its individual stages. Successive mineral stages started with higher temperatures than those at the end of the previous stage, suggesting a multiphase influx of ore forming fluids [19].

All post-brannerite processes only altered the original brannerite and redistributed uranium, forming coffinite. They did not add new uranium. Uranium-lead isotope dating yields an age of 135–130 Ma for primary brannerite, which correlates with the emplacement of the Early Cretaceous intrusions [182].

Archaean-Palaeoproterozoic granitized rocks are considered the most likely source of uranium. The pre-uranium gold is likely sourced from Mesozoic magma chambers of mantle material while the post-uranium gold and silver and the porphyry gold were likely derived from shallower magma chambers [182].

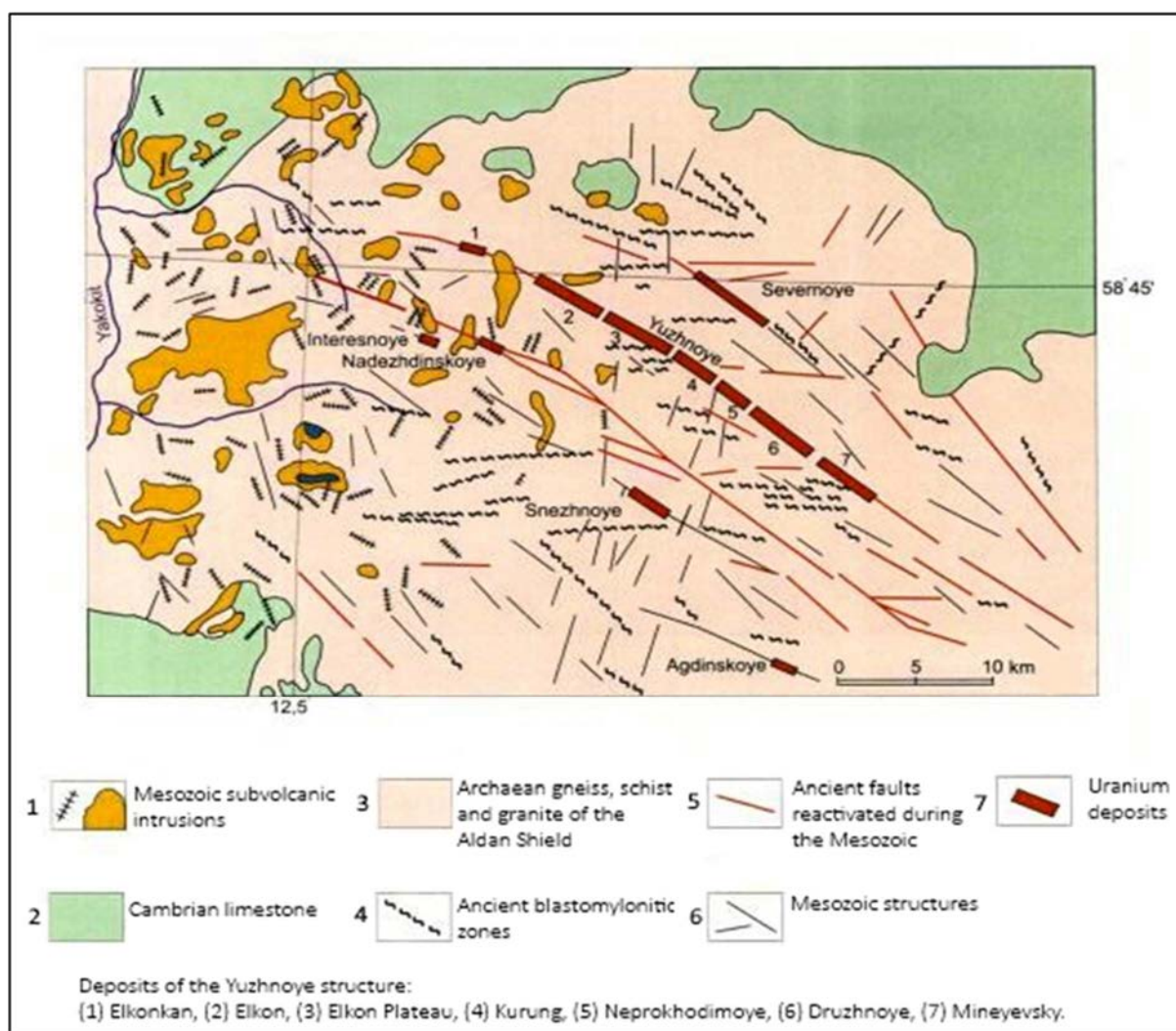


FIG. 71. Geological map of the Elkon district showing the location of the principal uranium zones and deposits) (adapted from Ref. [183]).

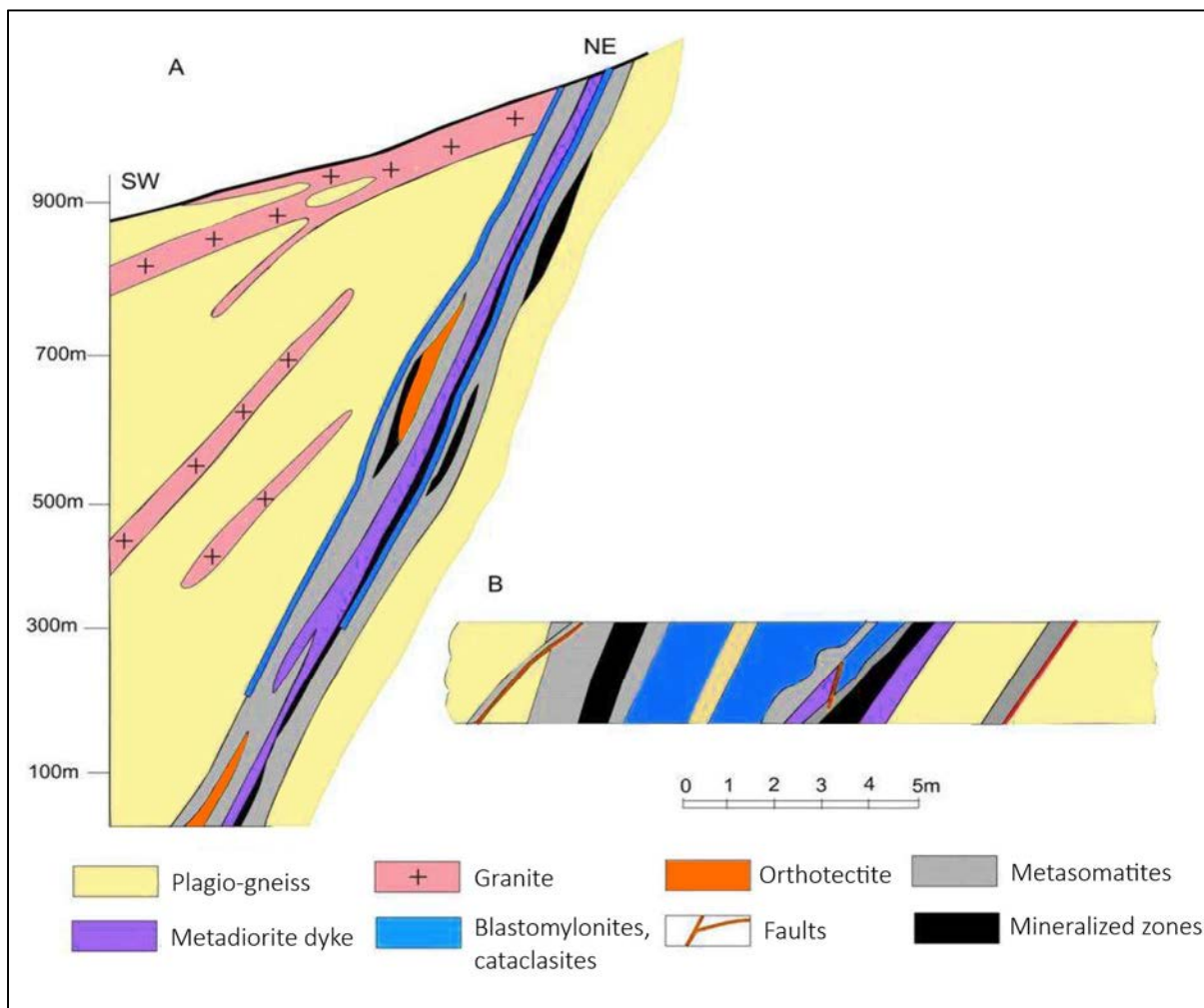


FIG. 72. Geological section across the Druzhnoye deposit) (adapted from Ref. [181]).

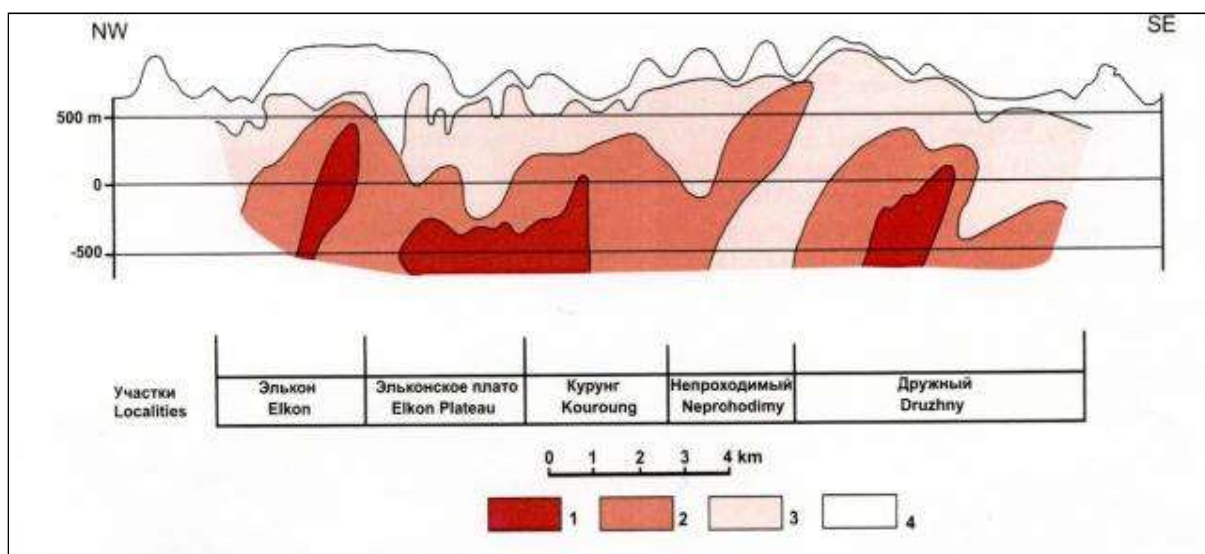


FIG. 73. Longitudinal section of the central part of the Yuzhnoye structure, (1) high grade ore, (2) average grade ore, (3) low grade ore, (4) barren rock [183] (reproduced courtesy of A. Boitsov, ARMZ/Uranium 1).

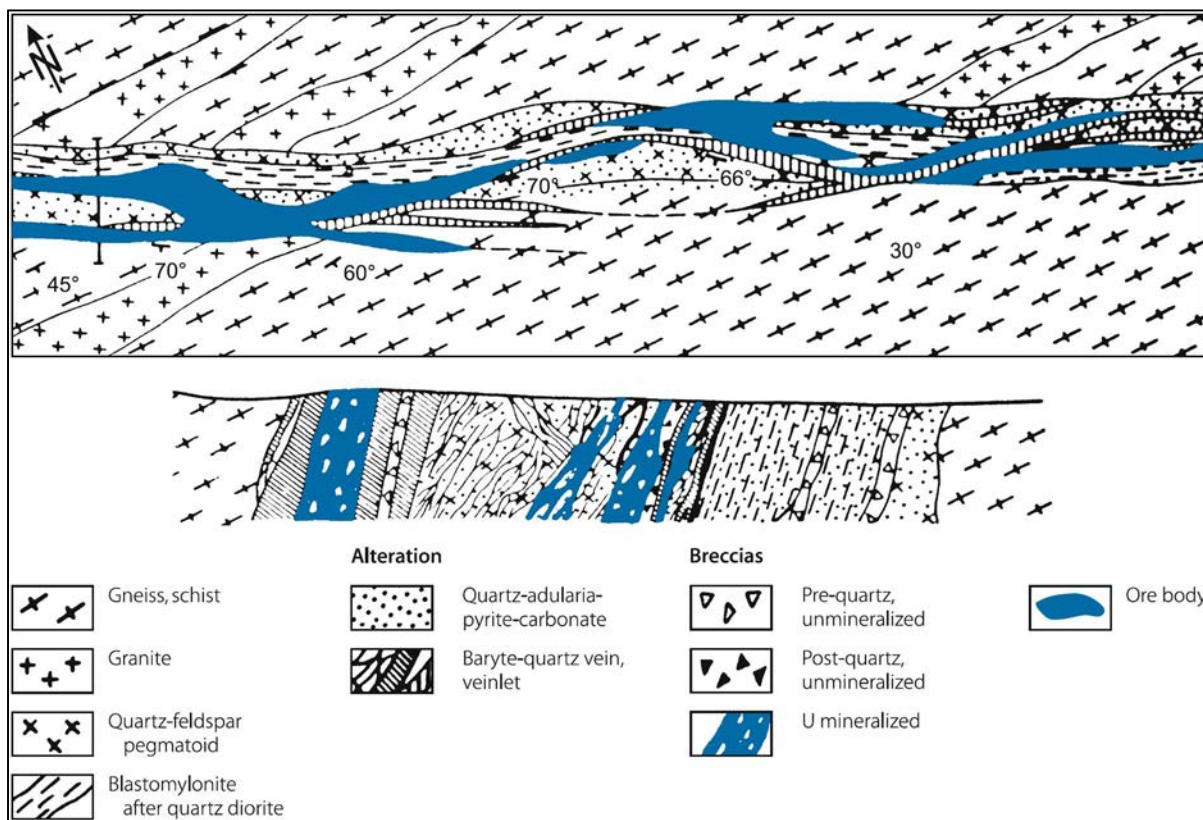


FIG. 74. Elkon district: (a) plan and (b) SW–NE cross-section across a uranium mineralized structure [22, 47] (reproduced with permission).

#### 3.5.4.4. The Coles Hill deposit (USA)

##### Introduction

The Coles Hill uranium deposit (also referred to as the Swanson deposit) is located in Pittsylvania County in southern Virginia, approximately 10 km NE of Chatham. It contains an estimated 62 886 tU grading 0.0545% U (using a cut-off grade of 0.020% U) hosted by two orebodies. The North orebody contains 31 728 tU at an average grade of 0.039% U and the South orebody 31 154 tU at a grade of 0.051% U [184].

The deposit was discovered in 1978. In 1979, Marline Corporation optioned the property and delineated the extent of the deposit through drilling programmes carried out in 1979–1984. The Marline option was allowed to lapse due to market conditions, combined with the moratorium on uranium mining in Virginia that was passed in 1982. In 2006, a newly formed corporation, Virginia Uranium Inc., acquired and leased the property and has undertaken several studies of the area. In 2015, the moratorium on mining was still in effect in Virginia.

##### Geological setting

The deposit lies just west of the Chatham Fault, a complex cataclastic zone up to 500 m wide that juxtaposes crystalline rocks of the Smith River Allochthon (SRA) on the west against Triassic sedimentary rocks of the Danville Basin to the east (Fig. 75). The SRA is a Palaeozoic thrust sheet consisting of Neoproterozoic pelitic schist, granitic and pelitic gneisses and amphibolite. These are intruded by the Martinsville Igneous Complex (MIC). The MIC consists of a ~445 Ma unit of granite and granodiorite with minor syenite and quartz diorite (Leatherwood granite) and a slightly younger

(~430 Ma) mafic intrusive unit (Rich Acres Formation) consisting of olivine gabbro, norite, gabbro and diorite [185–189]. The Coles Hill deposit occurs in deformed SRA footwall rocks immediately adjacent to and below the Chatham Fault Zone (Figs 76 and 77). Mineralization does not appear to extend beyond the zone of intense cataclasis and breccia into the Triassic sedimentary rocks.

The mineralized host rock consists of the strongly deformed Leatherwood granite and the lesser deformed Rich Acres Diorite (termed ‘amphibolite’ in most early reports) that intrudes the granite. A ductile fabric in the granite, sometimes referred to as ‘augen’ mylonite, appears to reflect early movement (possibly Palaeozoic) along the fault. The ductile deformation is overprinted by a series of brittle hydrothermal fractures that host the ore. The age of the brittle fabric has not yet been conclusively determined, but an association with Mesozoic reactivation and movement along the Chatham Fault Zone is the most likely interpretation [47].

Rocks within mineralized zones are Na-metasomatized and altered to varying degrees, in part pervasively, by carbonatization, chloritization, dequartzification, haematization, sericitization, silicification and zeolitization. Ubiquitous Na-metasomatism is reflected by: (i) clear albite rims around feldspar augen, (ii) riebeckite formation, in particular in amphibolites and (iii) small albite veinlets or clusters in augen gneiss and cataclastic rocks. Calcite, epidote and clinozoisite often occur in the immediate vicinity of plagioclase, indicating their derivation from the later. Ilmenite and/or sphene are partially altered to idiomorphic rutile and titanite is altered to anatase [47].

Haematization shows a correlation with uranium. In some cases it forms distinct halos around uranium veinlets. Amphibolite and amphibole–biotite gneiss are consistently stained red by haematite when mineralized. Mineralized augen gneiss commonly has a reddish hue, but haematite staining is also present in unmineralized augen gneiss. Most haematite is disseminated as minute particles in the fine-grained, cataclastic matrix. Haematite also reddens feldspar porphyroclasts. Limonitization is typically widespread in the weathering zone. Fractures varying from hairline to a few centimetres in width are filled with a variety of minerals such as apatite, baryte, carbonate, chlorite, gypsum, harmotome and other zeolites, haematite and quartz. Different mineral assemblages in discrete, cross-cutting fracture sets suggest different hydrothermal events [47].

## Mineralization

The Coles Hill deposit includes two major orebodies (Fig. 78). The internal structure of these orebodies is essentially a stockwork of uranium-bearing veinlets with narrow intervals of disseminated mineralization localized within the tectonized footwall zone of the Chatham Fault.

The North orebody is larger in volume but lower both in grade and uranium resource than the South zone. It contains 18 115 tU at an average grade of 0.042% U. The orebody is an irregularly shaped, more or less flattened spheroid, approximately 350 m in diameter and extends from the surface to a depth of 300 m. The upper contact is the base of the microbreccia and cataclasite of the Chatham Fault. The lower, western boundary extends into the lower mafic augen gneiss. The North deposit has a predominance of disseminated type ore, which forms wide and low grade zones of mineralization [47]. Weathering has affected the top of the North deposit, resulting in radioactive disequilibrium and the formation of abundant hexavalent uranium minerals in saprolite, but without significant depletion of uranium [189].

The South orebody contains 27 650 tU at an average grade of 0.06% U. The orebody is an irregularly shaped, flattened cylinder plunging 40° S. It is up to 300 m wide in an E–W direction, has a thickness of 150 m and is more than 700 m long (along the plunge axis). The deposit extends from the surface to about 500 m but is open at depth. It dips at a slightly lower angle than the host strata. On the western side, the lower contact lies at the base of the monzonite or middle augen gneiss unit. The eastern boundary is at the base of the protobreccia/microbreccia zone in the footwall of the Chatham Fault but mineralization does not extend into these rocks for more than a metre. Haematization and granularization of the host rocks essentially correspond to the margin of the orebody. Mineralization is of disseminated and vein types, with the majority of the uranium present in microfractures.

Disseminated uranium minerals are concentrated in narrow bands rarely more than a 0.25 m thick. Mineralization occurs in all rock types, but the highest grades are found in amphibolites, in narrow zones associated with calcite [47].

Most of the uranium at Coles Hill is present as coffinite, uranium oxides (uraninite or pitchblende, at least in part) and by U–Ti phases. One unusual aspect of the deposit is that uranium-bearing apatite is abundant and may constitute 4% or more of the reserves at Coles Hill. Hexavalent uranium minerals occur in oxidized, weathered zones, particularly in the North orebody. Associated sulphides are rare, consisting mainly of pyrite.

As described by Jerden [188], mineralization is mainly controlled by brittle fracture according to the following paragenetic sequence. The earliest event is strong Na-metasomatism that resulted in replacement and local rimming of all host rock feldspar by albite, the growth of sparry, neoblastic albite on fracture walls, the replacement of hornblende rims by riebeckite and the replacement of biotite by chlorite. This is followed by several uranium mineralization events. The earliest mineralization consists of coffinite and uraniferous apatite in chlorite-rich fracture fills. This is followed by calcite–uraninite and, finally, zeolite–uraninite fracture fills. Haematite occurs in all three mineralized vein types and is closely associated with uranium ores [47].

The mineralization is heterogeneous, with a tendency for strong mineralization to occur in the more mafic (and iron-rich) lithologies, such as amphibolites or in granites near their margins. However, some strongly mineralized areas are hosted by granite not associated with amphibolites. Although mineralization is restricted to Na-metasomatized rocks and hydrothermal fractures, not all Na-metasomatized rocks or fractures are mineralized. Similarly, although most phosphate-rich rocks are uraniferous, this is, again, not always the case [47].

At Coles Hill, uranium mineralization occurs in iron-rich lithologies (at least locally) and is spatially associated with haematite. This relationship suggests that the ore was deposited when oxidized,  $U^{6+}$ -bearing fluids became reduced to  $U^{4+}$  as they interacted with ferrous iron-bearing rocks and minerals. The reduced uranium precipitated as coffinite and  $U^{4+}$ -bearing oxides or was incorporated into apatite as  $U^{4+}$ .

Uranium–lead isotope analysis gives two principal apparent ages for uranium crystallization:  $562 \pm 5$  Ma for uranium oxide in amphibolites and 417 Ma for uranium oxide in augen gneiss [190]. Uranium–lead dating of euhedral zircons of the Leatherwood granite also indicates two ages: 1020 Ma for zircons, including corroded crystals, and 450 Ma for euhedral zircons [191]. It is suggested from the two zircon ages that the Leatherwood granite crystallized around 450 Ma, but has retained an inherited component, 1000 Ma old, that has probably been incorporated into the granitic magma by assimilation of rocks of Grenville age. The 417 Ma age is close to the 450 Ma age of the granite and is similar to the Acadian ages of shear zones identified throughout the Blue Ridge and Piedmont Provinces. The older, 562 Ma age is dubious and can be interpreted as the indication of an older uranium generation or a pre-dated value by older lead contamination [47].

#### Metallogenic aspects

The source of the uranium at Coles Hill is currently debated. One school of thought favours an origin from within the crystalline rocks of the SRA. Some granitoids in the SRA have elevated uranium levels and the abundant schists of the Fork Mountain Formation, some of which have a black shale protolith, are another possible source. Another model postulates the uranium source as being the sedimentary rocks of the Danville Basin. Uraniferous black shales are truncated along the Chatham Fault Zone and diagenesis of basin rocks suggests interaction with an alkaline, sodium-rich fluid [192].

No complete metallogenic model for the origin of the Coles Hill deposit has been established. Metallogenesis related criteria, as established to date, suggest [47]:

- (a) Structurally controlled uranium was introduced by hydrothermal solutions, but the origin, nature and physicochemical properties of the solutions forming the early and later uranium generations are largely unknown;
- (b) Alteration mineralogy and the presence of zeolite in pitchblende veinlets suggest that solutions, at least of late hydrothermal phases, were of moderate to low temperature;
- (c) The presence of apatite and calcite in the gangue mineral suite indicates solutions containing phosphate and carbonate complexes;
- (d) Coffinite reflects silica-bearing fluids;
- (e) Destruction of magnetite, ilmenite and possibly sphene indicate reducing reactions;
- (f) Transformation of uraninite to pitchblende and oxidation of sooty pitchblende indicate probably repeated oxidation processes.

Localization of the deposit within and adjacent to the intrusive Leatherwood granite and the approximately coeval timing of the emplacement of this granite with an early phase of uranium mineralization may suggest some relationship [47].

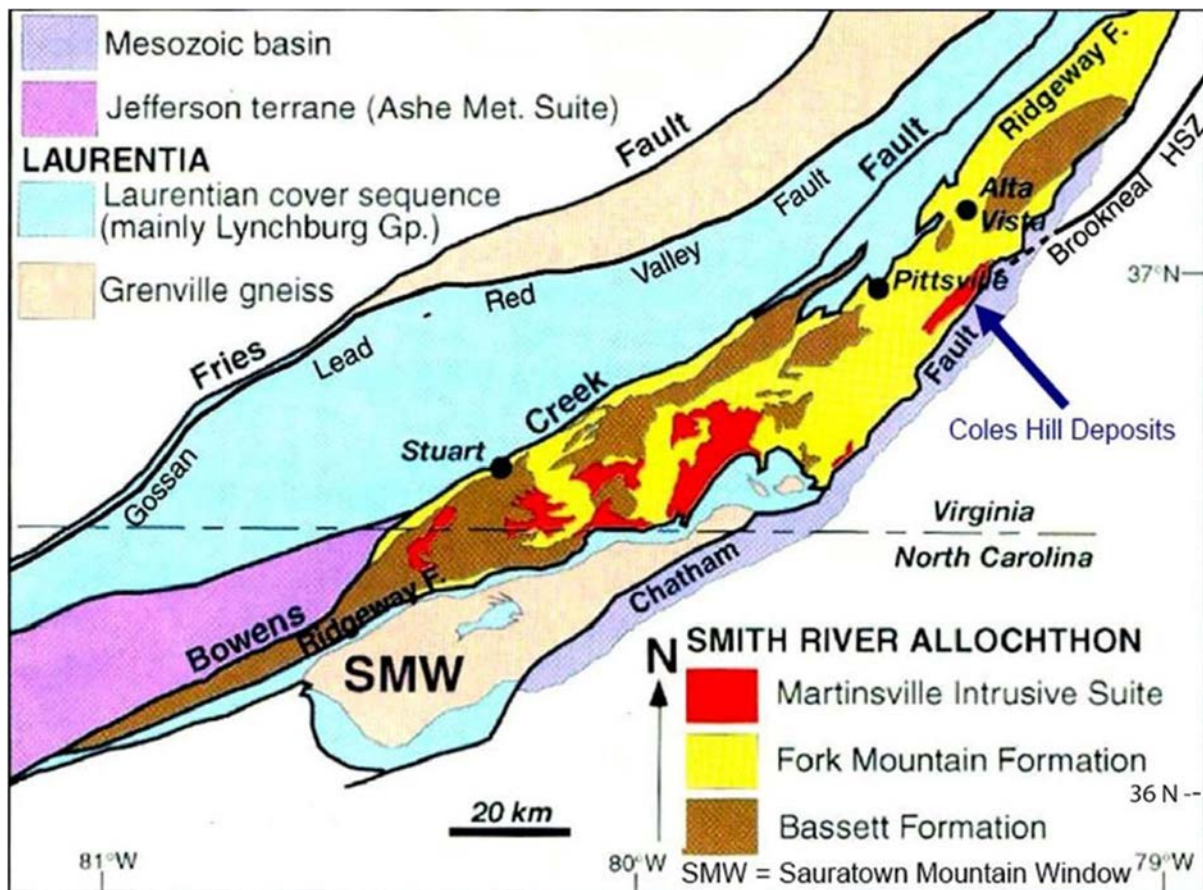


FIG. 75. Location of the Coles Hill uranium deposit in the western Piedmont region of Virginia, USA (adapted from Ref. [193]).

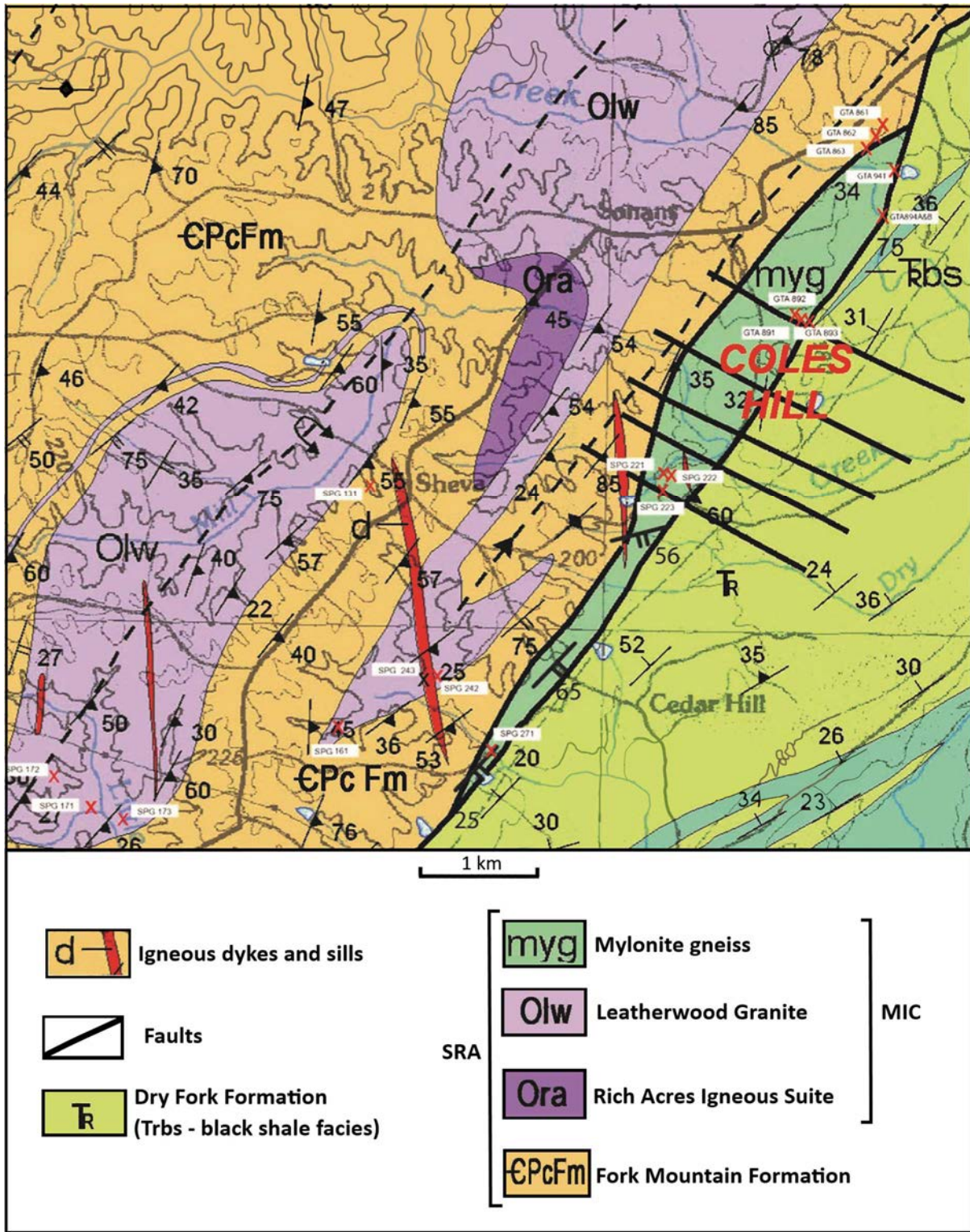


FIG. 76. Local geology of the Coles Hill deposit. Ordovician Martinsville Igneous Complex (MIC-including Leatherwood Granite, Olw and Rich Acres Igneous Suite, Ora); other units of the Smith River Allocthon (SRA), EPcFm - Fork Mountain Formation, myg — mylonite gneiss deformed rocks near the fault that hosts the deposit. Trbs: Triassic shale facies truncated at Chatham Fault, Tr: Dry Fork Formation (Triassic conglomerate, sandstone and mudstone facies truncated at Chatham Fault Zone) (adapted from Ref. [194]).

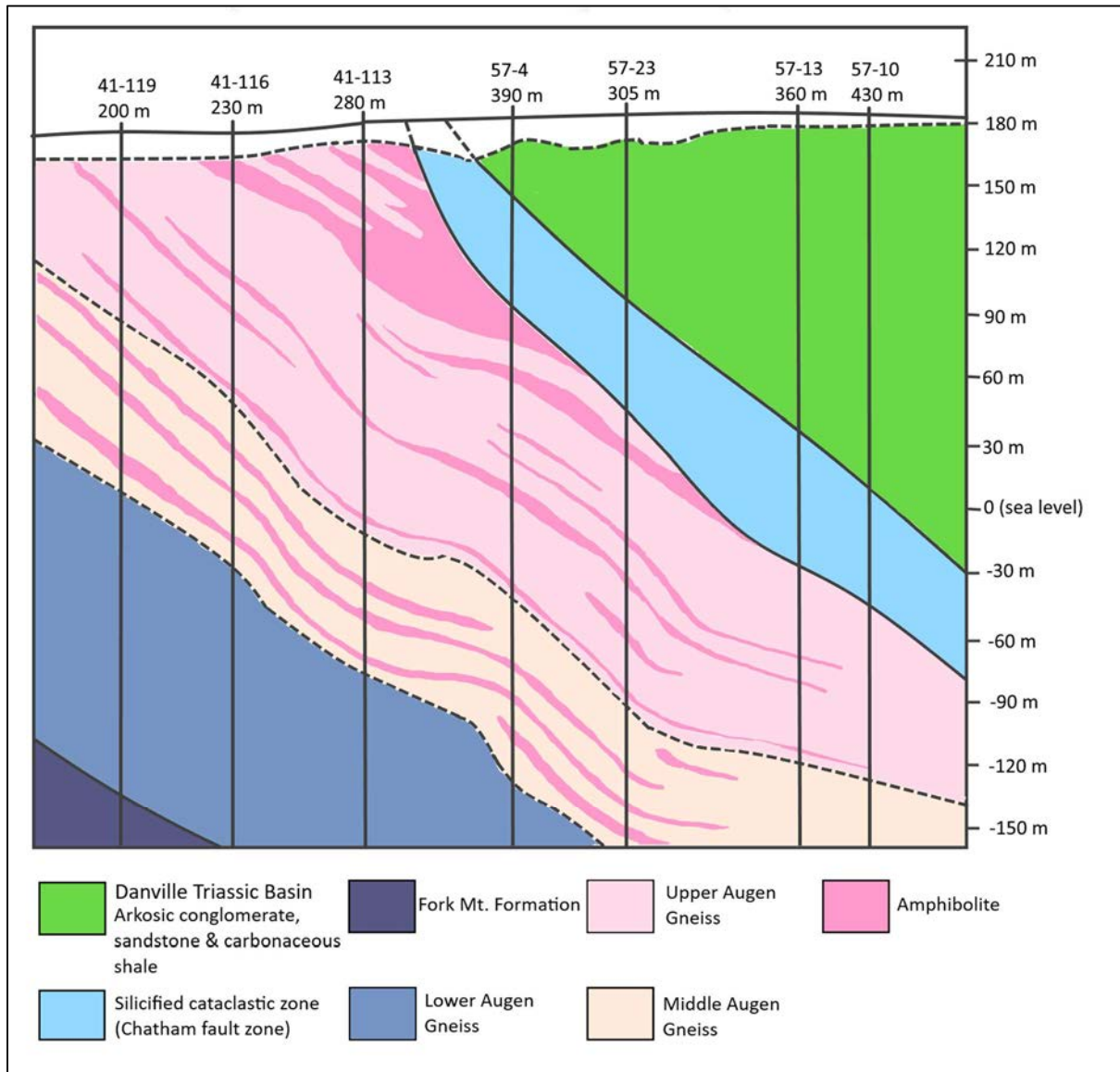


FIG. 77. Geological cross-section (E-W) of the Coles Hill deposit (adapted from Ref. [189]).

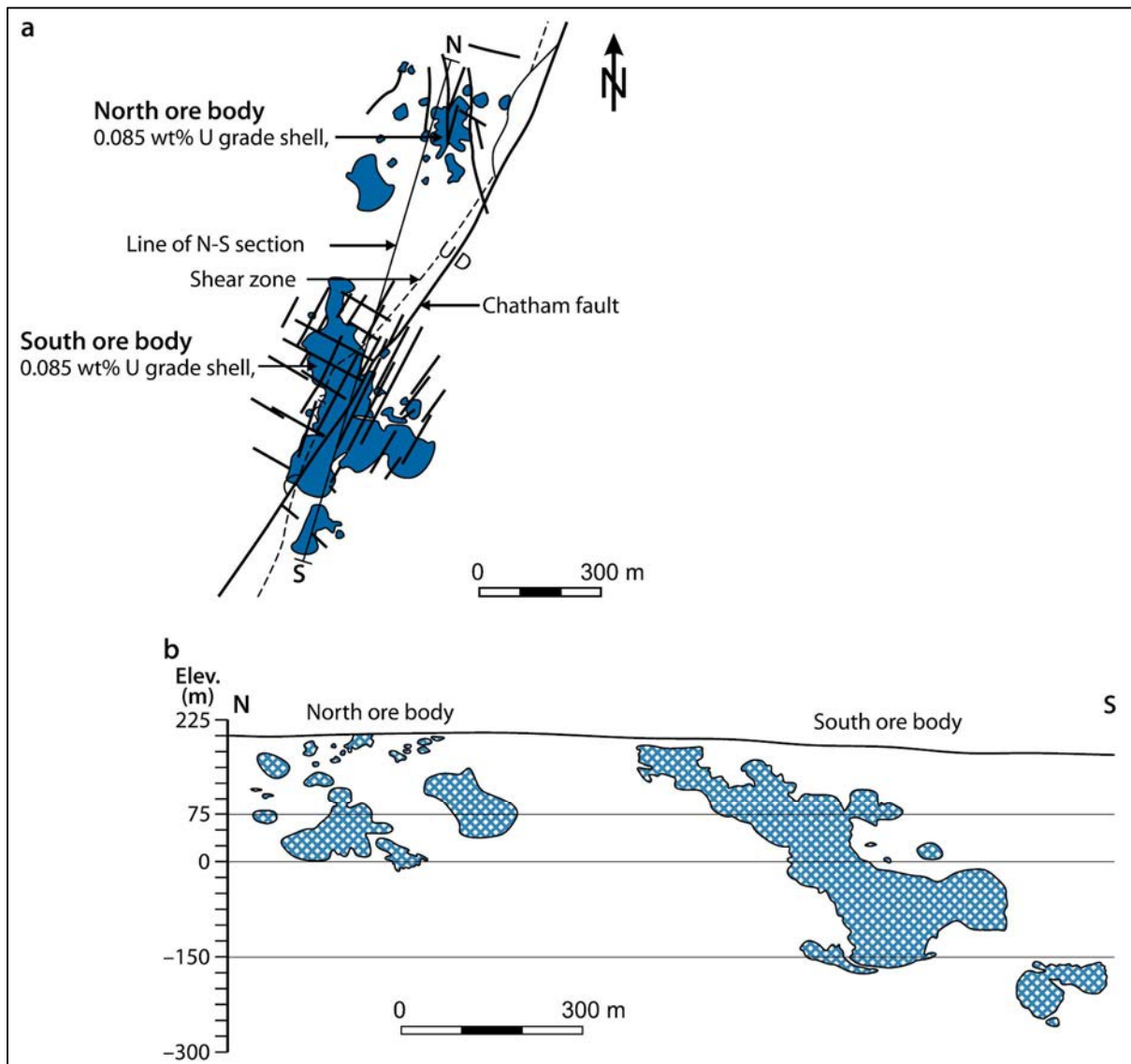


FIG. 78. Coles Hill deposit: (a) plan view of surface projected orebodies, (b) N–S section outlined by a cut-off grade of 0.084% U [47, 189] (reproduced with permission).

#### 3.5.4.5. Uranium–thorium deposits of the Tranomaro district (Madagascar)

##### Introduction

The Tranomaro district is located in southern Madagascar, about 90 km north-west of Tolanaro (Fort Dauphin) (Fig. 79). Thorianite mineralization was first discovered in 1947 during exploration for mica. Owing to the high uranium content (several per cent), the district was intensively explored by the French Commissariat à l’Energie Atomique. In the period 1955–1968, 1030 tU and 3220 t Th were produced by the open pit mining of several tens of small uranothorianite deposits. Most of the thorium production was sent to the USA. Since 2005, Pan African Mining Corporation has been conducting exploration in the Tranomaro district. Drilling indicates that the structures are still mineralized to a depth of 100 m below the open pits. Results at mine 37, one of the more than 100 known open pits, has returned 11 m grading 600 ppm U and 1099 ppm Th, and 6 m grading 1458 ppm U and 1540 ppm Th [195]. In June 2008, the company was bought by Asia Thai Mining Corporation Ltd and the project has been dormant since then.

## Geological setting

The geology of southern Madagascar consists of metasedimentary and metavolcanic rocks of Palaeoproterozoic age that were reworked and metamorphosed to granulite facies during the formation of the Pan-African Mozambique Belt, prior to the break-up of Gondwana [196–198]. The Mozambique Mobile Belt extends into Sri Lanka and southern India. The Highland Complex of central Sri Lanka contains comparable metasedimentary rocks of a similar metamorphic grade to those found near Tranomaro. Single zircon  $^{207}\text{Pb}/^{206}\text{Pb}$  ages for granulites, gneisses and granites in southern Madagascar record a widespread Pan-African metamorphic and magmatic event with an age range of 650–556 Ma [196].

The Tranomaro basement is divided into three blocks (Fig. 80) by N–S trending, vertical, lithospheric scale shear zones [199]. The western block consists of leptynites (felsic volcanics) of the Fort Dauphin Group, the central block consists of marble and pyroxenite of the Tranomaro Group and the eastern block contains granite and charnockite of the Anosyan Complex. All three blocks underwent granulite facies metamorphism (750–800°C) with pressure decreasing from 11 kbar in the western block to 8 kbar in the centre and to 4–5 kbar in the east.

Uranium–thorium mineralization in the Tranomaro area is located in the eastern, lowest pressure block [200, 201]. The Tranomaro gneiss is comprised of metapelite, commonly graphitic, abundant calc-silicate rocks and marble, as well as quartz feldspar gneiss, some of which represents former felsic volcanic rocks (Fig. 81). The sedimentary protoliths were deposited in a passive, epicontinental margin setting. The marble layers range from a few metres to a few hundred metres in thickness and several kilometres in extent. In the north-western part of the area, the marble layers form closed structures similar to those to the west and these have been interpreted by Martelat et al. [202] as the product of polyphase deformation. As a result of the high ductility of the marble layers, complex folding and boudinage of the more competent calc-silicate layers are common. Calc-silicate rocks are closely associated with marble. Polymineralic calc-silicate assemblages were formed by metamorphism of impure limestone or marl interlayered with the marble. Monomineralic calc-silicates have a metasomatic origin, resulting from element transfer between the marble and granitic intrusions or from fluid injections, resulting in isolated masses within the marble.

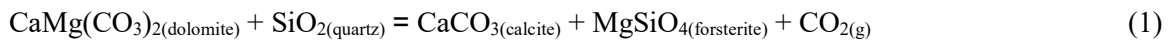
Granite intrusions are numerous, generally small in size and derived from dehydration melting of biotite-bearing gneiss at depth, as described in the western deeper level blocks. Large granitic intrusions occur in the Anosyan Ranges, east of the Tranomaro Block.

Metasomatic skarns are generally well zoned, with the following sequence that may extend from several metres to several tens of metres [45]:

- (a) Biotite  $\pm$  hypersthene granite;
- (b) Diopsidic syenite derived from granite from which quartz has been leached, silica has infiltrated into the enclosing marble, and Ca has migrated towards the granite to form diopside from biotite or hypersthene;
- (c) Scapolite, essentially consisting of the meionite end-member, with subordinate diopside, typically corresponding to an endoskarn;
- (d) Pyroxenite, essentially composed of pure Ca (wollastonite) or Ca–Mg (diopside)  $\pm$  fluorine-rich phlogopite  $\pm$  scapolite, which corresponds to an exoskarn;
- (e) Marble, either pure carbonate or calc-silicate-bearing with a variety of minerals (forsterite, fluorine-rich phlogopite, diopside, dark green to light coloured spinel, fluorine-rich humite, wollastonite or pargasite) depending on the amount of detrital Al-silicates in the protolith. Minor exsolution of dolomite is locally observed in calcite, K-feldspar is sometimes present as small intergranular lenses and neither garnet nor graphite is present in the marble. Forsterite-bearing marble generally has an MgO content higher than 12wt%, whereas most diopsidic marble has an MgO content lower than 5wt%.

Granite is not always observed in the metasomatic zonation, e.g. the Marosohy occurrence. Here, the nearly monomineralic pyroxenite with minor spinel and residual calcite is in sharp contact with a calcite–dolomite–forsterite–spinel marble. The amount of dolomite in the marble decreases toward the pyroxenite and is accompanied by a relative increase in calcite and forsterite. Free dolomite disappears inside the marble and is only observed as exsolution textures in the calcite near the contact. At the contact, diopside forms in the absence of forsterite. The mineralogical zonation results from two successive reactions (Eqs (1) and (2)) induced by the infiltration of a siliceous fluid and the production of carbon dioxide [45]:

(i) Disappearance of dolomite:



(ii) New formation of diopside:



Under retrograde granulite facies conditions, fluorine-rich phlogopite, which is mined locally, is associated with calcite, diopside and occasional anhydrite, and forms veins and lenses cross-cutting pyroxenite. Late stage REE-rich and zircon-rich calcite veins cross-cut the calc-silicate complex. These may contain euhedral zircon crystals up to several centimetres long [45].

#### Mineralization

Uranium–thorium mineralized showings are known in metasomatic calc-silicate rocks [203–205]. The main ore mineral is uranothorianite, which occurs as euhedral crystals, predominantly in diopside pyroxenite, which is always the most mineralized layer, but also, occasionally, in meionitic scapolite and the adjacent marble.

Pyroxenites are coarse-grained and are developed as a series of planar lenses corresponding to primary bedding. These lenses typically have thicknesses of one metre to a few metres but may be as much as 80–100 m thick and range from ten to a few hundred metres in length (Fig. 82).

The uranothorianite is typically present as millimetre size crystals but may locally reach several centimetres and be present as irregular disseminations or as layers. Uranothorianite may also be present in phlogopite lenses or as inclusions in calcite crystals. Some carbonate has been remobilized and several orebodies are covered with a secondary limestone crust. Two main types of mineralization have been distinguished (Fig. 83) [206]:

- (i) *Disseminated uranothorianite in pyroxenite*: Occurs in 1–10 m long lenses with abundant euhedral crystals (Ambindandrakemba, Amboanemba, Marosohy orebodies);
- (ii) *Uranothorianite associated with phlogopitic zones*: Occurs as (a) disseminations in phlogopite veins near the margins of the pyroxenites (Morafeno orebody), (b) disseminations within pegmatoidal calcite–phlogopite–anorthite pods (Marosohy, Betanimera, Ampiha orebodies) and (c) disseminations in fine-grained phlogopitic pods (Eroboka orebody).

The mineralized pyroxenite may also form lenses from a few metres to several tens of metres in length, not closely related to any visible intrusion. For example, in the Marosohy profile, the U–Th mineralization increases rapidly from the barren marble (3.8 ppm Th) towards the contact (up to 2000 ppm Th) and reaches a maximum in the pyroxenite (4000 ppm Th). Several centimetre sized uranothorianite crystals may also occur in the veins with phlogopite. Both REE–Th–U enriched hibonite and corundum may crystallize in some extremely aluminous metasomatic rocks [207]. More rarely, the uranothorianite has been observed within secondary silica associated with altered phlogopite or in true pegmatites. Secondary alluvial deposits are widespread in the Tranomaro district. Metallogenic aspects

Two main stages of metasomatism have been identified in the Tranomaro region [207]. The first stage includes an aluminous diopside–scapolite–meionite–titanite–spinel–wollastonite–corundum–uranothorianite assemblage that records pressure–temperature conditions of 5 kbar and 850°C at 565 Ma [196]. This is the main phase of U–Th mineralization. The second stage comprises hibonite enriched in F–phlogopite–F–pargasite–uranothorianite–REE and formed at 3 kbar and 800°C at 545 Ma [208], but this stage is of minor importance for the mineralization.

The similarity of the ages and of the pressure–temperature conditions demonstrates the synchronicity between granulite facies metamorphism and fluid circulation responsible for the first stage of metasomatism and U–Th mineralization. Fluid inclusions in minerals from gneiss and skarn are CO<sub>2</sub> enriched [204]. Primary inclusions in growth zones of euhedral corundum crystals have isochores that intersect the pressure–temperature field defined by geothermobarometry on silicate minerals, indicating that they are synchronous with the peak metamorphic conditions [204, 207].

Carbon dioxide was not the only fluid involved in the metasomatic reactions. In the Tranomaro metasomatic zones, the hydroxyl sites of phlogopite, pargasite, humite and apatite are nearly saturated with fluorine, suggesting that fluoride complexes may have simultaneously transported Th, U, REE, and Zr, which all appear to be mobile during these metasomatic conditions, together with Si and Ca [209]. In particular, most of the Th/U ratios of the mineralized rocks are between 2 and 3, close to the average crustal ratio and thus exhibiting no strong difference in mobility between U and Th. In addition, unmixed aqueous brines may have coexisted with the carbonic fluids, as shown by Touret [209] for other granulite terranes, but not yet identified in the Tranomaro area.

The  $\delta^{13}\text{C}$  values almost 0‰ for the Tranomaro marbles are typical of marine carbonate and thus do not provide evidence for extensive streaming of mantle derived fluids during granulite facies metamorphism. Localized but strong fluid flow occurred in the metasomatic mineralized zones, but also without any contribution of a deep seated carbon source as evidenced by the carbon isotopic compositions of infiltrated marble and pyroxenite.

The oxygen isotopic composition of pyroxenite is consistent with a crustal origin for both the metasomatic fluids and the U–Th mineralization, but rock-buffered fluids for marble. In addition, the neodymium isotopic composition of metasomatized marble is similar to that of the metasedimentary rocks and granite intrusions, indicating that the source of the REE is likely to be either from the marble or from the crustal host rocks [210].

One postulated source for the U–Th is via synsedimentary preconcentration of Th, U, Zr and REE in marl. This is unlikely, however, because in sediments these elements are found mainly in detrital monazite (for Th, U and REE) and zircon (for Zr) that occur as placer deposits in relatively coarse siliciclastic sediments. Marl, even that with a significant detrital component, never possesses high levels of these elements.

Another possible source, based mainly on the association of U with Th–REE–Zr and the presence of carbonate rocks with pyroxenite, could be a metamorphosed carbonatite protolith. For example, the U–Th mineralization in Phalabora (South Africa) is associated with carbonatite and pyroxenite, and uranothorianite is the main ore mineral [211]. However, U and Th concentrations in carbonatite are much lower, reaching only 25 ppm U at Phalabora, and such an origin does not account for the zoning observed across the different lithologies. Moreover, carbonatite bodies have high niobium contents that are not observed in the Tranomaro pyroxenite and carbonate rocks, and the carbon isotopic composition of the Tranomaro marble is typical of marine carbonate rocks.

Consequently, the geological, geochemical and isotopic data are most consistent with a synmetamorphic origin for the Th–U–REE–Zr mineralization, although these elements, especially U, are not typically enriched in granulite facies rocks [212]. The classic metasomatic zonation observed between the granite injections and marble is predominantly controlled by the exchange of Ca and Si between the two lithologies, as well as by the isotopic compositions of the metasomatic rocks. This implies that the Th–U–REE–Zr mineralization is most likely derived from metasomatic fluids

exsolved from granitic magmas injected in the Tranomaro metamorphic series or from fluids derived from devolatilization reactions occurring at depth during granulite facies metamorphism. The simultaneous mobility of U, Th, REE and Zr is probably due to the high fluorine contents of the fluids as a result of the dehydration of biotite [45].

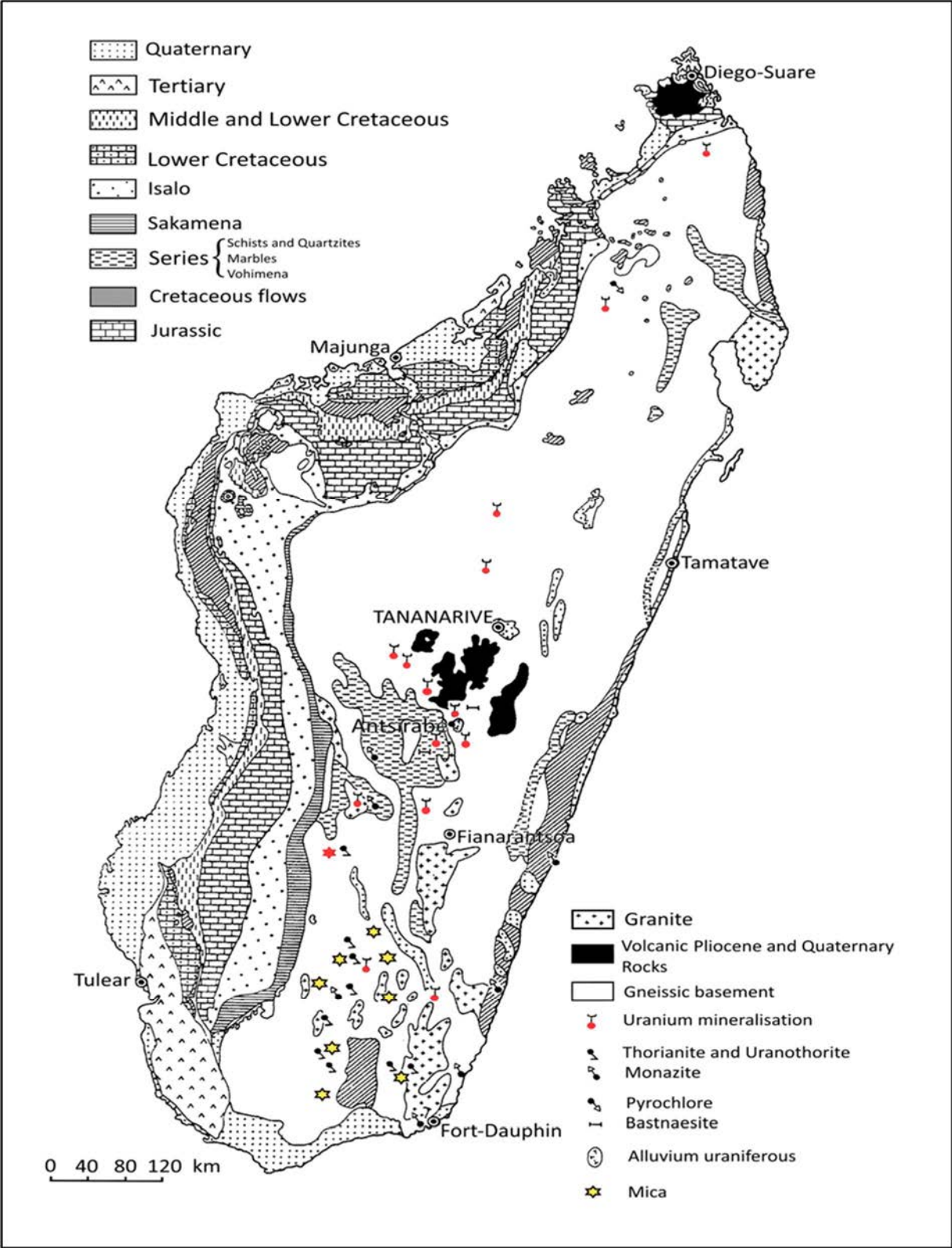


FIG. 79. map of Madagascar showing location of radioactive occurrences (adapted from Ref. [206]).

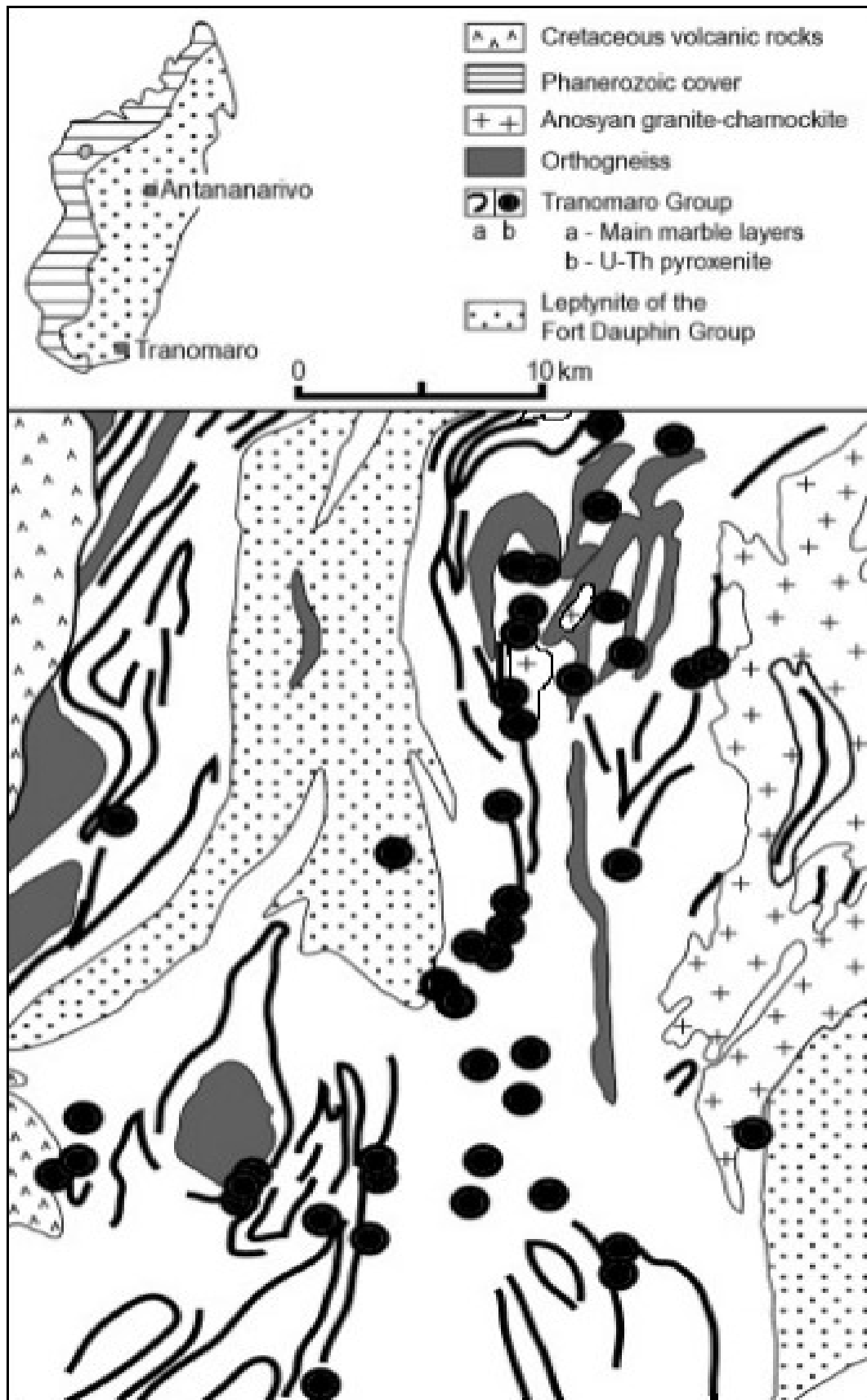


FIG. 80. Simplified geological map of the Tranomaro area. Only the largest granitic intrusions are represented (the N-S extension represents about 100 km) (adapted from Refs [42, 211] and reproduced with permission).

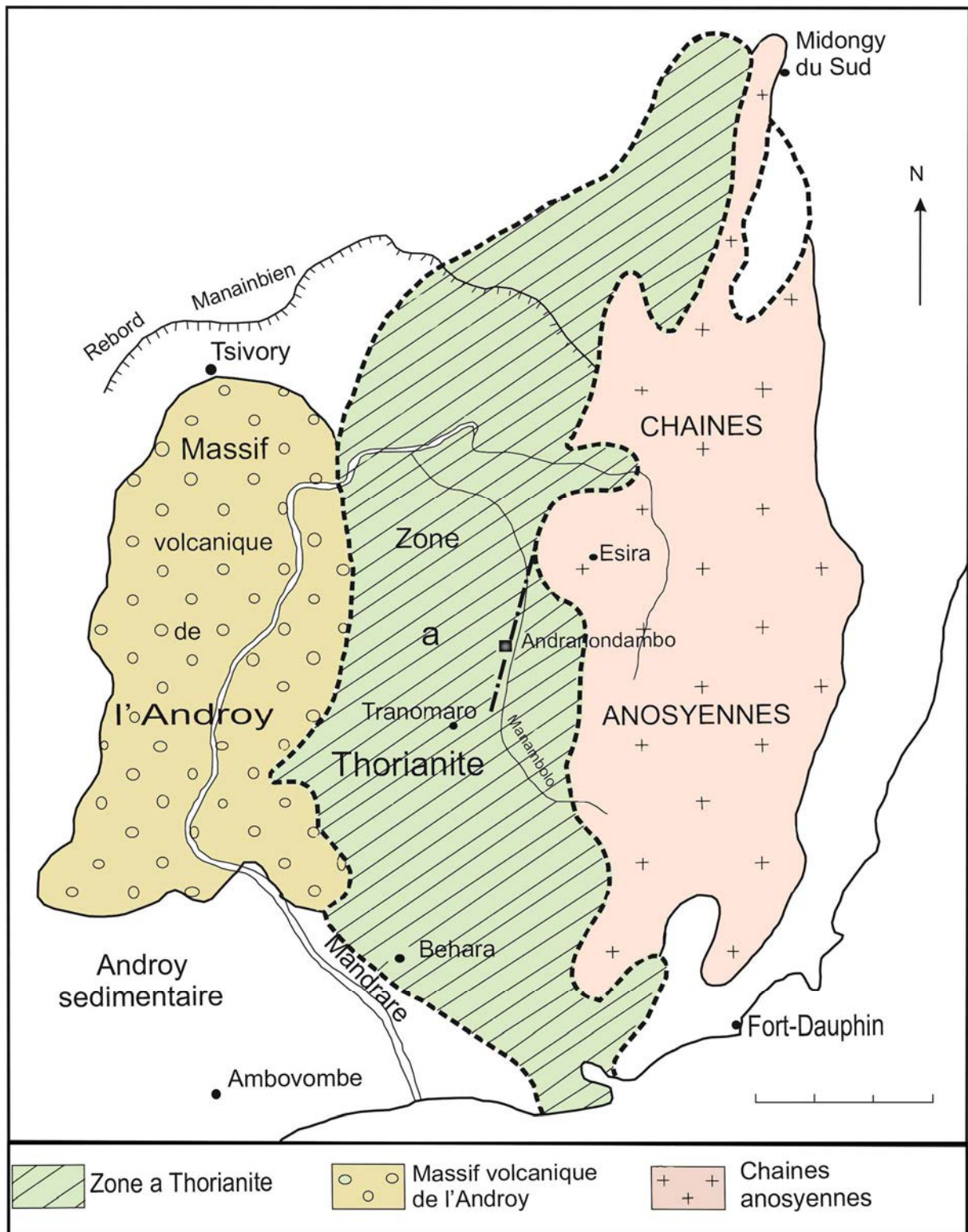


FIG. 81. General geological map showing the location of the uranothorianite zones in south Madagascar (adapted from Ref. [206]).

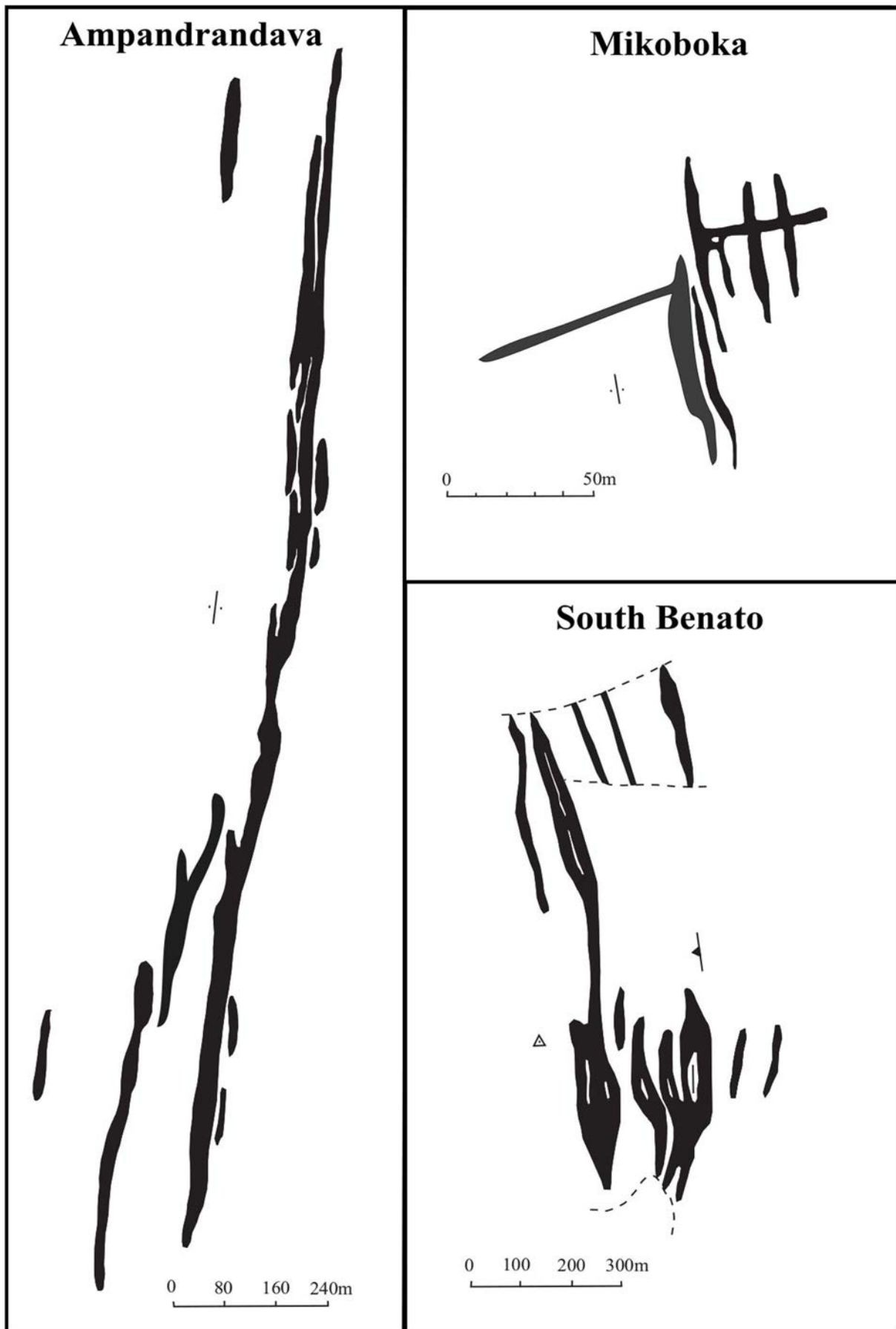


FIG. 82. Some typical pyroxenite mineralized structures (adapted from Ref. [206]).

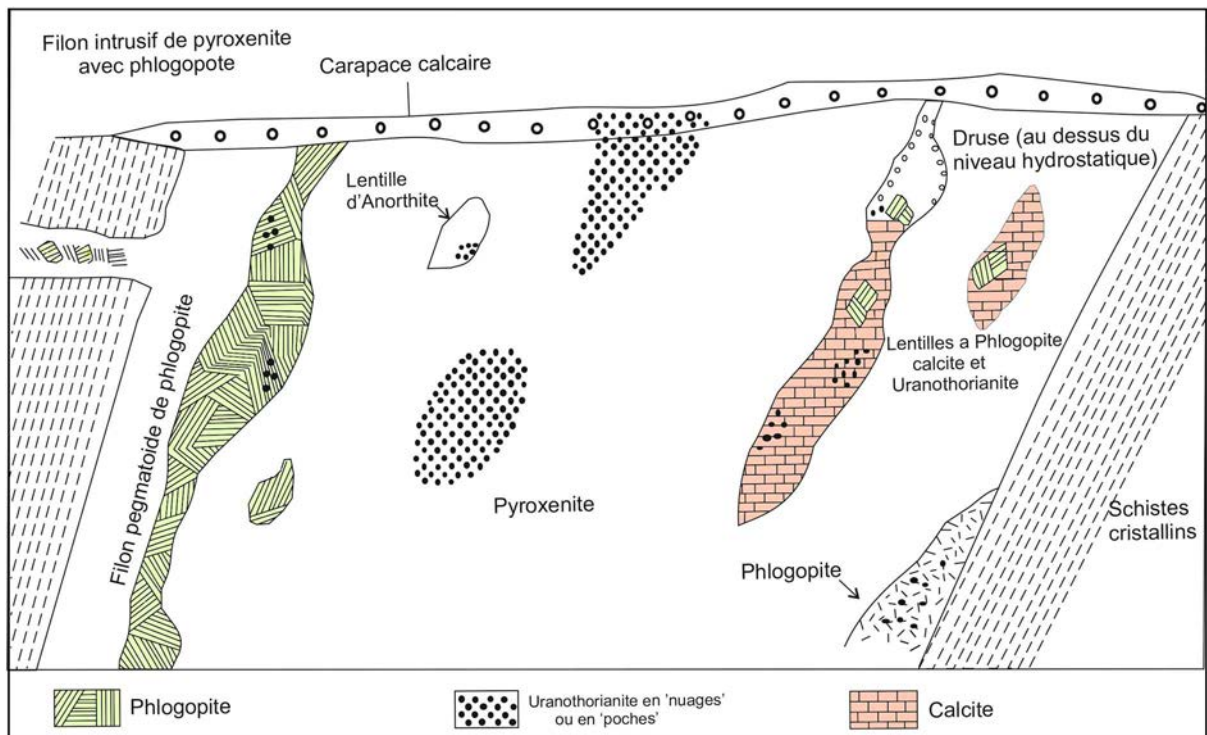


FIG. 83. Vertical schematic cross-section through a pyroxenite layer showing the various types of mineralization found in the Tranomaro district (adapted from Ref. [206]).

3.6. METAMORPHITE DEPOSITS

3.6.1. Definition

Metamorphite deposits consist of veins, stockworks and shear zones within metasedimentary–metavolcanic formations of various ages (Fig. 84). The vein modes are similar in structural control, ore and gangue mineral associations, and wall rock alteration to perigranitic deposits. Major differences include absence of granitic or other magmatic complexes and greater continuity of mineralization [19].

There are 111 metamorphite deposits listed in the UDEPO database. The largest district of this type is found in the Kokshetau region in northern Kazakhstan, where 27 deposits have been delineated with resources in excess of 200 000 tU. Total production between 1957 and 1998 is estimated to be of the order of 30 000–35 000 tU. Other important districts are the Itataia district (Brazil), with resources of more than 120 000 tU, the Singhbhum Cu–U Thrust Belt (India), with resources of about 70 000 tU hosted in 21 deposits, the the now depleted Uranium City district (Canada) with past production of 30 000 tU and the depleted Shinkolobwe deposit (Democratic Republic of the Congo), with production of 25 500 tU (Table 19). In 2015, uranium production from this deposit type from Kazakhstan, India, the Czech Republic and Romania is estimated to be of the order of 1000 tU (representing about 1% of world production).

TABLE 19. PRINCIPAL METAMORPHITE URANIUM DEPOSITS (as of 31 December 2015)

Deposit	Country	Resources (tU)	Grade (U %)	Status
Itataia district	Brazil	121 800	0.080	Development
Shinkolobwe	Democratic Republic of the Congo	25 500	0.50	Depleted
Kamyshevoye	Kazakhstan	21 700	0.12	Partially depleted
Manybaiskoye	Kazakhstan	21 400	0.086	Depleted
Rozna	Czech Republic	19 800	0.12	Production
Ace–Fay–Verna	Canada	18 900	0.21	Depleted
Zaozernoje	Kazakhstan	17 400	0.12	Partially depleted
Vostok	Kazakhstan	15 000	0.143	Production
Grachevskoye	Kazakhstan	14 200	0.17	Partially depleted
Chaglinskoye	Kazakhstan	14 000	0.070	Dormant
Schwartzwalder	USA	12 650	0.37	Partially depleted
Tinef	Algeria	11 752	0.075	Dormant
Lac Cinquante	Canada	11 550	0.45	Exploration
Mary Kathleen	Australia	10 260	0.11	Depleted
Gunnar	Canada	10 200	0.17	Depleted
Abankor	Algeria	9 134	0.32	Dormant
Narwapahar	India	9 074	0.050	Production
Zvyoznoye	Kazakhstan	9 000	0.17	Development
Malundwe	Zambia	8 821	0.0735	Development

### 3.6.2. Geological setting

Metamorphite deposits have been separated into three main subtypes: (i) stratabound deposits; (ii) structure-bound deposits, and (iii) marble-hosted phosphate deposits.

#### 3.6.2.1. Stratabound deposits

The synmetamorphic mineralization resulted from regional metamorphism of uraniferous sediments. It consists of disseminated uranium with a strata-concordant distribution in small lenses erratically scattered in metasediments. This type of deposit is not common. Resources are small to medium and grades low (Forstau, Austria).

#### 3.6.2.2. Structure-bound deposits

Monometallic veins comprise uranium (pitchblende, uraninite, coffinite) and gangue minerals with traces of other metallic minerals form stringers, veinlets and veins within larger tensional structures, particularly in horsetail fractures. Mineralization is relatively continuous but grades are highly variable (Schwartzwalder, USA; Kokshetau district, Kazakhstan; Beaverlodge district, Canada; Rozna, Czech Republic).

Polymetallic veins/stockworks comprise uranium (pitchblende, uraninite, coffinite) associated with Co, Cu, Fe, Mo, Ni, Pb, Zn and gangue minerals occur in veins, stockworks, breccia matrix as well as replacement masses and disseminations and aggregates in broken host rocks. Major faults are barren. Mineralization is fairly continuous but highly variable in grade and magnitude. Resources are small to

high and grades low to high (Shinkolobwe, Democratic Republic of the Congo; Kokshetau district, Kazakhstan; Lac Cinquante and Eldorado Mine, Canada).

The Kokshetau uranium region (Kazakhstan) is located in the Kokshetau Massif, which is a segment of the Caledonian North Tien Shan Fold Belt of the Ural–Mongolian orogenic system. About 27 deposits have been delineated in the crystalline rocks. They consist of structurally-controlled mineralization of vein–stockwork morphology [19]. Vein–stockwork mineralization may be either monometallic or polymetallic. By-products include Mo, Sc, Y, REE and phosphorous. Depth extension can be more than 1500 m.

In deposits associated with shear zones, orebodies consist of stringers and low grade disseminations of uranium minerals (mainly pitchblende and coffinite) without or with only minor gangue, within small, narrow structures that group to form lenticular ore shoots subparallel to the strike of the host strata. Prominent shear and breccia zones control the position and dimension of ore shoots. Classical veins are rare. Resources are low to medium and grades low (Rozna, Czech Republic).

### 3.6.2.3. Marble-hosted phosphate deposits

Marble-hosted phosphate deposits are exemplified by Itataia (Brazil), which is a complex hydrothermal metasomatic Cambrian–Ordovician uraniferous collophane (cryptocrystalline hydroxyapatite) deposit, hosted by Precambrian metamorphic rocks. Two major ore types have been identified, massive collophanite, and collophane veins and stockworks in marble, gneiss and episyenite. Another example is Nuottijarvi (Finland).

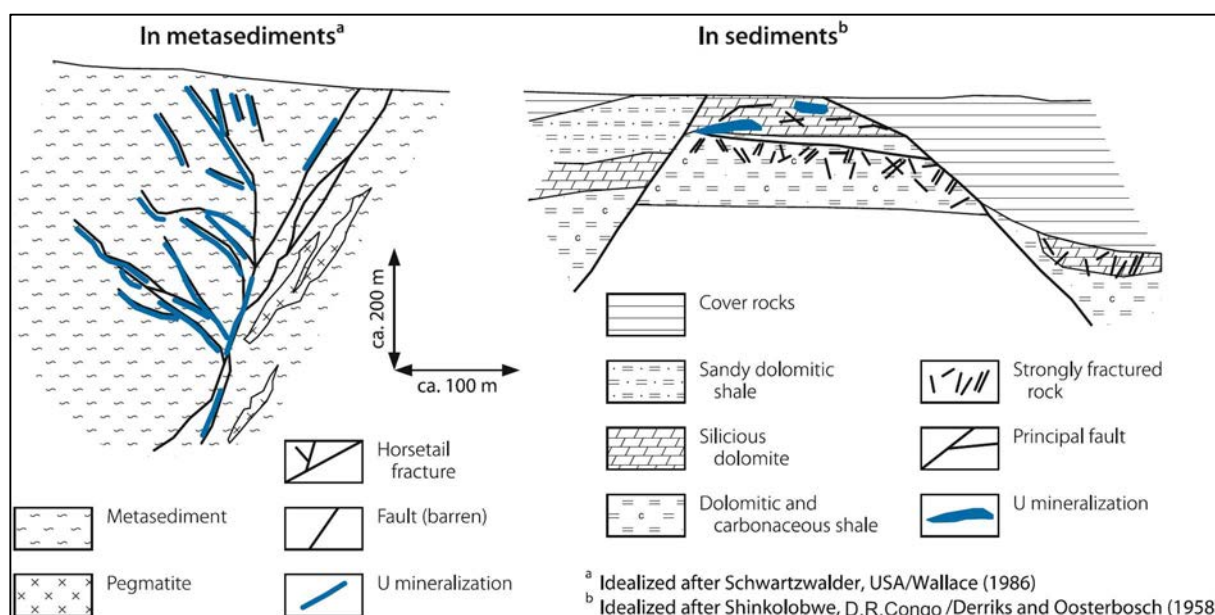


FIG. 84. Metamorphic uranium deposits [19] (reproduced with permission).

### 3.6.3. Metallogenesis

In all examples, mineralization is hosted by metamorphosed supracrustal rocks found in orogenic belts. As illustrated by the Beaverlodge district (Canada), Dahlkamp [19] notes that deposits of this type exhibit both structural and lithological control in that the vein, breccia and disseminated pitchblende is hosted by moderately to steeply dipping structures that are concordant to the folded

metasedimentary schist and gneiss. The Hudsonian age for these deposits is similar (slightly younger) to the age of metamorphism of the host rocks.

In the Beaverlodge district, as in other districts of this type, the dominant mineralization type is simple, with pitchblende in veins and associated with quartz, carbonate and chlorite with minor amounts of base metal sulphides. The less common complex or polymetallic ores contain pitchblende with a complex suite of Co–Ni arsenides, selenides and native metals [213] that typically form late in the paragenetic sequence.

Deposits feature extensive pre-ore albitization and syn-ore haematization, chloritization, epidotization, carbonatization, sericitization, and silicification. The alteration and mineralization are reasonably continuous to considerable depths (>1600 m). Interpreted temperatures of formation range greatly between high temperature early stages (440°C) down to 80°C in the late stages at Beaverlodge. Similar ranges are observed for other deposits of this type. The abundance of carbonate in the gangue suggests that the uranium was transported as carbonate complexes [214].

Some general similarities of metamorphite deposits with metasomatite and perigranitic deposit types in terms of mineralization morphology, gangue, wall rock alteration and host lithologies suggests some similarities of process or depositional conditions. A possible model is that uranium was leached from the metamorphic rocks during uplift and erosion in the waning stages of the orogeny. Uranium and complex ores were deposited in structures due to cooling and destabilization of the uranyl-carbonate complexes due to fluid evolution or water–rock interaction.

### **3.6.4. Description of selected deposits**

#### *3.6.4.1. The Forstau deposit (Austria)*

##### Introduction

The Forstau deposit is located in the Austrian Alps on the eastern margin of the Hohe Tauern tectonic window. It occurs within a narrow belt of Permian schists containing uranium mineralization and deposits along a trend of about 10 km. A 4 km section was explored by drilling and a 1 km section by underground workings. Resources are estimated to be of the order of 1000–2000 tU at a grade of 700–800 ppm U.

Several Permian uranium deposits are known in the Eastern Alps. These are sandstone type, but they exhibit some special features as a result of the orogenic environment of their deposition and of subsequent transformations. Only Forstau has been investigated by drilling and underground development. Geological resources of Austrian deposits (Forstau, Rettenegg, Fieberbrunn, Muhlbach and others) are estimated to be of the order of 2000–20 000 tU for each. The uranium content in all the deposits varies significantly from place to place, between 0.005 and 2% U. The average grade is about 800 ppm U [214].

##### Geological setting

Regional structure is extremely complicated. It can be represented as a very thick pile of overthrust complexes, from bottom to top, of Helvetic nappes (unmetamorphosed Triassic), lower Austro-Alpine nappes, the central zone of which contains the uranium-bearing Permian schists, upper Austro-Alpine nappes (Triassic carbonates), super Alpine nappes (Triassic special facies) and dolomites (Julian Alps/Triassic limestones and marls).

Most uranium deposits and occurrences in the Eastern Alps are hosted in sandstones and schists of the Lower Permian (Rotliegendes) (Fig. 85). Although fossils are absent from these variably metamorphosed beds, the ages can be defined from their stratigraphic position and lithofacies: the uraniumiferous series occurs between the Hercynian unconformity and the saline schist group with

gypsum of proven Zechstein age. In a few places, the frequent intercalation of felsic volcanic, associated tuffs and volcanogenic detritus is additional evidence for a Lower Permian age [215].

The mineralized Permian strata vary from quartz schist to sericite and chlorite schists. The uraniferous bed near Forstau occurs within a series of sericite–quartzite and sericite–chlorite schist that was metamorphosed during the Permian. Generally, the Lower Permian in the Alps is considered to be terrestrial. However, dolomitic nodules occur in the ore-bearing sericite schist of Forstau indicating some marine influence. In addition, the frequent occurrence of tourmaline needles in the quartzite at Forstau may be indicative of an originally high boron content of marine origin [215].

The facies, thickness and uranium content of the sequence are interrelated. Some typical sections of the Permian in the eastern part of the Austrian Alps are presented in Fig. 86. Generally, the uraniferous layers are found in the lower, predominantly schistose parts of the section, within the greater thickness of the Permo–Skythian. Palaeoreconstructions indicate that the zone of depression with the thicker and complete Permo–Skythian strata do not coincide with the E–W directed Alpine units but cut across these almost at a 90°. Deposition was controlled by the post-Hercynian relief, the pattern of which follows the N–S directed Hercynian structures (Fig. 87). Soft rocks such as phyllite form the comprise most of the basement and the basins, whereas harder rocks such as gneiss or Devonian limestone represent relative highs. The uranium-bearing beds are found in the depressions [215].

The above features are interpreted as marine ingress into erosional lows. In the morphological depressions, sand and mud were deposited under reducing conditions, the terrigenous material and the uranium originating from the adjacent ridges. These were covered by talus in the Middle Permian. The uniform transgression started with the Zechstein Sea as the precursor of the Triassic Sea.

The uraniferous bed near Forstau occurs within a series of sericite–quartzite and sericite–chlorite schist (Radstatt Series) that is epimetamorphic Permian. Whether this series is Lower Austro-Alpine or Middle Austro-Alpine, i.e. is related to a diapiric window or to an isoclinal synform within the gneiss of Schladming, remains controversial [215].

### Mineralization

The length of the uraniferous zone is at least 8 km in an E–W direction and the dip is 45–60° N. The cuts and drill holes have exposed a mineralized layer of about 2 m in thickness. The individual orebodies within this layer are lens shaped, with dimensions of 5–20 m along strike and down-dip (Fig. 88). The entire ore-bearing zone is oriented E–W, as are the other rocks in this area, whereas the individual ore lenses strike ENE–WSW, following the schistosity, at an angle of about 20° to the general stratification. Nevertheless, no discordance between ore and host strata has been observed on the walls of the drifts. The influence of microtectonics is, in any event, undeniable [214].

The genetic interpretation remains uncertain. The ore is better developed in intercalations of hard quartzite than it is in soft chlorite schist, but no roll type features have been observed. The ore layer is tabular, although deformed.

Uraninite and pitchblende are the two main uraniferous phases at Forstau, but some of the uranium occurs in compounds associated with black organic matter. Framboidal pyrite grains and small particles of base metal sulphides offer evidence of a reducing depositional environment. The diameter of the pitchblende grains is typically only 50–100 µm. In specimens from Forstau, former framboidal pyrite grains are coated by pitchblende or uraninite, the pyrite having been dissolved, whereas the organic material of the framboids was transformed to UO<sub>2</sub> or a U–C compound. In this manner, the former structure of the framboidal pyrite has been perfectly preserved. This indicates that hexavalent uranium solutions, probably diagenetic groundwater, penetrated into beds of reducing character [215].

There is no published age determination of the Forstau mineralization. In the Muhlbach deposit, an age of 90 Ma has been recorded in nodules of uraninite, indicating evidence of hydrothermal activity and metallogeny in the Eastern Alps during the Upper Cretaceous [215].

## Metallogenic aspects

Several Permian uranium deposits have been discovered in the Austrian Alps. Among them, only Forstau has been explored by drilling and underground workings. The Alpine tectonic movements had a marked effect on the shape of the sandstone type deposits, so their genesis is difficult to decipher in detail. The deposition of uranium was conditioned by the post-Hercynian relief of the Alps. The deposits formed in lagoonal basins, transverse to the E–W Alpine trend, and were originally tabular. The uranium was concentrated in organic matter.

The Alpine Orogeny displaced the original sedimentary distribution, such that the deposits are situated in different tectonic units and have been affected by folding, schistosity development and elongation of the ore layers in an E–W direction. Widespread metamorphism in the Alps had little effect on the uranium mineralization, which is generally considered as relatively mobile. One possible reason for this could be the adsorption and fixation of uranium by the organic matter during metamorphism. However, metamorphism affected the fabric of the ore-bearing schist and, therefore, its porosity. The latter controls the formation of secondary uranium minerals and probably also the extraction (recovery) properties [215].

Mineralogical–petrological comparison of the Austrian deposits identifies some differences in composition (uraninite, pitchblende, brannerite, thucholite, uranothorianite and Fe–Cu sulphides), which are controlled by variations in sedimentology and metamorphism. In all cases, part of the uranium occurs in compounds associated with black organic matter. Mineralization is accompanied by haematization.

Uranium mineralization was probably derived from an original preconcentration in Permian black shales that was subsequently remobilized during Alpine metamorphism. Owing to the persistence of reducing conditions, the remobilization from the original site to that of deposition may have been limited to local reconcentration in shear zones and in the hinges of folds.

The source of uranium in the sediments is uncertain. In the Forstau strata, no felsic volcanic rocks have been identified. Thus, the provenance may derive from Hercynian gneisses. The Gastein syenite gneiss contains up to 80–100 ppm U. In the gneiss terranes of Seckau and Koralpe, secondary uranium minerals have been found.

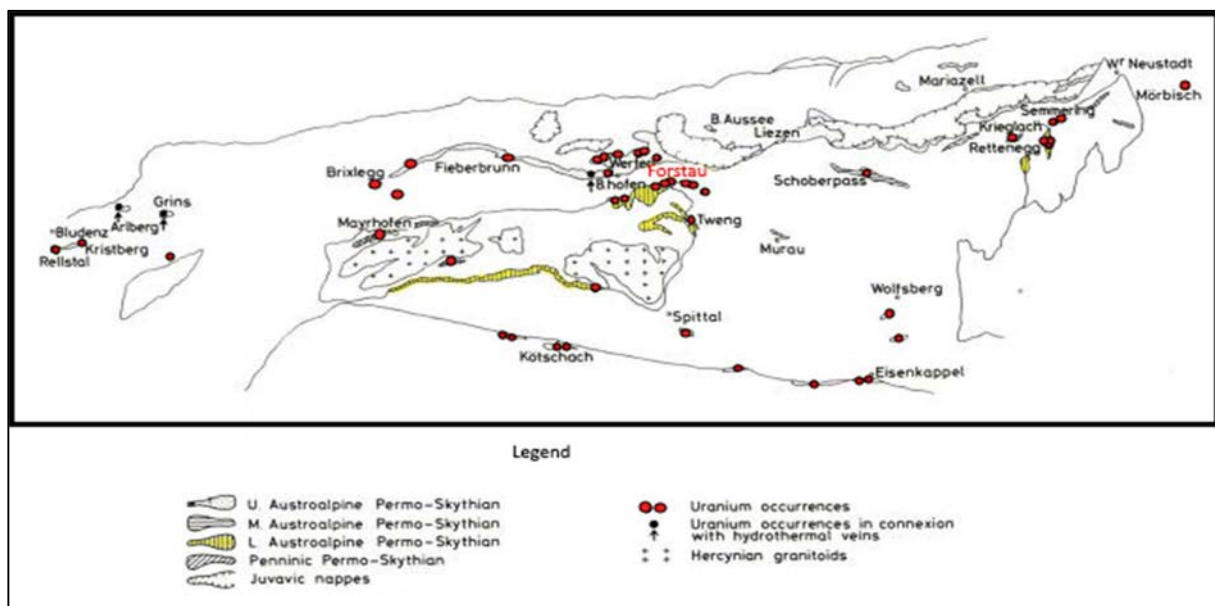


FIG. 85. Tectonic units and uranium occurrences in the Austrian Alps (the E–W extension of the map is about 500 km) (adapted from Ref. [215]).

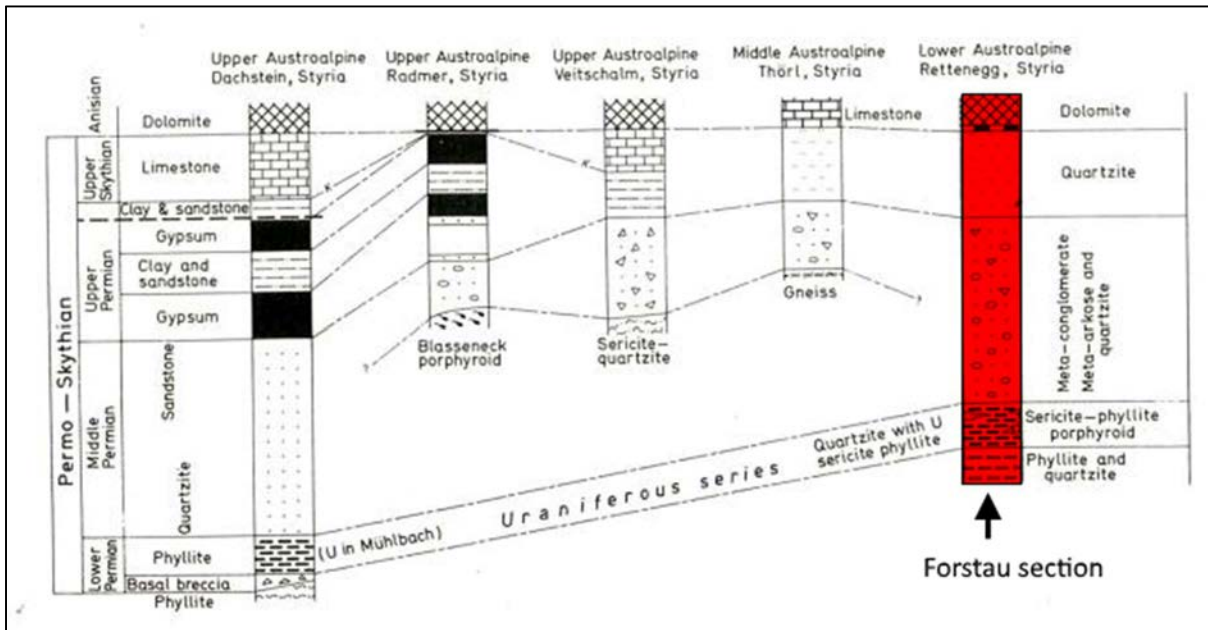


FIG. 86. Typical sections of Permian strata in the Eastern Alps. The Forstau section corresponds to the column on the right (adapted from Ref. [216]).

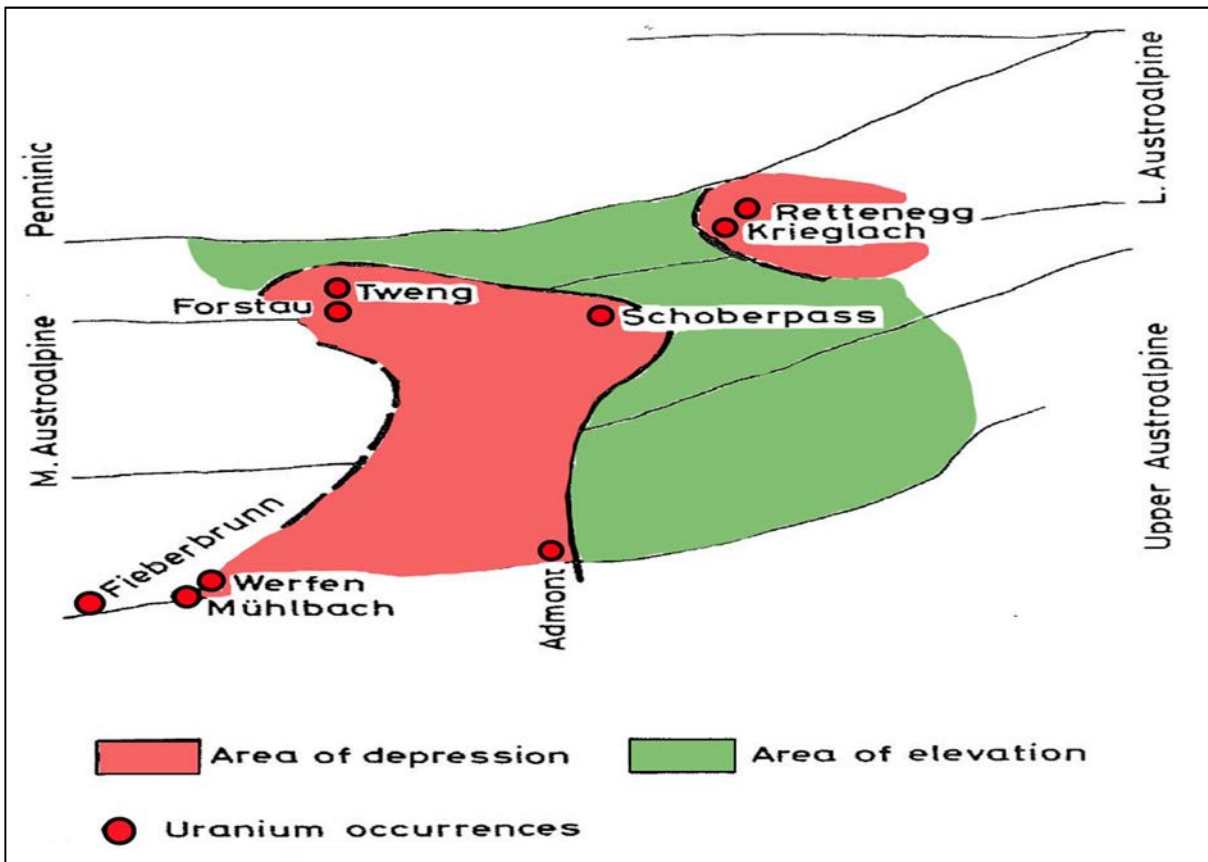


FIG. 87. Palaeogeographic setting of Permian uranium deposits in the Austrian Alps (adapted from Ref. [216]).

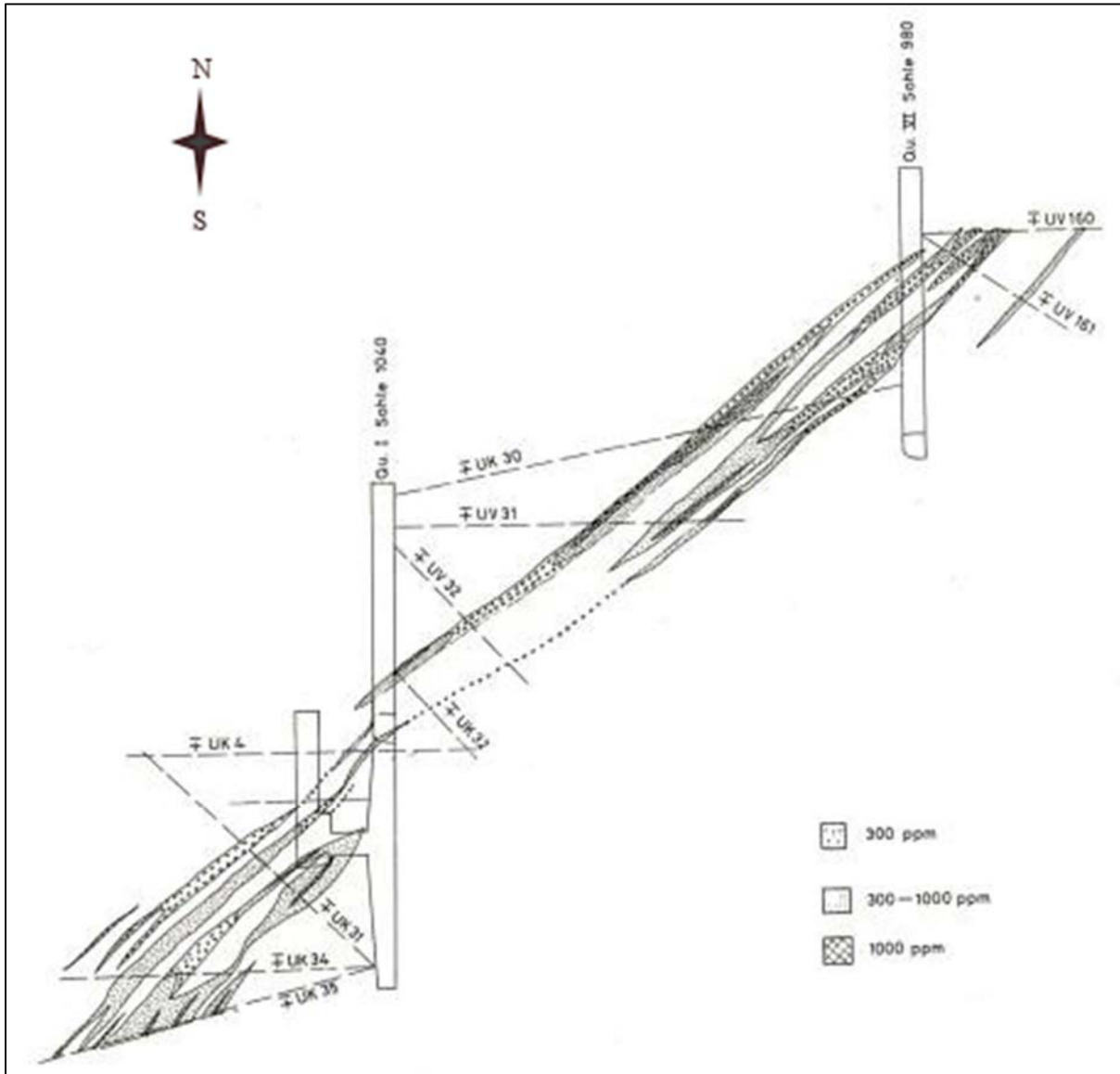


FIG. 88. Section across the Forstau deposit (adapted from Ref. [216]).

### 3.6.4.2. The Lac Cinquante deposit (Canada)

#### Introduction

The Lac Cinquante uranium deposit is located approximately 200 km south-west of Baker Lake, Nunavut, Canada, between Angikuni and Yathkyed Lakes (Fig. 89). Following earlier exploration success in the Baker Lake Basin, various companies began exploration in the Yathkyed and Angikuni sub-basins in the early 1970s.

After a 1975 helicopter radiometric survey identified radioactive conglomerates along the north-east margin of the Angikuni Sub-basin, Pan Ocean Oil staked claims in the area and undertook airborne magnetic and EM surveys, as well as ground scintillometer, magnetic and VLF surveys. Ground prospecting discovered pitchblende-haematite-carbonate veins in Archaean basement adjacent to the basin edge [217-219], which was the upper extent of the Lac Cinquante deposit. Pan Ocean Oil (later

Aberford Resources) extensively drilled the trend in the late 1970s and early 1980s [217] and defined a narrow vein system with a strike length of 400 m, which was drilled to a depth of about 300 m and hosting a resource of 4468 tU (not NI 43-101 compliant) [218]. Following the downturn in the uranium market from the mid-1980s through the 1990s, work ceased on the property. The deposit is situated on Inuit owned subsurface lands (Nunavut Tunngavik Inc). Kaminak Gold (later spun off as Kivalliq Energy Corporation) signed an exploration agreement to obtain the mineral rights to what is called the Angilak property in 2008. Since that time, it has undertaken ground and airborne geophysical surveys, geological mapping and prospecting, and diamond drilling.

A NI 43-101 compliant resource estimate based on the 2009–2011 drilling programmes was released in March 2012. Drilling in 2013 added additional resources to the Lac Cinquante deposit, amounting to a total of 11 550 tU at a grade of 0.45% U in the inferred resources category from the Main Zone and East and West Extensions. It has additional Ag, Mo and Cu credits. The new J4/Ray zone was defined with 6045 tU at an average grade of 0.585% U [219]. These two deposits lie on a NW–SE structural trend, now called the Lac 50 Trend. In 2015, exploration was still ongoing following the discovery of promising showings.

### Geological setting

The basement complex to the Angikuni Sub-basin consists of an Archaean granite–greenstone belt and high grade granitoid gneiss of the Hearne Province of the Canadian Shield. Following uplift and erosion of the Palaeoproterozoic Trans-Hudson Orogen, sediments and alkaline volcanic rocks were deposited in a series of fault controlled basins along the Snowbird Tectonic Zone. The largest is the Baker Lake Basin to the north-east while several smaller sub-basins are situated to the south-west, including the Angikuni and Yathkyed Sub-basins.

The Archaean basement is haematized and carbonate altered below the Angikuni unconformity [218]. The basin fill consists of a basal sedimentary breccia and conglomerate of the South Channel Formation, locally present Kazan Formation red bed sandstone (mainly in the north-east) and the Christopher Island Formation volcanic and volcanoclastic rocks, which comprise the majority of the basin [219].

The Lac Cinquante deposit is situated in Archaean greenstone belt basement intruded by feldspar porphyry and gabbro intrusions, adjacent to the Angikuni Sub-basin. The mineralization is hosted in metavolcanic (mafic to intermediate flows and tuffs with lesser felsic volcanic rocks) and metasedimentary rocks of the Henik Group [218]. The latter unit, called the graphitic tuff unit is an interflow tuffaceous sedimentary unit containing abundant chlorite, pyrite, chert and variable amounts of graphite and carbonaceous material. It ranges around 0.5–2 m in thickness and has been the loci of extensive foliation-parallel shearing and faulting, presumably at least in part during the Palaeoproterozoic Hudsonian Orogeny.

The dominant structural grain of the basement rocks is ENE trending (070–080°) with more subtle north-west trends [219]. However, the Lac Cinquante deposit is situated along a 110–120° striking, moderately south-west dipping (60°) VLF conductor (Fig. 90) related to the sulphidic–graphitic pelite horizon [218]. This metasedimentary unit exhibits strong foliation-parallel shears that host the majority of the mineralization. This is cut by north-east trending (040–060°) cross faults and veins.

### Mineralization

The Lac Cinquante deposit is a pitchblende vein system controlled by faults and shears along the narrow (~2 m), steeply dipping cherty metasedimentary unit (Fig. 91). Mineralization is found over a 3 km strike length in a vein system averaging about 1 m in width. The Main Zone of the mineralization is about 1400 m long, the Western extension is 600 m long, and the Eastern extension almost 600 m. According to Dufresne et al. [219], the true thickness of the zone is in the range 0.05–13.5 m, averaging 2.2 m. It is drill defined to a depth of about 265 m [217] but remains open at depth.

Although mineralization is relatively continuous along strike, the highest grades define pods plunging 30–40° to the north-west [218], possibly related to structural intersections.

Mineralization consists of disseminated pitchblende and base metals in strongly fractured cherty metasedimentary rocks, cross-cutting pitchblende veins, and gash veins consisting of pitchblende, quartz, carbonate, and sulphides. Uranium is present as colloform and sooty pitchblende, as both fracture fills and disseminations. It is often accompanied by Mo and Ag while Cu is present in the carbonate-bearing gash veins. Elevated Pb, Cu and Zn may be at least in part due to volcanic–hydrothermal processes related to the deposition and alteration of the chemical sedimentary unit. Little alteration is associated with mineralization, consisting mainly of chloritization with lesser, localized haematization, carbonatization, silicification and albitization [218].

#### Metallogenic aspects

The Lac Cinquante deposit is a metamorphic type, vein style pitchblende deposit hosted by moderately dipping brittle structures in polydeformed and metamorphosed basement rocks adjacent to a Palaeoproterozoic successor basin. In those respects it bears similarity to the deposits of the Beaverlodge district of northern Saskatchewan as it includes: narrow ore shoots in discrete fault zones, similar age of host rocks and alteration assemblages, similar grade and distribution of uranium minerals [219], as well as similar alteration assemblages and the presence of both monometallic and polymetallic deposits and showings. The only major difference between the deposits is the poorly developed haematization at Lac Cinquante.

Comparisons have been made with the polymetallic iron oxide breccia complex deposit type (also known as IOCG) [219], citing the extensional basin setting, proximity to a Proterozoic unconformity, haematization, polymetallic nature, presence of breccias and several other factors of similarity.

Western Mining Corporation did explore for this deposit class in 1995 [219], although it focused on the Angikuni Basin itself rather than in the Lac Cinquante area. However, Lac Cinquante bears little resemblance to Olympic Dam, with the lack of an association with large granitic intrusions, comparatively little brecciation and haematization, and a significantly different metal grade.

This area was also explored for unconformity uranium mineralization and some comparisons have been made. Similarities include both monomineralic and polymetallic mineralization styles, the strong structural control and the proximity to Proterozoic clastic basins. However, several factors are inconsistent with the model, including the lack of an established temporal association with the Angikuni Sub-basin, the lack of haematization at the unconformity, the lower ore grades and, most notably, the lack of strong clay alteration and other relatively low temperature alteration phases associated with mineralization [219].

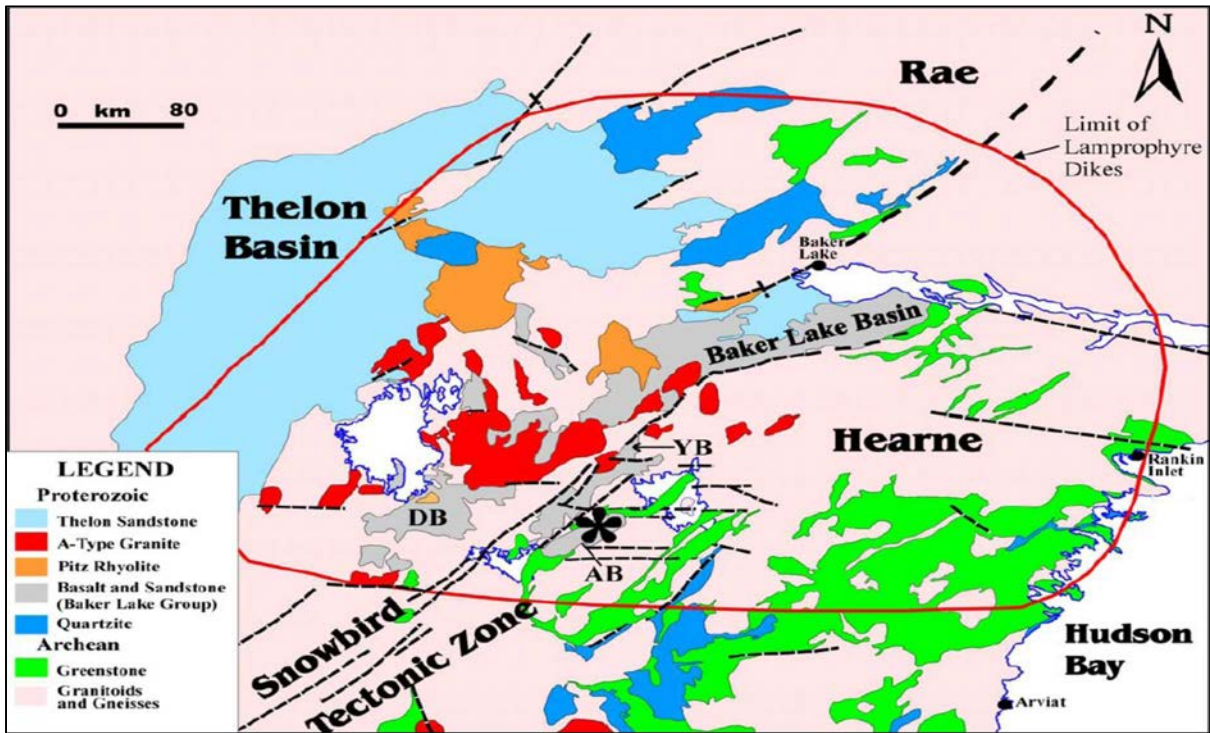


FIG. 89. Regional geology of the Baker Lake Basin occurring within the Snowbird Tectonic Zone. The 'flower' shape shows the location of the Lac Cinquante deposit [219] (reproduced with permission).

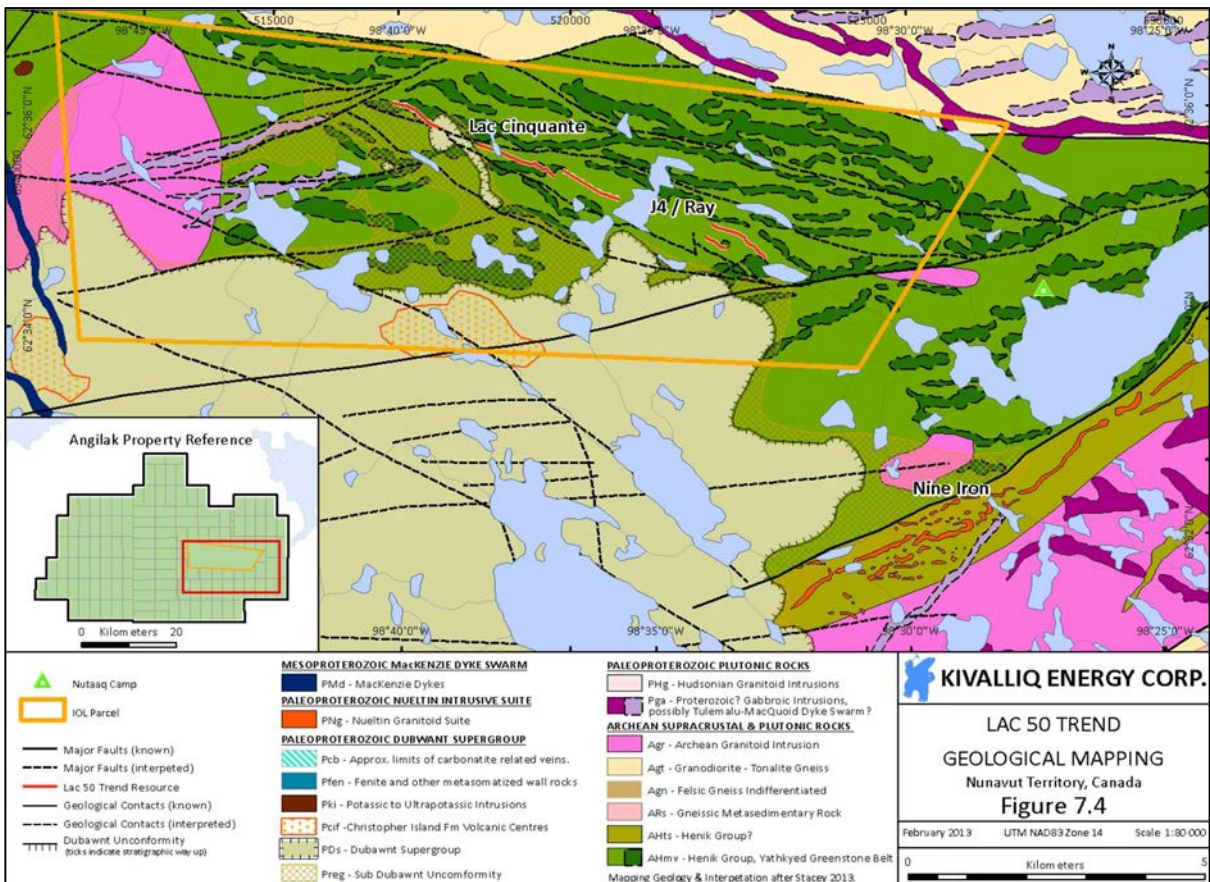


FIG. 90. Geology of the Lac 50 trend, along the Angikuni basin [219] (reproduced with permission).

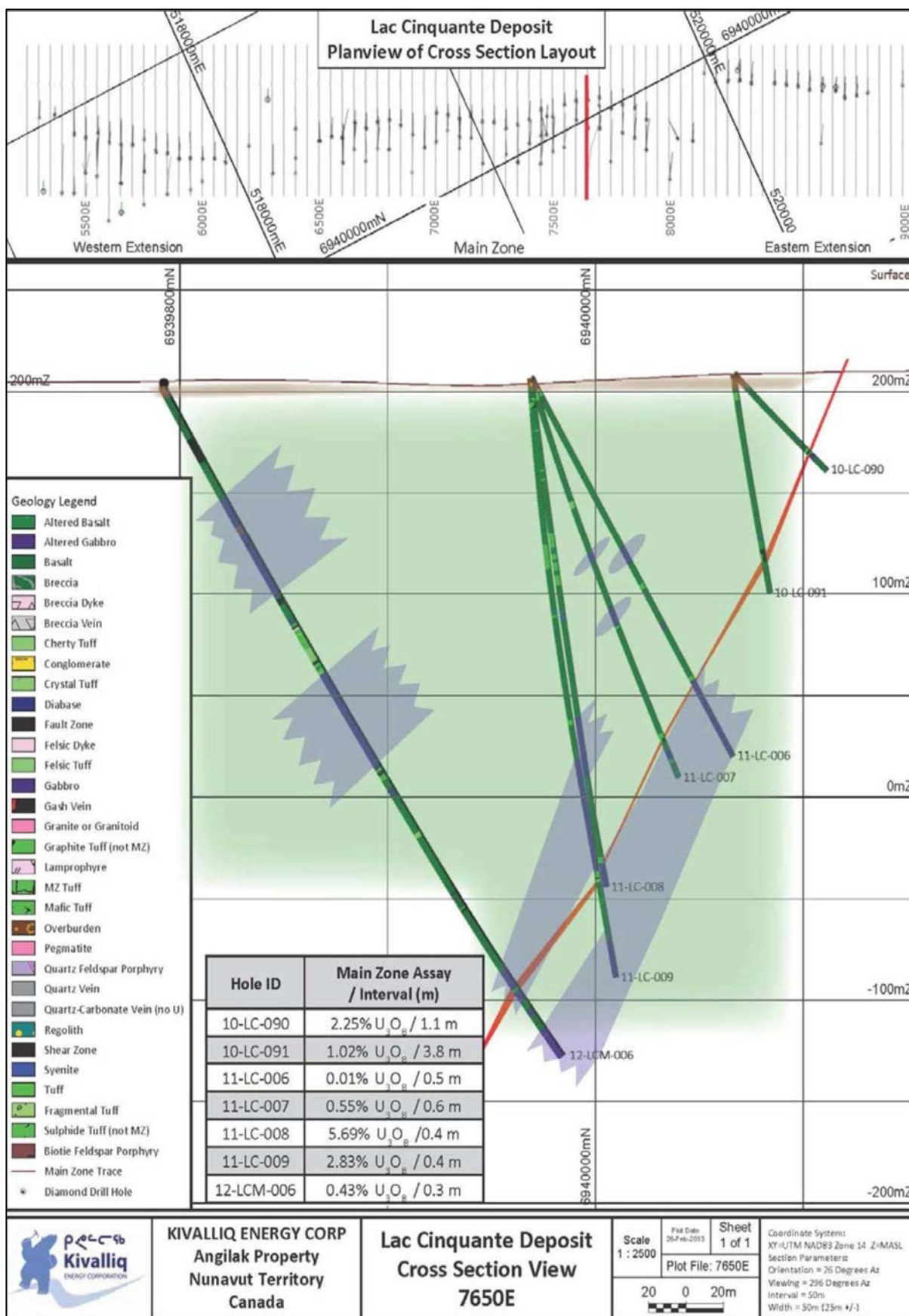


FIG. 91. Cross-section of the Lac Cinquante deposit, which is hosted in veins and fractures of the cherty metasedimentary unit (tuff) [219] (reproduced with permission).

### 3.6.4.3. *Eldorado mine, Port Radium (Canada)*

#### Introduction

The Port Radium uranium mine is located on the western edge of a peninsula on the eastern shore of the McTavish arm of Great Bear Lake in the Northwest Territories, Canada, approximately 430 km north-west of Yellowknife. As reported by Campbell [220], Cu–Co-bearing veins were first discovered in the area in 1899 by J.M. Bell of the Geological Survey of Canada. In 1930, G. Labine and E.C. St Paul discovered pitchblende–silver ores, which started a prospecting and staking rush. The Eldorado mine went into production in 1934 producing silver and radium ores. After closing in 1940, it reopened in 1942 as a uranium mine. Owing to the strategic value of uranium during the Second World War, Eldorado Nuclear was nationalized by the Canadian Government in 1943. The Eldorado mine produced uranium until 1960 [221]. Several other polymetallic deposits and occurrences are found in the area, most significantly the Contact Lake Ag–U occurrence and the Echo Bay silver mine [221].

#### Geological setting

The Port Radium mine is located in the western part of the Great Bear Magmatic Zone in Bear Province of the Canadian Shield [222]. The regional geology is shown in Fig. 92. As described by Hildebrand [223], Bear Province records the accretion, metamorphism and magmatism of the 2100–1800 Ma Wopmay Orogen along the western margin of the Slave Craton. The orogen includes four zones, from east to west: platform cover, the Asiatic Fold Thrust Belt, the orthotectonic zone and, on the west side of the Wopmay Fault, the Great Bear Volcano–Plutonic Belt. The southern part of the belt consists of high level plutonic rocks and deformed 1920 Ma sialic basement of the Holly Lake Metamorphics. The northern part records a shallower erosional level, consisting of volcanic and sedimentary roof cover rocks of the McTavish Supergroup.

The McTavish Supergroup consists of three units: (i) the lowermost Labine Group of intermediate lavas and pyroclastic rocks with lesser sediment and porphyritic intrusives, (ii) the Sloan Group dacite and rhyodacite tuff and (iii) the Upper Dumas Group mafic volcanic rocks and mudstone. The McTavish Supergroup is folded along NW trending axes and is cut by NE trending strike-slip faults that post-date the magmatism [223].

The Labine Group consists of four formations. The lowermost Port Radium Formation (the lower unit of the Echo Bay Group of Campbell [220, 224]) consists of a coarsening upward sequence of laminated sandstone and siltstone, tuff, minor conglomerate and carbonate. The overlying Echo Bay Formation consists mainly of massive and columnar porphyritic andesite breccia and flows, rhyodacite flows and epiclastic sediments (the age is reported as 1875–1860 Ma by Ruzicka and Thorpe [221]). Overlying and interfingering with the Echo Bay Formation are clastic sediments, rhyolite flows, ash flow tuff and andesite of the Cameron Bay Formation. This is capped by ash flow, crystal tuff and dacite flows with minor stromatolitic dolomite of the Feniak Formation [223].

The Labine Group is intruded by several generations of plagioclase and hornblende–plagioclase porphyritic intrusions representing subvolcanic magma chambers of the coeval volcanic rocks. Contact metamorphism in the country rock is up to amphibolite facies and metasomatism may be extensive [223]. Most noteworthy is the Mystery Island Intrusive Suite, consisting of sheets of medium-grained diorite, quartz syenite and granodiorite. It features zoned alteration halos up to 2 km wide, with an inner bleached and albitized zone, a central zone of apatite–actinolite–magnetite alteration and breccia, and an outer zone containing chalcopyrite and pyrite [223].

The Port Radium veins and fracture fillings are hosted mainly within the Port Radium and Echo Bay Formations but extend along strike to the north-east into the Cameron Bay Formation and granodiorite and to the south-west into biotite granite. Campbell [220, 224] noted a strongly stratabound nature, with most mineralization hosted in banded cherts of the lower Echo Bay Group. While this unit is

undoubtedly the main host, Jory [225] interpreted these as dacitic tuffs, based on the recognition that they were composed mainly of very fine albite, not silica. Hildebrand [223], however, interpreted them as sedimentary rocks that had undergone albitization.

The deposit is hosted in a NE trending, lozenge shaped fracture zone between Cobalt Island and Cross Fault Lake, as shown in Fig. 93. This fault and fracture zone lies along the 65° NW dipping Eldorado Shear Zone. The main block within the fault system consists of the Port Radium Formation (Lower Echo Bay Group of Campbell [220]), bounded to the south-east by Echo Bay Formation volcanic rocks and to the north by granite. The rocks of the Labine Group strike north-east and have a steep, south-east dip, but locally show complex fold patterns near the porphyry dykes and sills that intrude them [225].

### Mineralization

The Port Radium deposit consists of a number of lensoid bodies hosted in veins, breccia and shear zones. Veins may be greater than 1000 m long and extend to 500 m in depth. Between 1938 and 1960, the deposit produced 6000 tU at a grade of 0.3–0.6% U [222].

As described by Campbell [224], the Port Radium deposit consists of a NE trending fault and shear system with complex fracture systems within the lozenge, with the main zones being the No. 1 vein and Bear Bay Shear. Mineralization is of two types, hosted in: (i) shear zones, and (ii) fracture zones. Shear zones feature chlorite on slip planes and gouge on slip planes of the footwall. Mineralized zones range from 0.3 m to 12 m wide, recording several mineralization and brecciation events. Zones of this style include the Nos 1, 2, 4, 5 veins and Bear Bay Shear. Fracture zones feature no gouge but include fractures, breccias, vein filling and alteration. They range in width from several centimetres to 9 m. Examples include the Nos 3, 7 and 8 veins and branches of the No. 2 vein. The veins are narrow in massive rocks (granite, porphyry, diabase and metasomatized sediments) but branch and widen in the sedimentary rocks. Fig. 94 shows a cross-section of the Port Radium mine and Fig. 95 depicts a long section of the No. 2 vein.

Mineralization is contained within a steeply dipping quartz stockwork along NE trending faults termed the ‘Giant Quartz Veins’ by Campbell [220]. These vein–stockwork zones vary in width in the range 15–300 m and extend over lengths of several tens of kilometres [226]. These stockworks consist of a central zone of massive quartz and breccia flanked by an outer zone of stockwork quartz stringers in the brecciated and healed country rock [223, 226]. The last brecciation and quartz veining event was accompanied by specular haematite, pyrite, Cu sulphides and pitchblende [223]. Wall rock alteration consists of widespread haematization zoned inwards to argillic alteration, chloritization and carbonate. However, Campbell [224] reports that mineralized veins do not exhibit a consistent association to wall rock alteration.

The vein formation consists of a sequence of five stages [223, 225]:

- (i) Haematite and quartz (massive greenish or white);
- (ii) Pitchblende, quartz (brown or grey) and haematite exhibiting late brecciation (the main uranium mineralization stage);
- (iii) Quartz (grey jasper and brown quartz), Co–Ni arsenides and sulphides, minor pitchblende;
- (iv) Copper sulphides, galena, sphalerite, tetrahedrite, chlorite, clay, ± dolomite, both as vein and replacement styles;
- (v) Carbonate (dolomite, rhodochrosite, calcite), native silver, bismuth, ± chalcopyrite, pitchblende (the main silver mineralization stage).

Veins are mainly fracture infill but some replacement of wall rock is found along the margins. However, the pitchblende, silver and arsenide minerals are only infill [225]. Pitchblende is locally very rich and occurs in a number of forms, including colloform seams up to 2.5 cm wide, massive veins and lenses <65 cm wide, pods and lenses in quartz and chlorite shears, fragments in late veins

and rims around fragments of quartz or wall rock. Lenses are sharp, ranging from <30 m to >180 m in length, with stopes <1 m to 7 m wide and averaging about 1.3 m. Uranium is found in tensional openings along the veins, related to competency contrasts, bends, branches and steep sections. The No. 2a, 3 and 7 veins are the highest grade [225]. Silver is only found in vertical parts of the vein system.

Alteration is highly variable in width, ranging from 2.5 cm to 16 m. Most prominent are argillic, chlorite, haematite and carbonate, with minor silicification, sulphidization and apatite.

#### Metallogenic aspects

The pitchblende–silver-bearing veins of Port Radium are structurally controlled veins in a complexly faulted and fractured lozenge along a NE trending fault zone. The mineralization is mainly hosted in the sedimentary and volcanic rocks of the Port Radium and Echo Bay formations, along the margins of the porphyry intrusions. The fault systems widen substantially in the sedimentary and volcanic rocks in contrast to the more massive granitic and porphyry rocks. As indicated by Campbell [224], competency contrasts are the main ore control. Pitchblende and arsenide mineralization types are found only as infill, especially where the veins steepen.

The polymetallic mineralization shows a systematic progression of oxides (including pitchblende) to arsenides, sulphides, carbonates and, finally, native metals (Ag and Bi). This indicates a progression from oxidizing, near neutral to reducing, higher pH conditions over the period of vein deposition. Campbell [224] attributes the precipitation of uranium to destabilization of uranyl carbonate complexes causing release of CO<sub>2</sub> and precipitation of uraninite as colloids. The author also interprets the locally strong clay alteration as synchronous with the sulphide stage of mineralization, thus post-dating the pitchblende.

Fluid inclusion, mineralogical and isotope data [226] suggest that for mineralization at the nearby Echo Bay mine, early mineralization took place at about 120°C and later sulphide and silver mineralization was deposited at 200°C from fluids of approximately 30wt% NaCl equivalent. During vein deposition, fluids evolved from low pH to higher pH and lower Eh. A peak temperature of 480°C was determined for the third (arsenide) stage of mineralization [226].

The deposit is interpreted as a polymetallic example of structurally hosted vein mineralization in metamorphic rocks (metamorphite) although at a higher structural level than most examples. The polymetallic veins bear similarities to the arsenide uranium veins found in Europe, such as Jachymov in the Czech Republic [222]. However, at Port Radium, a genetic link between the mineralization and the intrusive rocks is tenuous. The age of the Port Radium veins is uncertain, based on the complex data presented by Ruzicka and Thorpe [221]. The authors conclude that the veins formed between 1775 and 1665 Ma, with isotopic resetting at 1500 and 1420 Ma. However, the authors indicate that it is possible that primary pitchblende could have an age of 1500 Ma. These dates are all younger than the 1875–1860 Ma age of igneous activity of the Great Bear Magmatic Zone reported by Ruzicka and Thorpe [221] and the 1875 Ma age of the Labine Group [223] and its subvolcanic intrusive rocks.

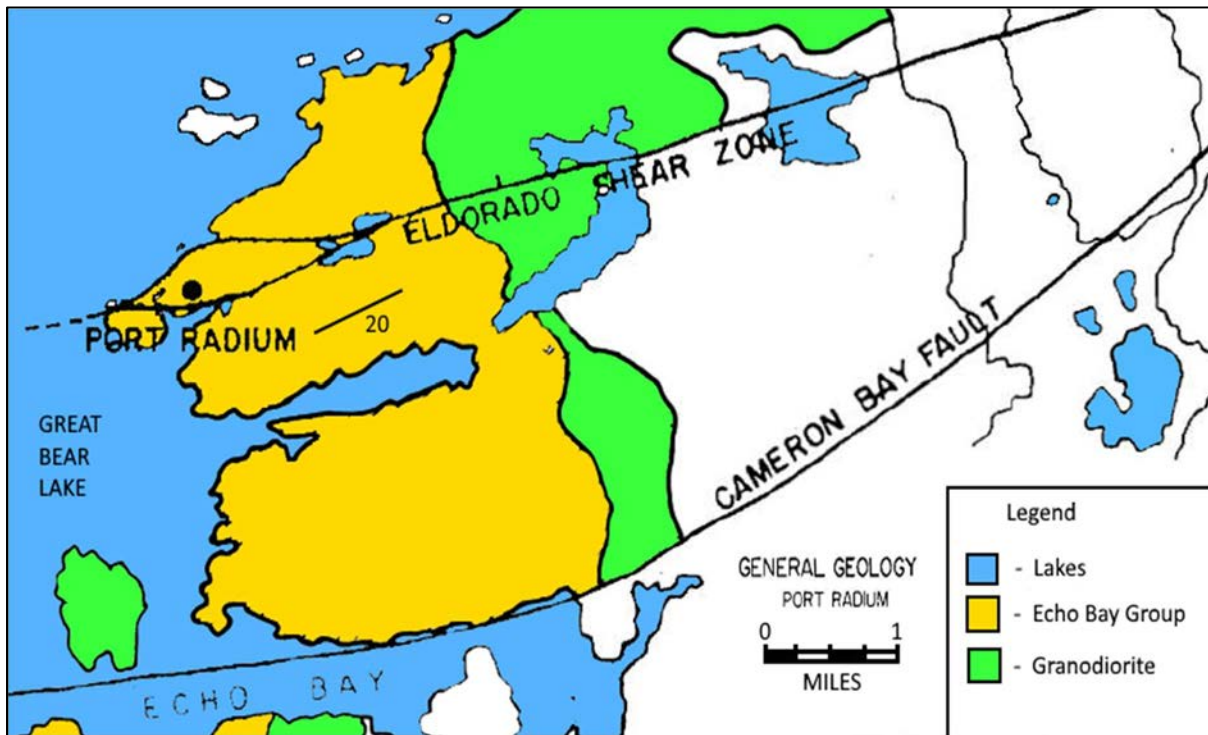


FIG. 92. Regional geology of the Wopmay Orogen showing the location of the Port Radium mine on the eastern shore of Great Bear Lake (adapted from Ref. [225]).

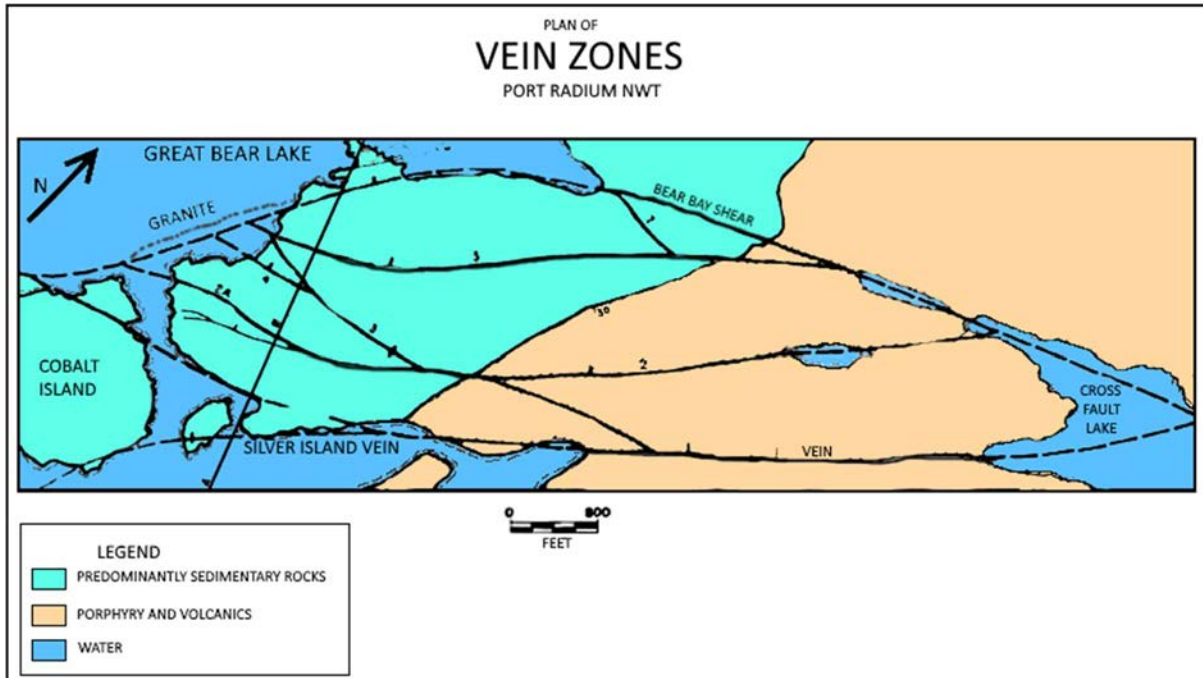


FIG. 93. Geology of the Port Radium mine showing the NE trending vein system (adapted from Ref. [225]).

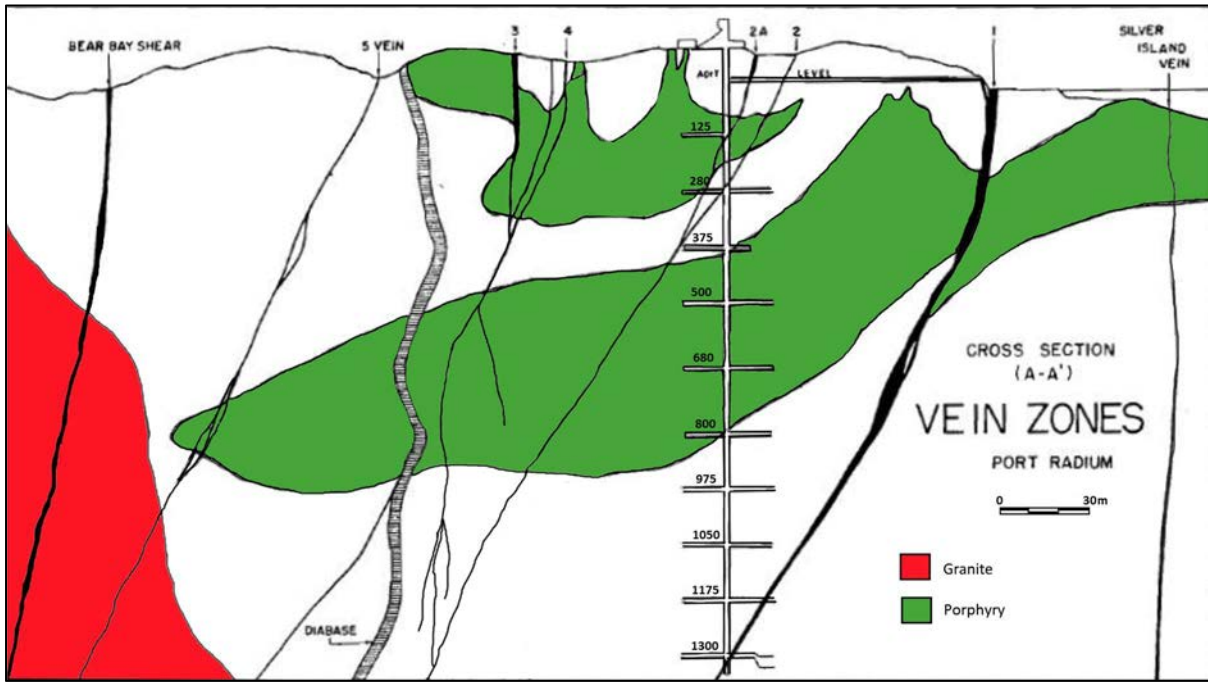


FIG. 94. Cross-section of the Port Radium mine (adapted from Ref. [225]).

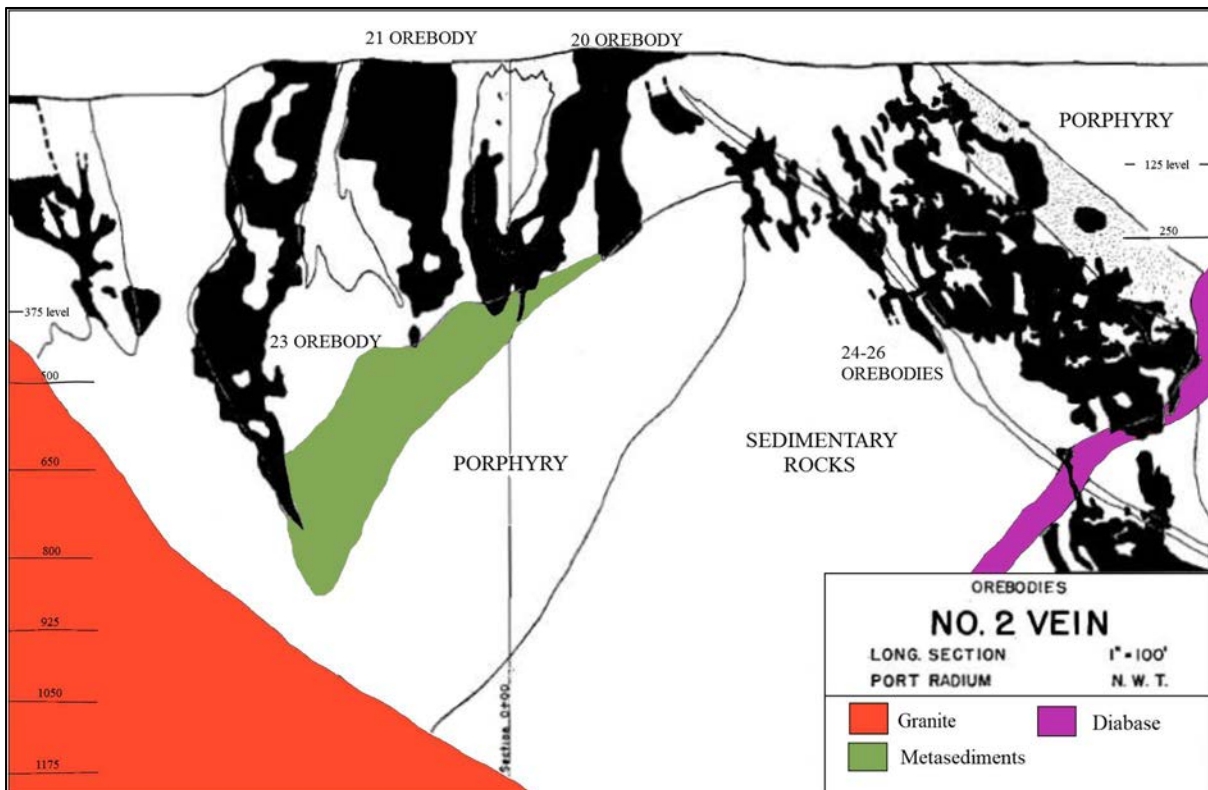


FIG. 95. Longitudinal section of the No. 2 vein of the Port Radium mine (adapted from Ref. [225]).

#### 3.6.4.4. *The Schwarzwald deposit (USA)*

##### Introduction

The Schwarzwald deposit is located in the east–central Front Range, approximately 20 km NW of Golden, Colorado (Fig. 96). It was discovered in the 1940s and was developed as a hard rock underground mine. Cotter Corporation, a subsidiary of General Atomic, acquired the mine in 1965. From 1953 through 2000, the 750 m deep mine produced about 7500 tU at a grade of 0.408% U. Total resources of the deposit to a depth of 900 m are estimated to be 12 650 tU at an average grade of 0.37% U. The mine has faced many environmental issues since its closure.

##### Geological setting

###### *Local geology*

The Schwarzwald uranium deposit is hosted by Palaeoproterozoic lithologies (Idaho Springs Formation) that were subjected to tight to isoclinal folding and regional amphibolite grade metamorphism about 1750–1700 Ma (Figs 97–99). Dykes of aplite and tourmaline–garnet-bearing pegmatite of Silver Plume age (1400 Ma) cut the metamorphic rocks.

Phanerozoic sedimentary rocks occur about 500 m east of the deposit. Unconformable red bed facies of Pennsylvanian age form the basal sedimentary unit. Marine and continental sediments of Permian–Cretaceous age rest upon the red beds. Regolithization of the crystalline basement rocks extends from the Pennsylvanian unconformity to a depth of as much as 30 m.

Four major lithological units of Palaeoproterozoic age constitute the stratigraphic sequence at the Schwarzwald deposit: (i) mica schist; (ii) garnet–biotite gneiss; (iii) quartzite, and (iv) hornblende gneiss. The Schwarzwald host rocks were probably derived from submarine pyroclastic rocks and iron- and sulphide-rich pelitic sediments similar to other Precambrian iron formations. Sediments were deposited in a restricted shallow basin in close proximity to submarine volcanic centres [227].

Hornblende gneiss and mica schist are thick and regionally extensive. Garnet–biotite gneiss and quartzite form a narrow transition zone between hornblende gneiss and mica schist. The original thickness of the transitional rocks is difficult to determine owing to intense folding and faulting, but is probably between 15 and 100 m [47].

###### *Structural geology*

The deposit is located in an area with a complex array of structural dilation zones, branching fault systems, deflections and intersections between the East and West branches of the NW–SE trending Rogers Fault System (Fig. 96).

The structural setting of the Schwarzwald deposit is dominated by two distinct fold and fault elements [47]:

- (i) An isoclinally folded synform with a nearly vertical axial plane and a steeply plunging fold axis. In the synform nose, the original thickness of ore hosting garnet–biotite gneiss and quartzite units of the transition zone is almost doubled to more than 100 m, whereas elsewhere mica schist occupies the fold core, bounded successively by garnet–biotite gneiss, quartzite, and hornblende gneiss;
- (ii) A set of two major, approximately parallel faults (East and West Rogers Faults) interconnected by cymoid faults trending NNW–WNW (Illinois Fault) with a stacked series of tensional horsetail type fractures branching off into the hanging wall of the Illinois Fault (Fig. 98).

The East and West Rogers Faults belong to a regional structure system consisting of a number of NW–SE trending, steeply dipping faults. Both exhibit intense shearing and brecciation over a width varying between one metre and several tens of metres. The East Rogers Fault displaces the Proterozoic–Palaeozoic unconformity for more than 100 m. The West Rogers Fault cuts the synform.

The Illinois Fault System, which hosts the Schwartzwalder uranium veins, evolved through multiple tectonic events. As a result, a number of pre-ore and post-ore subparallel faults trending between WNW and NNW are developed (Fig. 97). Wright [228] identified at least two successive periods of faulting in Proterozoic time: (i) an early, pre-Silver Plume period reflected by faults intruded by pegmatites of Silver Plume age, which parallel the Illinois Fault in its footwall and also associated horsetail fractures and (ii) a subsequent Proterozoic stage that apparently caused the drag of the synform. Later stage faults must have been reactivated several times, namely in pre-Laramide to early Laramide time to permit the entry of mineralizing fluids in Laramide time, and later on repeatedly during mineral deposition, as documented by ore textures.

Horsetail fractures developed in a stacked fashion in competent rocks on the hanging wall side of, and apparently ‘rooted’ in, the pre-ore Illinois Fault. Wright [228] considers horsetail fractures to be of Laramide age. He describes two sets of horsetails: one striking due N–S and the other NW–SE. Both dip easterly at changing attitudes, varying between steep and almost flat, and both are mineralized. No tensional horsetails exist in the incompetent footwall block. Displacement along the post-ore Illinois Fault has truncated many horsetail veins below the 13th level of the mine [47].

Dykes of clastic material are a characteristic feature of the Schwartzwalder deposit. These dykes invaded many structures and veins with the exception of the post-ore Illinois Fault. The latter is notably devoid of any clastic dykes. The dykes vary in width from a few centimetres to a metre and are composed of altered wall rocks and antecedent vein material cemented by a microcrystalline matrix of rock flour and authigenic, fine-grained carbonate and adularia. Three generations of clastic dykes characterized by variations in colour are present [47].

#### *Host rock alteration*

Altered wall rocks are typically bleached and are overprinted by reddish colouration along veins. Alteration is mineralogically uniform throughout the 900 m vertical interval of the mine but it is nowhere extensive or pervading far into the wall rock. It may locally be absent, even adjacent to pitchblende-bearing veins.

Wallace [227] describes two successive assemblages of wall rock alteration:

- (i) Early carbonatization and sericitization pseudomorphically replace all mafic minerals in the host rocks within 2 m of veins, indicating a large influx of CO<sub>2</sub> and concomitant loss of SiO<sub>2</sub>. Carbonate–sericite alteration products are of pale yellow–green colour and extend for as much as two metres from fractures into adjacent wall rocks but without destroying primary rock textures. Sericite and Ca–Mg–Fe carbonates, mainly siderite, ankerite and dolomite, are the principal alteration products, with minor amounts of chlorite, paragonite, kaolinite, albite and leucoxene. Siderite, marcasite and pyrite replace pyrrhotite and the first two replace pyrite of both metamorphic and alteration origin. Although carbonate and sericite pseudomorphically replace mafic rock constituents, they do not severely affect felsic minerals. A critical parameter for the relative intensity of this alteration type is the abundance of mafic minerals in any given wall rock [47];
- (ii) Subsequent haematization and potassium feldspathization (adularia) replace pre-existing alteration minerals immediately adjacent to veins. Haematite–adularia alteration consists essentially of these two minerals, but adularia can be locally absent. Alteration extends, as a reddish asymmetric halo, up to 20 cm into the wall of most fractures but is missing on one or both sides along many vein segments. It is restricted to rocks changed by type (i) alteration where it overprints the earlier formed assemblage as well as relict feldspars. haematitization

also affected pre-ore breccia fragments. In areas of most intense alteration of this type, along the Illinois and Rogers Faults, most quartz and all primary textures are destroyed and a hard, microcrystalline intergrowth of haematitized adularia with irregular patches of carbonates is formed [47].

## Mineralization

Schwartzwalder vein mineralization occurs predominantly in the Illinois, West Rogers and associated horsetail structures. The ore consists essentially of pitchblende accompanied by a number of other minerals. Trace elements include As, Ba, Cu, Mo, Pb, Sb, Sr, Th, V and Zn.

Multiple stages of mineral deposition and associated and coeval stages of fracturing/brecciation have been identified. Three main successive paragenetic stages and several sub-stages of hypogene uranium and base metal mineralization have been described: (i) sulphide–carbonate–adularia; (ii) pitchblende–coffinite–carbonate–adularia–sulphide; (iii) calcite–sulphide [227]:

- (i) *Stage i* mineralization is minor. It includes two mineral assemblages: (1a) haematite–chalcedony–carbonate, which formed contemporaneously with the second stage of alteration and (1b) carbonates, mainly dolomite, non- to slightly haematitic adularia, and base metal sulphides, including chalcocite, chalcopyrite, galena, pyrite and zoned yellow sphalerite;
- (ii) *Stage ii* is the principal uranium phase and produced the bulk of the vein fillings. Pitchblende and coffinite are the only uranium minerals. Pitchblende is paragenetically intergrown with an unnamed Fe–Mo–As–sulphide mineral. The mineral, formerly referred to as jordisite or molybdenite, is characteristic for horsetail ore, whereas it is markedly rare in fractured ore along the Illinois and West Rogers Faults. Wallace [227] subdivides stage ii into three substages:
  - (a) *Substage IIa* mineralization with ankerite–dolomite and non-haematitic adularia followed by pitchblende, pyrite, chalcopyrite, galena and the Fe–Mo–As–S mineral. Coffinite replaces pitchblende. All minerals commonly form a black, very fine-grained mixture filling voids in breccia zones and fractures;
  - (b) *Substage IIb* mineralization consists of colloform pitchblende intergrown throughout with minor amounts of disseminated sulphides including chalcopyrite, pyrite, galena and Fe–Mo–As–sulphide. Gangue minerals are ankerite, dolomite and non-haematitic euhedral adularia. Pitchblende and the other minerals fill the interstices between breccia fragments of reopened veins;
  - (c) *Substage IIc* mineralization is composed of a carbonate–sulphide assemblage with carbonate far more abundant than sulphides. The assemblage fills voids and fissures which remained open after pitchblende deposition. The principal sulphide and gangue minerals are the same as in substages IIa and IIb except that pitchblende is absent. Sulphide additions include yellow sphalerite, marcasite and minor amounts of tennantite, niccolite, rammelsbergite, arsenopyrite and a Pb–Mo sulphide. Gangue minerals are quartz–amethyst, chlorite, fluorite and calcite. Calcite was the last mineral to form.
- (iii) *Stage iii* mineralization comprises a coarse-grained assemblage of calcite–sulphide, predominantly pyrite and marcasite with minor chalcopyrite. These minerals fill vugs and fissures in uranium veins and in post-ore structures such as the post-ore Illinois Fault.

Supergene mineralization is limited to the uppermost part of the deposit, above the first level. Complete transformation of pitchblende into hexavalent uranium minerals is virtually restricted to within 10 m of the surface.

Uranium ore is distributed intermittently, mainly in the steeply dipping Illinois Vein and in associated east dipping horsetail structures in its hanging wall. Some ore occurs in the Washington Vein, which parallels on the footwall side and joins the Illinois Vein at depth (Fig. 98).

Depth extension of the Illinois Vein system as known from mining to the 20th level and from drill intersection is more than 700 m below the present day surface. Wallace [227] attributes this deep penetration to down faulting of some vein sections. Mineralization within the Illinois Vein itself extends intermittently from the surface to the 15th and 16th levels. At this depth, the structure narrows from a width of about 5 m with relatively good ore grades to a width of about 1 m which is devoid of ore except for some brecciated ore at the footwall boundary. Unmineralized breccia and dykes of cream coloured clastic material fill the structure from the 16 and 17 levels and below. Carbonate–sericite alteration continues in a narrow but persistent zone in wall rocks beyond the extent of the uranium to at least the 19th level [47].

The width of mineralized veins varies from millimetres to several metres. Horsetail veins average about 0.5 m in width and commonly contain high grade ore. The Illinois Vein has a width of up to 15 m, but ore, although of large minable tonnage, is of relative low grade. The length of ore shoots may be as much as 100–200 m, as within cymoid loops of the Illinois Vein. Horsetail veins, which root on cymoid bends, can have corresponding economic strike lengths and dip extensions of more than 150 m [228].

Uranium grades are highly variable as is reflected in the values of annual ore production and lay within the range 0.46–1.32% U (average 0.67% U) during the period 1953–1965 (cumulative production 830 tU) and 0.178–0.76% U (average 0.39% U) for the period 1966–2000 (cumulative production 6650 tU) [47]. Contents of trace elements can exceed 100 ppm for As, Ba, Cu, Sb, Sr, V and Zn, and several thousand ppm for Mo, Pb, and Th [228].

Ludwig et al. [229] report well-defined U–Pb isotope ages of  $69.3 \pm 1.1$  Ma for a suite of ore samples from the Titan Vein, a structure in the horsetail section of the Schwartzwalder deposit. The U–Pb isochron intercepts suggest that mineral components derived from a source dated at 1900–1600 Ma, which is equivalent to the age of the metamorphic host rocks. Other geochronological data of the Schwartzwalder deposit and surrounding terrane include:

- (a) U–Pb ages of  $68 \pm 2$ , 61 and 52 Ma [230]. These ages are considered the most reasonable ages for pitchblende from above the 6th level;
- (b) Fission tracks: 68.9–59.4 Ma, average  $63.1 \pm 2.2$  Ma, on apatite from fresh and altered wall rocks adjacent to 9-1 vein [231, 232].

#### Metallogenetic aspects

The Schwartzwalder and similar uranium vein deposits in the east and central part of the Front Range apparently evolved by complex multiphase processes in a terrane characterized by the coincidence of favourable metallogenetic parameters and its geological history.

The Schwartzwalder uranium is classified as a vein type uranium deposit in metamorphic rocks (metamorphite). Mineralization exhibits two main controls: large tensional faults with associated horsetail fractures and an affinity to distinct lithologies [47].

Hypotheses for mineralization range from Proterozoic/Silver Plume time to Mesozoic/Laramide time. Genetic models include processes initiated by magmatic centres such as the Silver Plume or Laramide intrusives of the nearby Colorado Mineral Belt, to hypogene processes that generated convective cells leaching uranium and other metals from Proterozoic country rocks and to supergene processes active along the Phanerozoic unconformity and deriving uranium from red beds of the Pennsylvanian Fountain Formation or other sources [47].

Wallace [227] narrowed the conceivable processes of ore formation to convective hypogene fluids leaching ore elements from the surrounding Proterozoic rocks and depositing them in distinct structurally conducive rock units during early Laramide time. The basic assumptions for the uranium source, nature of fluids, precipitants, pressure–temperature and hydrodynamic conditions are

supported by numerous data [47]. The criteria and conclusions of Wallace [227] may be summarized as follows. Uranium and the other metals are believed to have been derived from the metamorphic host rocks. Whole rock uranium values in the abundant hornblende gneiss, which is thought to have originated from submarine volcanic flows and pyroclastic rocks interbedded with clastic and chemical sediments average 1–4 ppm U with maximum values of 52 ppm U. Garnet–biotite gneiss contains an average of 5–10 ppm U (maximum 88 ppm U), quartzite 1.7–27 ppm U and mica schist 2–6 ppm U. Wallace [227] favours the extensive hornblende gneiss unit as the most likely source of uranium.

Indirect evidence such as the isotopic composition and lack of known viable magmatic sources also support the assumption that vein hosting metavolcanic and metasedimentary rocks were the most likely source of uranium and other ore related metals [47].

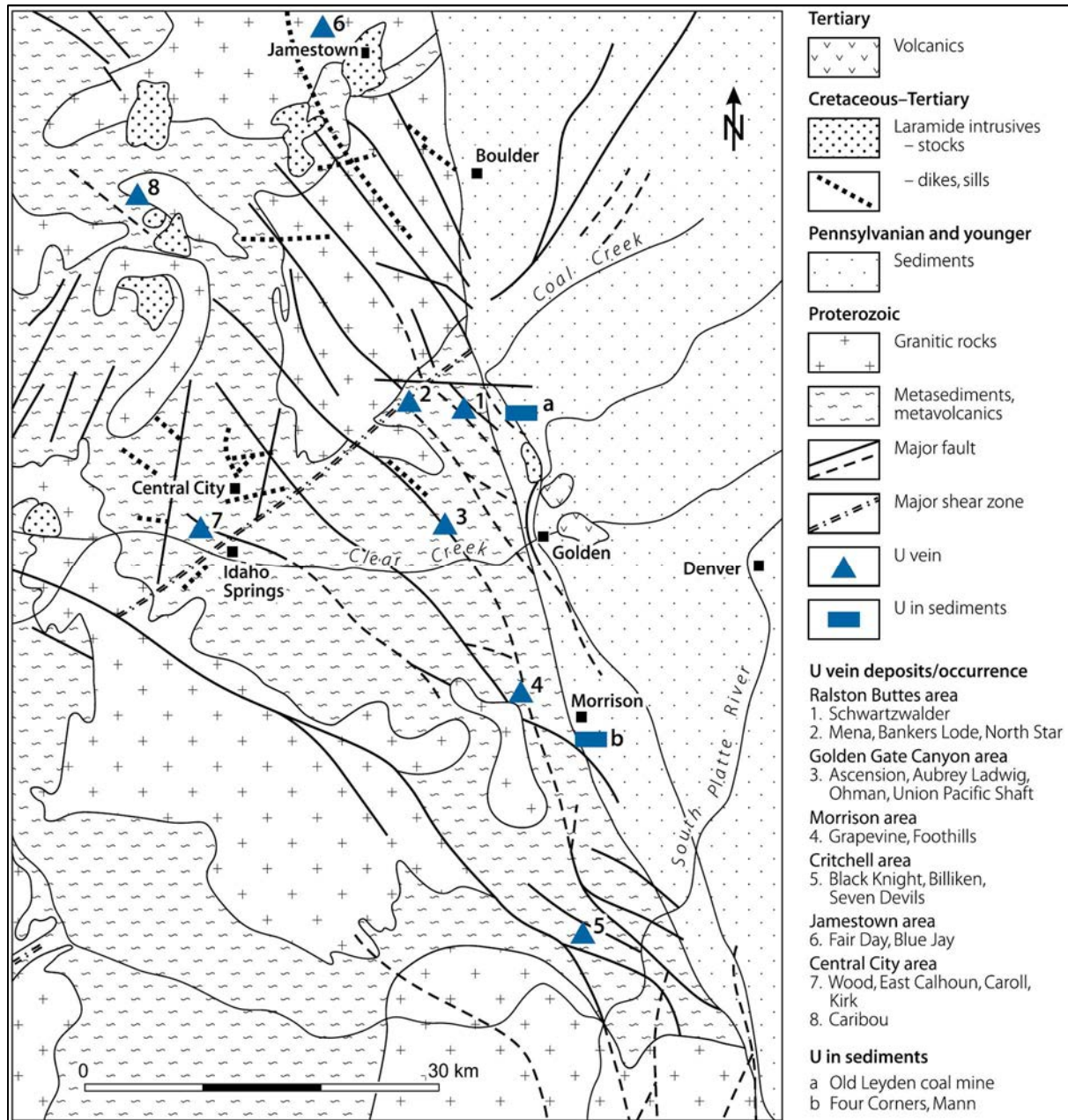


FIG. 96. Geological map of the east and central part of the Front Range showing the location of uranium deposits and major occurrences [47] (reproduced with permission).

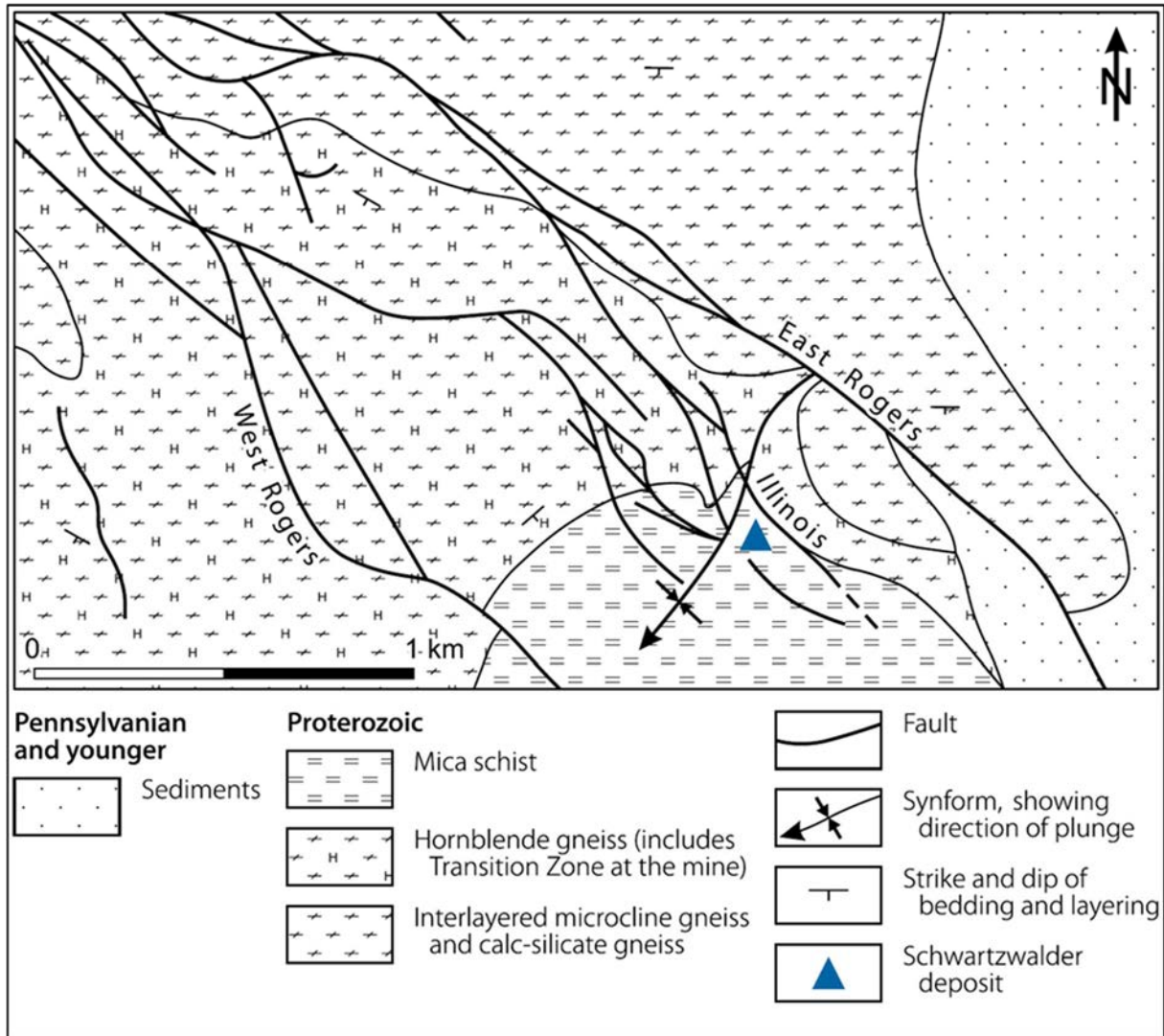


FIG. 97. General geological-structural map of the area surrounding the Schwartzwaldler mine [47] (reproduced with permission).

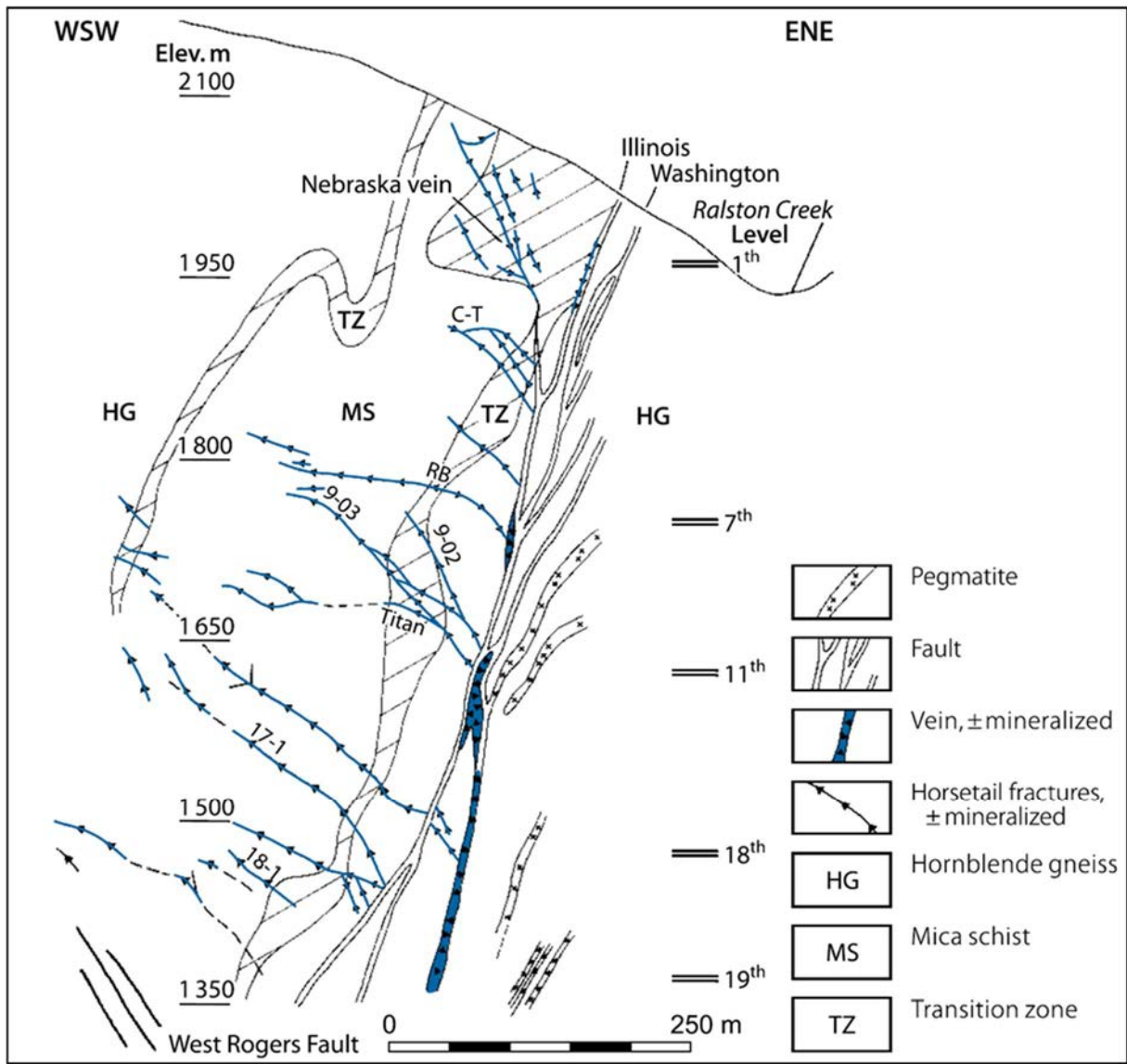


FIG. 98. Schwartzwalder mine: geological cross-section showing the principal veins, structures and horsetail fractures and their lithological position [47] (reproduced with permission).

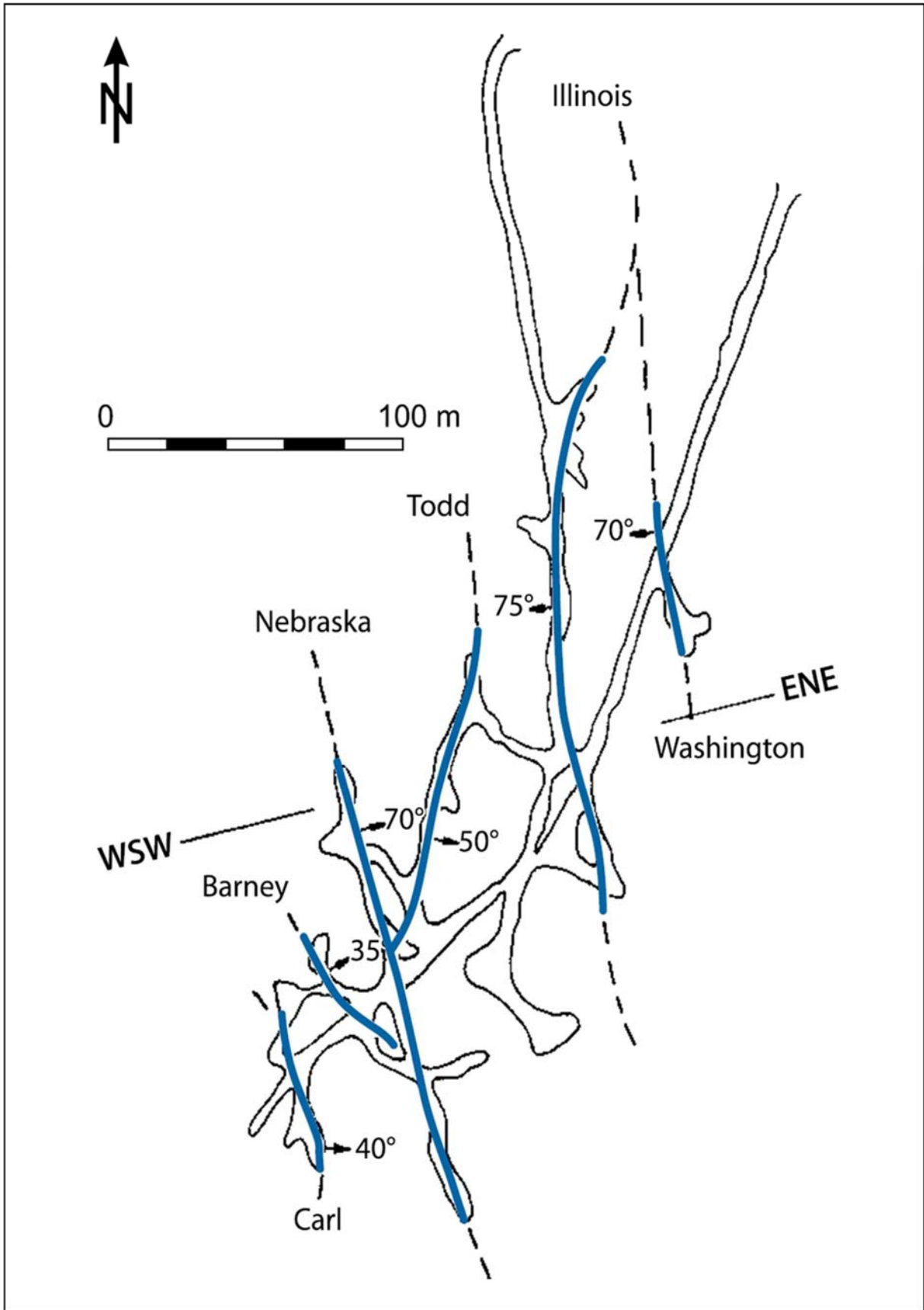


FIG. 99. Schwartzwaldler mine: plan view of the first level, showing the distribution of major veins and mine workings [47] (reproduced with permission).

### 3.6.4.5. The Itataia–Santa Quitéria deposit (Brazil)

#### Introduction

The phosphorous–uraniferous Itataia mineralization was discovered in 1976 by NUCLEBRAS. It is located in the central part of the Ceará State (north-eastern Brazil), 170 km south-west of Fortaleza, the capital, and 45 km south-east of Santa Quitéria (Fig. 100). More than 12 uranium–phosphate occurrences have been discovered in the area, including the largest one, Itataia, also known as Santa Quitéria. Itataia is a hydrothermal metasomatic Cambrian–Ordovician uraniferous apatite deposit, hosted by Precambrian metamorphic rocks. It is Brazil’s largest uranium resource with 121 800 tU at an average grade of 0.08% U, including smaller satellite deposits (Alcantil, Serotes Beixos), and is also the highest grade phosphate deposit. Phosphate resources exceed 14.5 Mt P<sub>2</sub>O<sub>5</sub> at a grade of 11% P<sub>2</sub>O<sub>5</sub>. The Th content of the phosphatic ore is 140 ppm.

Two major ore types have been identified: (i) massive collophanite and (ii) collophanite (cryptocrystalline hydroxyapatite) as veins and stockworks in marble, gneiss and syenite. Other uranium occurrences in the district are associated with feldspathic episyenite and are comparable with the Espinharas deposit, which is located about 500 km SE of Itataia in a similar geological environment [47].

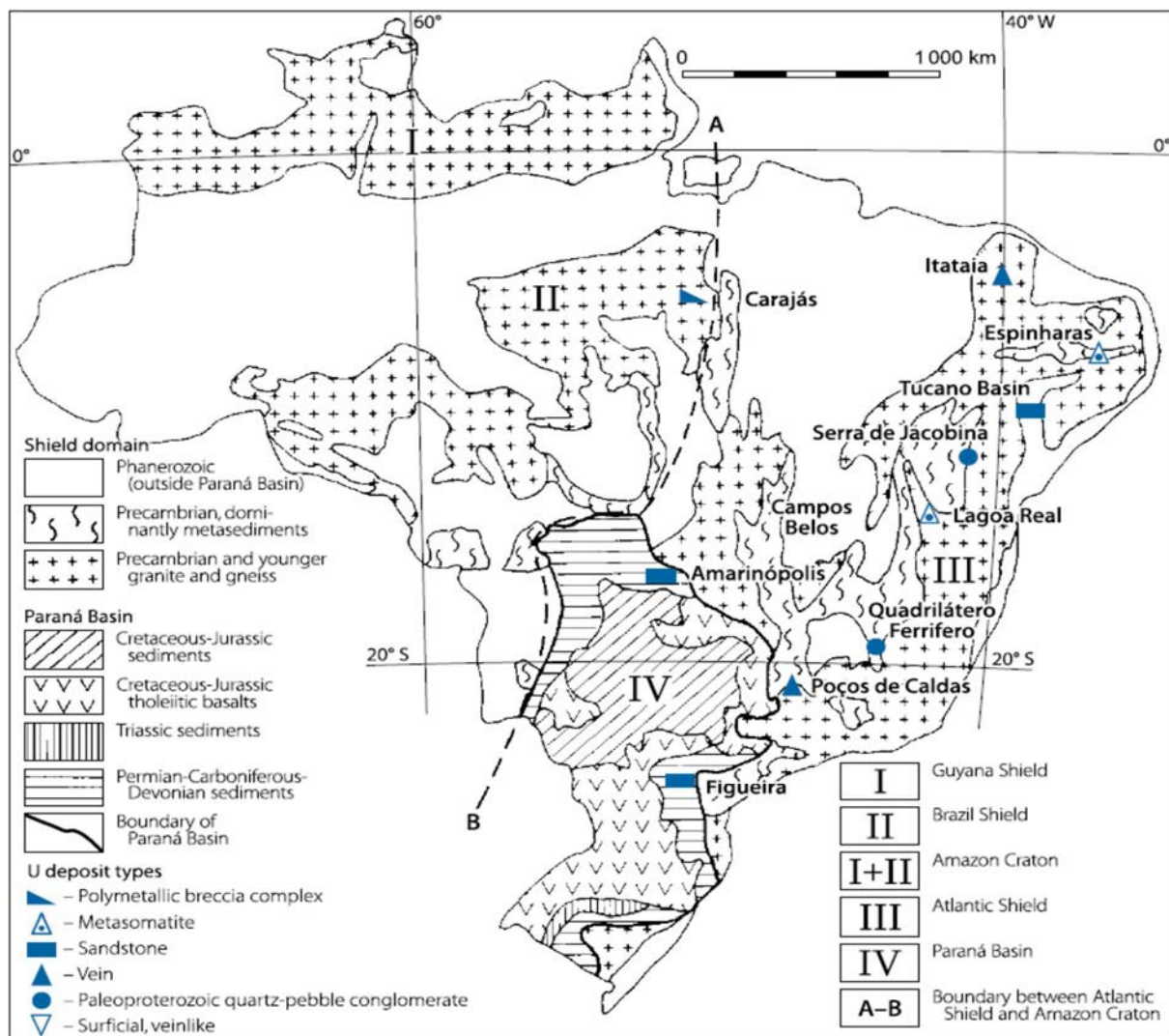


FIG. 100. Location of the P–U Itataia deposit (Brazil) [19] (reproduced with permission).

Itataia represents one of the world's largest concentrations of uranium associated with phosphatic rocks. Uranium production is dependent on phosphoric acid production. Since 2008, a partnership between State-owned *Indústrias Nucleares Brasileiras* and *Galvani Indústria, Comércio e Serviços Ltda* was established, aiming at the combined extraction of uranium and phosphate from an open pit. The plant will operate at full capacity after 3–4 years and is expected to produce 240 000 t of phosphate and up to 1500 tU annually [233].

Calcitic limestone may also be recovered as a by-product. Around 32 Mt are present in the main orebody, with another 46 Mt not related to the phosphate–uranium mineralization. Approximately 300 Mm<sup>3</sup> of marble with no detectable uranium could also be exploited.

### Geological setting

Two major geotectonic domains of the Precambrian Atlantic Shield dominate the central Ceará State, the Archaean Santa Quitéria–Tamboril Complex and the Palaeoproterozoic Jaguaribeana Fold Belt (Fig. 101). At least four orogenic/metamorphic events have affected the region at approximately 2500 Ma, 2000 Ma, 1300 Ma and 600 Ma.

The Itataia uranium mineralization was first detected by NUCLEBRAS and described by Mendonça et al. [234]. The authors defined a Precambrian transgressive metasedimentary sequence, with lower migmatite overlain by quartzite, gneiss and crystalline limestone, which comprises the Itataia Group. Formally, four formations were defined: (i) Serra do Céu Formation — migmatite, leptinite and gneiss, (ii) barren quartzite of the Laranjeiras Formation, while the two upper formations, (iii) Barrigas Formation — gneiss and migmatite and (iv) Alcantil Formation — marble and calc-silicate rocks, are mineralized.

Several generations of late to post-tectonic granite were emplaced during the Neoproterozoic Brazilian Orogeny. Autochthonous, synorogenic catazonal granite (650 Ma) of interpreted anatectic derivation is found in the older complexes. Late orogenic granites (550 Ma) are rare in the Itataia region. Post-orogenic, leucocratic, peraluminous granite intruded along dilational zones and boundaries between tectonic domains such as the Jaguaribeana Fold Belt and the Santa Quitéria Complex date to 510–450 Ma. These granites are present as stocks and apophyses with associated pegmatite dykes.

The Itataia Group is cut by large granitic and pegmatitic apophyses, episyenitized with dequartzification associated with Na-metasomatism. The entire assemblage (gneiss, marble and episyenite) was impregnated by uraniferous collophane, infilling voids and replacing marble and episyenite [235].

The mineralization is hosted by the calc-silicates and by saccharoidal marble. Gneiss and migmatite can host minor uranium mineralization.

### Mineralization

Two main ore types have been recognized: (i) massive, uniform collophane, and (ii) stockworks of collophane in marble, gneiss and episyenite. Collophane, a cryptocrystalline hydroxyapatite, is the principal uraniferous mineral and also the phosphate phase. No discrete uranium mineral has been detected to date. The massive collophane rock is referred to as a collophanite [236] and is the most important mineralization phase at Itataia.

Saad [237] defined collophanite as a reddish–brown rock with cream coloured and black patches, massive aphanitic to botryoidal texture, with small voids filled with ochre-yellow powder. It may form elongate orebodies, stockworks or fracture fill in marble. Other associated minerals are calcite, graphite and ankerite in marble, and albite, microcline, chlorite, zircon and calcite in episyenite. Table 20 presents the mineralogical composition of collophanite.

TABLE 20. MINERALOGICAL COMPOSITION OF THE COLLOPHANITIC ORE [238]

Mineral	Proportion (%)
Apatite	88.70
Quartz/chalcedony	5.32
Ore minerals	2.21
Limonite/goethite	1.88
Clay minerals/sericite	0.93
Muscovite	0.86
Titanite	0.26

Episyenite forms elongate bodies concordant to the fold axes in the metasedimentary rocks. The episyenite is a leucocratic, medium- to coarse-grained rock with breccia-like texture, essentially composed of albite and always mineralized with collophane. This phase is intergranular, filling up to centimetre size voids and forming massive veins. Despite sharp and well-defined contacts, the collophane mineralization post-dates the albite [239].

Netto [238] concludes that the episyenite results from Na-metasomatism of the gneiss, whereby Na-metasomatism is a consequence of tectono-magmatic reactivation of Precambrian terrains that leads to an environment favourable for the concentration of uranium.

The carbon-rich breccia is a dark grey (also termed ‘black ore’), aphanitic variety composed of apatite, clay minerals, calcite, chalcedony, zircon and organic matter. It contains cream coloured fragments, containing predominantly feldspar, but also graphite lamellae, sulphides and apatite without a defined shape, and is cut by carbonate veinlets [236].

The mineralization process is believed to be related to the Brazilian (Pan-African) Orogeny and linked to ring-like granitic intrusions of Itaperuaba type (550–450 Ma), which are also albitized and uranium enriched [240].

The Itataia deposit has a complex geometry but can be divided into two main orebodies (Figs 102 and 103). The main orebody has an ellipsoidal shape, extending 800 m in an E–W direction and 400 m in a N–S direction, crops out on the top of a hill, extends to 180 m depth and dips to the east. The second orebody is not very well defined. It occurs in the lowlands (around 100 m below the hilltop), extends 800–900 m in a NW direction, is 100–200 m deep and thins out to the N, NE and E [237].

The characterization of the mineralization of the Itataia deposit is based on the examination of 250 representative samples and classifies the deposit into three main ore types, whose mean chemical compositions are presented in Table 21:

- (i) Collophanite: comprising massive orebodies, tens of metres in size, associated with/or forming stockwork fillings in fractures in marble;
- (ii) Episyenite: disseminated collophane and/or apatite which may also occur in calc-silicate rocks, marble and gneiss;
- (iii) Dark carbonaceous and zirconium-rich material, cementing breccia where the fragments are mostly feldspathic, although graphite, sulphides, collophane and apatite are also frequent [240].

TABLE 21. MEAN CHEMICAL COMPOSITION OF THE THREE ORE TYPES (wt%) [238]

	Collophanite	Breccia	Episyenite
SiO <sub>2</sub>	15.67	32.09	38.69
TiO <sub>2</sub>	0.09	0.33	0.23
Al <sub>2</sub> O <sub>3</sub>	3.43	8.22	33.00
MgO	1.59	1.62	1.43
FeO	0.62	0.89	1.18
Fe <sub>2</sub> O <sub>3</sub>	3.68	4.58	1.71
CaO	37.28	21.48	11.83
Na <sub>2</sub> O	0.69	1.28	6.30
K <sub>2</sub> O	0.11	0.19	0.62
P <sub>2</sub> O <sub>5</sub>	26.35	11.23	7.05
S	0.14	0.42	0.08
C	1.19	4.44	0.79
U <sub>3</sub> O <sub>8</sub> (ppm)	1 890	6 310	940
Th <sub>2</sub> O (ppm)	160	650	100
Cl (ppm)	103	106	129
F (ppm)	11 713	6 294	3 577
Zr (ppm)	1 205	10 394	674
Y (ppm)	315	619	91
Yb (ppm)	49	74	19
Sc (ppm)	12	38	21

### Metallogenic aspects

Itataia is an epigenetic, structurally controlled deposit with a uraniferous phosphate ore unique in both type and metallogenesis. The principal ore controlling or recognition criteria of the deposit include [47]:

- (a) Association with highly uraniferous (average 26 ppm U), peraluminous granite of post-orogenic, final Brazilian origin;
- (b) Proximity to lineaments;
- (c) Position along a reverse fault with a wide cataclastic aureole;
- (d) Principal host rock is cataclastic marble and calc-silicate rock along with subordinate episyenite and gneiss;
- (e) Strong deuteric and retrograde metamorphic alteration of host rocks, including episyenitization of granite;
- (f) Ore consists almost exclusively of uraniferous collophane which, together with gangue minerals, form collophanite;
- (g) Collophanite occurs in massive concentrations in veins and veinlets, which aggregate as stockworks;
- (h) Massive collophanite extends from the current surface to a depth of 150 m or more;
- (i) Disseminated mineralization persists to a depth in excess of 300 m.

Angeiras et al. [241] propose a metallogenic model which includes four stages of development:

- (i) Intrusion of post-orogenic peraluminous uraniferous granite in dilation zones along lineaments during the waning stages of the Brazilian Orogeny. The intrusion probably inflicted intense hydraulic fracturing on the country rocks. In the Itataia area, the granite occurs as apophyses and dome shaped stocks. A larger body is believed to exist at depth, below the Itataia–Santa Quitéria deposits;
- (ii) Late magmatic–deuteric processes imposed feldspar episyenitization on granite and Na-metasomatism associated with greenschist facies retrograde alteration of all host rocks. Introduction of Na and remobilization of P, U and other elements was facilitated by the circulation of geochemically complex fluids, as deduced from minerals with P, U, Na, Zr and Ti [239]. Crystallization of analcime during the final phases indicates final temperatures of about 250–200°C. This step led to a preconcentration of U and P within episyenite to grades averaging 800 ppm U and 11% P. These elements form uraniferous apatite;
- (iii) Local scale cataclasis and brecciation of the host rocks created open spaces for later mineral emplacement. It is not known if this deformation resulted from normal tectonic displacement or in response to karst development and subsequent collapse of karst structures, as may be speculated from the size and configuration of large ore shoots developed essentially in marble;
- (iv) Precipitation of uraniferous collophane associated with calcite, ankerite and quartz, which partly crystallized in pores within collophanite, and of apatite crystals in voids within episyenite. Most intense collophane precipitation, however, happened at lower temperatures of 50–130°C, by void filling and replacement of marble and episyenite.

The most probable source of the uranium was the fertile post-orogenic granites emplaced along dilation zones coincident with earlier large regional faults, which caused intense hydraulic fracturing. The origin of phosphorous is still enigmatic. It is assumed that uranium may have been transported as chloride complexes since the mineralizing solutions were rich in chlorine. The provenance of chlorine is unknown.

In summary, the mineralization at Itataia is related to a significant metallogenic event at the end of the Brazilian Orogeny. Mineralization is believed to have formed by post-magmatic fluid circulation triggered by cooling of a deep seated granitic pluton. Ore forming fluids may have been of supergene or hypogene origin, or a mixture of the two. Mineral deposition took place in pulses, as inferred from the zoning of apatite and collophane crystals [47].

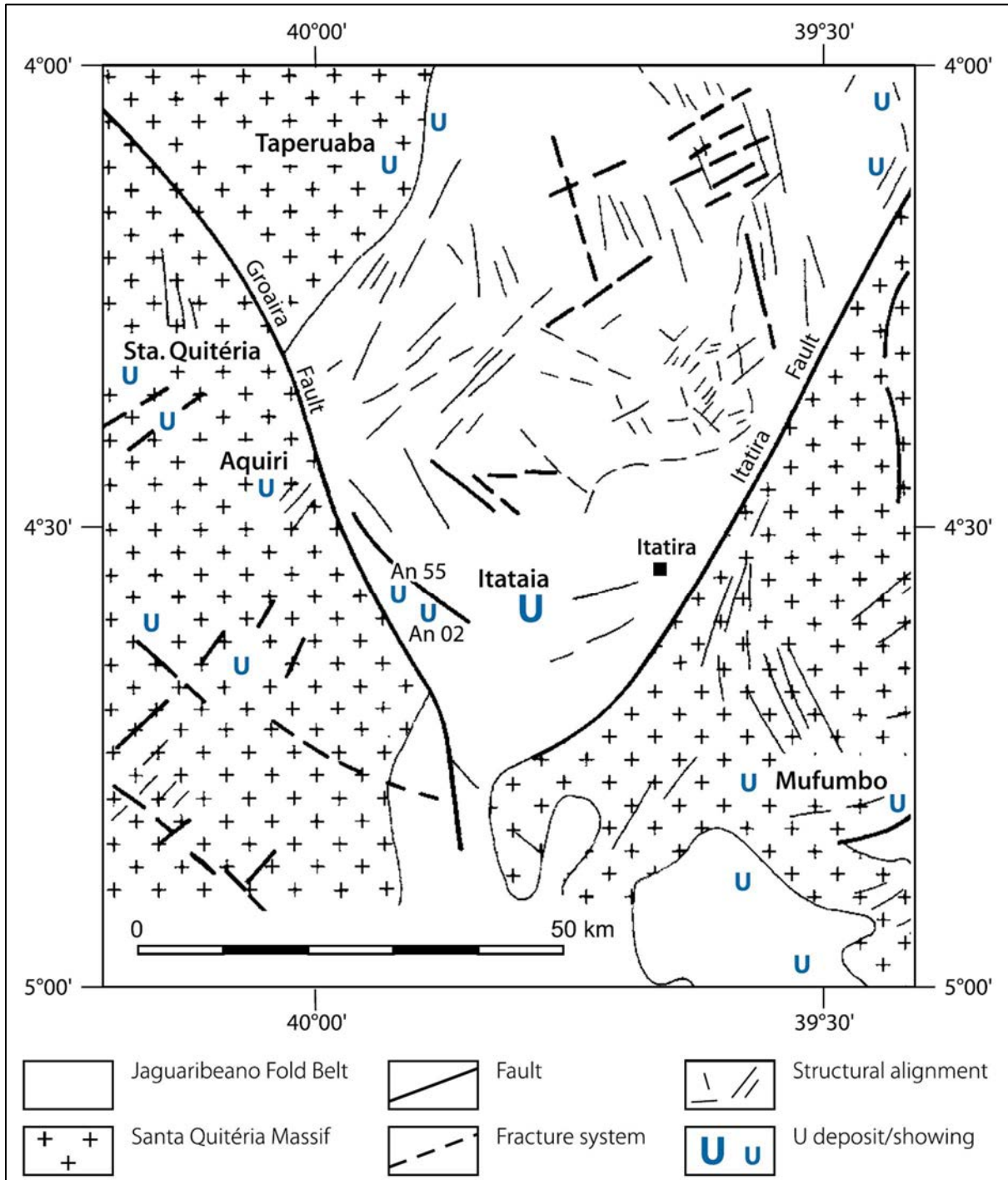


FIG. 101. Generalized geological map of the Central Ceará region showing the location of the Itataia–Santa Quitéria deposit [47] (reproduced with permission).

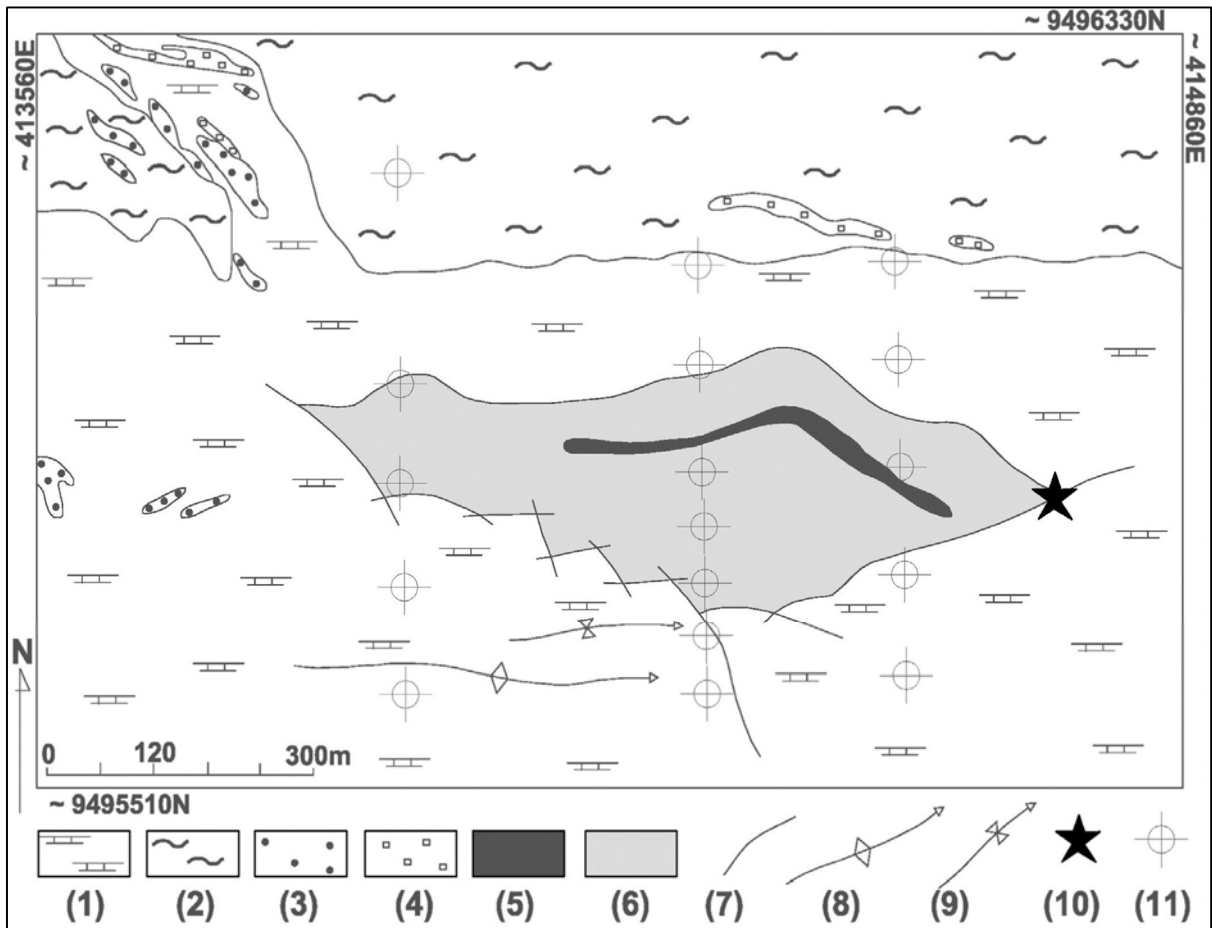


FIG. 102. Principal geological features of the Itataia uranium deposit area: (1) phlogopite–diopside calc-silicate rocks and marbles, (2) garnet–sillimanite metapelites, (3) uraniferous collophanite veins, (4) quartz feldspathic rocks, void-filling mineralization, (5) massive uraniferous collophanite, (6) stockwork and disseminated uraniferous collophanite in marble and calc-silicate, (7) contacts and faults, (8) antiform, (9) synform, (10) location of sample NCC-99, (11) site of drilling [47] (reproduced with permission).

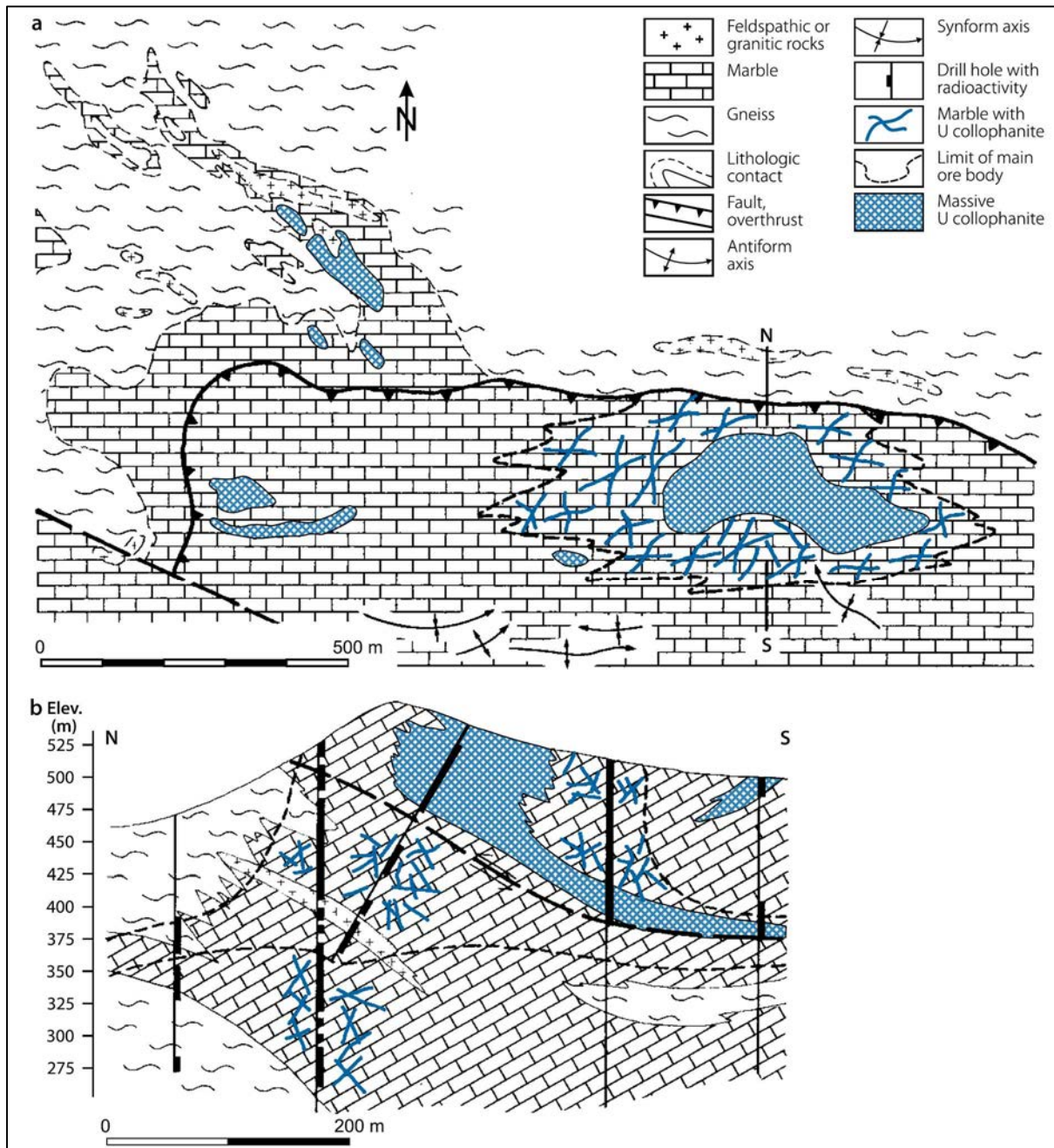


FIG. 103. Itataia–Santa Quitéria deposit: (a) geological map with distribution of uraniferous collophanite lodes, (b) geological N–S section across the main uranium orebody [47] (reproduced with permission).

### 3.7. PROTEROZOIC UNCONFORMITY DEPOSITS

#### 3.7.1. Definition

Uranium deposits associated with Proterozoic unconformities consist of massive pods, veins and/or disseminations of uraninite spatially associated with major erosional unconformities that separate Archaean–Palaeoproterozoic metamorphic basement from overlying Palaeoproterozoic–Mesoproterozoic siliciclastic basins. These represent world class deposits with a 2015 production of

15 020 tU (25% of world production) from four deposits, Ranger (1700 tU) in Australia, and McArthur River (7354 tU), Eagle Point (1621 tU) and Cigar Lake (4345 tU) in Canada. Their resources (RAR + IR) were estimated in 2014 at 663 900 tU (12% world resources) at a cost of less than US \$130/kg U [5].

As of 2015, 103 deposits associated with a Proterozoic unconformity were listed in the UDEPO database. These are located in Canada (63), Australia (35), India (4) and the Russian Federation (1). Two major provinces can be distinguished: the Athabasca Basin in Canada with geological resources of 1 027 000 tU and the Pine Creek Orogen in northern Australia with geological resources of 460 000 tU (Table 22).

TABLE 22. PRINCIPAL PROTEROZOIC UNCONFORMITY DEPOSITS (*as of 31 December 2015*)

Deposit	Country	Resources (tU)	Grade (% U)	Status
McArthur River	Canada	261 000	19.50	Operating
Ranger 3	Australia	179 790	0.084	Depleted
Cigar Lake	Canada	135 040	16.59	Operating
Jabiluka 2	Australia	120 500	0.46	Dormant
Arrow	Canada	77 457	2.229	Exploration
Key Lake	Canada	69 800	2.60	Depleted
Ranger 1	Australia	48 700	0.35	Depleted
Triple R	Canada	40 611	1.28	Exploration
Millenium	Canada	40 310	3.19	Exploration
Eagle Point	Canada	36 720	1.17	Operating
Kintyre	Australia	30 530	0.127	Dormant
Ranger 3 Deeps	Australia	37 200	0.19	Dormant
Phoenix	Canada	27 450	4.54	Exploration
Andrew Lake	Canada	22 755	0.377	Dormant
Roughrider	Canada	22 300	4.01	Exploration
Rabbit Lake	Canada	21 000	0.23	Depleted
McClellan Lake	Canada	17 500	4.14	Dormant
Kiggavik	Canada	15 560	0.27	Dormant
Kianna	Canada	15 340	1.20	Dormant
Midwest	Canada	13 850	3.83	Dormant

The Proterozoic unconformity deposits include three subtypes of variable importance (Fig. 104):

- (i) **Unconformity-contact deposits.** Except for the low grade Karku deposit (Russian Federation), these all occur in the Athabasca Basin (Canada). Deposits are situated at the base of the sedimentary cover, directly above the unconformity. They form elongate pods to flattened linear orebodies typically characterized by a high grade core surrounded by a lower grade halo. Most of the orebodies have root-like extensions into the basement. While some mineralization is open space infill, much of it is replacement style. Mineralization also often extends up to several tens of centimetres into the overlying sandstone cover along breccias

and fault zones, forming so-called ‘perched mineralization’. Deposits can be monometallic (McArthur River) or polymetallic (Cigar Lake). Deposits are medium to large or very large (1000–200 000 tU) and are characterized by their high grades (1–20% U);

- (ii) **Basement-hosted deposits.** Deposits are both stratabound and structure-bound in metasedimentary rocks below the unconformity on which the basal clastic sediments rest. The basement ore typically occupies moderate to steeply dipping brittle shear fractures and breccia zones for hundreds of metres along strike length and extends down-dip for several tens of metres to more than 1000 m below the unconformity, as with the Jabiluka deposit (Australia). Disseminated and vein uraninite–pitchblende occupies fractures and breccia matrix but may also replace the host rock. High grade ore is associated with brecciated graphitic schist. These deposits have small to very large resources (300–200 000 tU) at medium grade (0.10–0.50% U), although some deposits (Millennium and Nabarlek) may have grades of several per cent. Examples of basement-hosted deposits include Kintyre, Jabiluka and Ranger (Australia), Millennium and Eagle Point in the Athabasca Basin and Kiggavik and Andrew Lake in the Thelon Basin (Canada). Two large basement-hosted deposits were recently discovered in the western part of the Athabasca Basin: Arrow (77 457 tU) and Triple R (40 611 tU). Except for some mineralization of the recently discovered Angularli deposit in Arnhem Land [242], all of the Australian unconformity deposits are basement-hosted;
- (iii) **Stratiform structure-controlled deposits.** In India, a special class of uranium deposit, referred to as ‘unconformity proximal deposits’ by Indian geologists (herein termed stratiform structure-controlled), have been identified in the Cuddapah Basin [243]. These consist of flat ore lenses that occur along structures parallel to the unconformity that separates Archaean K–U–Th enriched granites from the Mesoproterozoic metamorphic Srisaïlam Formation. Resources are estimated at 15 000–20 000 tU at grades ranging between 0.04 and 0.10% U. Resources of individual deposits such as Chitrial and Lambapur are in the range 1000–8000 tU.

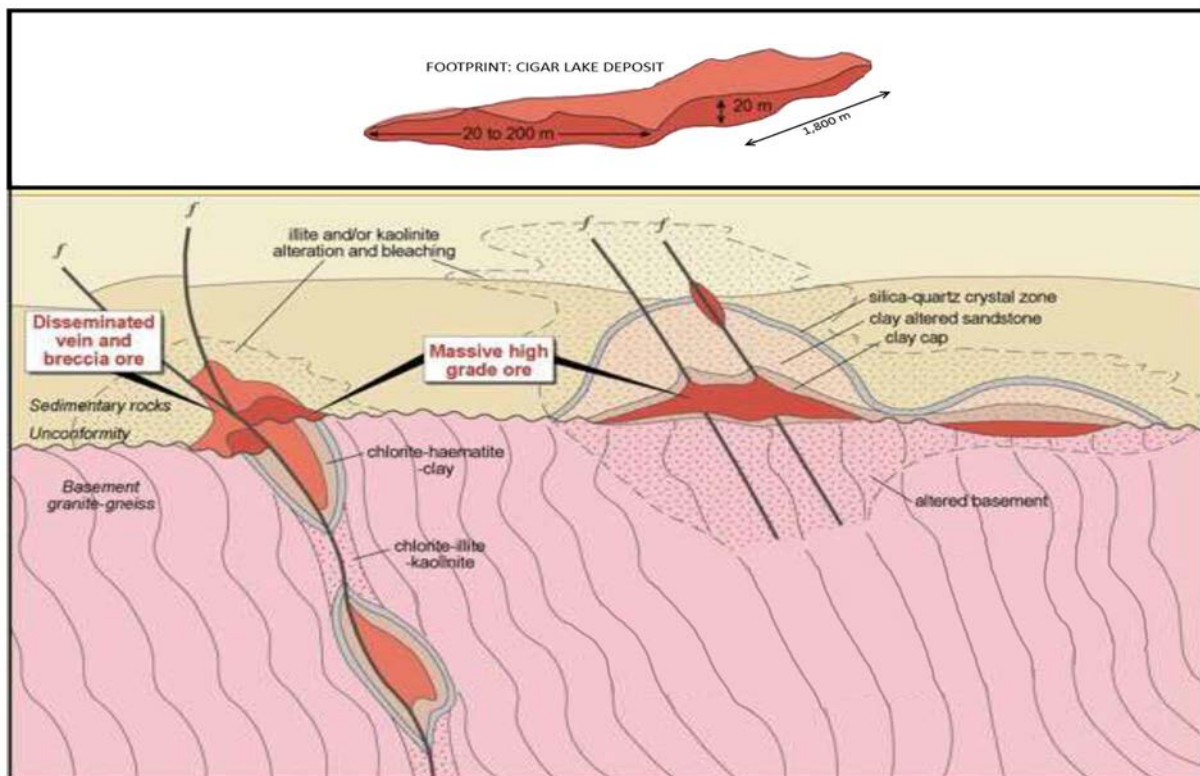


FIG. 104. Schematic representation of the Proterozoic unconformity deposits with the three subtypes: basement-hosted, unconformity-contact and stratiform structure-controlled (adapted from Ref. [244]).

### 3.7.2. Geological setting

Although Proterozoic unconformity-related deposits are geologically diverse in their details, they share some unifying characteristics. In Australia, the basement rocks are Palaeoproterozoic metasedimentary rocks mantling Archaean K–U–Th enriched granitoid gneiss domes. The overlying sandstone of the Kombolgie Subgroup in the Alligator Rivers region consists of a thick sequence (1–2 km) of flat lying clastic basin filling sediments that were deposited in fluvial, aeolian and marine settings. They are of Late Palaeoproterozoic age, as indicated by radiometric ages of the underlying Plum Tree Creek volcanics at 1822 Ma and intrusion of the Jimbu microgranite and of the Oenpelli dolerite at 1720 Ma [245]. In the Rudall region of Western Australia, where the Kintyre deposit is located, these sediments (Coolbro Sandstone of the Throssell Group) are Meso- and Neoproterozoic and have been folded.

In Canada, graphitic pelite, which is stratigraphically low in the metasedimentary sequences of the western Wollaston and eastern Mudjatik basement domains, unconformably overlies older tonalitic granitoid gneiss. Many significant deposits are located at the metamorphosed contact between Archaean granitoid gneiss and graphitic metapelites. These graphitic units are less competent than proximal quartz-rich lithologies and so were more strongly affected by regional deformation.

The overlying Athabasca Basin is interpreted as an intracontinental basin, although it is capped by marine sandstone and carbonate units. The Athabasca Group makes up the sedimentary basin fill and consists of flat lying, quartz-rich sandstone and conglomerates that are interpreted to have been deposited in major river systems and in near-shore to shallow marine shelf environments [246]. The sedimentary fill in the basin is currently 1–2 km thick. Temperature estimates derived from fluid inclusions, however, indicate that the sedimentary sequence reached a thickness of ~5 km during peak diagenesis [247]. Deposition of the Athabasca Group commenced before 1644 Ma, constrained by the age of tuffaceous beds in the Wolverine Point Formation [248]. Rainbird et al. [248] estimate that sedimentation began around 1740–1730 Ma, which is based on the metamorphic ages of titanites as young as 1750 Ma in the basement rocks. Similarly, basal units of the Thelon Basin have a maximum age of 1750–1720 Ma [249].

The style of high grade unconformity-related deposits at the unconformity, as seen at McArthur River and Cigar Lake, has not been found to date in the Pine Creek Inlier in northern Australia. Most Australian unconformity-related uranium deposits in the Alligator Rivers, Rum Jungle and South Alligator Valley fields are stratabound and are hosted by breccia zones, faults and shear zones.

The high to very high grade deposits (5–15% U) occur in clay altered sandstone immediately above the unconformity (Cigar Lake) and span the faulted unconformity (McArthur River). Mineralization commonly extends into the altered basement rocks and can be either monometallic (uranium) or polymetallic (U+Ni+Co+As+Mo+Pb and/or traces of Au–Pt–Pd). Bitumen and radioactive bitumen (thucholite) often occurs in the mineralized zones.

Deposits immediately below the unconformity are usually medium to high grade (0.3–2.0% U) and are predominantly monometallic (Eagle Point, Millennium and Jabiluka). The uranium mineralization occurs in faults and fracture zones in altered metasedimentary rocks that contain graphite.

The host rocks are pelitic, arkosic, calc-silicate and carbonate-bearing sediments that have been metamorphosed to amphibolite facies in the Athabasca Basin and in the Alligator Rivers Uranium Field, but only to greenschist grade at Rum Jungle and the South Alligator Valley Uranium Field. Retrograde metamorphism (greenschist facies) overprints many of these host rocks. Palaeoweathering of the crystalline basement rocks is recorded in the basement of the Athabasca Basin. Similarly, in the Alligator Rivers region, a regionally extensive palaeo-saprolitic profile, commonly more than 50 m thick, is observed in the basement.

Intense alteration of the host rocks (mainly chloritic, but also sericitic, argillic and carbonate alteration) surrounds the mineralization. Some of these deposits (Jabiluka, Koongarra and Ranger) contain gold mineralization and minor Pt–Pd mineralization. Some smaller deposits are polymetallic, such as those in Rum Jungle which contain Cu, Pb, Co and Ni.

Uranium–lead geochronological studies on pitchblende have indicated an age of 1737 Ma for mineralization at Ranger [250]. Recent geochronology for the Jabiluka deposit shows that massive uraninite first precipitated at about 1680 Ma [251]. The Sm–Nd ages for mineralization at the Nabarlek and Koongarra deposits lie in the range 1600–1650 Ma [252]. Recent regional mapping and geochronological studies have dated the Kombolgie Subgroup to 1822–1720 Ma, bracketing it with the U–Pb age of the pitchblende at Ranger and the intrusion of the Jimbu Microgranite (1720 Ma). The main mineralization at Jabiluka, Koongarra and Nabarlek formed after deposition of the Kombolgie Subgroup.

Athabasca Basin uranium deposits record one or two main hydrothermal ore related events around 1550–1500 Ma and 1350–1300 Ma that were overprinted by further alteration and uranium remobilization events dated at approximately 1200–1150 Ma, 900 Ma and 300–200 Ma [253].

### 3.7.3. Metallogenesis

Conventional models for unconformity-associated uranium deposits invoke high grade diagenetic to hydrothermal processes. There is sufficient diversity in unconformity associated deposit characteristics to require multiple variants or end-members of a main model [254]. These models propose that oxidizing, uranium transporting basinal fluids, heated by a high geothermal gradient, attained 200°C (at a depth of 5–6 km) at the unconformity and reacted with basement graphite causing uranium precipitation due to the mixing of reduced and oxidized fluids [255–261]. Precipitation was primarily focused by structural and physicochemical traps [256] that operated at fixed locations over very long periods of time [257], possibly of the order of hundreds of millions of years. Zones of fluid mixing are characterized by alteration haloes that contain illite, kaolinite, dravite, chlorite, euhedral quartz and, locally, Ni–Co–As–Cu sulphides.

Deposits formed after the deposition of at least the basal sandstone formations as the uranium and alteration minerals are found throughout the local stratigraphic columns.

The fragmentation of the supercontinent Columbia, associated with the development of anorogenic magmatism and continental rifting, which began at 1.6 Ga and continued until its final break-up at about 1.2 Ga, represents a major geodynamic event that may have been responsible for a critical change in the fluid regime operating in the Athabasca Basin and linked to the formation of uranium mineralization [262].

In Canada, fluid circulation associated with the intrusion of later Mackenzie dykes (1267 Ma) [262] caused the partial recrystallization of uraninite. Stable isotope compositions of the alteration minerals (illite, chlorite and kaolinite) in conjunction with their paragenesis indicate that oxidized basinal fluids were derived primarily from evolved seawater and leached uranium from the overlying sandstones of the Athabasca Formation and transported it into the basement via infiltration along fracture zones associated with reverse faults. Graphitic units in the basement and pre-ore alteration served as physical (fractured zones) and chemical (reductant) traps for the uranium mineralization.

The various conventional models all attempt to account for the combined efficiency of source, transport and deposition of uranium, as summarized by Cuney et al. [263]. There are two main sources proposed for the uranium: the basement rocks and the sandstone. These have been summarized by Jefferson et al. [253]. Primary sources in the basement include radiogenic S-type granites and pegmatites, metasedimentary domains with abundant pelite, the uranium content of which is well above Clarke values, pegmatites and previous uranium enrichments. Regions relatively well endowed with uranium, such as the Wollaston and Mudjatik Domains of the Trans-Hudson Orogen in Canada

and the Pine Creek Geosyncline in Australia, have a much better chance of generating world class deposits given favourable subsequent conditions. Intermediate stage reservoirs of uranium were the fluids and the sediments derived from the sources already noted. The shortcoming of this model, however, is that there is a lack of evidence for large scale oxidized fluid interaction with these uraniferous basement rocks, which would be required to leach the uranium at the relatively low temperatures of deposit formation. In addition, the mechanism for precipitation of basement derived uranium at the unconformity, with its higher oxidation state (higher uranium solubility), is problematic.

A number of workers have proposed that the basin sediments were the main source of the uranium. Opponents of this theory reject the basin filling strata as a significant source of uranium, noting that minerals capable of yielding uranium are absent and that the nearby, unaltered basement uranium contents are much higher. However, as summarized by Jefferson et al. [253], the proponents of this model posit that uranium was derived from detrital heavy minerals in the sandstone, mainly monazite, which is highly metamict. Mass balance calculations indicate that with typical uranium contents of monazite, the monazite content of the Athabasca Group, and estimates of the sandstone volume, such a leaching model could theoretically account for the uranium discovered in the Athabasca Basin. However, given the great uncertainties with regard to the efficiency of the precipitation process, the extent of closed system behaviour (i.e. what proportion of the uranium leached from the basin would remain in the basin) and the unknown total amount of uranium present, such theoretical calculations are far from proof.

### **3.7.4. Description of selected deposits**

#### *3.7.4.1. Basement-hosted deposits*

#### **The Ranger deposits (Australia)**

##### Introduction

The Ranger uranium deposits (Ranger 1 No. 1 and Ranger 1 No. 3) are located in the Northern Territory of Australia, about 250 km east of Darwin. The mine lies within the Alligator Rivers Uranium Field, close to the boundary between the Kakadu National Park and the Arnhem Land Aboriginal Reserve. Energy Resources Australia Ltd, which is majority owned by Rio Tinto Ltd, operates the Ranger deposits as open pit mines.

The Ranger deposits were discovered in 1969 by an airborne survey. The mine commenced operation in 1980 and since then about 107 000 tU at an average grade of 0.26% U were produced. Production in 2015 was 1700 tU. Open pit mining started with orebody No. 1, which was depleted in 1994 after having produced 51 660 tU at a grade of 0.29% U. Excavation of the nearby orebody No. 3 started in 1997 and was depleted in 2015. The life of the Ranger plant was extended to 2020 enabling treatment of large stockpiles of lower grade ore. In 2009, Energy Resources of Australia announced the discovery of Ranger No. 3 Deeps with resources of 37 200 tU at a grade of 0.19% U. Construction of a decline to explore the deposit, which is situated between 250 and 550 m below the surface was approved in 2011 and started in 2013. Owing to the low price of uranium, the project was suspended in 2015. In total, resources for the Ranger deposits are in the order of 260 000 tU.

##### Geological setting

##### *Regional geology*

The Ranger deposits are located in the north-east section of the Pine Creek Orogen, which is a Palaeoproterozoic inlier covering an area of 66 000 km<sup>2</sup>. The Pine Creek Orogen is dominated by a succession comprising carbonates and carbonaceous, clastic and volcanogenic sedimentary rocks

deposited on Neoproterozoic crystalline basement. These formations have been regionally metamorphosed, deformed and intruded by syn- to post-tectonic granitic rocks and mafic bodies.

The Alligator Rivers Uranium Field is characterized by inliers of the Archaean Nanambu Complex and is surrounded by highly deformed sedimentary rocks of the Kakadu Group, Cahill Formation and Nourlangie Schist, which have been metamorphosed to middle–upper amphibolite facies (Fig. 105). Rocks of the Nanambu Complex are predominantly granite or granitic gneiss with minor amphibolite. Uranium–lead dating of zircon and whole rock Rb–Sr dating produced an age of  $2470 \pm 50$  Ma for the Nanambu Granite [264]. The north-eastern section of the Alligator Rivers Uranium Field contains a mixture of deformed high grade metasedimentary rocks known as the Myra Falls Metamorphics and syntectonic granitic gneiss of the Nimbuwah Complex, intruded during the period 1840–1820 Ma by post-tectonic granitoids, including the Jim Jim and Nabarlek Granites [265].

Metaquartzite and arkose of the Kakadu Group are presumed to have unconformably overlain the Nanambu Complex, but deformation and metamorphism has resulted in partial assimilation into the granitoid gneiss. The Cahill Formation conformably overlies the Kakadu Group or has a tectonized contact with the Nanambu Complex. The Cahill Formation and the Myra Falls Metamorphics host all the known uranium deposits and prospects of the Alligator Rivers Uranium Field.

The Nanambu Complex and the metasedimentary rocks were uplifted and eroded before deposition of the thick Katherine River Group Mesoproterozoic sandstone and intercalated mafic volcanic rocks. A 20–60 m thick palaeoweathering profile (regolith) is preserved immediately below the unconformity with the sedimentary cover. The regolith has an upper portion of strong red haematitic alteration that grades downward through greenish chloritic alteration into fresh basement rocks.

Overlying the steeply dipping Palaeoproterozoic metasedimentary basement is the flat lying Kombolgie Subgroup, part of the Katherine River Group. The Kombolgie Subgroup consists of sandstone and conglomerate interlayered with two volcanic units: the Nungbagarri Formation and the Gilruth Member. The Subgroup is predominantly composed of sandstone and arkose that were deposited in fluvial and aeolian environments with occasional marine incursions that deposited marine sandstone and evaporite. The lowermost unit of the Kombolgie Subgroup, the Mamadawere Sandstone, is composed of coarse-grained sandstone and conglomerate with abundant trough cross-bedding. This lower stratigraphic unit is interpreted to represent deposition in high energy braided river systems.

Uranium–lead ages of zircons of the volcanic strata at the top of the Katherine River Group indicate a minimum age of 1712–1705 Ma [250]. Volcanic rocks of the Edith River Group, below the unconformity, give a maximum age of deposition of 1822 Ma. Correlations between the Kombolgie Basin and the McArthur–Mt Isa Basins suggest that the Kombolgie Basin began to form at about 1793 Ma [266, 267]. Large sills and dykes of dolerite (Oenpelli Dolerite) intruded the metamorphic basement and the Kombolgie Subgroup at 1725–1720 Ma [268].

### *Local geology*

The Ranger deposits are hosted in the lower member of the Cahill Formation, close to the contact with the underlying Nanambu Complex (Fig. 106). Lithologies within the mine area have been informally subdivided by the local geologists into the Footwall Sequence, the Lower Mine Sequence (LMS), the Upper Mine Sequence (UMS) and the Hangingwall Sequence (Fig. 107). The oldest, the Footwall Sequence, is part of the Archaean basement of the Nanambu Complex and is composed of schist, gneiss and granite. It is exposed in No. 1 pit (Fig. 108). The LMS (300 m) consists of thick carbonate units interbedded with schist (Lenticular Schist) and chert. The UMS (500 m) comprises quartz–feldspar–biotite schist and microgneiss with sparse carbonate beds. The sequence contains numerous faults and thrusts. The Hangingwall Sequence comprises micaceous quartz–feldspar schists intercalated with amphibolite units (Zamu Dolerite). Layering dips 15–40° to the east and there is a strong schistosity subparallel to the bedding that corresponds with the regional S2 foliation. Quartz–

feldspar–tourmaline pegmatite bodies cross-cut the foliation of the metamorphic rocks but predate the mineralization. One of the intrusions has been dated at  $1847 \pm 1$  Ma [269]. Dolerite dykes and veins have also intruded the metamorphic basement and are interpreted as having the same age as the Oenpelli Dolerite ( $\sim 1720$  Ma).

The geological interpretation described by Hein [270] for the Ranger deposits is markedly different from that of previous studies. The most important differences are:

- (a) The Lenticular Schist and other schist layers, interpreted as discrete stratigraphic units, are fault rocks produced by shearing.
- (b) The contact between the granitic gneiss sequence (Footwall Sequence) and overlying sequences is an unconformity that trends NNE–NNW. The unconformity is locally sheared and faulted.
- (c) A metavolcanic sequence is recognized in the place of the lower carbonate unit of the LMS. This sequence has a distinct volcanic facies consisting of basalt, hyaloclastite and autobreccia. It is generally chloritized, kaolinized adjacent to faults and shears, and locally carbonate altered and ferruginized.
- (d) The breccia types described by various authors can be divided into two groups: (i) volcanic breccias including hyaloclastite and autobreccia, confined to the metavolcanic sequence and (ii) tectonic breccias, B<sub>2</sub> and B<sub>4</sub>, associated with failure of the hangingwall–footwall rocks adjacent to shears and thrusts in D<sub>2</sub> and normal faults in D<sub>4</sub>.
- (e) A set of previously unreported granitic dykes cross-cuts the sequences of the No. 1 open pit.
- (f) Pegmatite veins form a conjugate set in contrast to the previous interpretation of four categories. It is believed that they formed during a period of E–W compression similar to that of D<sub>2</sub>.

The deformation history of the rocks of the Ranger mine began with regional diastathermal (extensional) greenschist facies metamorphism (D<sub>1</sub>). The D<sub>2</sub> resulted in the development of NNE–NNW trending mesoscopic folds (F<sub>2</sub>) and a network of thrusts and dextral reverse shears. These were accompanied by ductile–brittle deformation. The D<sub>3</sub> is associated with the development of WNW–NW trending mesoscopic folds (F<sub>3</sub>), a weakly defined axial planar cleavage (S<sub>3</sub>) and sinistral reactivation of D<sub>2</sub> shears. In contrast, D<sub>4</sub> involved block displacement on normal faults during a period of E–W extension [270]. This final event represents brittle–ductile and brittle deformation.

To the south of the Ranger area, the Mamadawerre Sandstone (basal unit of the Kombolgie Subgroup) unconformably overlies the Cahill Formation. Chloritized sandstone/conglomerate remnants have also been described in the Ranger No. 3 pit. However, according to Hein [270], the Kombolgie Subgroup does not crop out west of the Ranger No. 3 orebody nor on the western wall of the pit. The author's interpretation is that the quartzite unit present in the pit represents the basal quartzite unit of the metasedimentary sequence.

## Mineralization

Uranium mineralization is hosted in parts of the LMS and UMS, the Lenticular Schist, pegmatite veins and mafic dykes. In both orebodies, primary uranium mineralization occurs as uraninite veins and disseminations with accessory coffinite and brannerite [271].

Mineralization generally occurs as subhedral to euhedral uraninite grains (often pitted with chlorite or quartz inclusions) as granular masses and as veins and veinlets of variable thickness. Petrographic observations indicate that the uraninite fills voids, hairline fractures and breccia interstices and also forms irregular masses. Filamental growths, originating from uraninite masses, are also observed and these generally interfinger with chlorite/sericite. Botryoidal uraninite formed during alteration and/or remobilization of earlier generation uraninite. During mineralization, fluid–rock interaction has

produced massive magnesian chloritization, sericitization and haematization with subordinate quartz, pyrite and dolomite and, in some cases, the primary mineral fabric has been completely obliterated.

Secondary uranium minerals in weathered ore include saleeite, sklodovskite, torbernite and kasolite. Lateritic ore mainly contains torbernite and saleeite. Gold has been reported from both orebodies and occurs as free grains associated with uraninite. Platinum and paladium have also been recorded.

#### *No. 1 orebody*

The orebodies exhibit a strong structural control. In the No. 1 orebody, the dominant feature is a synformal structure formed by the thinning of LMS carbonate relative to UMS rocks (Fig. 107). The LMS in the synformal hinge is predominantly chert, the origin of which is interpreted as carbonate dissolution and silica replacement. The UMS rocks within the synform are extensively brecciated, particularly near the UMS–LMS contact. The contact itself is folded.

Chlorite altered pegmatoids have intruded all mine sequence rocks and occur as pods and NE striking dykes. The pegmatoids may be weakly mineralized, are affected by ore related alteration assemblages and are offset by syn-mineralization faults. Dolerite dykes, correlated with the Oenpelli Dolerite, occur as thin veins, steeply dipping bodies or irregular blocks within UMS and LMS rocks. According to Kendall [272], dolerite dykes are intruded along faults associated with primary uranium mineralization and the author describes one example of uranium mineralization cross-cutting a dolerite dyke.

Two main types of ore grade uranium mineralization have been observed. The first averaged 0.85% U and occurred as four parallel vein or reef type structures within the UMS, near the LMS contact, which is marked by zones of intense brecciation and chloritization. The second type, surrounding the high grade zone, averaged 0.13% U and occurred as finely disseminated pitchblende occurring through the remainder of the UMS in the orebody and within the LMS on the western limb of the synform. In addition, the UMS schist to the east of the brecciated zone contained very low grade uranium mineralization (less than 0.025% U), which was locally concentrated within brecciated and chloritized zones [272].

#### *No. 3 orebody*

In the No. 3 orebody, the UMS is a ‘monotonous’ succession of thinly laminated quartz–chlorite schist containing a few thin chert bands. Pegmatoid bodies in UMS and LMS rocks are either steeply dipping, 1–3 m wide, NE striking dykes, or variably deformed and altered pods up to 250 m wide. Narrow dolerite dykes and veins also occur, but not in the same quantity as in the No. 1 orebody. Drilling and pit mapping shows the broad ‘ramp-and-flat’ geometry of the LMS–UMS contact, which is steeper on the western and eastern sides and sub-horizontal beneath the main orebody (Fig. 107). In the west wall of the pit, a faulted outlier of haematitic, chloritized and brecciated Mamadawerre Sandstone occurs between the LMS and UMS. The east side of this outlier is a reverse fault with UMS in the hangingwall. Locally steeply dipping beds within the sandstone indicate folding associated with the reverse fault [265].

The most continuous and the highest grades in the mine occur within 3–5 m of the LMS–UMS contact, almost wholly within the UMS. At depth to the east, the high grade zone is situated further above the contact and continues to the eastern limit of the pit (Fig. 107). The high grade mineralization is described as a zone of intense brecciation [272]. Above the flat portion of the contact, there is a broader zone of mineralization within the UMS that exhibits strong structural control. Reverse faults mapped in the pit can be matched to nearly linear zones of higher grade mineralization, which generally occurs in the footwall of the faults. These reverse faults can be traced down-dip to the LMS–UMS contact. Two pods of uranium mineralization occur within the LMS, well below the UMS contact (Fig. 107), within chlorite veins that infill brecciated carbonate.

Pegmatite bodies are barren or very weakly mineralized and are commonly altered to massive quartz–chlorite or chlorite rock. The sense of offset of the pegmatite dykes across faults is consistent with reverse movement. The margins of pegmatite pods are commonly sheared, most probably as a result of strain partitioning during reverse faulting [265].

Reverse faulting, kink folding and mineralization post-date development of the pervasive schistosity, the intrusion of quartz–feldspar pegmatites, development of the Ranger syncline, steeply dipping normal faulting and deposition of the Kombolgie Sandstone. The LMS–UMS contact appears to be the principal fault surface in a westerly directed thrust system. Dilation and brecciation is most intense along the low angle plane of the fault. Changes in the geometry of the LMS–UMS contact resulting from pre-mineralization folding, faulting and LMS carbonate dissolution, controlled the fracturing of the UMS and, therefore, mineralizing fluids to form the orebody [265].

#### Metallogenic aspects

Except for the Angularli uranium discovery in north Arnhem Land [242], which has some mineralization occurring in the sandstone cover, all deposits are basement-hosted. Leaching of uraniumiferous Archaean and Palaeoproterozoic granitic basement rocks is considered to be the main source of uranium, which is present in refractory minerals such as monazite, zircon and accessory uraninite, as well as leaching of uranium-bearing clastic sediments of the sandstone cover. A Sm–Nd isotope study [252] indicates that the Archaean Nanambu Complex may have been involved in the ore forming hydrothermal system in the case of the Ranger deposits. Polito et al. [251, 273] suggested that the metalliferous fluids, originating from the Kombolgie Sandstones, are responsible for the formation of the deposits.

A recent study [274] using a large set of geochemical data at Ranger 3, in conjunction with petrographic studies, investigates the alteration pattern around the deposit. The geochemistry indicates strong zonation and fractionation associated with a large alteration halo around the deposit and with fault planes that cross-cut and bound the deposit. It also shows the existence of broad geochemical zones in the schist formations surrounding the mineralization. The strongest alteration is characterized by massive chloritization with dominant magnesian chlorites (clinocllore) and is associated with the highest grade mineralization. The central zone of Mg alteration overprints a biotite–muscovite–K–feldspar assemblage, displaying increasing loss of Na, Ba and Ca towards the mineralization. For the authors, the alteration patterns, in conjunction with the REE fractionation and the mineralogy, suggest mass transfer dominated by fluid up-flow driving deposition of uraninite and HREE within a chloritic ore zone. Also of interest, the authors state that the spatial extent of the alteration zones, the mobility of alkalis above the system and the indication of upward fluid flow could be applied to develop new vectors for the exploration of Proterozoic unconformity deposits, particularly beneath the thick Kombolgie Sandstone cover, in the case of Australia.

At Ranger, mineralization is hosted in D<sub>4</sub> faults and breccias that locally cross-cut mafic dykes. An age of  $1737 \pm 20$  Ma was determined by Ludwig et al. [250] for primary uranium mineralization from U–Pb dating of uraninite in selected samples from Ranger 3. The emplacement of mafic dykes in the pits can be correlated with the emplacement of the regional Oenpelli Dolerite, around 1725–1720 Ma. The basal Mamadawerre Sandstone of the Kombolgie Subgroup has an age between 1822 and 1720 Ma. Gold and platinum group elements were precipitated at the same time as the uranium.

Polito and Kyser [275] dated retrograde Fe-rich chlorite in the outer alteration zone at Nabarlek as 1750 Ma, which they interpreted as being due to early alteration along faults by fluid inflow from overlying aquifers in the Mamadawerre Sandstone. This 1750 Ma event is within the margin of error for the age of primary mineralization at Ranger. Studies of Rb–Sr, U–Pb, Pb–Pb and Sm–Nd of uraninite and inner alteration zone minerals at Jabiluka and Nabarlek produced consistent ages of primary mineralization in the range 1650–1610 Ma.

Post-mineralization remobilization of uraninite at 1380–1300 Ma and 1190–1100 Ma is recorded by U–Pb, Pb–Pb and Rb–Sr systems in Jabiluka and Nabarlek [273]. Younger uranium mineralization at 900–800 Ma is indicated by U–Pb ages of uraninite from Ranger, Jabiluka, Nabarlek and Koongarra.

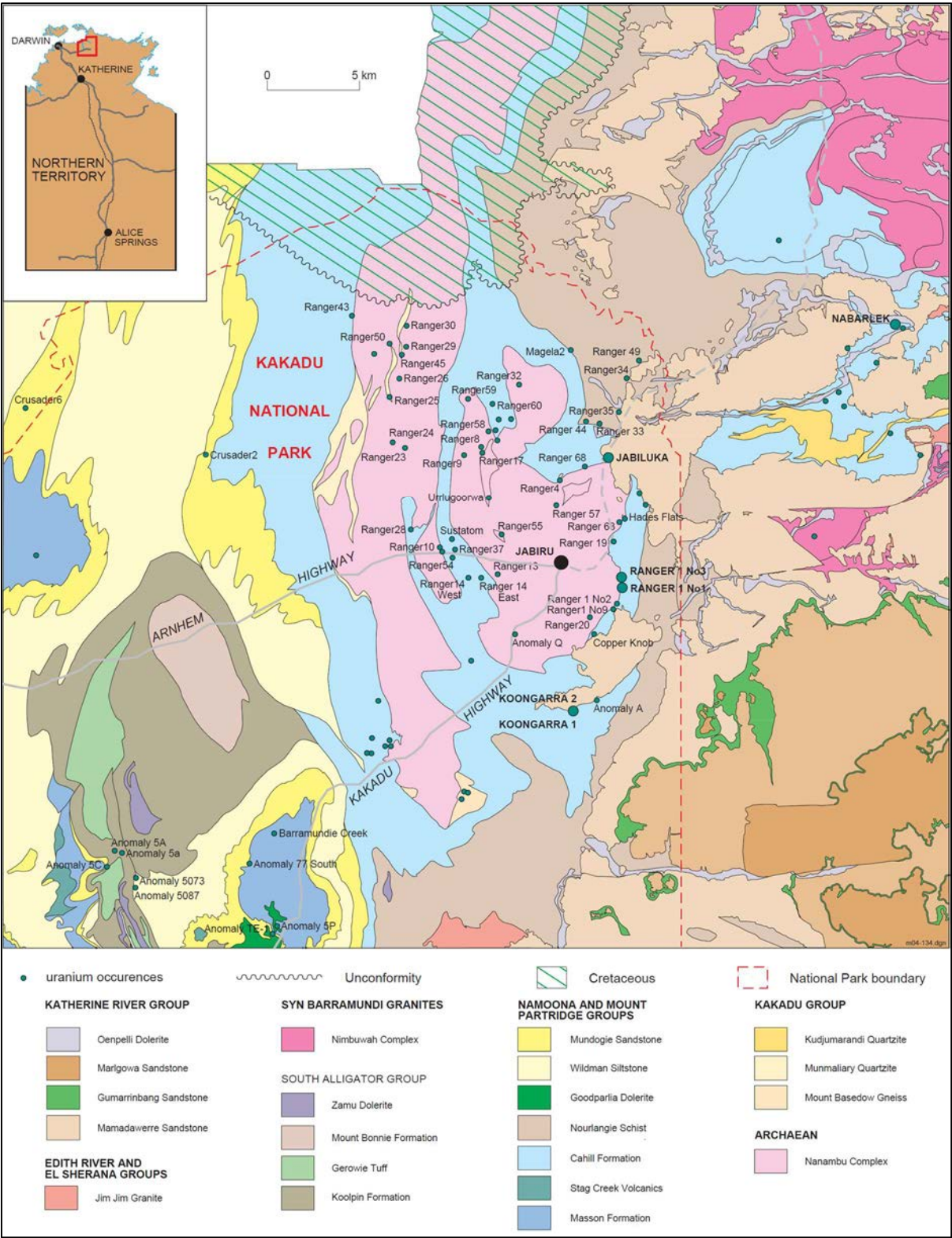


FIG. 105. Geology and uranium deposit occurrences in the Alligator Rivers Uranium Field [265] (reproduced with permission).

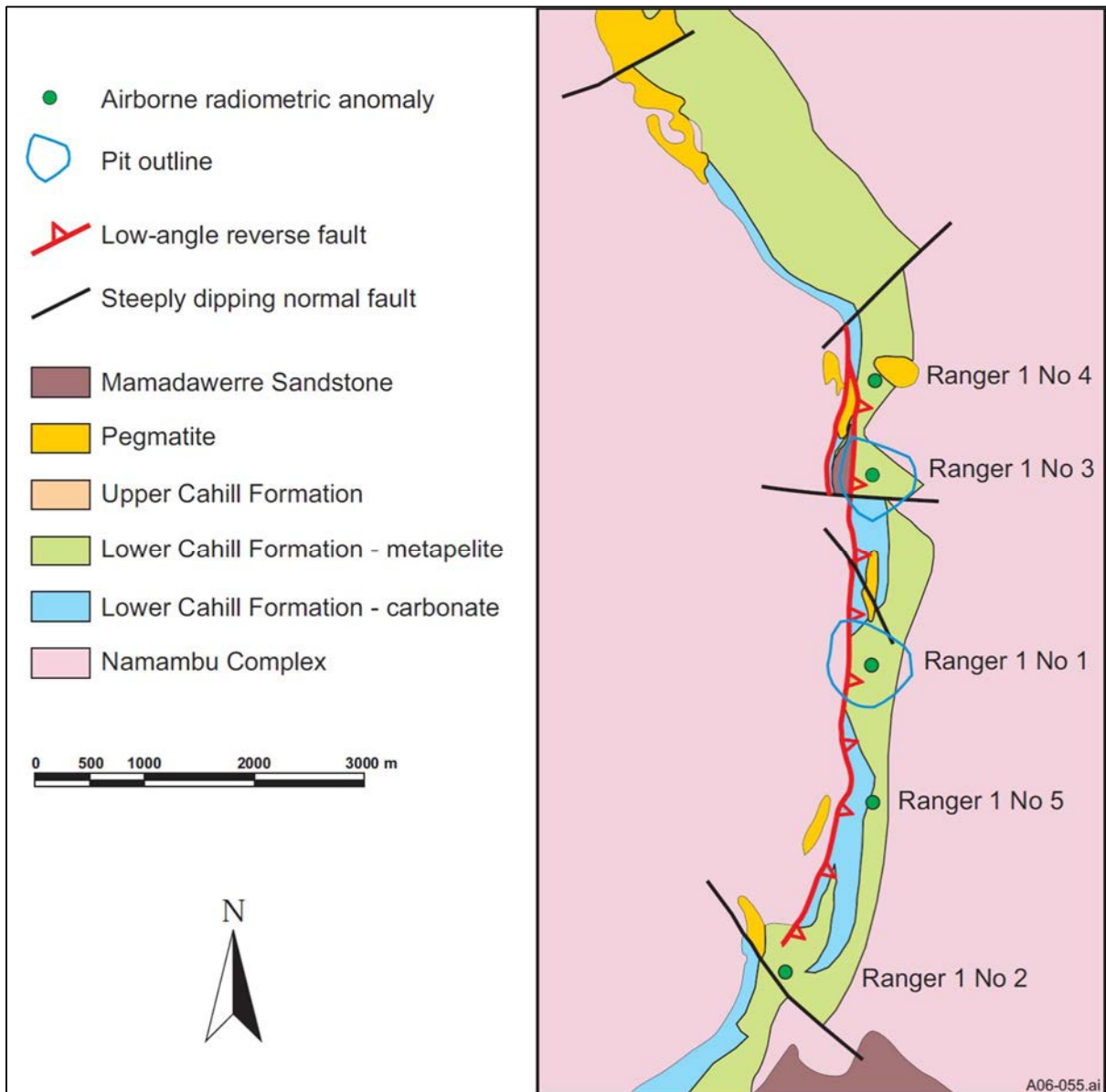


FIG. 106. Detailed geology of the Ranger area [265] (reproduced with permission).

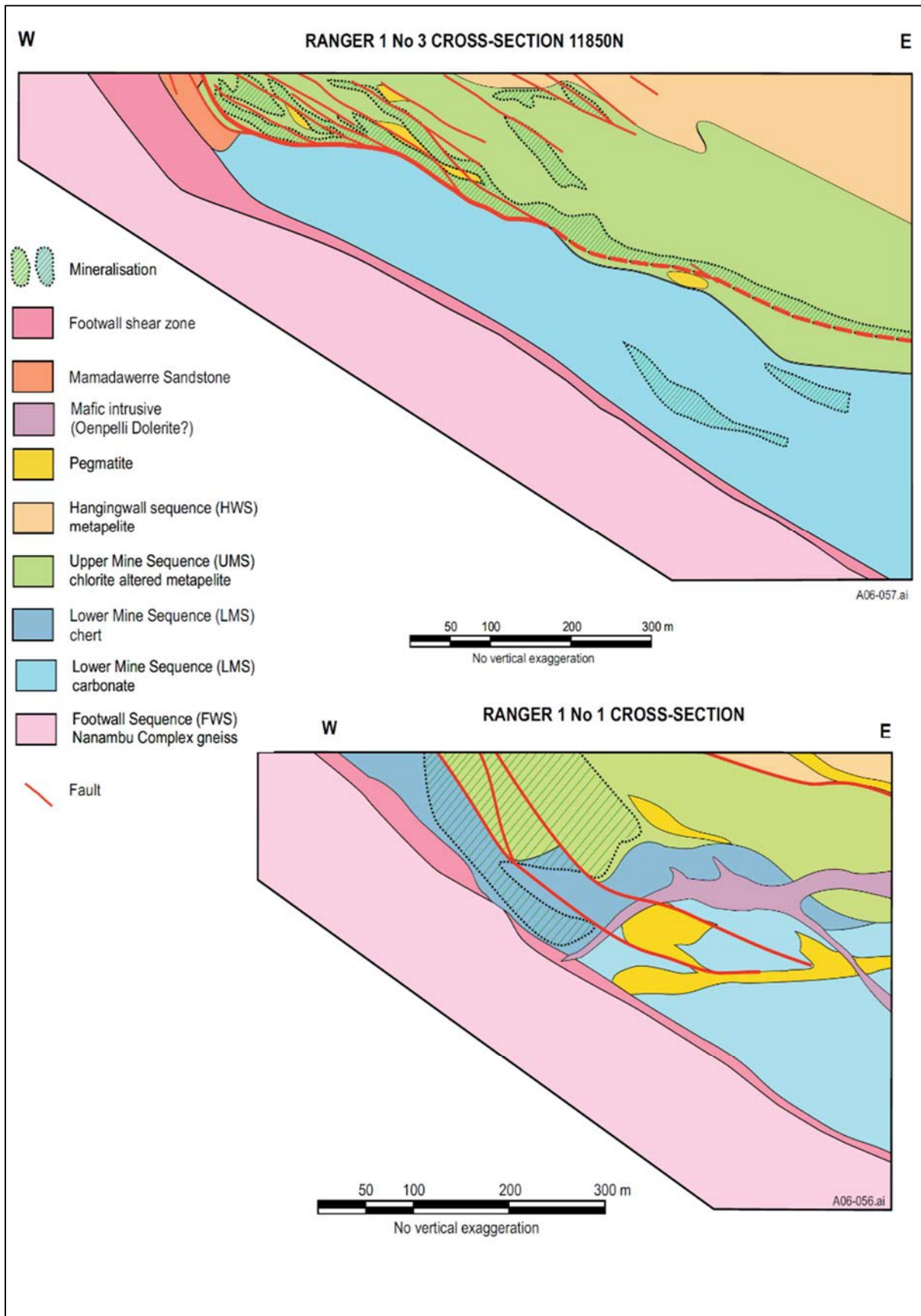


FIG. 107. Geological E–W cross-sections through Ranger deposits Nos 1 and 3 [265] (reproduced with permission).

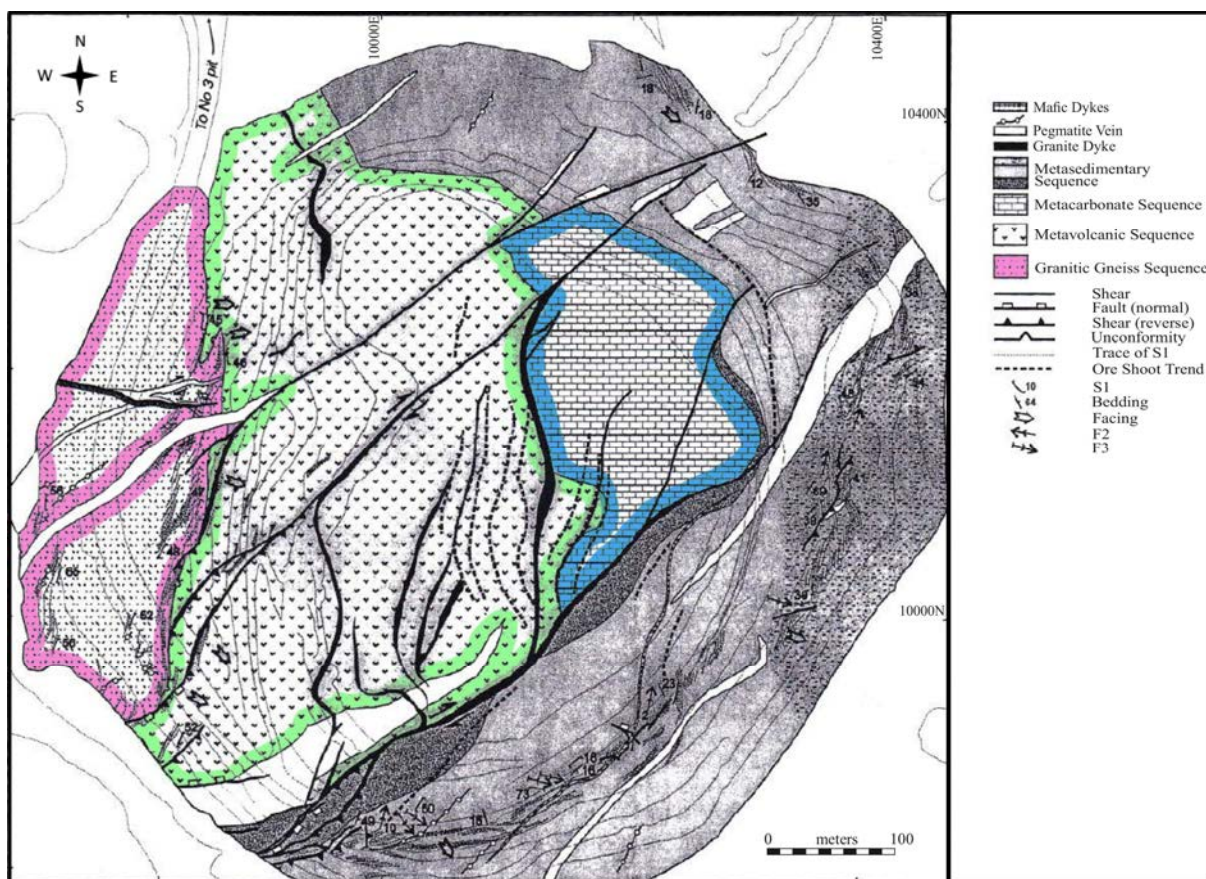


FIG. 108. Geology of the Ranger No. 1 pit (adapted from Ref. [270]).

## The Andrew Lake deposit (Canada)

### Introduction

The Andrew Lake deposit is located approximately 100 km west of Baker Lake, Nunavut (Canada) (Fig. 109). Along with the Kiggavik, End Grid and other deposits, it is found on the Kiggavik Project lease, which is a joint venture between AREVA (64.8%), JCU (33.5%) and Daewoo (1.7%), with AREVA being the operator. The present Kiggavik Project was formed by amalgamation of the former Kiggavik and Sissons Schultz South Projects.

Exploration began in the eastern Thelon region in the late 1960s. Metallgesellschaft started exploration in the project area in 1974 and discovered radioactive cobbles in a frost boil at Kiggavik during follow-up of a helicopter-borne radiometric survey [276]. Urangesellschaft Canada, as the Canadian subsidiary, continued exploration in 1975 and named the new discovery Lone Gull, which was subsequently renamed Kiggavik. Over the next three years, Urangesellschaft Canada discovered the Main Zone (1977), the Centre Zone (1978) and Granite Grid (1984). On the Sissons Schultz South project to the south of Kiggavik, diamond drilling programmes discovered mineralization at Bong in 1984, End Grid in 1987, Andrew Lake in 1988 and Jane in 1992.

A feasibility study for the two Kiggavik deposits was undertaken in 1989 but a 1990 referendum held in Baker Lake voted against development of the Kiggavik mine. In 1993, COGEMA Resources Canada Inc. (now AREVA Resources Canada Inc.) became the operator of the joint venture. A prefeasibility study was completed in 1997 and the project was put under care and maintenance. In 2005, AREVA Resources Canada began stakeholder consultations and in 2006 established a local

office in Baker Lake and initiated a viability study. Exploration and development drilling, along with a conduct of a feasibility study, have been ongoing since 2007. In 2015, the project was dormant. The Andrew Lake deposit contains 22 754 tU at a grade of 0.377% U.

### Geological setting

The deposits are located 7–22 km south of the margin of the Thelon Basin, an 80 000 km<sup>2</sup> Palaeoproterozoic, intracratonic sandstone basin deposited in the Rae Province of the Canadian Shield. The Rae and adjacent Hearne Provinces together make up what was formerly known as the Churchill Province of the Canadian Shield. They represent Archaean crust that was cratonized during the Late Archaean, but was extensively reworked during the Palaeoproterozoic Trans-Hudson Orogeny. The Rae Province basement in the eastern Thelon records a complex stratigraphic and tectonic history.

The simplified bedrock geology of the area is shown in Fig. 110. The oldest rocks in the area are high grade Archaean granitoid gneiss and intrusive rocks. The Woodburn Lake Group is the oldest recognizable metasedimentary and metavolcanic sequence in the area, consisting of ~2796–2752 Ma old greenschist–granulite facies, felsic to intermediate volcanic rocks, komatiite, banded iron formation, chert, psammite and quartzite [277–280]. Unconformably overlying the Woodburn Lake Group in the north is the ~2.45–1.90 Ga Amer Group. It has been metamorphosed to greenschist facies and consists of a lower orthoquartzite sequence, a middle sequence of dolomitic limestone interbedded with mudstone and an uppermost sequence of schist and feldspathic sandstone [280–282]. In the eastern Thelon region, the upper, predominantly metasedimentary portion of the supracrustal sequence (quartzite and feldspathic wacke with lesser phyllite, oxide facies iron formation and mafic volcanic rocks), formerly considered to be Upper Woodburn Lake Group has recently been interpreted as Palaeoproterozoic Ketyet River Group, a correlative of the Amer Group [280].

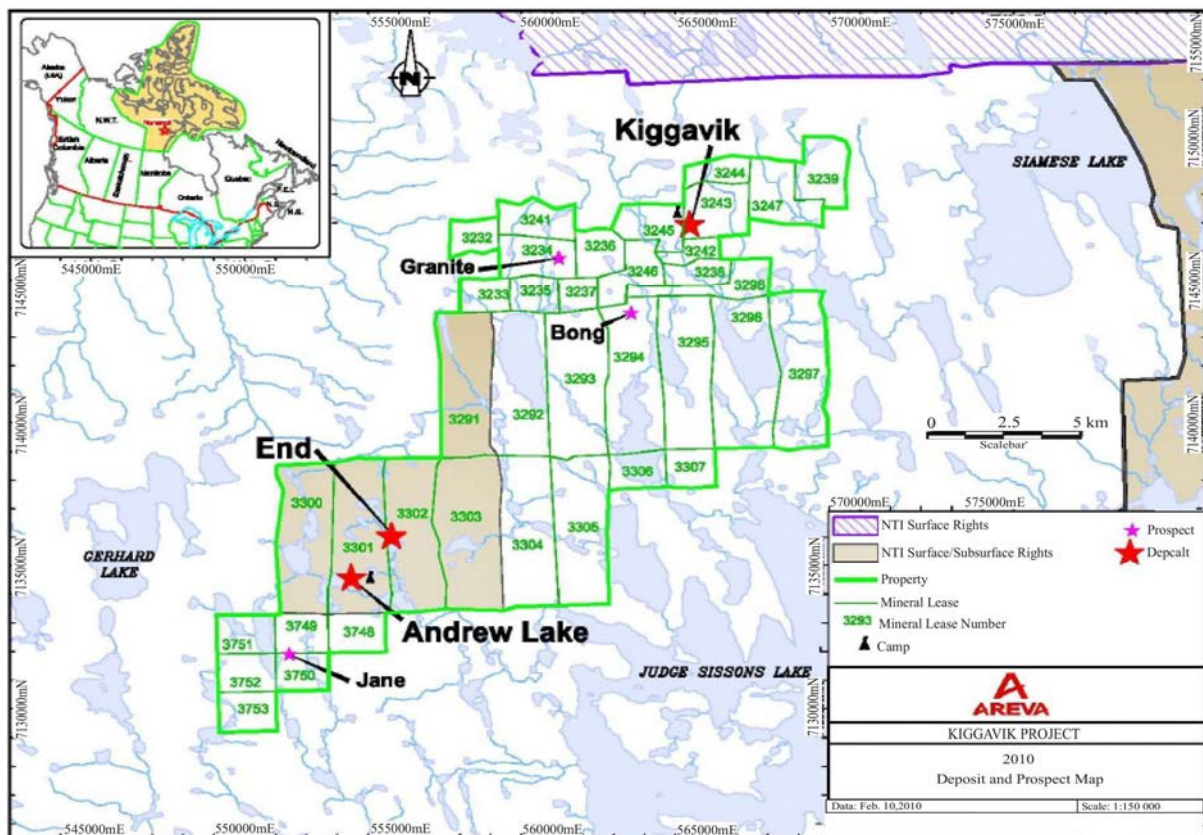


FIG. 109. Location of Andrew Lake and other deposits of the Kiggavik Project [283] (reproduced with permission).

The Trans-Hudson Orogeny (~1900–1820 Ma) led to widespread metamorphism, tectonism and granite/syenite to lamprophyric plutonism throughout Churchill Province [284, 285]. The intrusion of the Hudson Suite occurred between 1845 and 1795 Ma and is interpreted as a syn- to post-orogenic middle crustal level melt closely associated with Martell Syenite intrusions and lamprophyre dyke emplacement [279]. Subsequent to the tectonic activity and related plutonism was the deposition of the Dubawnt Supergroup in early structurally controlled basins and later, an extensive intracratonic basin.

The Baker Lake Group (the lowermost group of the Dubawnt Supergroup) is restricted to the Baker Lake Basin and related sub-basins (Angikuni and Yathkyed) forming a south-westward trend in the southern Rae Province, paralleling the Snowbird Tectonic Zone. The Baker Lake Group comprises (from bottom to top) the South Channel, Kazan/Angikuni, Christopher Island and Kunwak Formations [249]. The South Channel Formation is a coarse alluvial, red bed sequence and is overlain by fine-grained sandstone of the Kazan and Angikuni formations. The Christopher Island Formation is characterized by minette lava flows as well as pyroclastic and epiclastic rock units. The Kunwak Formation consists of conglomerate, sandstone and siltstone.

At approximately 1.765–1.750 Ga, crustal extension and anorogenic basaltic magma upwelling in the lower crust led to the generation of Nuelin Granitoid Suite plutons and related Pitz Formation rhyolite flows [284]. Intermingled with the Nuelin granites are the McRae Lake diabase dykes, a plagioclase- and magnetite-rich gabbro with minor pyroxene  $\pm$  olivine. The (1.76 Ga) Wharton Group sedimentation is synchronous with the felsic plutonism and volcanism, occurring in both the Baker Lake Basins and extending to the north-west, below portions of the Thelon Basin. It comprises the Amarook and Pitz Formations. The Amarook Formation consists of a basal conglomerate, which is overlain by large scale, cross-bedded sandstone. The Pitz Formation is a coarsening upwarda sequence beginning with rhyolite flows and tuffaceous units followed by sandstone and conglomerate [284].

The Barrenslund Group is the uppermost and most widespread part of the Dubawnt Supergroup. It is dominated by the Thelon Formation which has been dated at ~1.72 Ga and which has an estimated thickness of 1.9 km. It is an unmetamorphosed, sub-horizontal succession of quartz-rich conglomerate, sandstone, siltstone and mudstone that is interpreted to represent alluvial fan, fluvial, minor shallow marine and aeolian sedimentation. The Thelon Formation is overlain by the 10 m thick Kuungmi Formation, an amygdaloidal, shoshonitic basalt, and the 40 m thick Lookout Point Formation, a siliceous, stromatolitic dolomite with minor interbeds of quartz arenite. These contrasting lithologies suggest a depositional transition from a fluvial, terrestrial environment to a stable, continental platform. Intruding into all the aforementioned rock units is the ~1.25 Ga Mackenzie Diabase Dyke Swarm, which has a general NNW–SSE trend [286].

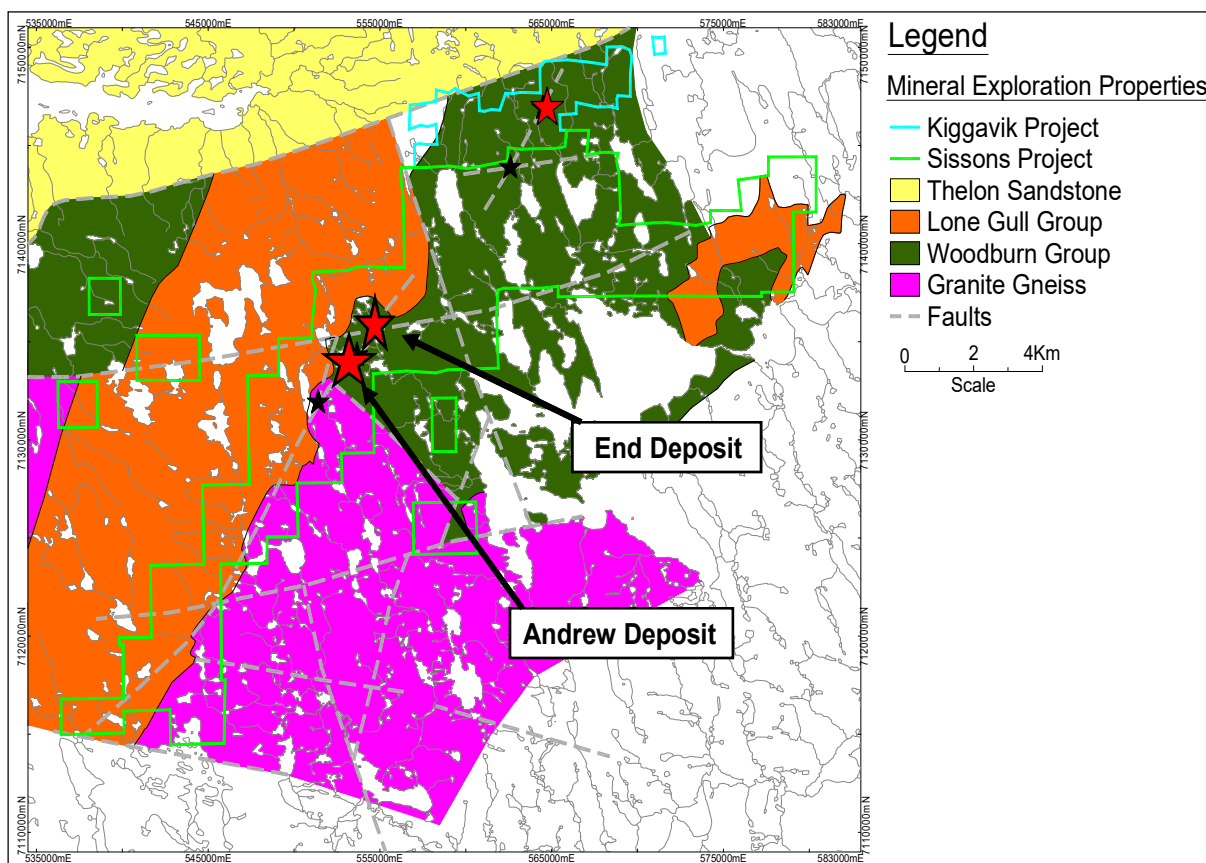


FIG. 110. Geology of the Andrew Lake deposit area [287] (reproduced with permission).

## Mineralization

The mineralization of the deposits in the Kiggavik Project area is all hosted in the basement rocks, but considering the close proximity to the basin and the younger age of the mineralization, it is believed that they formed below the sub-Thelon unconformity. The uranium deposits are generally hosted along a north-east trend a few kilometres south of the Thelon Basin margin. The deposits are all structurally controlled. The dominant structures are ENE trending ( $\sim 065^\circ$  strike), subparallel to the Judge Sisson Fault and the Thelon Fault that forms the southern boundary of the basin, approximately 1.5 km north of Kiggavik. These are cross-cut by NNW and NE trending faults ( $\sim 045^\circ$ ) [276, 287]. Some of the deposits are located at the intersections of these structures. As shown by Reilly and Wheatley [287], at the district scale, the Andrew Lake, End Grid and Jane deposits are located along the NE trending, moderately to steeply SE dipping Andrew Lake Fault, which cross-cuts the regional scale, ENE trending Judge Sissons Fault. The End Grid deposit is located at this intersection. The Andrew Lake deposit is located approximately 2 km south-west of End Grid and Jane is located 2 km south-west of Andrew Lake. Although the Andrew Lake deposit lies along the Andrew Lake Fault, the actual ore controlling structures are smaller, subsidiary splays, approximately 60 m in the footwall below the main trace of the Andrew Lake Fault [287].

The Andrew Lake deposit consists of three separate lenses, an upper lens containing the majority of the resource, a lower lens in the footwall to the fault, and a new lens continuing southwards from the upper lens [283]. The orebody is 450 m long, approximately 100 m wide and 300 m in vertical thickness. The deposit is the largest of the Kiggavik Project and contains 22 754 tU at an average grade of 0.377% U.

The mineralization at Kiggavik, Bong, End Grid and Andrew Lake is almost always hosted in strongly altered metasedimentary rocks of the Woodburn Lake Group with a lesser amount in the underlying granite and granitic gneiss. The main host is the lower part of the Woodburn Lake Group, referred to by Fuchs et al. [276] as the ‘dirty quartzite’. This is a historical field term used for the mixed package of metagreywacke and mica-rich quartz–feldspar gneiss capped by pelite and banded iron formation. It is overlain by a relatively pure, massive white quartzite with some bands of chlorite–sericite schist named ‘orthoquartzite’. The mineralization at Andrew Lake is located near the base of the metasedimentary unit, extending into the underlying Hudson granitoid and (the lower lens), below the quartz breccia into the underlying migmatized orthogneiss and paragneiss (significantly less well foliated than the overlying metasedimentary rocks) (Fig. 111).

Mineralization is structurally controlled along steeply dipping faults and is enveloped by an intense clay alteration zone. Alteration, from periphery to core consists of: (a) an outer zone (greenish–grey) of weak clay alteration typified by alteration of plagioclase to illite and biotite to chlorite, gradational to (b) an inner zone of strong clay alteration where K-feldspar and plagioclase are altered to illite ± montmorillonite and celadonite and ferruginous chlorite is altered to magnesian chlorite, ranging from strongly oxidized (red) to reduced (bleached) in the inner parts and finally to (c) a proximal white zone of sericite with lesser quartz and sudoite (magnesian chlorite), accompanied by desilicification in the ore zone. The combination of strong clay alteration and desilicification results in very diagnostic resistivity and gravity low geophysical responses [288].

Ore zones exhibit strong structural control with lenses following the host structures or structural intersections. Some exhibit a plunge along these trends. The boundaries of the orebodies are very sharp. Mineralization consists of disseminations, blebs and veins of pitchblende and coffinite. The Kiggavik Centre Zone contains colloform aggregates and rosettes in open fractures as well as fine-grained disseminations. It is often accompanied by limonite, interpreted as an alteration product of pyrite, which is present as corroded grains [276]. Weyer et al. [289] describe a paragenesis of rutile and leucoxene followed by pyrite and/or marcasite, followed by pitchblende which rims quartz veinlets, coats and infills fractures in chlorite and sulphide grains and replaces marcasite and sometimes rutile. Sooty pitchblende and coffinite follow and replace pitchblende. The ores are clean, monomineralic pitchblende but contain geochemical enrichment of Ni, Bi, Ag and Pb [271]. The Andrew Lake and End Grid deposits also contain significant (although uneconomic) enrichment of gold and platinum [287].

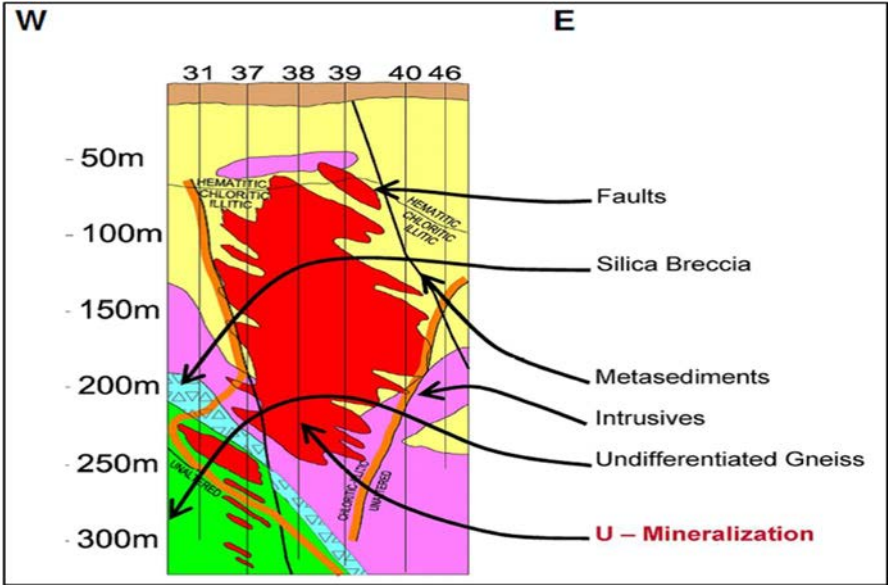


FIG. 111. Ore zone cross-section of the Andrew Lake deposit [283] (reproduced with permission).

## Metallogenic aspects

Whole rock K–Ar dates from altered rocks range from 1658 and 1563 Ma for the least altered to between 1358 and 1073 Ma for the most altered rocks at Kiggavik [276]. Uranium–lead age determinations from mineralization at the Kiggavik Main Zone give an oldest age of 1403 Ma [289]. Considering the uncertainties with these ages, the alteration and mineralization likely formed together (also indicated by field observations) and as they are younger than the Thelon Basin, they are presumed to have formed at the unconformity.

The nature of the alteration assemblage places some constraints on the ore forming process. The intensity of the clay alteration indicates that the altering and mineralizing fluids reacted strongly with the host rocks at relatively low temperatures. However, the dominantly illitic nature of the clays (with only rare kaolinite) suggests that the pH was moderate, essentially buffered by feldspar. The mineralization is also situated in reduced (or bleached) rock, proximal to sharp redox boundaries, suggesting the importance of reduction of uranium in the depositional process. The ore-related haematite is typically brick red in colour, distinct from the strong maroon haematization proximal to the sub-Thelon unconformity and major structures.

The uranium deposits of the eastern Thelon region display several similarities to the basement-hosted variety of unconformity type uranium deposits of the Athabasca region. These include: high grade mineralization; monomineralic pitchblende with only geochemical enrichments of base metals, strong structural control of mineralization, strong clay and haematite alteration, predominantly metasedimentary host rocks and formation beneath large Palaeoproterozoic, mature, intracratonic sandstone basins following the Trans-Hudson Orogeny. However, there are differences from the Athabasca model including: much more intense and extensive clay alteration, lack of a spatial association with strongly graphitic fault zones (although minor graphite and carbonaceous material may be locally present), lower grades than the Athabasca deposits (although still very high compared with other deposit classes), lack of known mineralization spanning the unconformity into the Thelon sandstone and lack of polymetallic (Ni–Co–As) examples. Nevertheless, the similarities in style, the interpreted attendant geological processes and the relationships with respect to the same broad geological events suggest that these deposits belong to the same genetic model [289].

### 3.7.4.2. *Unconformity-contact deposits*

#### **Fracture-controlled: The Shea Creek deposits**

##### Introduction

The Shea Creek project is located 15 km south of the former Cluff Lake uranium mine and 30 km east of the Alberta border in north-western Saskatchewan (Fig. 112).

Exploration was carried out between 1969 and 1985 by various companies. The early programmes were largely of a regional nature. Cogema Resources (now AREVA Resources Canada) initiated exploration activities on the Shea Creek project in 1990 utilizing modern, deep penetrating airborne geophysical surveys. Subsequent ground surveys identified a large NNW trending graphitic conductor, the Saskatoon Lake Conductor, which has a strike length of 25 km. Several electromagnetic conductors were drilled in 1992, intersecting narrow intervals of uranium mineralization.

Systematic drilling between 1993 and 2000 resulted in the discovery of the Colette (1996) and Anne (1994) deposits. Kianna was then discovered in 2004 and 58B Area in 2005. As of 2013, total resources amounted to 36 900 tU, located in four deposits: Anne (10 540 tU at 1.61% U), Colette (5180 tU at 0.64% U), Kianna (19 895 tU at 1.26% U) and 58B (1288 tU at 0.59% U) [291].

The Shea Creek project is a joint venture between AREVA (51%) and UEX Corporation (49%). It is dormant as of 2015.

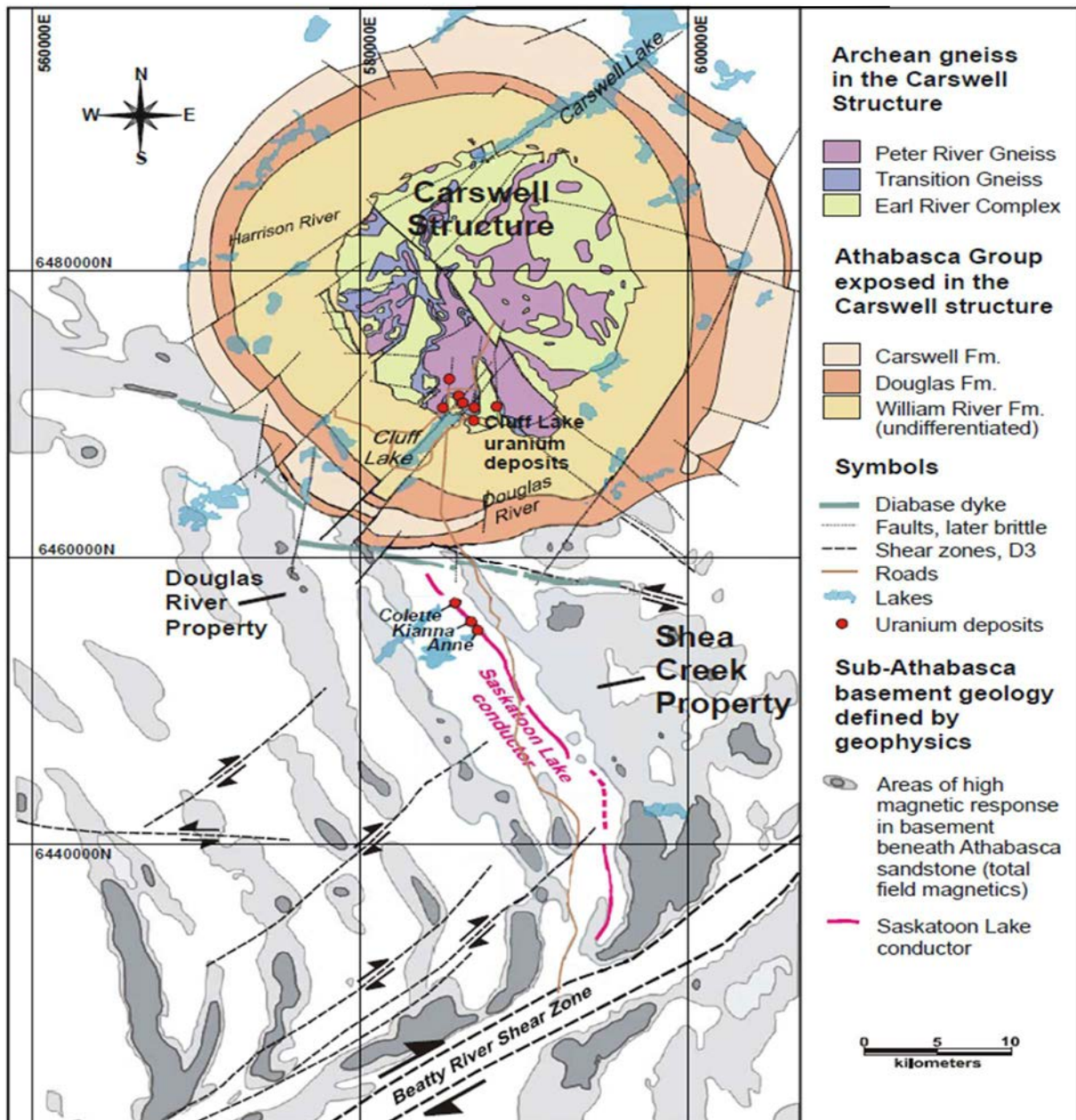


FIG. 112. Geological setting of the Shea Creek project (adapted from Ref. [290]).

### Geological setting

The Shea Creek project lies within the western part of the Athabasca Basin of northern Saskatchewan. Two dominant lithological formations are present:

- (i) A polydeformed, metamorphic basement of Archean and Palaeoproterozoic age;
- (ii) A flat lying to shallowly dipping, 400–800 m thick, undeformed, supermature, quartz sandstone cover of the Late Palaeoproterozoic–Mesoproterozoic Athabasca Group.

Basement rocks in the western part of the Athabasca Basin consist of Archean–Palaeoproterozoic orthogneisses and paragneisses of the Lloyd Domain, part of the Rae Province. On the Shea Creek project, basement lithologies trend NNW and dip moderately to the WSW. They comprise an alternating sequence of graphitic gneiss, dioritic gneiss and pelitic gneiss (Karen Lake Assemblage)

which were metamorphosed to amphibolite facies. The latter lithology includes the Saskatoon Lake Conductor, a graphite-bearing pelitic gneiss which is spatially associated with uranium mineralization. The pelitic gneiss, which hosts most of the mineralization, is 40–80 m thick and consists of a basal graphitic pelitic gneiss with overlying, alternating garnetiferous gneisses and aluminous pelitic gneiss. The hangingwall and footwall to the pelite consist of felsic garnetiferous granitic gneiss. A conformable metabasalt unit occurs in the Anne area.

The Shea Creek basement was affected by at least two main periods of deformation prior to the deposition of the Athabasca sandstone cover. The first period occurred during the 1950–1900 Ma Taltson–Thelon Orogeny, followed by polyphase regional deformation and the formation of regional shear zones during the Hudsonian Orogeny between 1900 and 1740 Ma.

The folded, metamorphosed basement sequence was eroded and then unconformably overlain by the flat lying, quartz arenite dominated Athabasca Group sandstone between 1769 and 1500 Ma. The uppermost tens of metres of the basement gneiss are affected by a regional palaeoweathering profile.

The structural styles and ages vary substantially and include early regional ductile and brittle structures that predate the deposition of the Athabasca Group, as well as post-Athabasca brittle structures [292]. The Saskatoon Lake Conductor is a SE trending SW dipping graphitic interval interpreted to be a large scale reverse fault oriented subparallel to the main foliation and dipping 30–50° SW. It is the earliest mineralization related structure (associated with the Colette, Kianna, Anne and 58B deposits). Several later generations of faults and fractures offset the Saskatoon Lake Conductor. All of the faults sets are steeply dipping to vertical. Semi-brittle, stylolitic faults extend into the basal Athabasca sandstone where they locally overprint mineralized chlorite matrix breccias, indicating that this fault activity may have coincided with, and locally outlasted, alteration related to uranium mineralization. The NE and E–W trending steeply dipping fault sets coincide with the areas of highest grade uranium mineralization at the unconformity and are host to, or control, the underlying uranium mineralization in the basement rocks [290].

The Athabasca Group consists of three orthoquartzite clastic sequences bounded by unconformities: the lower Fair Point, the intermediate Manitou Falls–Wolverine Point and the upper Locker Lake–Carswell Sequence [293]. These orthoquartzite sequences consist mainly of medium- to coarse-grained, fluvialite, quartz-rich sandstone, conglomerate and minor siltstone that underwent deep burial to a maximum of 4–5 km [294]. The age of sedimentation of the Athabasca Group is Late Palaeozoic–Mesoproterozoic, possibly in the range 1720–1650 Ma [295].

The sandstone is dominated by monocrystalline quartz. Zircon, Fe-tourmaline, Fe–Ti oxides and rare detrital white mica are accessory minerals. No feldspar grains have been reported. The major diagenetic features comprise pore sealing by quartz overgrowths and crystallization of kaolin minerals along the kaolinite to dickite phase boundary. Minor haematite with rare siderite and pyrite is also present. Alteration mineralogy of the host rocks is dominated by illite with variable amounts of sudoite, trioctahedral chlorite, dravite, drusy quartz and minor amounts of alumino–phosphate–sulphate minerals.

In summary, most of the uranium bodies are associated with extensive quartz dissolution, enrichment in clay minerals (especially illite) and collapse of the sandstone cover. Silicified zones, notably as fractures and breccias filled with drusy quartz, are also common, but restricted to the zones around the major desilicified zone. Silicification pre-dates mineralization and related host rock alteration [296].

## Mineralization

Uranium mineralization is found in four deposits, Colette, 58B Area, Kianna and Anne, occurring along a 3 km strike length of the Saskatoon Lake Conductor at depths of 650–1000 m below the current surface (Fig. 113). Mineralization has also been intersected 2 km south of the Anne deposit.

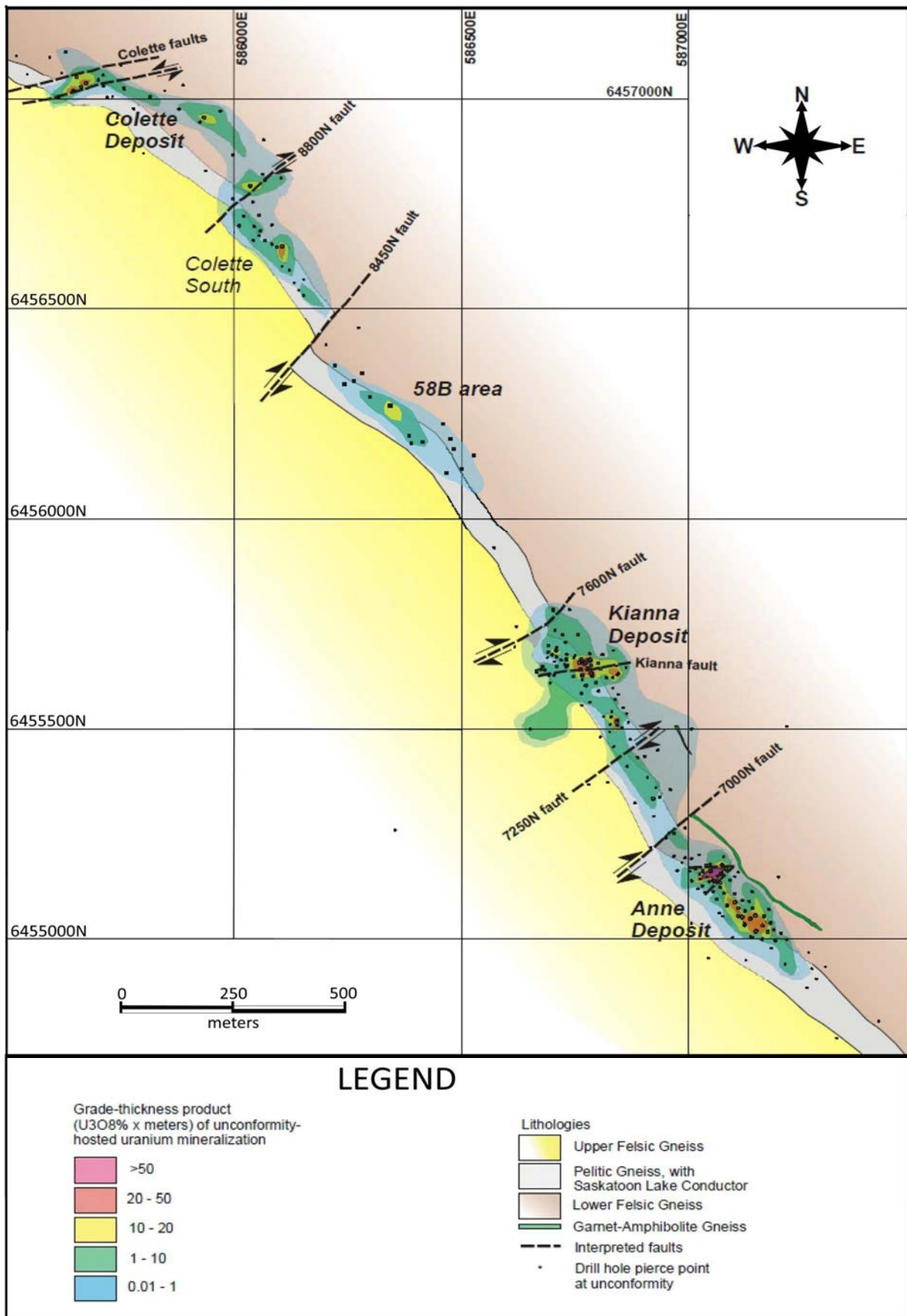


FIG. 113. Geology of the Shea Creek property showing the location of the deposits (adapted from Ref. [290]).

Three types of mineralization have been described on the basis of their positions with respect to the unconformity and their overall morphology [290]:

- (i) Unconformity-hosted mineralization is the most widespread style. It corresponds to shallow dipping zones developed in the lowermost sandstone cover immediately above the unconformity or straddling the unconformity and extending downwards for several metres into the underlying basement. The mineralization is elongate in plan view, extending at the unconformity over a width of 40–150 m. In high grade areas, mineralization consists of massive, nodular and blebby pitchblende  $\pm$  coffinite  $\pm$  uraniferous silicates in a haematite–clay matrix that grades between 4 and 30% U over intervals of several metres. In lower grade areas, mineralization may be disseminated in chlorite–clay–dravite alteration. Mineralization is often associated with chlorite–dravite dissolution breccias in the basal sandstone;
- (ii) Basement mineralization is the second most extensive type of mineralization occurring in the Anne and Kianna deposits and in the Colette South area. It is mainly developed in granitic gneiss for up to 200 m below the unconformity and vertically below the unconformity-hosted mineralization. Minor mineralization is also present in the pelitic gneiss. Basement mineralization is variable in style and morphology and is associated with areas of intense white to pale green clay–chlorite alteration. It can be either concordant or discordant in style, with the two styles often occurring together or branching off from one another. Concordant basement mineralization (southern Anne and Colette South) forms shallow to moderate dipping lenticular zones that are parallel or subparallel to the foliation in the granitic gneiss. Where present, the metabasite unit may be preferentially mineralized. Discordant basement mineralization, which is best developed at Kianna and in the northern part of the Anne deposit, consists of steeply dipping, easterly trending zones of disseminated, nodular and locally massive replacement style pitchblende  $\pm$  coffinite  $\pm$  haematite  $\pm$  uraniferous silicates and by sets of pitchblende  $\pm$  quartz  $\pm$  clay veinlets. Interaction between concordant and discordant mineralization forms oreshoots that plunge moderately to shallowly to the WSW;
- (iii) Perched mineralization is the least extensive. It consists of flat lying to shallowly SW dipping lenses of disseminated to massive pitchblende–coffinite–haematite–clay mineralization that is developed within the sandstone for up to 60 m above the unconformity. Perched lenses may occur stacked above unconformity mineralization with no associated faulting or they may occur along or at the termination of SW dipping faults where they project upwards into the sandstone from the underlying pelitic basement.

Where best developed and of highest grade, all three mineralization styles may be vertically stacked on top of one another (Fig. 114). Pre-Athabasca basement structural architecture probably plays an important role in localizing the higher grade areas.

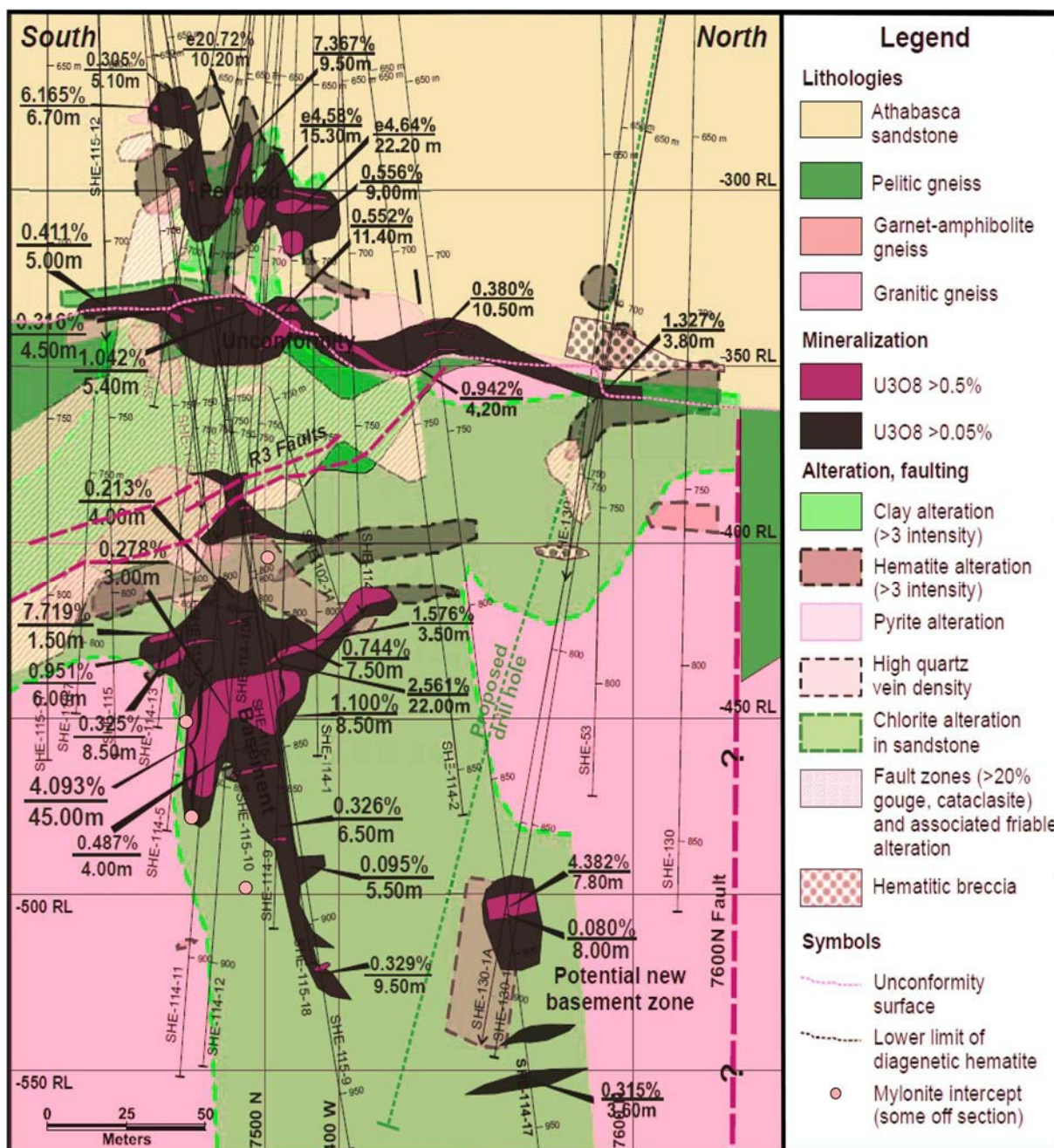


FIG. 114. Vertical geological section through the Kianna deposit (adapted from Ref. [290]).

Metallogenic studies suggest that pitchblende (botryoidal uraninite) is the dominant uranium-bearing mineral in the three types of mineralization. The common paragenetic sequence consists of early pitchblende locally accompanied by brannerite, which are replaced by secondary pitchblende + coffinite ± boltwoodite or other uraniferous silicates. In addition to pyrite and/or marcasite, uranium mineralization is accompanied by small quantities of Ni-As minerals (gersdorffite, nickeline and rammelsbergite), chalcopyrite and galena. Concentrations of Ni and As are typically highest in basement mineralization.

Elevated Au values are also commonly present (20.79 g/t Au over 2.40 m, 14.02 g/t over 3.30 m and 13.75 g/t over 2.50 m). The morphology and true thickness of the intervals of high gold content are as yet undetermined. High gold grades frequently, but not always, occur in areas of higher grade uranium

mineralization and can be present both in unconformity and basement mineralization in the three deposits. Native gold grains, both encapsulated in pitchblende, sometimes in association with bismuth tellurides, and also free in the surrounding clay alteration have been identified in samples from basement and sandstone-hosted mineralization [290].

Mineralization is associated with extensive clay alteration affecting the lower sandstone and extends downwards into the basement. Principal clay minerals are illite, chlorite, kaolinite and dravite. Often an early phase of illitization is evident, while kaolinite is paragenetically late. Extensive areas of chlorite–clay–dravite matrix breccias occur along the unconformity in the basal sandstones and are spatially associated with unconformity-hosted mineralization. The occurrence of both pitchblende fragments in the breccias and the overprinting of the breccia matrix by pitchblende–coffinite assemblages indicate a syn-mineralization timing which was also coeval with reverse faulting. Clay alteration in the basement envelops the mineralized zones and outlines their general morphology.

Potassium–argon dating was carried out on illite samples from sandstone and basement rocks in the vicinity of, and away from, the Shea Creek deposits. The intermittent hydrothermal activity induced several generations of authigenic illite dated at  $1453 \pm 2$ ,  $1330 \pm 20$  and about 1235 Ma [297]. These episodes coincide with the dates recorded by the uranium oxides of the Anne and Colette deposits and dated by the U–Pb method at about 1330 and 1275 Ma [298]. These ages are significantly younger than the ages recorded for the McArthur, Cigar Lake and Sue deposits (1550–1440 Ma). An event at  $380 \pm 5$  Ma was also recorded in samples from massive ore zones. This event may be attributed to the beginning of the Athabasca Basin uplift, inducing the percolation of meteoric water into the basal formations of the basin. Part of the polymetallic mineralization (Ni–Co–S–As) might have been deposited during this stage.

#### Metallogenic aspects

The Shea Creek deposits show similar characteristics to the other unconformity type deposits of the Athabasca Basin. The association of Fe and Cu sulphides and Ni–Co arsenides with the uranium mineralization is similar to what has been observed in the ‘so-called’ sandstone-hosted egress type deposits involving a stronger basement fluid input [299].

The Shea Creek mineralization is associated with areas of clay alteration and sandstone desilicification locally above the mineralization and peripheral silicification which together may be detectable through resistivity surveys [290]. Alteration patterns are comparable to other unconformity type uranium deposits in the Athabasca Basin.

Nickel arsenides are more abundant in basement zones and therefore mineralization at Shea Creek has more similarities to the monomineralic type seen in the eastern Athabasca Basin than the Ni–arsenide association observed at Midwest Lake or Cigar Lake.

#### **Clay-bound: The Tamarack deposit (Canada)**

##### Introduction

The Tamarack deposit (formerly known as the Collins Creek deposit) is located in the eastern part of the Athabasca Basin in northern Saskatchewan, Canada. It is located approximately 20 km west of the Rabbit Lake mine (Fig. 115). The deposit is part of the Dawn Lake Project, a joint venture between Cameco Corporation (57.466%) (the operator), AREVA Resources Canada (23.086%) and JCU Canada Exploration Co. Ltd (19.448%). The project has been actively explored since 1977.

The Q8 conductor trend has been explored using electromagnetics and other ground geophysical surveys, boulder surveys and diamond drilling. Low grade mineralization was first intersected in 1999. As uranium prices began to rise, exploration efforts were renewed in 2001. Additional drilling discovered higher grades and delineated the orebody. As of 2015, the project remains dormant.

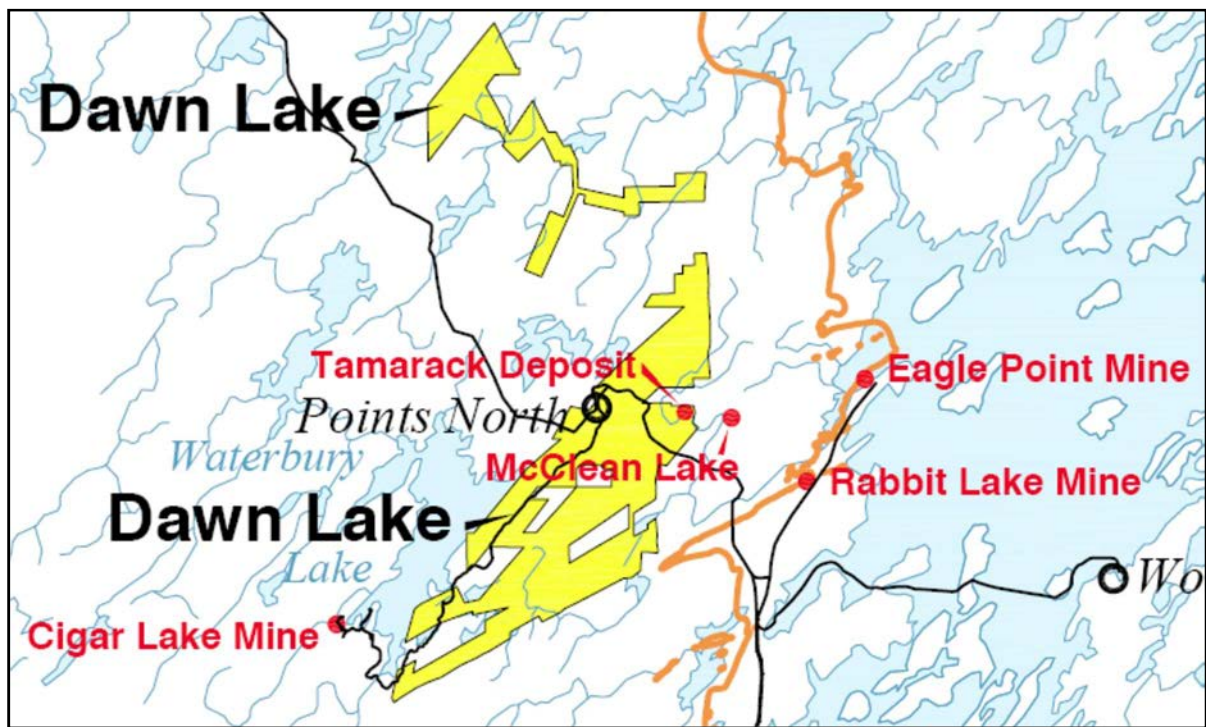


FIG. 115. Location of the Tamarack deposit and the Dawn Lake Project, northern Saskatchewan, Canada (source: G. Zaluski, CAMECO) (reproduced with permission).

#### Geological setting

The Athabasca Basin of northern Saskatchewan and Alberta lies upon Archaean and Palaeoproterozoic crystalline basement (Canadian Shield) rocks of Churchill Province that were metamorphosed during the Trans-Hudson Orogeny. This structural province consists of the Rae Province in the west and the Hearne Province in the east, joined along the Snowbird Tectonic Zone, a long lived, NE trending regional scale tectonic zone that underlies the Athabasca Basin. The eastern half of the Athabasca Basin lies upon the western part of the Hearne Province, which corresponds to the Cree Lake Zone of Lewry and Sibbald [300]. From west to east, this zone includes three NE trending domains: the Virgin River, Mudjatik and Wollaston domains.

The amount of preserved supracrustal cover and the intensity of deformation increases eastwards, with the Wollaston Domain consisting of a belt of strongly folded and faulted metasedimentary rocks with a strong, NE trending structural grain cored by elongate, doubly-plunging Archaean basement domes. This contrasts with the Mudjatik Domain to the west, which is characterized by a dome and basin fold interference pattern with narrow, arcuate keels of supracrustal rocks preserved between Archaean granitoid gneiss domes [301].

Most of the uranium deposits are hosted in the Wollaston Domain or the Wollaston–Mudjatik Transition Zone, the latter representing a gradual change of structural style between the two domains. The Wollaston Domain is dominated by metasedimentary rocks of the Wollaston Group. Summarized by Sibbald [302], the group consists of three main subdivisions. The lower pelitic unit is dominated by biotite-rich pelite with variable amounts of sillimanite, cordierite and garnet. Some of the pelitic gneisses are strongly graphitic, especially near the base. This is overlain by an arkosic gneiss unit consisting of arkose, with lesser semi-pelitic gneiss and variable quantities of calc-silicate minerals, giving rise to calc-arkosic and calc-semi-pelitic units and, locally, calc-silicates. The latter are often found associated with plagioclase, predominantly albite with minor proportions of calc-silicate

minerals. The uppermost unit of the Wollaston Group is a quartzite–amphibolite unit consisting of quartzite with concordant amphibolite beds, sillimanite-bearing quartzite, calcareous arkose/semi-pelite, and minor calc-silicate, marble and pelite. This upper unit is restricted to the Wollaston Lake area and is considered correlative with the Hidden Bay assemblage. The Wollaston Group basement in the Dawn Lake Project area is similar to the pelitic and arkosic units discussed above, although with a greater proportion of calc-silicate-bearing rocks and pegmatite.

Following Hudsonian metamorphism, deformation, erosion of the orogen and regolith development, the Athabasca Group was deposited in a large intracratonic sedimentary basin in Late Palaeoproterozoic time. The group records an early period of predominantly fluvial sedimentation, transitional westwards and upwards into marine depositional environments [303].

The eastern part of the basin is comprised of a thick sequence of quartz arenite, pebbly sandstone and conglomerate of the Manitou Falls Formation, which has been subdivided by Ramaekers [304] into four lithofacies, the MFa, MFb, MFc, and MFd, which record a fining upwards sequence of early conglomerate and sandstone deposited in a high energy braided stream environment followed by more distal fluvial, and in the MFd, marginal marine sedimentation.

The basement rocks were affected by complex polyphase folding and faulting during the Trans-Hudson Orogeny. Some of these faults have undergone post-Athabasca reactivation, as evidenced by offsets of the sub-Athabasca unconformity [300, 301] and the presence of brittle fault fabrics. These post-Athabasca reactivated faults are a first order control on uranium mineralization [305, 306].

At Tamarack, the basement geology consists of an ENE trending, southerly dipping package of Wollaston Group metasedimentary rocks (Fig. 116) [307], consisting of an upper unit dominated by biotite ± cordierite gneiss with <2% graphite and a lower pelitic to psammitic unit with abundant graphite (generally >4%) [308]. Calc-silicate bands are found in both units and both are cut by abundant dykes and sills of granite pegmatite. Subparallel to the basement stratigraphy is an old ductile high strain zone (Hudsonian mylonite), exceeding 10 m in width, developed in pegmatite, showing dominantly reverse, dip-slip kinematic indicators. Subparallel, semi-brittle graphitic shears with oblique dextral reverse movement are developed in the adjacent metasedimentary basement rocks [308, 309].

The deposit is controlled by the intersection of the sub-Athabasca unconformity with the 080–085° striking, 50–70° dipping Tent Seal Fault that defines the Emperor Lake Conductor, a brittle post-Athabasca breccia and graphitic shear zone 20–100 m wide [307]. Slickenside lineations on the fault surface indicate a dominant strike-slip displacement [308]. This fault is offset by a series of NE trending, sinistral faults that also offset the mineralization [304].

The deposit is overlain by 190 m of quartz arenite and conglomerate of the Manitou Falls Formation. Mineralization is found both above and below the unconformity. Post-Athabasca displacement is indicated by 5–10 m of movement across uplifted blocks, creating E–W ridges at the unconformity [307].

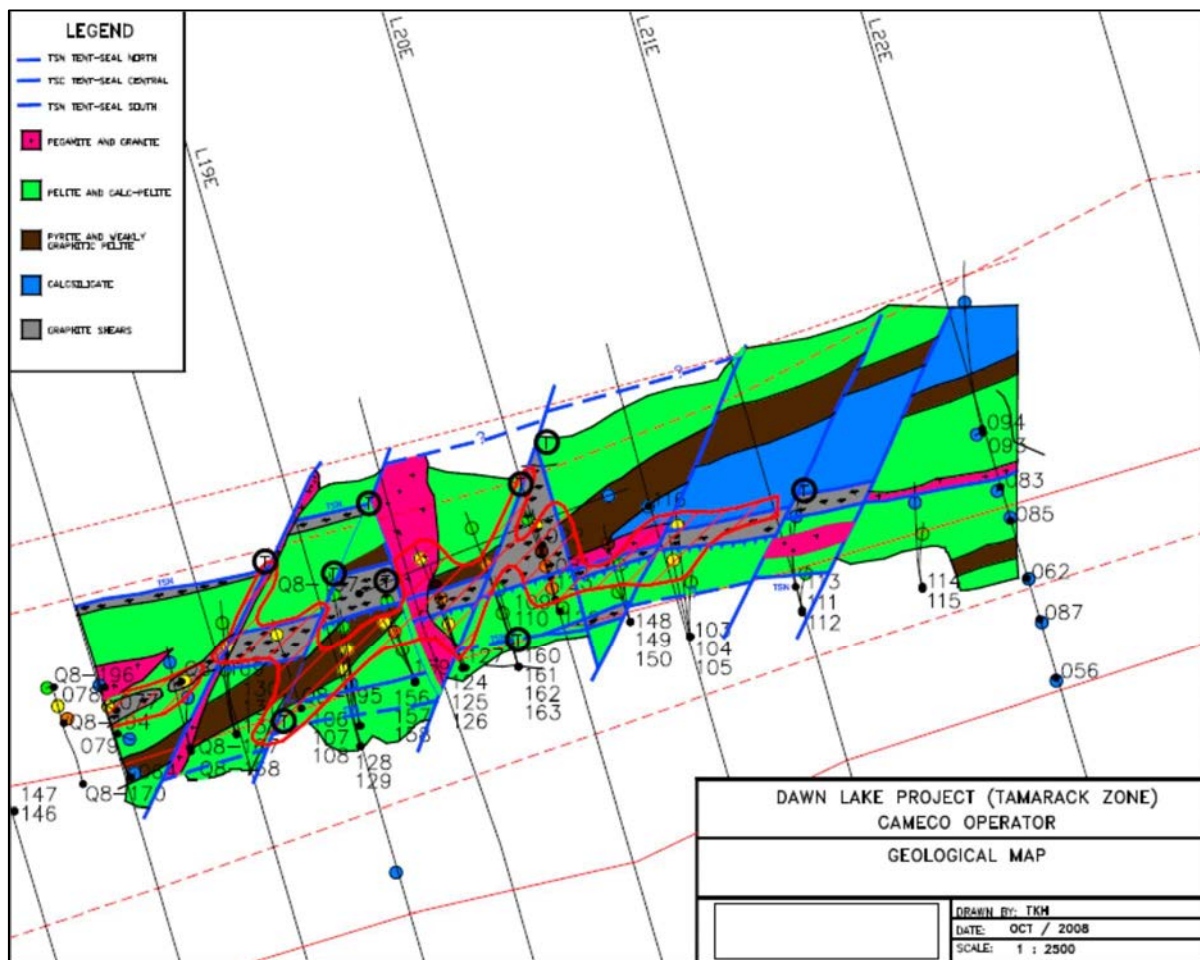


FIG. 116. Basement geology of the eastern part of the Tamarack deposit (source: G. Zaluski, CAMECO) (reproduced with permission).

### Mineralization

The Tamarack orebody is approximately 700 m long, located at the intersection of the Tent Seal Fault and the sub-Athabasca unconformity, creating an elongate, cigar shaped orebody. Summarized from Baudemont [307], the majority of the mineralization forms a zone spanning the unconformity, replacing the lower sandstone as well as the immediately underlying basement (Fig. 117). Rarely, mineralization is found along structures deeper in the basement, to depths of 5–15 m below the unconformity. The most favourable areas are at the tops of small (<10 m) ridges created by small thrust folds intersecting the unconformity. As for other classic unconformity deposits, significant quantities of Ni, Mo and Co are locally present, often associated with cross-cutting structures. Locally, mineralization is found perched in the sandstone, 15–35 m above the unconformity. These are associated with cross-cutting faults and are separated from the main zone of mineralization by a barren interval. This perched mineralization is considered to have been remobilized and exhibits a stratigraphic control.

Alteration includes haematization, pyritization, chloritization, argillization and desilicification. Quartz dissolution is noted in the sandstone above and immediately to the north of the mineralization. This is best shown by structure contours of a quartz-pebble conglomerate horizon approximately 35 m above the unconformity, which shows significant (locally up to 35%) volume reduction, as well as strong ‘sanding’ caused by dissolution of quartz cement [307]. Strong, brick red hydrothermal haematite alteration, accompanied by clay alteration, forms a halo to the mineralization, mainly in the sandstone

but also affecting the immediately underlying basement. A reduced zone of chlorite and pyrite/marcasite alteration is found close to the mineralization. A reduced basement alteration assemblage of sericite, sausserite and chlorite penetrates the basement, which is the footwall to the main fault zone [308].

Alteration clays are predominantly illite with minor kaolinite in the mineralization. A uranium halo is present in the overlying sandstone, with more than 5 ppm  $U_{\text{partial}}$  extending as high as the conglomerate marker horizon (35 m) and a level of 1 ppm  $U_{\text{partial}}$  extending well into the upper sandstone, in some cases to the subcrop. This halo spans a width of more than 40 m at the unconformity [308].

The indicated resource for Tamarack is 6895 tU at a grade of 3.75% U [310]. Grades are locally very high, in excess of 40% U in narrow intervals of many holes. The mineralization consists mainly of pitchblende, occurring as massive replacements and as blebs along haematite fronts. The highest grade portions of the deposit (especially in the west-central area) contain massive uraninite with abundant sulphides and arsenides (niccolite). A common feature is so-called 'worm rock', consisting of irregular blebs and disseminations of black pitchblende with bleached, clay-rich margins, intermingled with brick red haematite. Secondary uranium minerals are very rare [306].

#### Metallogenic aspects

The Tamarack deposit exhibits the geological characteristics typical of classic Athabasca unconformity deposits where the mineralization spans the sandstone-basement unconformity-contact.

High grade mineralization is found as an elongate, sub-horizontal orebody following the intersection of the unconformity with a graphitic basement fault reactivated during post-Athabasca time. This subtype of deposits is characterized by high grades (>2% U) of polymetallic uranium mineralization, with a strongly developed clay and haematite halo. The polymetallic nature is interpreted as a result of mixing of oxidized, uranium-bearing fluids from the sandstone mixing with base metal-, arsenic- and sulphide-rich reduced fluids sourced from the basement.

Although the deposit matches the characteristics of the class very well, some minor differences may be noted. As demonstrated by Baudemont [307], the mineralization shows strong evidence of control by, or influence of, NE trending cross-structures on high grade zones.

While dominantly reverse dip-slip displacement is typical of most unconformity deposits, the Tent Seal Fault that controls Tamarack displays mainly strike-slip displacement from post-Athabasca time. This results in only minor unconformity displacement and limited penetration into the basement along the fault. In this respect, Tamarack is similar to Cigar Lake.

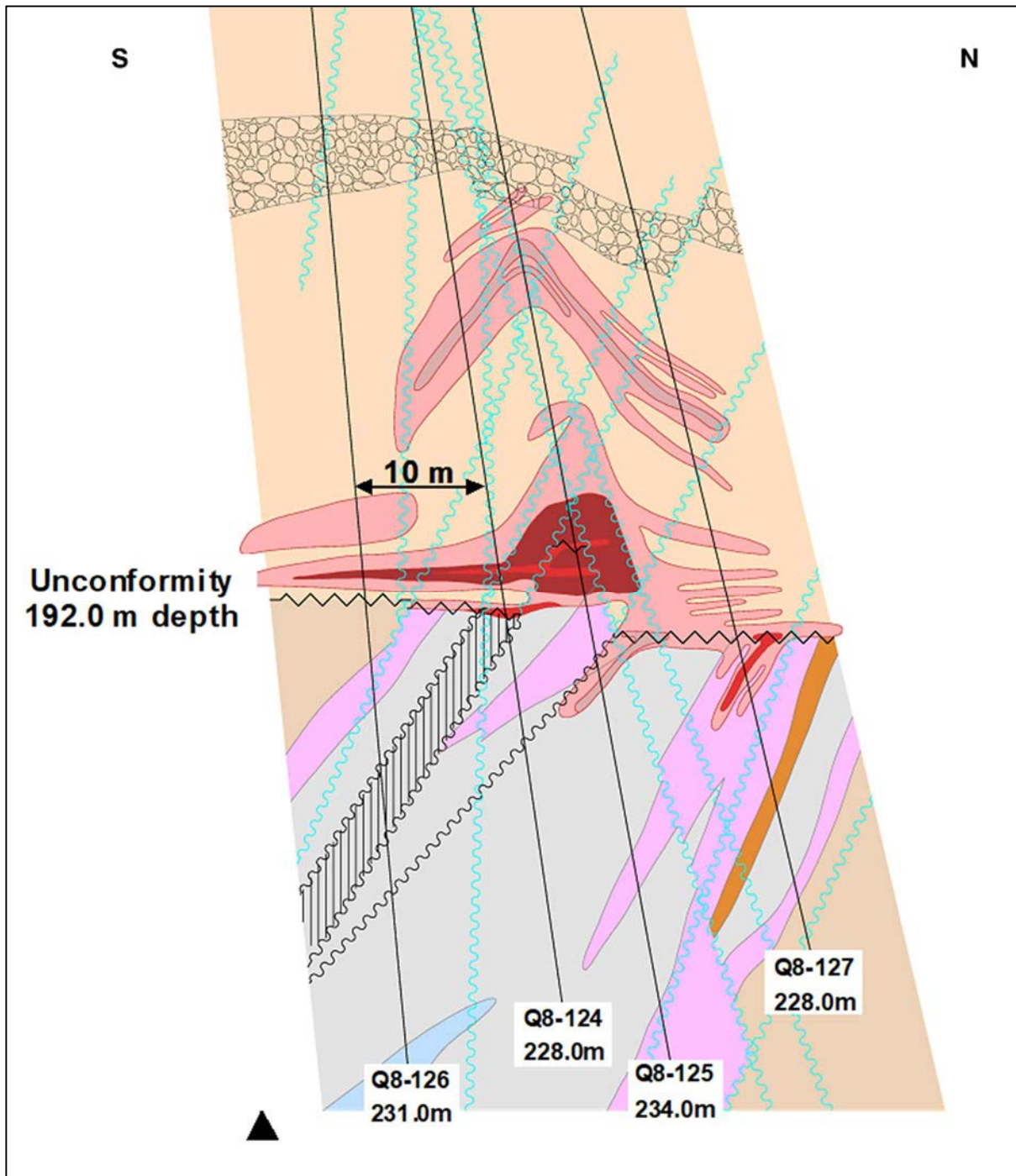


FIG. 117. Tamarack deposit cross-section showing the location of mineralization (source: G. Zaluski, CAMECO) (reproduced with permission).

### Stratiform fracture-controlled: Deposits of the north Cuddapah Basin (India)

#### Introduction

The discovery of high grade, large tonnage uranium deposits associated with the Mesoproterozoic basins of Canada [311] and Australia, prompted exploration for unconformity type uranium deposits in some of the Proterozoic basins of India during the early 1990s. Consequently, the Proterozoic Cuddapah Basin in the eastern Dharwar Craton was identified as one of the promising targets for such

deposits. Intensive uranium exploration in this basin has resulted in the discovery of uranium mineralization at the unconformity-contact between sediments and basement crystalline rocks. Four low grade, low tonnage deposits, namely Lambapur, Peddagattu, Chitrial and Koppunuru (Table 23), have been discovered in the peripheral areas of the northern part of the Cuddapah Basin (Fig. 118). Subsurface exploration is still ongoing in the peripheral areas of the basin to establish additional uranium resources in the adjoining areas of these deposits and in the deeper parts of these sub-basins.

TABLE 23. URANIUM DEPOSITS OF THE CUDDAPAH BASIN (*as of 31 December 2015*)

Deposit	Resources (tU)	Grade (% U)	Status
Chitrial	5000–10 000	0.05–0.10	Exploration
Koppunuru	700	0.070	Exploration
Lambapur	1 370	0.094	Exploration
Peddagattu	6 000	0.040	Exploration

Uranium mineralization associated with unconformities has been discovered only in the younger sediments of the Cuddapah Supergroup, i.e. the Srisailam Group and the Neoproterozoic Kurnool Group in the Palnad sub-basin. The younger formations of the Cuddapah Basin are restricted to the northern and central part of the basin. These deposits differ from the classical unconformity associated deposits of Australia and Canada by the absence of a Palaeoproterozoic sedimentary sequence below the Mesoproterozoic sediments, confinement of uranium mineralization mostly within the basement granitoids at the unconformity surface, absence of mineralization continuity extending to deeper parts of the basement granitoids along the fractures and the occurrence of uranium mineralization even in the Archaean granitoids and the Neoproterozoic sediments.

#### Geological setting

The crescent-shaped Cuddapah Basin occupies an area of 44 500 km<sup>2</sup> and contains a 12 km thick sequence of sedimentary and volcanic rocks belonging to the Palaeoproterozoic–Neoproterozoic Cuddapah Supergroup and Kurnool Group. The Cuddapah Basin is a mosaic of six sub-basins, ranging in age from Palaeoproterozoic to Mesoproterozoic to Neoproterozoic, i.e. Papaghni, Chitravati, Nallamalai, Srisailam, Kurnool and Palnad, in order of ascending age [312].

The western margin of the basin is marked by an unconformity where the formations are resting on Archaean gneisses, narrow linear greenstone belts and granites of Archaean–Palaeoproterozoic age. The eastern margin of the basin is marked by a thrust contact, where the older Archaean gneisses and Dharwar metasedimentary rocks have been thrust over the rocks of the Cuddapah Basin. The sediments of the Cuddapah Supergroup and Kurnool Group are unmetamorphosed, unfossiliferous and predominantly composed of arenaceous to argillaceous sediments with subordinate calcareous and dolomitic rocks. In the northern margins of the Cuddapah Basin, the basement is comprised of Archaean schists and gneisses, Palaeoproterozoic granites, mafic dykes, pegmatites and quartz veins. Major faults affecting the basement, as well as the overlying sediments, generally trend NNE–SSW and ENE–WSW.

Potassium–argon radiometric data obtained on mafic dykes from the south-west and north-west margins of the Cuddapah Basin suggest at least four separate periods of dyke emplacement dated at 1760–1730, 1500–1400, 1100 and 650 Ma [313]. The Sm–Nd, Rb–Sr and Pb–Pb isotopic systematics of whole rocks and mineral separates from tholeiitic mafic dykes of the Mahbubnagar Dyke Swarm intruding the granitic basement of the Cuddapah Basin suggest that the dykes were emplaced at 2170 Ma, marking an episode of crustal extension and fracturing which ultimately resulted in the formation of the Cuddapah Basin [314].

*The Srisailam sub-basin*

The Neoproterozoic Srisailam Formation, the youngest unit of the Cuddapah Supergroup deposited in the Srisailam sub-basin, forms a prominent plateau extending to about 3000 km<sup>2</sup> in the northern part of the Cuddapah Basin. It is mainly an arenaceous unit with subordinate shale intercalations. The sediments display sub-horizontal to gently south-east dips and attains a maximum thickness of 300 m. Along the northern margin, sediments of the Srisailam Formation directly overlie the basement rocks which consist of Archaean gneiss and Palaeoproterozoic granite (2268 ± 32 Ma to 2482 ± 70 Ma) [315]. Along the south-eastern margin, the Srisailam Formation overlies the Nallamalai Group of sediments with an angular unconformity. Along its northern fringes, the Srisailam sub-basin has a highly dissected topography with several flat lying sediment outliers rising 100–150 m above the general topography. The Lambapur, Peddagattu and Chitrial uranium deposits are located in three such peripheral outliers of the Srisailam sub-basin.

The basement granites/gneisses are intruded by three sets of mafic dykes, which are older than the Srisailam Formation. The Srisailam Formation consists of a lower, pebbly, gritty, arenite horizon, overlain by shale and shale/quartzite intercalations, followed by massive quartzite. The thickness of the Srisailam Formation varies around 5–70 m, with gentle dips of 3–5° to the south-east.

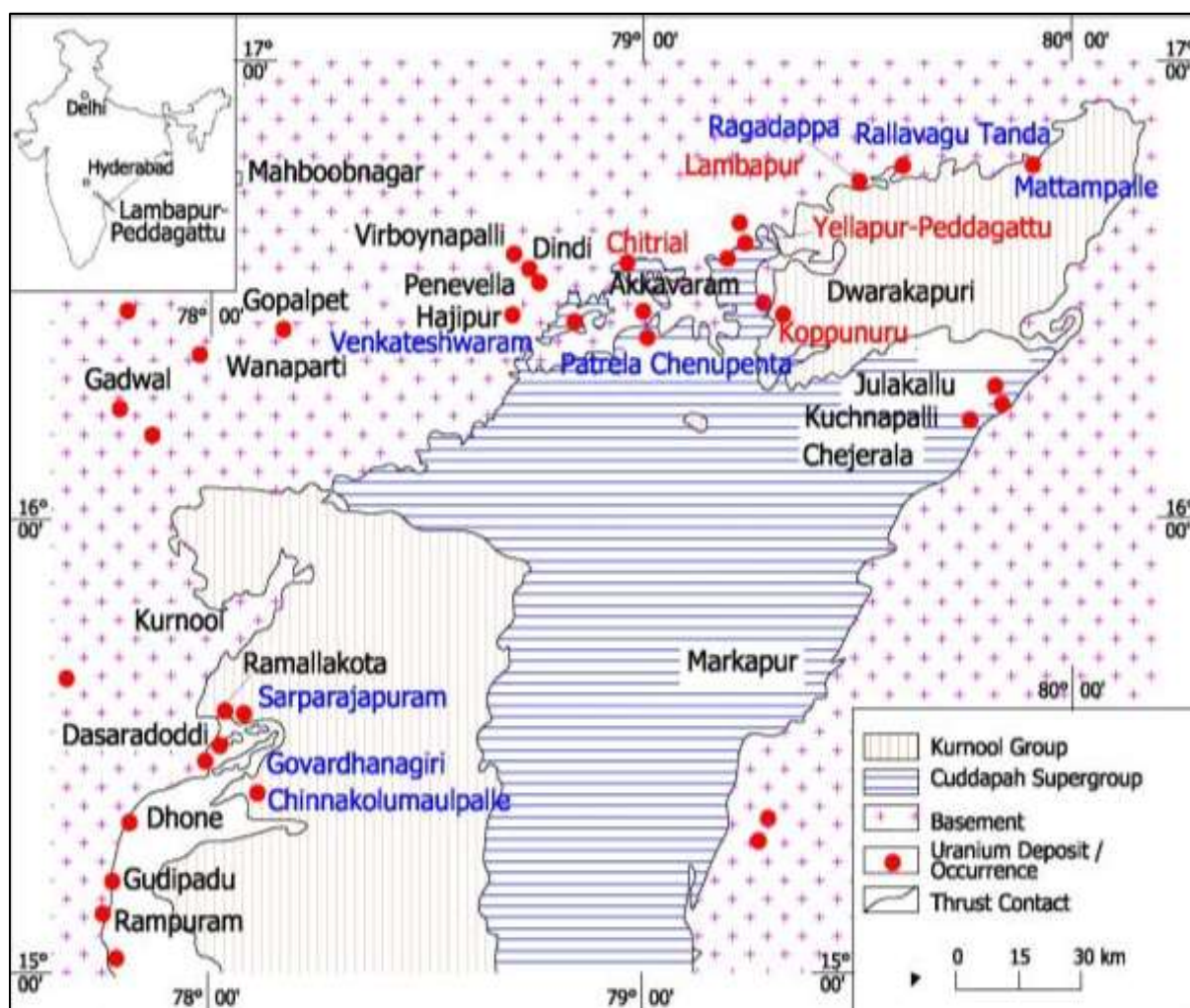


FIG. 118. Geological map of the northern part of the Cuddapah Basin showing the location of uranium deposits and occurrences (reproduced courtesy of A. Chaki).  
*The Palnad sub-basin*

The Neoproterozoic Palnad sub-basin extends over 3400 km<sup>2</sup> and consists of arenaceous, argillaceous and calcareous sediments (equivalent to the Kurnool Group in the main Kurnool sub-basin) unconformably overlying basement granite and gneiss. The sediments consist of the Banganapalle quartzite/shale, Narji limestone/calcareous shale, Owk shale and Paniam quartzite. The thickness of the sediments varies from 10 m to 450 m, with gentle south-easterly dips.

The basement granite/gneiss is essentially composed of quartz, plagioclase and alkali feldspar with accessory biotite, apatite, monazite and allanite. A thin (1–2 m) palaeosol is developed on the granite surface (represented by haematization and illitization). Mafic dykes (<1–60 m in width) trending N–S, E–W and NW–SE and quartz veins trending N–S cross-cut the basement rocks.

### Mineralization

In 1990, uranium anomalies located by ground radiometric surveys occurring along the unconformity between basement granite and overlying Srisailam sediments in the Lambapur outlier along the northern edge of the Srisailam sub-basin led to the first major breakthrough in the search for unconformity-related uranium deposits in the Cuddapah Basin. Detailed exploration at Lambapur and in adjacent outliers resulted in the discovery of three uranium deposits at Lambapur, Peddagattu and Chitrial. Continuity of basement geology and proximity of the major uranium deposits in the Srisailam sub-basin to the adjacent Palnad sub-basin led to the extension of uranium exploration into the Palnad sub-basin as well. This eventually resulted in the discovery of the Koppunuru uranium deposit [316], close to the unconformity between the basement granite and sediments of the Kurnool Group (Fig. 119).

The deposits (referred to as ‘unconformity proximal’ by Indian geologists) consist of flat ore lenses of varying thickness that occur at a depth of 1–60 m below the unconformity that separates Archaean basement granite from the Middle Proterozoic Srisailam Formation.

At Lambapur (Fig. 120), uranium mineralization is predominantly (85%) hosted in chloritized granite and locally in gritty quartzitic sandstone at the base of the Srisailam Formation. Mafic dykes and quartz veins within the granitic basement can also be mineralized close to the unconformity. In addition, the quartz veins also contain some lead and copper mineralization.

The granite is a leucocratic to mesocratic, equigranular, medium- to coarse-grained rock. It is composed of quartz, orthoclase, microcline, plagioclase and/or perthite with subordinate amounts of biotite, chlorite, apatite, zircon, allanite, ilmenite, magnetite and rare hornblende. Radioactive minerals identified include zircon, allanite and monazite. Microperthitic microcline shows post-crystalline deformation with fractures hosting clusters of chlorite, sphene and epidote, with secondary development of uranophane. The uranium (10–116 ppm, averaging 27 ppm U) and thorium (11–61 ppm, averaging 35 ppm Th) contents of the granite are high, with U/Th ratios in the range 0.34–2.32. Geochemical studies of the granites of these areas indicate that they are potassic ( $K_2O/Na_2O > 1$ ), peraluminous ( $A/CNK: 1.05–2.18$ ) and low calcic granite, without showing significant differentiation and probably formed by partial melting of silicic crustal material.

The host Srisailam arenite varies from feldspathic sandstone to arkose. The alkali feldspar contents are as high as 40% in some samples. Uraninite and secondary uranophane are hosted by fractures within these arenites.

Interpretation of drilling data indicates that the richest portions of the orebody are confined to prominent NNE–SSW and NW–SE fracture trends in the basement. In the opinion of Indian geologists, these two sets of fractures have played a major role in concentrating uranium at Lambapur. The fracture intensity within the granite, and the intersection of the fracture zones with the unconformity, are believed to control the location, grade and shape of the mineralized zones. The vertical fractures are filled with drusy quartz and kasolite associated with galena. In the south-eastern part of the Lambapur Inlier, the highest grade mineralization is oriented parallel to a NNE trending

mafic dyke, which is highly sheared on its eastern margin and cut by abundant quartz veins. The role of the mafic dykes, which may have served as a significant heat source, is not yet understood.

Characteristic uranium minerals in the Lambapur and Peddagattu deposits are uraninite, pitchblende, kasolite and uranophane, together with minor galena, chalcopyrite and pyrite. The primary uranium mineralization is interpreted as epigenetic hydrothermal in nature [317]. Locally, blebs of organic matter have also been observed in fractures in the granite.

#### Metallogenic aspects

The Lambapur, Peddagattu and Chitrial uranium deposits have similar lithostructural settings and similar styles of uranium mineralization, and their interpreted geological and geochemical controls are comparable. Features of hydrothermal activity, both in the basement and in the overlying sediments, is evidenced by high sulphide concentrations. Fluid inclusion studies of quartz occurring in mineralized granite indicate that highly saline solutions at a temperature of 100–200°C are responsible for deposition of the uranium [318].

Samarium–Neodymium isochron dating of uraninite from the Lambapur area indicates an age of  $1327 \pm 170$  Ma [315, 319]. On the basis of the above evidence, it is inferred that uraniferous hypothermal to mesothermal solutions derived from the basement rocks were responsible for the mineralization. The localization of the mineralization near the unconformity surface and mostly in the underlying granitoids is attributed to the restricted passage of hot groundwater below the shale layer of the Srisailam Formation, resulting in uranium deposition.

Vertical fractures and shears in the basement granitoids acted as conduits for the uraniferous solution. It may be noted that no significant thermal or deformation events affected the area after the deposition of the Srisailam Formation.

Unlike the Canadian unconformity type deposits, the Chitrial, Lambapur, Peddagattu and Koppunuru deposits do not overlie graphite-bearing Proterozoic metasedimentary basement rocks, only granitic basement. In addition, the Australian and Canadian deposits are localized along an unconformity between Late Palaeoproterozoic–Mesoproterozoic basins and underlying Palaeoproterozoic basement. For the unconformity associated deposits of the Cuddapah Basin, the Archaean–Mesoproterozoic unconformity forms the loci of uranium mineralization in the case of the Lambapur, Peddagattu and Chitrial deposits, whereas in the case of the Koppunuru deposit, uranium mineralization is located at the Archaean–Neoproterozoic unconformity-contact [320].

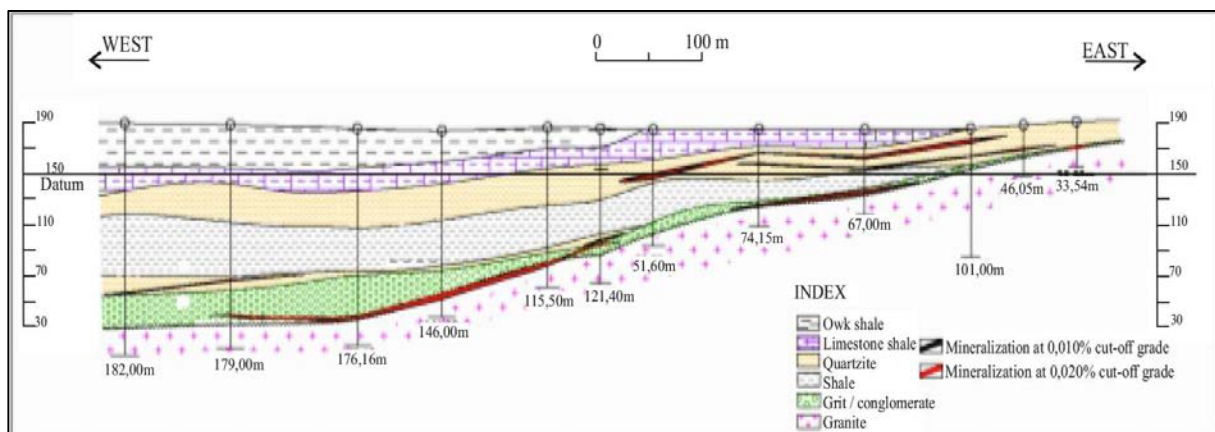


FIG. 119. Geological cross-section of the Koppunuru deposit (reproduced courtesy of A. Chaki).

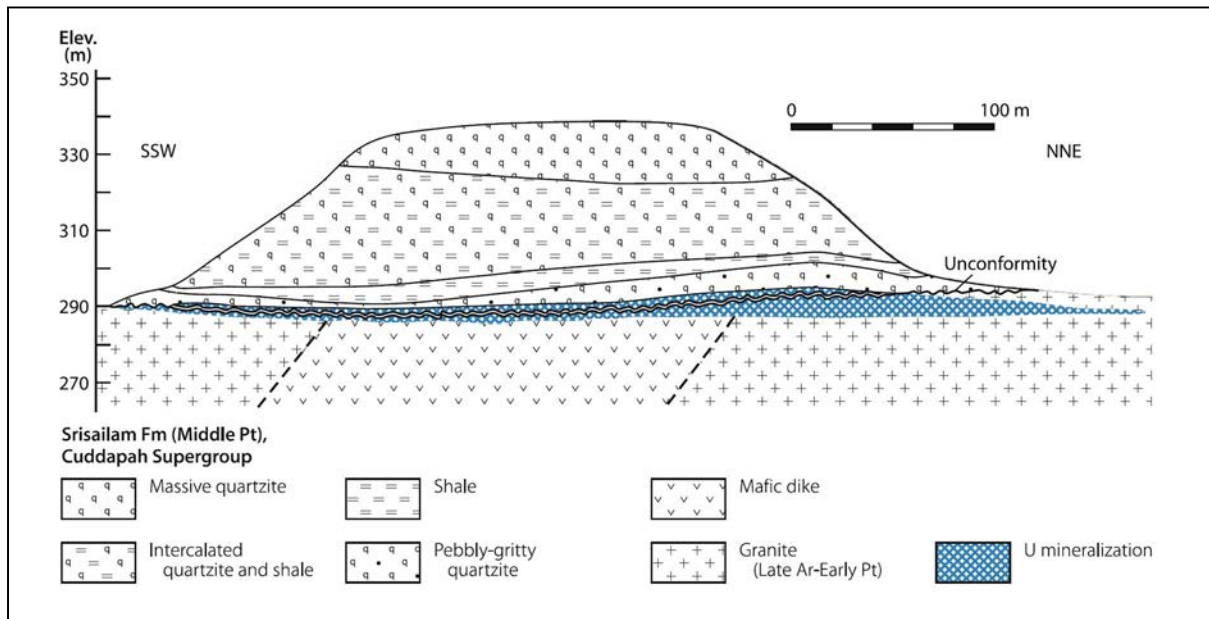


FIG. 120. Generalized geological section through the Lambapur deposit, Cuddapah Basin [19] (reproduced with permission).

### 3.8. COLLAPSE BRECCIA PIPE DEPOSITS

#### 3.8.1. Definition

The host structures for this type of uranium deposit, collapse breccia pipes, form initially by solution and collapse of caverns in a karst environment. Hundreds, perhaps thousands, of these solution-collapse breccia pipes occur in northern Arizona, USA, although not all the pipes are mineralized. Exploration in the region has shown that only a small percentage of the identified breccia pipes contain economically significant uranium mineralization. However, some of these breccia pipes contain the highest grade uranium ore in the USA. The breccia pipes of northern Arizona are believed to have formed through a sequence of steps: (i) dissolution and karst (cave) development in the Redwall Limestone unit (Fig. 121), (ii) collapse of the cavern ceiling (which forms the broken rubble) and (iii) progressive collapse stopping upwards into the overlying formations over time, forming a rubble filled column (breccia pipe). The pipe-like structures are typically less than 90 m in diameter. Mineralized pipes contain high concentrations of uranium, copper, silver, lead, zinc, cobalt and nickel minerals [321–323].

From 1951 to 1969, uranium production in the Grand Canyon region of northern Arizona derived from four breccia pipes (Fig. 122): (i) the Orphan Lode (or Orphan); (ii) Hacks (or Hack Canyon); (iii) Ridenour, and (iv) Chapel [324, 325]. Except for the Orphan Lode mine, all production was modest during this time period. The Orphan Lode mine produced about 1654 tU in 1956–1969 at an average ore grade of 0.36% U.

Exploration for breccia pipe uranium deposits was undertaken in the Grand Canyon region throughout much of the 1970s and uranium mining resumed in the 1980s. Breccia pipe deposits that were mined or thoroughly drilled during the 1980s had average grades of 0.36–0.92% U (Table 24) and the deposits ranged in size around 165–2700 tU [326]. From breccia pipe mines of this region, combined uranium production has totalled 8960 tU (as of January 2011). This total included production from the Orphan Lode pipe in 1956–1969 and mining during the 1980s and up to the early 1990s at the Hack 1,

Hack 2, Hack 3, Pigeon, Hermit, Kanab North and Pinenut mines (Fig. 122). The Arizona 1 deposit is currently being mined for its 368 tU with an average grade of 0.58% U.

Sixteen collapse breccia pipes deposits are recorded in the UDEPO database (Table 24), all of them located in the USA. The most recent breccia pipe mines of northern Arizona (1980s to present) have been underground operations (Tables 25 and 26).

TABLE 24. COLLAPSE BRECCIA PIPE DEPOSITS (*as of 31 December 2015*)

Deposit	Country	Resources (tU)	Grade (% U)	Status
Hack 2	USA	2695	0.60	Dormant
Pigeon	USA	2300	0.60	Depleted
Orphan Lode	USA	2050	0.36	Depleted
Kanab North	USA	1500	0.50	Dormant
Sage	USA	1400	0.72	Dormant
Hermit	USA	1000	0.85	Depleted
Faith	USA	900	0.16	Dormant
Canyon Mine	USA	627	0.83	Development
Pinenut Mine	USA	560	0.42	Dormant
Hack 1	USA	550	0.45	Dormant
EZ 1	USA	435	0.44	Dormant
Hack 3	USA	430	0.43	Dormant
Arizona 1	USA	405	0.56	Depleted
EZ 2	USA	380	0.37	Dormant
DB 1	USA	347	0.37	Dormant
Wate	USA	341	0.64	Dormant

### 3.8.2. Geological setting

The breccia pipes of northern Arizona are rooted in the Redwall Limestone (Mississippian) and cross-cut the Grand Canyon stratigraphy up to the Chinle Formation (Triassic). Some pipes extend vertically as much as 1200 m. The uraninite–sulphide orebodies are most often hosted in the breccia pipes at the stratigraphic horizons of the Esplanade Sandstone, Hermit Formation and Coconino Sandstone (Fig. 121). The ore minerals are confined to the breccia pipe column and the enclosing fracture zones (ring fractures): the mineral deposits do not usually extend more than a few metres into the surrounding sedimentary wall rocks. The principal form of alteration in the rocks surrounding the deposits is bleaching through removal of iron oxide minerals, turning otherwise red sandstones and siltstone into a bleached, white colour.

Breccia pipes in northern Arizona have not been observed in rock units younger than about 200 Ma (Triassic). The breccia clasts in the pipes are consistently blocks and pieces of rock units from stratigraphically higher positions relative to the surrounding stratigraphy. That is, all rocks within the breccia column (pipe) have fallen downward. In contrast to many other types of mineral deposits classified as breccia pipes, no igneous rocks are associated with the northern Arizona breccia pipes and no igneous processes contributed to their formation.

The breccia pipes are typically about 60–120 m in diameter, although, a pipe's surface expression on the plateau is usually much larger, often comprising a circular topographic depression several hundred metres or more in diameter. The collapse structure at the surface may be surrounded by a raised rim with inwardly dipping strata. However, some pipes have little expression on the plateau surface. In addition, buried or 'blind' breccia pipes exist and these pipes are rooted in the Redwall Limestone (Fig. 121) but do not extend upwards to the plateau surface.

### Mineralization

The primary ore mineral in the northern Arizona breccia pipe deposits is uraninite (UO<sub>2</sub>). The uraninite is intergrown with numerous sulphide and oxide minerals variably enriched in copper, iron, vanadium, zinc, lead, silver, molybdenum, nickel, cobalt, arsenic and selenium (Fig. 123) [321, 322]. The uraninite and other ore zone minerals are generally fine-grained, mostly less than 1 mm across.

The principal gangue minerals include Ca–Mg–Fe carbonates, Ba and Ca sulphates, phosphates and silicates. Alteration types include bleaching, pyritization, dolomitization, calcitization, gypsum/anhydrite formation, minor silicification, commonly desilicification and magnesium depletion (dolomite dissolution).

The sulphide mineralization may predate the uraninite in the breccia pipes and have a different origin. Petrographic studies suggest that the uranium mineralization occurred late in the paragenetic sequence, after most of the base metal sulphides were deposited. A large set of U–Pb isotopic analyses from the Hack 1, Hack 2, Kanab North, EZ-1, EZ-2, Arizona 1, Pinenut and Canyon pipe orebodies shows that the main uranium mineralizing event occurred about 200 Ma. Data from Canyon and Pinenut pipes, however, indicate at least one earlier phased of mineralization at approximately 260 Ma [327]. Dating of pitchblende from the Orphan Lode mine yields a minimum age of 141 Ma [328]. Kredweld and Carisey [329] report U–Pb ages of 184 and 165 Ma for ore from the EZ-2 pipe.

Ubiquitous altered hydrocarbons occur in all ore-bearing pipes although in highly variable quantities. The highest concentrations are typically found from the lower part of the Toroweap Formation downwards to the upper part of the Hermit Formation.

### 3.8.3. Metallogenic aspects

While the mineralogy and chemistry of the breccia pipe pitchblende–sulphide deposits of northern Arizona are well characterized, the origin(s) of their mineralizing fluids is still debated. Two main models for ore deposition are generally postulated: (i) flow of basin fluids upwards through the porous breccia column, driven by a regional hydraulic head [330] or (ii) downwards flow of mineralizing fluids from the top of the breccia pipes, percolating down through the breccia column during the Upper Triassic. This latter model would genetically link the formation of the breccia pipe deposits to stratabound uranium deposits commonly found in the basal sandstones of the Chinle Formation. In the first model, basinal brines moved upwards through the breccia pipe under artesian flow and mixed with uranium-bearing, oxidizing waters that flowed laterally through red bed sandstones, such as the red beds in the Supai Group strata (Fig. 121).

The compositions and types of sulphide minerals intergrown with the uraninite are similar to those found in mid-continental (United States) Mississippi Valley type deposits. Therefore, by analogy, this may indicate a basinal brine origin or influence on their formation. Fluid inclusion analyses on sphalerite and dolomite associated with the ore indicate formation temperatures of 80–173°C [321, 322]. These fluid temperatures are typical of fluids heated only by depth of burial in a basin and not influenced by magmatic or hydrothermal processes. In the model proposed by Wenrich and Titley [330], these observations are considered as evidence for a basinal brine origin for the metals (Cu, Pb, Zn, Ag, Co, Ni and As) bound with sulphur, which are abundant in collapse breccia pipe uranium deposits.

No viable uranium source has yet been established but it is postulated that uranium sources may have been: (i) crystalline Proterozoic basement underlying the Arizona Strip area; (ii) crystalline Proterozoic rocks already cropping out in Triassic time in the Mogollon Highland at the southern margin of the Colorado Plateau; (iii) fluvial channel sediments of the lower Chinle Formation of Triassic age, which covered NW–SE trending part of the Arizona Strip area; (iv) fluvial sediments of the Jurassic Morrison Formation found to the east and north-east of the Arizona Strip, and (v) altered volcanic material forming the bentonitic component of the Petrified Forest Member of the Chinle Formation [47].

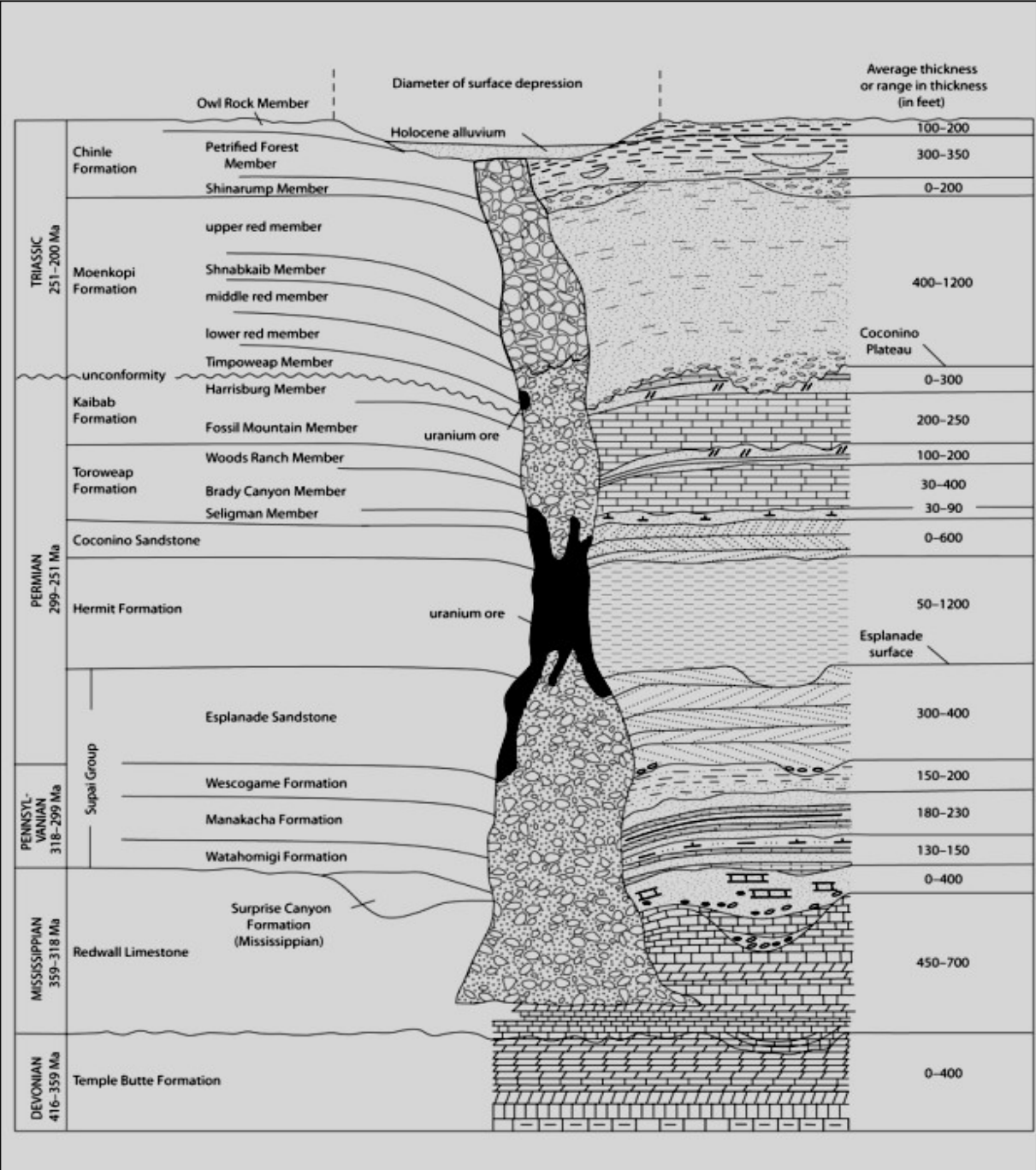


FIG. 121. Schematic representation of a solution collapse breccia pipe in northern Arizona, USA, showing the relation of the breccia pipe to the surrounding strata and uranium orebodies (diagram is not to scale). The width across a breccia pipe is typically 60–120 m [19] (reproduced with permission).

### 3.8.4. Description of a selected deposit: The Canyon deposit (USA)

#### Introduction

Although the price of uranium dropped dramatically in the early 1980s, existing purchase contracts and the high grades of the breccia pipe deposits in northern Arizona made mining economically viable. During the 1980s and early 1990s, several breccia pipe deposits were mined for uranium (Table 24), the Hack 1, Hack 2, Hack 3, Pigeon, Hermit, Kanab North and Pinenut pipes. Mining at the first five breccia pipes was completed and the sites were reclaimed. The Kanab North breccia pipe deposit (Fig. 124) was also mined, but minor amounts of uranium ore remain and the site has been on standby status since 1992. The Pinenut deposit was partially mined (Tables 25 and 26); the mine has been on standby status since 1989. The Arizona 1 breccia pipe was developed with a shaft by 1992, but operations ceased before ore was produced. Energy Fuels Inc. reopened the mine in December 2009 and, up to the beginning of 2013, had produced 462 tU at a grade of 0.53% U [331].

In the late 1980s, surface operations at the Canyon breccia pipe were developed and a shaft collared to a depth of 15 m in preparation for underground mining. Owing to a steep decline in uranium prices, further development of the mine was suspended and no ore was extracted. Energy Fuels acquired the deposit from Denison Mines in 2012 and sunk a shaft with production scheduled to start in 2017. The Canyon breccia pipe is located about 10 km south-east of Tusayan, Arizona, (Fig. 122). Reserves amount to 627 tU with a grade of 0.83% U [331]. Copper and silver will be extracted as co-products.

#### Geological setting

The surface expression of the Canyon breccia pipe, on the Coconino Plateau, corresponds to a sage covered, elliptical clearing in a ponderosa pine forest. The boundaries of the clearing define a shallow basin that overlies the collapse structure. The clearing is about 610 m long by 490 m wide. The underlying breccia pipe averages less than 60 m in diameter. The pipe narrows within the horizons of the Coconino Sandstone and Hermit Formation [332], as shown schematically in Fig. 121.

The outcropping stratigraphic unit of the Canyon breccia pipe is the Harrisburg Member of the Kaibab Formation (Fig. 121). As the Canyon breccia pipe is rooted in the Redwall Limestone, its vertical extent from its base within a collapsed cavern in the Redwall Limestone up to the plateau surface is approximately 830 m.

#### Mineralization

Drilling of the Canyon breccia pipe by Energy Fuels in the 1980s defined a zone of abundant sulphide minerals (the 'sulphide cap') near the contact of the Toroweap Formation and the underlying Coconino Sandstone [332]. The drilling revealed that uranium mineralization extends for at least 490 m vertically through the breccia pipe, from the lower Toroweap Formation down to the upper Redwall Limestone. The orebody has a reported grade of 0.83% U for a resource of approximately 627 tU. This ore occurs mainly in the Coconino, Hermit and Esplanade Formations within the pipe [332].

Uraninite (UO<sub>2</sub>) is the primary uranium ore mineral and many sulphide minerals are intergrown with the uraninite [321, 322]. The sulphides include sphalerite (ZnS), galena (PbS), rammelsbergite (NiAs<sub>2</sub>), nickeline (NiAs), gersdorffite (NiAsS), cobaltiferous gersdorffite [(Co,Ni)AsS], bravoite [(Ni,Fe)S<sub>2</sub>], stibnite (Sb<sub>2</sub>S<sub>3</sub>), chalcopyrite (CuFeS<sub>2</sub>), pyrite (FeS<sub>2</sub>), arsenopyrite (FeAsS), tennantite–tetrahedrite [Cu<sub>10</sub>(Fe,Zn)<sub>2</sub>(As,Sb)<sub>4</sub>S<sub>13</sub>], siegenite (CoNi<sub>2</sub>S<sub>4</sub>), vaesite (NiS<sub>2</sub>), millerite (NiS), skutterudite (CoAs<sub>3</sub>), linnaeite (Co<sub>3</sub>S<sub>4</sub>), molybdenite (MoS<sub>2</sub>), lautite (CuAsS) and enargite (Cu<sub>3</sub>As<sub>4</sub>). Gangue minerals include baryte, quartz, kaolinite, calcite, dolomite, ankerite, siderite, anhydrite and fluorite.

Isotopic U–Pb analyses of uraninite from the Canyon breccia pipe suggested two main phases of uranium mineralization; one at about 200 Ma and an earlier event of about 260 Ma [327]. Petrographic studies suggest that in most of the breccia pipe deposits, the uranium mineralization occurred after

most of the Co, Cu, Fe, Mo, Ni, Pb and Zn mineralization. However, some copper-, lead- and zinc-bearing minerals in the Canyon pipe deposits appear to have formed after uraninite [333].

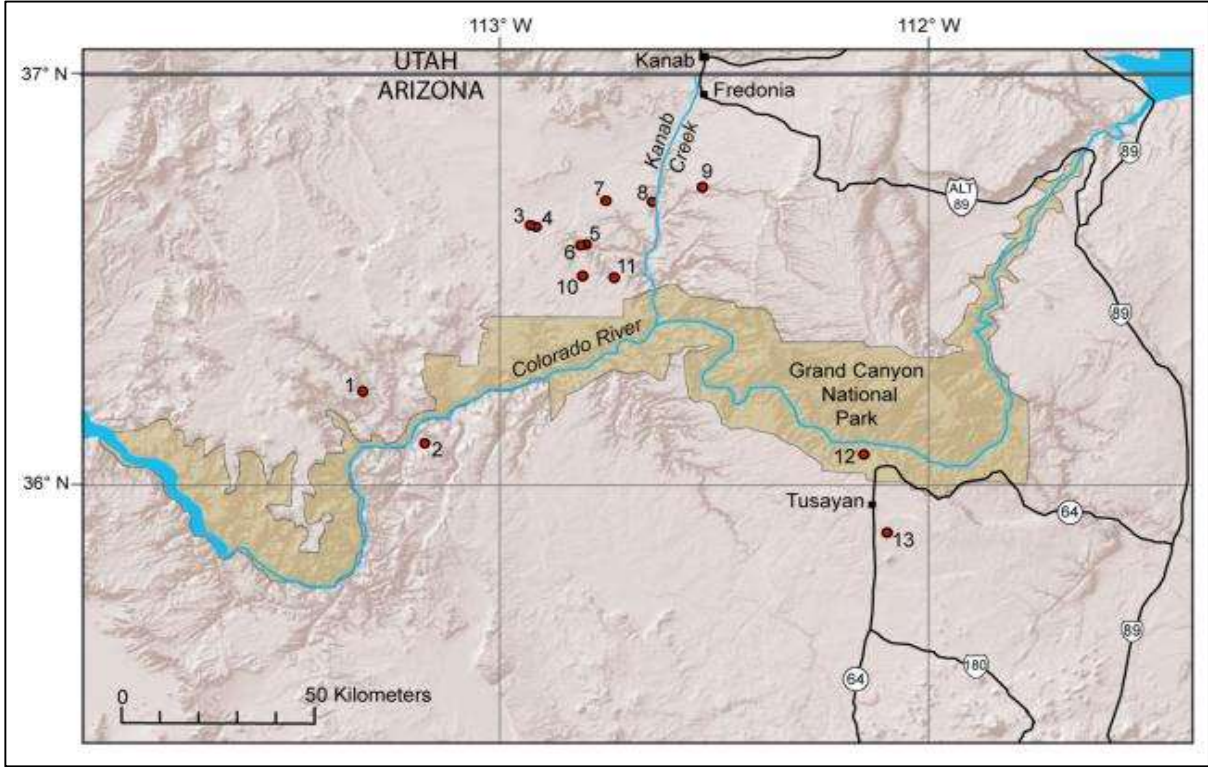


FIG. 122. Index map of the Grand Canyon region of north-western Arizona, USA, showing the solution collapse breccia pipe uranium deposits that have been mined in this region. The uranium mines are: (1) Chapel, (2) Ridenour, (3) EZ-2, (4) EZ-1, (5) Hack Canyon and Hack 1, (6) Hack 2 and Hack 3, (7) Hermit, (8) Kanab North, (9) Pigeon, (10) Arizona 1, (11) Pinenut, (12) Orphan and (13) Canyon. Hundreds of breccia pipes have been mapped in this region (see Plate 1 of Alpine, <http://pubs.usgs.gov/sir/2010/5025/>). An undetermined number of these breccia pipes are mineralized and some contain economic uranium mineralization [334] (reproduced with permission).

TABLE 25. PRODUCTION FROM SEVEN MODERN (1980s and 1990s) BRECCIA PIPE MINES IN NORTHERN ARIZONA, USA (adapted from OTTON and VAN GOSEN [326])

Mine	Production (M/lb U <sub>3</sub> O <sub>8</sub> )	Production (tU)	Average grade (% U)	Status
Hack 2	7.0	2693	0.59	Reclaimed site
Pigeon	5.7	2192	0.55	Reclaimed site
Kanab North	2.77	1065	0.45	Standby status since 1992
Hack 1	1.42	546	0.45	Reclaimed site
Hack 3	1.12	431	0.42	Reclaimed site
Hermit	0.55	212	0.64	Reclaimed site
Pinenut	0.526	202	0.86	Standby status since 1989

TABLE 26. INFERRED URANIUM RESOURCES ESTIMATED TO EXIST WITHIN PREVIOUSLY MINED OR SUFFICIENTLY DRILLED BRECCIA PIPE DEPOSITS IN NORTHERN ARIZONA, USA  
(adapted from OTTON and VAN GOSEN [326])

Mine	Resources (M/lb U <sub>3</sub> O <sub>8</sub> )	Resources (tU)	Grade (% U)	Status
Arizona 1	1.2	462	0.63	Operating
Canyon	1.6	627	0.83	Development
Pinenut	0.873	336	0.37	Operating
Kanab North		Minor reserves remain		Standby since 1992
EZ-1	0.436	168	0.46	Undeveloped
EZ-2	0.428	165	0.36	Undeveloped



FIG. 123. Example of uranium ore from a solution collapse breccia pipe in northern Arizona, USA. This breccia is from the Pigeon (mine) breccia pipe. The sample contains 0.606% U, 0.25% As, 0.13% Zn, 0.07% Ni and many other metals. Uraninite (UO<sub>2</sub>) is the principal uranium mineral. Photograph courtesy of B. Van Gosen (reproduced with permission).



*FIG. 124. Kanab North (breccia pipe) mine site above Kanab Creek, north-central Arizona, USA. The mine has been on standby status since 1992. From 1988 through 1990, the mine produced 1065 tU from a breccia pipe deposit with an average grade of 0.4% U. Photograph courtesy of D. Bills, US Geological Survey and taken on 25 August 2009 (reproduced with permission).*

### 3.9. SANDSTONE DEPOSITS

#### 3.9.1. Definition

Sandstone uranium deposits occur in carbon- and/or pyrite-bearing fluvial (less commonly marine), arkosic, medium- to coarse-grained sandstones that contain, are interbedded with and are bounded by less permeable horizons. The primary uranium minerals are predominantly pitchblende, coffinite and, to a lesser extent, uranium-bearing vanadates and phosphates [335–337]. Uranium is precipitated under reducing conditions caused by the presence of a variety of reducing agents within the sandstones (for example, carbonaceous material, sulphides, hydrocarbons and ferromagnesian minerals such as chlorite). Major known sandstone deposits range in age from Palaeozoic to Tertiary. There are also small Precambrian sandstone deposits associated with carbonaceous matter of probable algal origin and deposits associated with mafic dykes and sills intruding Proterozoic sandstones.

Sandstone uranium deposits are amenable to conventional open pit and underground mining methods, for example the Arlit district (Niger), or by in situ leaching and heap leaching (Australia, China, Kazakhstan, the Russian Federation, the USA and Uzbekistan).

A total of 662 uranium deposits associated with sandstones are recorded in the UDEPO database. In 2015, 55% (33 520 tU) of world production was derived from sandstone deposits.

### 3.9.2. Geological setting

Sandstone uranium deposits are divided into five main subtypes (Fig. 125) which are listed below along with representative examples:

- (i) Basal channel subtype: Dalmatovskoye, Khiagdinskoye (Russian Federation) and Beverley (Australia);
- (ii) Tabular subtype: Akouta, Imouraren and Arlit (Niger), Coutras (France) and Ambrosia Lake and Colorado Plateau (USA);
- (iii) Roll-front subtype: Moinkum, Inkai and Mynkuduk (Kazakhstan), Crow Butte and Smith Ranch (USA) and Bukinay, Sugraly and Uchkuduk (Uzbekistan);
- (iv) Tectonic-lithologic subtype: Mikouloungou (Gabon) and Mas Lavayre (France);
- (v) Mafic dykes–sills in Proterozoic sandstone subtype: Matoush (Canada) and Westmoreland district (Australia).

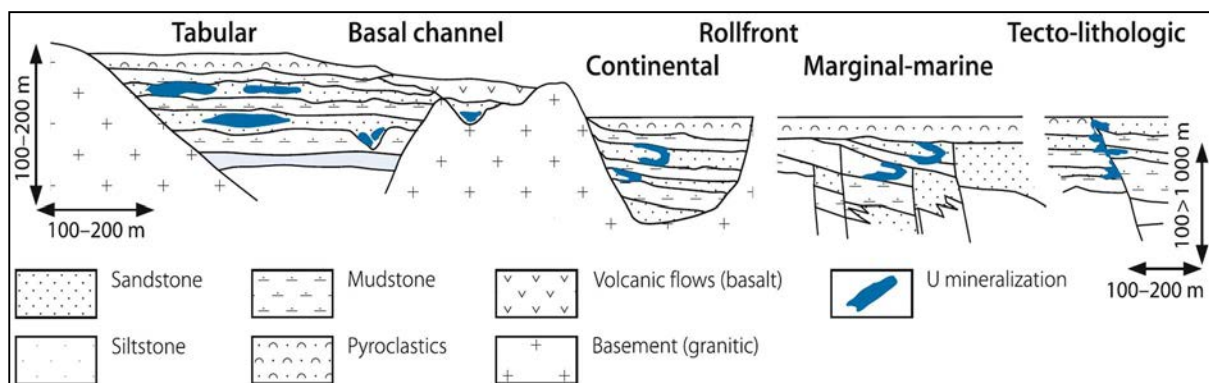


FIG. 125. Sandstone-hosted uranium deposits [19] (reproduced with permission).

With few exceptions, sandstone uranium deposits are of diagenetic–epigenetic, low temperature origin. Groundwater chemistry and migration are instrumental in leaching uranium from source rocks and transporting it in low concentrations to a chemical interface commonly provided by reducing or precipitating agents where it is deposited. Essential parameters that control these processes include a uranium source, host rock lithology and permeability, groundwater chemistry amenable to leaching and transporting uranium, depositional environment, adsorptive/reducing agents and an arid to semi-arid climate.

Fluvial, first cycle feldspathic or arkosic sandstones (weakly mature) of limited thickness (<10 m) interbedded with layers of fine-grained, low permeability clastic sediments deposited in intracratonic basins provide the most favourable host rocks for large, relatively high grade sandstone-hosted uranium deposits. Marginal marine environments are also prospective, but to a lesser degree. The presence of uraniferous tuffaceous material either as a constituent of the host sandstone or in overlying strata may enhance the favourability of a fluvial sequence owing to its potential as a uranium source rock. Felsic volcanic and crystalline terrains are also considered to be potential uranium source rocks for sandstone uranium deposits.

The feldspar component of the host rocks, though probably of no direct importance in the mineralizing process, indicates a granitic source from which the uranium may have originated combined with an environment of rapid erosion and sedimentation providing the required hydrological conditions, particularly permeability for adequate groundwater migration. Impermeable or less permeable strata or

other barriers may be instrumental in vertically and laterally channelling uraniferous fluids to favourable sites of deposition, while at the same time prohibiting widespread flushing and dilution of fluids.

Uranium is soluble in large quantities only in its hexavalent state. Therefore, uranium transporting fluids must be sufficiently oxygenated to keep the uranium in solution for transport, but at the same time limited in oxidizing potential so that the reduction and precipitation of uranium generates high enough grades and in sufficiently high quantities to be commercially important. Complexing agents such as carbonate ions are important for enhancing the solubility and mobility of the uranyl ion in neutral to alkaline groundwater in either oxidizing or reducing conditions [338].

Hexavalent uranium in solution must be reduced to the tetravalent state in order to form commercially significant concentrations of pitchblende or coffinite, the principal uranium minerals in most reduced sandstone deposits. Under certain conditions, uranium minerals may also precipitate in an oxidizing environment when complexing agents such as vanadium compounds are present to fix the uranyl ion in the form of uranyl vanadates that are quite stable in oxidized rocks. A reductant is required to convert (reduce) hexavalent uranium to tetravalent uranium. Many substances have been invoked as uranyl reductants, including partially coalified vegetal matter, woody fragments (coalification not higher than sub-bituminous), amorphous organic matter (humate), petroleum, so-called 'dead oil', 'sour' natural gas, hydrogen sulphide and pyrite or other sulphides. Bacterial activity is considered by some authorities to be an important factor in producing a reducing environment.

### **3.9.3. Basal channel sandstone deposits**

#### *3.9.3.1. Definition*

The palaeodrainage systems that host basal channel sandstone deposits consist of channels, several hundreds of metres in width, filled with thick, permeable alluvial-fluvial sediments. The uranium mineralization is predominantly associated with detrital plant debris in orebodies that display, in plan view, an elongated lens or ribbon-like configuration and in cross-section, a lenticular or, more rarely, roll shape. Typical examples of basal channel deposits include those at Dalmatovskoye and Khiagda (Russian Federation) and at Beverley and Four Mile (Australia).

In 2015, 78 basal channel sandstone deposits were recorded in the UDEPO database. Of these, 24 are located in the USA and 16 in the Russian Federation. Three deposits are currently producing, Dalmatovskoye and Khiagda (Russian Federation) and Semizbai (Kazakhstan). The sizes of the deposits vary from a few hundred tonnes to 19 000 tU for the largest one, Ryst Kuil (South Africa), with grades ranging between 0.02 and 0.20% (Table 27).

#### *3.9.3.2. Geological setting*

Basal channel sandstone deposits occur in poorly consolidated, highly permeable, fluvial to lacustrine, carbonaceous gravels and sands deposited in palaeovalleys incised in basement rocks of generally granitic composition and capped by plateau basalts and sediments. They are transitional between surficial deposits and sandstone-hosted deposits. Uranium is leached from the granitic basement and precipitated by reaction with the organic matter during groundwater percolation through permeable sediments between low permeability basement rocks and capping basalt. The basal channel subtype is referred to as 'palaeovalley' or 'infiltration' type uranium deposits in the terminology of Russian Federation geologists.

TABLE 27. MAIN BASAL CHANNEL SANDSTONE URANIUM DEPOSITS (as of 31 December 2015)

Deposit	Country	Resources (tU)	Grade (% U)	Status
Ryst Kuil	South Africa	19 300	0.088	Exploration
Semizbai	Kazakhstan	17 400	0.057	Operating
Four Mile West	Australia	16 155	0.028	Development
Malinovskoye	Russian Federation	15 000	0.050	Exploration
Beverley	Australia	13 820	0.0229	Care and maintenance
Hansen	USA	11 500	0.090	Dormant
Khiagda	Russian Federation	11 300	0.055	Operating
Four Mile East	Australia	11 155	0.026	Development
Khokhlovskoye	Russian Federation	10 000	0.050	Exploration
Zheglvskoye	Russian Federation	7 900	0.062	Exploration
Dobrovolnoye	Russian Federation	7 400	0.056	Dormant
Dalmatovskoye	Russian Federation	6 800	0.041	Operating
Tetrakskoye	Russian Federation	6 400	0.047	Exploration
Boyer	USA	6 240	0.0555	Exploration
Chengzishan	China	6 000	0.05–0.10	Dormant
Sherwood Mine	USA	5 800	0.080	Depleted

### 3.9.3.3. Description of selected deposits

#### The Khiagda deposit (Russian Federation)

##### Introduction

The Khiagda deposit is located in the Vitim district, about 150 km north of the town of Chita. It is situated on the Amalat Plateau, in the upper part of Vitim River system. The deposit includes the Khiagda orefield and some other isolated deposits and occurrences hosted by recent channels. Resources in the Vitim district are estimated at 52 000 tU, while speculative resources are of the order of 100 000 tU [339].

##### Geological setting

The Khiagda orefield constitutes the major portion of the Vitim district. It is situated 150 km north of the town of Chita and covers an area of 250 km<sup>2</sup>. It consists of eight deposits with similar geology: Khiagda, Tetrakhsokoye, Vershinnoye, Dybryn, Namaru, Koretkonde, Istochnoye and Kolichikan (Fig. 126). The distance between deposits varies between 1.5 km and 6.0 km. The resources of the Khiagda orefield total 44 800 tU. Total speculated resources are estimated to be about 60 000 tU. Khiagda, the largest deposit, contains about 15 500 tU. Resources at Tetrakhsokoye are in excess of 5000 tU and the other deposits contain between 1500 and 5000 tU each. Their grades average between 0.05 and 0.3% U. However, there are no definite boundaries between the deposits. Each of them consists of several closely situated orebodies.

Proterozoic metamorphic rocks (schist, gneiss and migmatite) intruded by Palaeozoic granite constitute the basement of the Vitim district. The old peneplain was deeply weathered by a semi-arid to arid climate and incised by a palaeodrainage system. The system consists of tributary channels combining into two major ancestral rivers which bound the margins of the Buysiuchan Plain. More

than 50 m of Oligocene–Miocene sediments, predominantly of colluvial and, along thalwegs, of alluvial provenance, fill the palaeochannels. The sediments consist of grey and multicoloured carbonaceous clay–siltstone, sandstone, conglomerate and tuff with some intercalated lignite seams. Grey facies contain pyrite and are enriched in plant debris. Carbon content averages about 0.8%  $C_{org}$ . A cover of 10–30 m, locally up to 250 m thick, Quaternary tuffaceous sand and gravel intercalated with or overlain by basalt lenses or sheets overlies the older rocks [47].

Originally grey host rocks are oxidized to multicoloured facies in which pyrite, siderite and organic matter are replaced by iron hydroxides. The oxidation front developed from the sides of the palaeovalleys. Bleaching due to reduction has produced a whitish facies along the interface of grey and multicoloured rocks.

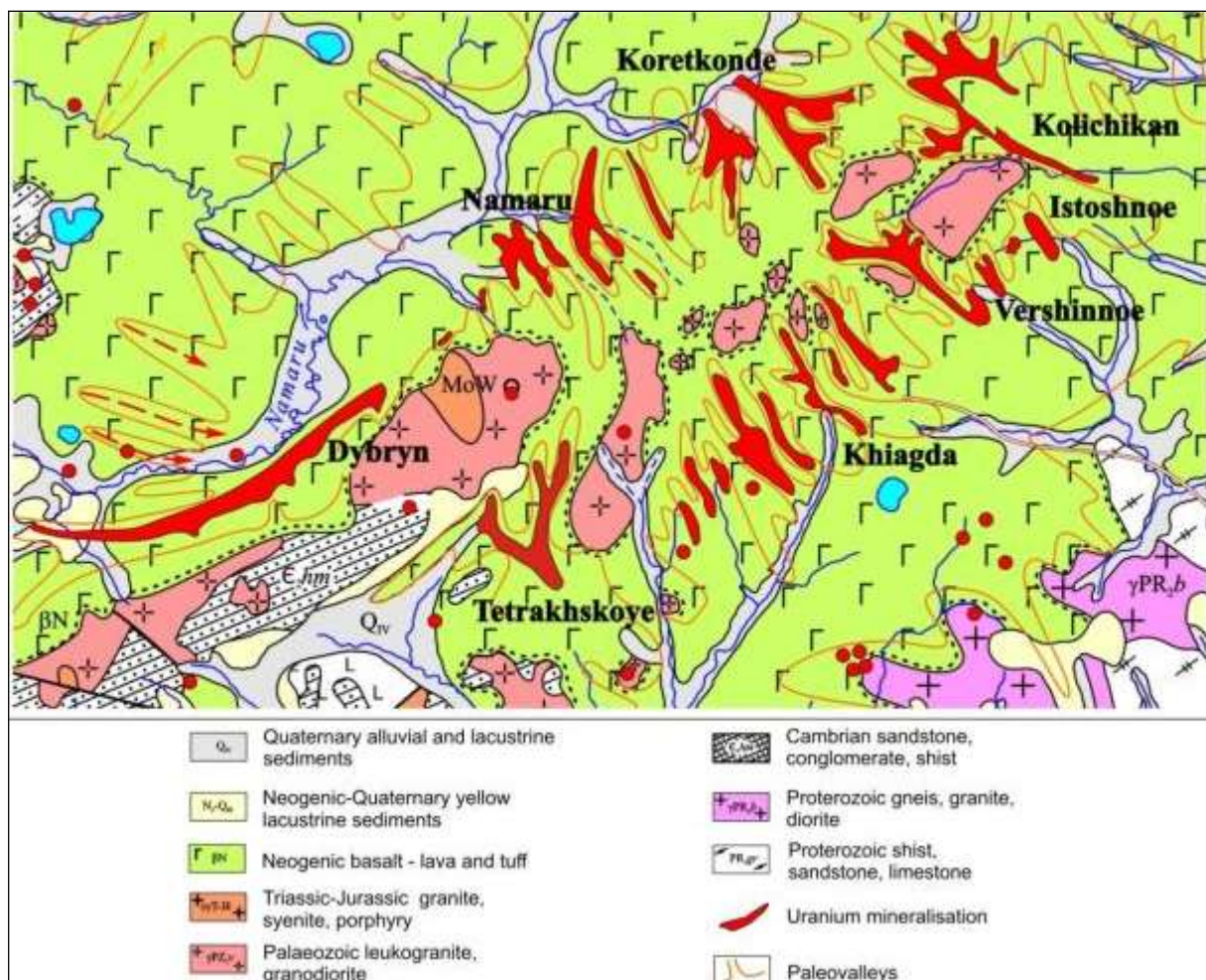


FIG. 126. Geological map of the Khiagda orefield (reproduced courtesy of A. Boitsov, ARMZ/Uranium I).

### Mineralization

The principal uranium minerals comprise oxides, coffinite and, rarely, ningyoite. Some uranium is also adsorbed onto carbonaceous matter and clays. Dating of uranium minerals yields ages ranging from 25 Ma to Recent. Associated elements present in orebodies in concentrations of 5–400 times the Clarke values include Mo, Zn, Co, Zr, Cu, Y, Sc and lanthanides. Minor phases include arsenopyrite, galena, marcasite, pyrite, sphalerite and haematite.

Uranium deposits are restricted to channel sections underlain by granite. Channels in metamorphic terrains are barren of uranium but may contain gold. Ore minerals occur as disseminations, mostly in sandstone and conglomerate in basal parts of the palaeochannel.

Individual deposits contain several hundred tonnes to more than 5000 tU. They consist of orebodies which are ribbon-like in plan view, trending along channel axes, and in cross-section exhibit elongated roll or lens shapes. Orebodies are up to 3 km long, 150–400 m wide and from less than 1 m to a maximum of 23 m thick. They occur commonly at depths of 150–200 m. Ore grades range from 0.01 to 0.5% U.

The Khiagda deposit is the largest deposit of the district and contains about 15 500 tU. Mineralization occurs in permeable, poorly consolidated Neogene fluvial sediments filling relatively narrow tributary palaeovalleys. The basement consists of Palaeozoic granite. Ore-hosting sediments are capped by basalt of Neogene–Quaternary age (Fig. 127).

The thickness of the ore-hosting horizon varies from several metres up to 120 m and the depth varies around 60–240 m (averaging 170 m). Mineralization occurs in lens and lenticular (ribbon-like) orebodies. Single orebodies are 850–4100 m long, 15–400 m wide and 1–20 m thick. The principal minerals are pitchblende, coffinite and sooty pitchblende, mainly present as disseminations.

The Khiagda uranium deposit is mined as an in situ recovery mining operation. The potential capacity of the processing plant is 2000 tU/year.

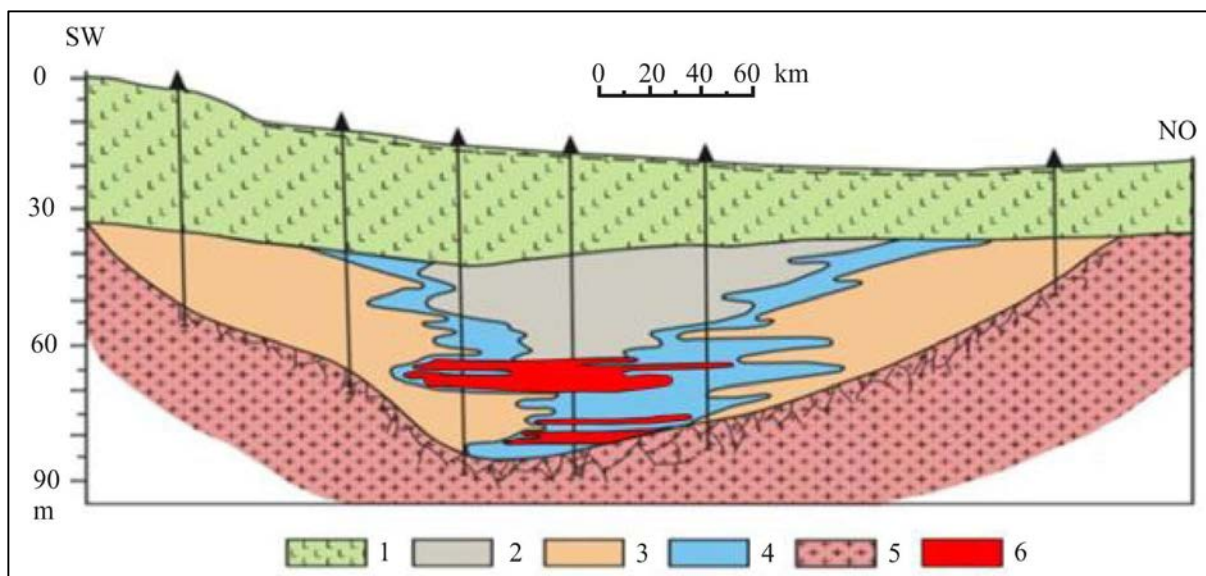


FIG. 127. Typical cross-section through the Khiagda deposit: (1) basalt; (2–4) Neogene permeable sediments (sand, silt, clay); (2) grey; (3) oxidized yellow; (4) reduced white); (5) granite, and (6) uranium orebodies (reproduced courtesy of A. Boitsov, ARMZ/Uranium 1).

#### Metallogenic aspects

Uranium ore formation is considered to be of epigenetic origin, resulting from the infiltration of oxygenated, uranium-bearing vadose water. The porous, predominantly sandstone channel facies served as the conduit through which the fluids migrated. Precipitation of uranium occurred where the solutions encountered sufficiently high concentrations of carbonaceous matter to establish a redox front along which the dissolved hexavalent uranium was reduced and deposited. The ribbon-like

configuration of the orebodies, stretching along the axes of valleys suggests that the mineralizing fluids entered the valley from the flanks [19]. Palaeozoic granite of the basement is favoured as the most likely source of uranium. Granitic facies contain uraninite and have elevated uranium background values reportedly of up to 80 ppm U. Another potential source is the tuffaceous constituents of the cover sediments [19].

### **3.9.4. Tabular sandstone deposits**

#### *3.9.4.1. Definition*

Tabular uranium deposits consist of uranium matrix impregnations that form irregularly shaped lenticular masses within reduced sediments. The mineralized zones are largely oriented parallel to the depositional trend. Examples of tabular sandstone deposits include Hamr-Stráz (Czech Republic), Imouraren, Akouta and Arlit (Niger) and the deposits of the Colorado Plateau (USA) (Table 28).

A total of 306 tabular sandstone deposits are recorded in the UDEPO database. The resources of individual tabular uranium deposits vary widely, ranging from clusters of relatively small deposits in the 300–1500 tU range, which is typical of the Saltwash vanadium–uranium deposits, to intrinsic and extrinsic carbon-related deposits that exceed 50 000 tU. Original resources at Arlit and Akouta in Niger, the two largest known intrinsic carbon-related districts, exceeded 50 000 tU each, with average grades of 0.35% and 0.50% U, respectively.

Cumulative production through 2015 from the Akouta underground mine (mill capacity 1600 tU/year) and the Arlit open pit mine (mill capacity 2700 tU/year) totalled approximately 140 000 tU. AREVA is the operator of both operations in Niger and is developing the very large Imouraren deposit which has resources in excess of 200 000 tU.

Uranium production from extrinsic carbon-related deposits in New Mexico is estimated to have totalled approximately 124 200 tU. The largest single known deposit in the Ambrosia Lake district, Mt Taylor, has resources totalling 16 150 tU, with an average grade of 0.42% U. Mining at Mt Taylor was suspended in 1990. Most of the mining in the Ambrosia Lake district was undertaken by underground methods.

TABLE 28. PRINCIPAL TABULAR SANDSTONE DEPOSITS (as of 31 December 2015)

Deposit	Country	Resources (tU)	Grade (% U)	Status
Imouraren	Niger	276 200	0.07	Care and maintenance
Ambrosia Lake	USA	64 970	0.144	Partially depleted
Dasa 1-2-3	Niger	64 680	0.048	Exploration
Nyota	United Republic of Tanzania	55 135	0.025	Dormant
Rietkuil	South Africa	54 960	0.043	Exploration
Akouta	Niger	53 500	0.35	Operating
Gorgon Main	Botswana	51 667	0.0178	Dormant
Mt Taylor Mine	USA	47 000	0.21	Dormant
Hamr	Czech Republic	40 000	0.070	Dormant
Stráz	Czech Republic	40 000	0.070	Depleted
Jackpile-Paguate	USA	39 400	0.20	Depleted
Akola	Niger	35 000	0.35	Operating
Gorgon West	United Republic of Tanzania	34 845	0.0134	Dormant
Mecsek	Hungary	32 800	0.12	Depleted
Serule NW	Botswana	30 107	0.0199	Dormant
Osecna-Kotel	Czech Republic	30 000	0.070	Dormant
Ebala	Niger	30 000	0.22	Dormant
Tamgak	Niger	30 000	0.30	Operating
Kayelekera	Malawi	29 100	0.080	Care and maintenance
Gorgon South	United Republic of Tanzania	28 105	0.0184	Dormant
Koenigstein	Germany	27 810	0.084	Depleted
Marianne-Maryline	Niger	26 090	0.125	Exploration
Cliffside	USA	25 000	0.14	Dormant
Pecs	Hungary	24 652	0.084	Dormant
Imskoye	Russian Federation	23 500	0.058	Dormant
Beaufort Ouest	South Africa	23 000	0.080	Dormant
Erdos Basin	China	21 600	0.030	Exploration

### Geological setting

Tabular sandstone deposits occur in several broadly similar geological settings. For purposes of this discussion, tabular deposits are subdivided into the intrinsic and extrinsic carbon class subtypes and the vanadium-uranium deposit class subtypes. The source of the uranium reductant and associated minerals provides the main basis on which the class subtypes are defined.

#### **Class subtype 1: Intrinsic carbon-related deposits**

The uranium mineralization in intrinsic carbon-related deposits is associated with detrital carbonaceous debris that was deposited contemporaneously with the host sandstone. Examples of this

deposit type include Arlit and Akouta (Niger) and Coutras (France). These deposits typically occur in reduced continental sandstones. The uranium, which was introduced into the host sandstones by laterally circulating groundwater, is closely associated with detrital plant debris, which acted as a reductant.

### **Class subtype 2: Extrinsic carbon-related deposits ('Grants type')**

The uranium mineralization in extrinsic carbon-related deposits is associated with redistributed carbonaceous matter (e.g. humate), which post-dates deposition of the host sandstone. The uranium deposits of the Ambrosia Lake district in New Mexico, USA, are the best examples of extrinsic carbon-related tabular uranium deposits. The host sandstones in the Ambrosia Lake district were deposited by W–E flowing fluvial systems that deposited a broad alluvial fan that extends across a large part of north-western New Mexico. Major orebodies at Ambrosia Lake are restricted to the braided, straight and sinuous channel facies within the fan complex.

The uranium mineralization in Ambrosia Lake, which resulted from interaction between uranium-bearing groundwater and elongate humate masses, consists of submicroscopic coffinite with minor amounts of amorphous urano-organic clay complexes in a matrix of dark coloured, amorphous carbonaceous matter that impregnates and partially replaces the sandstone. The carbonaceous matrix of the ore has been identified as degraded humate, i.e. humic acids derived from decaying plant debris that were introduced into the host sandstone by laterally migrating groundwater. As the humic acids migrated they began to condense or polymerize and form into gel-like substances that adhered to the host sand grains [340].

The approximate chemical composition of humate is  $(C_{15}H_{16}O_8NS)_n$  [340]. The humate material resembles amorphous carbon, having lost most of its hydrogen and oxygen. The humate masses were shaped by groundwater flow, streamlining them to minimize flow resistance. As the humate masses took form, lack of circulation and the concentration of organic matter increased the reducing state of their interiors. The humate was able to capture the uranyl cations by ion exchange. The adsorbed, organically bound uranium was reduced and fixed within the humate masses. Within the Ambrosia Lake district, there are also many examples of uranium ore associated with plumes of humic material directly associated with carbonized logs or organic 'trash' accumulations (intrinsic carbon). However, the extent of locally derived humic material is minimal in the Ambrosia Lake district. Conversely, the regional scale of the humate masses in the Ambrosia Lake district makes them unique among worldwide sandstone deposits.

The uranium in the Ambrosia Lake district was probably sourced from devitrification of volcanic ash in overlying sediments. The uranium orebodies are typically elongate, parallel to the original transport direction of the host sands and to the shape of the humate masses.

### **Class subtype 3: Vanadium–uranium deposits ('Saltwash type')**

Saltwash type uranium deposits are unique among sandstone-hosted uranium deposits in that either vanadium or uranium can be the dominant commercial commodity, depending on fluctuations in commodity prices. The main examples of this deposit class subtype are the deposits of the Henry Basin and UraVan Mineral Belt districts (USA). The host rocks for the vanadium–uranium deposits are continental fluvial sandstones. The host sands are reduced and contain carbonaceous plant debris similar to intrinsic carbon-related deposits.

The source of the uranium for the UraVan deposits was probably devitrification of tuffaceous sediments overlying the host sandstone units. The source of the vanadium is more problematic. Three sources have been proposed: (i) alteration of ilmenite and magnetite within the host sands and/or adjoining crystalline highlands; (ii) diagenesis of overlying sediments, and (iii) leaching from distant sedimentary and/or crystalline terrains [341].

#### 3.9.4.2. *Metallogenesis*

Regardless of which class subtype they belong to, tabular uranium deposits have many characteristics in common. They typically parallel bedding and their overall shape is controlled by the shape/distribution of the reductant, intrinsic or extrinsic carbon, and they are frequently elongated in the direction of host sediment transport. Tabular deposits also have similar metallogenic histories, regardless of class subtype. The uranium was likely sourced from devitrification of volcanic tuff, which was either admixed in the host sands or in overlying beds, or was leached from highlands underlain by felsic volcanic or crystalline terrains. Uranium was introduced into the host sands by laterally circulating oxidized groundwater and was precipitated by reduction arising from contact with carbonaceous material.

The source of the vanadium in the vanadium–uranium deposits is more problematic. One of the more widely held hypotheses suggests that the association of vanadium and uranium resulted from the mixing of two groundwaters with different chemistry, one containing organic complexes and vanadium derived from alteration of ilmenite and magnetite, the other containing  $U^{6+}$  species [342]. The uranium was reduced by  $V^{3+}$ , resulting in  $U^{4+}$  and  $V^{5+}$ .

Individual extrinsic carbon orebodies range from 500 m to 4 km long, 50–300 m wide and up to 20 m thick. Individual vanadium–uranium deposits of the Saltwash type are typically small, ranging from 100–500 m long, 10–50 m wide and 1–10 m thick.

#### 3.9.4.3. *Description of selected deposits*

##### **The Amer Lake deposit (Canada)**

###### Introduction

The Amer Lake deposit is located 145 km north of Baker Lake, Canada (Fig. 128). Uranium showings were discovered in 1969 when the Aquitaine Company of Canada undertook a regional airborne radiometric survey. This was followed up in 1970 by a detailed airborne radiometric survey, mapping and prospecting in the Amer Lake area along with 6825 m of diamond drilling (37 holes) that defined the Main and Faucon deposits [343]. Several other showings (Main East, A, B, C, D and E) were also discovered [344]. Cominco explored the area in 1977 through mapping, prospecting, relogging and resampling of Aquitaine drill holes as well as conducting additional drilling at the A, B and Faucon showings. Uranerz Exploration and Mining explored adjacent areas from 1976 through 1981 using airborne radiometrics, prospecting, mapping, ground geophysics and diamond drilling at the Split Lake and Horned Lake showings [343].

In 2006, Diamonds North optioned the property from MPH Consulting and transferred it to Uranium North. Exploration in 2007–2009 included compilation, airborne magnetic and radiometric surveys, drill hole relocation, soil geochemistry, prospecting, mapping and reverse circulation drilling [338]. A NI 43-101 compliant resource estimate was produced in 2009 by Uranium North Resources, the operator. In February 2013, Uranium North and Diamonds North were amalgamated to become Adamera Minerals Corporation. As of 2015, the project has been dormant.

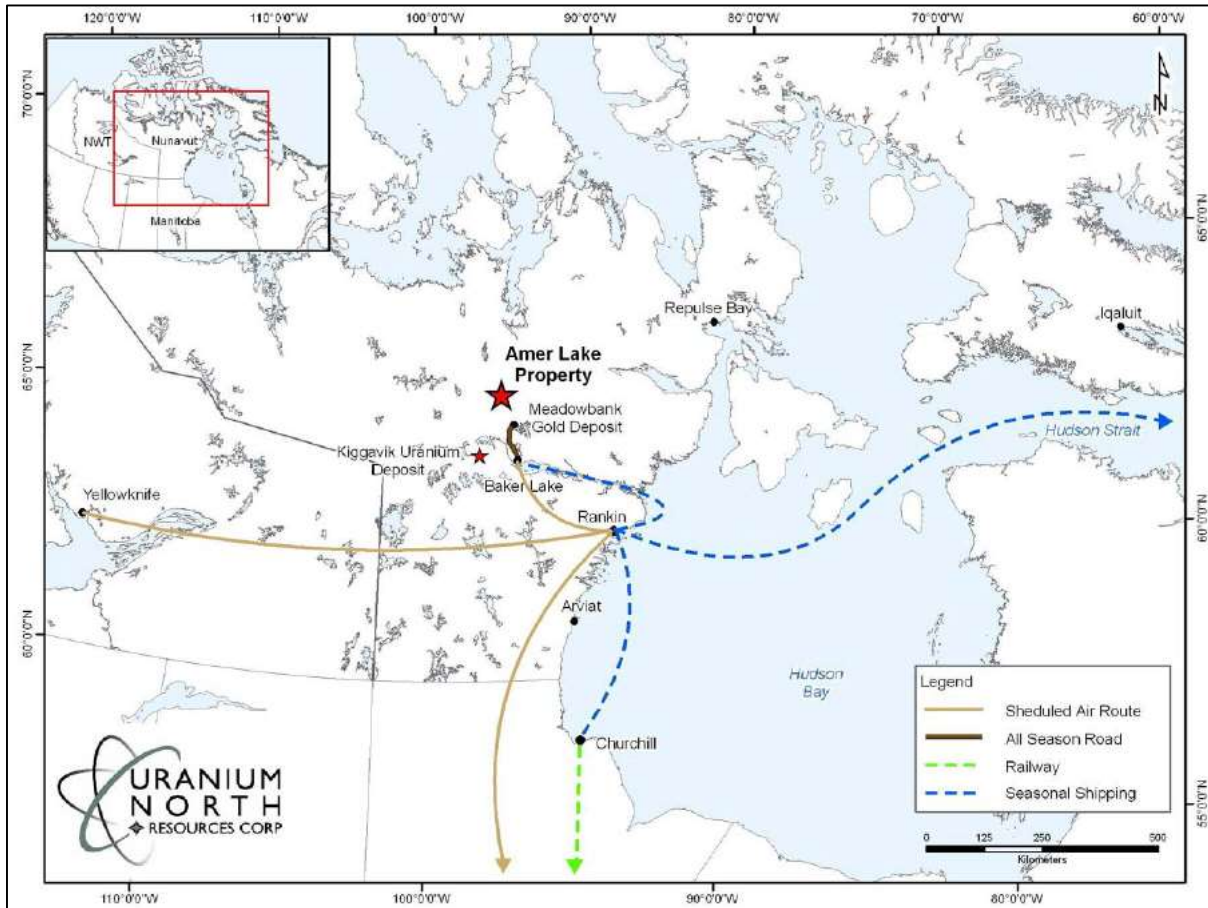


FIG. 128..Location of the Amer Lake deposit [343] (reproduced with permission).

### Geological setting

The Amer Belt is a 140 km long, ENE trending syncline overlying polyphase deformed Archaean basement consisting of orthogneiss, migmatite, granite, paragneiss and infolded metavolcanic rocks [345]. The 2.45–2.1 Ga Amer Group unconformably overlies the Archaean basement and was deformed and variably metamorphosed during the ~1.91–1.80 Ga Trans-Hudson Orogeny [345]. It is affected by north-west verging thrusts and north-west trending brittle faults. The area was intruded by 1830–1800 Ma granite plutons and was partially overlain by the Palaeoproterozoic Baker Lake and Thelon Basins.

The Amer Group consists of lower and upper clastic units deposited in a nearshore marine environment. According to Young [346], the stratigraphy is as follows. The lower clastic series consists of a basal schist and conglomerate unit, the Umiujalik Lake Formation. This is overlain by the Ayagaq Lake Formation, consisting of orthoquartzite with interlayered purple-green mudstone, silty quartzite, dolomite and subarkosic arenite, recording sedimentation in a shallow marine stable shelf environment. Vesicular and amygdaloidal basalts of the Five Mile Lake Formation are locally interlayered with the quartzite.

The upper clastic sequence conformably overlies the quartzite, recording sedimentation in a deepening marine basin followed by shallow marine to tidal settings. The lowermost unit, the Resort Lake Formation, consists of pyritic mudstone and siltstone with graphitic lenses. This is overlain successively by: siliceous dolomite and subarkosic sandstone (Aluminum River Formation), the Three

Lake Formation (siltstone, quartz arenite, pyritic mudstone and dolomite), the Oora Lake Formation (feldspathic sandstone, quartz arenite, mudstone and dolomite), the Showing Lake Formation (rhythmically interbedded feldspathic sandstone, mudstone and dolomite) and, finally, the Itza Lake Formation arkose and subarkosic sandstone.

The belt was subjected to folding, faulting and metamorphism during the Trans-Hudson Orogeny. The oldest deformation produced northerly directed thrusts and west plunging folds. This was followed by SW trending folds, NE trending normal faults and, finally, NW trending, vertical normal faults. Metamorphic grade is typically mid-greenschist facies (biotite grade) but ranges from sub-greenschist to a maximum of lower amphibolite in the north-east [344].

### Mineralization

All of the uranium showings are hosted within the Showing Lake Formation in the Amer Lake Belt Syncline (Fig. 129). The Main Zone deposit consists of low grade, stratabound and stratiform uranium mineralization in sandy interbeds of the Showing Lake Formation (Fig. 130). The mineralization is contained in a series of stacked dark grey to red sandstone lenses separated by laminated arkosic and dolomitic siltstone [338]. The mineralized horizons span an interval of 40–70 m in strata that dip to the south (10–40°) and extend over a 1700 m strike length. It is cut by a series of NW striking, NE dipping reverse faults that offset the mineralization by up to 30 m [343].

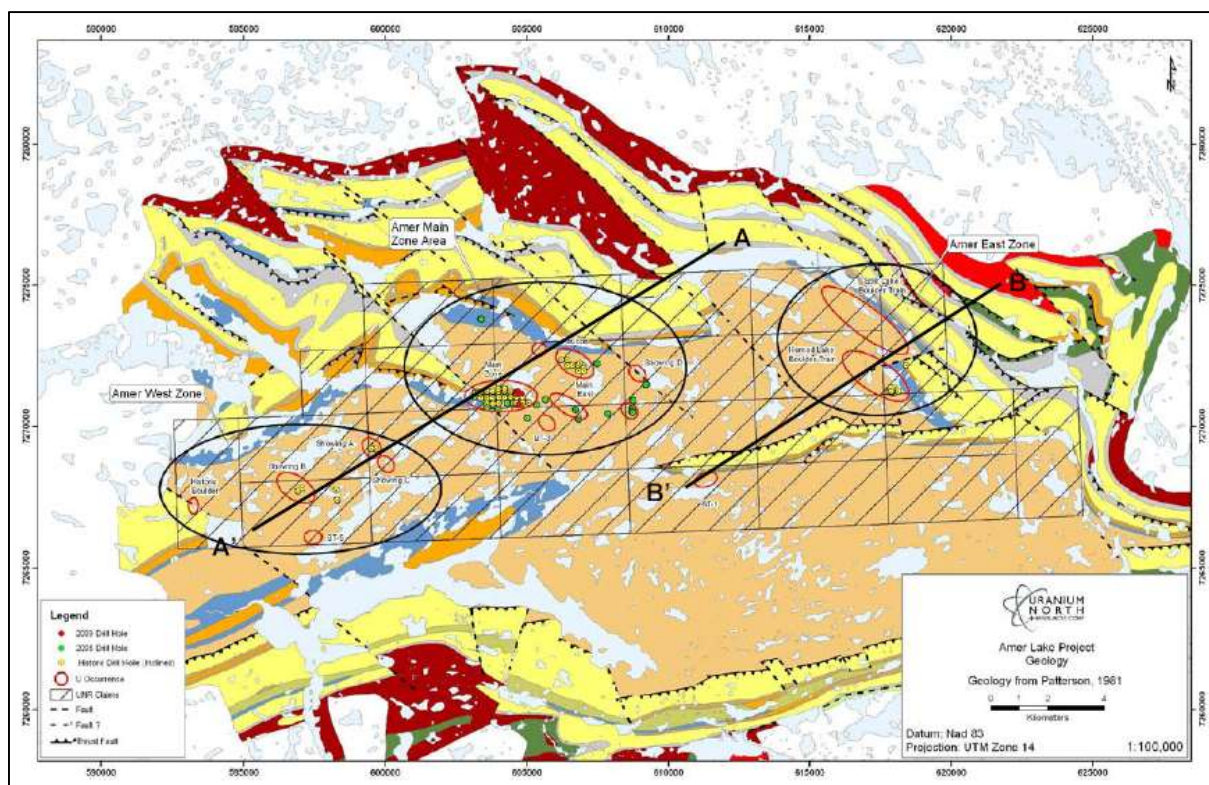


FIG. 129. Amer Lake Belt Syncline showing the location of uranium showings and deposits [343] (reproduced with permission.)

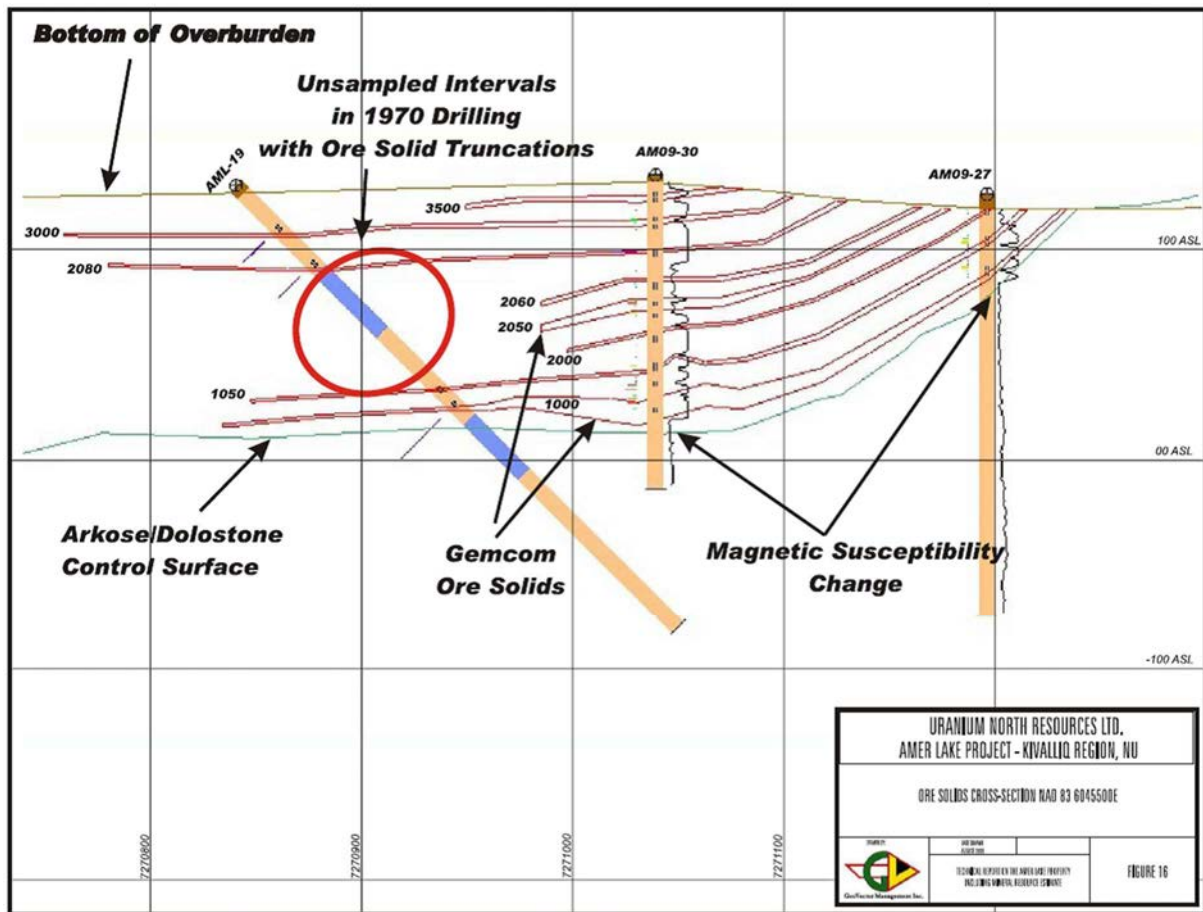


FIG. 130. Ore zone cross-section of the Amer Lake Main Zone deposit [343] (reproduced with permission).

A NI 43-101 compliant resource estimate was made in 2009 using historical drill data and the 2008–2009 reverse circulation drilling campaign [343]. A range of cut-off grades was used. The inferred resource is 3737 tU at an average grade of 0.076% U (cut-off grade of 0.04% U) or, using a cut-off grade of 0.0085% U, the resource rises to 7435 tU.

As described by Armitage [344], mineralization is contained in white to red arkosic beds, the latter colour being due to the oxidation of magnetite and pyrite. No other alteration is observed. The mineralization consists of very fine-grained uraninite, brannerite and, locally, uranophane. It is found as disseminations (up to 2 mm) and concretions up to 2 cm and, locally, may be structurally upgraded. Mineralization is found mainly in the lower part of the Showing Lake Formation as disseminated pitchblende, coffinite and a U–Ti phase (brannerite?) accompanied by pyrite, chalcopyrite with traces bornite, covellite and chalcocite [345]. Mineral shapes suggest that the magnetite is diagenetic and is altered to haematite and replaced by the Fe–Cu sulphides in the ore zone. The mineralized zones are enriched in Cu, Ag and Mo while base metals (Cu, Zn and Pb) are enriched in the interbedded carbonates of the mineralized zones compared with background areas. Both U and Cu correlate positively with Fe [345].

In addition to the Main Zone, several other similar showings are present. Faucon, approximately 1.5 km to the north-east, was drilled by Aquitaine and Cominco. It consists of low grade mineralization in orange–red arkosic units interbedded with siltstone. Faults offset the mineralization. Main East is a 1–2 m thick laminated siltstone which contains uraniferous concretions and, to the south, narrow lenses

of radioactive, silty arkose are present. Some mineralization along ‘whispy’ arkosic lamellae appears to be deformed into rods [346]. Showings A through E consist of outcrops and boulders with radioactive arkose interbedded with siltstone. In several of these, mineralization is deformed (westerly plunging lineations) and faulted. The Horned Lake and Split Lake showings are located approximately 12 km east of the Main Zone. These consist of laminated arkose and siltstone with magnetic and radiometric anomalies. Uranerz Exploration and Mining drilled 14 holes at Horned Lake in 1981.

Amer Lake mineralization has yielded U–Pb and Pb–Pb dates of about 1835 Ma, which are interpreted to reflect isotopic re-equilibration during the Trans-Hudson Orogeny [347].

#### Metallogenic aspect

The Amer Lake deposit and related showings are interpreted as Palaeoproterozoic examples of tabular/peneconcordant type sandstone-hosted uranium deposits, with some structural remobilization. Uranium mineralization is interpreted to have occurred during diagenesis of the host interbedded arkosic sandstone and siltstone. Mineralization is affected by Hudsonian deformation, metamorphism and faulting, and therefore must be either pre- or syn-deformational. Diagenetic magnetite (which gives an elevated magnetic expression to the host strata) is interpreted as being the main reductant for the uranium since the mineralization-related Cu sulphides and pyrite replace magnetite rather than pyrite or Fe–Ti minerals [345]. In addition, pitchblende, coffinite and the Ti–U phase are intergrown with authigenic carbonate, albite and quartz, indicating that the mineralization was synchronous with early cementation. The high copper contents compared with typical tabular sandstone deposits could be a reflection of the near-shore marine environment of the host sediments, similar to that of red bed Cu deposits [345].

### **The Kayelekera deposit (Malawi)**

#### Introduction

The Kayelekera deposit is a Karoo age, sandstone-hosted deposit located 52 km west of the provincial town of Karonga, in the far north of Malawi (Fig. 131). The project is held by Paladin Africa Ltd (85%), a wholly-owned subsidiary of Paladin Energy Ltd, and by the Government of Malawi (15%).

In 1987, Agip Exploration located a number of airborne radiometric anomalies and discovered uranium secondary minerals in outcrop near the village of Kayelekera. The Central Electricity Generating Board took over the area in 1983 and a full feasibility study was completed in 1991, assessing the viability of a conventional open pit mining operation.

The project was abandoned in 1992 owing to the significant drop in the price of uranium. In 1997, Balmain Resources Pty Ltd obtained an exploration licence on the area and in 1998 Paladin Energy acquired the Kayelekera project from Balmain [348].

In 2010, total resources of the deposit at a cut-off grade of 300 ppm U were 17 835 tU at an average grade of 680 ppm U. The mineralization is not fully delineated in extension and at depth, with additional mineralization identified below the current mine units. Production started in 2009 and production for 2013 amounted to 1101 tU. The mine was designed to have an annual production of 1270 tU [349], but as a result of low uranium prices, it was placed on care and maintenance in 2014.

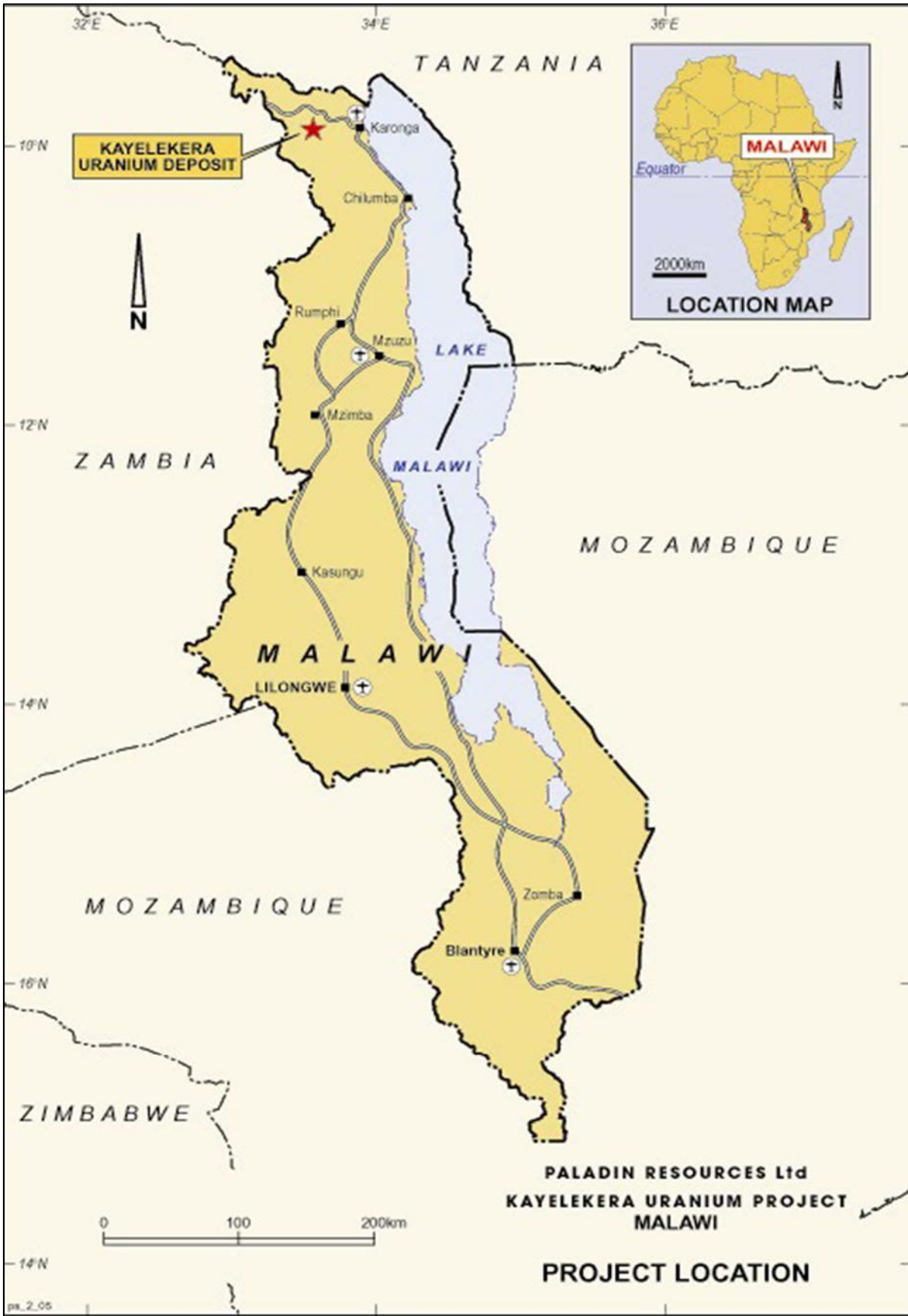


FIG. 131. Location of the Kayalekera deposit, northern Malawi (source: Paladin Energy) (reproduced with permission).

## Geological setting

Northern Malawi is underlain by metamorphic and igneous rocks of the Malawi Basement Complex, the main components of which are gneisses and intrusive rocks of the Misuku Belt that form the south-eastern extension of the Ubendian Mobile Belt of south-western part of the United Republic of Tanzania. The Precambrian basement was subjected to four episodes of deformation in the Late Precambrian and Early Palaeozoic, during the Irumide and Mozambique Orogenies [350]. A long period of erosion of the Misuku Belt was interrupted in the Early Permian by the deposition of Karoo sediments upon an irregular topography initially under glacial and periglacial conditions. Faulting and subsidence accompanied Karoo sedimentation, which ended with the initiation of the Gondwana erosion cycle in the Early Jurassic.

The Karoo strata, which probably covered much of the area by the Middle Permian, are now found in several partially or totally fault bounded basins. The North Rukuru Basin, in which the deposit is located, is a N–S elongate basin about 50 km long with a maximum width of 6.5 km. It contains a thick (at least 1500 m) sequence of Karoo sedimentary rocks and is broadly parallel to the Malawi segment of the Lake Malawi Rift [348].

The Karoo rocks of the North Rukuru Basin consist of a thick succession of clastic sediments which are divided into two distinctly different formations: (i) the Basal Beds Formation, consisting of tillite horizons with overlying sandstone and varved shale horizons and (ii) an overlying thick series of alternating arkosic sandstone and mudstone of the North Rukuru Sandstone and Shale Formation (Fig. 132). The Basal Beds Formation represents glacial and glacio-lacustrine sedimentation whilst the North Rukuru Sandstone and Shale Formation was deposited in a subsiding basin with lakes and braided and meandering river systems [348].

The uranium deposit is hosted in the Kayelekera Member, the uppermost part of the North Rukuru Sandstone and Shale Formation that is preserved in the basin. The Kayelekera Member has a maximum thickness of 150 m. Eight separate arkosic units with intervening mudstone and silty mudstone beds have been defined (Fig. 133). The succession is indicative of cyclic sedimentation within a broad, shallow, intermittently subsiding basin. Each cyclothem generally passes upwards from coarse, reduced facies arkose through oxide facies red bed mudstone into reduced facies, grey–black carbonaceous silty mudstone. Thin coaly horizons are present within some cyclothem.

The arkose units average about 8 m in thickness and are generally coarse-grained and poorly sorted with a high percentage of fresh pink feldspar clasts. In reduced facies intersections, the pink feldspars contrast with the dark green pyritic carbonaceous matrix. Individual arkose units may contain several upwards fining sequences ranging from quartz–feldspar pebble conglomerate to medium- or fine-grained micaceous arkosic sandstone. Current bedding is common. Carbonaceous debris, as layers on cross-stratification surfaces, disseminations and as lenses several centimetres in length is commonly present in association with pyrite in reduced facies arkose [348].

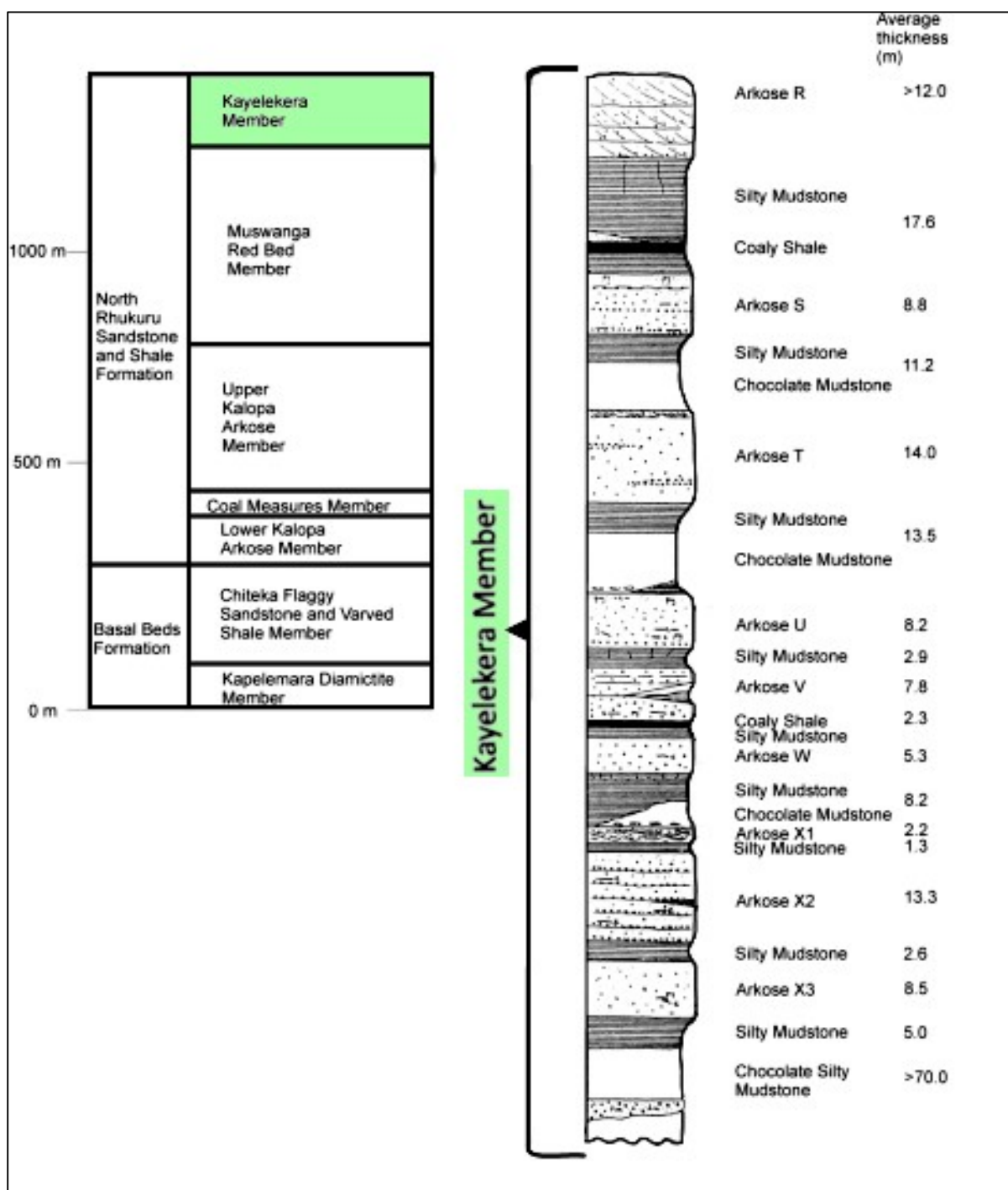


FIG. 132. Generalized stratigraphic sequence of the Karoo strata in the northern North Rhukuru Basin and of the Kayelekera Member hosting the Kayelekera uranium deposit (adapted from Ref. [348]).

The red bed mudstone is a red to chocolate-brown coloured, homogenous, massive, fine-grained sediment. In the lower units, calcareous concretions and calcite veins are common. These sediments appear to have accumulated in a subaerial environment as extensive floodplain mud flats.

The grey carbonaceous mudstone units comprise a range of lithotypes, including light to dark grey homogenous mudstone, grey silty mudstone, sometimes with calcite veins, silty mudstone with

multicoloured, angular mud clasts, laminated bedded carbonaceous pyritic black shales, fine-grained ripple cross-stratified carbonaceous sandstone and coal-bearing shale [348].

The Muswanga Member is folded into gentle synclines. The Kayelekera Member and the uranium deposit occupy the core of one of these synclines with an axial trace parallel to the eastern basement fault. Faults within the Karoo Basin are predominantly steep normal faults. A series of steep, closely spaced normal faults with a combined throw in excess of 100 m mark the eastern margin of the deposit.

#### Mineralization

Lenses of uranium mineralization occur within arkose units S and T, the arkose–mudstone units U, V, W and the arkose units X1 to X3 up to a depth of 100 m (Figs 132 and 133). The lenses appear to be stacked vertically along an axis approximately parallel to the synclinal axis of the fault-bounded structure. Mineralization is offset, but not confined, by the fault. Most of the mineralization is contained within the arkose units, but some secondary mineralization occurs in the mudstone immediately below the mineralized arkoses adjacent to faults (Fig. 133).

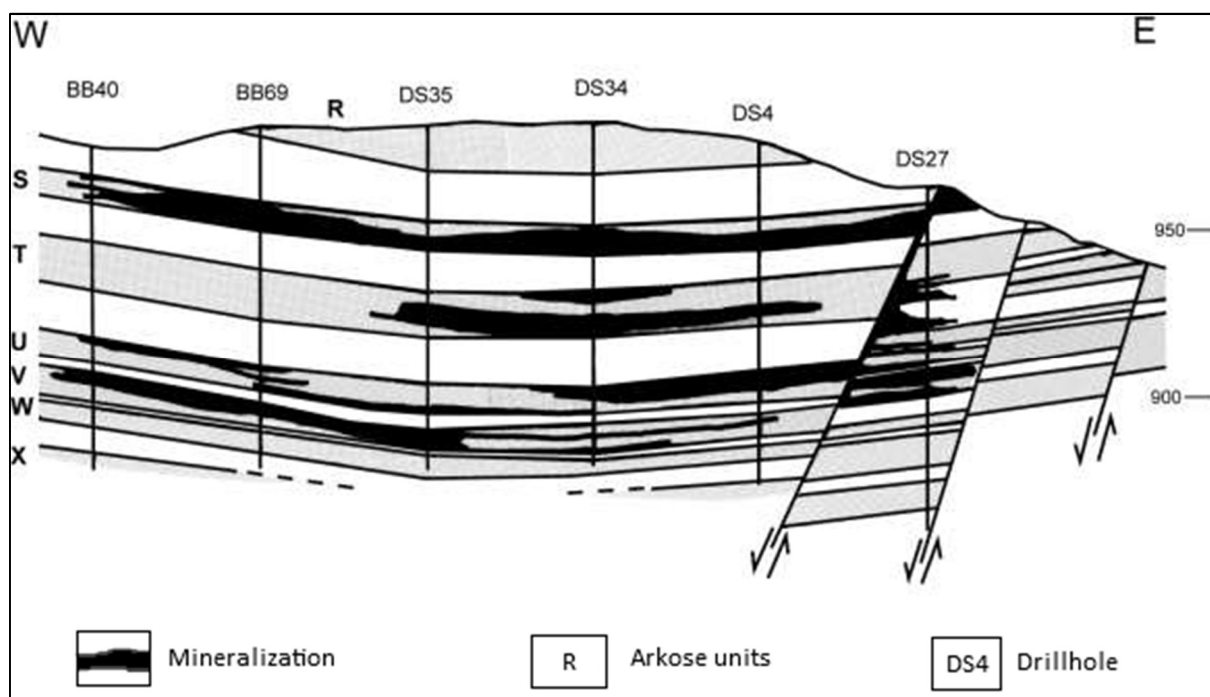


FIG. 133. Longitudinal section of the Kayelekera deposit. (R to X: arkose units, black indicates mineralization) (adapted from Ref. [348]).

Mineralization has been classified into three types based on the basis of visual identification of the redox state of the host lithology: reduced ore, (oxidized ore and mixed oxidized–reduced ore). Detailed studies have established three modes of occurrence: (i) organic matter, (ii) secondary microcrystalline titanium oxide and (iii) secondary minerals.

Coffinite is the main primary uranium mineral present in the reduced facies. It is often associated with organic debris and/or pyrite and is finely intergrown with chlorite and clay, which fills the pore space of the arkose. The highest concentrations of uranium are found in bands and layers of organic debris where coffinite occurs as euhedral crystals in open spaces within collapsed cell structures or interstices in authigenic pyrite framboids. Mineralization therefore post-dates the main period of diagenetic

compaction [351]. Small quantities of extremely fine-grained uranium oxide, probably uraninite, have been identified in some reduced and transitional mineralized zones. A titanium–uranium mineral, either betafite or tanteuxenite, has also been identified in minor quantities. Secondary minerals (meta-autunite, boltwoodite and uranophane) are present in the oxide facies, originating from oxidative, near-surface weathering of the primary uranium minerals [343]. Gangue minerals are principally feldspar, quartz, haematite and pyrite, with minor amounts of carbonaceous material and calcite. Chemical analyses indicate single element (uranium) enrichment with no evidence of associated or indicator elements.

#### Metallogenic aspect

The uranium contained in the Kayelekera deposit was probably derived from the erosion of granitic rocks to the south-west, some of which feature high levels of radioactivity. The nearest is the Kapola Granite, which has anomalous U and Th and is responsible for elevated values of these elements in the north Rukuru drainage basin [351].

Where unaffected by surface weathering or oxidized groundwater circulation, the arkose of the Kayelekera Member is reduced, preserving the organic and pyritic fractions of the rock. Under these conditions, the relatively insoluble uranium remained throughout the rocks in low concentrations as a low grade protore associated with carbonaceous-rich zones. Following rift faulting and associated folding, the uranium was mobilized by oxidized groundwaters and redeposited in ore grade concentrations at the redox front within reduced arkose in preserved structural basins [348].

The Kayelekera uranium deposit is considered by some authorities to be a variant of the roll-front type sandstone deposit model. The presence of carbonaceous debris and pyrite in the reduced arkose facies and the redox-related mechanism of uranium remobilization and re-deposition are similar. However, the basin structure has led to the concentration of uranium in a structural low in a series of stacked arkose horizons in comparison to the classic roll-front type of deposits that are generally formed in extensive, gently dipping strata and are rarely multi-layer deposits. Also, the mineralization is surprisingly continuous and strongly controlled by the lithology [348].

### **3.9.5. Roll-front deposits**

#### *3.9.5.1. Definition*

Roll-front deposits are zones of uranium matrix impregnations that cross-cut sandstone bedding and extend vertically between overlying and underlying horizons of lower permeability. In cross-section, roll-front deposits are crescent-shaped and are convex in a down-gradient direction.

A total of 243 roll-front sandstone deposits are recorded in the UDEPO database. The largest ones are located in Kazakhstan (Chu-Sarysu and Syr Daria Basins) and Uzbekistan (Kyzylkum district) (Table 29). Large districts are also present in the USA (Wyoming and Texas). In 2015, about 29 000 tU (48% of world production) originated from this type of deposit which is mined by in situ recovery methods. Kazakhstan is the world's largest uranium producer, having produced 23 800 tU in 2015, essentially from roll-front sandstone deposits.

TABLE 29. PRINCIPAL ROLL-FRONT SANDSTONE DEPOSITS (as of 31 December 2015)

Deposit	Country	Resources (tU)	Grade (% U)	Status
Inkai	Kazakhstan	209 340	0.043	Operating
Mynkuduk	Kazakhstan	203 400	0.040	Operating
Budennovskoye	Kazakhstan	128 269	0.066	Operating
Moynkum	Kazakhstan	71 566	0.056	Operating
Kharasan	Kazakhstan	58 453	0.098	Operating
Zoovch Ovoo	Mongolia	54 640	0.023	Exploration
Uchkuduk	Uzbekistan	49 280	0.129	Operating
Sugraly	Uzbekistan	43 050	0.172	Operating
Bukeenai	Uzbekistan	33 100	0.058	Operating
Karamurun	Kazakhstan	31 630	0.060	Operating
Irkol	Kazakhstan	30 200	0.045	Development
Suluchekinskoye	Kazakhstan	28 800	0.090	Dormant
Smith Ranch	USA	26 200	0.086	Operating
Yili Basin	China	26 000	0.060	Operating
Tortkuduk	Kazakhstan	24 480	0.10	Operating
Imskoye	Russian Federation	23 500	0.058	Dormant
Kendrick	USA	19 830	0.041	Exploration
Four Mile NE	Australia	19 550	0.254	Development
Zarechnoye	Kazakhstan	18 900	0.056	Operating
Bayinwula	China	17 500	0.010–0.05	Exploration
Sheep Mountain	USA	17 150	0.055	Dormant
Jacpot Mine	USA	16 600	0.18	Dormant
Highland	USA	16 500	0.095	Operating
Assarchik	Kazakhstan	15 400	0.059	Dormant

### 3.9.5.2. Geological setting

Roll-front deposits can be subdivided into three types based on occurrence either in intracratonic basins filled with continental alluvial–fluvial sediments or in mixed fluviomarine sediments along coastal plains. Reductants may consist of detrital carbon, extrinsic hydrocarbons or H<sub>2</sub>S and/or Fe sulphides that originated from influx of H<sub>2</sub>S into the host sand [19]. The most probable sources for the uranium are uraniferous granitic rocks and uraniferous volcanic and volcanoclastic rocks.

*Continental basin, uranium associated with intrinsic reductant (Wyoming type):* uranium occurs as disseminations at the down-gradient side of redox fronts related to detrital carbonaceous debris in arkosic and sub-arkosic sandstone. The sediments were deposited in intracratonic or intermontane basins in spatial proximity to rocks containing anomalous uranium concentrations, such as tuff and granite. Most deposits occur in sequences of interbedded fluvial sandstone and volcanic-rich sediments. The shape of deposits is strongly controlled by the hydrology of the host rocks. Some deposits have long tabular limbs overlying and/or underlying carbonaceous-rich clayey–silty sediments. Resources are small to large and of medium grade [19].

*Continental to marginal marine, uranium associated with intrinsic reductant (Chu-Sarysu type, Kazakhstan):* deposits are similar to deposits in continental basins but host lithologies correspond to a

sequence of mixed continental and marginal marine origin. Resources are medium to very large but grades are generally low.

*Marginal marine, uranium associated with extrinsic reductant (South Texas type):* uranium is concentrated in roll-type deposits near faults and in contact with pyrite/marcasite-bearing sandstone on their down-gradient side. The sandstone on the up-gradient side of deposits is haematite- and/or limonite-bearing except for certain deposits that occur entirely within reduced, pyrite-bearing sandstones. This latter type probably reflects the post-ore introduction of H<sub>2</sub>S along faults. Hydrogen sulphide introduced before ore formation prepared the host for roll-front development. Host environments include point bars, lateral bars and crevasse splays in fluvial sequences, and barrier bars and offshore bars in marine settings. Resources are small to medium and grades low to medium [19].

### 3.9.5.3. *Metallogenesis*

The mineralized zones consist of elongate and sinuous bands approximately parallel to the strike of the strata and perpendicular to the direction of sedimentary deposition and groundwater flow. Redox interfaces control the setting and configuration of these zones. The mineralized zones are convex down the hydrological gradient and exhibit diffuse boundaries with reduced sandstone on the down-gradient side and sharp contacts with oxidized sandstone on the up-gradient side [19].

Oxidation processes associated with the ore forming process include bleaching of the normal grey sandstone, elevated Se, V and Mo contents, higher CaCO<sub>3</sub>, organic carbon and sulphate contents and destruction of heavy minerals, particularly pyrite and magnetite. Ore minerals are uraninite and coffinite, which occur as coatings on sand grains, void fillings in sandstone and replacement of organic matter.

Harshman and Adams [352] comprehensively reviewed the formation of roll-front sandstone deposits in Wyoming and elsewhere. They note an inconsistent correlation between uranium and organic carbon within roll-front systems, indicating that other mechanisms for precipitation of uranium must exist. Microbes existing in two very different Eh and pH environments on either side of a very sharp redox front have been proposed as a mechanism for ore deposition [353]. The biogenic process is self-perpetuating and needs only oxygen, pyrite, CO<sub>2</sub> and organic matter to complete the oxidation, migration and reduction cycle required in this dynamic system.

The role of microbes as a critical element in the formation of roll-front type uranium deposits is exemplified by results from sandstone-hosted deposits in the Xinjiang region of north-western China [354]. Several deposits consisting of uraninite and coffinite have textures indicating that they were biogenically precipitated and that they pseudomorphically replaced fungi and bacteria. Uranium is interpreted to have been reduced enzymatically by these microorganisms. A similar model was proposed by Arthur et al. [355] for the Tono uranium deposit (basal channel) in Japan. The redox environment in which the uranium was deposited is believed to have been controlled by microbially mediated sulphate reduction, oxidation of organic matter and precipitation of sulphide minerals.

### 3.9.5.4. *Description of selected deposits*

#### Sandstone-hosted roll-front deposits in the USA

##### Definition

Sandstone-hosted roll-front deposits form at the interface between oxidized and reduced sedimentary rocks in Cretaceous–Tertiary clastic sediments throughout the western USA. The deposits form along reaction fronts in typical C-shaped rolls, although the geometry of these deposits is highly variable and dependent on local geology.

The best known roll-front deposits are in the Texas Gulf Coast marginal marine and Wyoming intracratonic basin provinces. Roll-front deposits are also described in the Cheyenne Basin along the eastern front of the Rocky Mountains in Colorado (Keota, Grover and Centennial deposits), north-west Nebraska (Crow Butte deposit), northern Black Hills (Hauber deposit), southern Black Hills (Dewey-Burdock deposit) and the Grants Mineral Belt in New Mexico (Crownpoint and other deposits) (Fig. 134). In addition, scattered roll-front deposits accompany other types of sandstone-hosted uranium mineralization throughout the western USA. In these basins, discontinuous roll-front deposits are found along redox reaction fronts that may extend for several hundred kilometres. Deposits range in size from 1 to 20 000 tU and in grade from approximately 0.06–0.22% U. Mineralization pinches and swells along strike so deposit bounds may be somewhat arbitrary and grades may be highly variable. This type example includes an overview of major US provinces followed by more detailed descriptions of both the Kingsville Dome and Rosita deposits in Texas and other important deposits of the Gulf Coast Province.

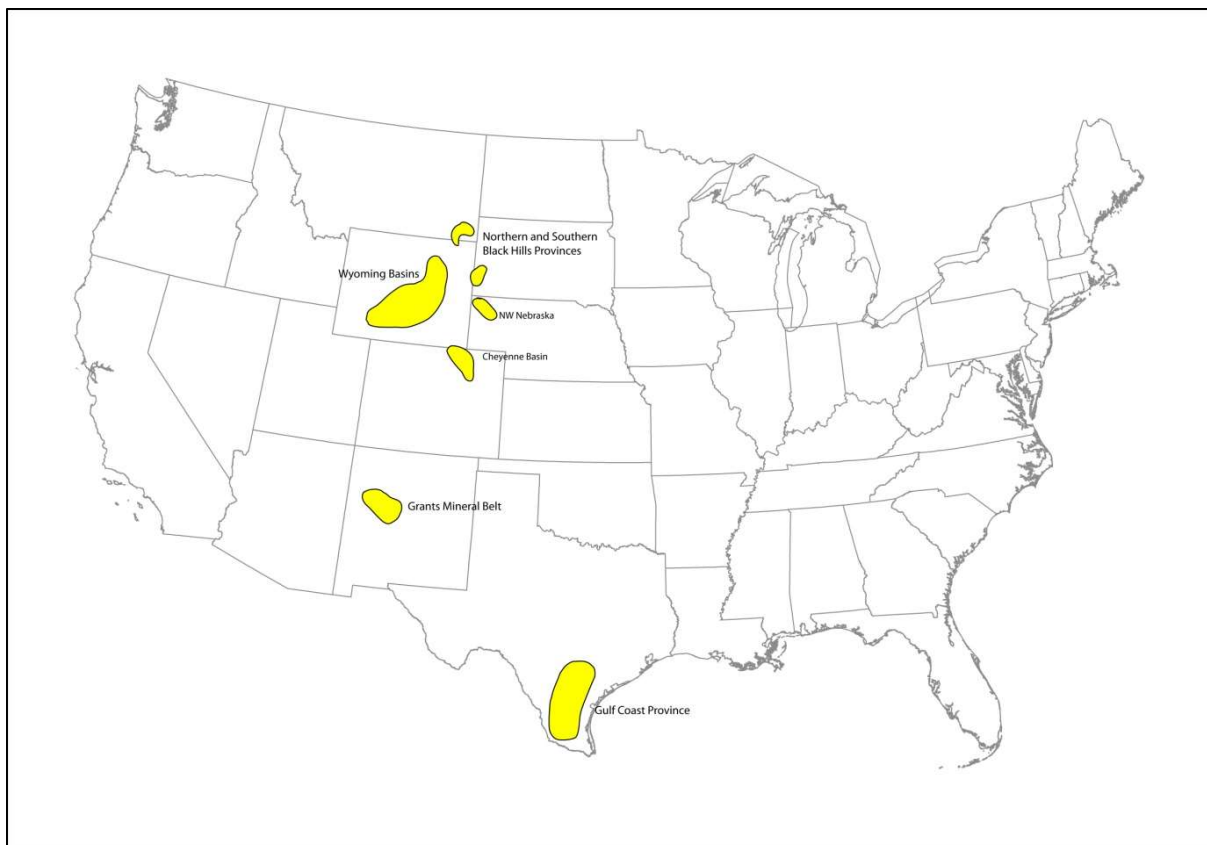


FIG. 134. Principal sandstone-hosted roll-front uranium provinces of the USA (reproduced courtesy of S. Hall).

Most current US uranium production is from sandstone-hosted roll-front deposits, with active mines in the Texas Gulf Coast, north-west Nebraska and Wyoming Basin provinces. An estimated 85% of reasonably assured resources in the USA are sandstone-hosted deposits [169], the majority of which are roll-front type deposits. In the Texas Gulf Coast Province, approximately 27 000 tU have been produced, about 5% of total US production, and another 15 500 tU remain, about 4% of known reserves mineable at <US \$260/kgU [356]. Between 77 000 and 80 000 tU have been mined from the Wyoming Basin area, with between 72 000 and 149 000 tU remaining [357]. In New Mexico, more than 130 000 tU have been produced from several different types of sandstone-hosted uranium deposit in the Grants Mineral Belt, with an estimated 155 000 tU remaining [358].

Historically, roll-front deposits have been mined using open-pit and underground methods. Owing to their low grade, erratic distribution and higher costs of open-pit and underground mining, most

sandstone-hosted deposits are currently mined using lower cost in situ recovery techniques. Although acid and ammonium lixiviants were formerly used in some pilot projects in the 1970s, now only alkaline lixiviants are used in the USA and these typically comprise some combination of oxygen and carbon dioxide or bicarbonate which is added to groundwater in order to oxidize and mobilize the uranium.

### Geological setting

Sandstone-hosted roll-front uranium deposits in the USA have many features in common: an indeterminate uranium source, similar ore mineralogy and geochemistry from basin to basin and a reductant that causes uranium to precipitate out of solution. Variations in possible uranium source, detailed mineralogy and geochemistry, the number of reaction fronts present in the basin and, most importantly, the type of reductant create unique deposits that characterize each major US roll-front province.

### Wyoming Basins

In the four major basins that make up the Wyoming Basin Province, roll-front deposits are hosted in Jurassic–Oligocene sandstones, with mineralization mostly in the Palaeocene Fort Union and Eocene Wasatch, Wind River and Battle Spring Formations. These units are fluvial, mostly arkosic, continental sandstones with interbedded clay and siltstone deposited adjacent to rapidly eroding upland areas as a result of Laramide uplift. Roll-front deposits are found in the more permeable facies of alluvial fans that are stacked and separated by less permeable siltstones and claystones. Coal beds are common in the lower Wasatch and Fort Union Formations in the Powder River Basin. Roll-front deposits are associated with the leading edges of oxygenated groundwater plumes flanking the edges of the Powder River, Wind River, Great Divide and Shirley Basins (Fig. 135).

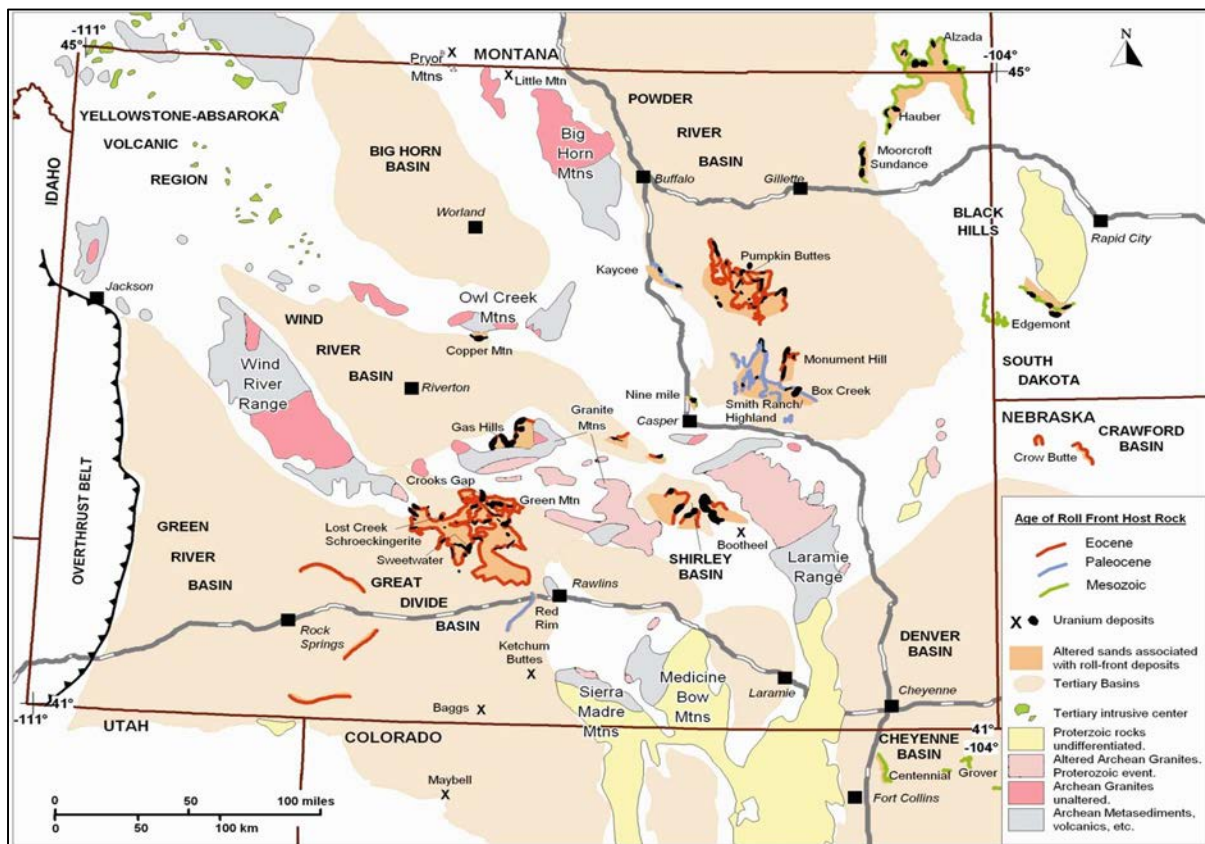


FIG. 135. Uranium deposits in the Wyoming Basin Province [357] (reproduced with permission).

Groundwater flow is controlled by palaeo-topographic highs such as the Casper Arch south-west of the Powder River Basin and the Granite Mountains adjacent to the Shirley, Wind River and Great Divide Basins. Oxygenated groundwater, flowing from high to low levels, mobilized uranium that is believed to have originated from volcanic ash within the sediments [359] or from granitic rocks in upland areas adjacent to the basins [360–363]. The uranium was precipitated from solution where reducing conditions were encountered within the basins. These include the presence of organic debris and pyrite common in the arkosic host sandstone of the Wyoming Basins, with some influence from hydrocarbon seepage into the sandstone of the Gas Hills area. The ages of roll-front deposits in the Wyoming Basins lie between 43 and 1.8 Ma, and the locations of most deposits coincide with Eocene drainage systems [357].

### *Grants Mineral Belt*

Roll-front deposits in the uranium-rich Grants Mineral Belt formed as oxygenated groundwater remobilized pre-existing tabular sandstone deposits. The oxygenated groundwater was derived from the Zuni Uplift that formed south-west of the basin during the Early Tertiary. The tabular deposits are blanket-like orebodies, less than 2.5 m thick, averaging >0.17% U and having sharp ore–waste boundaries. Tabular deposits are hosted in Jurassic sandstones of the Morrison Formation and are associated with humates. Roll-front deposits in the Grants Mineral Belt formed along redox fronts that trend roughly E–W across the mineral belt. These deposits are found in sandstone of both the Jurassic Morrison Formation and the Cretaceous Dakota Sandstone and are typically greater than 2.5 m thick, with grades in the range 0.10–0.25% U [358]. In total, it is estimated that 130 780 tU have been mined from sandstone deposits in the Grants Mineral Belt, and an estimated 155 000 tU remains. Of this, the total resource contained in roll-front deposits is in excess of 25 000 tU [358]. Uranium that was not remobilized by groundwater in the basin was left behind as ‘remnant’ ore. Such mineralization is likely to have remained in a place where it was less easily dissolved by groundwater, either in areas of lower primary permeability of the sandstone or else in zones of lower secondary permeability caused by stronger calcite and silica cementation. Two possible sources for uranium have been identified in the Grants Mineral Belt: (i) Proterozoic granites in the Zuni Mountains south of the district and (ii) Jurassic volcanic ash that originated south-west of the district and is interbedded with the host sandstone [358].

### *Black Hills Province*

Uranium roll-front deposits have been described in Cretaceous sandstones lying along the northern and southern flanks of the Laramide Black Hills Uplift (Fig. 135). In the northern Black Hills, roll-front deposits ranging between 1.5 and 5 m thick are found along a redox front greater than 40 km long and hosted within the Cretaceous Lance Formation and Fox Hills Sandstone [364]. Individual mineable deposits along this trend contain between 1500 and 4500 tU. In the southern Black Hills, roll-front deposits are located along redox fronts that extend for tens of kilometres in the Cretaceous Lakota and Fall River Sandstones [365]. These sandstones, deposited as fluvial sequences along a broad flat plain in a marginal marine environment, are typified by abundant channels with associated crevasse splays and floodplains.

Uranium roll-front deposits are more commonly situated along the margins of those anastomosing channels through which groundwater flowed, down-gradient, from the Black Hills Uplift. Deposits are typically C-shaped, a few tens of metres wide and several hundred metres long. The rolls are stacked and separated by less permeable overbank deposits. The Dewey-Burdock deposit in this region contains an inferred resource of 4461 tU with an average grade of 0.15% U [366]. The uranium source of the southern Black Hills may have been volcanic tuffs in the Tertiary White River Formation that overlies the host Cretaceous sandstones [365]. Alternatively, it has been proposed that uranium may have been derived from older sedimentary and granitic units in the Black Hills, from which it migrated into overlying channel sands via sedimentary breccia pipes that commonly cross-cut the strata [367].

### *North-western Nebraska*

Sandstone of the Tertiary Chadron Formation in north-western Nebraska hosts the Crow Butte roll-front deposit that contains a total resource of more than 11 000 tU at an average grade of 0.25% U [368]. Roll-front deposits are localized along the margins of palaeovalleys or the edges of sandstone channels [369, 370]. Pyrite within the Chadron Formation may have been the dominant reductant [371] as the organic content of sandstones at Crow Butte is very low [368]. This pyrite may have formed through bacterial reduction of iron, with the bacteria consuming organic matter deposited at the margins of sandstone channels [369, 371]. The uranium source in this region, as in the Powder River Basin of Wyoming, is thought to be tuffaceous rocks of the White River Group [369].

### *Cheyenne Basin*

A significant uranium roll-front system formed in the Cretaceous Fox Hills and Laramie Formations of the Cheyenne Basin, located in northern Colorado and southern Wyoming (Fig. 135) [372]. Although only minor uranium from the Grover in situ recovery pilot project has been produced from this basin, several deposits, including the Centennial deposit (4800 tU resources averaging 0.08% U) have been delineated. The Upper Cretaceous Fox Hills and Laramie Formations were deposited as offshore barrier island and deltaic marine complexes with roll-fronts mapped continuously over 50 km in various parts of the basin [373].

### Metallogenesis

Uranium roll-front deposits are generally believed to form in response to chemical changes wherein alkaline, oxidizing groundwaters with high uranium contents encounter chemically reducing environments in the host sandstone. The type of reductant varies depending on the local geology but is typically pre-ore carbon, sulphide, or hydrocarbons present within the sandstone. Although the geochemical cells associated with roll-front deposits are complex, variable and mineralogically unique, some general patterns are evident in roll-front deposits from different areas. Sandstones on the oxidized side of the roll are typically pink and haematite-bearing. Where present in the pre-ore sandstone, calcite has been leached, carbon destroyed, feldspar altered to montmorillonite or nontronite and iron and magnesium silicates altered or destroyed during oxidation.

In oxidized sandstones, iron is present as a ferric species and sulphur is found more often as sulphate rather than sulphide. Closer to the roll-front, siderite, ferroselite and goethite increase in abundance. In the ore zone, the sandstone becomes enriched in Mo, Se, V, Co, Mn and As minerals. Ferrous iron predominates and the organic carbon content increases. Uranium may be in the form of discrete minerals, typically uraninite, coffinite, zippeite, tyuyumunite or carnotite, or may be intergrown with iron oxy-hydroxides or oxides. Uranium minerals are present: (a) as coatings on sand grains; (b) interstitially in the sandstone matrix; (c) within feldspar grains or lithic clasts, and (d) intergrown with clays. Selenium minerals such as ferroselite form on the oxidized side of the roll-front. Uranium minerals are typically concentrated at the redox interface and molybdenum (as molybdenite) is common on the reduced side of the roll (Fig. 136). Vanadium, where present, is found on the oxidized side of the roll-front, adsorbed onto iron oxides or as uranium vanadates. Arsenic is present as a trace element in pyrite on the reduced side of the roll-front and is adsorbed onto iron oxides on the oxidized side of the roll. Carbonate cement at the roll-front interface is more common in younger Tertiary deposits in the USA, making them less amenable to acid leach mining techniques. Down-gradient (reduced) sandstones are grey coloured and contain fresh organic material and/or sulphides, unaltered feldspar, titanomagnetite and iron/magnesium silicates. Clays on the reduced side of the front are sodic and calcic montmorillonite. Sulphides such as jordisite, pyrite and marcasite increase with distance from the roll.

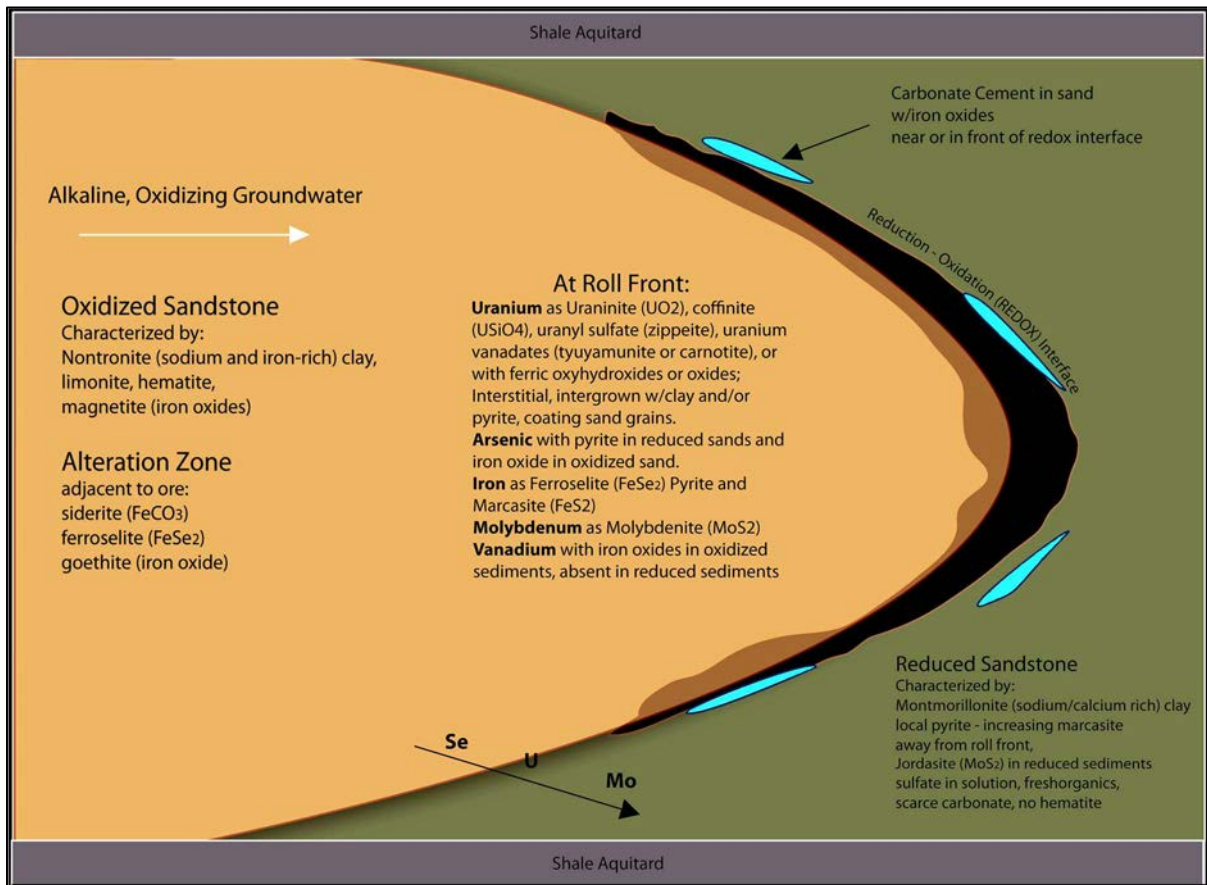


FIG. 136. Mineralogy of an idealized roll-front deposit (adapted from Refs [374–378]).

There is some mineralogical evidence that reduction of uranium may be facilitated or influenced by native bacterial communities within sandstones. Framboidal pyrite in roll-front deposits in Wyoming is believed to have been formed by bacteria, providing possible evidence that bacterial communities were active in these environments [378]. Sulphur isotope studies of deposits from Wyoming basins corroborate the view that bacteria were active in reducing sulphur to form sulphides in roll-front deposits [379]. On the reducing side of roll-fronts, anaerobic bacteria reduce  $\text{H}_2\text{S}$  to form sulphides and biological processes increase the pH and precipitate calcite, creating conditions conducive to uranium precipitation. On the oxidized side of the rolls, aerobic bacteria oxidize sulphide to sulphate and ferrous iron to ferric iron, creating a low pH, high Eh environment that favours oxidation and mobilization of uranium and vanadium [353]. Biological activity also raises bicarbonate concentrations in the water which promotes dissolution of uranium, vanadium, selenium and other redox sensitive elements. Bacteria may not have been as active in organic-poor sequences such as in the Texas Gulf Coast Province [380].

#### *Kingsville Dome and Rosita mines, Texas Gulf Coast Province*

##### Introduction

Among the best studied uranium deposits in the USA are the roll-front deposits of the Texas Gulf Coast Province that have been mined almost continuously since the 1970s. These deposits are found in Tertiary rocks along the Gulf Coast of Texas to the west of the palaeohigh known as the San Marcos Arch (Fig. 137) [376, 381].

Uranium has been mined from the Whitsett Formation (Eocene), Catahoula Formation (Oligocene), Oakville Sandstone (Miocene) and Goliad Sand (Pliocene) [376]. The Oakville Sandstone has been the most prolific, producing 7200 tU, followed by the Goliad Sand from which 2800 tU were mined and the Catahoula Formation which produced 2300 tU (Fig. 138). Additional production reported from Texas (41 000 tU) likely originated from early open-pit mines as well as the three in situ recovery mines developed in the Whitsett Formation, with some contributions from uraniumiferous lignite. Currently identified reserves are dominated by deposits hosted by the Goliad Sand (6300 tU), followed by the Oakville Sandstone (25 tU). No remaining reserves are reported from the Catahoula or Whitsett Formations.

The first uranium deposits mined in Texas were in the Whitsett Formation, which crops out along the northern portion of the province. Uranium was identified in this formation by airborne radiometric survey. Regional groundwater sampling from existing wells is typically used as a reconnaissance technique to target roll-fronts in Texas. Many deposits were also initially identified from gamma anomalies in Tertiary rocks in oil and gas wells. Once prospective ground is identified, follow-up logging and sampling of rotary drill cuttings is standard practice. Drill holes are also commonly logged using prompt fission neutron technology to directly measure the  $^{235}\text{U}$  content.

The Kingsville Dome and Rosita mines extracted uranium from roll-front deposits in the Goliad Sand (Figs. 137 and 138). The Kingsville Dome mine is located about 13 km south-east of Kingsville and the Rosita mine is 30 km north-west of Alice. Kingsville Dome was mined intermittently from 1987 until 2009 with the development of at least 14 well fields, producing in total of 1672 tU. In all, 1019 tU was produced from Rosita between 1990 and 1999 and during a short period of production in 2008. At Kingsville Dome, uranium mineralization was discovered during oil and gas exploration that focused on locating structural traps related to the Kingsville Dome salt diapir. Many deposits in south Texas formed adjacent to known structures and above structural highs caused by salt domes [382, 383]. However, some deposits appear to have formed without an externally sourced reductant [384–386].

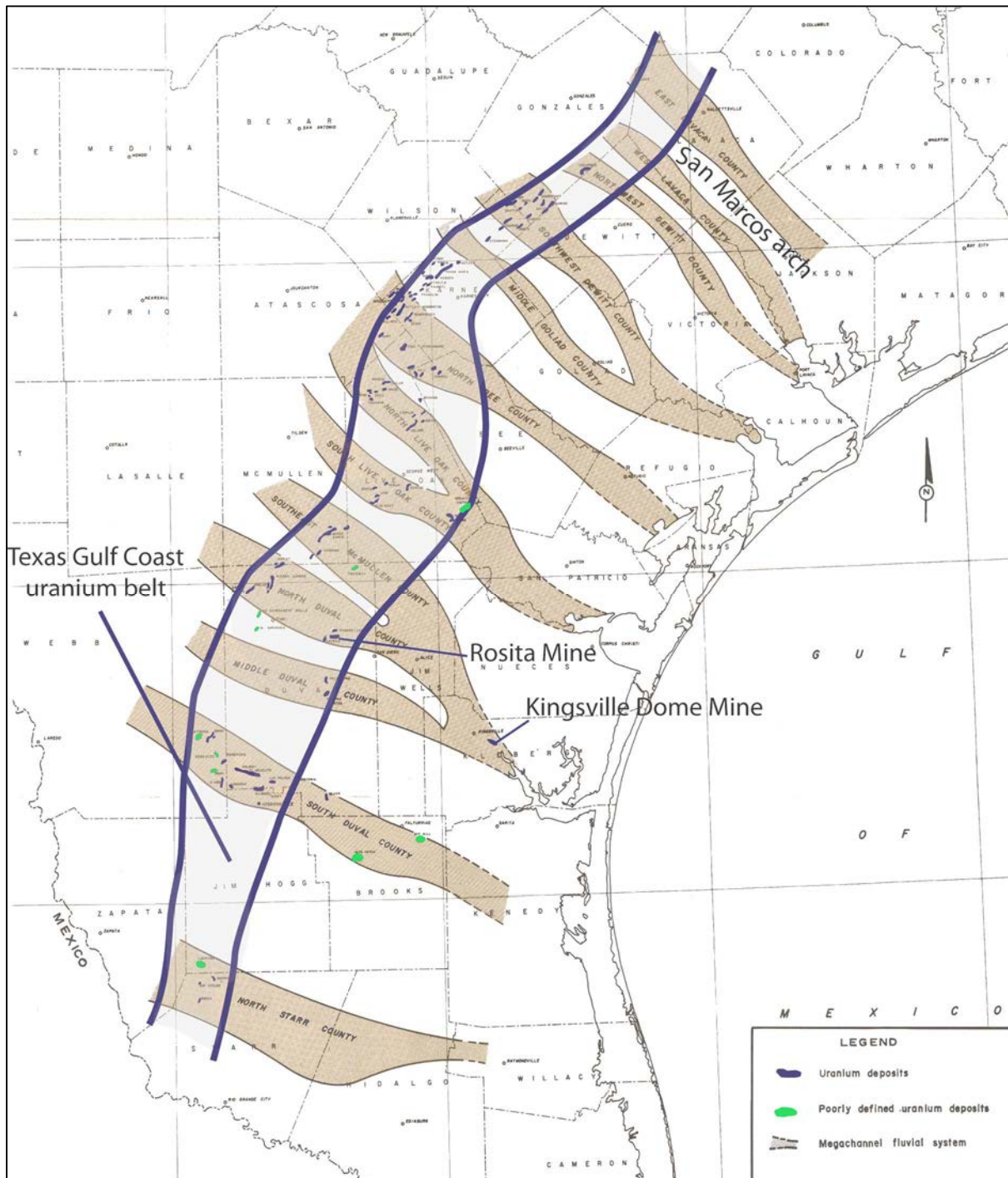


FIG. 137. Location of uranium deposits in south Texas showing major palaeochannels [387] (reproduced with permission).

System Series	Geologic Unit	Lithology	Uranium		
Quaternary	Holocene	Floodplain and fluvial terrace deposits			
	Pleistocene	Deweyville Formation, Beaumont Formation Montgomery Formation, Bentley Formation, Willis Formation	Sand, gravel, silt clay		
Tertiary (part)	Pliocene	Goliad Sand	Sand, conglomerate, calcareous sand basal medium to coarse sandstone strongly calcified		
		Fleming Formation	Calcareous clay and sand		
	Miocene	Oakville Sandstone	Calcareous, crossbedded, coarse sand, some clay, silt and reworked sand and clay pebbles near base		
		Oligocene	Catahoula Formation	Chusa Tuff Member	
	Soledad Conglomerate Member			Calcareous tuff, bentonitic clay, some gravel and varicolored sand near base	
	Fant Tuff Member				
	Eocene (part)	Whitsett Formation	Frio Clay	Light-gray to green clay, local sand filled channels	
			Fashing Clay Member	Clay, some lignite and sand	
			Tordilla Sandstone Member	Very fine sand	
			Dubose Member	Silt, sand, clay and lignite	
Deweessville Sandstone Member			Mostly fine sand, some carbonaceous silt and clay		
Conquista Clay Member			Carbonaceous clay		
Dilworth Sandstone Member	Fine sand				

FIG. 138. Stratigraphic position of uranium deposits (marked yellow), within Tertiary units of south Texas [381] (reproduced with permission).

## Geological setting

The Goliad Sand in the area of both Kingsville Dome and Rosita consists of a series of coarse-grained, calcareous sandstones interbedded with claystone and siltstone [382]. Finer grained sandstones are well indurated, whereas coarser grained sandstones are poorly consolidated [374]. The sandstones are mostly litharenites comprised of mixed sedimentary, volcanic and metamorphic rock fragments. Sparite and micrite carbonate cements are common. At Rosita, white calcareous clay balls are found in finer grained sandstones and claystone [374]. The porosity of the Goliad Sand at Kingsville Dome varies in the range 29–41%, with a mean of 33% [382, 388].

The Goliad Sand is a fluviodeltaic unit along the South Texas Coastal Plain [388]. Correlations of drill logs across the property indicate an upwards coarsening sandstone that prograded across mudstone and was subsequently capped by younger mudstone. At Kingsville Dome, the mudstone is interbedded with channel fill or barrier bar sandstone lenses. Further inland, at Rosita, the mudstone is interbedded with fluvial channel sandstone with abundant crevasse splays. The presence of foraminifera and glauconite indicates shallow shelf, coastal bay, lagoon and estuarine environments proximal to an active shoreline [374, 382]. The clastic material was likely transported a short distance to the site of deposition, as indicated by the preservation of metastable volcanic rock fragments and carbonate clasts and the euhedral shape of quartz and feldspar grains. The climate during deposition of the Goliad Sand was likely arid, as evidenced by the preservation of carbonate clasts [381].

The Kingsville Dome deposit is made up of multiple roll-fronts, ranging in width around 9–20 m and situated 200–250 m below the surface in a confined sandstone aquifer. Regional groundwater flow, which transported uranium for the roll-front deposits, is naturally in an eastwards direction, towards the Gulf Coast. However, a cone of depression near Kingsville has now formed in response to water withdrawal for municipal and industrial uses [382].

Uranium orebodies in south Texas typically exhibit C-shaped rolls, with individual shapes controlled by local variations in sandstone facies and by the location of reductants. Individual orebodies are reasonably small, usually less than 5 m thick, pod-like and can be traced discontinuously over several kilometres. They are typically stacked and show traces of ‘ghost rolls’ upgradient from the present-day location created by the relatively young and actively migrating mineralized fronts. Deposits range from about 30 to about 3900 tU in size and average 0.07–0.08% U [1, 47].

## Mineralization

At Kingsville Dome, uranium is present in the interstices between sandstone grains in classic C-shaped roll-fronts typical of the Gulf Coast. Uranium minerals fill spaces between sand grains in rocks with the greatest transmissivity. A defined redox front trends NW–SE along the south-west flank of the Kingsville Dome. Individual rolls are about 9–20 m wide. Ghost rolls defined by radioactive uranium progeny are found within barren oxidized zones 15–30 m up-gradient of the mineralized roll-front deposits. As this was such an actively migrating system, the use of prompt fission neutron logging to directly measure  $^{235}\text{U}$  is critical to define the shape, position and grade of mineable roll-fronts.

Within roll-front deposits at Kingsville Dome, uranium ore phases include uraninite and amorphous uranium minerals, possibly pitchblende. They are associated with titanium oxide, marcasite, pyrite and calcic montmorillonite. Uranium is also adsorbed onto clay minerals in the sandstone. Pyrite and marcasite replace detrital ilmenite or titaniferous magnetite. The paragenetic sequence includes: (i) pre-ore authigenic K-feldspar, kaolinite, montmorillonite, calcite, pyrite and leucosene; (ii) ore stage pyrite, marcasite, uraninite, iron oxy-hydroxide and calcite, and (iii) post-ore authigenic gypsum and baryte. Hydrogen sulphide and methane gases, which were responsible for creating the reducing conditions that preceded deposit formation, dissolved detrital ilmenite throughout the sandstone and liberated iron that subsequently formed pre-ore sulphide and titanium dioxide [382].

At Rosita, uranium formed late in the paragenetic sequence and was accompanied by the formation of montmorillonite clay and calcite cement [374]. In this deposit, uranium is associated with titanium derived from detrital titanomagnetite. Significant amounts of carbonaceous material are not present at either Kingsville Dome or Rosita.

Hydrogen sulphide and methane gas originating from hydrocarbon reservoirs deeper in the section at Kingsville Dome created reducing conditions that were responsible for the formation of roll-front deposits in that area [382]. Fault zones formed the pathways for movement of these reductants from the oil and gas reservoirs that underlie the Tertiary strata [387]. The reductant at Rosita is believed to be iron sulphides formed by normal diagenetic processes within the host rocks and from H<sub>2</sub>S from petroleum accumulations deeper in the section which migrated upwards along faults into the Goliad Sand [374].

Detailed studies of the mineralogy and stable isotope systematics of other deposits in south Texas show isotopically heavy pre- or post-ore pyrite that likely formed from sulphur originating from hydrocarbons deeper in the sedimentary section. Isotopically lighter marcasite and pyrite formed as part of the ore forming process by partial oxidation of pre-ore sulphides [380]. However, some other deposits formed in response to reduction related to the presence of lignite and other organic matter in the local sandstone [386].

On the basis of disequilibrium studies, uranium mineralization at Kingsville Dome is dated between 159 000 years and 1 Ma. However, uranium migration continues to the present-day. Other roll-front deposits in Miocene sandstones in the Texas Gulf Coast Province have been dated at 5.07 Ma using uranium–lead dating techniques [389].

The source of uranium for Gulf Coast roll-front deposits is poorly understood, but is thought to be derived from volcanic rock fragments eroded from highland areas to the south-west or from air fall ash interbedded with the host sandstone [376, 387]. The NW trending San Marcos Arch near Victoria which marks the eastern limit of known uranium deposits in Texas may have controlled the easternmost distribution of these volcanoclastic sediments or of the volcanic ash, effectively limiting economic concentrations of uranium to areas west of this palaeohigh. Deposits may also have formed from weathering and reconcentration of uranium in exposed Catahoula Formation or similar uranium-rich tuffs.

Alkaline groundwater likely leached uranium from source rocks, transporting it down-gradient as uranium reaction fronts. Dissolved carbonate, derived from micritic clasts and diagenetic overgrowths in sandstone, likely acted as a complexing agent in the groundwater, aiding in the efficient transport of uranium in solution. Uranium was transported and formed deposits in sandstone facies with the highest transmissivity. These sandstones are generally organic-poor, which allowed uranium to be transported through the section without reduction en route [376, 390]. The climate during the Tertiary in south Texas was arid to semi-arid, an environment in which biological productivity was low, yielding organic-poor sandstones critical for uranium movement through the section. Arid to semi-arid conditions favoured alkaline groundwater capable of leaching uranium from tuff and volcanoclastic clasts within the sedimentary section [376]. This model fits well with detailed mineralogical studies of the Kingsville Dome and Rosita deposits. Alkaline groundwater moved eastwards through the Goliad Sand and encountered reducing conditions adjacent to the areas upwarped by doming and faulting at Kingsville Dome and by deep faulting at Rosita, thereby localizing deposits in these two areas. Continued H<sub>2</sub>S and methane influx locally resulted in reduction of the host sandstone. At the Vasquez deposit, ore phase minerals are enclosed by late stage pyrite in the host Oakville Sandstone, leading to difficulties in uranium recovery by in situ leach oxidation.

## *The Budenovskoye deposit (Kazakhstan)*

### Introduction

The Budenovskoye uranium deposit is located in the south-western part of the Chu-Sarysu Depression, Suzak district, approximately 400 km north-west of Shymkent and 200 km east of Kyzyl-Orda (Fig. 139).

The deposit extends for about 75 km in a N–S direction. To the north it is separated from the Inkai uranium deposit by a barren or weakly mineralized interval about 20 km long and is limited to the south by the Karatau Range. It is subdivided into the northern (Saumalkolsky) and southern (Kabanbulaksky) subfields. The Budenovskoye deposit is the southern continuation of the Inkai deposit [27].

The Budenovskoye mineralization was discovered in 1979. Exploration in the northern subfield was undertaken between 1987 and 1990 by ‘Unit 7 of the Geological Exploration Expedition’, on a 3.2–6.4 km drill line spacing with drill holes 50–100 m apart. Exploration in the southern subfield by ‘Unit 5 of the Geological Exploration Expedition’ between 1982 and 1986 included initial and more detailed drilling (up to an 800 m line spacing with a drill spacing of 50–200 m). Up to 1990, a total of 88 575 m was drilled in the northern and southern subfields.

As a result of historical exploration activities, uranium resources were estimated at 151 000 tU for the northern subfield and 204 000 tU for the southern subfield. Thus, total in situ resources are more than 350 000 tU at an average grade of about 0.07% U. Owing to the widespread occurrence of oxbow lakes and floodplain marshes along the Shu River, the northern subfield is not considered a priority project for development.

The southern subfield is operated by Kazatomprom and is divided into six mine sites (Fig. 140). The 2015 production from Budenovskoye 1-2-3-4 amounted to 3700 tU.

### Geological setting

The Budenovskoye deposit is located in the Chu-Sarysu depression, which represents a large Cretaceous basin up to 250 km wide extending northwards from the foothills of the Tien Shan Mountains for over 1000 km. The basin is underlain and flanked by folded Early Proterozoic formations, which are exposed at the south-west margin where the Karatau Mountains separate the Chu-Sarysu Basin from the parallel Syr Darya Basin. The platform consists of continental sediments up to 320 m thick and Palaeogene marine sediments up to 200 m thick that are overlain by red sandy clay sediments of Oligocene–Quaternary age. The basin is an asymmetric syncline with a broad, gently sloping north-east limb and an uplifted south limb (forming the Karatau Mountains) [27]. The axis of the basin is parallel to its south-west margin (Fig. 141).

The Budenovskoye uranium mineralization is hosted in three upper Cretaceous horizons, namely the Jalpak, Inkuduk, and Mynkuduk:

- (i) The lowest Mynkuduk horizon is located about 620–800 m below the surface and consists of coarse-grained grey alluvial sediments at the base where the uranium mineralization is hosted, grading upward into fine-grained sands. Total thickness of the Mynkuduk horizon is 40–90 m;
- (ii) The Inkuduk horizon is composed of coarse basal gravel grading upward into fine- to medium-grained sand, with interbedded clay beds 105–130 m thick, at depths of between 530 and 670 m;
- (iii) Overlying the Inkuduk horizon at typical depths of between 470 m and 615 m, the Jalpak horizon consists of medium-grained grey–green sands grading upwards to red and brown clays 20–80 m thick.

The above units meander in plan, in bands 27–67 km long, 50–1500 m wide and 0.5–20 m thick. The mineralized bands average 4–6 m in thickness. The overlying Palaeogene sediments consist of 140–220 m of grey–green clay and siltstone overlain by 200 m of Neogene sand and clay. There is up to 60 m of Quaternary alluvial sand, clay and loam. In plan, the mineralized deposits are represented as ‘weaving ribbons’ of varying width and length controlled by the oxidation zone boundary (Fig. 140).

The widths of the deposits may vary from tens of metres to one kilometre, often dependent on the thickness and frequency of the internal confining layers that complicate the boundary of the zone of formation oxidation thinning in the stratigraphy. The extended upper limb of a roll complicated by stepwise ‘sliding’ of the geochemical boundary is usually observed when the thickness of the horizons is considerable and several confining lenses are available in the area of the zone of formation oxidation boundary thinning. Multi-stage bodies and extended limbs consisting of a number of mineralized lenses, which are also found in abundance between the limbs, are typical of the deposit stratigraphy and confirm the extreme complexity of the enclosing rock sequence. The rolled parts of various widths are encountered practically everywhere, with the exception of the Mynkuduk.

### Mineralization

The Jalpak horizon occurs at a depth of between 470 m and 615 m and is subdivided into the Lower Jalpak subhorizon (75–80 m thick) and the Upper Jalpak subhorizon (25–35 m thick). Uranium mineralization has only been recorded in the Lower Jalpak subhorizon. It can be traced over 60 km and is 500–1500 m wide.

The maximum total thickness of the mineralized horizons is 5.8 m at a grade of 0.076% U. The mineralized deposits are confined to medium-grained sands with pebble and gravel lenses, with a relatively high carbonized organic content.

The Inkuduk horizon occurs at a depth of between 530 and 670 m has an average thickness of 85 m. It can be traced for over 35 km along strike. The mineralization varies between 0.5 and 20.9 km in width. The mineralized horizons are up to 20.9 m thick with a grade up to 0.098% U, hosted by coarse sand with gravel.

The Mynkuduk horizon typically lies at a depth of between 620 m and 800 m and is approximately 35 m thick. It is typically composed of coarse sand, sandy gravel and fine gravel. Rare, thin (up to 1 m thick) layers of clay and sandy shale are found within the horizon, increasing in frequency upward. The uranium mineralization of commercial interest varies between 200 and 800 m wide in plan and has a total thickness of up to 12 m containing up to 0.120% U. It is hosted by coarse-grained, poorly sorted grey sands and has been traced for over 55 km along strike.

The mineralized horizons are typically shaped as lenses and, to a lesser extent, rolls. The mineralization is hosted by sand with an uneven grain size distribution, typically coarse- to medium-grained, with possibly a significant fine content. Acid resistant minerals predominate in the mineralized sands (averaging 98.5%). Quartz is the major mineral (up to 62%), with feldspar (up to 17%), fragments of siliceous rocks (up to 18%), mica and ‘phytoleims’ (organic matter). Clay minerals, including montmorillonite, kaolinite and mica, are found within the matrix. Accessory minerals and authigenic minerals include ilmenite, pyrite, calcite, siderite, tourmaline, garnet, apatite and rutile.

Coffinite and pitchblende are the main uranium minerals, found as cements and grain coatings. In the Inkuduk horizon, the coffinite and pitchblende are typically found in a 50:50 ratio. The chemical composition of the mineralized horizons is typically silicate (81–85% SiO<sub>2</sub>, 7–10% Al<sub>2</sub>O<sub>3</sub>, 1.9–2.4% Fe<sub>2</sub>O<sub>3</sub>, 2.3–2.7% K<sub>2</sub>O and 0.5–1% Na<sub>2</sub>O).

The carbonate content of the Budenovskoye deposits is less than 1% CaCO<sub>3</sub>. The Jalpak, Inkuduk and Mynkuduk horizons form a single aquifer with no continuous impermeable layer separating them, thus

representing a single aquifer 200–245 m thick with filtration coefficients (hydraulic conductivity) of 2.9–7.2 m/d. The piezometric surface is orientated SSE–NNW.

The aquifer is recharged in the Karatau Mountains. The subsurface water in the south has 0.5–1.5 g/L of dissolved solids, increasing to 1.8 g/L at Karatau and 3.5–3.6 g/L in the north (at the Inkai deposit). The groundwater features an absence of dissolved oxygen, low negative values for redox potential, the presence of hydrogen sulphide and near-neutral to alkaline conditions. Dissolved mineral concentrations in the aquifers are typically:

- $2.5 \times 10^{-4}$  g/L uranium;
- $8.2 \times 10^{-10}$  g/L radium;
- $1.0 \times 10^{-5}$  g/L molybdenum;
- $1.4 \times 10^{-4}$  g/L zinc;
- $1.8\text{--}2.0 \times 10^{-7}$  g/L rhenium.

#### Metallogenic aspect

The Kazakhstan deposits are considered roll-front deposits but are of an exceptional size. The geology and genesis of roll-front uranium deposits have been studied since the 1960s. These deposits are typically found in Cenozoic intermontane basins where uranium occurs in the form of mineralized roll-fronts emplaced at the redox interface in continental sandstones containing detrital carbonaceous material.

Epigenetic deposits are formed by down-dip migration of oxidizing solutions, with a concentration of uranium mineralization occurring at the redox front. The highest grade portion of the front is in the main part of the C-shape, with lesser grades found on the upper and lower limbs. The sandstone behind the front is altered but essentially barren.

The most favourable host rocks are friable, fine- to coarse-grained arkosic sandstones containing pyrite and carbonaceous material. Interbedded mudstone, claystone and siltstone are often present. Sand and silt channels with cross-bedding are also common.

Below the water table, unaltered sandstone is light grey to greenish grey with abundant pyrite and carbonaceous material, while the altered sandstone is reddish or greenish yellow, with no pyrite and little carbonaceous material. The roll-front alteration penetrates the sandstone down-dip. The fronts vary widely in size and shape and commonly have lateral ranges of several kilometres and thicknesses of several metres. Within any one formation, there may be many individual beds that contain roll-fronts.

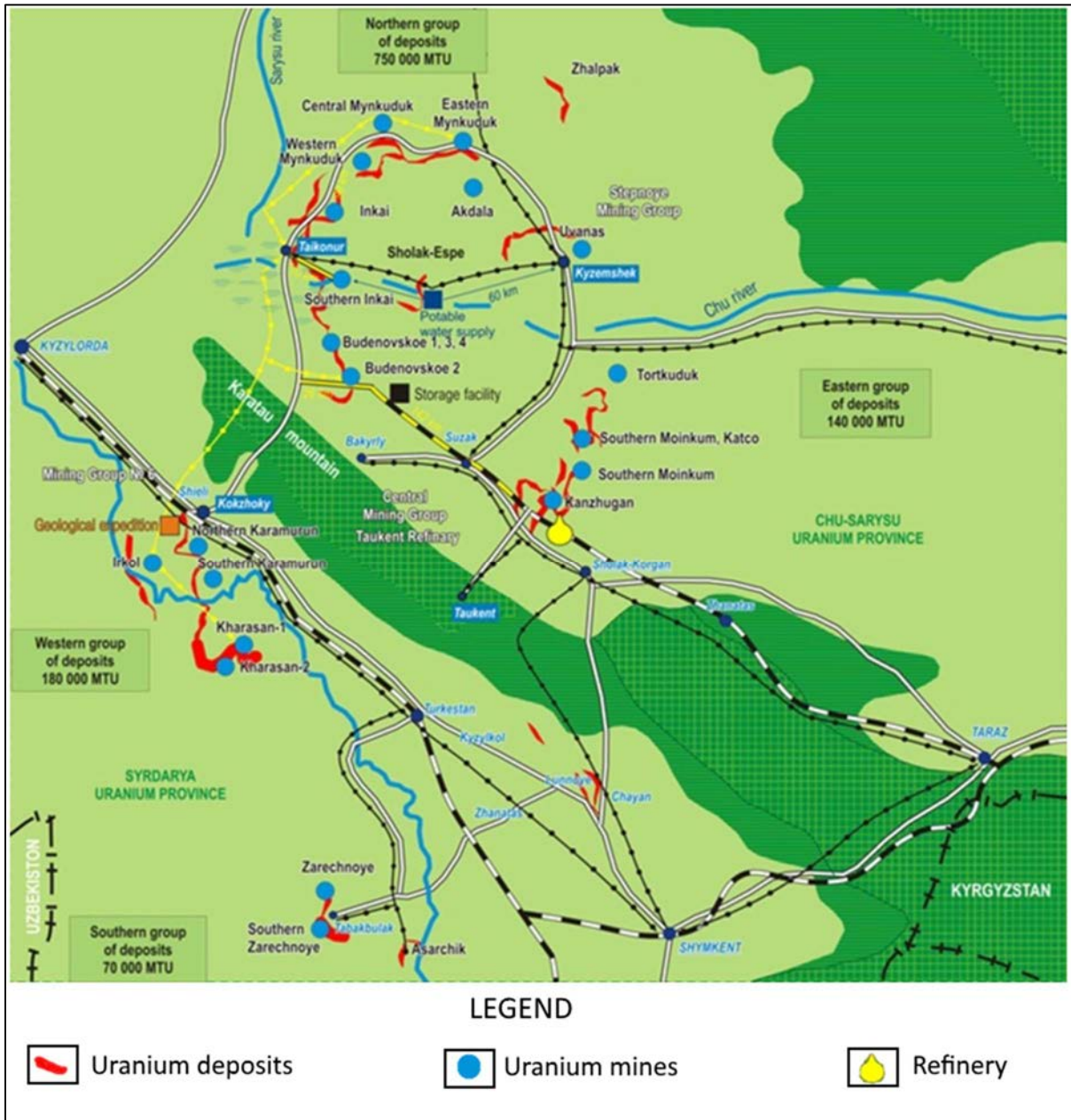


FIG. 139. Location of the Budenovskoye deposit (reproduced courtesy of A. Boitsov, ARMZ/Uranium I).

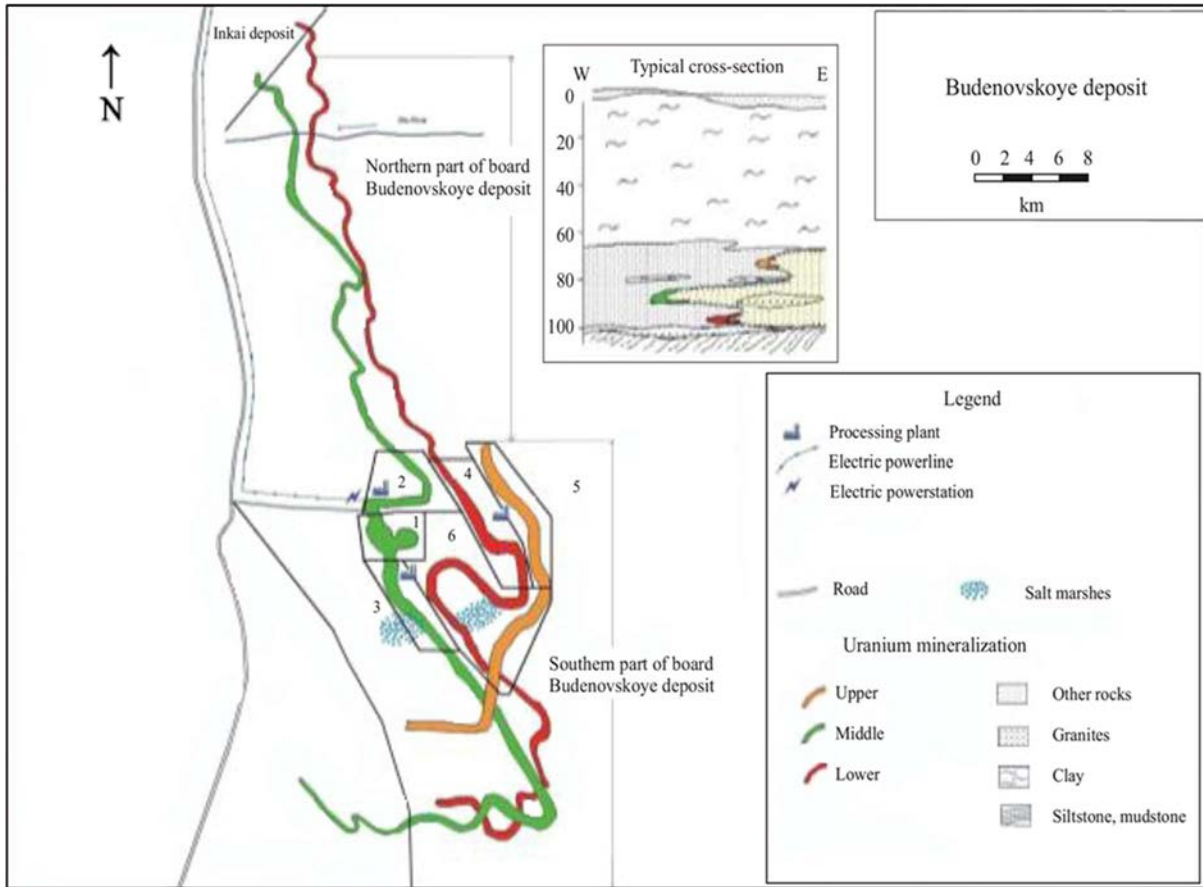


FIG. 140. Plan and typical cross-section of the Budenovskoye deposit (reproduced courtesy of A. Boitsov, ARMZ/Uranium 1).

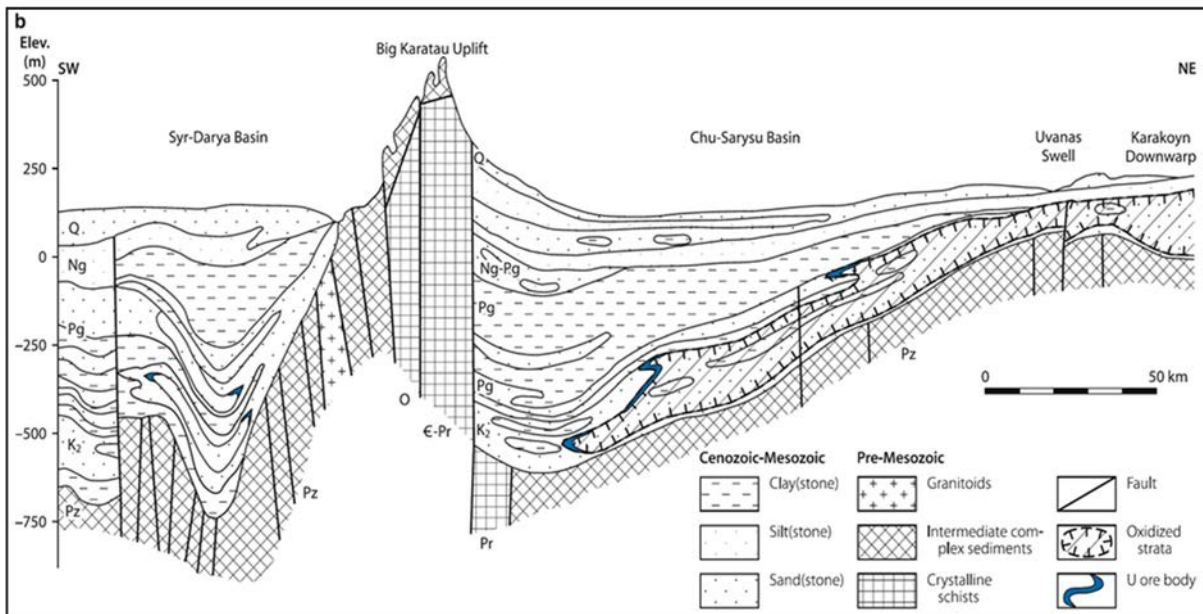


FIG. 141. Geological cross-section (NE-SW) showing the location of the redox front and related uranium deposits [19] (reproduced with permission).

### 3.9.6. Tectonic-lithologic sandstone deposits

#### 3.9.6.1. Definition

Tectonic-lithologic sandstone deposits are discordant to the surrounding strata. They occur along permeable fault zones with linguiform impregnation of the adjacent clastic sediments (i.e. tongue-like impregnations extending away from faults into the surrounding country rock). Thick, steeply dipping orebodies referred to as 'stack' deposits can result from redistribution of primary uranium into permissive hosts such as fault zones or permeable sedimentary units by younger processes, for example, in the Grants Mineral Belt. They may also originate by the introduction of primary uranium, as interpreted for some deposits in Gabon (Mikouloungou).

Twenty-four tectonic-lithologic sandstone deposits are recorded in the UDEPO database (Table 30). Most of them are located in two areas, the Lodève district (France) and the Franceville Basin (Gabon). Both of these deposits are now depleted but exploration has been restarted in Gabon. Resources are small to medium (100–10 000 tU) and grades are low to medium (0.10–0.40% U).

These deposits are probably more common than previously thought, in particular in the USA. For example, in the Morrison Formation sandstones of the Grants Mineral Belt, tabular or roll-type primary mineralization is frequently redistributed along faults forming stack orebodies which usually cross-cut sandstone strata concentrating in or along steeply dipping faults of Tertiary age or younger [47].

TABLE 30. PRINCIPAL TECTONIC-LITHOLOGIC SANDSTONE DEPOSITS (as of 31 December 2015)

Deposit	Country	Resources (tU)	Grade (% U)	Status
Oklo	Gabon	14 800	0.37	Depleted
Ust-Uyuskoye	Russian Federation	13 160	0.092	Dormant
Mas Lavayre	France	12 250	0.31	Depleted
Sernoye	Turkmenistan	7 000	0.45	Depleted
Mounana	Gabon	5 760	0.49	Depleted
Bagombé	Gabon	5 420	0.027	Exploration
Buyanovskoye	Russian Federation	5 300	0.108	Dormant
Tréviels	France	3 102	0.13	Depleted
Boyindzy	Gabon	2 470	0.31	Depleted
Okelobondo North	Gabon	1 990	0.42	Depleted
Okelobondo South	Gabon	1 335	0.35	Depleted
Failles Sud	France	1 377	0.216	Depleted
Mas d'Alary	France	1 280	0.17	Depleted
Mikouloungou	Gabon	1 135	0.38	Depleted

#### 3.9.6.2. Description of selected deposits of the Lodève Basin (France)

##### Introduction

The Permian continental Lodève Basin is located in the southern part of the Massif Central, 45 km west of Montpellier. Its total area is approximately 250 km<sup>2</sup>. It features an eroded depression, surface bounded to the west by the Montagne Noire, to the north and north-east by the Larzac causses (limestone plateaus) and to the south it disappears under the Cenozoic Languedoc Plain.

The first mineralized outcrop was discovered in 1957 within Thuringian formations by carbone radiometric prospecting [391]. Before mining, total reserves of the basin were estimated at 18 000 tU at an average grade of 0.22% U. Between 1981 and 1997, 14 240 tU were produced from 12 underground (12 860 tU at 0.313% U) and open pit (1380 tU at 0.303% U) mines. The largest deposit was Mas Lavayre which produced 12 250 tU and was mined to a depth of 310 m.

### Geological setting

The Lodève Basin is a monoclinical structure dipping gently (10–15°) to the south (Figs 142 and 143). It is limited along its western, southern and eastern boundaries by major E–W and NNE–SSW trending Hercynian faults which were reactivated during the Pyrenean Orogeny. Towards the north, the Permian sediments of the basin unconformably overlie strongly folded Precambrian schists and Cambrian dolomite of the Lodève Uplift. The Permian basinal formations are cross-cut by a network of E–W trending normal faults with ‘wedge and strip’ geometry. These faults play an important role in the distribution of uranium deposits.

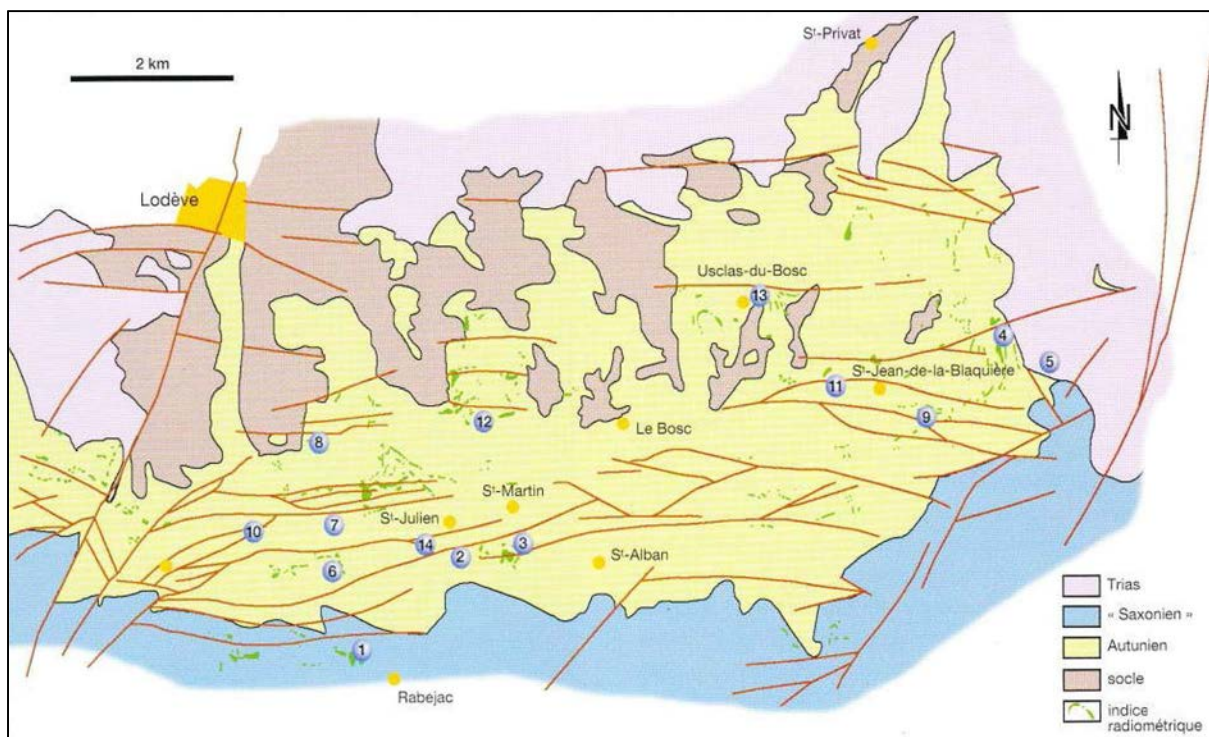


FIG. 142. Geological map of the Permian Lodève Basin showing the location of the uranium deposits [392] (reproduced with permission).

The Permian units correlate with the classical succession found across the European Hercynian period. At the base, Carboniferous strata (Stephanian Series) with coal beds is only present in the southern, deepest part of the basin. It is overlain by the fluviodeltaic Autunian, Saxonian and Thuringian Series with a thickness of at least 2500 m. The coarse detrital facies, at the base of the Permian sedimentary sequence, was deposited on a palaeosurface that cuts the Cambrian basement and displays a dome and basin pattern. South striking, parallel valleys are present on the southern side of the Lodève Uplift [393].

The Autunian contains most of the uranium deposits. With a maximum thickness of 650 m, it comprises four units:

- (i) A basal conglomerate (0–80 m thick) with dolomitic clasts, irregularly deposited along the palaeovalleys;
- (ii) A grey unit (150 m thick);
- (iii) A grey–green–red unit (150 m thick);
- (iv) An upper red unit (300 m thick).

The entire basal conglomerate was produced by the erosion of the Cambrian dolomite with very limited transport of the eroded material. The overlying three units are each composed of a succession of elementary sequences of variable colour and thickness. The sequences have identical lithologies, with sandstone at the base, a central bituminous layer and pelites at the top. Sandstone is very fine-grained with a silty matrix and generally cemented by carbonates. The grey–black bituminous layer, called ‘couche’, alternates in composition between very fine-grained, millimetre thick laminae of carbonate-bearing sandstone and organic-rich carbonates often becoming dolomitic towards the top of the sequence, with sedimentary structures indicative of shallow water to emergent conditions (mud cracks, rain drop casts, ripple marks and vertebrate tracks). About 50 such sequences have been identified in the Autunian. Their thicknesses vary from 1 to 15 m but they show remarkable continuity across the entire basin [394].

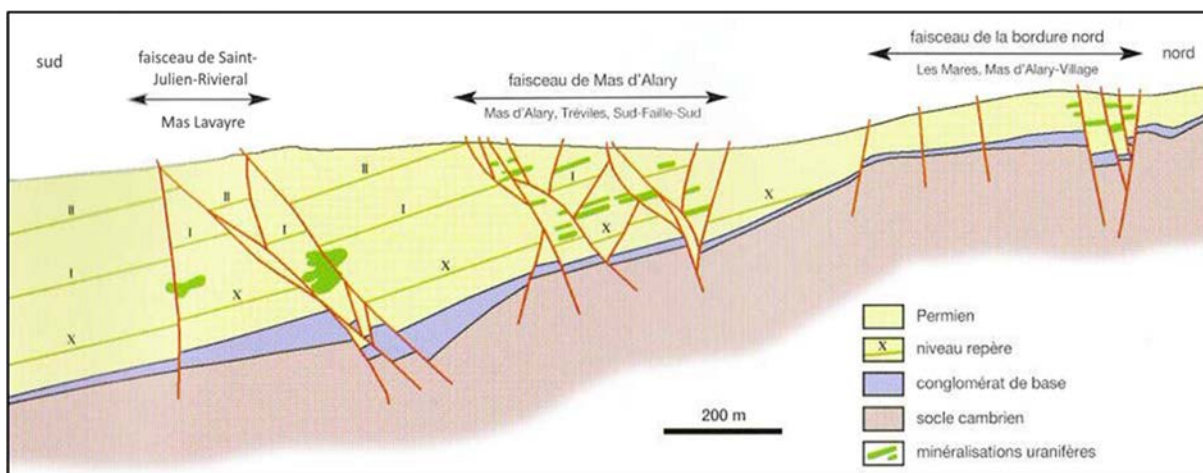


FIG. 143. Geological cross-section of the north margin of the Permian Lodève Basin showing the location of mineralization associated with the main fault systems [392] (reproduced with permission).

In addition, 20 volcanic ash beds (cinerites), centimetres to decimetres thick, are intercalated within the Autunian strata. White in colour, they constitute excellent marker horizons throughout the entire basin. Ash beds change from potassic (sanidine, microcline) to sodic (albite, analcite) towards the top of the series. During diagenesis, the original textures of the ash marker beds have been completely destroyed. The location of the volcanoes is not known [394].

The Autunian is overlain by a minor unconformity and more than 1500 m of Saxonian Series sediments. They are very uniform across the basin, consisting of a thin basal conglomerate overlain by 50–100 m of fine-grained sandstone. The bulk of the series is composed of claystone, occasionally carbonate-rich, with some intercalations of carbonate cemented sandstone. This unit exhibits regional continuity. The Saxonian series is brick red in colour with some greenish intervals at the top and features mud cracks and vertebrate tracks. It is overlain by discordant Triassic formations.

The base of the Autunian series is rich in organic matter. A small portion of it is detrital, derived from plants and trees (*Walchia* trunks and fragments), but the majority of the organic matter originates from lacustrine and marine plankton and algae. It is present as well stratified kero-bituminous schists within

the couche facies or as bitumen which has migrated within fractures. It is erratically distributed throughout the series, even within an individual layer. There is no variation in the composition between the uraniferous and the barren horizons [394]. The Autunian shales have matured to the point of oil generation by burial and thus are excellent hydrocarbon source rocks. The migration of hydrocarbons from the shales into reservoir horizons (breccias, faults, sandstones and dolomites) has created a reducing environment in the facies originally unfavourable to uranium. These liquid hydrocarbons evolved into almost insoluble solid bitumen [395]. This transformation may have been caused by radiation from the uranium (dehydrogenation of the organic matter and destruction of the amino acids) or else (since certain bitumens are barren) by bacterial decay related to either meteoric water (aerobic bacteria) or connate saline water (anaerobic bacteria).

Compaction is very important in a sequence as fine-grained as the Permian of Lodève. Compaction ratios are estimated at 1–3 for the sandstone and as much as 1–50 for the pelites or the couches [396]. Circulating fluids and soluble elements moved through the basin, following the more favourable zones such as thickened detritus-rich zones (palaeovalleys), faults and joints, playing an important role in concentrating minerals. Porosity and permeability are very low because of the fine grain size but also because of the clogging of pore space by diagenetic phenomena, such as carbonation and, especially, albitization. As a result, the claystone and sandstone are almost totally impermeable. Only the couche facies, owing to its fine bedding, has retained some permeability, permitting circulation of meteoric and compaction water. Post-diagenetic dissolution along the base of the Autunian and Cambrian strata developed karst and cellular dolomite where the hydrocarbons are frequently found [394].

The original nature of the Autunian sediments is often obscured by the effects of diagenesis. Feldspars are dominant (45–55% within the sandstones, couches and cinerites (volcanic ash-rich rocks) and 20–30% within the pelites). They range from potassic at the base to sodic towards the top. The detrital K-feldspars are found in greatest quantity in the grey Autunian sediments where they have best resisted the saline brines produced by compaction, while Na has been leached. Newly formed albite, present throughout the series, becomes dominant in the red layers where the K-feldspars disappear. Quartz is secondary in abundance (15–20% in the sandstones and cinerites where it is authigenic, 2–10% in the pelites and couches). Clay minerals (from 10% in the sandstones to 65% in the pelites) evolved similarly to the feldspars. Montmorillonite dominates in the upper portion and grades to illite–montmorillonite towards the base. Diagenetic illite is the only clay mineral present in the lower portion of the Autunian strata. Kaolinite is confined to the red facies. Carbonates are abundant (20% in the sandstones and couches, 5% in the pelites). Calcite dominates throughout the flood plain sediments (red Autunian), while the lagoonal sediments (grey) are dolomitic. Within the grey Autunian, abundant evidence of epigenetic sulphate crystals in the carbonates, caused by bacterial action, are observed [394].

The Lodève Basin is located in a depression zone bordered to the east, south and west by late Hercynian transverse faults related to NW–SE compression, while to the north, the sediments of the basin are discordant on the Cambrian basement. The basin thus initiated at a very early stage as a half-graben and formed a weaker zone favourable for subsidence. These faults were reactivated from Stephanian to present times, influencing the nature and distribution of the sedimentary rocks. Lastly, Palatinian deformation indicates a stress regime of N–S extension which later influenced the syn- and post-diagenetic structures [394].

### Mineralization

In the Lodève Basin, uranium is found in 14 deposits (Fig. 142) of variable importance, with Mas Lavayre (12 250 tU) containing more than 75% of the reserves. Other deposits include Mas d'Alary and Treviels (1500 tU combined), Mares, Mas d'Alary, Capitoul, Rouvayret, Hémies, La Plane, Rabejac, Campagnac, Puech Buissou, Failles Centrales et Sud, each representing a few tens to a few hundred tonnes of uranium. One deposit, Saint Jean de la Blaquière, was never mined owing to strong local opposition.

Three major parameters — tectonic, stratigraphical and sedimentological — have controlled the location of mineralization:

- (i) *Tectonic*: most of the economic mineralization is associated with three major tectonic structures, Saint Julien-Riviéral, Mas d'Alary and the north border. These 070–110° striking structures are complex, anastomosing normal fault systems (tectonic bundles). Mineralization is preferentially located in the zones where the faults bend or intersect;
- (ii) *Stratigraphical*: most deposits are situated within the lower grey Autunian and in the grey–red Autunian. Only the Rabejac deposit is located in Saxonian formations;
- (iii) *Sedimentological*: mineralization is preferentially located at the base of the largest sandstone–siltstone sedimentary sequences.

In the Lodève Basin, mineralization is present as stratabound bodies and/or veins. Four types of mineralization have been recognized: (i) stratabound couche type mineralization; (ii) couche–fault mineralization; (iii) mineralization (pods) associated with large fractures, and (iv) veins [393] (Fig. 144).

Stratabound couche type mineralization (type 1) is contained in organic-rich layers with bitumen. Uranium was deposited syngenetically and then concentrated through successive accretionary events during diagenesis. Uranium grade may reach 0.20% U with bed thicknesses of one to a few metres. This mineralization type is common in the upper couches, where the oxidized environment accentuated this phenomenon by liberating most of the available uranium.

Couche–fault mineralization (type 2) is characterized by uranium enrichments in layers intersected by faults. Faults constitute an oil trap and increase the fracturing of the rock. Mineralized structures are thin (a few metres) but continuous for tens to hundreds of metres. Uranium grades are highly variable and may reach 1–2% U. This type of mineralization prevails in most of the Lodève deposits. This includes the small deposits with an average grade of 0.10–0.20% U as well as the larger part of the underground ore at Mas Lavayre.

Mineralization (pods) associated with large fractures (type 3) is associated with intense fracturing developed near the main faults with the formation of cataclastic breccias. Breccias are impregnated by a mixture of microgranular pitchblende and bitumen which are trapped within the pore space of the matrix. Uranium mineralization, which may reach grades of several per cent, migrates beyond the couches to form an almost continuous mineralized lens over an area ranging from several metres to several tens of metres. An example is the central part of the Mas Lavayre orebody, located at the junction of two faults.

Vein mineralization (type 4) is uncommon and only present in the northern part of the basin, near the contact with the Cambrian basement. Mineralization is limited to fractures with limited lateral extent. Rock alteration is more significant than in the other types and organic matter is scarce or absent.

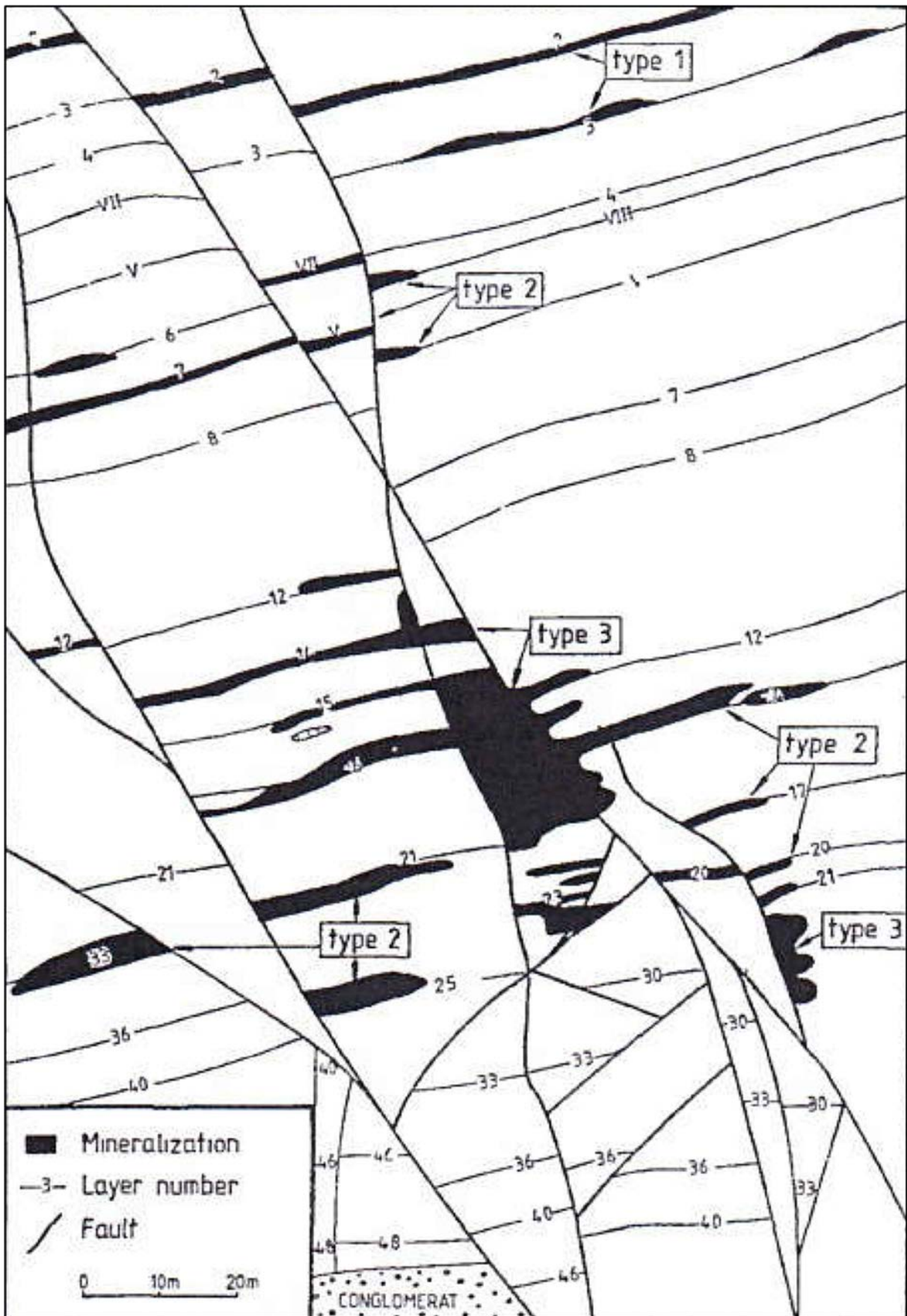


FIG. 144. Mineralization types in the Lodève Basin [394] (reproduced with permission).

Microscopically, mineralization is present in several habits:

- (a) Conformable to the stratification, which is underlined by alternating organic-rich pelite and carbonate seams. Uranium mineralization, difficult to distinguish from the organic matter, is present as diffuse, cryptocrystalline masses or small veinlets within the pelitic seams;
- (b) As microgranular uranium oxides (pitchblende) located at the margin of bitumen impregnations in the carbonate or sandstone facies;
- (c) Filling microfractures: uranium oxides are intimately mixed with argillaceous cryptocrystalline products and migrated organic matter. In this case, the surrounding rocks may be impregnated outwards from the microfractures.

Pitchblende and coffinite are associated with abundant sulphides, mainly pyrite and sphalerite. Pyrrhotite and galena are rare. Carbonate and quartz are common in fractures. Molybdenum can be found in the upper portion of the Autunian while zirconium may occur in the lower part [394].

Metallogenic aspects

#### *Origin of uranium*

The couche facies contains anomalous uranium concentrations within very large volumes, thus representing a very important metal reservoir. Three sources have been invoked for the origin of the uranium [393]:

- (i) Syngenetic uranium deposited during the sedimentation of the Lodève Basin. This uranium probably originated from the erosion of uraniumiferous Hercynian leucogranites, which are well represented in the Massif Central;
- (ii) Numerous cinerite layers intercalated within the Autunian series indicate nearby active felsic ignimbritic volcanism. Such ignimbrites are easily altered and can release their uranium into the sediments;
- (iii) Deeply sourced hydrothermal origin associated with E–W basement faults. Economic mineralization is always associated with these faults. Fluid inclusion studies of sphalerite indicate the presence of two hydrothermal fluids, a low temperature brine (130–140°C) and a hydrothermal fluid with temperatures of 240–250°C circulating during the mineralizing event [397]. Such a syndimentary hydrothermal event, even if it were not associated with uranium, could have played an important role during the preconcentration phase.

#### *Uranium concentration*

During the Autunian, syndimentary trapping of uranium associated with organic matter create a preconcentration in the couches. At the time of subsidence and burial, organic matter matured and generated hydrocarbons. This bitumen migrated along permeable zones in the couche facies and along extension zones created by the syn- and post-sedimentary structures, preferentially, the E–W normal faults. Bitumen was trapped in the most porous rock reservoir, the fractured and brecciated fault zones, as well as the couche facies. Some uranium may have been transported in the form of organo-metallic complexes [394]. The uraniumiferous fluids in the sediment were also expelled and followed the same path as the bitumen.

Precipitation of uranium was favoured in the open spaces in the fault zones by pressure reduction and a strongly reduced environment. This was accentuated by a process of concentration through repetitive cycles of oxidation–reduction due to the maturation of organic matter and in the permeable zones, by fluids (connate water) expelled by compaction or by meteoric water that rose along the faults in the bedrock.

Uranium–lead isotopic studies on uraniferous strata indicate two U–Pb mobilization phases for the base of the Autunian series:  $73 \pm 6$  Ma and  $108 \pm 5$  Ma [398]. The oldest phase is the most clearly expressed. No ‘relic’ feature indicating a Permian age could be recognized in the U–Pb system. The first uranium mobilization has been dated at 170 Ma, during extension of the continental crust. This phase, coinciding with burial metamorphism, induced circulation of mineralized fluids and caused illite recrystallization in the Permian pelites and dolomitization at temperatures of 100–200°C. Alkaline basalt volcanism has been dated at  $155 \pm 6$  Ma in the nearby Permian Rodez Basin [399]. Mid-Jurassic extension is related to the opening of the Tethys Sea. Finally, during the Pyrenean N–S compression phase around 110 Ma, displacement parallel to the sedimentary layering, affected the previous fault system, raising temperatures and causing local remobilization of uranium and bitumen.

### **3.9.7. Mafic dykes/sills in Proterozoic sandstone**

#### *3.9.7.1. Definition*

Deposits hosted by mafic dykes/sills in Proterozoic sandstone consist of U–(Au) mineralization. Eight deposits of this type are recorded in the UDEPO database (Table 31). They are situated within the Westmoreland district, McArthur Basin (Australia) and within the Otish Basin (Canada). Other prospects are known in the Gandi district, Cuddapah Basin (India), in the Alligator Rivers Uranium Field (Australia) and in the Nonacho Basin (Canada).

TABLE 31. DEPOSITS ASSOCIATED WITH MAFIC DYKES IN PROTEROZOIC SANDSTONE  
(as of 31 December 2015)

Deposit	Country	Resources (tU)	Grade (% U)	Status
Redtree	Australia	12 350	0.071	Dormant
Matoush	Canada	10 395	0.47	Dormant
L	Canada	5 065	0.42	Dormant
Junnagunna	Australia	4 365	0.067	Dormant
Huarabagoo	Australia	3 270	0.084	Dormant
Outcamp	Australia	800	0.136	Dormant
Sue	Australia	570	0.136	Dormant
N 147	Australia	450	0.30	Dormant

#### *3.9.7.2. Geological setting*

Mineralization is confined to Palaeoproterozoic–Mesoproterozoic intracratonic basins such as the McArthur Basin (Australia) for mineralization located in the Westmoreland district and in the Alligator Rivers Uranium Field (Australia), the Otish Basin (Canada) and the Cuddapah Basin (India).

The Palaeoproterozoic–Mesoproterozoic McArthur Basin in northern Australia is a large, thick (5–10 km) intracratonic basin, mostly composed of unmetamorphosed sedimentary and volcanic rocks that were deposited between 1800 and 1575 Ma. In the Westmoreland district, the basal Westmoreland Conglomerate is up to 1800 m thick and is conformably overlain by the mafic Seigal Volcanics. Dolerite dykes and minor sills, which may have been feeders of the lava flows, intrude along NE trending fault and fracture zones that cut the basal detrital unit. The Westmoreland uranium deposits (Redtree, Junnagunna and Huarabagoo) lie along the Redtree dyke zone. The primary phase of mineralization occurred between 1655 and 1606 Ma.

Further north, in the Alligator Rivers Uranium Field, the lower Katherine River Group (Kombolgie Formation), which is 3–4 km thick, includes mafic volcanic flows interbedded with sandstone units. It has been intruded by large lopolithic intrusions (Oenpelli Dolerite) at 1725–1720 Ma. Small deposits and prospects (N-147, U-42, Arrara and Caramal) are associated with the mafic sills. In Arnhem Land, an age of 1579 Ma was obtained on uraninite crystals from a mineralized quartz vein intersecting an Oenpelli Dolerite sill [400].

The Otish Basin is situated in Quebec, Canada, and is part of a Palaeoproterozoic continental to marginal marine sedimentary system that formed along the edge of the Superior Craton. The age of the sediments is constrained to a maximum age of 2140 Ma and a minimum age of 1730 Ma by the overlying and intruding Otish Gabbro, which is associated with the uranium mineralization. Mineralized zones are highly variable in size and shape and consist of: (a) stratabound mineralization in the sandstone units subparallel to the contact with the overlying mafic volcanic rocks and/or parallel to the contacts with sills, (b) discordant mineralization in steeply dipping zones adjacent to the contacts with mafic dykes and (3) mineralization associated with steep faults and fractures in the altered mafic dykes. Stratabound mineralization may grade into steeply dipping zones of mineralization adjacent to the contact with mafic dykes. Primary uranium mineralization follows the intrusion of the dykes and is dated to between 1725 and 1710 Ma.

The Cuddapah Basin in India occupies an area of 44 500 km<sup>2</sup> and contains a 12 km thick sequence of sedimentary and volcanic rocks belonging to the Palaeoproterozoic–Neoproterozoic Cuddapah Supergroup (1900–1400 Ma) and Kurnool Group. Uranium mineralization is associated with chloritized, linear mafic dykes intruding the basal arenaceous Gulcheru Formation. Potassium–argon radiometric data obtained on mafic dykes suggest at least four separate periods of dyke emplacement, 1760–1730, 1500–1400, 1100 and 650 Ma. Primary mineralization consists of uraninite and brannerite associated with albite.

### 3.9.7.3. *Metallogenesis*

Mineralization is best classified as a separate deposit subclass, empirically defined as uranium associated with mafic dykes in Proterozoic sandstone. For this type of deposit, the Proterozoic sandstones are much older than the host rocks of typical sandstone uranium deposits and fossilised plant matter is absent and thus very different in term of genesis from the four other subtypes of sandstone deposit. Also, gold values of economic significance are reported from various areas in Canada and Australia associated with uranium mineralization.

The most common uranium mineralization in the Otish Basin (Canada) is epigenetic with a dominant structural control. The best examples are the Matoush deposit in the western central part of the basin and the L deposit. Uranium mineralization is mainly present as pitchblende and is controlled primarily by fractures, but also by favourable lithologies. It is assumed that circulating diagenetic fluids leached the regolith from the basement and led to extensive dolomitization and concentration of uranium. Mineralization at the L deposit consists of a mineralized lens where gabbro meets carbonate rocks. It is believed that mineralized fluids travelled along the southern gabbro contact until they reached the carbonate horizon, which acted as a cap rock and trapped the mineralization underneath. Fractured gabbro margins likely provided sufficient permeability for fluid circulation. Other mineralized zones are hosted within the gabbro and represent subvertical fault or fracture corridors with a steep dip to the south.

Uranium mineralization in the Westmoreland region (Australia) consists of uraninite with haematite and illite and occurs within a zone of chlorite alteration that formed prior to the uraninite. Oxygen and hydrogen isotopic compositions of syn-mineralization illite suggest that uranium was transported to the site of deposition by a basinal brine which evolved from evaporated seawater [401]. The relatively impermeable mafic dykes coupled with higher fluid flow created by faults that offset these dykes by up to 30 m provided the structural trap that focused the uranium-bearing brine. The Fe<sup>2+</sup> in the Fe-rich

chlorite adjacent to the mafic dykes and flows may have been the chemical reductant that reduced the hexavalent uranium to precipitate uraninite.

#### 3.9.7.4. *Description of selected deposits*

### **Deposits of the Westmoreland district (Australia)**

#### Introduction

The Westmoreland district straddles the boundary between Queensland and the Northern Territory, about 100 km south of the Gulf of Carpentaria coastline and 390 km NNE of the mining town of Mt Isa.

Mineralization was first indicated by an airborne survey of the Bureau of Mineral Resources in 1956 and found the same year to occur as secondary mineralization in quartz arenite of Carpentarian age. The area was optioned in 1967 by Queensland Mines, which undertook a major exploration and drilling programme. By 1969, three orebodies had been delineated (the Jack, Garee and Langi lenses of the Redtree deposit). Exploration continued in the Westmoreland area until 1982.

In 1990, CRA Ltd (now Rio Tinto Ltd) started a new phase of exploration that resulted in the discovery and delineation of the Junnagunna and Huarabagoo deposits. Owing to low uranium prices, the project was relinquished in 2000.

In 2004, Laramide Resources Ltd acquired the project and since then has been conducting exploration work. In 2009, total mineral resources of the project were estimated at 19 980 tU at an average grade of 0.07% U [402], hosted within five deposits. In addition, gold values of economic significance are reported from various areas associated with uranium mineralization. The project was dormant as of 2015.

#### Geological setting

The Westmoreland project is situated in the Palaeoproterozoic–Mesoproterozoic McArthur Basin. It is a large intracratonic basin with sediments that preserve a history of fluid interaction associated with mass transport of K, Fe, Mg, Zn, Pb, Cu, U and Ag [396]. The McArthur Basin is a 5–10 km thick sequence of mostly unmetamorphosed sedimentary and volcanic rocks that were deposited between 1800 and 1575 Ma [403].

The oldest rocks in the Westmoreland region are Palaeoproterozoic quartz–feldspar–mica schists and gneisses of the Murphy Metamorphics. These metamorphic rocks are essentially a sequence of shale, siltstone, greywacke and volcanic rocks deposited along a plate margin and metamorphosed to greenschist facies and consisting of quartz–albite–muscovite ( $\pm$  biotite) schist and gneiss. Uranium–lead data from detrital zircon suggest a maximum depositional age of  $1853 \pm 4$  Ma for the Murphy Metamorphics [404].

Palaeoproterozoic felsic lavas and ignimbrites (Cliffdale Volcanics) unconformably overlie the metamorphic rocks (Fig. 145). The lower sequence of the Cliffdale Volcanics is dominated by coarse, poorly sorted ignimbrites of dacitic and rhyolitic composition. The light coloured ignimbrites are rich in quartz phenocrysts while in the dark varieties, feldspar is abundant and quartz is minor to absent. Minor phases include biotite, actinolite, sphene and magnetite. The upper sequence consists essentially of flow banded alkali rhyolite and minor tuff [405].

The Nicholson Granite Complex (Fig. 145) can be divided into two broad suites based on chemical and mineralogical composition. Group A includes granodiorite, granite and adamellite; the dominant rock type is porphyritic biotite  $\pm$  hornblende-bearing adamellite containing mafic xenoliths. The groundmass includes quartz, plagioclase, perthite, hornblende and biotite with accessory titanite,

apatite, zircon and monazite. Group B includes granite, adamellite and alkali granite; the dominant rock type is phaneritic biotite–muscovite granite with rare hornblende. Zircon, apatite and fluorite are common accessory minerals but titanite is rare [405]. The upper units of the Clifffdale Volcanics and the Nicholson Granite have been dated at  $\sim 1840$  Ma<sup>1</sup>. Multiphase intrusions of the Nicholson Granite Complex (granite and adamellite) intrude the metamorphic rocks and Clifffdale Volcanics.

The basal unit of the overlying McArthur Basin, the Westmoreland Conglomerate (Fig. 146), is a fluvial unit more than 1200 m thick comprised of arkose, conglomerate and quartz arenite. The Westmoreland Conglomerate has been subdivided into four stratigraphic units [406]. Most of the uranium mineralization is hosted within the upper unit (Ptw4 unit), which is a porous, coarse-grained sandstone, conglomeratic in part, and 80–90 m thick. Uranium–lead dating of detrital zircon from the Westmoreland Conglomerate has returned maximum depositional ages of  $1865 \pm 7$  Ma for the lower section and  $1843 \pm 4$  Ma for the upper section [404]. Basaltic lavas of the Seigal Volcanics conformably overlie the Westmoreland Conglomerate, followed by dolomite, sandstone, mafic and felsic volcanic rocks of the upper part of the Tawallah Group.

Aphyric, medium-grained dolerite dykes and minor sills intrude along NE trending fault and fracture zones that intersect the Westmoreland Conglomerate. The most significant of these are the Redtree and the Northeast Westmoreland dyke zones (Fig. 146). The Redtree dyke zone is over 15 km long and consists of a complex series of dykes, with individual dykes generally less than 20 m wide. The Westmoreland uranium deposits (Redtree, Junnagunna and Huarabagoo) lie along the Redtree dyke zone.

#### Mineralization

This style of deposit consists of uraniferous (auriferous) veins in Proterozoic sandstone with overlying mafic to felsic volcanics. The sandstones are also intruded by mafic dykes believed to be coeval with the overlying mafic volcanics. The deposits occur in four main geological settings (Fig. 147) described as types 1–4 [21]:

- (i) Type 1 consists of stratabound mineralization in the sandstone, subparallel to the contact with:
  - The overlying mafic volcanic flows;
  - The contacts with intermediate sills.
- (ii) Type 2 consists of discordant, steeply dipping zones of mineralization adjacent to the contacts with mafic dykes. Stratabound mineralization may grade into steeply dipping zones of mineralization adjacent to the contacts with mafic dykes;
- (iii) Type 3 consists of mineralization associated with fractures in the altered mafic volcanic rocks;
- (iv) Type 4 consists of mineralization associated with shear zones within altered felsic volcanic rocks.

Pitchblende is the dominant primary uranium mineral. It occurs in massive and colloform textures. Haematite is almost invariably associated with pitchblende and together they replace the clay or quartz matrix of the host sandstone. In volcanic units, pitchblende occurs as replacements along the edges of veins which are often filled with quartz. Small grains of gold up to 10  $\mu\text{m}$  in diameter have been observed. Rare grains of pyrite, marcasite, chalcopyrite, bornite, gersdorffite (NiAs) and safflorite (CoAs<sub>2</sub>) have also been observed [405].

---

<sup>1</sup> M. Ahmad, Northern Territory Geological Survey, personal communication.

The Redtree uranium deposit occurs at the south-western end of the Redtree dyke zone. It consists of both horizontal and vertical mineralization (Fig. 148) with an indicated resource of 12.86 Mt of ore at an average grade of 0.076% U and an inferred resource of 4.47 Mt at an average grade of 0.06% U [407]. The horizontal mineralization is up to 15 m thick and is entirely hosted by sandstone. It is associated with chlorite and minor haematite alteration. The mineralization thickens and steepens near the dyke, where it is 30–40 m thick.

The Junnagunna uranium deposit occurs at a fault intersection west of the Redtree dyke zone and south of the NW trending Cliffdale Fault (Fig. 146). Uranium mineralized zones in the Junnagunna deposit are predominantly flat lying and concentrated within the upper unit of the Westmoreland Conglomerate, just below the Seigal Volcanics (Fig. 148). Minor discordant mineralization occurs within the Westmoreland Conglomerate adjacent to the Redtree dyke. Limited mineralized zones also occur on the northern side of the Cliffdale Fault and the eastern side of the Redtree dyke zone. Junnagunna has an indicated resource of 4.36 Mt of ore at an average grade of 0.068% U and an inferred resource of 2.15 Mt at an average grade of 0.068% U [407].

The Huarabagoo uranium deposit is located approximately 3 km north-east of the Redtree deposit (Fig. 148) and is a zone of vertical mineralization in a structurally complex area of the Redtree dyke zone (Fig. 146). In this zone, there were multiple injections of smaller dykes (steeply dipping and horizontal) associated with the two main vertical dykes. Most of the mineralization is hosted within the Westmoreland Conglomerate adjacent to the dykes, and the remainder is hosted in the dykes. The Huarabagoo deposit has an indicated resource of 1.46 Mt ore at an average grade of 0.076% U and an inferred resource of 2.41 Mt at an average grade of 0.10% U [407].

The Long Pocket prospects are hosted within the sandstone (Fig. 148). Mineralization occurs as a number of horizontal lenses, 0.5–5 m thick along the upper and lower contacts of a subhorizontal dolerite sill ~5 m thick. Approximately 90% of the mineralization is hosted in sandstone along the contact and the remainder is within the sill. Recent drilling of the Long Pocket prospects has given a best intercept of 4 m at 0.25% U.

#### Metallogenic aspects

The Proterozoic sandstones are much older than the host rocks of typical sandstone uranium deposits and fossilised plant matter is absent. Uranium mineralization in the Westmoreland region consists of uraninite with haematite and illite and occurs within a zone of chlorite alteration that formed prior to the uraninite. Oxygen and hydrogen isotopic compositions of syn-mineralization illite suggest that uranium was transported to the site of deposition by a basinal brine evolved from evaporated seawater [401]. Fluid inclusion studies indicate that mineralization occurred at temperatures of  $190 \pm 70^\circ\text{C}$  [408].

Illite  $^{40}\text{Ar}/^{39}\text{Ar}$  ages and  $^{207}\text{Pb}/^{206}\text{Pb}$  ages of uraninite suggest that mineralization occurred at  $1655 \pm 83$  and  $1606 \pm 80$  Ma and was later remobilized at 1150 and 850 Ma [401]. The relatively impermeable mafic dykes, coupled with higher fluid flow created by fault ramps that offset these dykes by up to 30 m, provided the structural trap that focused the uranium-bearing brine. The  $\text{Fe}^{2+}$  in the ferruginous chlorite adjacent to the mafic dykes and flows may have been the chemical reductant that reduced the hexavalent uranium to precipitate uraninite.

For Polito et al. [401], the similar mineralogy, paragenesis and geochemistry to the deposits from the East Alligator River Uranium Field suggest that they may be supraconformity equivalents to the East Alligator River Uranium Field. The coincidence of this uranium mineralization indicates that a period of regional uranium (Au) mineralization occurred in the Late Palaeoproterozoic after deposition of the Kombolgie Sandstone cover.

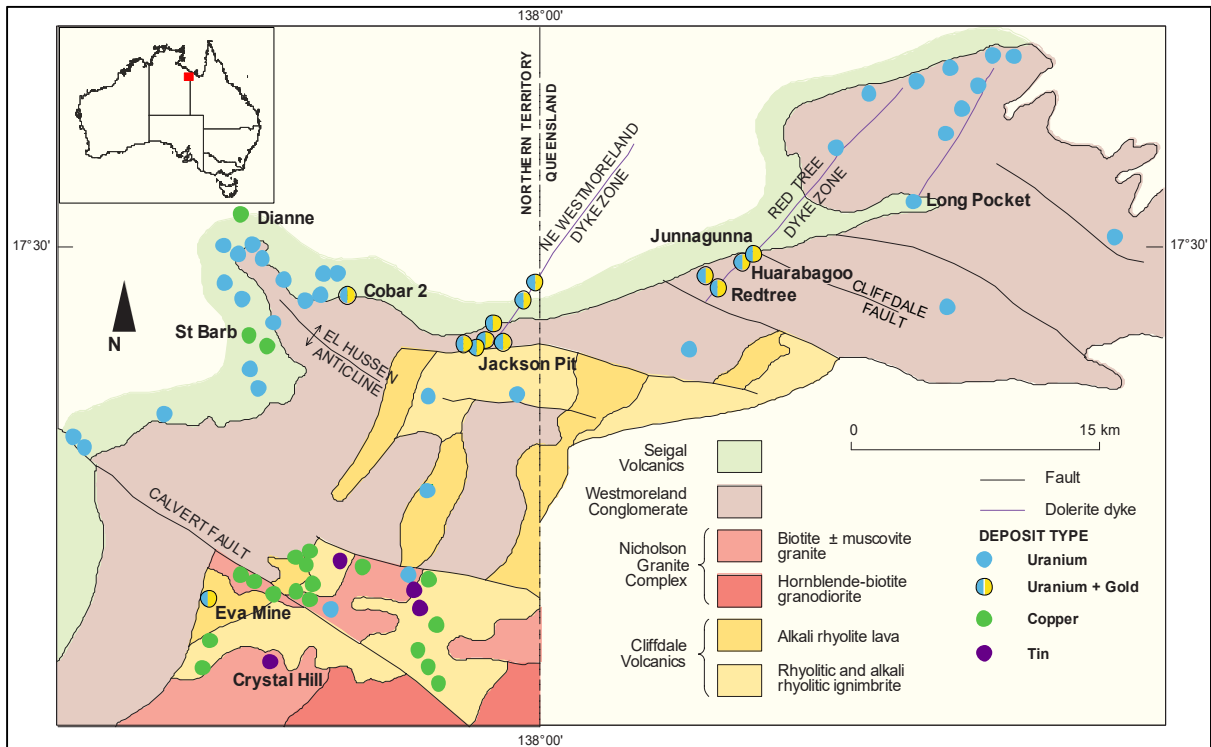


FIG. 145. Geological setting of mineral deposits and occurrences in the Westmoreland Uranium Field [265] (reproduced with permission).

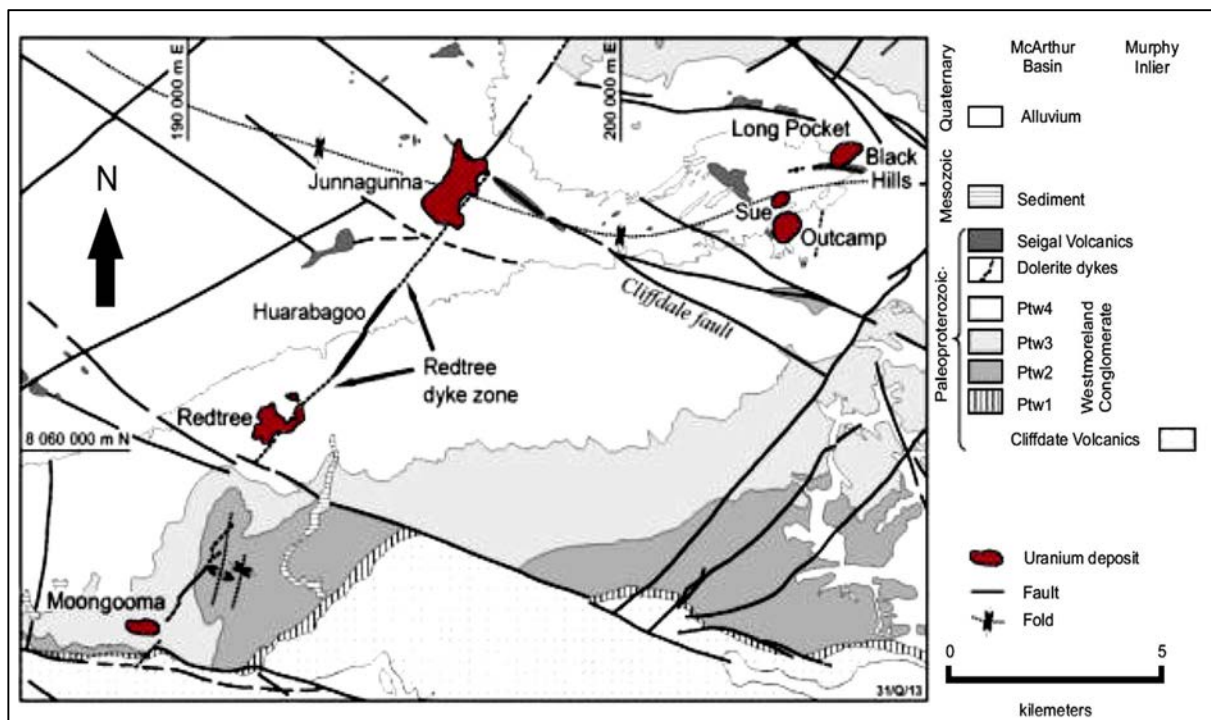


FIG. 146. Location and geology of the Westmoreland uranium deposits (adapted from Ref. [409]).

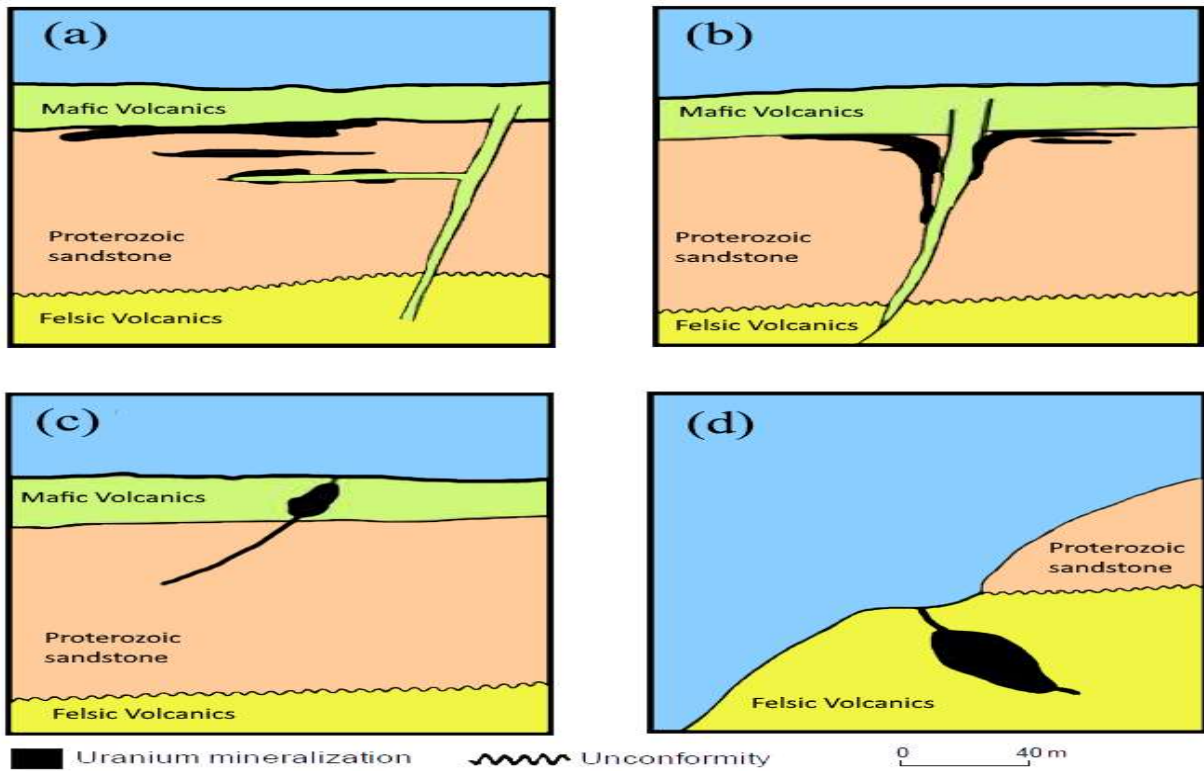


FIG. 147. Geological setting and (a) Type 1, (b) Type 2, (c) Type 3 and (d) Type 4 mineral occurrences in the Westmoreland Uranium Field (adapted from Ref. [21]).

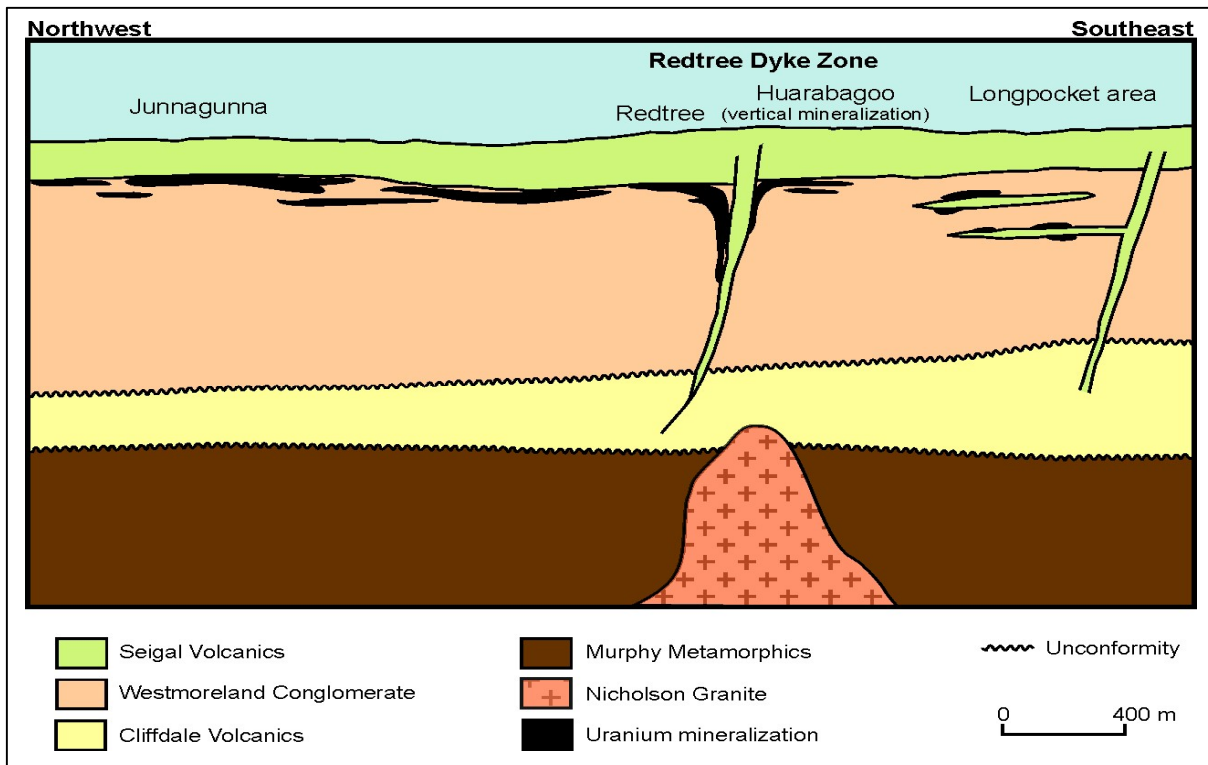


FIG. 148. Diagrammatic cross-section of uranium deposits of the Westmoreland region [410] (reproduced with permission).

## The Matoush deposit (Canada)

### Introduction

The Matoush uranium deposit is located in the Otish Mountains of northern Quebec, Canada, approximately 265 km north-east of Chibougamau and approximately 200 km north-east of Mistissini. The deposit location and the regional geology are shown in Fig. 149. Summarized from Cook and Ross [411], the earliest uranium exploration took place from the mid-1960s to the mid-1970s for palaeo quartz-pebble conglomerate deposits, using an Elliot Lake analogue. Exploration in 1980–1985 targeted unconformity-type deposits similar to those of the Athabasca Basin. This was undertaken by Uranerz Exploration and Mining (Uranerz), SERU Nucleaire, SOQUEM, Pan-Continental, Esso Minerals and others. The Matoush prospect in the western central part of the Otish Basin was discovered in 1980 by Uranerz as a surface showing and was explored by mapping, prospecting and sampling, conducting airborne and ground geophysics and diamond drilling 23 holes [21]. The deposit was explored by Uranerz in 1980–1984 and abandoned in 1985. Mineralization was defined over a 900 m strike length as pitchblende veins occurring along a strongly altered mafic dyke intruded along a NNE trending subvertical fault (the Matoush Fault). The best intercept, in drill hole AM-15, was over a 16 m section which graded 0.81% U.

The lease was acquired by Ditem Exploration Inc. and explored for diamonds following the discovery of the Renard kimberlites in 2002. The claims were optioned by Strateco Resources Inc. in 2005, which now owns 100% of the property [411]. Strateco has explored the property and several adjacent projects since 2006. The 2012, NI 43-101 compliant resource estimate includes 2990 tU at a grade of 0.66% U in the indicated category and 7438 tU at 0.36% U in the inferred resource category [412]. Strateco is seeking regulatory and community approvals to develop a decline for underground exploration. In March 2013, the Government of Quebec announced a moratorium on uranium exploration and development while a review of safety, environmental and social issues was undertaken. The project is on care and maintenance with little hope of restarting in the near future.

### Geological setting

The Otish Basin is located along the southeastern edge of the Superior Province of the Canadian Shield, along its boundary with the Grenville Province. The basement rocks consist of quartz-feldspar gneiss and amphibolite (Epervanche Complex) and volcanosedimentary supracrustal belts (greenstone belts) of the Tichegami Group, all of Archaean age [413]. These rocks were metamorphosed to amphibolite facies during the cratonization of the Superior Province in the Kenoran Orogeny (~2500 Ma). This has resulted in an E–W trending structural grain with a subvertical foliation. The basement has undergone retrograde metamorphism near the Grenville Front [413].

The Otish Basin and the correlative Mistassini Basin are part of a Palaeoproterozoic, continental to marginal marine sedimentary system that formed along a passive margin on the edge of the Superior Craton. The system records a transition from fluvial, terrestrial sedimentation in the north-east (Otish Basin) to marginal and open marine in the south-west (Mistassini Basin). The sequence also records a marine transgression with marine sedimentation at the top of the Otish Basin. The age of the sediments is constrained by a maximum age of 2140 Ma (NNE trending Mistassini dykes in the underlying basement [414]) and a minimum age of 1730 Ma by the overlying and intruding Otish Gabbro [415]. An age of  $2172 \pm 1.7$  Ma was recently obtained by CAMECO on the Otish Gabbro<sup>2</sup>. Thus, the age of sedimentation of the basin is between 2510 Ma (age of mafic dykes intruding the Archaean basement) and 2172 Ma. This age is correlative to the Huronian Supergroup containing the palaeo quartz-pebble conglomerate deposits in Ontario.

---

<sup>2</sup> G. Zaluski, personal communication, 2012.

The geology of the Otish Basin is shown in Fig. 150. The basin records sedimentation of the Otish Group, which comprises two formations. The lower unit, the Indicator Formation is composed mainly of quartz-pebble conglomerate, pebbly sandstone, feldspathic sandstone and quartz arenite representing a decreasing energy fluvial system. Locally the basal conglomerate is polymictic [413], containing locally derived clasts of the Tichegami Group basement. The Indicator Formation varies in thickness from about 330 m to more than 760 m in the western part of the basin [411]. The overlying Peribonca Formation is preserved in the northeastern part of the basin. It is notably red in colour and consists of a lower unit of well-sorted sandstone with minor conglomerate and dolomite, and is cemented by dolomite [416]. The upper unit consists of red arkose and argillaceous sandstone. The maximum observed thickness is 380 m [411]. Otish Gabbro sills and dykes form extensive outcrops in the north-eastern part of the basin, but form only narrow dykes in the basement. The Otish Gabbro consists mainly of gabbro with lesser olivine gabbro, porphyritic basalt and amygdaloidal dolerite [413].

The Matoush deposit is hosted in an altered mafic dyke and the adjacent Indicator Formation sandstone overlying granitic basement. As described by Cook and Ross [411], the Indicator Formation in the deposit area is about 800 m thick. The distal fluvial sediments were deposited in a braided stream environment and include two alternating lithofacies. The Active Channel Facies (ACF) consists of massive to weakly cross-bedded, coarse-grained sandstone, pebbly sandstone and conglomerate in fining-upward cycles. The Channel Bar Facies (CBF) consists of medium- to coarse-grained, cross-bedded and well sorted subarkosic sandstone. Four ACF cycles separated by three CBF units are identified in the Matoush area, numbered sequentially (ACF 1 through ACF 4) from top to bottom. The mineralized lenses of the Matoush deposit are preferentially developed in the ACF facies, probably because of their greater permeability (although all units are generally well silicified).

The Otish Group sediments in the deposit area are essentially flat lying, cut by N–S and NE trending subvertical faults. The Matoush Fault Zone is oriented at  $007^{\circ}/085^{\circ}$  and is traceable in airborne magnetic and VLF data for more than 20 km. Bedding contacts are not vertically offset across the fault zone, indicating that either there has been little displacement or that it is dominantly strike-slip [411]. In support of the latter, Rhys [417], cited in Cook and Ross [411], noted that mineralization is found in a dilational bend of the fault system, suggesting dextral displacement. The Matoush Fault Zone is intruded by a mafic dyke that, although locally fresh, is usually strongly altered.

### Mineralization

The Matoush deposit consists of 13 zones controlled by the intersection of the almost N–S trending Matoush Fault (intruded by a mafic dyke quite possibly younger than the Otish Gabbro) with the ACF units of the Indicator Formation. A schematic cross-section showing the geometry of the mineralization and geological controls is shown in Fig. 151. Cook and Ross [411] describe the main characteristics of the mineralization in the AM-15 zone at Matoush.

The AM-15 zone is a subvertical, tabular body at the intersection of the Matoush Fault Zone and the ACF 3 unit. It has an overall strike length of 300 m and a vertical extent of 50–100 m at a depth of 175–275 m. As a whole, it exhibits a shallow plunge of  $15^{\circ}$  to the south and some mineralization is found in the overlying CBF 3 and CBF 4 units. Within the AM-15 zone, the resources are found in four approximately vertical lenses, the Main, South, Upper and North Lenses. The largest is the Main Lens, an ovoid shaped body with a 235 m strike length, 50 m down-dip extent and 2–15 m (averaging 7.5 m) thickness. The other lenses exhibit similar geometry.

The indicated resources (2994 tU at a grade of 0.66% U) are contained in the AM-15 and MT-34 zones, while the inferred resources (7438 tU at 0.36% U) are found in the AM-15, MT-02, MT-06, MT-22, MT-34 and MT-36 zones [412]. As shown in the longitudinal section in Fig. 152, these zones span a 13.5 km strike length along the fault, dominantly in the ACF 3 and ACF 4 units but also extending into the adjacent units.

The mineralization of the AM-15 zone is dominantly replacement style disseminations and clots of pitchblende but higher grade areas consist of semi-massive pitchblende in veins with euhedral quartz, amphibole, haematite and tourmaline [411]. Secondary uranophane is also present. Minor phases include coffinite, pyrite and a number of Cu, Ni and Pb sulphides, arsenides and selenides [415]. Although the mineralization is found on both sides of the fault, it is preferentially found on the eastern side. The AM-15 zone is situated at a bend in the structure, interpreted as a dilational zone during dextral displacement along the Matoush Fault [417].

As described by Cook and Ross [411], alteration around the mineralization consists of a weak outermost halo of haematite and limonite surrounding an intermediate halo up to 10 m wide of pale green to emerald green vanadium- and chromium-bearing phyllosilicate alteration in dominantly bleached sandstone. The inner zone (several metres to 10 m wide) is dark greenish grey, consisting of magnesium chlorite and disseminated pitchblende, with patchy limonite and haematite. This is the main part of the ore zone. The innermost alteration zone consists of mottled and banded tourmaline alteration within two metres of the Matoush Fault and Dyke. Late white clay alteration is present along the fault and in the dyke and adjacent sandstone. This appears to post-date all mineralization, but it is unclear whether it is late stage hydrothermal alteration or the product of a much later event, which has been superimposed on the fault system.

#### Metallogenic aspects

Mineralization at Matoush is contained within 13 lenses, all proximal to the Matoush Fault and Dyke. The mineralization and alteration overprints the dyke and therefore post-dates it [411]. While some of the lenses are hosted in the CBF strata of the Indicator Formation, the vast majority are found in the ACF units. This is attributed by Cook and Ross [411] as being a result of the higher permeability of these units, controlling fluid flow of oxidized, basinal brines carrying the uranium to the fault and dyke, where the uranium is reduced and precipitated. Strateco has identified strong alteration similar to that found at Matoush over an extensive strike length of the fault within the ACF units, although it is not continuously mineralized. The controls on the sites of mineralization are not well understood.

The Otish Basin has been explored for unconformity uranium deposits because of general similarities to the Athabasca Basin, including the presence of a mature quartz-rich sandstone basin of Proterozoic age unconformably overlying Archaean metamorphic basement rocks. The Camie River occurrence of the Cameco Corporation and AREVA Resources Canada Inc. joint venture is an example of unconformity uranium mineralization along the southern margin of the basin. It has been postulated that Matoush represents an unconformity variant or perched mineralization, considering the host basin, the polymetallic nature of the mineralization and some similarities in the alteration. However, as noted by Cook and Ross [411], the mineralization of AM-15 occurs more than 520 m above the unconformity, where no significant mineralization or alteration is present. The unconformity-type variant model, therefore, is unlikely.

Discordant U–Pb isotope data from mineralization at Matoush reported by Hohndorf et al. [414] gave intercepts of  $1359 \pm 28$  and  $622 \pm 40$  Ma. The upper age was interpreted by the authors as the primary Matoush mineralization age, from remobilization of earlier ~1730 Ma mineralization. This model of remobilization of earlier mineralization is only speculative. Alternatively, these dates could represent a primary mineralization age or else only isotopic resetting of older mineralization with little remobilization.

The Matoush mineralization is best classified as a separate deposit subclass, empirically defined as uranium associated with mafic dykes in Proterozoic sandstone. Other examples are present in the Otish Basin, such as the L deposit discovered by Cogema Resources (the deposit now owned by Abitex Resources). The uranium deposits of the Westmoreland area of Queensland and Pandanus Creek in the Northern Territory of Australia are other possible analogues.

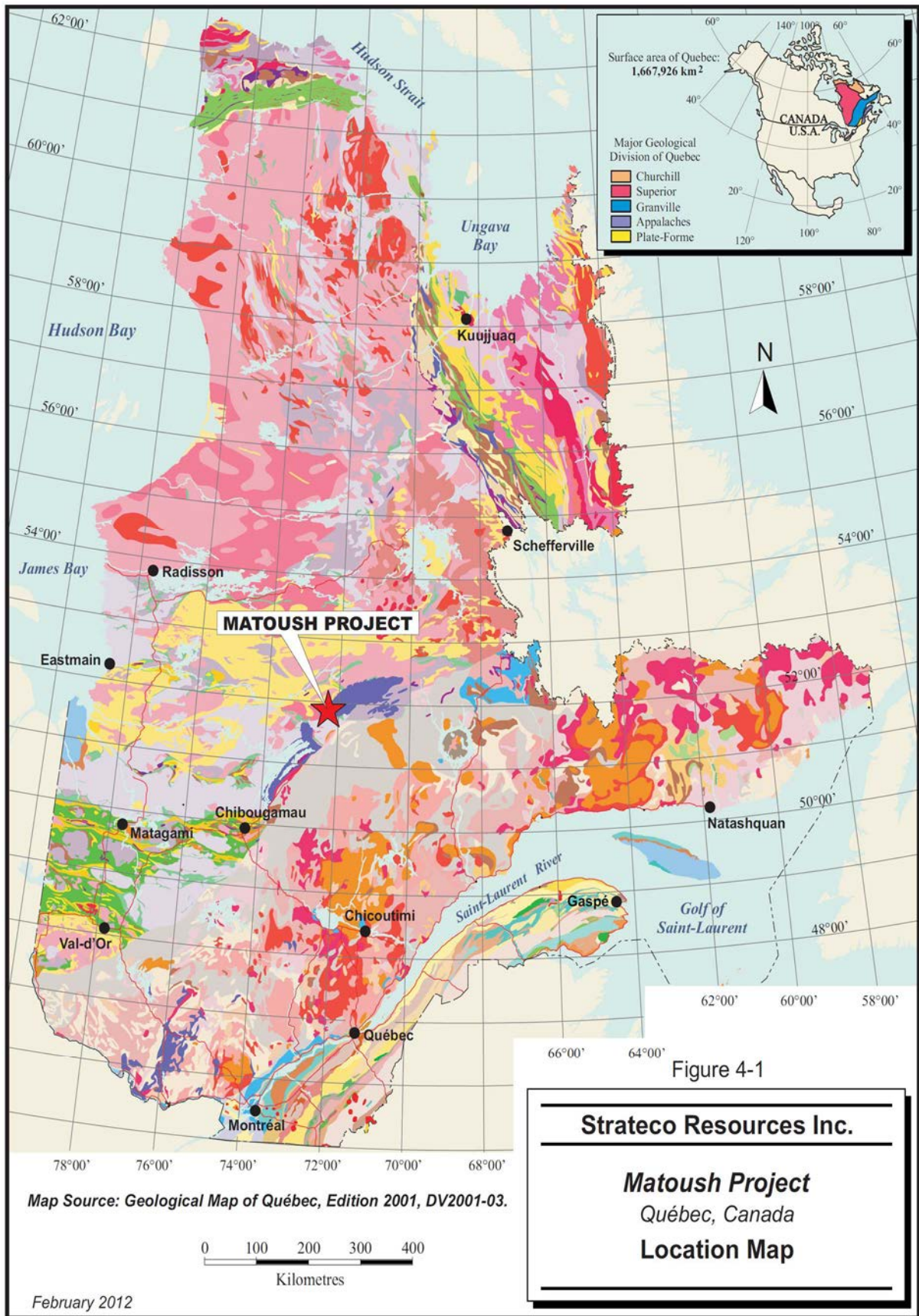


FIG. 149. Regional geology of the Otish Basin, Canada, showing the location of the Matoush deposit [411] (reproduced with permission).

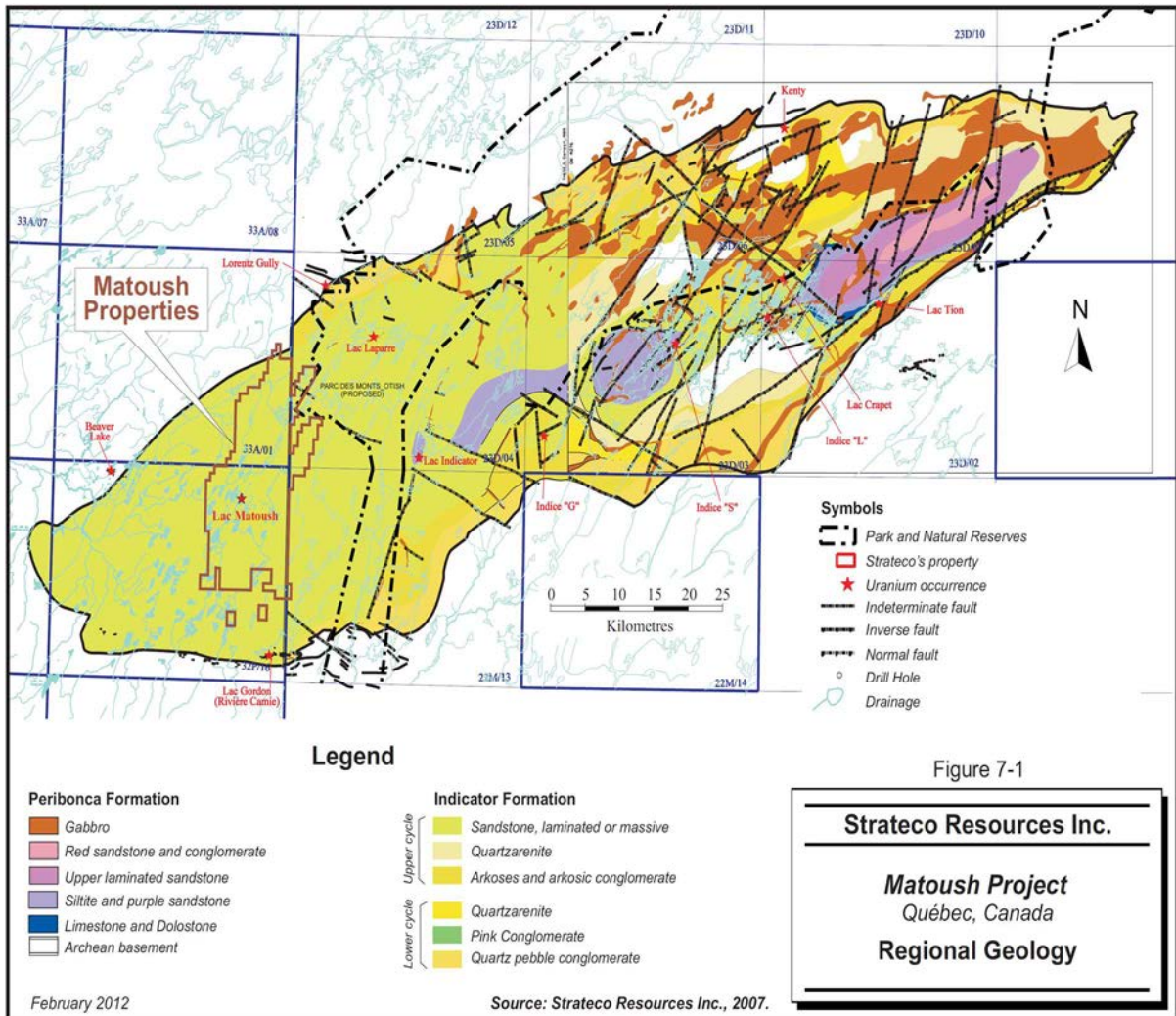


FIG. 150. Geology of the Matoush area [411] (reproduced with permission).

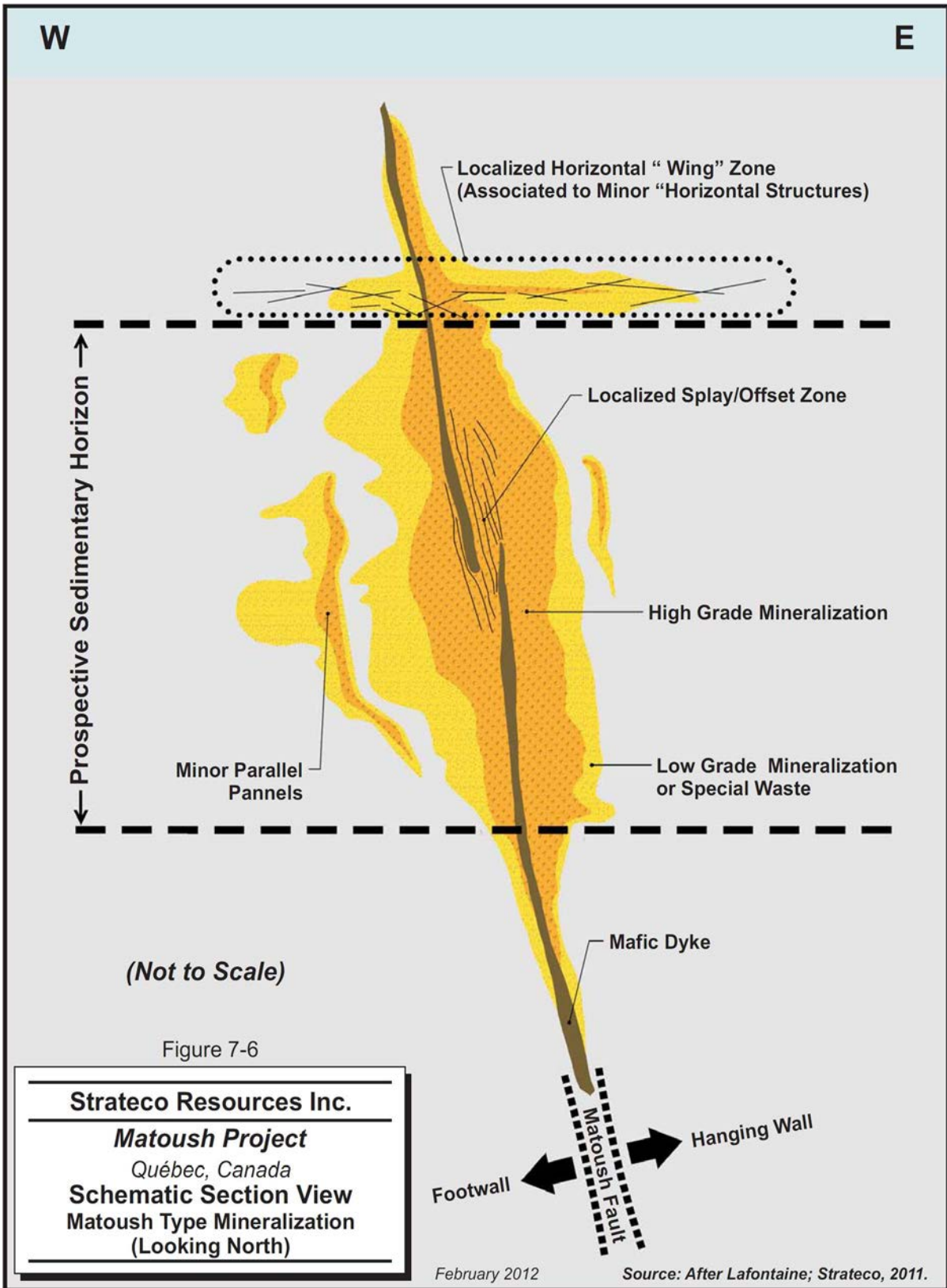


FIG. 151. Schematic cross-section of Matoush style mineralization [411] (reproduced with permission).

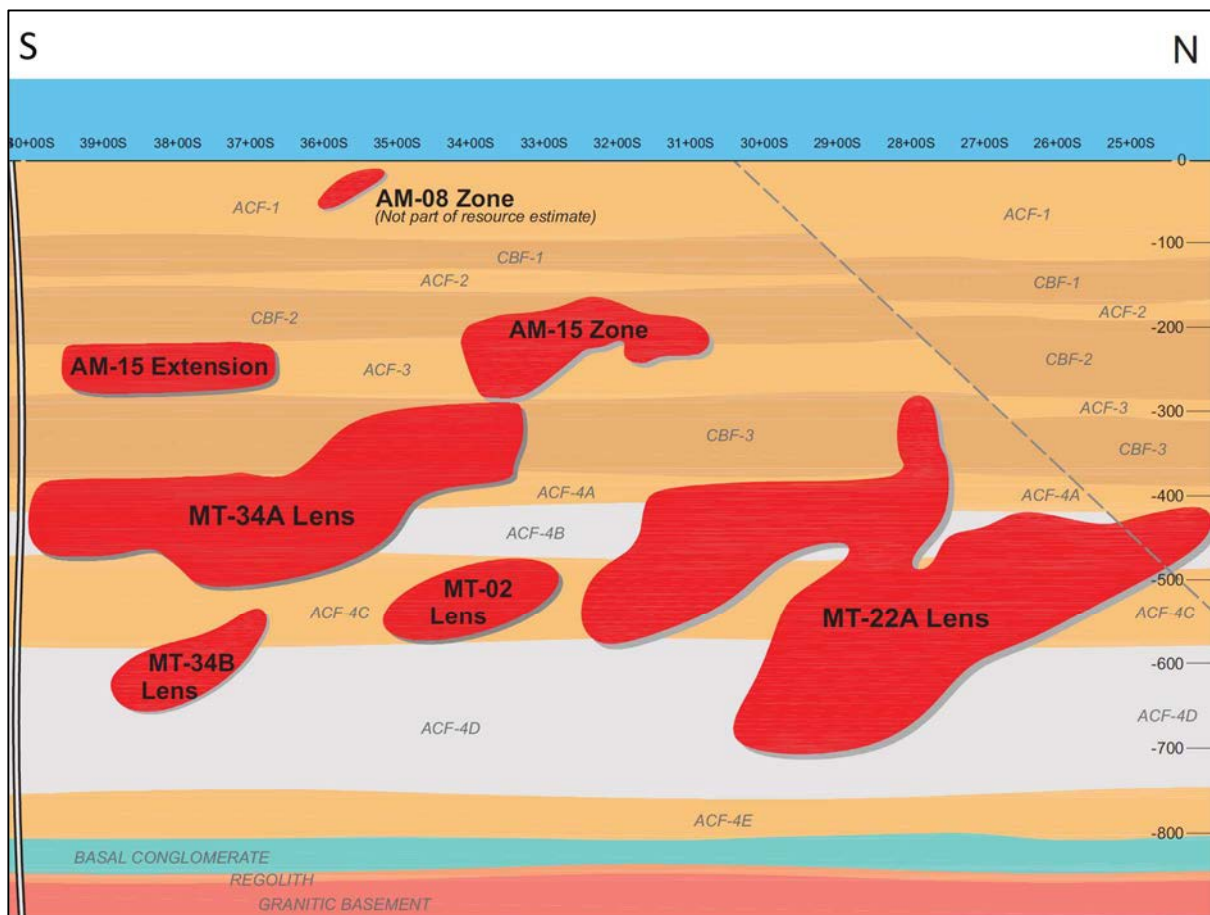


FIG. 152. Longitudinal cross-section of the Matoush deposit, along the Matoush Fault [412] (reproduced with permission).

### 3.10. PALAEO QUARTZ-PEBBLE CONGLOMERATE DEPOSITS

#### 3.10.1. Definition

Palaeo quartz-pebble conglomerate uranium deposits are defined as stratiform and stratabound deposits of uraninite and brannerite hosted in pyrite-rich quartz-pebble conglomerates. They are restricted to Early Proterozoic intracratonic basins (older than 2.3–2.4 Ga) developed on Archaean basement assemblages. Host rocks for this deposit type generally consist of cross-bedded, oligomictic quartz-pebble conglomerate beds with a pyritic matrix interbedded with quartzite and argillite beds. This suite of lithologies typically occurs as basal units in fluviodeltaic braided stream systems. Pyrite is the main detrital and authigenic heavy mineral, with pyrite contents generally varying between 3 and 15%. These deposits can be of detrital or hydrothermal origin.

The UDEPO database lists 88 palaeo quartz-pebble conglomerate deposits, with 60 in South Africa, 25 in Canada, 2 in Brazil and 1 in Ukraine. In Canada, 138 500 tU were produced from 12 mines between 1956 and 1996. Remaining geological resources are estimated at 325 000 tU. In South Africa, about 160 000 tU have been produced since 1952 as a by-product of gold mining. Production in 2015 amounted to 393 tU from two mines: Vaal Rivers and Ezulwini-Cooke. Geological resources are estimated to be of the order of 1 500 000 tU (Table 32).

TABLE 32. PRINCIPAL PROTEROZOIC PALAEO QUARTZ-PEBBLE CONGLOMERATE DEPOSITS  
(as of 31 December 2015)

Deposit	Country	Resources (tU)	Grade (U %)	Status
Free State Geduld	South Africa	277 450	0.039	Dormant
Vaal Reefs	South Africa	195 645	0.0272	Dormant
Denison	Canada	185 000	0.10	Dormant
Dominion Reefs	South Africa	96 525	0.041	Dormant
Ezulwini-Cooke	South Africa	94 200	0.0238	Operating
Freddies	South Africa	93 330	0.0115	Dormant
Hartebeestfontein	South Africa	82 570	0.0330	Operating
Potchefstroom	South Africa	62 810	0.025	Dormant
Riet Kuil–Dominion	South Africa	51 711	0.039	Exploration
Banana Lake	Canada	51 436	0.030	Dormant
Driefontein	South Africa	45 600	0.0150	Development
Quirke	Canada	45 000	0.10	Closed
Western Holdings	South Africa	44 900	0.0145	Dormant
Stanleigh	Canada	41 000	0.07	Closed
West Rand tailings	South Africa	37 944	0.0052	Dormant
Vaal River tailings	South Africa	35 842	0.0076	Dormant
Buffelsfontein–Hartebeestfontein tailings	South Africa	27 806	0.007	Dormant
Harmony		27 115	0.0086	Exploration
Moab Khotsong	South Africa	25 055	0.070	Dormant
Nordic	Canada	23 000	0.09	Dormant

### 3.10.2. Geological setting

Two economic subtypes of palaeo quartz-pebble conglomerate uranium deposit have been identified: Au-dominant (Witwatersrand Basin, South Africa) and U-dominant (Blind River-Elliot Lake area, Canada) (Fig. 153) [18, 19]. Other areas that have been explored for their Proterozoic quartz-pebble conglomerate-type uranium mineralization include the southern Lake Superior region, the conglomerates of the Black Hills and southeastern Wyoming (USA), the conglomerates of the Koli area in eastern Finland, the Moeda and Jacobina Formations in Brazil and conglomerates in Ghana and in Western Australia.

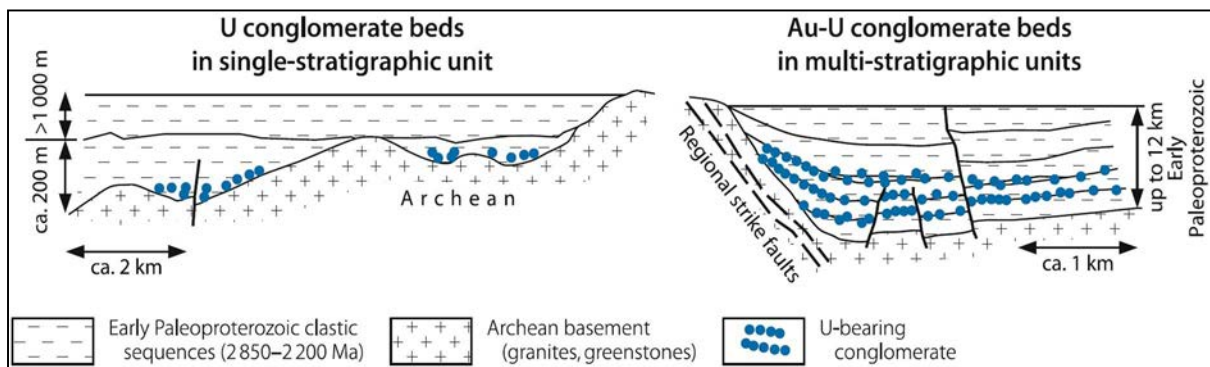


FIG. 153. Palaeoproterozoic quartz-pebble conglomerate deposits [18] (reproduced with permission).

*U-dominant type: The Elliot Lake–Blind River area deposits (Canada)*

The Elliot Lake–Blind River district is located in southern Ontario at the southern margin of the Canadian Shield (Fig. 154). Detrital heavy minerals (dominated by uraninite and REE minerals) and later formed authigenic phases occur as disseminated matrix components in pyritic (5–20wt%), oligomictic quartz-pebble conglomerate horizons (termed ‘reefs’), which vary in thickness from 0.5 to >3.5 m. Quartzite beds are interbedded with the conglomerate. This suite forms the basal section of a sequence about 50 m thick, found in palaeovalleys scoured into Archean basement. Uraninite, uranotorite, uranotorianite, monazite and xenotime are the prevailing detrital minerals. Authigenic minerals include U–Ti oxide phases (brannerite), coffinite, thucholite and, locally, gummite. Uranium was the primary commodity produced, with occasional recovery of Th and some REE, particularly Y. In 1986, Denison Mines built a plant with an initial rated capacity of 150 t annual production of yttrium.

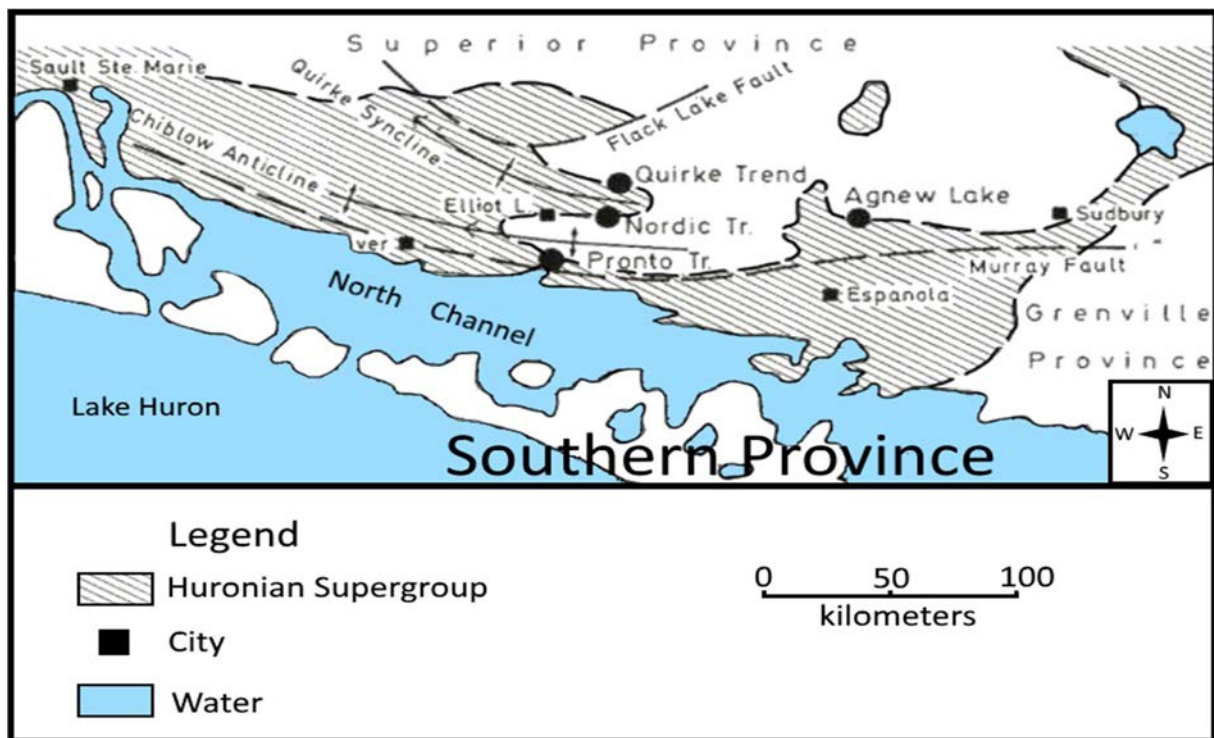


FIG. 154. Blind River–Elliot Lake–Agnew Lake area: distribution of the Huronian Supergroup (hatched) and position of uranium production centres (black circles) (adapted from Ref. [418]).

*Au-dominant type: The Witwatersrand Basin deposits (South Africa)*

The Witwatersrand Basin covers an area of 50 000 km<sup>2</sup> which is underlain by more than 8000 m of slightly metamorphosed strata of the Dominion Group and Witwatersrand Supergroup which host ore-bearing, quartz-pebble conglomerate and the Ventersdorp Supergroup, which is only slightly mineralized. The strata rest unconformably on granitic gneiss as well as on ultramafic and metasedimentary rocks of the Swaziland Supergroup of the Archaean Kaapvaal Craton, with a palaeosol just below the unconformity.

Gold-uranium ore and associated minerals in the Witwatersrand deposits occur as detrital and redistributed matrix components in oligomictic quartz-pebble conglomerate horizons in multi-stratigraphic cycles within six large fluviodeltaic fans on the northern and western sides of the Witwatersrand Basin. The ore-hosting fluvial fans are up to 40 km long, 90 km wide across the distal fan base, and are several thousand metres thick. The source of the detrital uranium minerals is believed to have been Archaean granitic basement rocks, such as the unusually uraniferous, hydrothermally altered granites identified in the hinterland of the Witwatersrand Basin (Fig. 155).

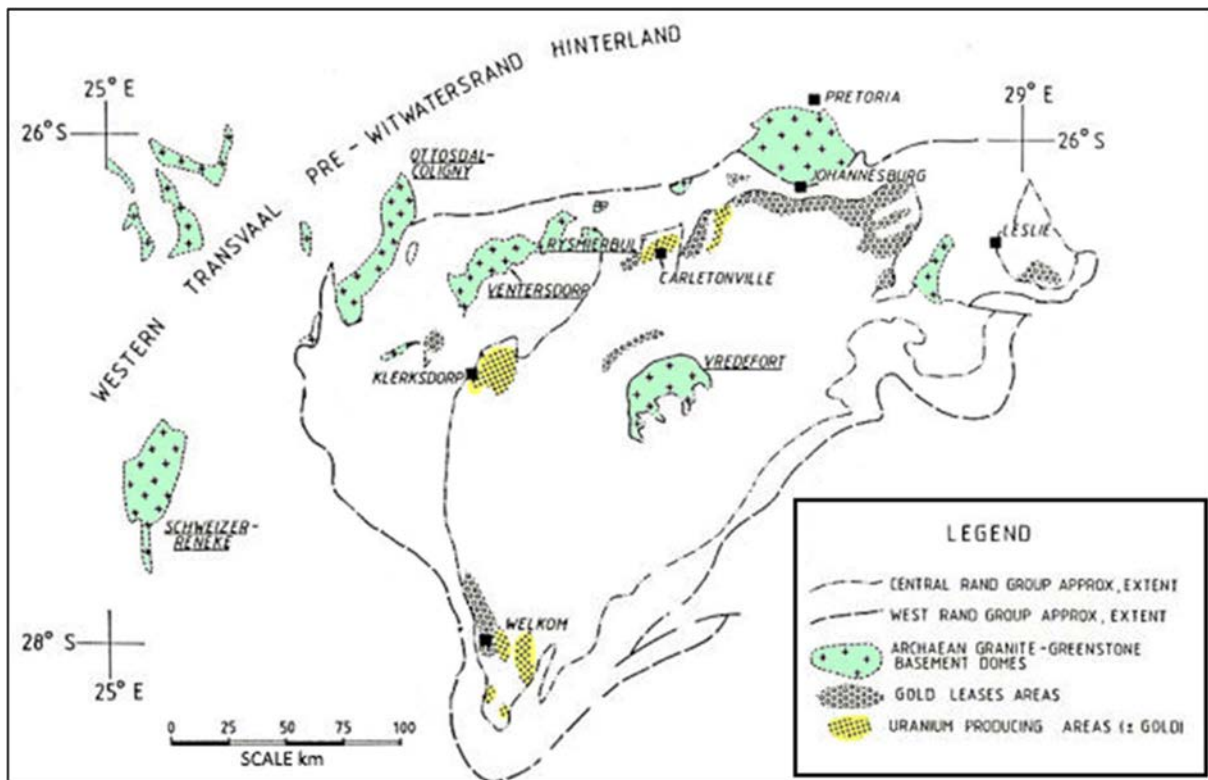


FIG. 155. The Witwatersrand Basin, South Africa (adapted from Ref. [419]).

On a regional scale, uranium mineralized reefs occur in all four stratigraphic systems that fill the Witwatersrand Basin. Large concentrations of uranium are restricted to distinct, narrow zones however, that occupy only about 2% of the entire Upper Witwatersrand System within a belt trending parallel to the former coastline. The most productive reefs occur in the Bird Reef Stage of the Upper Witwatersrand System, which has yielded about 80% of past production.

Host rocks within the Witwatersrand Basin consist of pyritic, oligomictic quartz-pebble conglomerate beds that are commonly only a few centimetres to several tens of centimetres thick, which are

interbedded with quartzite, arkose, shale and volcanic units. Carbonaceous material occurs in several horizons. Detrital ore minerals include uraninite, uranothorite, native gold, and platinum elements (Os, Ir, Ru, Pt). Post-depositional modification of the placers created several generations of authigenic ore and associated minerals including brannerite and thucholite. Uraninite grains from Witwatersrand ore have apparent U–Pb ages of  $3065 \pm 100$  Ma, similar to the age of granites surrounding the Witwatersrand Basin and a secondary age of 2040 Ma that is coeval with the emplacement of the Bushveld Complex and the large Vredefort impact structure.

On a local scale, the ore minerals are preferentially concentrated in conglomerate beds less than 30 cm thick that were deposited: (i) immediately above local intraformational unconformities or unconformities, particularly where conglomerates fill depressions or scours in underlying rocks; (ii) near the base of conglomerate beds that overlie distinct, partly carbonaceous argillaceous/shaly units, and (iii) in generally parallel ‘pay streaks’ characterized by densely packed, well rounded and well sorted pebbles predominantly of quartz with variable amounts of uranium and other heavy minerals [419].

Individual deposits are several hundred to several thousand metres long, several tens to several hundred metres wide and 5–200 cm thick. They contain up to several tens of thousands of tonnes of uranium at average grades ranging of 0.01–0.03% U and locally up to 0.15% U. Resources including production total >500 000 tU. Uranium production began in the Witwatersrand Basin in 1952 and cumulative production through 2012 totalled 170 000 tU. Gold values in the Witwatersrand Basin range from <1 to 25 ppm Au. Uranium is recovered as a by-product of gold mining operations except in a few depleted mines, such as Afrikander/Vaal Reefs, with grades of 0.12% U and 1.1 ppm Au.

### **3.10.3. Metallogenesis**

Placer uraninite, the principal primary uranium phase, is locally associated with gold, REE and/or other detrital metallic oxide and sulphide minerals. The variable ore mineralogy is a function of different geological source provinces. Fluvial transport and accumulation of uraninite depended on the reduced state of the Earth’s early, oxygen-poor atmosphere prior to a gradual increase in oxygen content in the Earth’s atmosphere. Post-depositional redistribution and mineral crystallization mainly by diagenetic processes led to the formation of modified placers composed of a suite of authigenic ore and associated minerals, including brannerite, rutile, anatase, coffinite, pyrite and others.

In the Witwatersrand Basin, the source of Au and U has been a matter for debate ever since the beginning of mining more than a century ago and it remains a controversial topic. Numerous genetic models have been proposed from palaeoplacer, magmatic, metamorphic, syn- or post-depositional hydrothermal models to impact induced, synsedimentary microbially mediated formation to precipitation from seawater and H<sub>2</sub> degassing of the Earth’s core. Depiné et al. [420] have completed the first systematic analyses of the trace and REE distribution in uraninites from various gold-bearing conglomerates of the Central Rand Group. They confirm a placer origin for the uraninites in the light of their high Th contents and their chondrite normalized REE patterns being incompatible with post-sedimentary hydrothermal genetic models. They point to a derivation of the detrital uraninites from a high temperature, magmatic, granitic to pegmatitic source. They also mention that uranium phases such as brannerite and other minerals such as pyrite and gold show evidence of partial, short range mobilization of originally detrital particles by post-sedimentary fluids.

### **3.10.4. Description of a selected deposit: The Denison mine deposit (Canada)**

#### *Introduction*

The Denison mine deposit is located in the Elliot Lake district, Ontario, Canada. The original claims containing the Denison mine deposit were acquired by Denison in 1954. The property covered the down-plunge extension of the near surface mineralized zones that were developed through the Nordic

mine (Fig. 156). Surface drilling the same year resulted in the discovery of the Denison deposit. The mine was brought into production in 1957 and total production until mine closure in 1992 was 55 325 tU at an average grade of 0.105% U. In 2007, a new estimate of the remaining resources in the developed and undeveloped sections of the deposit was carried out, indicating resources of 79 000 tU at an average grade of 0.046% U (cut-off grade of 300 ppm U) [421].

### *Geological setting*

The Elliot Lake area lies within Precambrian rocks of the Canadian Shield of northern Ontario, on the boundary between the Southern and Superior Provinces. The Southern Province consists of a thick sequence of clastic sediments with minor marine limestone and volcanic rocks. The clastic sequence is referred to as the Huronian Supergroup with an aggregate maximum thickness of as much as 15 km [422]. It is divided into four groups that form southward thickening wedges. In ascending order, these are the Elliot Lake Group (4000 m), the Hough Lake Group (3700 m), the Quirke Lake Group (2400 m) and the Cobalt Group (5000 m). The sediments were deposited during the Palaeoproterozoic (2450–2115 Ma) on Archaean metavolcanic and metasedimentary rocks and granitic intrusive rocks of the Superior Province.

The Elliot Lake Group, containing the only volcanic succession, also includes fine-grained pelitic sediments, arenaceous units and pyritic quartz-pebble conglomerate beds. The majority of the uranium mineralization is hosted at the base of the sequence, in the Matinenda Formation, non-conformably overlying palaeosol mantled Archaean rocks. The Huronian sediments were intruded by sills and dykes of the Nipissing Diabase (2115 Ma). Sediments and diabases were deformed and metamorphosed during the Penokean Orogeny (1850–1750 Ma).

Huronian rocks are folded to form a gently westward plunging, folded syncline designated as the Quirke Syncline. It is flanked to the north and east by Archaean granite and to the south by Archaean mafic metavolcanic and metasedimentary rocks.

Thrust faults occur within the host rocks at the Denison mine. The Quirke Lake overthrust is located in the hanging wall of the deposit. A thrust fault is located directly above the conglomerate beds in the Pecors argillite, offsetting the Nipissing Diabase and the sediments (Fig. 156).

### *Mineralization*

Although the coarser grained quartzite beds of the Lower Matinenda Formation commonly contain low grade uranium mineralization, the higher grade uranium mineralization is hosted within the beds of quartz-pebble conglomerate along with disseminated pyrite in the matrix. Generally, the uranium grade increases with increasing pyrite content. The uranium-bearing conglomerate beds are found within thicker sections of the Matinenda Formation that are located over depressions in the underlying basement. The Matinenda Formation is divided into two members, the lower Ryan Member, which hosts the uranium mineralization, and the upper Stinson Member, which consists of massive quartzite. The thicker sections of the Ryan Member are termed ‘channels’ and these generally strike WNW. The Denison mine is located within the Quirke Channel, which also hosts the Quirke, Panel, Spanish American and Stanrock mines.

The Denison mine consists of two zones, the Main Zone and the Upper Zone. Each consists of multiple conglomerate beds containing uraniferous, pyrite quartz-pebble conglomerate reefs. The zones are separated by 40 m of quartzite (Fig. 156). The reefs strike between 105° and 120° and dip 0–60° south [421].

The uranium-bearing minerals are uraninite and brannerite, which occur along with pyrite, monazite, zircon and rutile in the matrix of the conglomerate, interstitial to the quartz pebbles. The uraninite is generally concentrated at the base of the conglomerate beds with the largest pebbles, whereas brannerite, rutile, monazite and zircon are mainly concentrated in the upper portions of the beds.



The quartz pebbles, uranium minerals and other heavy minerals were deposited in areas where the velocity of the streams were reduced, forming conglomerate beds within delta fans. Peripheral to the conglomerate beds, poorly sorted feldspathic sand and silt were deposited. The character of these peripheral sediments is indicative of wave action on delta margins and offshore deep water conditions [425]. The conglomerate beds are intercalated with coarse-grained sandstone with scattered pebbles and siltstone. At the Denison mine, the highest uranium grades occurred to the lee of basement highs where the flow was more abruptly reduced [421].

Robinson and Spooner [426] suggest that post-depositional modification of the uranium occurred in three stages: (i) leaching of iron from detrital ilmenite-magnetite grains and mobility of U, Th, REE and Si. Uraninite was replaced by coffinite and quartz, detrital monazite was altered to uranothorite and uranium reacted with  $TiO_2$  to form brannerite; (ii) precipitation of secondary pyrite, and (iii) formation of secondary quartz and sericite. The authors suggest that post-depositional modification of the detrital uraninite was limited in the conglomerate and uranium was not significantly mobilized. There is no indication that significant, secondary uranium deposits were formed.

### 3.11. SURFICIAL DEPOSITS

#### 3.11.1. Definition

Surficial uranium deposits are broadly defined as young (Tertiary–Recent), near surface uranium concentrations in sediments or soils which have not been subjected to deep burial and may or may not have been cemented to some degree [427]. These deposits usually have secondary cementing minerals, the approximate order of importance being calcite, gypsum, dolomite, ferric oxide, strontianite and halite.

Surficial uranium deposits have been identified in various parts of the world. In 2012, 62 surficial deposits were recorded in the UDEPO database with 18 of them in Australia and 15 in Namibia. Also included in this category are peat deposits such as Flodelle Creek (USA) and Kamushanovskoye (Kyrgyzstan) and uncommon pedogenic fracture-filled deposits such as Beslet (Bulgaria).

Only one deposit is in production: Langer Heinrich (Namibia) has been producing uranium since 2007, with a production of 1937 tU recorded in 2015. The Wiluna project (Australia) is at an advanced stage of development. Trekkopje in Namibia produced some uranium in 2012 and 2013, but was subsequently put on care and maintenance. In 2015, total resources of surficial deposits in Namibia were 200 000 tU hosted in 15 deposits and 100 000 tU in Australia hosted within 18 deposits.

Surficial deposits are usually low grade (100–400 ppm U) (Table 33), with the exception of Yeelirrie (Australia), with an average grade of 0.127% U. The deposits located to date vary considerably in size from a few hundred tonnes for the smallest ones to 67 000 tU for Langer Heinrich. Owing to their location at the surface and to the soft nature of the host rocks, these deposits have gained considerable interest from mining companies.

TABLE 33. PRINCIPAL SURFICIAL URANIUM DEPOSITS (*as of 31 December 2015*)

Deposit	Country	Resources (tU)	Grade (% U)	Status
Langer Heinrich	Namibia	66 605	0.051	Operating
Marenica	Namibia	53 130	0.0082	Pre-feasibility
Yeelirrie	Australia	55 600	0.111	Pre-feasibility
Klein Trekkopje	Namibia	42 360	0.012	Care and maintenance
Siwaqa	Jordan	29 330	0.0505	Dormant
Khan Azzabib	Jordan	13 230	0.0804	Dormant
Tubas Red Sand	Namibia	10 935	0.0125	Dormant
Lake Maitland	Australia	9 355	0.047	Development
Ain Sder	Mauritania	7 662	0.030	Exploration
Aussinassis	Namibia	6 960	0.020	Exploration
Oued el Foule	Mauritania	6 930	0.030	Exploration
Thatcher Soak West	Australia	6 539	0.059	Exploration
Dusa Mareb	Somalia	6 400	Unknown	Dormant
Manyoni–Zone C1	United Republic of Tanzania	6 122	0.0125	Exploration
Centipede	Australia	5 005	0.048	Exploration

### 3.11.2. Geological setting

Four main deposit subtypes have been identified: peat bog, fluvial valley fill, lacustrine–playa, and pedogenic fracture-fill (Fig. 157). The karst cavern subtype which was defined and included in this type by Dahlkamp [18] has been moved in this classification to the carbonate type.

Peat bog deposits are formed in humid climatic regions where uranium accumulates in vegetal organic and clay-rich shallow depressions (swamps, bogs and muskegs). No discrete uranium minerals occur. Resources are small and grades low (Kamushanovskoye (Kyrgyzstan), Flodelle Creek (USA)). Significant uranium accumulations have been described in British Columbia (Canada) although without published resource details.

Fluvial valley-fill deposits occur in valleys, flood plains and deltaic environments (Fig. 158). Mineralization in duricrusted valley sediments forms flat lying lenses up to several metres thick, with most of the mineralization located immediately beneath the present-day water table. Valley-fill deposits have the greatest economic potential of all the surficial deposits so far discovered. They are known in Australia, Namibia, Mauritania, South Africa, Somalia and China.

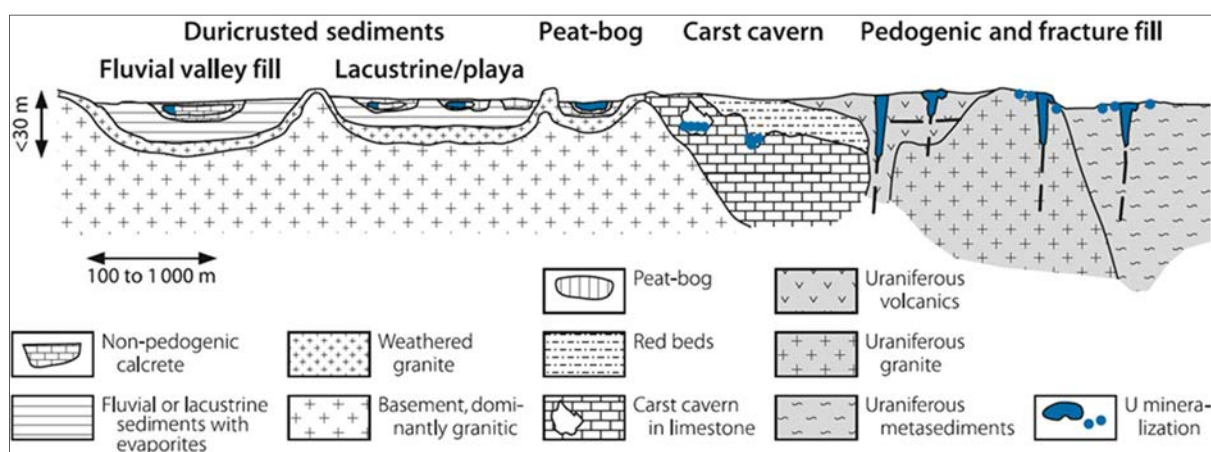


FIG. 157. Surficial uranium deposit subtypes [18] (reproduced with permission).

Playa deposits form in flat portions of arid basins that periodically flood and accumulate detrital and evaporite sediments. Mineralization is similar to fluvial valley-fill mineralization. They occur in Australia, Chile and South Africa. Pedogenic fracture-fill deposits are not common and have only been described in Bulgaria. They occur in weathered zones overlying bedrock. The decomposed material is entirely of in situ origin and may be cemented by one or other minerals and associated uranium. Allogenic pedogenic deposits occur in soils developed from transported material of fluvial or aeolian origin. Small occurrences of this deposit type are found in Mauritania.

Uranium mineralization in fluvial valley-fill and lacustrine–playa deposits is generally hosted in calcretes (calcium and magnesium carbonate). This style of mineralization constitutes the majority of surficial deposits. The calcrete bodies are interbedded with Tertiary sand and clay, which are usually cemented by calcium and magnesium carbonate. Calcrete deposits form in regions where uranium-rich granites were deeply weathered in a semi-arid to arid climate.

In Australia, surficial calcrete-related uranium deposits occur in valley-fill sediments along Tertiary drainage channels (Yeelirrie, Centipede, Hinkler and Lake Way) and in playa lake sediments (Lake Maitland and Lake Austin). These deposits overlie Archaean granite and greenstone basement of the northern portion of the Yilgarn Craton. Calcretes occur as elongate sheets occupying central tracks in trunk valleys and form important aquifers. They vary in width from a few hundred metres to 3–5 km or more and may be 100 km in length. Thicknesses are usually 5–10 m but may exceed 30 m along the axis. They frequently lead to playa lakes where they broaden out into deltaic platforms. Calcretes frequently form positive relief features in the valleys, being raised and mounded to 3 m or more above the flanking alluvial plain. Calcretes also frequently exhibit karst features, with evidence of slumping and caving due to the dissolution of carbonates [428]. The main uranium mineral is carnotite (hydrated potassium uranium vanadium oxide), formed as late stage precipitates in cavities with coatings of calcite, dolomite, silica and/or sepiolite. Carnotite may also be finely disseminated, particularly in quartz–clay units.

Several calcrete-hosted uranium deposits also occur in the central Namib Desert on the coastal plain of Namibia, the largest being the Langer Heinrich deposit. Other deposits are Trekkopje, Marenica, Tubas and Aussinanis (Table 33). The deposits are found in palaeovalleys of ancient rivers that flowed westwards from the Great Escarpment during the Late Cretaceous and Early Tertiary (88–25 Ma). The Namib Desert is extremely dry and all of the major surficial uranium deposits occur within the 100 mm isohyets. The arid environment has promoted preservation of the uranium deposits [429]. Uranium in the Namib Desert occurs in the form of the mineral carnotite but soddyite has also been reported. Carnotite occurs interstitially along grain boundaries, filling cavities and is most abundant in zones of high porosity. The age of the uranium mineralization is difficult to establish. Geological relationships suggest that a Late Tertiary age is likely [430].

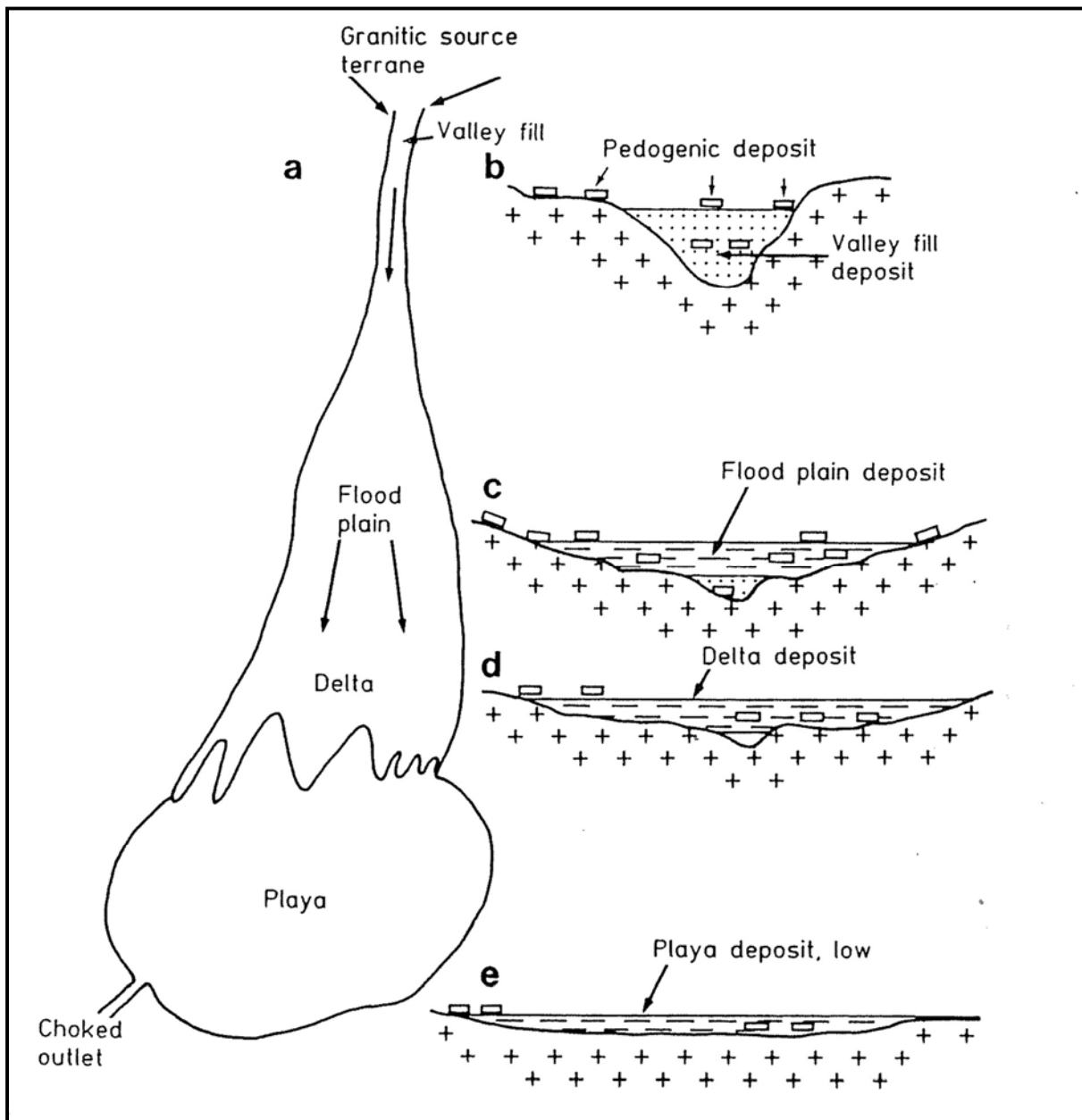


FIG. 158. Schematic representation of the location of valley-fill, flood plain, deltaic and playa deposits within a drainage system [427] (reproduced with permission).

### 3.11.3. Metallogenesis

In Australia, the distribution of uranium deposits strongly suggests that granitoids were the source of uranium, potassium and probably vanadium in the carnotite [428]. Fresh granitoids in the Yilgarn Block typically contain 3–8 ppm U and therefore represent an adequate source. Vanadium is probably derived from mafic minerals in the granitoids, probably via secondary accumulations in clay and iron oxides. The basin that hosts the deposits had low relief, a low drainage gradient and a large catchment area, including deeply weathered granitic rocks. Distribution of calcrete/dolocrete is mainly in axial segments of large channels, becoming less well developed at playa margins.

Uranium released from weathering granitoids is transported in groundwaters as uranyl carbonate complexes. Vanadium is transported as a tetravalent cation. Precipitation of carnotite occurs where concentrations of uranium and potassium have been elevated by evaporation and where vanadium is

oxidized to the  $V^{5+}$  state. Isotopic disequilibrium and ore textures in the Yeelirrie deposit suggest that uranium continually dissolved and reprecipitated during an extended period in the Late Pleistocene and Holocene. The age of mineralization is not known for any of the deposits, but the most geologically reasonable models suggest that uranium was deposited around 0.75–0.1 Ma.

A general model for calcrete-hosted uranium deposits involves deposition upstream of local barriers formed by uplifted basement blocks or by local constrictions in the channel. These constrictions allow the depressions to be temporarily flooded, conducive to formation of calcrete and diminishing phreatic water circulation. The stabilized phreatic lens promotes dolomitization of the original calcrete and concentration of uranium and vanadium, which precipitate as carnotite during evaporation in arid to semi-arid climates [431].

### 3.11.4. Description of selected deposits

#### 3.11.4.1. Peat bog: The Kamushanovskoye deposit (Kyrgyzstan)

##### Introduction

The Kamushanovskoye project is located in northern Kyrgyzstan, near the border with Kazakhstan. The project area is situated about 60 km north-west of the capital Bishkek and 100 km to the north-east of the Kara Balta Soviet processing plant (Fig. 159).

The deposit represents an unusual style of uranium mineralization as it is hosted in peat deposits in back-swamp areas of the Chu River. The peat deposits were initially explored for their potential as fuel during the 1960s and were found to be uraniferous. International Mining Company Invest (IMC) acquired the property in 2006 for its uranium potential and has been exploring the property. In 2012, resources were estimated at 2214 tU at an average grade of 0.037% U. Large, potentially mineralized areas remain to be tested within the licence. The deposit was dormant as of 2015.

IMC proposes to construct a simple mining operation at Kamushanovskoye. The uraniferous peat will be directly loaded onto road trucks for transport to the uranium processing facilities at Kara Balta. The peat will be incinerated and the resultant ash will be treated with acid to recover the uranium [432].

##### Geological setting

The Kamushanovskoye deposit lies within Quaternary sedimentary deposits on the floor of the Chu River valley. The river represents the border between Kyrgyzstan and Kazakhstan. On a regional scale, the area is part of a Neogene–Quaternary basin extending 650 km WNW from Tokmak in Kyrgyzstan into Kazakhstan (Fig. 159). Roll-front uranium deposits are known from the Neogene and Quaternary deposits on the western side of the basin and in some adjacent basins. The eastern Kyrgyzstan segment of the basin is bounded to the south by the 3000–4800 m Kirgiz Range and to the north-east by the 1500–2000 m Kendyktas Range (Fig. 159). The basin opens and widens to the WNW with a low relief surface falling from 1000 m to below 500 m.

The Neogene and Quaternary sedimentary infill buries older topography and shows extensive areas of outcrop of Lower and Middle Pleistocene sediments. This surface is dissected by the present-day Chu River drainage, which flows along the northern margin of the basin. Upper Pleistocene and Holocene deposits are restricted to this drainage system. The Chu River descends from the western end of the Terskey Ala Too mountain range in central Kyrgyzstan and enters the basin at its south-eastern end. The river flows along the northern margin of the basin and eventually terminates in seasonal salt pans at the far west end of the basin in Kazakhstan. Most tributaries in the Kyrgyzstan portion of the basin begin in the Kirgiz Range, descending and joining the Chu River from the south. Minor tributaries flow south from the Kendyktas Range. The Chu River valley probably controls groundwater flow in the Quaternary basin-fill sediments [432].

The Kirgiz and Kendyktas Ranges represent the main sediment sources for the basin infill. They display a sequence ranging from Riphean to Carboniferous. Large parts of the Riphean–Ordovician succession are intruded by granitoids. Vein, stockwork and porphyry style mineral deposits are abundant. Three uranium deposits within granitoid intrusions are reported, but the style of deposit is unknown [432].

At Kamushanovskoye, the Chu River valley is approximately 5 km wide. The valley floor has an elevation of just below 550 m and is approximately 20 m lower than the surrounding terrain. There is a well-defined bluff marking the valley limit. Short streams are locally incised into the surrounding terrains but most of the surface is flat. Lower Pleistocene sediments crop out on the south side of the valley but Upper Pleistocene sediments crop out along the Kazakhstan (north) side of the valley.

The valley floor at Kamushanovskoye consists of five distinct zones (Fig. 160) [432]:

- (i) Zone 1: The modern river forms a meander belt 1.5 km wide along the northern side of the valley. This zone incorporates the border with Kazakhstan on the north-east side of the current river;
- (ii) Zone 2: A reed marsh occurs as a <1 km zone along the southern side of the modern meander belt. The uraniferous peat deposits at sites 1 and 2 occur within this zone;
- (iii) Zone 3: An abandoned meander belt occupies the central part of the valley. Crop markings show meander patterns with similar wavelength and channel width to the present-day river;
- (iv) Zone 4: A zone of reed marsh, 0.5–2.0 km wide, with no significant natural river channels flowing through it. This zone contains uraniferous peat deposits at sites 3 and 4 along the south-western margin. The south-western margin with zone 5 exhibits a scalloped pattern similar in scale and form to the meanders in zones 1 and 3. The northern margin with zone 3 is irregular. Locally, zone 4 merges with the fill of meanders in zone 3 and also partly overprints meander loops;
- (v) Zone 5: A zone of flat, cultivated land marking the southern side of the valley. This zone is generally >1 km wide, although locally very narrow or absent at the south-eastern end of Kamushanovskoye. No evidence of channels or meander patterns is seen. The southern margin of the zone is marked by bluffs forming the boundary of the main valley. This zone may mark a relict of Upper Pleistocene sediment on the south side of the valley.

This arrangement of sedimentary zones does not persist upstream or downstream. Upstream, south-east of Kamushanovskoye, the modern meander belt occupies the south side of the valley, the implication being that favourable sites for peat preservation will be on the Kazakh side. Marshy vegetation appears to occupy a much greater proportion of the valley width downstream, north-west of Kamushanovskoye. The Chu River is dammed 35 km downstream from Kamushanovskoye to form a reservoir at Aul Ayt-Kozha and it is unclear whether the extensive marsh vegetation is natural or the result of a rise in the water table due to the formation of the reservoir. The downstream section of the Chu River valley is in Kazakhstan flowing to the north-east about 2.5 km downstream of Kamushanovskoye. Both the modern and abandoned meander belts show varying states of preservation of meander loops, suggesting a history of small scale migration of the belts [432].

The following sequence of fluvial events is inferred for the Kamushanovskoye area [432]:

- (a) Incision of the Chu River valley;
- (b) Infill of the valley by Late Pleistocene sediment, forming zone 5 and the surface north of zone 1;
- (c) Incision of the Chu River valley forming the scalloped margin on the north-eastern side of zone 5;
- (d) Sediment infill and development of a raised meander belt, forming zone 3. Peat accumulation probably began during this phase;
- (e) Avulsion results in the main Chu River channel switching to zone 1 from zone 3. Formation of the scalloped margin on the north-east side of zone 3. Peat accumulation in zone 4 to infill

back-swamp areas and some abandoned meander channels. Wet areas suggest that peat or peaty sediment accumulation is continuing to the present-day;

- (f) Generation of a modern raised meander belt in zone 1. Peat accumulation in zone 2 is inferred to infill back-swamp areas of the zone 1 meander belt. Peat accumulation in zone 1 is thus inferred to span a shorter time interval than for the peat in zone 4.

Peat accumulations can be developed as sequences interspersed with other sediments. Lake environments may alternate between open water and low lying wet ground with layering reflecting changing vegetation and modes of decay. Changes in the course of meandering river systems, such as the Chu River, may result in peat erosion and the deposition of alluvial sediments. The result of the influx of sediment-bearing water may result in alluvial sediment intercalated within peat or layers of peat with dispersed sedimentary particles. Additionally, drying events can lead to the formation of thin layers of extremely decomposed vegetation [432].

### Mineralization

At Kamushanovskoye, uranium mineralization occurs over a wide area of the back-swamp peat deposits. From the available geological information, a channelized system of peat- and silt-filled meander bends occurs, which has been preserved within the wider alluvium-filled meander belts of the Chu River. Of particular significance at Kamushanovskoye is the migration of the current course of the Chu River to the north-east, resulting in a wide belt of meanders and back-swamps on the Kyrgyz side of the border. The geological setting of Kamushanovskoye is consistent with other Quaternary uranium occurrences and peat is a known geochemical trap site for uranium [432].

Four mineralized areas have been defined, named sites 1–4 (Fig. 161). Site 4 comprises a north-west trending elongate peat body about 2400 m in length and with a maximum width of 400 m. The north-western extensions are water flooded zones. The site is clearly defined as a distinct dark green vegetated area on Google Earth images.

On Soviet geological sections, two peat layers are systematically present, separated by dark grey to black silt with vegetation ‘residuals’ (Figs 162 and 163). The upper peat is made of undecomposed vegetation. It has a flat top below modern reed litter. Thickness varies in the range 0–1.65 m, reflecting gradual changes in the depth to the base. The lower peat shows semi-decomposed vegetation. Thickness varies in the range 0–3.45 m. The maximum thickness occurs in a narrow section of the deposit, possibly marking a scour depression. Both top and bottom surfaces undulate. The upper peat is present in every hole while the lower peat occupies a more restricted area, locally pinching out as indicated on the geological cross-sections. Fully decomposed peat is only shown in section IV, where it forms a third layer of peat. The dark grey to black silt layer usually overlaps the lower peat horizon. The base of the sequence is marked by medium-grained sand with pebbles. Peat can lie directly on this surface or may be separated from it by black clay [432].

Uranium enrichment at Kamushanovskoye can occur through the full thickness of peat right to the surface, while in other full peat sections there is only a low uranium content throughout. This distribution shows that:

- (a) Uranium deposition was ongoing after the topmost peat was deposited;
- (b) Uranium deposition is in part discordant to the peat and silt layering.

There are no published data on the detailed repartition of uranium or grades.

## Metallogenic aspect

The Kamushanovskoye deposits are found in narrow and restricted back-swamp environments between marginal bluffs and a raised meander belt. The individual deposits are similar in size to the montaine examples but are located on a major river and the surrounding terrain includes extensive, earlier Quaternary sediments that lie slightly above river level. The nearest bedrock outcrops occur to the north, up to 20 km away and are drained by small tributary streams [432].

Quaternary accumulations of uranium are mostly associated with peat or peaty sediments, although some are associated with evaporation of surface or groundwater. Peat-hosted, geologically recent uranium accumulations are reported from Canada, Sweden, the United Kingdom and the USA, and the former Soviet Union (Russian Federation and Kyrgyzstan). Studies of peat-hosted uranium accumulations show that much uranium is derived from regional groundwater carrying uranium as uranyl bicarbonate complexes. Uranium deposition in sedimentary hosts is known to be controlled by the presence of organic matter capable of adsorbing  $U^{6+}$  or reducing  $U^{6+}$  to  $U^{4+}$ . This is likely to be a major mechanism at Kamushanovskoye.

Culbert and Leighton [433] report uranium concentration in pans and alkaline lakes in the dry zone of Washington (USA) and British Columbia (Canada). Tixier and Beckie [434] report evaporative concentration of groundwater at Prairie Flats, British Columbia, but suggest that it is not an important factor in uranium concentration at that site. A contribution of this type, as a result of evapotranspiration during reed growth, may occur at Kamushanovskoye. Most pre-Quaternary sediment-hosted uranium deposits are modified and further concentrated by later solution and redeposition. The events are usually attributed to the flow of oxidizing groundwater dissolving the uranium, which is then reprecipitated at interfaces with organic-rich sediment or reducing groundwater. These interfaces are commonly marked by a boundary between reduced, grey coloured, sediments and orange, yellow or bleached sediments. Any such alteration at Kamushanovskoye is likely to be restricted to the pebbly sands below the uraniferous peat.

A peat-hosted deposit at Flodelle Creek, Washington (USA) was mined from 1983. Shawe et al. [435] note that surficial uranium deposits have not been widely exploited in the USA, although they form potentially large, low grade, resources. This report does not specifically mention the Flodelle Creek deposit. Culbert and Leighton [433] report significant accumulations of uranium in peat in British Columbia, Canada. They note that some preliminary feasibility studies for extraction had been released in 1979, but that exploration for uranium had subsequently been banned in British Columbia.

Studies of channel uranium deposits in Australia suggest that weathering of granitoid igneous rocks in headwater areas provide uranium-bearing waters. Granitoid intrusive rocks and hard rock uranium mineralization in the surrounding mountain ranges provide similar sources for the Kamushanovskoye deposits. These felsic igneous rocks are also likely to be major contributors of sediment to the basin fill and provide a source of uranium-bearing accessory minerals to the groundwater system. They also contribute to the sediment fill of a Neogene intermontane basin in the upper reaches of the Chu River [432].



FIG. 159. Map showing the location of the Kamushanovskoye licence [432] (reproduced with permission).

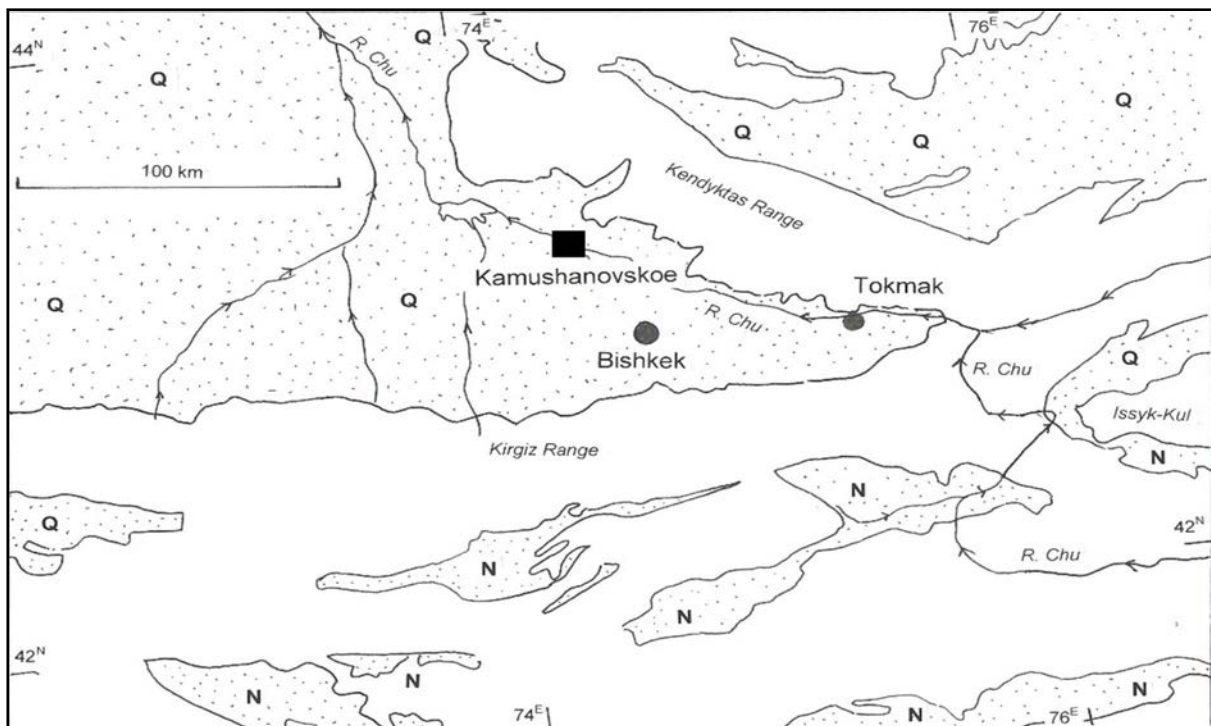


FIG. 160. Quaternary geology of the Kamushanovskoye area in northern Kyrgyzstan [432]. (Q: Quaternary sediments, N: Neogene sediments, white areas indicate basement formations) (reproduced with permission).

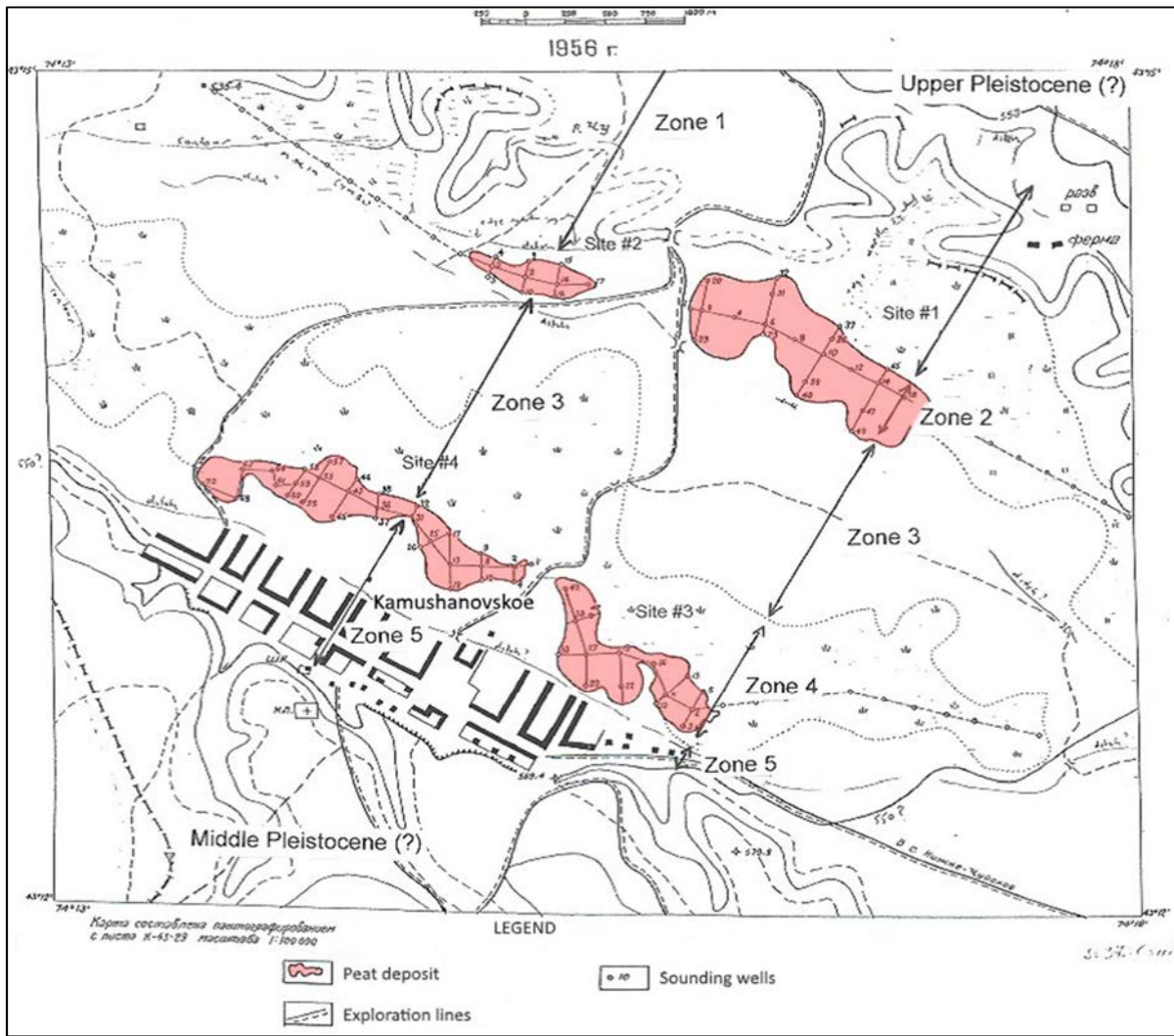


FIG. 161. Soviet era map of Kamushanovskoye showing the four peat sites and interpreted fluvial zonation [432] (reproduced with permission).

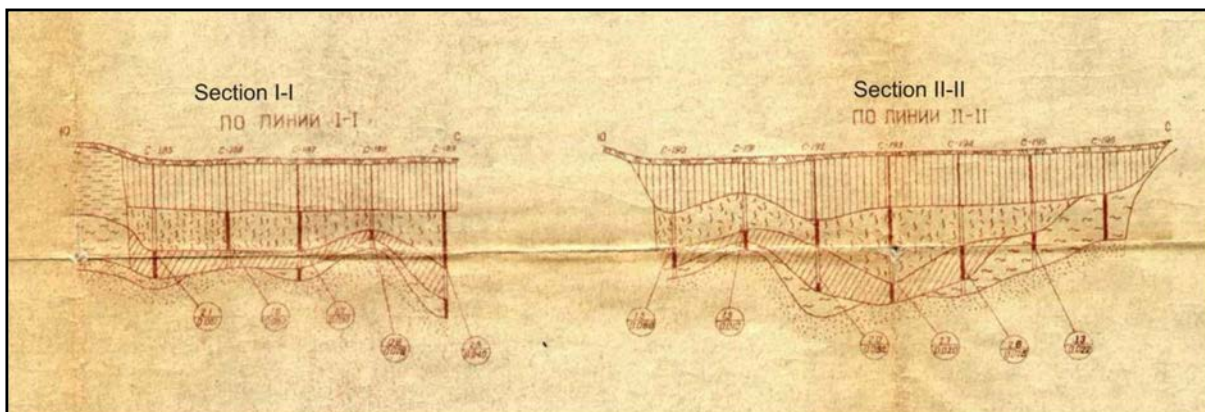


FIG. 162. Soviet era sections I and II from Kamushanovskoye Site 4 (from top to bottom: thin loam layer, undecomposed peat, silt, semi-decomposed peat and sand forming the basement) [432] (reproduced with permission).

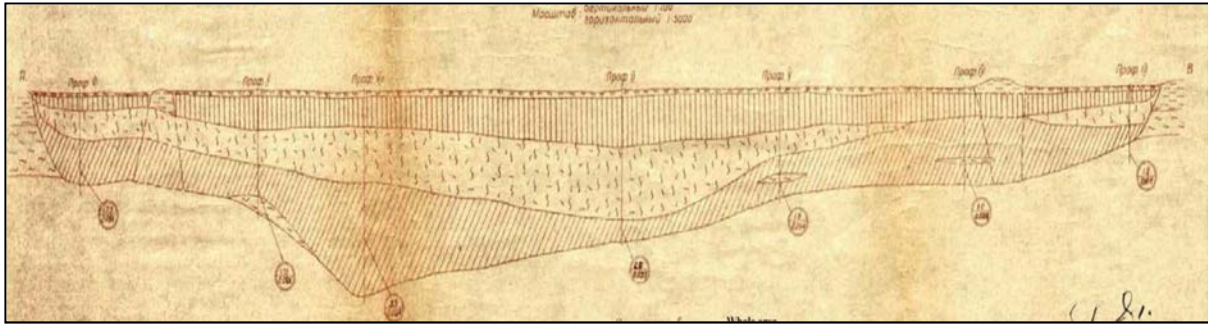


FIG. 163. Soviet era section through Kamushanovskoye Site 4 (from top to bottom: thin loam layer, undecomposed peat, silt, semi-decomposed peat and sand forming the basement) [432] (reproduced with permission).

### 3.11.4.2. Fluvial valley: The Langer Heinrich deposit (Namibia)

#### Introduction

The Langer Heinrich deposit is situated in the Gawib River valley, 90 km east of Swakopmund and 40 km south-east of the Rössing uranium mine. The deposit was discovered in 1973 as the result of a government sponsored airborne radiometric survey, although it was not developed until 38 years later due largely to the depressed uranium price. The project was acquired in 2002 by Paladin Energy Ltd and construction began in 2005 and the mine opened in 2007. In 2014, a 25% stake in Langer Heinrich was sold to CNNC Overseas Uranium Holdings Limited, a wholly owned subsidiary of China National Nuclear Corporation.

Langer Heinrich is a sandstone- and conglomerate-hosted uranium deposit occurring within palaeochannel sediments in an extensive Tertiary palaeodrainage system. Total resources are estimated to be 66 605 tU at an average grade of 0.051% U [436]. The deposit is currently being mined in seven open pits within the 15 km length of the palaeodrainage system. Production in 2015 totalled 1937 tU and cumulative production since 2006 is 12 825 t U.

#### Geological setting

As already noted, the Langer Heinrich project is a calcrete-hosted secondary uranium deposit associated with valley-fill sediments in an extensive Tertiary palaeodrainage system in the Gawib River valley. It consists of seven contiguous mineralized zones (designated 1 to 7) within the 15 km length of the palaeodrainage system (Fig. 164).

The Namib Desert lies within the Neoproterozoic Damara Orogenic Belt and consists of metamorphosed sedimentary and volcanic rocks. Various syn- to post-tectonic granites and alaskites have intruded the Damara rocks, some of them containing high concentrations of uranium. The lowermost rocks of the Damara Sequence that crop out in the area are pink quartzites of the Etusis Formation (Nosib Group). The quartzites form the Langer Heinrich Anticlinorium, which is a major structure. Unconformably overlying the quartzite are rhythmically interbedded metapelite, metagreywacke and calc-silicate beds of the Tinkas Member (Khomas Subgroup).

The orogenic Salem Granite has intruded the Damara Sequence and covers large areas north of the Langer Heinrich Mountains. To the south of the mountains, the Bloedkoppie Granite has intruded the belt. It is a leucocratic, late tectonic to post-tectonic member of the Salem Granite Suite and typically contains 8–12 ppm U with values up to 80 ppm U. The Bloedkoppie Granite is of the same age as the alaskite ( $509 \pm 1$  Ma as determined from uraninite [437]) and may be related [429].

The Langer Heinrich valley is a portion of a 13 km long E–W trending palaeochannel which transects the Bloedkoppie Granite in the east and the Komass Schist in the central and western parts. The surficial sediments in the Gawib River valley comprise the Langer Heinrich and Bloedkoppie Formations. Headward erosion by the Gawib River initiated by uplift during the Pleistocene resulted in exposure of the Langer Heinrich Formation, which contains a wide range of lithologies [430]. Calcrete terraces within the valley indicate an original sediment thickness of 60 m. Subsequent erosion in the central and eastern portions of the palaeochannel removed 30–40 m of the original sediments. Bedding of the fluvial sediments within the palaeochannel is sharp and lenticular. Cross-bedding is present, with vertical lithology changes being rapid and irregular. Sorting is poor to moderate and the sequence is normally graded. The sediments consist mainly of siltstone, conglomerate and breccia with either a silty or calcareous matrix. Sedimentary cycles typically consist of a basal conglomerate or breccia followed by alternating siltstone, conglomerate, breccia and calcareous arkose. The beds vary from a few decimetres to a few metres thick. Towards the top, the calcareous arkose (calcrete) becomes dominant [429].

### Mineralization

The mineralization is hosted by the fluvial sediments of the palaeochannel. In general, the bulk of uranium mineralization is confined to the Langer Heinrich Formation, with only a small amount occurring in the Bloedkoppie Formation. It consists of several thin, tabular bodies along the length of the palaeochannel, generally a few metres above the bottom of the channel fill. In vertical section there is only one ore-bearing zone (Figs 165 and 166) which has irregular, gradational hangingwall and footwall contacts. The grade of the mineralization is generally highest in the centre of the zone. Mineralization is not controlled by lithology and occurs within all the sediment types [429].

Uranium occurs as irregularly distributed carnotite. It occurs as thin films lining cavities and fracture planes and as grain coatings and disseminations. Carnotite specks up to 2 mm in diameter are irregularly distributed within the calcium carbonate matrix [438]. The calcite-cemented sandy grits typically contain the highest grades of mineralization. Mineralization is located near the surface in bodies 1–30 m thick and between 50 and 1100 m wide, depending on the width of the palaeovalley.

### Metallogenic aspects

In Namibia, surficial uranium deposits occur in fluvial and pedogenic environments on the coastal plain of the Namib Desert. The desert is extremely dry and this arid environment has preserved the deposits.

The paragenetic carnotite/calcite relationship in the Langer Heinrich Formation indicates that several ages of calcite precipitation took place, probably starting in the Late Tertiary. The carnotite appears to predate the Pleistocene uplift that caused the downcutting of the Gawib River and its precipitation likely took place during the Late Tertiary [430]. The Bloedkoppie Granite and the associated pegmatites are the probable source of the uranium in the Langer Heinrich Formation.

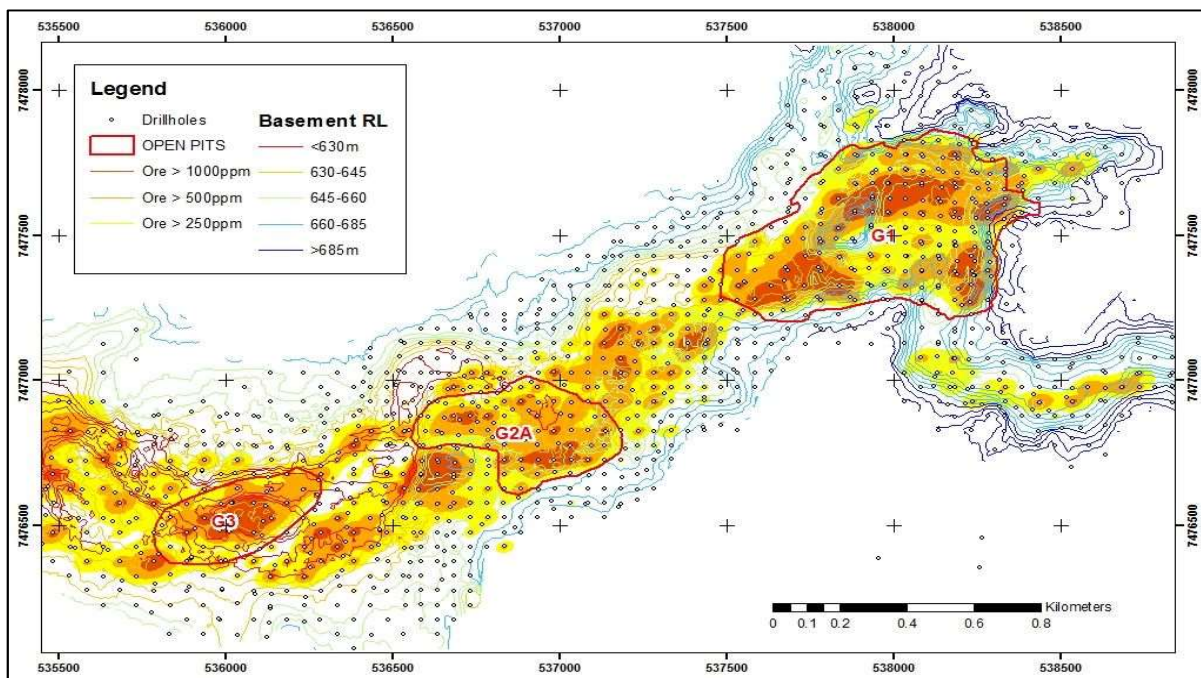


FIG. 164. The Langer Heinrich deposit [436] (reproduced with permission).

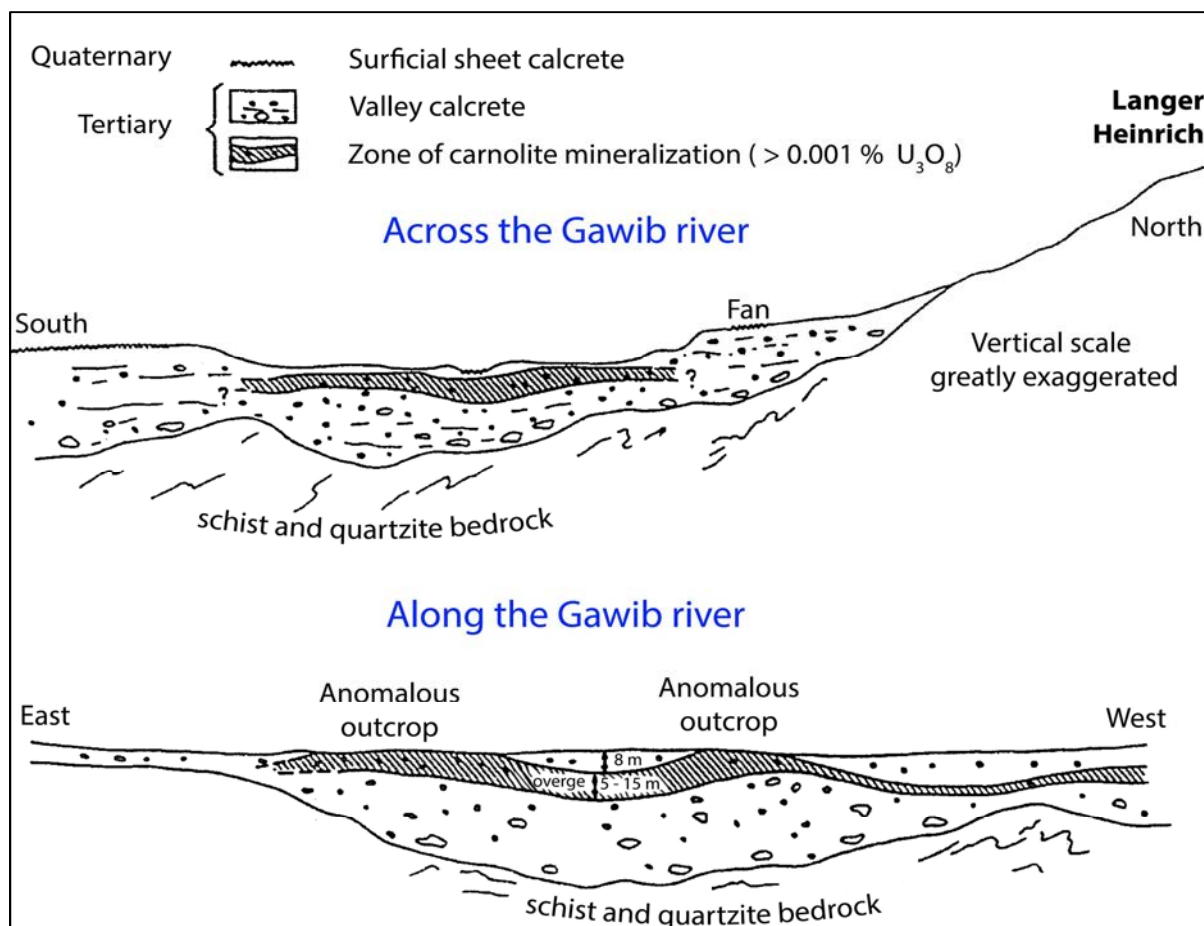


FIG. 165. Diagrammatic section of the Langer Heinrich deposit (adapted from Ref. [429]).

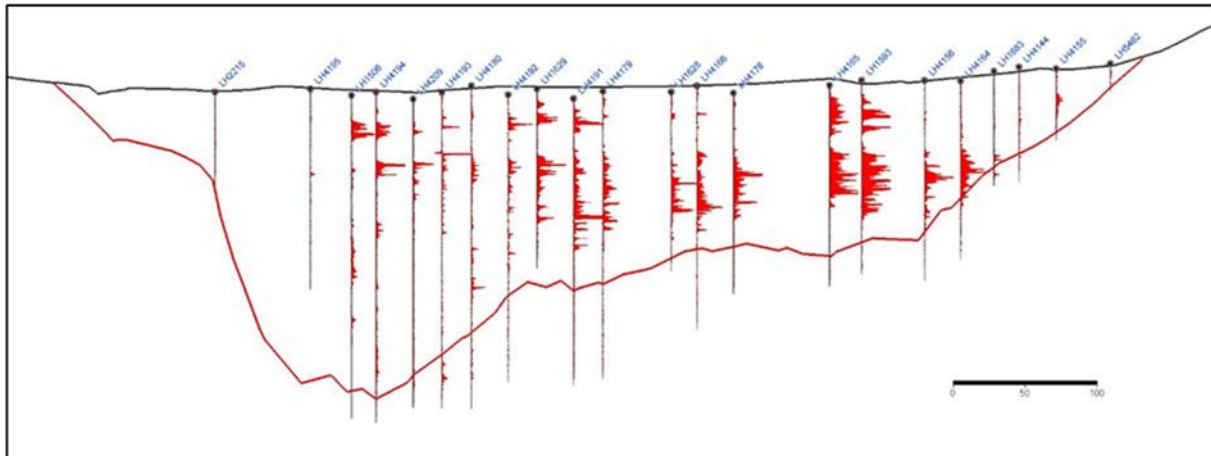


FIG. 166. Cross-section of the Langer Heinrich deposit (reproduced courtesy of E. Beker, Paladin Energy).

#### 3.11.4.3. Lacustrine–playa: The Lake Way Centipede and Millipede deposits (Australia)

##### Introduction

The Lake Way deposit is part of the Wiluna uranium project operated by Toro Energy Ltd and comprises six defined uranium deposits. The project area is situated in Western Australia, 16 km south-east of Wiluna and about 800 km north-east of Perth (Fig. 167).

The Lake Way uranium deposit, which is located along the north shore of the lake (Fig. 168) was discovered in 1972 by Dehli International Oil Corporation and Vam Ltd during an aerial spectrometer survey. As of 2012, resources amounted to 4731 tU at an average grade of 460 ppm U. The Centipede–Millipede deposits, with aggregate resources of 7662 tU at a grade of 455 ppm U, are situated on the south-western side of the lake. A small deposit, Lake Way South, has been delineated by Encounter Resources Ltd between the two deposits. In addition, Toro Energy has three other deposits in its Wiluna regional resource, Dawson-Hinkler, Lake Maitland and Nowthanna, which it is continuing to evaluate. As of the end of 2012, total resources of the five deposits, at a cut-off grade of 170 ppm U, were estimated to be 32 340 tU at a grade of 410 ppm U [439].

The project would involve mining up to 2 million tonnes of mineralized ore over an anticipated mine life of about 17 years, producing up to 680 tU annually from three deposits [440]. Prefeasibility estimates and the process engineering phase of the definitive feasibility study are complete for mining of the three shallow (open pit to a depth of 10 m) calcrete deposits for which all government environmental approvals have been received. First production is planned for 2018.

##### Geological setting

In Australia, surficial deposits are found only in calcrete. The main uranium-bearing calcrete deposits are in Western Australia, in the Archaean Yilgarn Craton.

The Wiluna Project lies on the internal plateau of Western Australia and is characterized by remnant salt lakes and extensive tracts of featureless, undulating sand plains, interspersed with higher areas of bedrock. Duricrusted granitoid outcrops are commonly bounded by erosional escarpments and deeply weathered mafic rocks are covered by laterite, forming low, rounded hills. The maximum relief in the region is generally less than 100 m and within the mineralized area relief is less than 10 m [441].

The regional geology of the Wiluna area consists of Archaean bedrock dominated by granite and gneiss on the east and mafic volcanic rocks of the Norseman–Wiluna greenstone belt on the west. Lake Way overlies the contact between the two units (Fig. 169). The Archaean rocks are typically deeply weathered and are covered by recent alluvium, sheetwash, sand plain and calcrete.

Rocks in the main catchment area consist of adamellite and gneissic biotite granite. Airborne reconnaissance surveys over the Mount Cleaver adamellite outcrops show an anomalous radiometric response three to five times higher than those of other granite exposures in the area. The medium-grained adamellite consists of quartz (30%), microcline (30%), plagioclase (30%) and biotite (7–10%). Altered monazite, ilmenite, zircon and magnetite are selectively associated with the biotite. Zircon (>1%) is surrounded by metamict alteration envelopes. Trace elements of weathered samples are as follows: U = 12 ppm, Th = 40 ppm, V = 50 ppm, Zr = 120 ppm, La = 150 ppm and Ce = 300 ppm [441].

The Lake Way and Centipede deposits are associated with broad palaeochannel deltas that empty into the Lake Way hypersaline playa, which itself represents the remnants of a major primary palaeodrainage system of predominantly Tertiary age.

Most of the mineralization consists of carnotite that has been deposited within carbonated, reworked, fluvial clastic sediments occupying the southern extremity and peripheral areas of the Uramurdah–Negrara drainage. In addition, significant mineralization also occurs along the southern edge of the valley-fill calcrete and in the younger chemical delta carbonates at the edge of Lake Way. Mineralization is not lithologically controlled but is directly related to sediment permeability (primary or secondary), water table depth and rate of groundwater evaporation [441].

Fluviodeltaic sediments consist of an interfingering and transitional sequence of carbonated sand, silt, clay and calcrete. Quartz sand grains are subangular, dark brown to grey and vary in grain size from very fine to grit, becoming more argillaceous towards the delta area. Reworked carbonate fragments and nodules are common and carbonaceous material is found lining fossil root tubes. Carbonated silts and clays are typically brown to light grey, thinly bedded and strongly arenaceous. Thin lenses of sand, grit and reworked calcrete fragments are present [441].

The dominant minerals in the clay-sized fractions are very fine-grained quartz and dolomite. Kaolin is the main clay mineral but smectite and smectite–illite mixed layer clays may locally be present. Accessory and trace minerals include gypsum, kaolin, feldspar, attapulgite, halite, mica, illite and goethite.

Calcretes are generally light to dark grey, but the younger, more massive and dolomitic calcretes in the chemical delta are distinctly brown. Quartz grains are common as inclusions and sepiolite is found lining cavities and fractures. Oolitic and spherulitic carbonate forms occur at or near the surface on the lake margins and are composed of aragonite crystals, often coated with or in a sepiolite matrix. Some reprecipitation of carbonate is apparent within the calcrete, where clear microcrystalline calcite is present as growths in voids and on fracture planes. Fluviodeltaic sediments associated with the calcretes are subject to carbonate replacement, especially those immediately above the water table [441]. Karst features, dissolution voids, shrinkage cracks and coarse, irregular bedding provide for rapid infiltration and movement of groundwater towards the local base level.

### Mineralization

The uranium mineralization is located in shallow deposits hosted in calcrete, dolomite, silt, clay and sand. These deposits were formed within the palaeochannel drainage system and so follow the palaeochannels. Present-day drainage has eroded these channels, resulting in a complex discontinuous orebody. The mineralization usually occurs at or in close proximity to the current water table, typically 1–2 m below ground level. The total thickness of mineralization generally does not exceed 6–7 m.

The uranium mineralization at Lake Way is distributed throughout a calcrete/dolomite, carbonated silty clay and carbonated sand sequence, which can attain a thickness of 40 m. The mineralization occurs at, or in close proximity to, the current water table, typically at a depth of approximately 2 m below the surface and in some places extends to a depth of 12 m. This calcrete/carbonated sequence is overlain by 2 m of alluvium (Fig. 170). There appears to be no preferred host rock to the mineralization.

Uranium mineralization at both deposits is dominated by carnotite, which has been precipitated and preserved within the lower reaches of tributary palaeochannels, as a result of subtle changes in groundwater chemistry and evaporation. Most of the visible uranium mineralization occurs in the form of micro- to cryptocrystalline carnotite (grain size of less than 0.04 mm). The carnotite is found as coatings on bedding planes, infillings between sand and silt grains, fissure fillings within calcrete and dolomite and infillings of tubular voids in buried soil profiles. The carnotite appears to have been precipitated on any available surface. Some carnotite crystals are present in an argillaceous matrix with micro- to cryptocrystalline calcrete or micro-oolitic and spherulitic carbonate (aragonite). Both the crystalline and the oolitic calcrete are distinctly separate and younger than the massive valley-fill calcrete and are more prevalent in the associated clay/silt horizons. Leaching tests indicate that a small fraction of the carnotite may be associated with recent silicification [441].

The mineralization at Centipede and Lake Way generally occurs in a number of flat lying, irregular lenses at or close to the current water table, typically 1–5 m below the surface. The mineralization varies in thickness up to about 6.5 m and lies beneath 1–15 m of overburden. The mineralization can be found in most rock types including calcrete, dolomite, sand and clay.

Disequilibrium studies showed a range of values from 1:1.02 to 1:1.16. Maximum disequilibrium was recognized in the chemical delta where the mineralization is considered to be slightly younger and probably derived from the higher, more northerly deposits. Most of the mineralization occurs in the 1–6% total dissolved salts (TDS) zone. No commercial mineralization has been found in the lake, where groundwater contains up to 20% TDS, or in the northern area, where groundwater contains less than 0.5% TDS [441].

#### Metallogenic aspect

Calcrete uranium mineralization is in the form of carnotite, which is believed to have precipitated from groundwater in areas where the water table in the palaeodrainage aquifers rises close to the surface, promoting evaporation and concentration of uranium, potassium and vanadium. Such areas are also characterized by carbonate precipitation, mounding and lateral spread of calcrete.

Several parameters are suggested as having influenced the formation of the surficial uranium deposits of Western Australia:

- (a) Separate uranium and vanadium groundwater aquifers;
- (b) Change of carnotite solubility with change in pH;
- (c) Evaporation of groundwater;
- (d) Local increase in  $K^+$  activity;
- (e) Change in partial pressure of  $CO_2$ ;
- (f) Dissociation of uranyl carbonate complexes;
- (g) Redox controlled precipitation.

Several of these factors are likely to be involved in the genesis of any individual deposit, but the importance of redox control on the movement of vanadium and an increase in potassium ion activity by evaporation of groundwater appear to be dominant processes in many deposits [428].

The distribution of the uranium deposits in Western Australia strongly suggests granitoids to be the source of U, K and probably V present in the carnotite. Fresh granitoids in the Yilgarn Craton usually contain 3–8 ppm U, within the range of 1–80 ppm U, and therefore represent an adequate source since

leaching due to weathering may extend to depths as great as 250 m. There is no evidence that the bedrock uranium content has significance and attempts to relate mineralization to specific uraniumiferous granites have not been successful. Assuming that some of the uranium is accessible, the factors in a weathering environment that control leaching, mobilization and precipitation have greater importance [428].

Vanadium is likely derived from mafic minerals in the granitoids, possibly via secondary accumulations in clays or iron oxides. Although greenstone belts, with their associated mafic rocks, are present in most catchments, there is no evidence that their presence has any control over the location or grade of the uranium mineralization [428].

Uranium released from weathering is transported in groundwaters as uranyl carbonate complexes. Vanadium is solubilized as a tetravalent cation complex. Precipitation of carnotite occurs where concentrations of uranium and potassium have been elevated by evaporation and where vanadium is oxidized to the pentavalent state. This may be where vanadium has diffused upwards from depth within the saturated zone under a redox gradient or where a subsurface bar has caused upwelling of such groundwaters to relatively oxidizing conditions, the accompanying effects being mounding and lateral spreading of the calcrete [428].



FIG. 167. Location of the Wiluna uranium project in Western Australia (adapted from Ref. [440]).

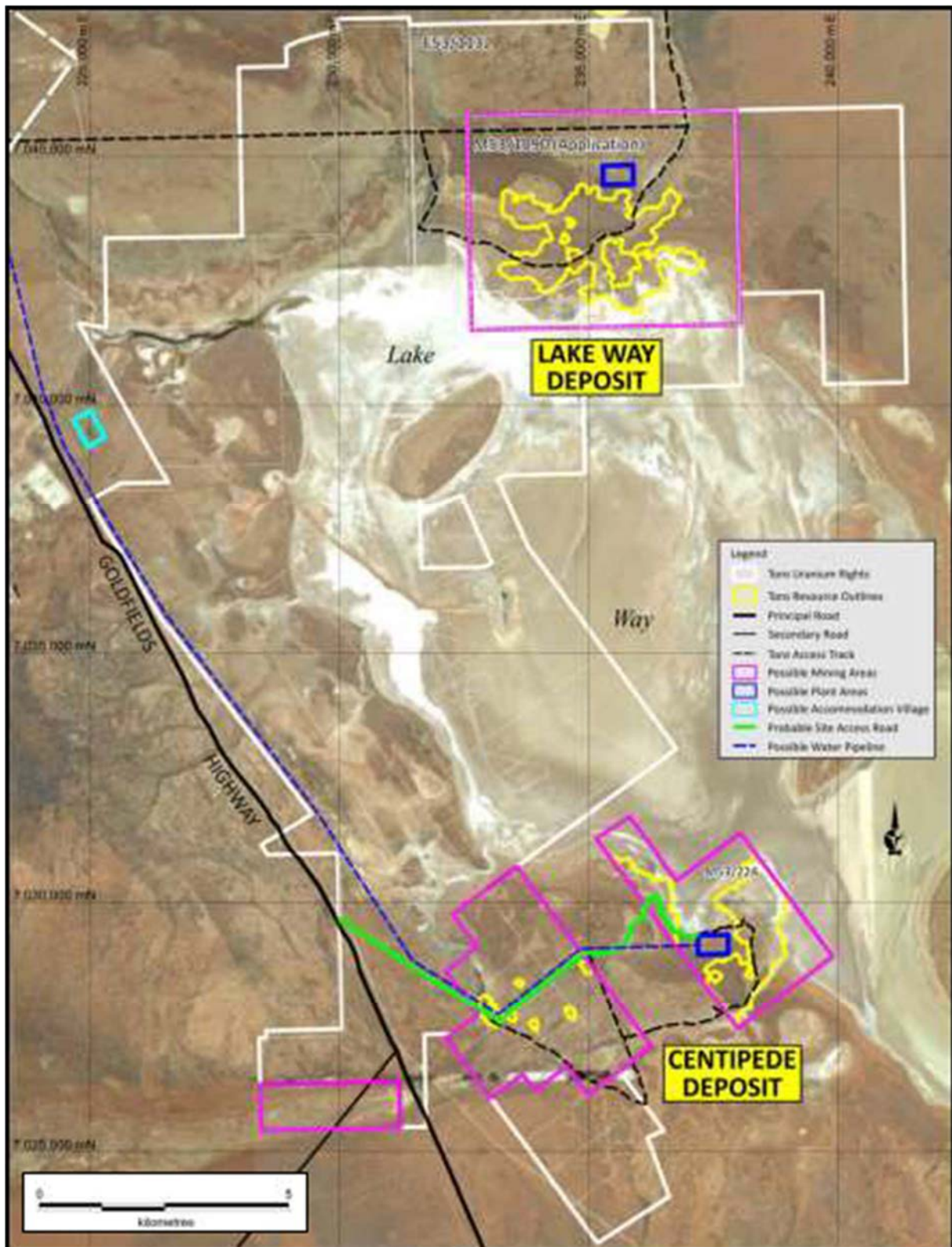


FIG. 168. Location of the Lake Way and Centipede uranium deposits (adapted from Ref. [440]).

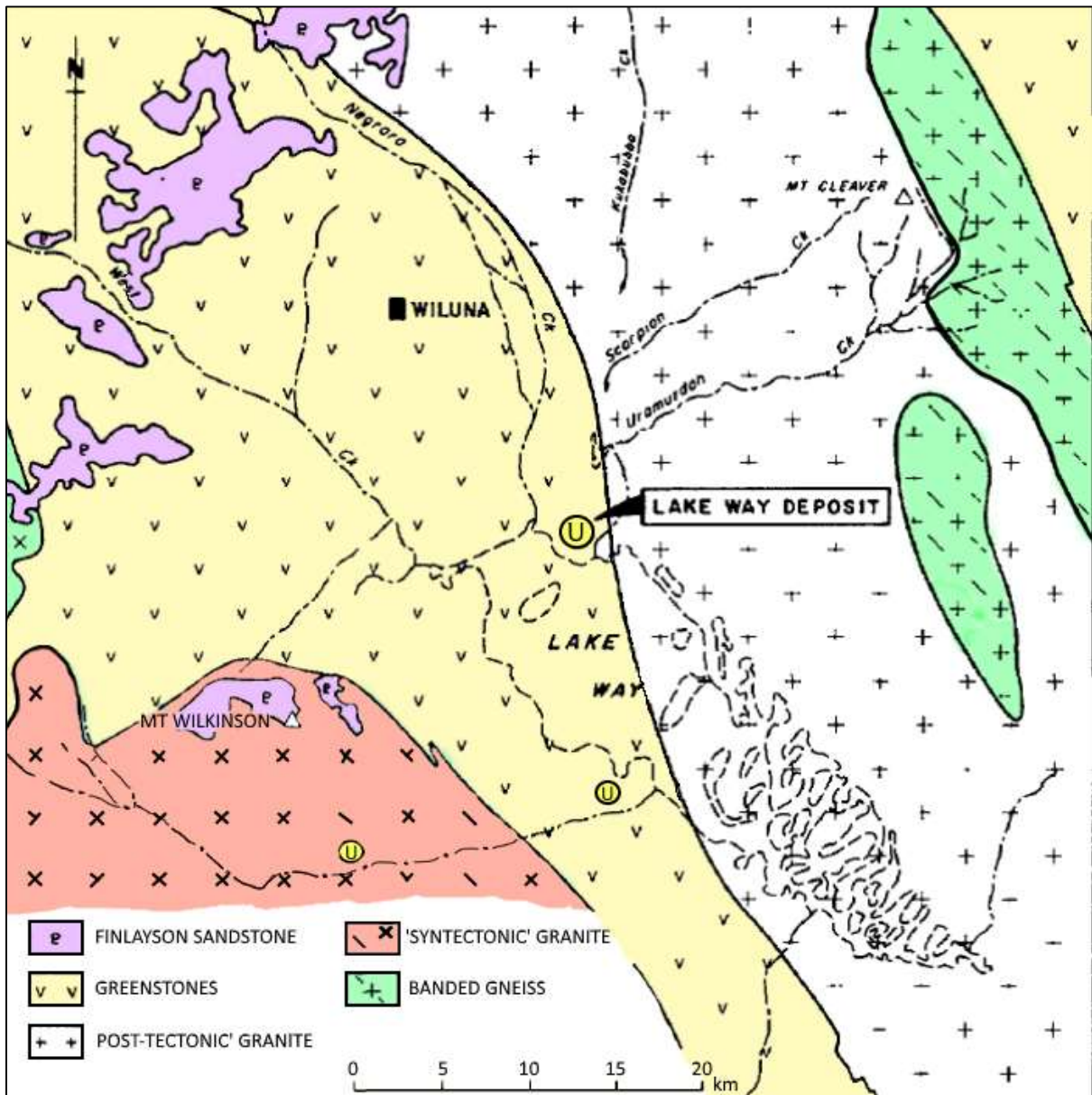


FIG. 169. Geology of the basement rocks in the vicinity of Lake Way (adapted from Ref. [441]).

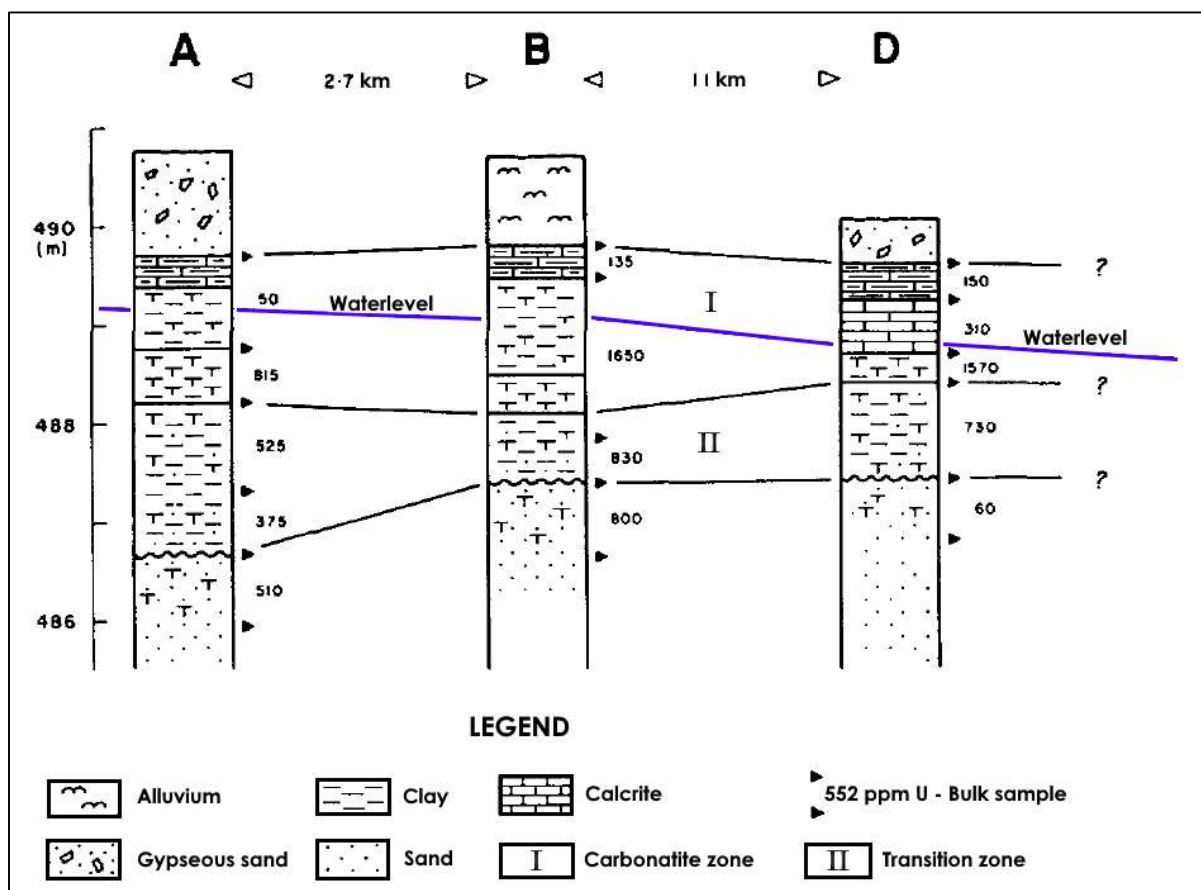


FIG. 170. Geological cross-section of the Lake Way deposit (adapted from Ref. [441]).

### 3.12. Lignite–coal deposits

#### 3.12.1. Definition

Lignite–coal uranium mineralization consists of paludal material composed of land plant debris mixed with coalified detritus and containing quantities ranging from traces to large amounts of syndepositional, uniformly disseminated uranium or epigenetic, irregularly distributed structurally controlled uranium. In both cases, uranium is adsorbed onto carbonaceous matter [18]. In general, lignite formations contain more uranium than coal formations.

The UDEPO database (2015) lists 35 lignite–coal deposits. Worldwide, lignite–coal deposits frequently display elevated uranium contents, although the uranium grades are typically very low (1–20 ppm U). Exceptionally, some strata can be enriched in uranium to levels exceeding 0.10%, such as in the Kazakhstan coal deposits. Hundreds of lignite–coal deposits and districts exist around the world, with 1600 localities listed in the IHS Global Coal Database.

Examples of uranium occurrences in lignite–coal formations include the deposits of North Dakota and South Dakota in the Northern Great Plains (USA), where geological resources are estimated at several million tonnes, the Serres Basin (Greece), Springbok Flats (South Africa), the Koldzhat and Nizhne Iliskoye deposits (Kazakhstan), the Stepnovskoye deposit (Russian Federation), the deposits at Mulga Rock (Australia), Daladi (China) and the Freital-Gittersee deposit (Germany) (Table 34).

TABLE 34. PRINCIPAL LIGNITE–COAL DEPOSITS/DISTRICTS (as of 31 December 2015)

Deposit	Country	Resources (tU)	Grade (% U)	Status
Northern Great Plains	USA	6 000 000/ 7 000 000	0.002–0.008	Dormant
East Ebro Valley	Spain	102 000	0.017	Dormant
Springbok Flats	South Africa	81 920	0.042	Exploration
Nizhne Iliskoye	Kazakhstan	60 000	0.098	Dormant
Koldzhat	Kazakhstan	37 000	0.162	Dormant
Stepnovskoye	Russian Federation	19 100	0.050	Dormant
Ambassador	Australia	14 437	0.0517	
Coyote Basin	USA	13 615	0.17	Dormant
Emperor	Australia	10 215	0.0424	
Luena Basin	Democratic Republic of the Congo	7 500	0.01–0.05	Dormant
Badyelskoye	Russian Federation	5 430	0.0382	Dormant
Belskoje	Russian Federation	5 000	0.026	Dormant
Briketno-Zheltuhinskoye	Russian Federation	5 000	0.035	Dormant
Serres Basin	Greece	4 000	0.01	Dormant
Freital-Gittersee	Germany	3 977	0.10	Depleted

Uranium extraction from lignite–coal is hampered by its binding to organic compounds, rendering it almost refractory as regards metallurgical extraction [17]. However, about 3700 tU at an average grade of 0.12% U were mined from the Freital-Gittersee deposit (Germany) and a small amount (550 tU) was extracted from lignites of the Dakota Plains (USA). In Harding County, South Dakota, grades from 0.1% U up to several per cent have been recorded in Palaeocene lignite layers. The Hilltop mine produced 232 tU at an average grade of 0.28% U. In Kyrgyzstan, small intermontane coal-bearing basins in the Tien Shan Mountains contain uraniferous lignite seams which have been mined for uranium. The Tuyuk-Suu deposit reportedly produced 2626 tU. Uranium is also concentrated in ash produced by coal-fired power plants. Sparton Resources, a Canadian company, intends to recover 125 tU annually from Chinese power plant ash. At the Sentinel project in North Dakota (USA), which has been explored by PacMag Metals Ltd, a small U–Mo–Ge deposit (Church) containing 330 tU at 0.014% U has been delineated within shallow Tertiary lignite seams [442]. Historical mining from a nearby pit produced 60 tU at a grade of 0.15% U.

### 3.12.2. Geological setting

Lignite–coal seams are interbedded with carbonaceous clastic sediments in paludal, low lying, poorly drained shallow depressions located either on coastal plains (paralic lignite) or within landlocked basins (limnic lignite). Uraniferous felsic pyroclastic material often overlies or is intercalated with the seams. Granites and other rocks with anomalous uranium contents are frequently found near these basins. Lignitic host beds are usually small (<2 m). Two deposit subtypes are distinguished [18] (Fig. 171):

- (i) *Stratiform* (North Dakota (USA), Nizhne Iliskoye (Kazakhstan)) uranium occurs as stratiform, syngenetic, uniformly disseminated, very low (20–150 ppm U) to medium (0.05–0.10% U) grade mineralization;

- (ii) *Fracture-controlled* epigenetic (Freital-type (Germany)) mineralization is spotty and irregularly distributed with strong grade variations. Grades are commonly a few hundred ppm U (0.03–0.15% U).

In joint/fracture-related deposits, host rocks correspond to pyritic, high ash lignite, sub-bituminous coal and non-marine carbonaceous mudstone and siltstone. Joints and fractures are common and intraformational unconformities often control uranium accumulation. No alteration is present. There are no discrete primary uranium minerals. Locally, secondary hexavalent uranium minerals may be present in joints and fractures. Uranium is adsorbed onto carbonaceous matter or bound in organic compounds (uranyl humate), particularly in cataclastic zones. Other metals present in anomalous amounts, but not necessarily correlative with uranium, may include As, Be, Cd, Co, Cu, Ge, Mo, Ni, Pb, Se, Ti, V, Y, Zr and REE.

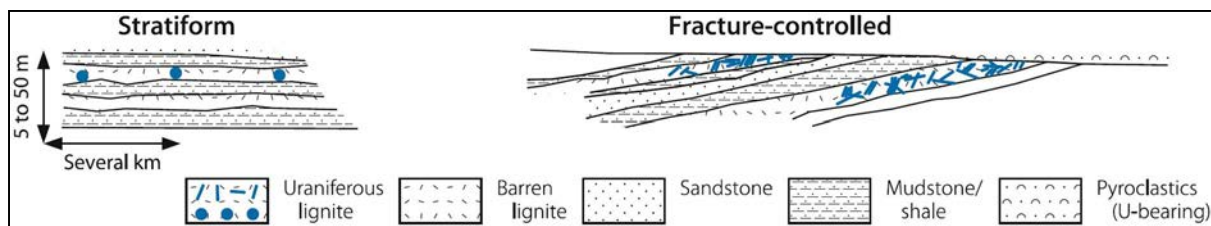


FIG. 171. Uraniferous lignite–coal deposits [18] (reproduced with permission).

### 3.12.3. Metallogenesis

Lignites and coal are favourable horizons for uranium accumulation when they originate from paludal, poorly drained shallow depressions with abundant vegetation and located either on coastal plains (paralic lignite) or within landlocked basins (limnic lignite). Uranium is believed to have been leached from surrounding rocks bordering the basins, such as granites and volcanics containing anomalous amounts of uranium. Two mechanisms have been invoked for transportation of uranium into the basins: (i) transport by surficial waters with precipitation by syngenetic adsorption onto organic material to form syngenetic mineralization and (ii) post-depositional, by groundwater migration into buried basins to form epigenetic mineralization. In this last case, infiltration occurred along permeable zones (joints, fractures) producing the irregular distribution of uranium.

### 3.12.4. Description of selected deposits

#### 3.12.4.1. Uraniferous coal–lignite deposits from Central Asia

##### Introduction

Central Asia contains several small to large uraniferous lignite–coal deposits. The largest uranium resources in the coal basins of this region are the Koldzhatsk (37 000 tU) and Nizhne Iliskoye (60 000 tU) deposits in Kazakhstan. Smaller uranium deposits and occurrences in coal basins in the Russian Federation are situated in the southern Urals (Donsk), Transbaikalia (Urtuisk), Kansk-Achinsk Basin (Berezovsk) and Primorski Krai (Rakovsk, Luzanovsk) (Fig. 172). The average uranium content of the uraniferous lignite–coal varies from a few tens to a few thousand parts per million.

According to Seredin and Finkelman [443], metalliferous lignite–coal deposits were generated by the circulation of uraniferous surface water and groundwater through sedimentary basins. The structure of the deposits and the uranium resources are directly related to the nature, type and duration of uranium-bearing water circulation in the basin. Large uraniferous lignite–coal deposits were formed by epigenetic infiltration after the onset of coalification during the lignite–sub-bituminous stage [444]. In

contrast, 'infiltration' and 'exfiltration' types that were formed during the peat accumulation and early diagenetic stages have resources of the order of one to two orders of magnitude smaller.

## Geological setting

### *Infiltration type: Syngenetic and diagenetic deposits*

These small uranium deposits and occurrences in lignite–coal beds have many features in common with modern uranium-bearing peat occurrences known in several countries. Uraniferous lignite–coal beds usually occur interbedded with impermeable clay layers, which exclude the epigenetic accumulation of uranium. Similar deposits have been described in the far eastern part of the Russian Federation and in the former Czechoslovakia. Their characteristic features are: (i) development in the marginal parts of coal basins, (ii) stratabound, lenticular shape of the orebodies, and (iii) prevalence of organically bound uranium with only a minor proportion of uranium in minerals [443].

### *Epigenetic deposits*

Epigenetic deposits are known worldwide in Palaeozoic, Mesozoic and Cenozoic coalfields. The Mesozoic and Cenozoic lignite and sub-bituminous coal contain the highest uranium resources. The deposits occur in the marginal parts of coal basins, in zones accessible to oxygenated waters with high uranium contents during arid periods. The deposits usually consist of a series of band-shaped ore lenses lying at the contacts between lignite–coal beds and oxidized sandstones. However, high uranium contents are not observed at the contacts between lignite–coal beds and clays. The orebodies are oriented parallel to the basin margins and range around 1–15 km long and 0.1–2 km wide. The near contact uraniumiferous lignite–coal layers are 0.1–0.5 m thick in most cases and rarely exceed 1–2 m [443].

Russian geologists distinguish two types of epigenetic uraniumiferous lignite–coal deposits based on the character of the meteoric water circulation: (i) ground infiltration deposits precipitated from unconfined water and (ii) bed infiltration deposits originating from confined water [444]. The two types of deposit differ from each other in their shapes and by the location of the orebodies in the coal sequences.

Uranium orebodies of the ground infiltration type and with monoclinally dipping coal beds are located only at the tops of these beds. Typical examples are the Nizhne Iliskoye deposit (Kazakhstan) (Fig. 173), which is similar to the South Dakota (USA) uranium concentrations. In deposits with steeply dipping coal beds, uranium mineralization is dispersed across their entire thicknesses. However, in this case, the mineralization usually pinches out within a few tens of metres [443].

The Nizhne Iliskoye deposit consists of 48 orebodies contained in a zone about 40 km long and 100–2000 m wide, located within a NW–SE trending graben. Orebodies occur at depths of 100–500 m (Fig. 173). They are lenticular and are mainly restricted to the upper 2 m of the Jurassic lignite seam. Lenses are less than 1–4 m thick and range in area around 0.1–3.2 km<sup>2</sup> and contain 0.05–2% U, averaging 0.1% U, 0.03% Mo, <30–60 ppm Ag and <2–5 ppm Re. Barren or weakly mineralized zones link the lenses. Mineralization is polymetallic, comprising primarily U–Mo with trace amounts of other metals. Uranium minerals are predominantly pitchblende and coffinite. A major fraction of the uranium is adsorbed onto carbonaceous matter in limonitized lignite [18].

Uranium orebodies of the bed infiltration type exhibit varying morphology. Classical rolls, as crescent-shaped orebodies, lie in the pinched out stratal oxidation zones in sandstones enriched with disseminated organic matter. A second style of orebody, found in sand horizons devoid of plant remnants, is lenticular uranium-bearing zones pinching-out dipwards [445]. In this case, the orebodies in the upper and lower parts of the coal beds occur not only near the oxidized, coarse-grained rocks, but also beneath the bleached and unaltered sandstones. However, the uranium content of the coal and the thicknesses of the mineralized zones gradually decrease with increasing distance from the margins

of the bedding controlled limonitization [446]. Some deposits, such as Koldzhatsk, consist of orebodies related to unconfined as well as confined water oxidation. The former was responsible for the generation of the largest orebody at the top of bed V, while the classical uranium rolls in sandstones and ambient coals are related to the latter. Therefore, this large deposit (37 000 tU) was formed by both unconfined and confined oxygen-rich waters [444].

The Koldzhatsk deposit is located near the border with China (Fig. 172). Underground exploration to a depth of 600 m took place between 1969 and 1978. The deposit is 16 km long and as much as 7 km wide and contains several Jurassic lignite seams with thicknesses of 3–23 m. Uranium occurs in seven horizons, three lignite and four sandstone. Uranium orebodies associated with lignite have tabular to lenticular shapes and the ore is almost exclusively found near the top of the lignite seams. Individual orebodies range between 0.5 and 15 km long, 20–2000 m wide and as much as 2 m thick. Grade is irregular, typically from 0.05 to >0.10% U. Pitchblende, sooty pitchblende and coffinite are the main uranium minerals. These are associated with molybdenum-bearing minerals, pyrite and marcasite [18].

### Mineralization

The metalliferous beds of epigenetic, infiltration deposits usually exhibit alteration zonation. A rear metal-bearing zone composed of oxidized, sooty, high ash coals enriched in iron hydroxides lies beneath limonitized sandstone. Uranium generally occurs in hexavalent form associated with organic material, and in some deposits is also incorporated in arsenates, vanadates, phosphates and carbonates. The rear zone is underlain by the front, uraniferous zone composed of pyritized coal with abundant epigenetic mineralization. Uranium generally occurs in the tetravalent state, in oxides (pitchblende) and silicates (coffinite). Unaltered coal with low uranium content underlies the front zone [443].

Uranium is variably distributed within the metal-bearing layers of epigenetic deposits. The highest concentrations are found in the upper zones, at the contacts with oxidized host rocks, and in the front zone at some distance from the oxidized horizons. In some cases, uranium of both valence states is evenly distributed across the two metalliferous zones [446].

### Geochemistry

Molybdenum, selenium, vanadium and rhenium usually accompany uranium in epigenetic infiltration deposits. However, the uraniferous coals are often enriched in other lithophile, chalcophile and siderophile elements. The rear and front uranium-bearing zones in the upper, uraniferous part of a thick (40 m) coal bed in the Nizhne Iliskoye deposit show different trace element associations. The limonitized coals have elevated V, Zr, Be, Y and REE, while pyritized varieties show high U, Mo, Ge and Tl. Some elements are accumulated in both zones (Se, Re and Co), i.e. in the rear zone and the upper part of the front zone. The concentrations decrease abruptly below. These elements are predominantly adsorbed in limonitized coals and bound in minerals in the pyritized varieties. Molybdenum and chalcophile elements are present in sulphides and arsenates (molybdenite, galena, sphalerite, tennantite, bravoite, linneite, realgar, etc.). Selenium occurs as ferroselite and As and Se may occur as native minerals [445].

### Conditions of formation

For Seredin and Finkelman [443], a combination of several favourable conditions is necessary for the formation of epigenetic infiltration uranium lignite–coal deposits. These conditions are:

- (a) Elevated uranium contents in the meteoric and unconfined waters and in confined groundwater;
- (b) Long term migration of these waters within the coal-bearing sediments.

Elevated uranium contents in water occur when: (a) the coal basins are surrounded by rocks anomalously enriched in uranium and (b) the climate is arid during ore formation. The highest uranium concentrations in groundwater are achieved when both factors act together.

Water migration is favoured by certain tectonic settings during the mineralization event and the period of accumulation of coal-bearing sediments. The optimal hydrological conditions for the formation of uranium mineralization are those typical of coal basins, with a high proportion of coarse sediments that serve as channels for migration of the uranium-bearing waters. Epigenetic uranium mineralization in coal basins is also controlled by basin evolution after the accumulation of the coal-bearing strata. The most favourable hydrodynamic regime is found where the sedimentation stage is followed by weak uplift of the region. The coal-bearing sequences undergo erosion and the lignite–coal beds and adjacent coarse-grained sediments are subjected to free (unconfined) and/or retarded (confined, stratal) water exchange [443].

#### Exfiltration type

The uranium deposits of this type have structural control, occurrence of metasomatic alteration in the basement rocks, high (up to 3–6 m) thickness of the uraniferous layers, short strike length and presence of uranium mineralization in multiple beds at different vertical levels and in the surrounding rocks. These uranium deposits are geochemically similar to the germanium-rich lignite–coal deposits and contain not only Ge, but also W, which is normally absent from the infiltration uranium–coal deposits [443].

Mineral springs with uranium contents two to three orders of magnitude higher than the average uranium content of groundwater in the supergene zone ( $0.56 \mu\text{g/L U}$ ) [447] are reported from many localities worldwide. For example, cool, carbonate springs discharging in northern Sweden into a peat bog and washing deep seated uraniferous iron ores contain up to  $700\text{--}1800 \mu\text{g/L U}$  [448].

All ore-hosting rocks contain finely disseminated marcasite. Quartz–carbonate veinlets fill fractures in the basement granite and can be traced to the Miocene uranium-bearing rocks. The ores are enriched in Ge (150–164 ppm) as well as uranium. The highest Ge (1670 ppm) and U (1.6%) values are found in lignite lenses in the basal conglomerate horizons. Uranium minerals consist of oxides and phosphates.

All these features may indicate the formation of mineralization from the discharge of volcanic-related hydrothermal waters at the base of coal deposits during a Pliocene–Quaternary pulse of volcanic activity. Sozinov [449] hypothesizes that uranium was leached from the basement granite by thermal waters. The southern orebody of the Luzanovsk germanium orefield is another example of an exfiltration uranium deposit [450]. Particularly high uranium contents (500 ppm U) are found in the bottom 1.5 m of coal beds lying near the granitic basement.

An exfiltration origin is also suggested for the uranium mineralization in lignite–coal beds within tuffaceous sedimentary rocks of the northern block of the Streltsovsk caldera in Transbaikalia [451]. This caldera contains significant vein and stockwork U–Mo volcanic deposits. Mineralization in the northern block consists of stratabound orebodies controlled by faults and their intersections. Uranium contents are high in coal beds and in the underlying argillized tuff, tuffite and sandstone. Coffinite and uranium oxides in the coal occur as tiny hollow spheres and as thin films on the surface of organic matter and pyrite. The uranium mineralization is accompanied by finely disseminated molybdenite and native arsenic. On the basis of isotopic data, the mineralization age is close to that of the host rocks (150–160 Ma). Mashkovtsev et al. [451] suggest that the mineralization was syngenetic and formed by the discharge of hydrothermal solutions near the bottom of a marshy lake prior to the time when organic matter was overlain by a thick tuffaceous cover. These examples demonstrate a mechanism for the formation of uraniferous coal deposits from the discharge of cool or thermal mineral springs into sedimentary basins at the stage of peat accumulation and diagenesis of organic matter [443].

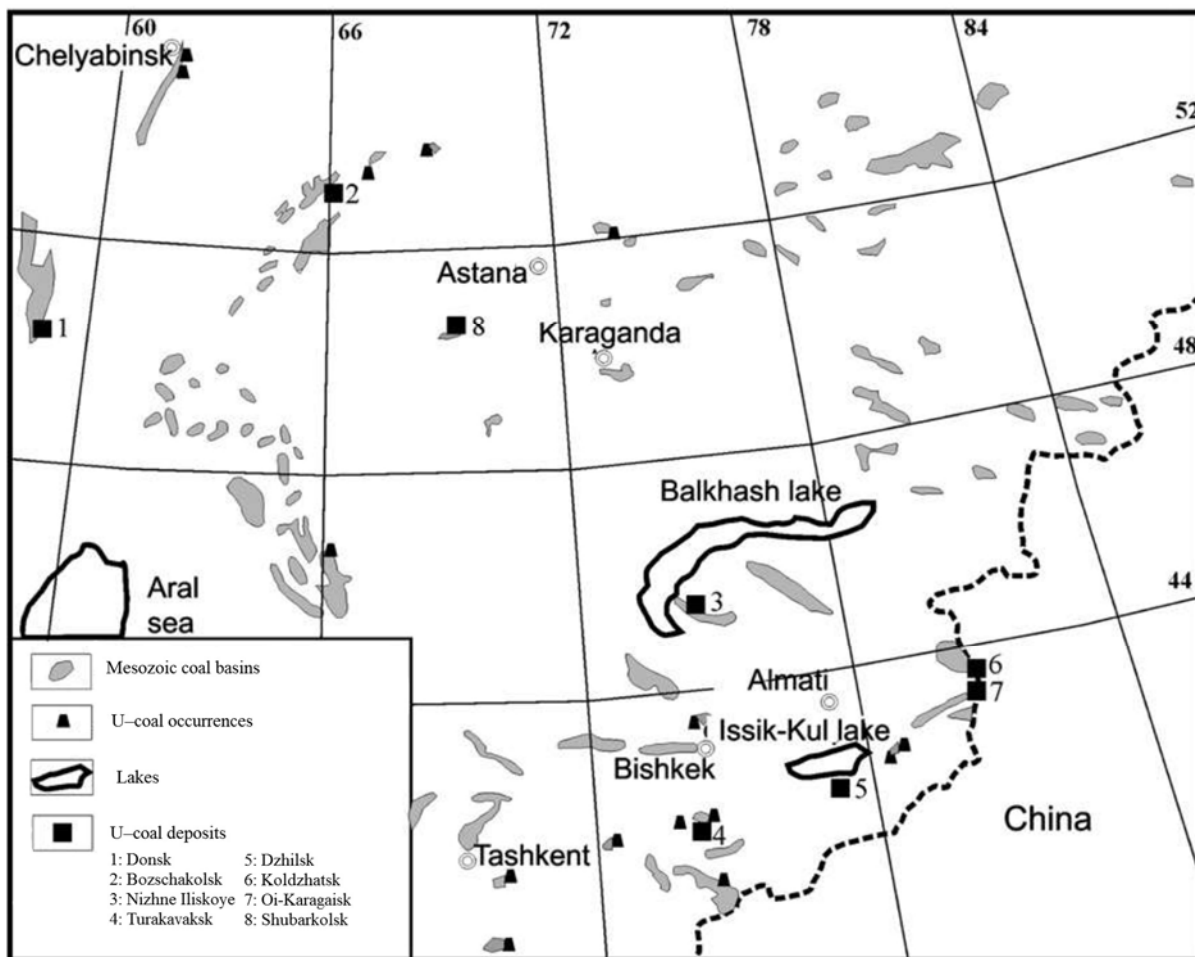


FIG. 172. Uraniferous coal deposits and occurrences in Central Asia (adapted from Ref. [443]).

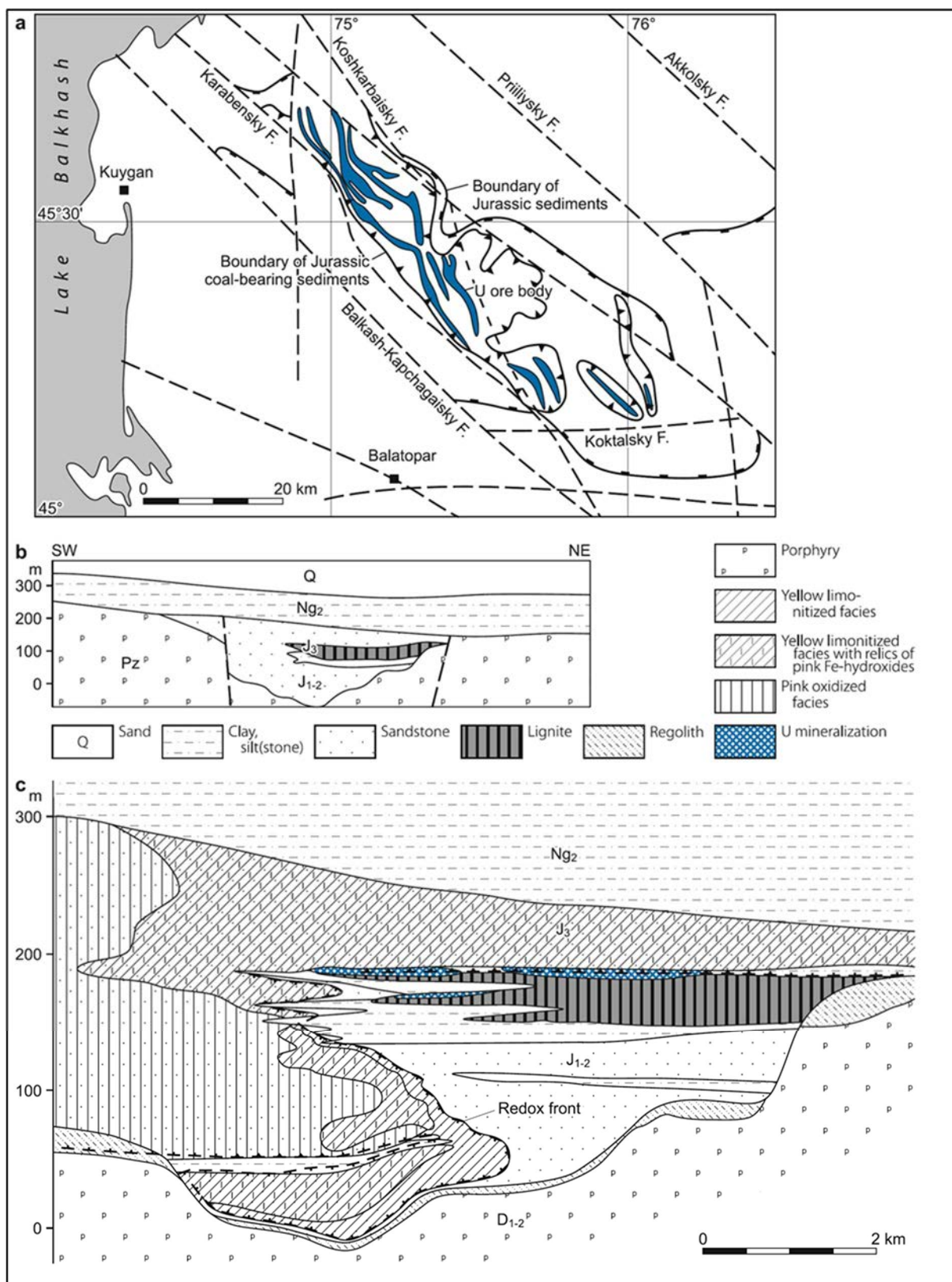


FIG. 173. Nizhne Iliskoye uranium deposit: (a) map of the graben showing uraniumiferous lignite seams; (b) regional lithostratigraphic section, and (c) geological cross-section with alteration features [18] (reproduced with permission).

### 3.12.4.2. *The Daladi deposit (China)*

#### Introduction

The Daladi deposit (deposit 509) is situated along the southern margin of the Yili Basin in the Junggar–Tien Shan Uranium Province. Uranium resources are of the order of 1000–2500 tU with grades of 0.10–0.20% U.

#### Geological setting

The Daladi uranium deposit is located in the Daladi Syncline, east of the southern margin of the Yili Basin. The syncline is 3.25 km long and 0.5–0.9 km wide. The topography is high to the south-west and low to the north-east. The formations dip about 10° and generally plunge to the north. The Daladi Syncline is asymmetric, with dips of 45–60° and up to 85° to the east and south-east limbs and dips of 20–45° to the west and south-west limbs. The Daladi Syncline and the Chabuchaer Syncline to the west were connected by a saddle anticline.

The main sedimentary package in the orefield is represented by the Lower–Middle Jurassic Shuixigou Formation (J1–2sh) which crops out on the east and south-east limbs of the Daladi Syncline. Elsewhere, the Shuixigou Formation is unconformably overlain by Pliocene sediments. Widespread Carboniferous–Permian felsic volcanic rocks are present to the south of the mineralized district.

The Shuixigou Formation, which hosts the Daladi deposit, has been subdivided into eight sedimentary cycles, including 12 coal seams. The cycles are transgressive system tracts, usually beginning with river bed subfacies and ending with valley flat or marsh subfacies. Although the individual cycles vary, the most common position of the coal seams (observed in seams 1–4 and 8–10) is at the top of these fining-upward cycles between the mudstone and the next overlying fluvial sandstone bed.

#### *Host rock alteration*

The Daladi uranium mineralization is hosted by the 1st, 9th and 10th lignite seams. They are 2–4 m in thickness and are composed of semi-dull coal, (64.4%), semi-bright coal (23.1%), fusite (5.9%), pyrite, kaolinite and other impurities (6.6%). The coal consists of 60–70% C, 3–5% H, 16–25% O, 0.7–1.3% N and 0.6–5% S.

The main alteration feature in the orefield is oxidation by groundwater. The alteration exhibits a vertical zonation comprising, from top to bottom, a strong oxidation zone, a weak oxidation zone, a redox zone and a reduction zone (Table 35).

The strong oxidation zone generally occurs in sandstone at a depth of 0–10 m and is characterized by a brown colouration. The weak oxidation zone generally occurs at the boundary between the sandstone and the underlying coal seam (depth of 10–30 m) and is characterized by yellow and buff colours. The oxidized coal seam contains some uranium mineralization. The redox zone generally occurs between 30 and 200 m and contains about 82% of the uranium mineralization. It is typically found at the top of the lignite-bearing horizon and is dull grey in colour and friable. Below 200 m lies the reduction zone, which is best developed in the mudstone below the lignite-bearing horizon and which is typically a grey-green colour. Only minor amounts of uraninite are present in this zone.

TABLE 35. VERTICAL OXIDATION FEATURES IN THE DALADI DEPOSIT

Zone	Sub-zone	Depth (m)	Wall rock	Colour	Minerals		Lithology and thickness (m)
					Uranium minerals	Associated minerals	
Oxidation zone	Strong oxidation zone	0–10	Sandstone	Brown	Silicate, phosphate, arsenate	Gypsum, jarosite	Sandstone 5–25
	Weak oxidation zone	10–30	Sandstone–coal	Yellow-buff (sandstone) Powder (coal)	Arsenate, vanadate	Limonite, baryte	
Redox zone		30–200	Coal	Grey, half bright	Uraninite	Limonite, pyrite	Coal 2–4
Reduction zone		>200	Coal–mudstone	Ash black (coal) Grey-green (mudstone)	Uraninite	Pyrite	Mudstone 3–12

### Mineralization

In the Daladi deposit, the uranium mineralization occurs mainly on top of the first coal seam and then in the 9th and 10th coal seams. Most of the orebodies are tabular, typically tens of metres long with the longest being 206 m. Thickness lies in the range 0.55–2.60 m. The ore-bearing coefficient is 0.58–0.84. The average grade is 0.279% U and the coefficient of variation of the grade is 59–146%.

In the mineralized zones, uranium is present in two forms. Uranium is present in black minerals, including uraninite. However, 80% of the mineralization in uraniferous coal deposits is dispersed, adsorbed onto materials such as coal, organic carbon, freshwater plants and clays in mudstone.

Two other metals are found in significant (economic) quantities. Selenium is present in its native form at an average grade of 0.044% Se, with estimated resources of 137 t. Molybdenum is present as molybdenum sulphide, with estimated resources of 154 t. Both elements exhibit a positive correlation with U, enriched in the uranium orebodies as well as being dispersed in the wall rocks (Table 36).

TABLE 36. LEVELS OF URANIUM, SELENIUM AND MOLYBDENUM IN THE 1st COAL SEAM OF THE DALADI DEPOSIT

Grade range (% U)	U (%)	Se (%)	Mo (%)
0.01–0.05	0.043	0.021	0.081
0.05–0.10	0.068	0.029	0.024
0.10–0.30	0.172	0.0313	0.064
0.30–0.50	0.361	0.135	0.0882
0.50–1.0	0.789	0.249	0.175
1.0–1.50	1.426	0.428	0.428

Uranium–lead radiometric dating of uraninite from the deposit has produced an age of ore formation of 7–5.5 Ma, indicating that the uranium mineralization occurred during the Late Miocene. At that time, the Daladi district was faulted into blocks and uplifted.

#### Metallogenic aspects

The uranium of the Daladi deposit is believed to have been derived from the widespread Carboniferous–Permian felsic volcanic rocks. The uranium content (6.2–9.6 ppm U) is far above the regional background and this type of rock could supply abundant uranium.

In the uplifted, faulted blocks, host rocks were elevated, down-dropped and denuded. This history was favourable for the development of phreatic water oxidation zones.

Uranium mineralization is related to the long depositional period. The Daladi district has two periods of deposition: one from Early–Middle Jurassic to Late Cretaceous and another from Late Cretaceous to Late Tertiary.

Studies have identified three formations representing sedimentary cycles in the southern part of the Yili Basin. The first formation represents a series of sedimentary half-cycles, with braided river sediments overlain by fan and swamp deposits. The second formation represents braided river delta and swamp sedimentation cycles. The third consists only of braided river delta sediments but different areas have different lithological and facies sequences. Coal-bearing beds of the Daladi deposit are found in the braided river to fan and swamp sequences, representing the sandstone–coal–mudstone framework. In this framework, sandstone directly overlies the coal seams and the sandstone has good permeability (coefficient of permeability of 0.5–1.5 m/d), allowing strong phreatic water oxidation. The coal beds are one to several metres thick, which are favourable for preconcentration and epigenetic enrichment of uranium. The uranium content of the coal seams was originally high (16–26.5 ppm U) and the mudstone (3–12 m thick) provided a stable, low permeability base.

Owing to favourable stratigraphy, structural setting and, most importantly, a favourable hydrogeological environment, strong phreatic water oxidation affected the Daladi district and developed deep phreatic water oxidation zones. Phreatic water carried the uranium from the upper sandstone and deposited it at the top of the coal seam, eventually forming a uranium deposit. Conversely, where oxidized phreatic water could not reach the coal seam, uranium mineralization did not form.

#### Deposit origin

The formation of the Daladi deposit can be divided into two stages:

- (i) *Uranium pre-concentration during sedimentation and diagenesis*: Uranium mineralization during the diagenetic stage consisted of the adsorption and enrichment of uranium by organic matter. At the syndimentary stage, during the formation of peat, the remains of terrestrial plants are broken down by aerobic bacteria, generating humic acids. Adsorption and ion exchange eventually generate uranium humic acid salts. During diagenesis with the deep burial of the ore-bearing rock, the peat changes into lignite, the dissolved oxygen in the formation waters gradually disappears and anaerobic bacteria become active again. This further decomposes the organic matter to produce CH<sub>4</sub>, H<sub>2</sub>S, H<sub>2</sub> and other gases, changing the formation waters from oxidized and acidic to alkaline and reduced. When uraniferous solutions migrate from the oxidizing environment to the reduction environment, both eH and pH change and the uranium is precipitated. This stage is characterized by uniform uranium mineralization at low grades which can be termed pre-enrichment;
- (ii) *Uranium accumulation during phreatic water oxidation*: The poorly lithified sandstone above the coal beds contains water and uranium. When the mineralized rock was uplifted near to the phreatic surface, the external oxidized uraniferous groundwater alters the grey coloured sandstone to maroon and leaches the uranium. The uraniferous groundwater

permeated into the underlying coal seam and was reduced, forming economic concentrations of uranium mineralization. In summary:

- Uranium mineralization at the top of coal seams is deposited by reduction from oxygenated, uraniferous groundwaters. Deposits are found where the sandstone overlying the coal seam is highly permeable and the highest grades occur near the top of the coal seam within 30 cm of the sandstone contact. Deposits do not form where the coal seam is overlain by impermeable mudstone;
- The main uranium mineralization is found at the top of coal seams overlain by permeable, oxidized sands. Sparse uranium is found in the underlying sandstone;
- The highest concentration of mineralization is found in flat lying or gently dipping beds. More steeply dipping stratigraphy is unfavourable;
- Radiography and fluorescent microscopy indicate that finely disseminated uranium minerals are distributed along fractures in the coal seams whereas agglutinated forms are most likely distributed in durain and the wood fibres of fusite;
- The distribution of uranium mineralization is variable; grades can locally reach 11.4–21% U in high grade areas;
- Ore formation was much younger than the host rocks. Ore from the Daladi deposit was isotopically dated to 7–5.7 Ma while the host rocks are the Lower–Middle Jurassic Shuixigou Formation (J<sub>1-2sh</sub>) with an age of 205–154 Ma.

#### 3.12.4.3. *The Mulga Rock deposits (Australia)*

##### Introduction

The Mulga Rock Project is located approximately 250 km ENE of Kalgoorlie, in Western Australia, on the south-west margin of the Great Victoria Desert. Since 2007, the project has been operated by Energy and Minerals Australia (EMA). It contains three uranium deposits occurring in Eocene palaeochannels and associated with lignite: Ambassador, Emperor and Shogun. They were discovered in 1979 by PNC Exploration Australia Pty Ltd during exploration drilling of an embayment along the south-west margin of the Gunbarrel Basin. In 1978–1990 over 2000 holes were drilled.

In March 2012, EMA announced the discovery of a fourth deposit located close to Ambassador, named Princess [452]. It is hosted within carbonaceous sandstone. Total resources at the end of 2015 in the four deposits amounted to 29 345 tU at an average grade of 435 ppm U. The deposits are polymetallic and also contain Ni, Co, REE, Y, Sc, V, Cu, Zn and Au. Some of these commodities could be recovered as by-products to the production of uranium. Drilling below the Emperor deposit has identified gold about 75 m below surface. In addition, it is estimated that more than 500 Mt of lignite resources are hosted within several deposits below, near, or a few kilometres south of Emperor.

In 2014, EMA changed its name to Vimy Resources Ltd. In the pre-feasibility study released at the end of 2015, it was indicated that the Mulga Rock Project will produce 1150 tU annually for 17 years. It is also planned to recover base metals (Cu–Zn–Ni–Co–Sc) during the processing of uranium ore.

##### Geological setting

The Mulga Rock deposits are located in the Narnoo Sub-basin, which corresponds to the south-western extremity of the larger Gunbarrel Basin (Fig. 174). The Narnoo Sub-basin is interpreted as a NW trending trough delimited on all sides by faulting. To the west, the Narnoo Sub-basin overlies the Archaean and Proterozoic granitoids of the Yilgarn Craton, and to the east, it overlies the Albany-Fraser Province. The Precambrian basement is overlain by deformed Neoproterozoic sediments of the Officer Basin, which in turn are overlain by the Phanerozoic Gunbarrel Basin. The region has been subjected to continental conditions since the Cretaceous, with planation and sedimentation under humid, followed by arid, conditions [453].

The Mulga Rock palaeochannel in which the deposits are situated was eroded down to the Lower Permian mudstone comprising the Paterson Formation, which represents the basal unit of the Gunbarrel Basin. The buried palaeochannel as outlined by drilling is 5–15 km wide and with a known extent of at least 100 km below the Tertiary cover rocks [454]. The western portion of the channel connects with the present-day drainage system of Lake Raeside and Ponton Creek, where several surficial deposits have been delineated. It likely extends for more than 400 km across the Yilgarn Craton (Fig. 174). The palaeochannel may follow even earlier drainage systems that were infilled during the Permian glaciation. Mapping of the basement geology suggests that there is a strong structural control on the palaeochannel, which has a trend similar to the strike of the Proterozoic basement [453].

Within the palaeochannel, up to 140 m of flat lying sand, silt and gravel unconformably overlie the mudstone of the Paterson Formation. In some areas, the mudstone has been removed by erosion and the younger sediments directly overlie the metamorphic units of the Albany-Fraser Province. Sediments range from Cretaceous to Tertiary in age. The sedimentary sequence defined at Mulga Rock is as follows [454]:

- (a) Basal Cretaceous lacustrine sediments (about 60 m thick), with a pebble gravel unit 2–3 m thick at the base, grading upwards into a sequence of quartz sand and sandy clay;
- (b) Tertiary fluviolacustrine sediments (about 80 m thick), conformably overlying the Cretaceous sands. The Tertiary sediments have been subdivided from top to bottom into three broad units: (i) oxidized upper fluvialite sands and interbedded lacustrine sediments (30 m); (ii) lacustrine to paludal sediments, kaolinitic clays overlying lignite (peat), clay-rich lignite and carbonaceous sands and clays (30 m), and (iii) basal fluvialite sand and gravel (40 m). The mineralization is hosted by the lignite and clay-rich lignite layers of Middle Eocene age.

The upper units have been strongly weathered and are variably ferruginized and silicified. Silcrete formation is locally intense. Oxidation extends to a depth of 20–30 m, with a sharp redox boundary between kaolinitic clay and lignite, close to the level of the water table. The oxidation is probably the result of weathering during warm and humid climates during the Oligocene–Middle Miocene period. The sequence has also been affected by later weathering, continuing to the present-day, under more arid conditions than those prevailing since the Middle Miocene [453]. Quaternary sediments, 2–20 m thick, consisting of aeolian sand, laterite and silcrete overlie the entire region.

#### Mineralization

At Mulga Rock, three deposits, Ambassador, Emperor and Shogun, have been defined (Fig. 175), which occur along the outer margin of a broad bend in a palaeochannel. The total areal extent of the three deposits is 7 km<sup>2</sup> at a cut-off grade of 0.03% U.

Most of the uranium mineralization is hosted by the lignite layers below the redox boundary at the base of the weathered zone and is entirely contained within the upper 1–2 m of lignite. The mineralized zones are flat lying and occur 20–50 m below the surface. There is no broad geochemical halo or surface radiometric expression (either local or regional in scale) [454].

At the Ambassador deposit, three major styles of mineralization have been recognized [455] (Figs 176–178):

- (i) Upper lignite, enriched in U, Ni, Co, REE, Sc, V and, locally, Su and Ag;
- (ii) Lower lignite and associated sandstone, also enriched in base metals;
- (iii) Basal sandstone-hosted mineralization.

Uranium has been adsorbed onto the organic matter within the lignite [454], similar to that recognized in many organic-hosted uranium deposits, including black shales and lignite-coal. The bulk of the uranium occurs as diffuse concentrations too fine to be resolved by scanning electron microscopy and disseminated evenly throughout the organic-rich sediments [456]. Uraninite, coffinite and brannerite associated with ilmenite are the principal authigenic minerals. In some places, uranium is precipitated as oxides and coffinite in leucoxenized ilmenite pseudomorphs. Ilmenite and rutile occur as needles in organic matter, indicating remobilization and precipitation [453].

More than 50 mineral phases have been described in the Shogun [456] and Ambassador [452, 457] deposits, with different element associations. Several authigenic sulphide minerals occur as discrete grains, spherules and irregular masses, including two pyrite phases, galena and sphalerite, as well as uranium sulphides and REE sulphides.

Associated with the uranium mineralization or underlying it are layers containing oily lignite, oil, Ni and possible values of Au, V, REE and other elements. Samples from only 10 holes were assayed for elements other than uranium in the past by PNC. The results indicated that all samples contain Ni-Co and locally Cu-Zn, suggesting that these elements might be widespread within the Ambassador deposit [452, 457]. Considerable enrichment of uranium (up to 3.4% U) occurs in a 1 m thick zone in the clay-rich lignite. Copper and Se, in addition to As, Sc and Tl, are also enriched. Just below the main uranium mineralization, Fe, Ce, Zn and several other transition metals are enriched. In addition, Th, REE, P, S and Se appear to be associated with amorphous organic matter, but the exact nature of the association has not been identified [453].

#### Metallogenic aspect

For Douglass et al. [453], it is likely that the Mulga Rock deposits formed from the convergence of a suite of redox active weathering processes and unique source and host rocks. The process was constrained within an extensive palaeochannel system incised into Permian and Proterozoic basement. During Tertiary weathering, uranium was likely leached from granitoids and metamorphic rocks of the Yilgarn and Albany-Fraser Provinces. Douglass et al. [453] indicate that a proximal source of uranium and trace elements is probable, as suggested by U-Pb isotopic signatures and U-Th disequilibrium and they favour a lamproite-carbonatite source. Such intrusions are common on the edge of the Albany-Fraser block and within the Yilgarn Craton.

Oxidized groundwaters within the sediments transported hexavalent uranium along the palaeochannel, which was subsequently fixed by adsorption occurring at the contacts with organic material in the peat layers. The lignite was probably formed in a palaeochannel wetland or coastal marine/estuarine environment, consistent with the prevailing Middle Eocene shoreline [453].

During the Cenozoic, weathering resulted in oxidation of the surface sediments to a depth of approximately 30 m. The uranium within these sediments was dissolved by oxidizing groundwaters, mobilized and re-adsorbed onto peat layers at the base of the oxidized zone. Repeated oxidation, downward movement and re-adsorption of the uranium were also assisted by seasonal fluctuations in the water table. Consequently, low grade mineralization, originally deposited in the organic-rich sediments, was subsequently concentrated by supergene processes that resulted in uranium accumulating within peat layers at the base of surface oxidation, which generally corresponded to the water table. The grade of mineralization and its thickness are controlled by the permeability and organic matter content of the host sediments. The highest grades and thickest zones of mineralization are developed within the more organic-rich and more permeable sediments. This process occurred within the past 300 000 years [453].

The Mulga Rock mineralization is in a state of radiometric disequilibrium that varies with depth below the surface. Oxidized sand and silt above the redox boundary are depleted in uranium compared with its progeny. In contrast, reduced sediments immediately below the redox boundary are enriched in uranium relative to its progeny [454].

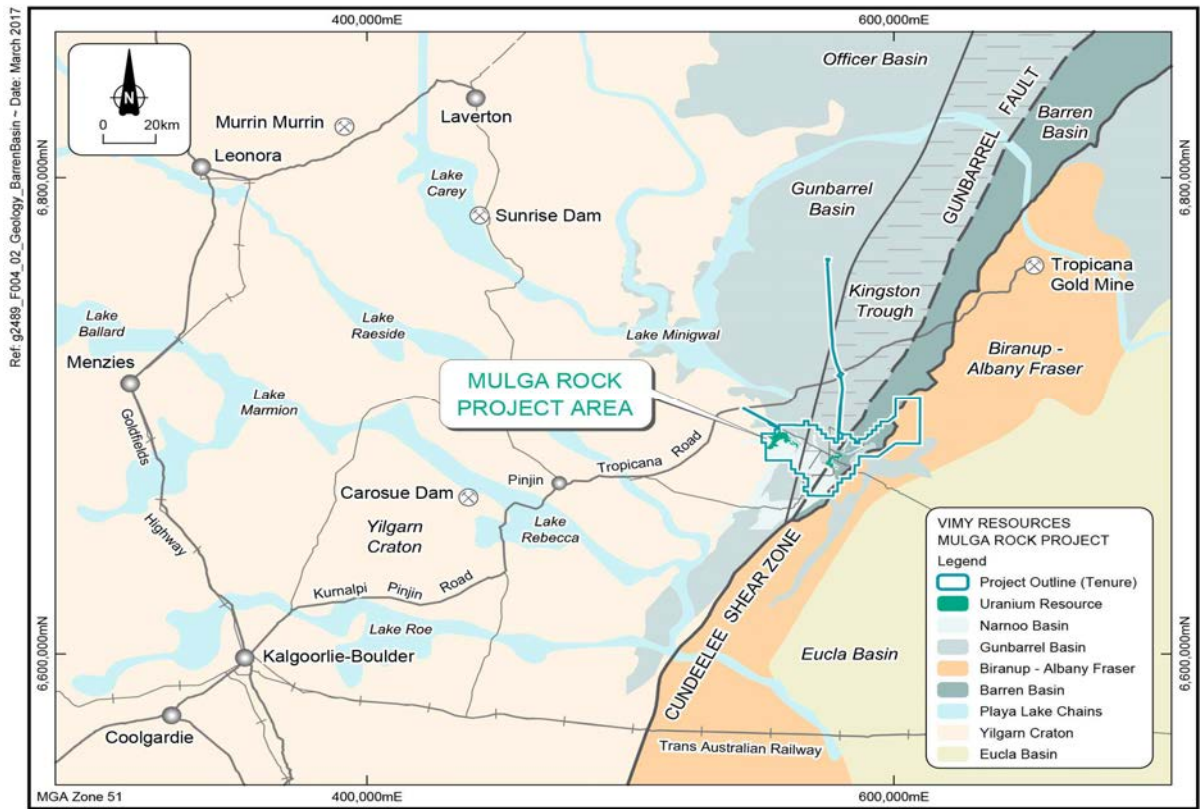


FIG. 174. Location of uranium deposits of the Mulga Rock Project (Australia) [455] (reproduced with permission).

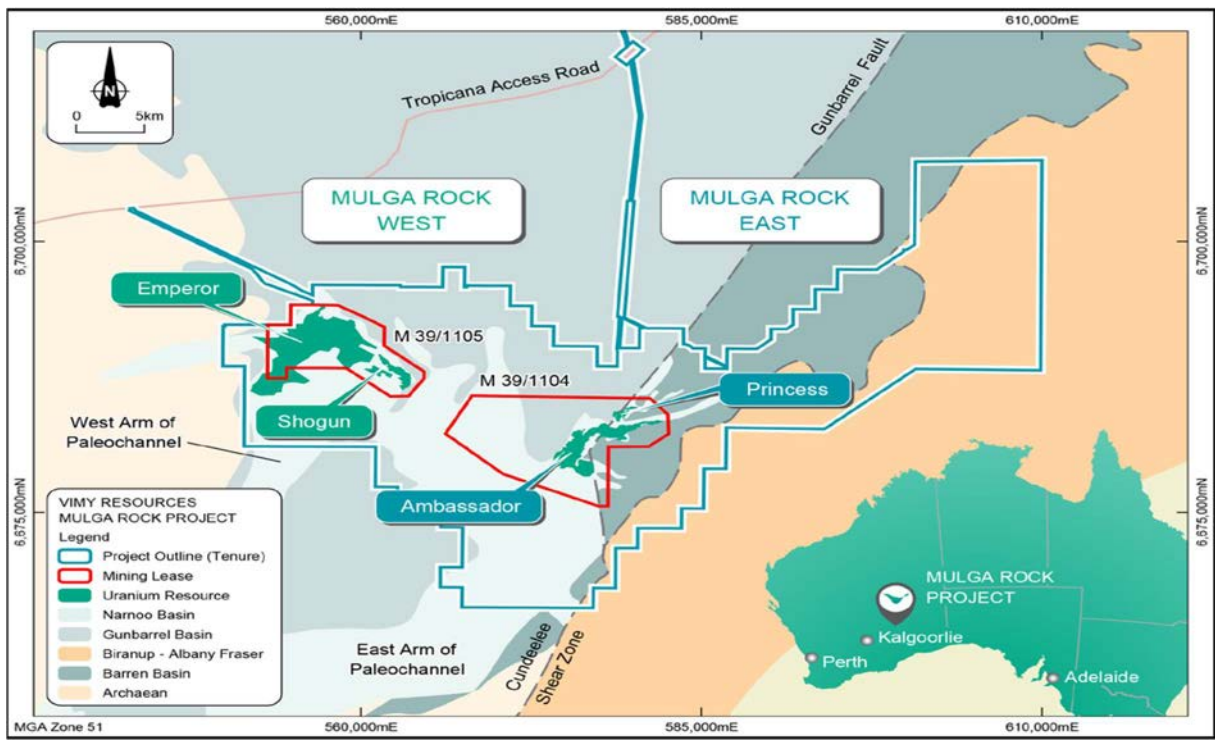


FIG. 175. EMA's lease holding showing location of the three deposits of the Mulga Rock Project [452] (reproduced with permission).

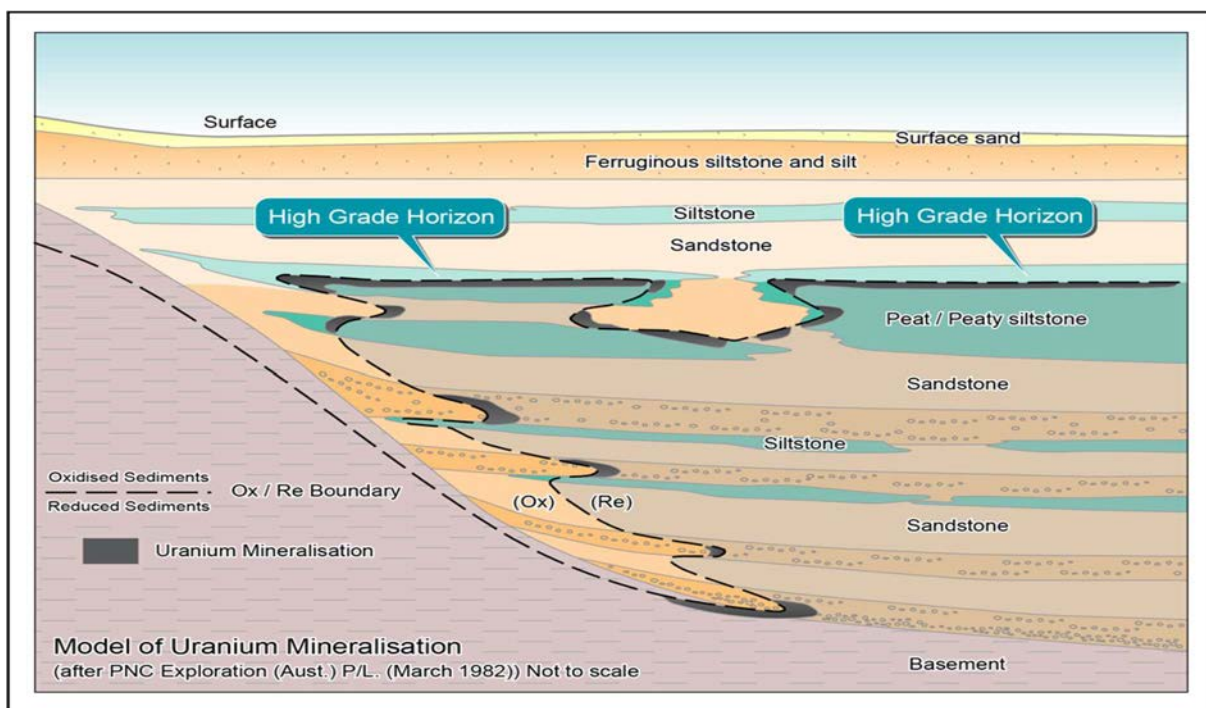


FIG. 176. Schematic geology and mineralization styles within the Narnoo sequence [455] (reproduced with permission).

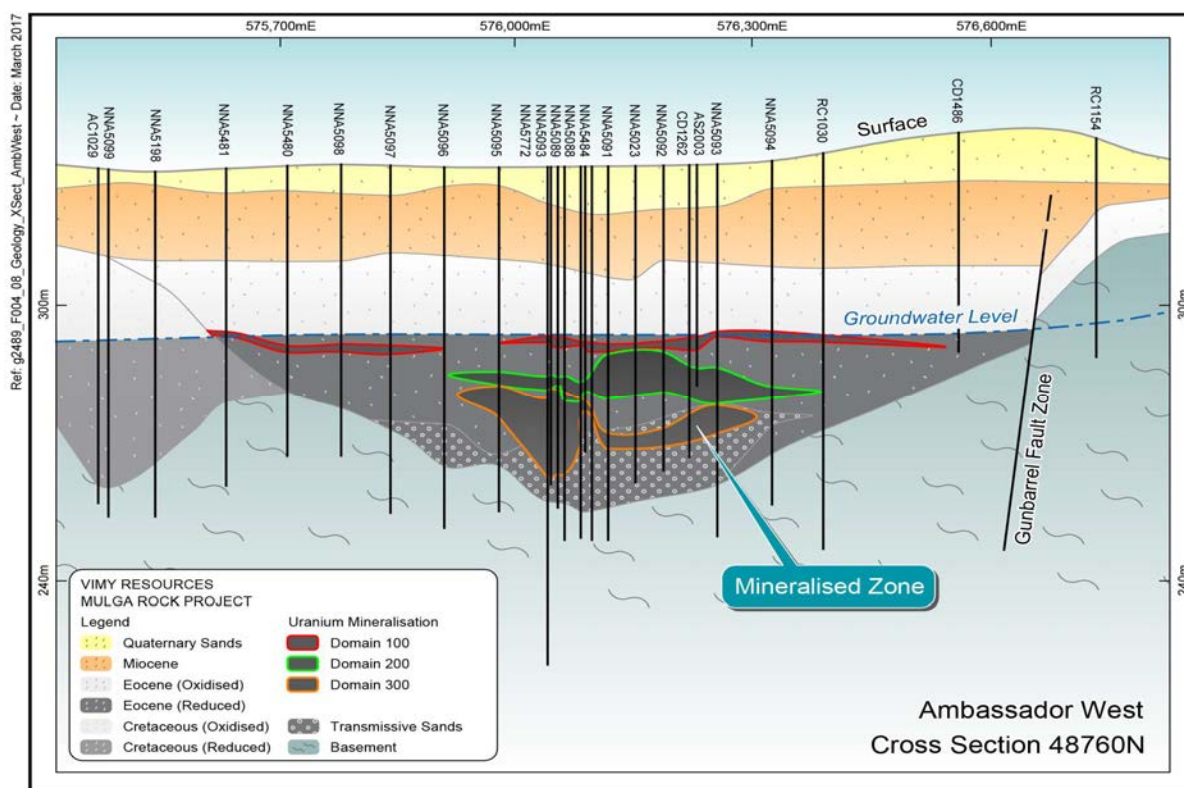


FIG. 177. Drill cross-section across the Ambassador deposit with interpreted stratigraphy [455] (reproduced with permission).

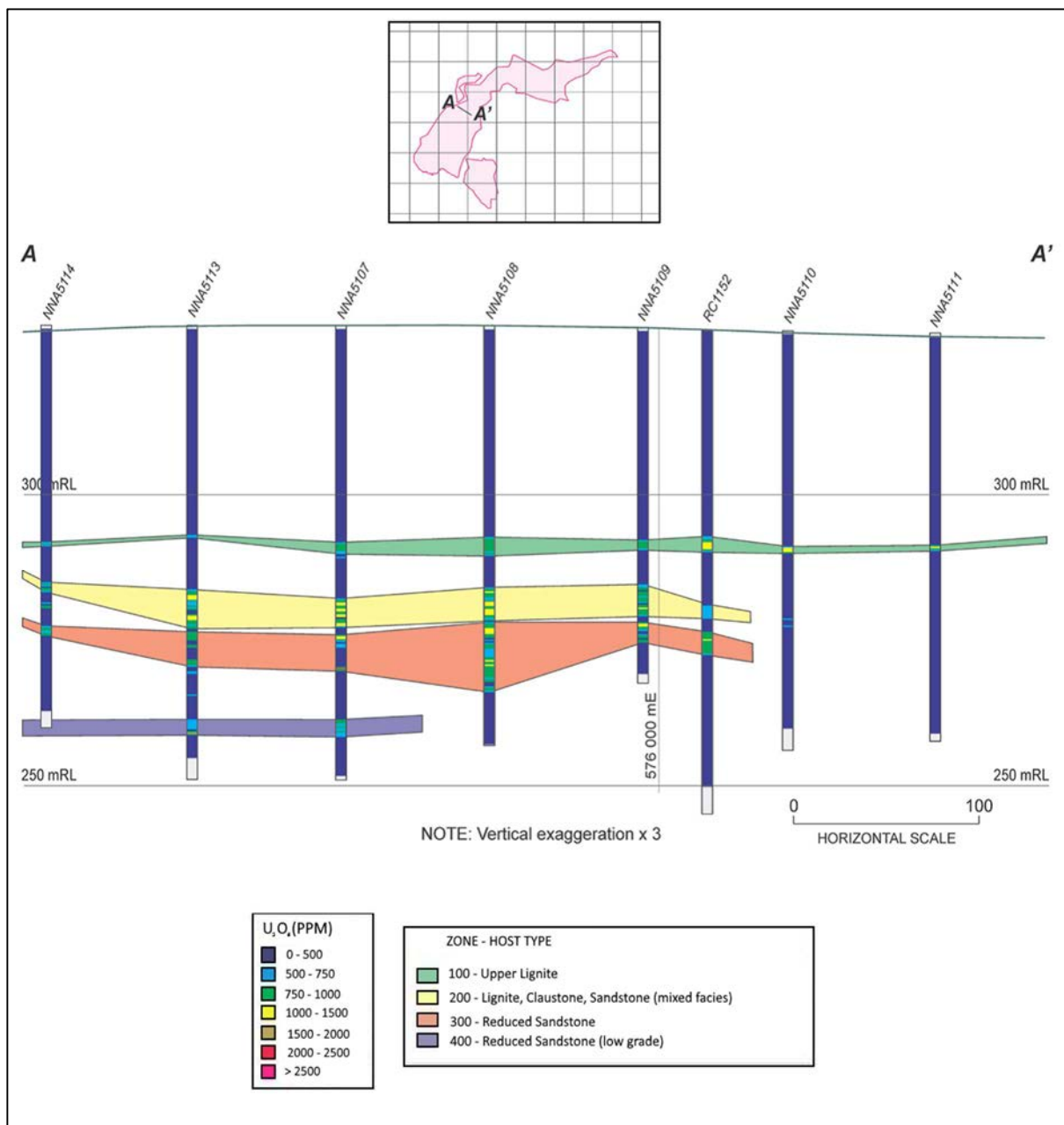


FIG. 178. Cross-section through the Ambassador deposit: interpreted mineralization along drilling fence (adapted from Ref. [455]).

### 3.13. CARBONATE DEPOSITS

#### 3.12.5. Definition

In 2015, 10 uranium deposits/districts associated with carbonate formations are recorded in the UDEPO database. They are highly variable in their size, grade and geological context (Table 37). About 10 000 tU were produced from various deposits in Kyrgyzstan and 2566 tU in the Todilto Limestone district (USA). Production has started in 2015 at the Tummalapalle deposit, India.

TABLE 37. CARBONATE DEPOSITS (as of 31 December 2015)

Deposit	Country	Resources (tU)	Grade (% U)	Status
Tummalapalle	India	90 962	0.04	Operating
Mailuu-Suu	Kyrgyzstan	10 000	0.10–0.20	Depleted
Tyuya-Muyun	Kyrgyzstan	3 750	0.05–0.10	Depleted
Todilto Limestone district	USA	2 566	0.20	Depleted
Maylisay	Kyrgyzstan	1 850	0.148	Depleted
Coneto-Buenavista	Mexico	975	0.05	Dormant
Bentou-Sanbaqi	China	650	0.10–0.20	Dormant
Shakaptar	Kyrgyzstan	650	0.05–0.10	Depleted
Pryor Mountains–Little Mountains districts	USA	650	0.20–0.50	Dormant

### 3.12.6. Geological setting

Carbonate deposits are hosted in limestone and dolostone. Three subtypes are distinguished on the basis of their structural setting, which is highly variable. Mineralization can be syngenetic stratabound or, more commonly, structure-related within karst caverns, fracture zones, faults and folds.

- (i) *Stratabound carbonate*: Only one deposit of this kind is known: Tumulappalle in India. The stratabound deposit is hosted in phosphatic dolostone and though the uranium grades are low (0.04%), the size of the deposit, with its considerable lateral and down-dip continuation, indicates that the area is likely to emerge as a major uranium province of the world;
- (ii) *Cataclastic carbonate*: Mineralization is structure-bound in organic-rich (bituminous/petroliferous) calcareous sediments. Ore zones are controlled by fracture intervals in intraformational folds and flexures (Mailuu-Suu, Kyrgyzstan; Todilto district, USA);
- (iii) *Palaeokarst*: Deposits are developed in solution collapse breccias occurring in limestone with intercalations of carbonaceous shale. Mineralization is preferentially concentrated along annular faults (Bentou/Sanbaqi, China) or may fill fractures and solution voids and impregnate the matrix of the cavern fill (Tyuya-Muyum, Kyrgyzstan; Pryor Mountains–Little Mountains district, USA).

### 3.12.7. Metallogenesis

Carbonates are typically unfavourable host rocks for uranium because of their low permeability and porosity and lack of precipitation agents such as organic material. Unusual geological circumstances associated with tectonic features are necessary to create uranium traps.

For McLemore and Chenoweth [458], uranium deposits of the Jurassic organic-rich Todilto Limestone in the Grants uranium region (USA) were deposited in a sabkha environment above the permeable Entrada Sandstone. Aeolian sediments of the transgressive Wanakak Formation produced intraformational folds locally in the soft muddy, limey, organic-rich Todilto beds before they were indurated and fractured. Uraniferous waters recharged from a highland to the south-west, percolated through the Entrada Sandstone and migrated into the Todilto Limestone by evaporative pumping. Uranium precipitated within intraformational folds and associated fractures in the limestone, wherever it encountered organic material [459, 460].

### 3.12.8. Description of selected deposits

#### 3.12.8.1. Syngenetic: The Tummalapalle deposit (India)

##### Introduction

Uranium mineralization associated with limestone is known in many parts of the world, but such mineralization generally occurs either as secondary encrustations or in association with apatite minerals. However, occurrence of discrete uranium minerals such as pitchblende and U–Ti–Si phases on a large scale in limestone or dolostone is not common. The south-western part of the Proterozoic Cuddapah Basin in India hosts uranium mineralization in a dolomitic limestone formation over a strike length of 160 km.

The mineralized dolomitic limestone horizon has been explored by drilling along a strike length of over 15 km on either side of Tummalapalle and about 2 km in the down-dip direction. In 2015, more than 90 000 tU at a grade of 0.04% U had already been established in a 15 km section of the belt. Mineral beneficiation experiments on this carbonate-hosted uranium ore have indicated 70–73% recovery of uranium by an alkali leach circuit. Although the uranium grades are low, the extensive nature of the deposit, with almost isotropic mineralization characteristics and considerable down-dip continuity, suggests that this part of the Cuddapah Basin is likely to emerge as one of the major uranium provinces of the world. The deposit also contains considerable amounts of molybdenum.

##### Geological setting

The crescent-shaped, Proterozoic Cuddapah Basin, a major geological entity in the Dharwar Craton of southern India is comprised of unmetamorphosed and unfossiliferous sediments of Palaeoproterozoic–Neoproterozoic age. The N–S trending basin covers an area of 44 500 km<sup>2</sup> and extends over a length of 450 km with a mean width of 150 km (Fig. 179) [461].

The Cuddapah Basin is characterized by quartzite–shale–limestone sequences with intermittent igneous units and has an aggregate thickness of 6–12 km. Apart from uranium, the basin is known for its diverse mineral potential, including baryte, asbestos, steatite, base metals and diamonds, as well as limestone and building stone. The Cuddapah Basin was formed by the coalescence of six smaller basins, namely the Papaghni, Chitravati, Nallamalai, Srisailam, Kurnool and Palnad sub-basins. The Papaghni Basin is of Palaeoproterozoic age while the Chitravati, Nallamalai and Srisailam sub-basins are of Mesoproterozoic age. The Kurnool and Palnad sub-basins are correlative and formed in the Neoproterozoic. The western part of the basin is undeformed, with a prominent non-conformity, whereas the eastern margin is thrust over by the crystalline basement rocks and, as a result, the Nallamalai Group in the eastern half of the basin has been subjected to folding.

The Papaghni Group forms the oldest unit of the Cuddapah Basin and the volcanic rocks associated with the sediments have been dated at 1800 Ma [462]. The Papaghni Group is comprised of a lower Gulcheru quartzite sequence and an upper Vempalle limestone sequence followed by volcanic rocks, together making a stratigraphic thickness of more than 2000 m.

The Vempalle Formation comprises shale, siltstone, sandstone and stromatolitic dolomite in the lower part and shale, chert and stromatolitic dolomite in the upper part. Uranium mineralization in this part of the basin is hosted by the impure dolomitic limestone of the Vempalle Formation. It extends from the village of Chalumpalli in the west to Maddimadugu in the east as a 160 km long belt extending along the western margin of the Cuddapah Basin. Uranium mineralization at Tummalapalle, Rachakuntapalle and Gadankipalle is found in the central part of the belt (Fig. 180) [463–466].

The mineralized carbonate is a phosphatic, siliceous, dolomitic limestone situated between the underlying massive dolomitic limestone and the overlying shale and cherty dolomitic limestone unit. Primary sedimentary structures such as mud cracks, ripple marks and stromatolites are observed in this

formation. The stromatolites include stratiform, domal and isolated oval structured varieties of *Stratifera* sp., *Collenia* sp. and *Oncolithic* sp., respectively.

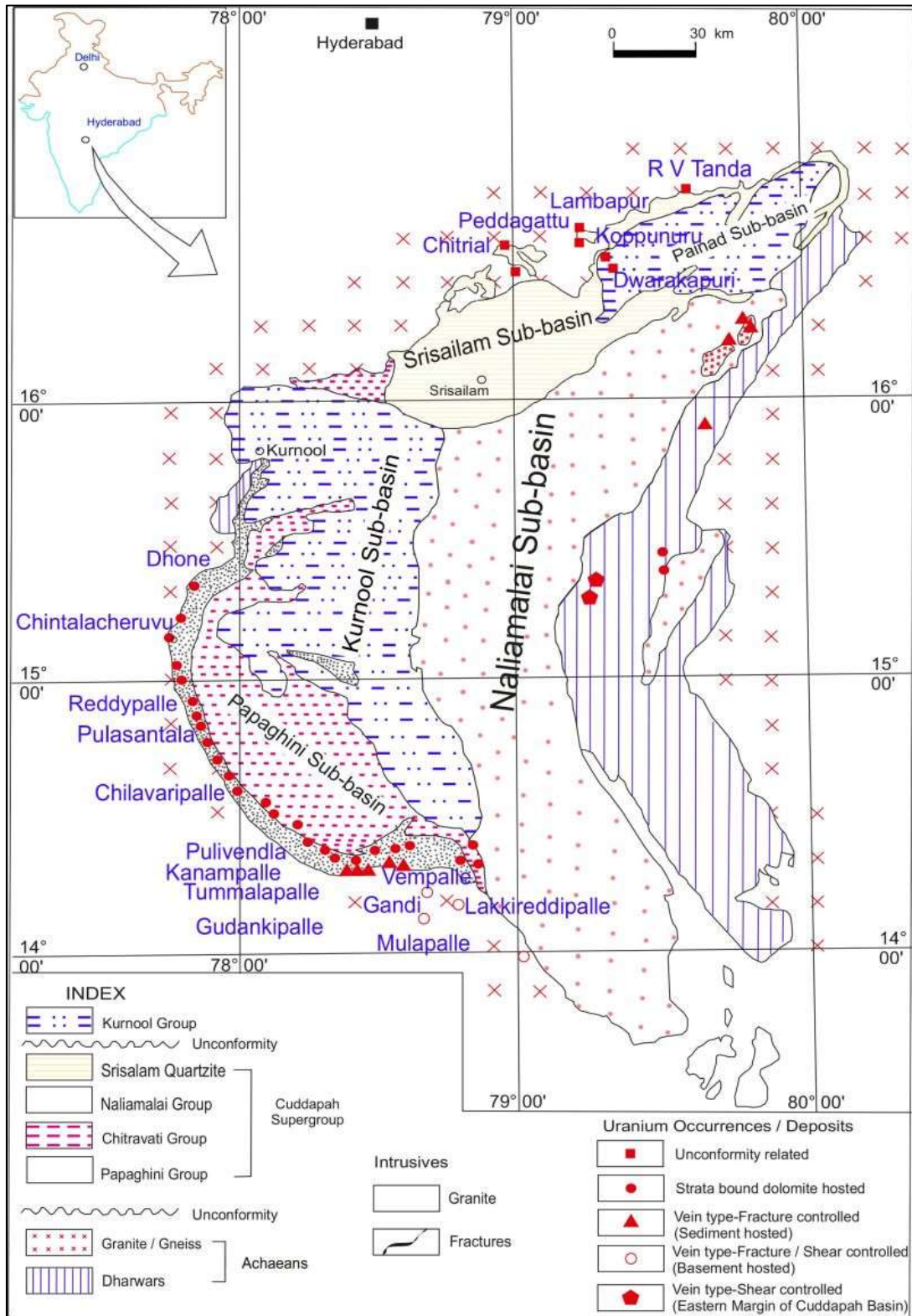


FIG. 179. Geological map of the Cuddapah Basin showing uranium deposits and occurrences. The Tummalapalle deposit is located along the southern margin of the basin.

The mineralized dolostone contains 0.025–0.25% U, with an average grade of about 0.04% U. In the majority of samples, radiometric disequilibrium is observed in favour of uranium in the range 6–100%. This has been corroborated by the ore from subsurface and drill core samples from Tummalapalle, Rachakuntapalle and Gadankipalle.

### Mineralization

The mineralized dolostone consists of 1–7 m thick, alternating bands of light to dark grey beds. The light grey beds are ultrafine and carbonate-rich whereas the medium to dark grey beds consist of coarse rhombic dolomite, ultrafine phosphate (collophane), brown organic matter, fine-grained opaque minerals and detrital quartz and feldspar, with authigenic development of dark pellets of micrite and collophane. Uranium mineralization occurs along bedding planes, carbonate–phosphate contacts, microstylolites, grain boundaries of clasts and within pelloids. The mineralization occurs in the form of ultrafine pitchblende (vanadium-bearing) in intimate association with pyrite and as disseminations in collophane-rich parts and as minor coffinite (vanadium-bearing) and U–Si–Ti phases. In addition, a small portion of the uranium is adsorbed onto collophane. The associated ore minerals include pyrite (arsenical and argentiferous), molybdenite, chalcopyrite, bornite, digenite and covellite.

### Metallogenic aspects

The uranium metallogeny of the Vempalle dolomitic limestone, and occasionally of the associated Gulcheru quartzite, has been interpreted as a polyphase genetic model involving three stages: syngenetic, diagenetic and epigenetic processes [467]. The impure nature of the dolomitic limestone appears to be one of the main controlling factors for uranium and molybdenum mineralization. The source of uranium for this deposit is likely to be the fertile basement granite at the south-western and western edges of the basin. Uranium liberated from the felsic crystalline rocks has been transported as uranyl carbonate/phosphate complexes in the shallow marine environment where the Vempalle dolomitic limestone was being deposited, as indicated by mud cracks, ripple marks, framboidal pyrite and stromatolites. A reducing environment was provided by pyrite, other sulphides and minor amounts of organic matter. Essentially, a syngenetic origin for this mineralization is postulated on the basis of field evidence such as the confinement of the mineralization to a single lithostratigraphic unit over a strike length of 160 km and with mineralization showing good continuity between drill hole intercepts (Fig. 181).

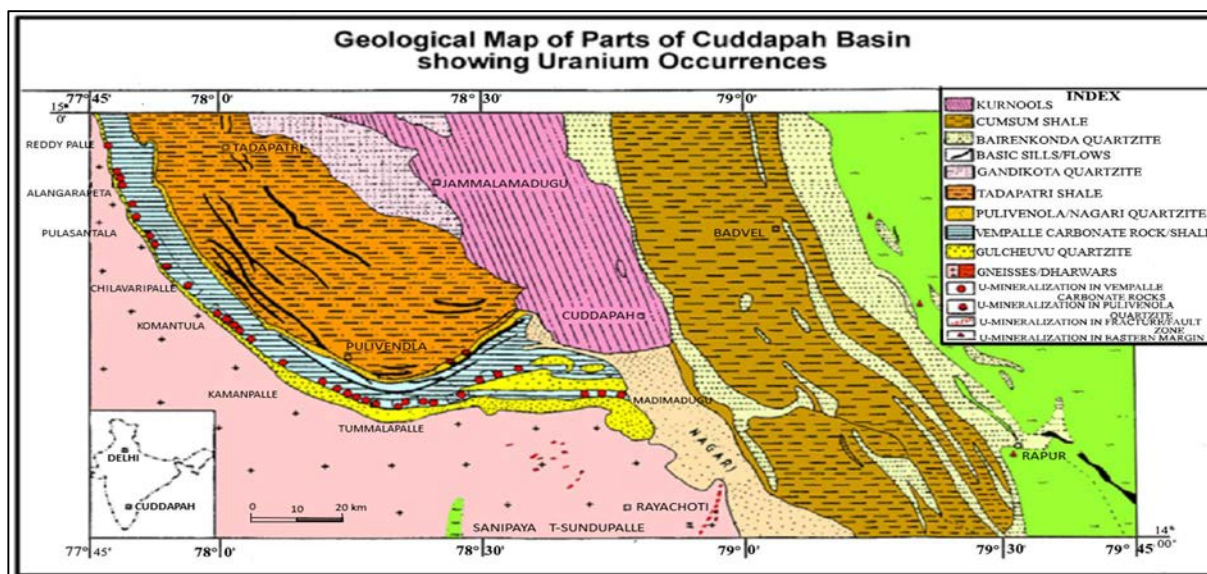


FIG. 180. Geological map of the southern part of the Cuddapah Basin showing uranium occurrences (reproduced courtesy of A. Chaki).

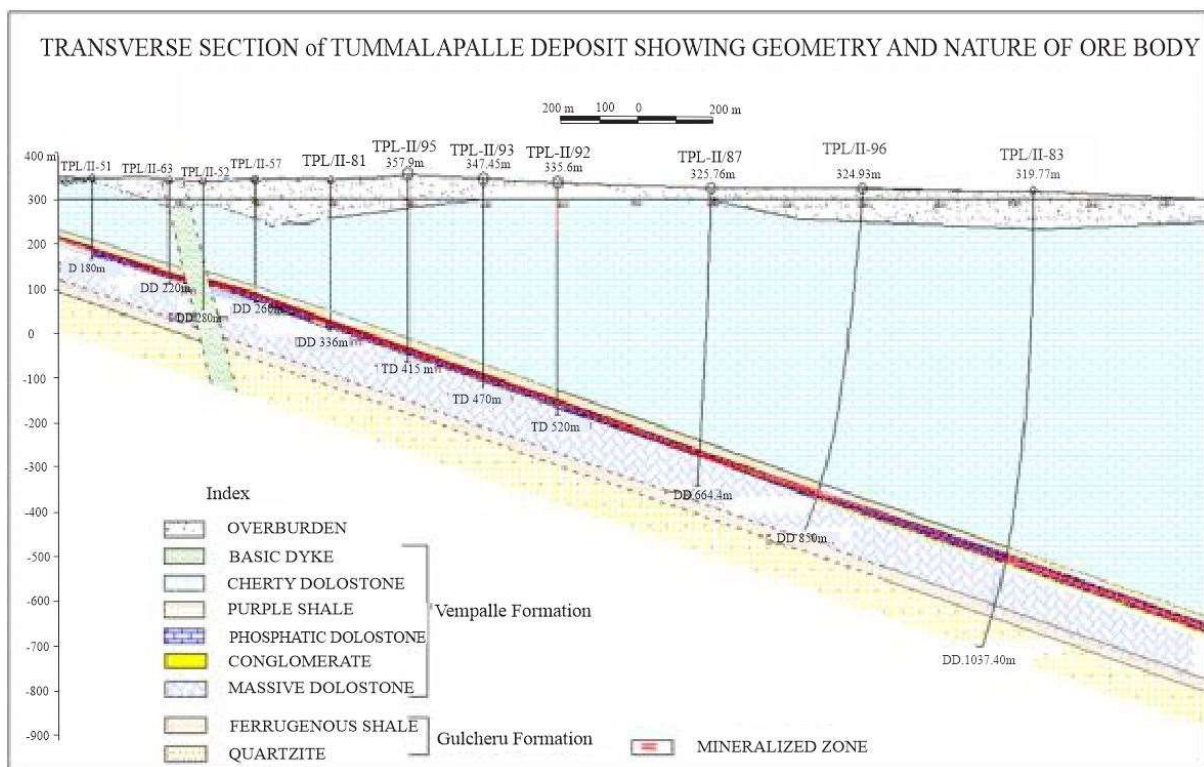


FIG. 181. Geological cross-section of the Tummalapalle deposit (reproduced courtesy of A. Chaki).

### 3.12.8.2. Bituminous–cataclastic: The Mailuu-Suu deposit (Kyrgyzstan)

#### Introduction

The depleted Mailuu-Suu deposit is located in western central Kyrgyzstan, near the north-east margin of the Fergana Valley. The deposit is hosted in fractured, petroliferous calcareous sediments and is defined as bituminous–cataclastic limestone type [18]. It produced about 10 000 tU. Ore grades ranged from 0.03% to over 0.5% U and averaged 0.11% U [468].

The Mailuu-Suu deposit consists of several discontinuous orebodies irregularly spread over a strike length of approximately 8 km. In addition to a number of smaller ore zones, approximately ten major orebodies have been identified, including the Bedre Sector in the north-western part of the deposit (Fig. 182).

#### Geological setting

A description of the Bedre sector, which contributed approximately 20% of the total Mailuu-Suu uranium production, has been provided by Roslyi [469].

Carbonate-hosted uranium mineralization is contained in Oligocene–Palaeocene bituminous/petroliferous calcareous sediments. The sediments are folded and orebodies are located on the limbs of anticlines, the crests of which are eroded. Host rocks include oolitic and dolomitic limestone, dolomite and marlstone intercalated with sandstone and gritstone.

The ore-hosting sequence is about 4–5 m thick and includes four units [18]:

- (i) *Hanging wall unit* (2.5 m thick): arenaceous–argillaceous continental sediments;
- (ii) *Upper limestone unit*: oolitic, stylolitic and detrital organic-bearing limestone;

- (iii) *Lower limestone unit* (2 m thick): argillaceous, dolomitic limestone with laminae of dolomitic marl;
- (iv) *Footwall unit*: dolomitic marl and pink arenaceous–argillaceous continental sediments.

Mineralized areas are characterized by intense structural disruption, including major faults, fractures/fissures and shear zones. A prominent, curvilinear E–W oriented, south dipping reverse fault with splay faults forms the southern boundary of the Bedre ore zone (Fig. 182). Fractures are particularly abundant in the upper limestone unit. Several fissure and shear fracture systems are distinguished. A series of NW–SE trending fracture zones extend in excess of 1000 m and change strike direction particularly along NE–SW oriented planes, which correspond to flexures of the limestone beds [18].

Alteration of ore-bearing calcareous sediments is reflected by reduction and oxidation phenomena [18]:

- (a) Pre-uranium reducing conditions of regional extent have altered red beds overlying and underlying the uranium-bearing calcareous unit to green and light grey colours, respectively, and possibly also caused pyritization of the limestone. In contrast, oxidation reflected by limonitization is the earliest alteration phenomenon within the ore-hosting carbonate unit but also overprinted locally reduced superjacent and subjacent strata.
- (b) Subsequent alteration of permeable limestone within the ore horizon includes leaching, argillization (hydromicazation) and bleaching. Iron was removed and redeposited as haematite and hydrohaematite at the margins of bleached zones. In a following stage, both limonitized and bleached rocks were recrystallized, with calcitization and minor pyritization.
- (c) Syngenetic uranium alteration is reflected by haematitization followed by pyritization. Both are associated with deposition of pitchblende and nivenite. Intense haematitization (interpreted as preceding the uranium) is found in front of the pitchblende–nivenite mineralization.
- (d) Post-uranium alteration phenomena include localized bitumenization, influx of viscous petroleum (maltha) and near surface limonitization.

#### Mineralization

The Bedre sector contains structure-bound uranium mineralization in carbonate beds in the footwall block of a reverse fault. Pitchblende, nivenite and sooty pitchblende are the principal uranium minerals. About 20% of the uranium is bound to post-uranium bitumens. The main gangue minerals are haematite and pyrite. Associated elements include As, Co, V, Mo, Ni and Pb.

Two varieties of ore assemblage are noted [18]:

- (i) An older, mottled black–pink coloured haematite–pitchblende–nivenite assemblage, which is practically free of pyrite and occurs in small lenses;
- (ii) A massive, black pyrite–pitchblende–nivenite assemblage cut by stringers of solid bitumens, which occurs within and correlates to a large extent with the outer margin of black pyritized rocks of the carbonate unit.

Uranium minerals of both assemblages occupy stylolites, sutures, microfissures and the interstices between carbonate grains, and coat voids, oolite grains and fragments of marine fossils. Microfissures and stylolites also contain greenish hydromuscovite and solid bitumens.

The host unit, up to 5 m thick, consists of altered, water- and hydrocarbon-bearing carbonate layers broken by faults and fractures. The upper 3–3.5 m contains ore zones composed of discontinuous, lenticular and roll shaped orebodies (Figs 183 and 184). Lenticular orebodies of mottled black–pink mineralization vary from <1 m to 10 m long and from a few centimetres to 0.5 m thick and extend up to 1–5 m into the wall rock. In zones of closely spaced shears, the ore lenses thicken appreciably and

merge into columnar lodes of higher grade ores. Ore lenses of this type are concentrated adjacent to shears within a 200 m long and up to 20 m wide ribbon-like ore zone.

Black pyrite–pitchblende–nivenite mineralization forms discontinuous lenses similar to those of mottled black–pink ore, but also crescent-shaped bodies. The ore lodes together form an irregular, winding band about 500 m long and up to 50 m wide controlled by a major fault, flexures of strata and attitude changes of shears. Large lenticular bodies are directly associated with an E–W fault along which they persist over a distance of approximately 200 m [18].

Roll type orebodies typically occur in oxidized zones. Rolls vary from a few metres to about 10 m wide, perpendicular to the strike of the strata and up to 3 m thick at the nose, while tails range from several centimetres to approximately 1 m thick. The larger, upper segment of the rolls is developed along continuous stylolites in beds near the top of the carbonate unit, while the commonly poorly developed lower part is hosted in less permeable dolomitic, argillaceous shale beds [18].

#### Metallogenic aspects

The origin of the uraniferous, bituminous limestone deposits at Mailuu-Suu is attributed to exogenic–epigenetic processes that were active in the Tertiary, with the principal ore forming stage occurring during the Miocene. Felsic volcanic rocks in the adjacent Karamazar region are favoured as the potential uranium source [18]. As proposed by Roslyi [469], the sequence of events involved in the metallogenesis of the Mailuu-Suu orebodies includes a number of distinct features.

Several alteration events preceded the main uranium stage. Alternating oxidation and reduction processes reflected by limonitization, haematitization, pyritization and hydromicazation are typical for this period. Subsequent mineralization stages include the deposition of a haematite–pitchblende–nivenite assemblage (mottled black–pink ore, practically free of pyrite) that was superimposed on recrystallized and limonitized host rocks. Infiltrating solutions caused intense haematitization in front of the developing pitchblende–nivenite mineralization. During a second, supposedly transitional mineralizing event, a suite of elements, including As, Co, Cr, Fe, Mo, Ni, Pb, S, U and V, were introduced and a pyrite–pitchblende–nivenite assemblage (black ore) was deposited. Deposition of this ore phase occurred in a band bordering pyritized limestone and overprinted all previous alteration types as well as the mottled, black–pink ore [18].

Post-ore block faulting during the Pliocene and Quaternary was associated with bitumenization of limestone as a result of oil infiltration along faults. This oil infiltration and related bitumenization is not considered essential for ore formation, but probably caused the discontinuation of the ore forming process and may have generated a geochemical barrier preventing the dissolution of the older uranium mineralization. A late, obviously recent ingress of viscous petroleum (maltha) formed a narrow maltha belt subparallel to the major faults. Current surface related oxidation is indicated by iron hydroxides and U–V micas in near surface fractures in limestone.

Felsic volcanic rocks and possibly granites of the Chatkal and Fergana Ranges located to the north-west and north of the deposit are considered the most likely sources of uranium and other elements [18].

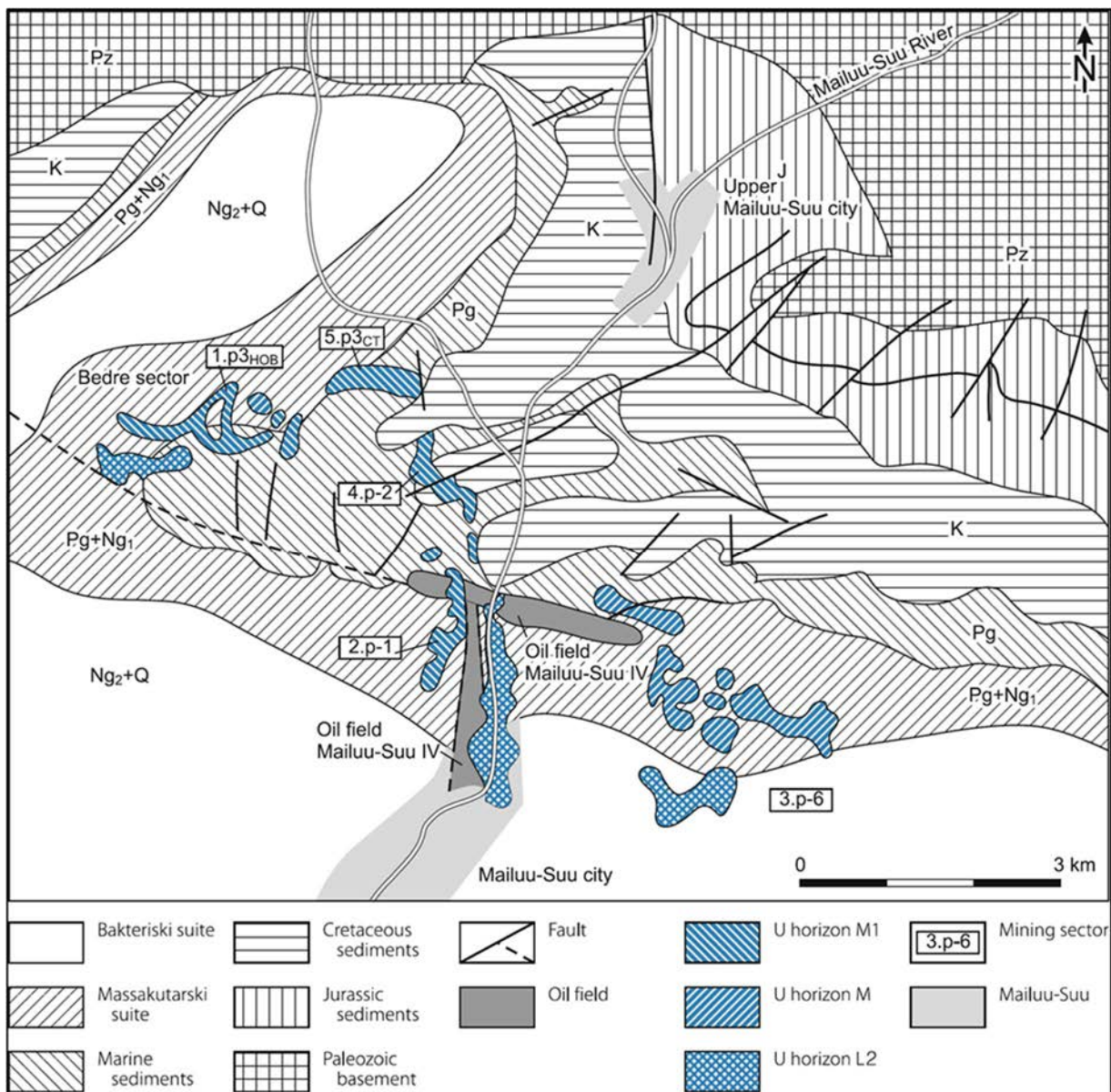


FIG. 182. Schematic geological map showing uranium mineralized horizons and sectors of the Mailuu-Suu deposit, Eastern Karamazar region [18] (reproduced with permission).

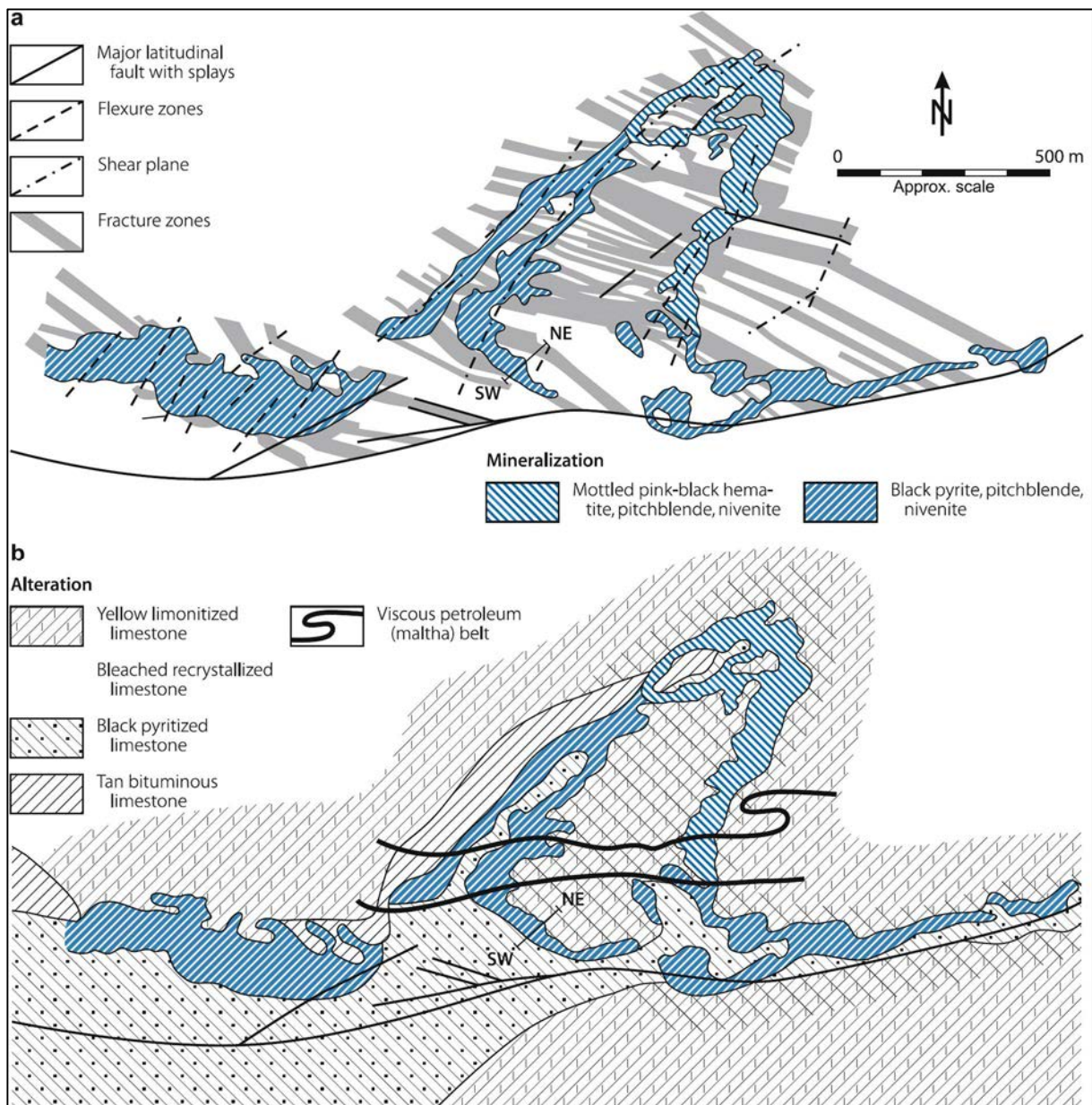


FIG. 183. Mailuu-Suu, Bedre sector: (a) structural pattern and distribution of mineral assemblages in the upper uranium mineralized carbonatic horizon, (b) associated wall rock alteration styles [18] (reproduced with permission).

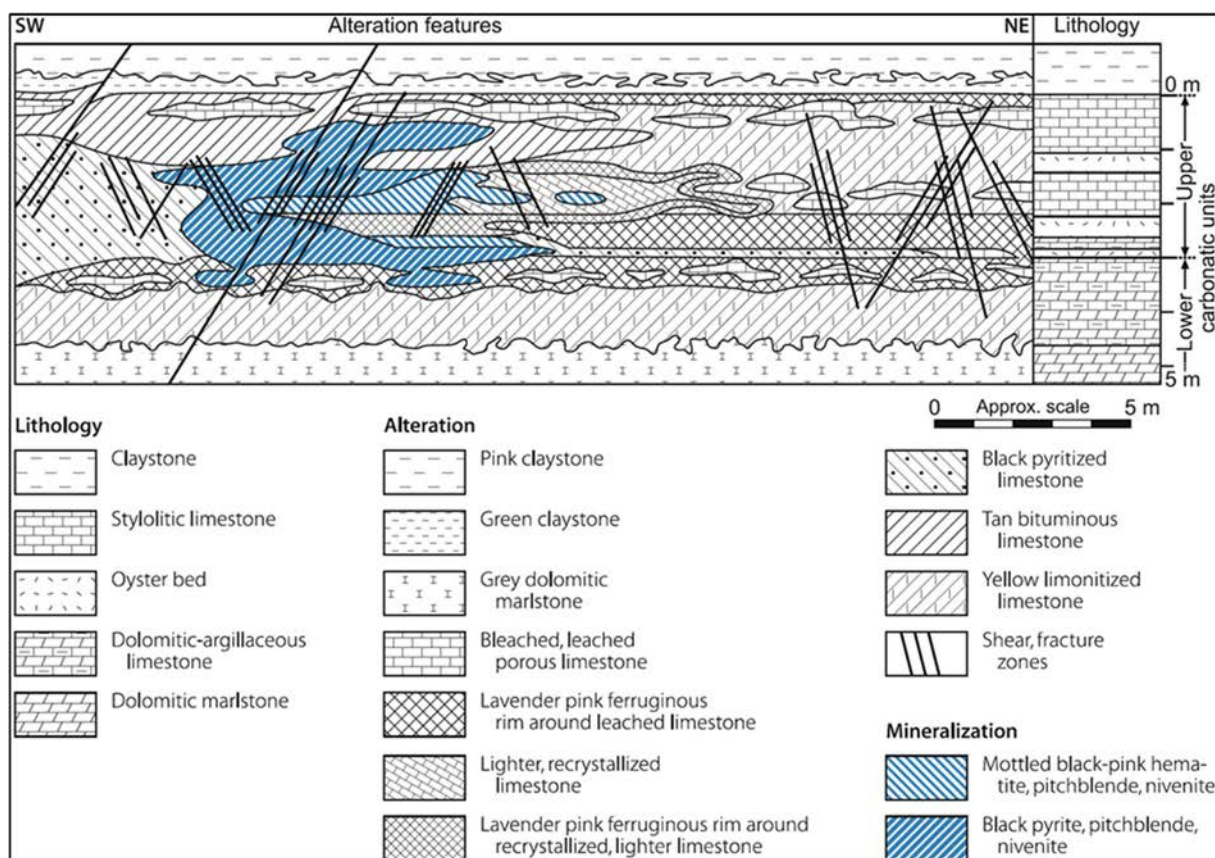


FIG. 184. Mailuu-Suu, Bedre sector, Eastern Karamazar region. A SW–NE section across a mineralized lode illustrating the distribution of the principal ore assemblages and related alteration features (left) combined with a stratigraphic column (right) [18] (reproduced with permission).

### 3.12.8.3. Palaeokarst: The Sanbaqi deposit (China)

#### Introduction

Discovered in 1973, Sanbaqi, also called Bentou or Benti, is located in Guiyang, in the south-east of Hunan Province. It is the largest of a group of six palaeokarst-hosted deposits in Lower Carboniferous limestone and represents an economically important, new type of uranium deposit for China.

The deposit was discovered in 1973 by airborne radiometric survey and subsequent ground follow-up of anomalies. It was explored over the period 1973–1991 [470]. Resources are estimated to be between 1500 and 5000 tU at a grade of 0.1–0.3% U.

#### Geological setting

Bentou is situated in the central south-western part of the South Hunan Synclinorium, which contains Upper Palaeozoic, mainly calcareous sediments with a thickness of 2500 m grouped into the lithostratigraphic units presented in Fig. 185. The Palaeozoic sediments were mildly folded (but not metamorphosed) by Indosinian tectonism that affected the region in the Late Triassic–Early Jurassic. Downfaulted Tertiary–Cretaceous basins occur in the vicinity of the deposit and are filled with continental sediments. Quaternary gravel, sand and clay form a veneer on top of the older strata. Several NW–SE and NE–SW trending high angle faults and fracture zones transect the site of the deposit. There are no igneous intrusions or extrusions at, or in the vicinity of, the deposit [18].

The location and formation of the orebodies are controlled by karst related solution collapse breccia cones or pipes in the Lower Carboniferous Shidengzi Formation. The host rock is an impure limestone with intercalations of marl and carbonaceous shale. The collapse breccias persist from the palaeosurface to depths of between 100 and 200 m and are filled with fragments of dolomite and sandstone from the Zhimenjiao and Ceshui Formations, embedded in a fine-grained matrix. The collapse fill is barren of ore. The Shingdengzi Formation rests conformably on the shale and dolomitic limestone of the Lower Carboniferous Yanguanji Formation [18].

### Mineralization

Orebodies occur at shallow depths along annular faults around the collapse structures (Fig. 185). Uranium mineralization is preferentially concentrated at intersections of carbonaceous marly micrite and fossiliferous micrite with intercalated silty micrite and biosparite. The marly beds are dark grey to black, rich in pyrite and contain 7–16 ppm U and 1.5–2.1wt% organic carbon.

Wall rock alteration is generally weak, extending for 0.1–1 cm from pitchblende veins and related fractures. Alteration products include authigenic quartz, hydromuscovite, chlorite, carbonates and pyrite as well as bleaching and yellow–green staining due to dumortieritization. Alteration consists of substantial additions of silica, iron and potassium, and a slight decrease in organic carbon [18].

Mineralization consists chiefly of pitchblende and uranium adsorbed onto carbonaceous matter, colloform pyrite and clay minerals. Associated minerals include pre-ore millerite, molybdenite, niccolite, pentlandite, ullmannite, dolomite and chlorite; pre- to syn-ore pyrite, goethite, haematite, chalcopyrite, galena and sphalerite, as well as dolomite, chlorite, quartz, clay minerals and rare fluorite; and post-ore antimonite. Calcite is ubiquitous. Uranium–lead dating of pitchblende yields ages of 135–119 Ma [18].

Fracture fillings and veinlets of pitchblende are typically 0.1–5 mm wide. Disseminated grains of pitchblende are 0.01–0.5 mm in diameter. A small proportion of uranium was adsorbed by the clay and organic carbon in the matrix. There are numerous submicroscopic pitchblende grains, less than 1 to 5  $\mu\text{m}$  in diameter, distributed along microfractures throughout the carbonaceous marl matrix [470].

The organic matter intimately associated with the uranium mineralization is chiefly of marine origin, with only a minor terrestrial component. The organic matter is of sapropelitic-humic origin. There are no fundamental differences between the genetic type of organic matter in background samples and samples spatially associated with uranium mineralization. The terrestrial organic matter in the ores may have been brought into the underground palaeo-caverns by palaeosurface waterflows during the palaeokarst episodes (Jurassic–Cretaceous age) when there was a dense forest in southern China [471].

Orebodies vary in morphology from tabular, lenticular, cone shaped, nested to irregular configurations with dimensions ranging from 10 m to several tens of metres in length and width, and several metres to tens of metres in thickness. Ore lodes are internally structured by networks of openings filled with fragments of wall rock and carbonaceous argillaceous matrix. Pitchblende occurs preferentially along fractures in solution voids and cavities, interstitially in granular material, and as partial replacement of the argillaceous matrix.

### Metallogenetic aspects

Min et al. [470] propose the following model for the formation of the Sanbaqi deposit. A palaeokarst related solution network controls the location and formation of the ore lodes. At least four episodes of karst development are identified: Late Triassic–Early Jurassic, Late Jurassic–Early Cretaceous, Cretaceous–Tertiary and Recent. The main uranium mineralizing phase was the second karst episode. This is supported by isotopic ages of two pitchblende samples at 134 and 129 Ma. These ages correlate with Yanshanian movements in south China that are thought to have opened or reactivated the annular faults during Late Jurassic–Cretaceous time. The new fractures provided pathways for solutions that

generated irregular solution cavities throughout the brecciated limestone. These openings were filled with clastic material, carbonaceous clay, drip stones, pitchblende and associated minerals. Mineralization in these reactivated fault breccias is also spatially related to the younger faults, referred to as 'ore-bearing tectonic belts' [18].

Mineralogical, fluid inclusion and isotopic data suggest that repeated pulses of hydrothermal activity generated the mineralization. Temperatures of ore formation lie in the range 150–181°C, as deduced from homogenization temperatures of fluid inclusions in ore stage calcite that range from 160° to 181°C and in post-ore calcite from 150° to 160°C. Data are interpreted to indicate a mixing of meteoric and metamorphic solutions. Salinities of fluid inclusions in ore stage calcite are distinctly different from those of calcite from unmineralized, brecciated limestone of the Shidengzi Formation.

Sulphur isotope compositions of vein pyrite in the ore range from 1 to -15.30‰  $\delta^{34}\text{S}$  and from 1 to -15.60‰  $\delta^{34}\text{S}$  for finely disseminated diagenetic pyrite in host rocks. This suggests that diagenetic pyrite of biogenetic origin was the most probable source of sulphur in the mineralizing fluids [18].

Redistribution of earlier formed ore minerals in an open system added to the complexity of the paragenetic sequence. Isotopic data, including U–Pb dating of pitchblende, suggest that younger episodes of mineralization were related to the later karst events during late Yanshanian tectonism in Cretaceous–Tertiary time and more recently [18].

The organic matter had both direct and indirect roles in the preconcentration of uranium and other ore forming elements in the source rocks and in palaeo-cavern fillings, as well as in subsequent precipitation of primary uranium minerals in the ores [466]. Palaeokarstification by groundwater played an important role in the localization and formation of the deposits and provided a channel for the mineralizing solutions and favourable sites for ore deposition. It also created protore containing as much as 200–600 ppm U by adsorption and reduction of uranium by organic matter and clays, which were accumulated in some parts of the extensive solution breccia along faults and in reworked breccias formed by repeated episodes of karstification [471]. With respect to potential sources of uranium and associated metals, Min et al. [470] favour carbonaceous shales of the Lower Carboniferous Shidengzi and Yanguanji Formations with Clarke grades of up to 16 ppm U.

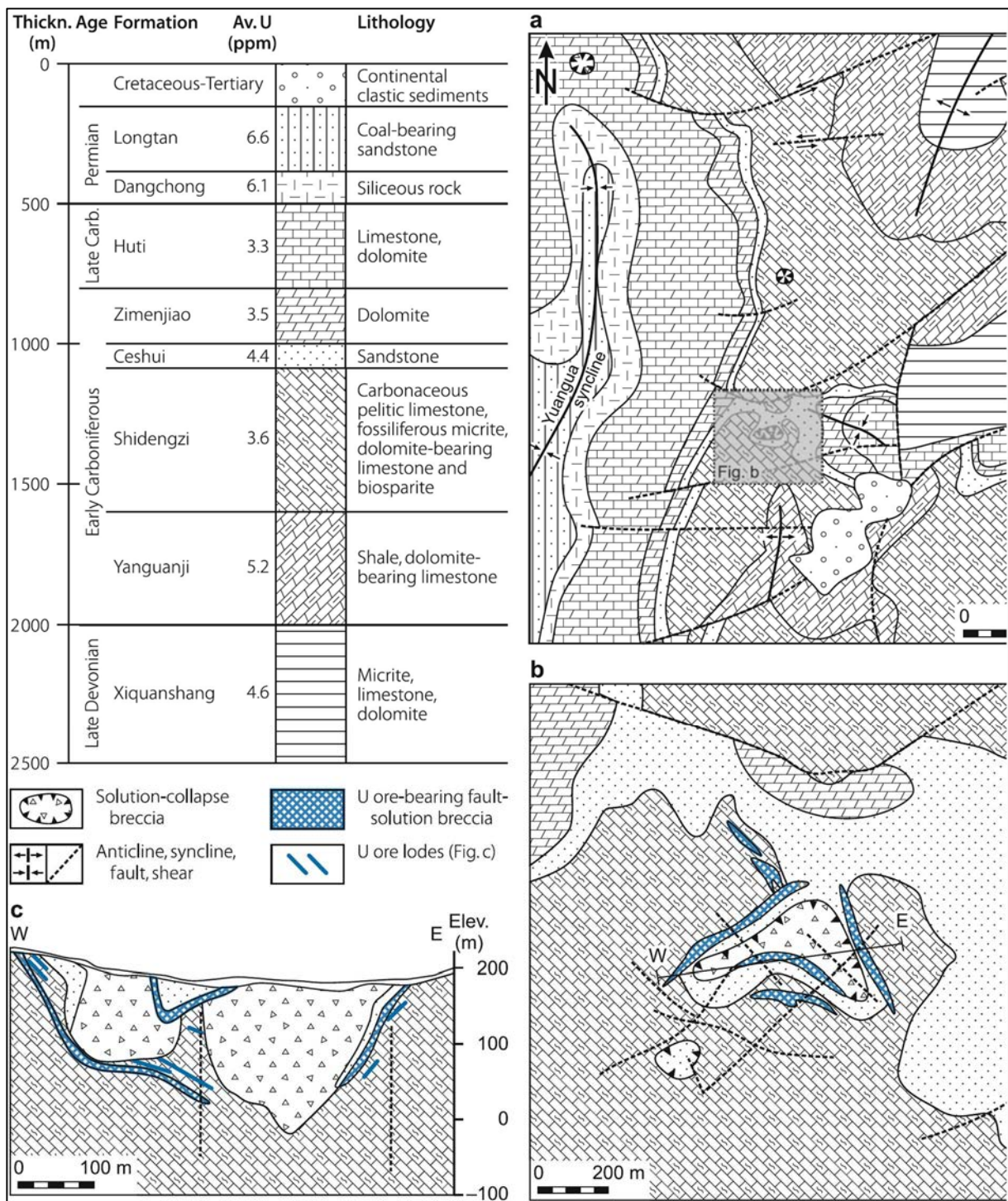


FIG. 185. Sanbaqi deposit: (a) and (b) geological maps exhibiting the lithostratigraphic and geotectonic setting of the palaeokarst uranium deposit in Carboniferous sediments; (c) W-E cross-section across fault-solution breccia bodies and related peripheral annular structures that control uranium mineralization [18] (reproduced with permission).

### 3.14. PHOSPHATE DEPOSITS

#### 3.12.9. Definition

The largest phosphate deposits consist of marine phosphorite of continental shelf origin containing synsedimentary stratiform, disseminated uranium in fine-grained apatite. Phosphorites contain very large uranium resources, albeit at a very low grade (50–200 ppm U). World uranium resources in phosphorites are estimated at 15–20 million tonnes. Examples of large phosphorite deposits include districts in Florida and the Phosphoria Formation (USA) and the Gantour, Meskala and Oulad Abdoum Basins (Morocco).

Other types of phosphorite deposit consist of organic phosphate, including argillaceous marine sediments enriched in fish remains that are uraniferous (Melovoye, Kazakhstan) and metamorphosed phosphorites, such as those occurring in the Tåsjö district (Sweden) (Table 38). Also, of particular interest because of their uniqueness, are the deposits of the Bakouma district (Central African Republic), which are uraniferous continental phosphate deposits. Rare biogenic phosphate deposits (guano) have also been described, such as the Minjingu deposit in the United Republic of Tanzania which has a high uranium content (400–1100 ppm U).

Large phosphate resources of intrusive magmatic origin are also present in peralkaline complexes and carbonatites. These occur as sheet and lenticular deposits of complex apatite ores associated with nepheline syenites and carbonatite deposits related to ultrabasic alkaline masses with complex apatite ores in the form of stocks and stockworks (refer to section on intrusive plutonic deposits).

On average, phosphates of sedimentary origin have higher concentrations of uranium (100–150 ppm U) and lower concentrations of thorium (20–35 ppm Th), whereas phosphates of magmatic or metamorphic origin have higher thorium (40–120 ppm Th) and lower uranium (25–35 ppm U).

Uranium has been recovered in the USA, in Belgium and in Israel as a by-product of phosphate production. In Florida, about 17 275 tU were produced between 1978 and 2000 from eight production centres.

The US Geological Survey dataset of world phosphate mines, deposits and occurrences [472] lists 1635 deposits, most of these marine phosphorites. As of 2015, only 57 phosphate deposits were listed in the UDEPO database, suggesting that uranium resources in phosphorites could be much more significant than previously thought.

TABLE 38. PRINCIPAL PHOSPHATE DEPOSITS/DISTRICTS (as of 31 December 2015)

Deposit	Country	Resource (tU)	Grade (% U)	Status
Phosphoria Formation	USA	5 000 000	0.006–0.020	Dormant
Oulad Abdoun Basin	Morocco	3 220 000	0.012	Dormant
Meskala Basin	Morocco	2 043 000	0.010	Dormant
Gantour Basin	Morocco	1 206 000	0.015	Dormant
East Florida	USA	270 000	0.010	Dormant
Swab	Iraq	245 000	0.007	Dormant
Central Florida	USA	225 000	0.010	Dormant
Dwaima	Iraq	193 000	0.007	Dormant
North-east Florida	USA	180 000	0.010	Dormant
Marbat	Iraq	148 000	0.007	Dormant
South Florida	USA	120 000	0.010	Dormant
Tebessa district	Algeria	120 000	0.006	Dormant
Nile Valley district	Egypt	118 500	0.007	Dormant
Uum Wu'al	Saudi Arabia	112 500	0.010	Dormant
North Florida	USA	90 000	0.010	Dormant
Shidiya Eshidia	Jordan	83 000	0.007	Exploration
Abu Tartur	Egypt	60 000	0.01–0.05	Dormant

### 3.12.10. Geological setting

In 2011, world phosphate resources were estimated to range between 65 [473] and 290 [474] billion tonnes. The distribution of resources is irregular: Morocco (46%), China (18%), USA (9%), South Africa 6.5%), Jordan (4.5%) and the Russian Federation (2%).

Phosphorites range in age from Palaeoproterozoic to Recent. The major period of phosphogenesis dated from about 800 Ma to the present. The principal phosphorite provinces are:

- (a) The Tertiary belt running W–E, from North Africa (Morocco, Algeria, Tunisia, Libya and Egypt) to the Middle East (Israel, Jordan, Syrian Arab Republic and Iraq);
- (b) The Tertiary deposits occurring along the Atlantic coasts of Africa (Morocco, Senegal, Togo and Nigeria) and the Americas (USA, Mexico, Brazil);
- (c) The Tertiary organic deposits from the Caspian Sea (Russian Federation, Kazakhstan);
- (d) The Permian Phosphoria Basin in the western USA;
- (e) The Proterozoic and Lower Palaeozoic phosphate basins of Australia, China and India.

Dahlkamp [18] distinguishes two main types of phosphorite deposits: (i) uraniferous organic phosphorite deposits (Mangyshlak type, Kazakhstan), and (ii) uraniferous minerochemical phosphorite deposits (Phosphoria Formation and Land Pebble types, USA).

Organic phosphorite deposits correspond to detritus from phosphatized fish remains in clay beds enriched in fish bones, fish scales and pyrite and melnicovite concretions. The mineralized beds are intercalated with a dark clay bed and occur in shallow marine, low energy Tertiary basins located in the northern Caspian Sea region. In Kazakhstan, resources are of the order of 70 000 tU at low grade (0.02–0.06% U) with associated REE and Sc. Further north, in the Ergeninsky region of the Russian

Federation, about 12 deposits are known with resources of the order of 60 000 tU and grades of 0.03–0.10% U.

Minerochemical phosphorite deposits consist of syndimentary stratiform disseminated uranium in marine phosphorite of continental shelf origin. The uranium is bound to cryptocrystalline fluor-carbonate apatite. These deposits represent very large uranium resources but at very low grade (20–300 ppm U) and are considered as unconventional uranium resources. The principal deposits of this type are in Morocco (6.5 Mt, 60–150 ppm U) and the USA in Florida (1.0 Mt, 80–120 ppm U) and in the Phosphoria Formation in Idaho (5 Mt, 60–200 ppm U). These deposits extend over large areas and exhibit a fairly uniform uranium distribution throughout any given bed.

Dahlkamp [18] recognizes two types of minerochemical uraniferous phosphorite (Fig. 186), bedded phosphorites (Phosphoria Formation type and Morocco) and Land Pebble type phosphates (Florida):

- (i) Bedded phosphorites consist of phosphatic shales with oolitic, pisolitic, pelletal and laminated textures interbedded with fine-grained passive margin facies such as black shale, mudstone and chert;
- (ii) Land pebble phosphates are composed of uranium enriched apatite pebbles within nodular phosphorite beds interbedded with fine- to medium-grained, shallow marine facies (sand and clay) and carbonate beds. They formed by local reworking and leaching of nodular phosphorites leading to secondary uranium enrichment in the pebbles.

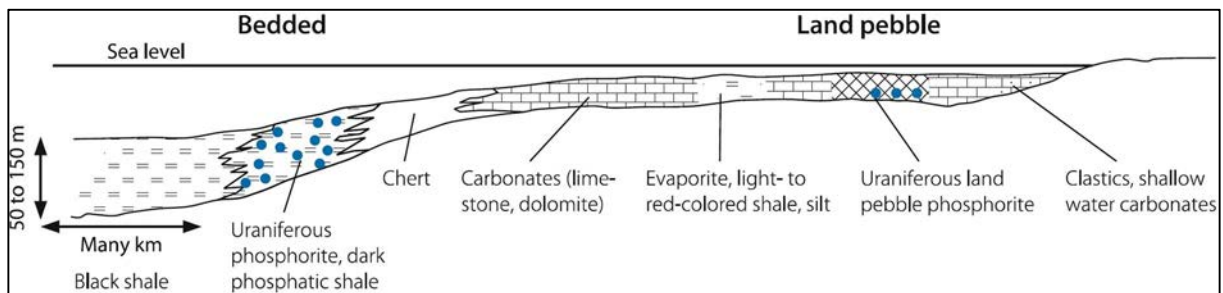


FIG. 186. Uraniferous minerochemical phosphorite deposits [18] (reproduced with permission).

The principal uranium-bearing mineral is cryptocrystalline fluor-carbonate apatite. There is a positive correlation between U and P when the concentration of both elements is relatively high. There is no ore related alteration other than weathering which can increase the grades.

In the Tåsjö district (Sweden), mineralization is confined in the Lower Ordovician Lycophoria Schist, a regionally metamorphosed phosphatic, calcareous sandstone with subordinate siltstone and shale, and lesser phosphorite concentrations. Rock constituents comprise varying quantities of carbonate (siderite), glauconite, phosphatic nodules (apatite) and quartz, in addition to organic matter and pyrite. Thin layers of massive phosphate occur locally in the basal part of the Lycophoria Schist, which varies in thickness in the range 0.5–10 m, with the greater intervals caused by structural thickening. Uranium and REE in the Lycophoria Schist are hosted by phosphatic intervals, with contents exceeding 13.8% P<sub>2</sub>O<sub>5</sub>, with lesser amounts present in less phosphatic lithologies. Brown–black carbonate–fluor–apatite is the principal uranium-bearing mineral. It constitutes 9–20% of the Lycophoria Schist and grades vary in the range 0.025–0.06% U and 0.11–0.24% REE [475].

Phosphorite occurrences of Palaeoproterozoic age have been recognized in various parts of the world including those in Michigan (USA), northern Australia, India and Finland. Deposits in Minnesota are especially interesting owing to their high uranium content but low metamorphic grade. These

occurrences contain 0.025–0.085% U and locally as much as 0.157% U. The uranium is closely associated with finely crystalline apatite. Uranium has also been involved in several episodes of remobilization and redeposition. These deposits are important as possible sources for epigenetic uranium deposits that may occur in Minnesota [476].

### 3.12.11. Metallogenesis

Only phosphates of shallow marine origin contain appreciable amounts of uranium. Uranium accumulation is interpreted as being due to syndimentary deposition of uranium from seawater and incorporation into phosphate minerals. Two favourable environments of sedimentation are recognized [16]:

- (i) Outer or distal shelf margin, where thick layers of bedded phosphorite developed within a pile of very fine-grained passive margin sediments, including black shale, carbonaceous mudstone, cherts beds and only minor carbonates (Phosphoria Formation, Idaho). The principal U–P mineral is cryptocrystalline fluor-carbonate apatite. Uranium (60–200 ppm) is considered to have been syngenetically incorporated into the apatite lattice by substitution for  $\text{Ca}^{2+}$  ions;
- (ii) Shallow marine, nearshore platform represented by lower grade (20–80 ppm U) phosphatic and nodular phosphorites. Fine- to medium-grained clastic sediments (clay, sand and glauconite) and shallow water carbonates have precipitated contemporaneously with phosphate.

The Land Pebble phosphorites (Florida) contain pebble and sand-sized grains of fluor-carbonate apatite enriched with up to 500 ppm U (locally higher). The enrichment is attributed to reworking and re-exposure of the apatite particles to uranium-bearing seawater during repeated marine transgressions.

### 3.12.12. Description of selected deposits

#### 3.12.12.1. *Organic phosphorous: deposits of the Precaspian region (Kazakhstan)*

##### Introduction

The Precaspian uranium region is located at the north-eastern margin of the Caspian Sea. Five partially mined deposits (Melovoye, Tasmurunskoye, Taybagarskoye, Tomakskoye and Sadyrnynskoye) have been delineated within the Karagiin orefield. Exploitation was by open pit methods and a total production of about 15 000 tU was recorded for the period 1959–1993. Remaining resources are estimated at around 65 000 tU, with most of these contained in the Melovoye deposit (43 820 tU) (Fig. 188). Ore grade is low, averaging 0.04–0.06% U, but the bone detritus is easily separated from the matrix and yields a concentrate with a uranium content 2–3 times higher and a phosphate content of about 30%  $\text{P}_2\text{O}_5$  [18]. In addition to U and P, REE and Sc were recovered from the detritus.

##### Geological setting

The deposits of the Precaspian region are unique and consist of uraniferous mineralization associated with fossil fish bones hosted in pyritic clays [18]. The Karagiin orefield comprises Cretaceous–Neogene marine sediments filling gentle basins lying unconformably on folded Jurassic and Permian–Triassic sediments. Mineralization is located within the Upper Oligocene Karagiin Member (Fig. 187), which is up to 400 m thick. The mineralized member is subdivided into three lithological units [18]:

- (i) Upper unit, up to 80 m thick, greenish-grey clay with disseminated pyrite concretions and intercalated mud beds;
- (ii) Middle (or fish) unit, 40–150 m thick, dark clay with beds enriched in pyrite and melnicovite concretions, fish bones and fish scales;
- (iii) Lower unit, up to 90 m thick, greenish-grey partly calcareous clay with rare shell and ‘mud eater’ fossils.



Minable uranium mineralization is restricted to the middle (fish) unit of the Karagiin Member. It contains between one and four stacked, uraniferous, phosphatic fish bone horizons which in some deposits feather out into several beds to form a horse tail pattern (Fig. 188).

Melovoye differs from the other deposits by its large size and characteristics. Sediments were deposited in a deep sea environment, which was more favourable for U, REE and Sc accumulation in bone phosphate and for Re incorporation in sulphides than in the Tomakskoye and Taybagarskoye deposits. Sedimentation forming the latter two deposits was coeval with that at Melovoye, but occurred under shallow marine conditions. This resulted in a doubling of the content of fish bone debris in ore beds, as reflected by the phosphate content and, locally, in a higher carbonate component [18].

The uranium-bearing unit extends south-eastwards, beyond the Precaspian mining district, but at greater depth. It is also found to the north-west of the Caspian Sea, where several uranium deposits are reported in the Russian Federation.

#### Mineralization

Uraniferous beds vary in thickness in the range 0.1–11 m and extend laterally for up to 18 km in length and several kilometres in width. Mineralization is found at the surface (Tasmurunskoye, Sadyrnynskoye) down to a depth of 240 m (Taybagarskoye). Melovoye covers an area of 89 km<sup>2</sup>. Uranium occurs in four horizons with abundant fish bones within a 20–60 m thick pyritic clay unit of the middle Karagiin Member.

Individual fish beds contain from a few per cent up to 75% fish bones, 1–25% P<sub>2</sub>O<sub>5</sub>, 10–60% sulphides and concentrations of U, La, Sc, Y, Co, Ni and Mo. Total REE content varies around 0.5–2.1%. Uranium ranges from 1 ppm to a few per cent, averaging 0.02–0.06% U. Phosphate is present in fossil fish bones and as a rock constituent. Uranium, scandium and REE are primarily incorporated in phosphatized fish bones detritus [18] and REE, phosphate and pyrite are recoverable as by-products to uranium.

The uranium and REE minerals present in the mineralized, bone-rich samples correspond to uraninite, coffinite, ningyoite, autunite and churchite. The presence of iron oxides and graphitized organic matter has also been detected. It is assumed that the contemporaneous occurrence of uranium and REE, which is not typical for sedimentary processes, resulted from secondary epigenetic processes and alternation of reducing and oxidizing environmental conditions [477].

#### Metallogenic aspect

A diagenetic concentration of uranium and other metals by adsorption onto phosphate and phosphatized fish bone detritus is accepted as the mineralization mechanism. Seawater is thought to be the source of the ore forming elements. The extensive accumulation of fish bones is attributed to a marked increase in hydrogen sulphide in seawater, resulting in a catastrophic impact on the fish population [18].

#### 3.12.12.2. *Minerochemical phosphorite: Central Florida Phosphate district (USA)*

##### Introduction

Uranium resources contained in the phosphorites in the USA are estimated to exceed 20 000 000 tU [473] with very low uranium content (<50–200 ppm U). Major phosphorite resources are located in both the south-eastern and north-western USA.

The Land Pebble Phosphate district of Florida, also called the Central Florida Phosphate district, is a part of the south-eastern phosphogenic province in the Atlantic Coastal Plain that extends from the

southern tip of Florida into the southern part of Virginia and includes deposits both on the land and in the adjacent parts of the continental shelf of the Atlantic Ocean. Total resources of phosphate in the province are exceptionally large, of the order of tens of billions of tonnes of phosphate pellets that contain on average about 25% P<sub>2</sub>O<sub>5</sub>. Identified resources in Florida, Georgia and North Carolina total about 8 billion tonnes of recoverable phosphate pellets with an average content of about 30% P<sub>2</sub>O<sub>5</sub> [478, 479].

In the Land Pebble district, uranium was extracted as a by-product of phosphate in eight processing plants over the period 1978–2000. Production totalled 17 275 tU. Although total resources of the district are estimated at some 500 000 tU or more, uranium resources estimated as being economic with respect to phosphate production may be in the range 100 000–200 000 tU [47]. Nukem and CF Industries are planning a 430 tU/year uranium recovery operation at CF Industries' facility at Plant City.

The uranium is normally recovered from the phosphoric acid (H<sub>3</sub>PO<sub>4</sub>) which yields about 28% P<sub>2</sub>O<sub>5</sub> by solvent extraction. A refinement of the old processes (by PhosEnergy using an ion exchange process) was announced in 2009 and reputedly offers uranium recovery costs of US \$25–30/lb U<sub>3</sub>O<sub>8</sub> (US \$55–66/kg U<sub>3</sub>O<sub>8</sub>), compared with historical costs of about twice this figure. Design and construction of a demonstration plant is complete and after undergoing final commissioning in Adelaide, South Australia, it was shipped to the USA. It is designed to operate for 5–6 months from late 2011 at a fertilizer plant [480].

#### Geological setting

Phosphorite in Florida is largely of shallow marine, nearshore platform provenance. In this environment, low grade phosphatic and uraniferous nodular and sandy phosphorite (10–20% P<sub>2</sub>O<sub>5</sub>, 20–80 ppm U) and fine- to medium-grained clastic sediments, as well as limestone and dolomite, were deposited. An exception in the uranium and phosphorous grades is the Land Pebble mineralization in the Bone Valley Formation [47].

The Pliocene Bone Valley Formation occurs in a restricted area on the southern part of the Ocala Platform (Fig. 189). Throughout its extent, the Bone Valley Member is a clastic unit consisting of phosphate grains of sand size or larger in a matrix of quartz sand, silt and clay. The lithology is highly variable, ranging from sandy, silty, phosphatic clays and relatively pure clays to clayey, phosphatic sands to sandy, clayey phosphorites.

The Bone Valley Formation is up to 15 m thick and the lower two thirds consists of phosphate pebbles and argillaceous phosphatic sand intercalated or interfingering with layers of fine- to medium-grained clastic sediments (clay, sand and glauconite), as well as shallow water limestone and dolomite. It grades upwards into sand and clay, 3–4 m thick, and rests upon limy sediments of the Miocene Hawthorn Formation (Fig. 190). The nodular phosphorite horizon, locally up to 10 m in thickness, referred to as Land Pebble phosphorite, is flat lying, crudely graded, reworked and composed of nodules and sand-sized grains of fluor-carbonate apatite mixed with clay minerals (smectite and montmorillonite) and quartz grains [47].

In general, it is poorly consolidated and colours range from white, light brown and yellowish grey to olive grey and blue-green. Molluscs are found as reworked, often phosphatized casts. Vertebrate fossils occur in many of the beds within the Bone Valley Member. Shark's teeth are abundant. Silicified corals and wood are occasionally present. The Bone Valley Formation is an extremely important phosphate deposit and has provided much of the phosphate production in the USA during the 20th century.

The areal extent of the lower Bone Valley Formation in which deposits of the Land Pebble district occur is about 2500 km<sup>2</sup>. Mineralized beds range in thickness from less than a metre to 10 m and average 5–7 m. The horizon is buried beneath a soil 'overburden' that is typically 5–10 m thick.

Mining of phosphate in the outcrop area began in 1888 and continues to the present-day. By the end of 2000, more than 850 km<sup>2</sup> had been mined in Florida.

The early Cenozoic rocks of Florida are not flat lying but form a series of highs (platforms) and lows (basins) (Fig. 191). The later Cenozoic sediments are thinnest over the highs and thickest in the lows. The oldest sediments exposed in Florida are exposed on the crest of the Ocala Platform, a major high feature in western central Florida. Other prominent highs include the Chattahoochee Anticline, Sanford High, Brevard Platform and the St. Johns Platform. The lows include the Okeechobee Basin, Osceola Low, Jacksonville Basin, the Gulf Trough and the Apalachicola Embayment. A major actively subsiding basin, the Gulf of Mexico Basin, lies west of the Florida Platform. To the east of the peninsula lie the Blake Plateau Basin and the Bahamas Basin [47].

### Mineralization

Uranium is concentrated at or near the base of the leached zone in which it occurs as stratiform disseminations, bound to cryptocrystalline calcium phosphate (principally fluor-carbonate apatite as francolite) in the form of sand-sized particles and nodules in beds mixed with quartz and clay minerals (Figs 192 and 193). Discrete primary uranium minerals are rare or absent. Although apatite grains and nodules are often enriched with up to 500 ppm U and 35% P<sub>2</sub>O<sub>5</sub>, and locally up to a few thousand parts per million of uranium at the bottom of the leached zones, the mineralized lower Bone Valley Member averages only 100–150 ppm U owing to the proportion of quartz and clay matrix [47].

Aluminous phosphates and Ca–Al phosphates (non-calcium phosphates) form unfavourable minerals for uranium accumulation. There is a positive correlation between U and P when the concentrations of both elements are relatively high and a negative correlation between uranium and the sedimentary carbonate content.

The main minerals of the Florida deposits are francolite, quartz, dolomite and clay minerals. Francolite is the only phosphate mineral that is economic. Iron and aluminium phosphate are characteristic of the uneconomic, highly weathered parts of the deposits. Quartz is the principal gangue mineral. Dolomite is a source of unwanted magnesium in fertilizer processes and mining is generally terminated when indurated dolostone beds are encountered. Clays are also a source of impurities and present a significant disposal problem [481].

### Metallogenic aspects

Uranium enrichment in the Land Pebble phosphorites of the Pliocene Bone Valley Member is attributed to reworking and corresponding re-exposure of the apatite particles to uranium-bearing seawater during repeated marine transgressions. The beginning of the Neogene not only marked a distinct change in sedimentation but also the initiation of phosphate deposition in Florida. The conditions leading to the deposition of marine phosphates are variable, but specific conditions are thought to be required. One of the most important factors is the upwelling of cold, nutrient-rich, phosphorus-bearing water from deep ocean basins. The increased phosphorus supply allows the rapid development of large populations of marine organisms such as plankton. As these organisms die and settle to the bottom, large amounts of organic material accumulate, mix with the sediments and are buried. It is thought that reactions within the sediments cause the formation of francolite. The subsequent development of economically significant phosphate deposits results from the reworking of the phosphatic sediments and the concentration of the phosphate by current and wave action.

Associated with the palaeogeographic history is the existence of an irregular, up to several metres thick, leached horizon developed within the Bone Valley Member by weathering. Its upper section is composed of aluminous phosphate and the middle section, dominated by Ca–Al phosphate, has released uranium, supposedly by acid solution leaching. Altschuler et al. [482] suggest that uranium reconcentration at or near the base of the leached zone, which comprised incipiently leached residual apatite, took place in response to neutralization of acidic fluids by calcium phosphate. Fixing of

uranium resulted from adsorption onto porous, partially leached, residual apatite leading to localized uranium concentrations of as much as several thousand parts per million. The distribution of uraniferous calcium phosphate and uranium poor Ca–Al phosphates and aluminous phosphates also reflect uranium grade zoning within the leached profile [47].

In summary, the phosphatic sediments of Florida are unconsolidated to partially consolidated sand, clay and carbonate rocks (dolomite, limestone). The deposition of phosphate was, in part, structurally controlled. Phosphate was deposited in basins on the flanks of structural or topographic highs. The economic deposits were reworked, concentrated and enriched after deposition. Uneconomic phosphatic carbonate rocks are abundant below the mine section and in the deeper parts of the basins [481].

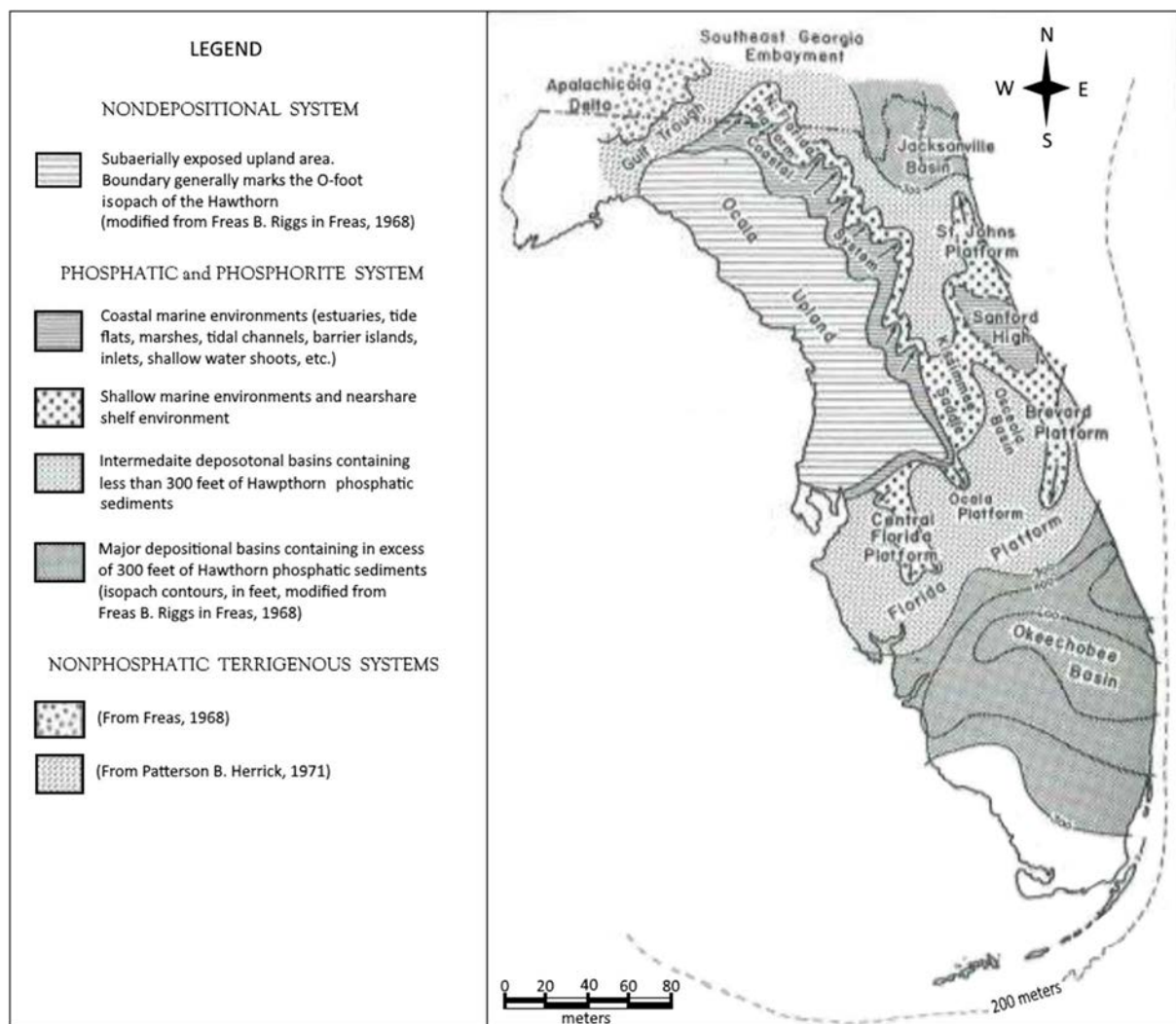


FIG. 189. Structural framework and resulting depositional environments for the phosphogenic portion of the Miocene of Florida (adapted from Ref. [483]).

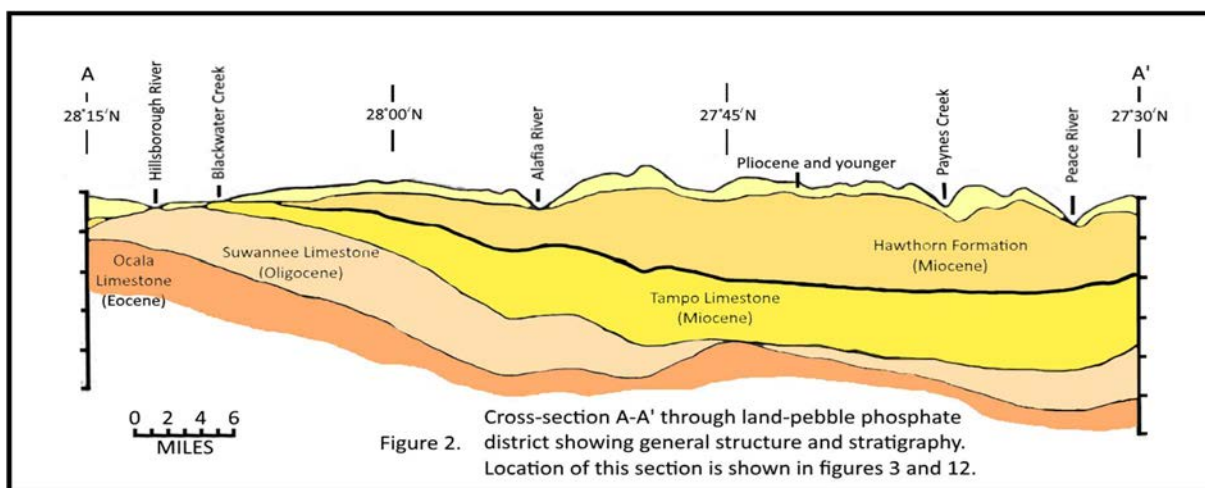


FIG. 190. Cross-section (A-A') through the Land Pebble phosphate district showing general structure and stratigraphy. Cross-section A-A' is also shown in Fig. 191 (adapted from Ref. [484]).

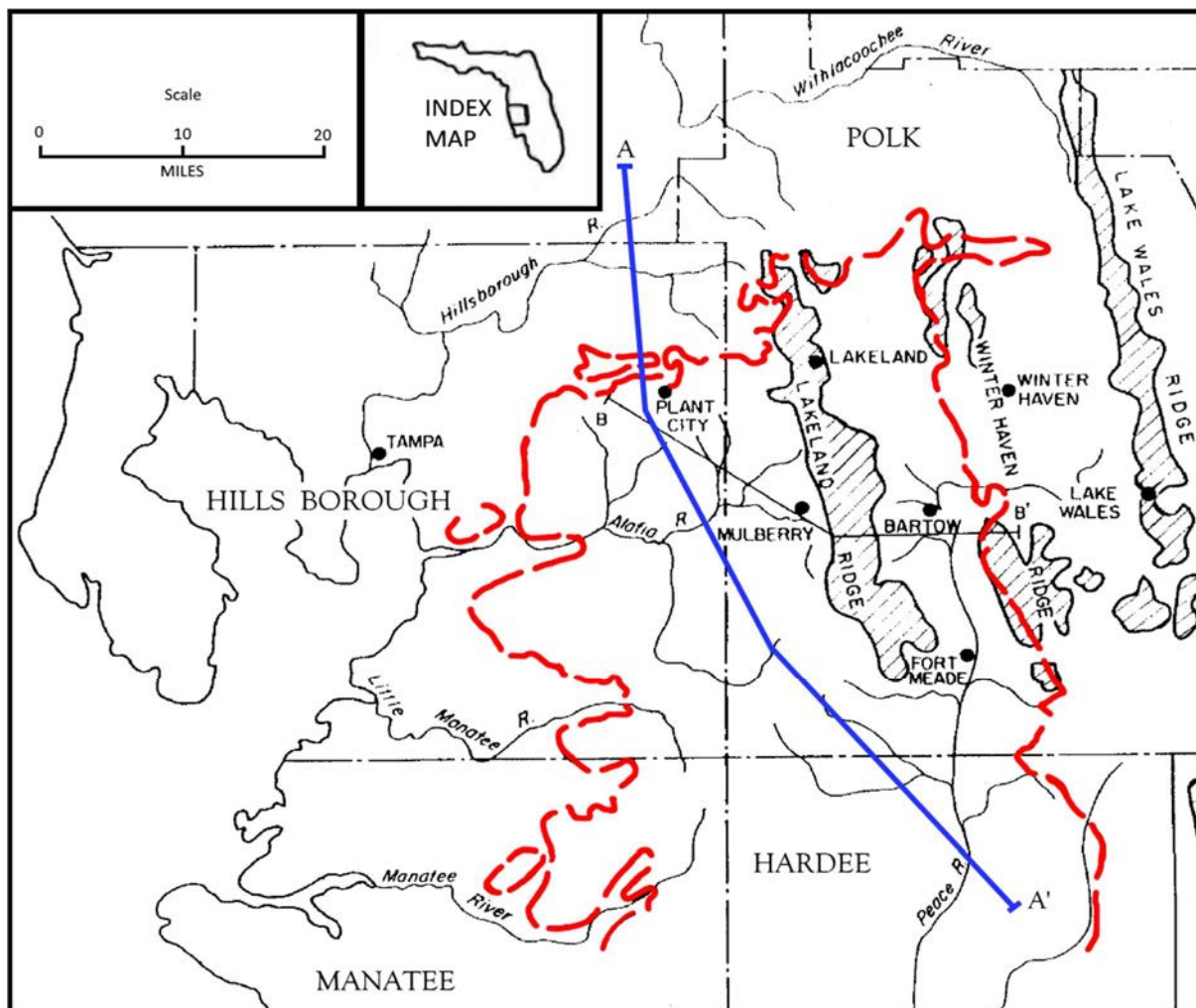


FIG. 191. Map of central peninsular Florida, showing limit of Land Pebble phosphate district (dashed lines) and topographic features. Shading indicates ridges > 50 m elevation (adapted from Ref. [484]).

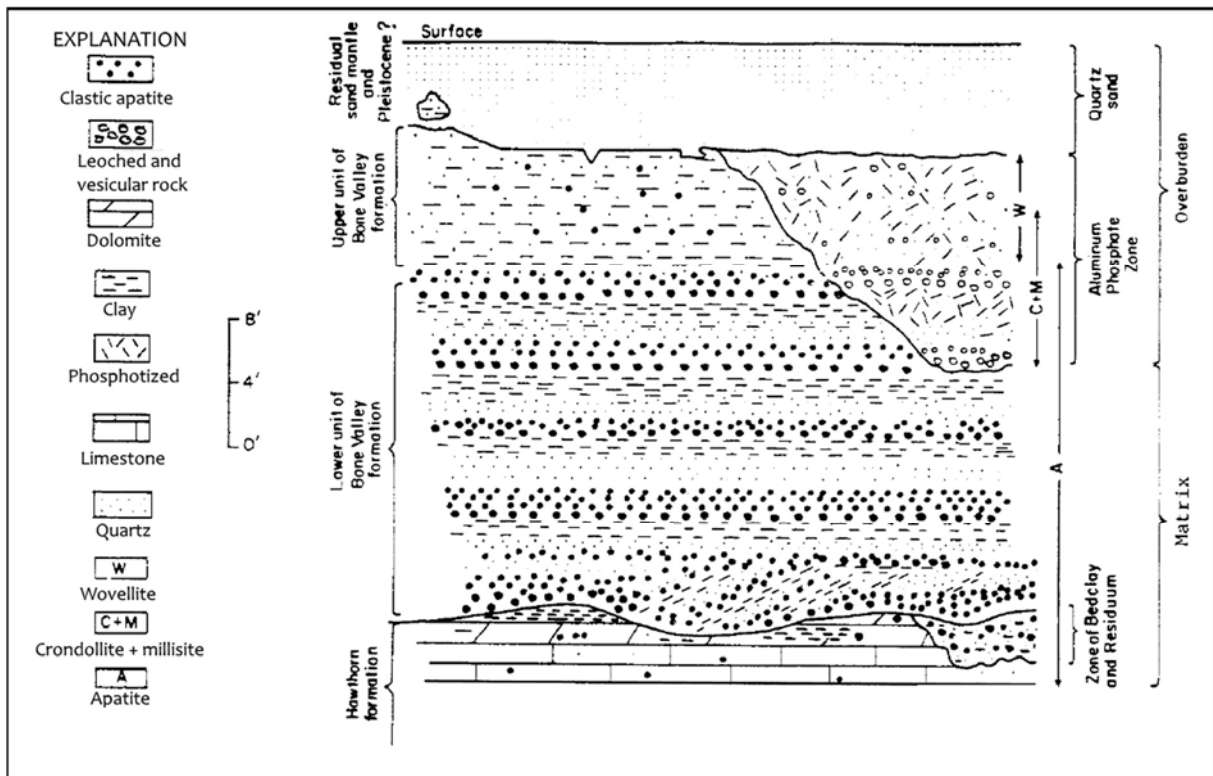


FIG. 192. Lithological and stratigraphic relations in the Land Pebble phosphate district (adapted from Ref. [484]).

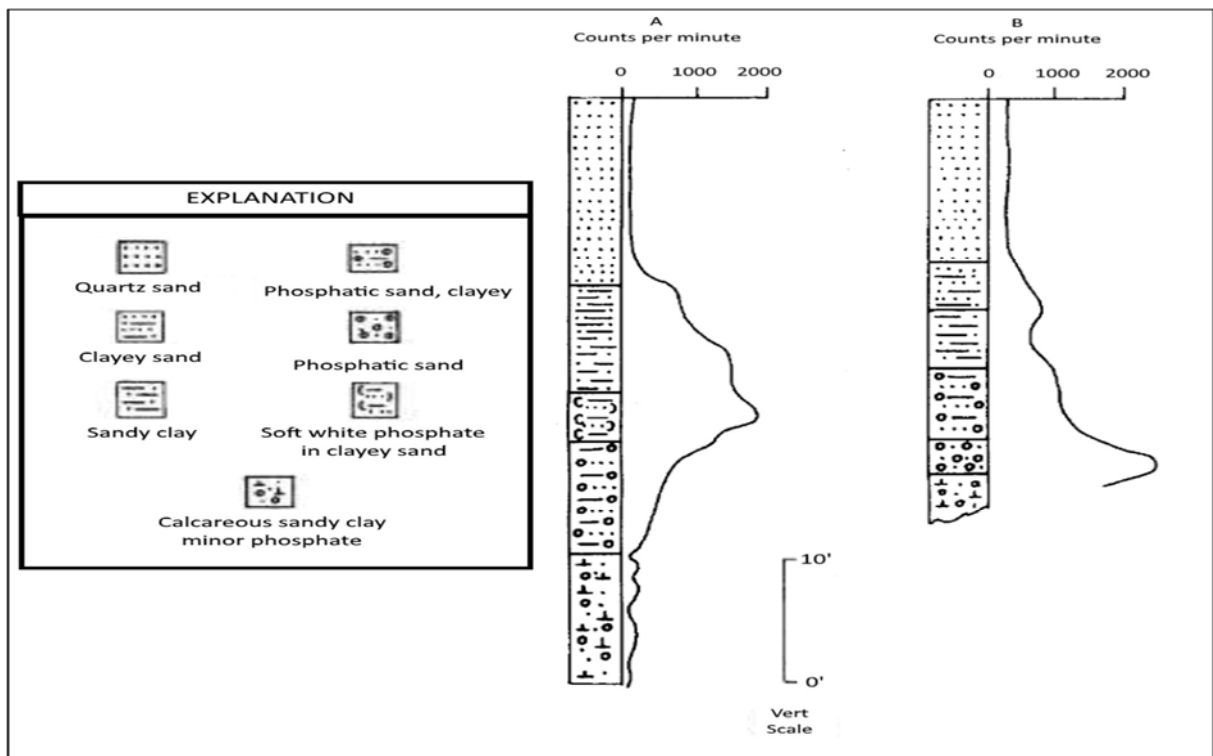


FIG. 193. Comparison of gamma ray logs of weathered and unweathered sections in the Land Pebble district (adapted from Ref. [484]).

### 3.12.12.3. Continental phosphates: The Bakouma deposits (Central African Republic)

#### Introduction

The Bakouma deposits are located in the Mbomou region, 550 km east of the capital Bangui and 4 km north-east of the town of Bakouma. The first anomaly was discovered in 1961 during a footborne follow-up of a systematic airborne radiometric survey carried out by the French Commissariat à l'Énergie Atomique and was extensively explored throughout the 1960s and 1970s. Ten uranium deposits (Patricia, Pama, Pato, Fosse, Paro, Palmyre, Pamela, Paloma, Pauline, Paquerette) were delineated in close proximity to one another, with total resources estimated at 17 000 tU with an average grade of 0.25% U [485]. The project was terminated in 1981 owing to processing difficulties and low uranium prices. Since 2007, the Bakouma project has been operated by AREVA, which has completed a significant exploration programme. In 2011, the mining project was suspended. Total resources stand at 36 400 tU at an average grade of 0.26% U with 11 510 tU at a grade of 0.138% U for the Patricia deposit only [486].

#### Geological setting

In the Bakouma area, the basement, which corresponds to the northern part of the Congo Craton (Fig. 194), is composed of Archaean granite and strongly metamorphosed Proterozoic gneiss overlain by the Bangui-Ketté System, comprising mica schist alternating with quartzite, which is in turn overlain by the Bougboulou Series with quartzite and micaceous schist. The Kembé-Nakando fluviodeltaic quartz sandstones are located above and are between 300 and 1000 m thick and they are deposited above a major unconformity. This formation, often coarse-grained and conglomeratic, contains oblique and cross-cutting units. It is overlain by thin layers of jasper and black to red pelite of the M'Bania Series, then by the red and beige clay, quartzitic conglomerate and black schist of the Bondo Series (Fig. 195). The black schist, which is interpreted as a tillite, marks the transition to the Bakouma carbonates [487, 488].

The Bakouma carbonates, which are only recognized in drill holes, have a thickness of about 200 m and are subdivided into four units [483], from bottom to top:

- (i) The basal dark grey to grey Bakouma Dolomite;
- (ii) The red to purple Palmyre Limestone;
- (iii) The blue-grey Bili Limestone;
- (iv) The Rocades Limestone and pelite.

The Palmyre Limestone contains on average 1–4% P<sub>2</sub>O<sub>5</sub> and locally up to 10% P<sub>2</sub>O<sub>5</sub>. The phosphate mineral is fine-grained apatite disseminated throughout the limestone. This phosphatic limestone is locally brecciated and locally enriched in uranium.

The Dialinga Series overlies the uppermost Rocades unit of the Bakouma carbonate series and is subdivided into three facies, a basal pyritic, black, pelitic facies, a well sorted sandstone facies and an upper micaceous pelitic facies. Deposition of the Rocades Limestone and the Dialinga Series indicates commencement of a marine regression, the end of Proterozoic sedimentation and the start of the Pan-African Orogeny (~700 Ma).

Major north-east to south-west oriented compression resulted in isoclinal folding followed by reverse faulting parallel to these structures. A final tectonic phase is characterized by the development of NE–SW extensional faults and intrusion of dolerites.

Post-orogenic erosion removed the Dialinga Series south of Bakouma. The Bakouma carbonate units were preferentially altered along faults, creating elongate, NE–SW oriented channels that were further developed through carbonate dissolution, resulting in the development of a karst environment.

During the Jurassic period, erosion of the Dialinga Series and Bakouma carbonates contributed to the formation of the unconformable detrital Mouka Ouadda Series. A system of E–W fractures developed during post-Cretaceous tectonism, inverting the general morphology and drainage direction. Erosion of the Bakouma carbonates continued and the karst structures were best developed at the junction of the two fault systems.

During the Eocene, the outlet of the Bakouma Basin was partially closed and lakes developed in the channels. The M'Patou phosphatized sediments hosting the uranium mineralization were deposited within the karst environment. The series is comprised of silicified to clayey silts that are partially indurated. A strong phosphate enrichment of the M'Patou Formation with important facies variations has been observed above some of the karst depressions, which can be 70–150 m wide and up to 80 m deep [485]. Ferruginous laterites overlie all sedimentary units.

### Mineralization

The Patricia deposit, which is the most explored orebody, is a sub-horizontal mineralized lens between 4 and 85 m thick, oriented NE–SW with a strike length of 850 m and a width of 100 m (Fig. 196). The top of the mineralization is 6–59 m below the surface and the base of the mineralization can extend to a depth of 106 m in some places.

At the Patricia deposit, Miauton [488] observes geological variations in the M'Patou Series, from thick (>50 m) phosphatized units in the north to thinner units with abundant chert in the south. The M'Patou Formation is composed at the base of black, pyritic and organic-rich argillite, clayey silt with indurated lenses of limestone, dolomite or chert overlain by red, orange or yellow silts more than 20 m thick. These silts are interbedded with indurated, strongly phosphatized lenses. Towards the top, indurated phosphatized lenses become less abundant and uraniferous secondary minerals such as torbernite and autunite occur frequently.

The M'Patou Formation is overlain by 20–30 m of red, orange or yellow silt composed of quartz and clay with illite or kaolinite. Interbedded lateritic layers are present and diagenetic phosphate is not observed. The silty unit grades into clay, which is, in turn, overlain by ferruginous gravel. The uppermost unit corresponds to 5–8 m of strongly indurated ferruginous laterite.

The uranium mineralization is present within weathered, very fine-grained sandstone and, locally, quartzite overlying limestone, sometimes pink in colour, and light grey dolomite. Minor mineralization is present within completely oxidized lithologies. Uraniferous phosphate minerals comprise autunite and torbernite as fracture coatings and as fine-grained disseminations of apatite. White, indurated masses of crandallite have also been described. In the mineralized phosphatic lenses, the  $P_2O_5$  content varies around 5–35%.

### Metallogenic aspects

The Bakouma deposits correspond to newly formed, continental, lacustrine uraniferous phosphate deposits hosted in fine-grained sediments and deposited within a karst environment. They represent the only known example of this type of deposit.

M'Patou sediments were deposited within a karst environment. It is suggested that during the deposition of the M'Patou Series, lake waters were reducing and strongly alkaline and on the slopes of the intracontinental basin the conditions were oxidizing and acidic. As a result, P, Si, Al and Ca were concentrated in the basin in the presence of organic matter. The magnesium in the dolomite probably inhibited the deposition of apatite. As the basin filled up, the influence of the dolomite decreased and the phosphate minerals were precipitated in the M'Patou sediments.

A geological model of continental origin is invoked for the uranium deposits of the Bakouma area. Deep NE–SW trending karst channels formed in locally phosphate enriched carbonate lithologies at

the intersection of fault structures. Host sediments derived from sediments bounding the channels were deposited in the karst channels and P, Al and Ca from the eroding sediments were transported and concentrated within organic horizons in the channels. As the basin continued to fill, the influence of magnesium from the dolomites decreased and the mineralization was deposited as fine-grained sediment.

The origin of the uranium is still controversial. For Mathieu (personal communication, 2010), the proximal phosphatic and uraniferous Palmyre Limestone, located on top of the Bakouma carbonates, represents the main source of uranium. The carbonates are locally brecciated, their cement is apatite-rich and they may contain up to 1000 ppm U. The U-P limestone is strongly dissolved by acidic water circulating through the Neoproterozoic Dialinga Series cover which contains sulphide-rich pelite layers. The Mouka Ouadda sandstone and the Dialinga pelite (black shale) represent other possible uranium sources.

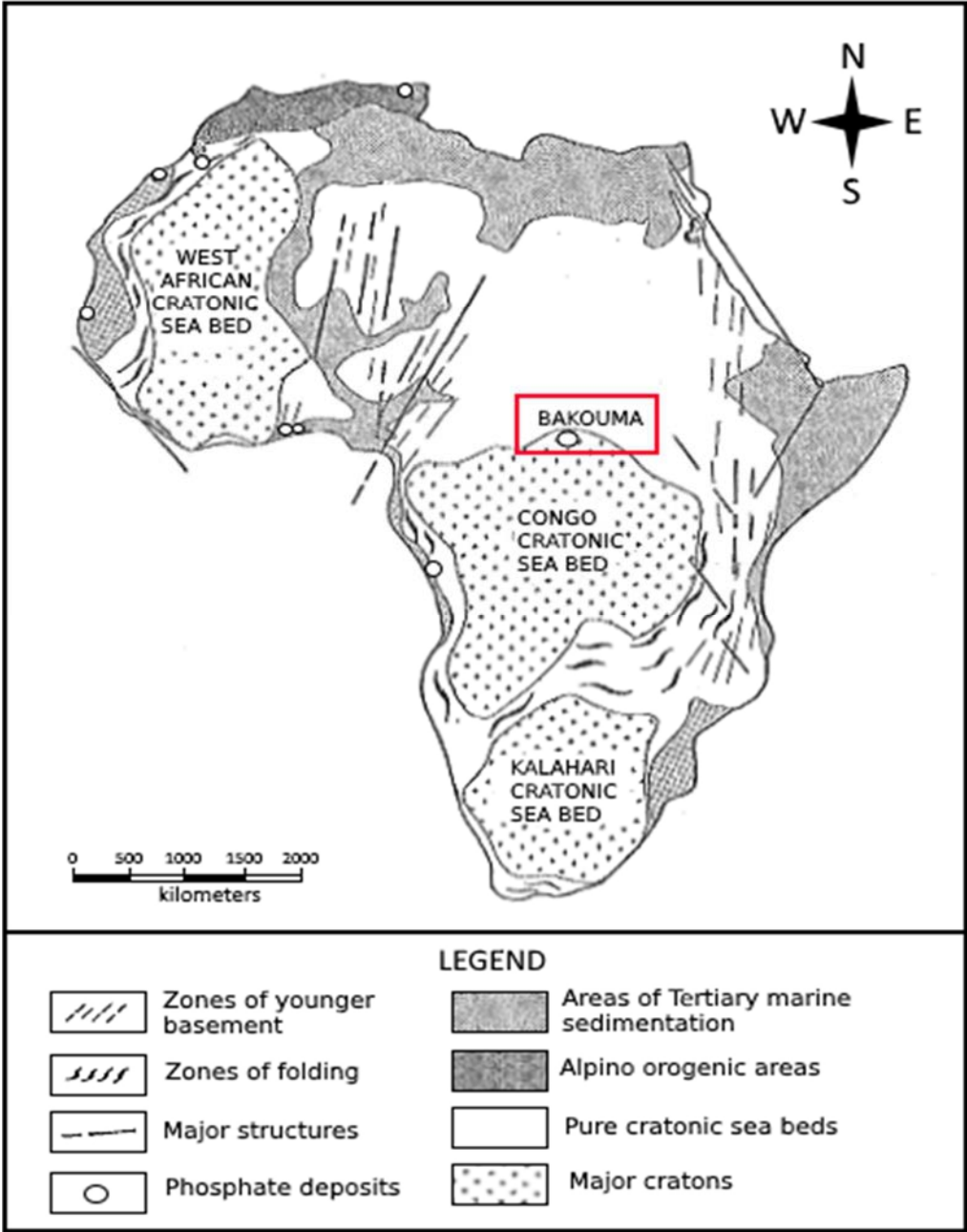


FIG. 194. Location of the Bakouma district, north of the Congo Craton (adapted from Ref. [488]).

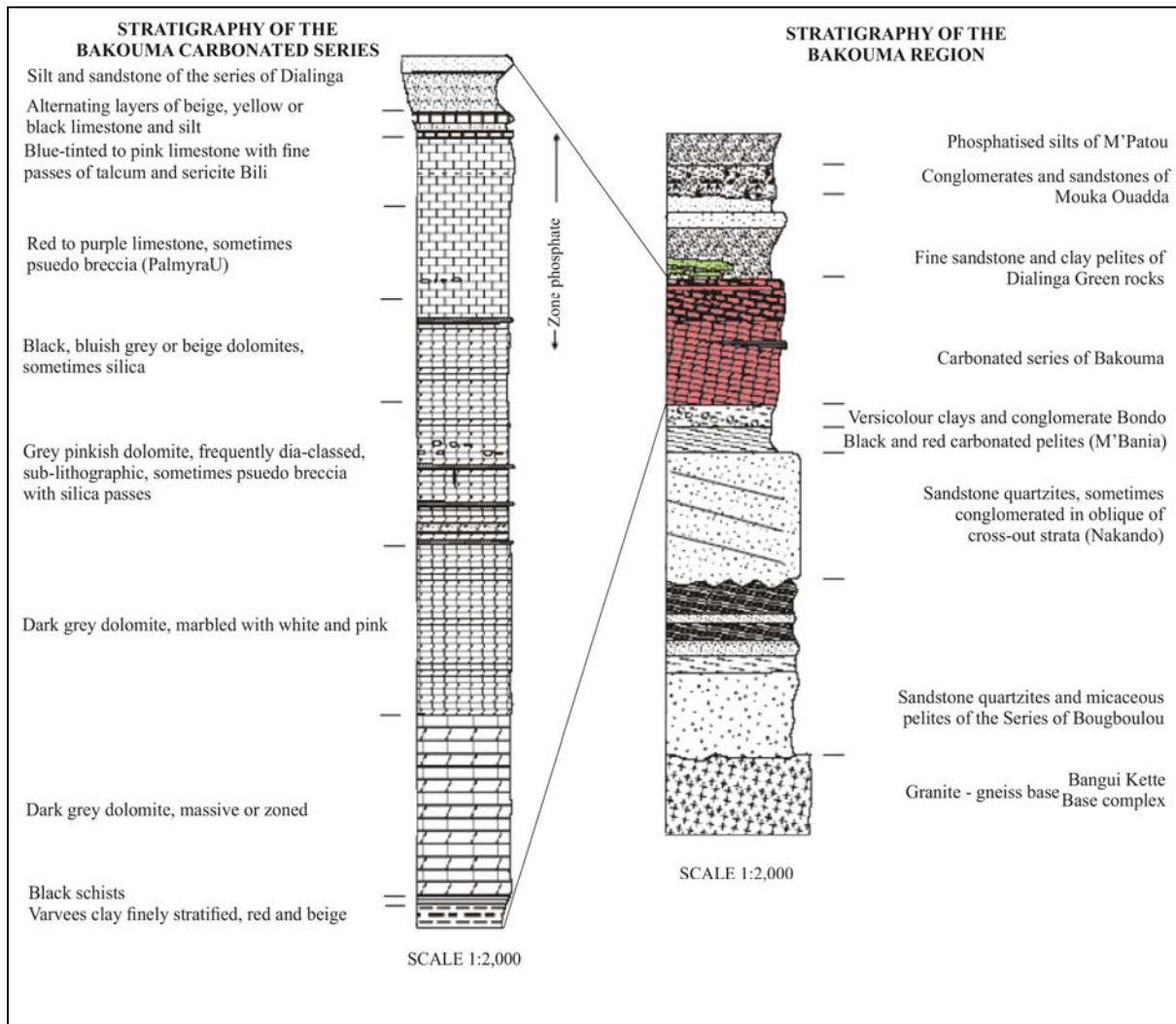


FIG. 195. Stratigraphic log of the Bakouma region with detailed stratigraphy of the Bakouma carbonate series (adapted from Ref. [488]).

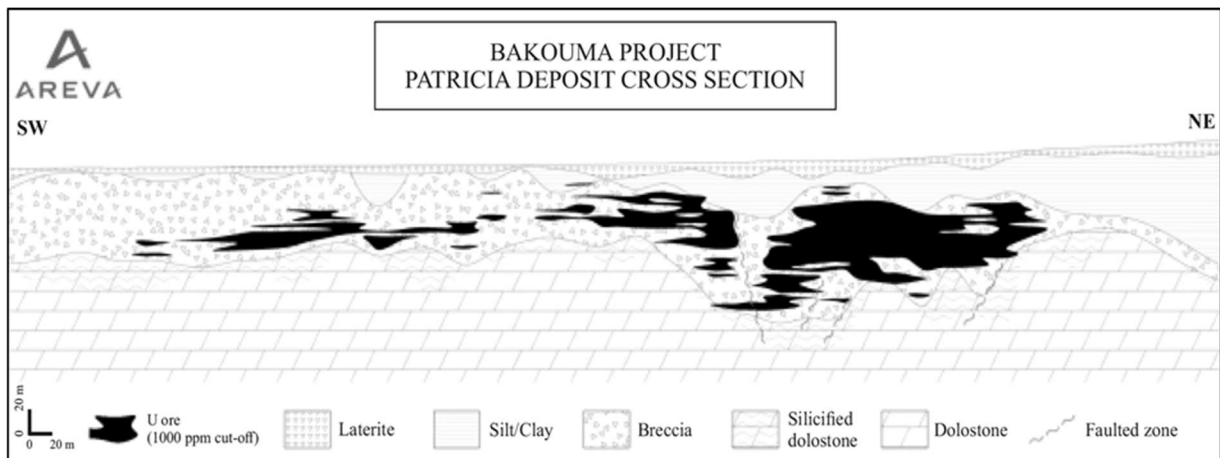


FIG. 196. Cross-section of the Patricia deposit, Bakouma district (source: AREVA) (reproduced with permission).

### 3.15. BLACK SHALE DEPOSITS

#### 3.12.13. Definition

Black shale related uranium mineralization consists of marine, organic-rich shale or coal-rich pyritic shale, containing syndimentary disseminated uranium adsorbed onto organic material. The size of the deposits is highly variable, ranging from small occurrences to covering very large districts. Grades are usually low to very low (30–500 ppm U) with notable structural enrichments (0.10–0.20% U) in some deposits. Major examples include the uraniferous Alum Shale in Sweden, the Chattanooga Shale and the Pennsylvanian Shale (USA), the Ziyuan orefield (China), the Auminzatau orefield (Uzbekistan), the Ogcheon Group (Republic of Korea) and the Gera-Ronneburg orefield (Germany) (Table 39).

The UDEPO database lists 50 black shale deposits/districts. These deposits have only ever been mined in Germany, in the Gera-Ronneburg orefield, which recorded a total production of 125 000 tU at an average grade of 0.085% U from 20 deposits. Numerous black shale deposits/districts are recorded around the world and many of these have anomalous values of various elements such as Ni, Mo, V, Cu, U, Zn, Ba, Ag, Au and platinum group elements.

TABLE 39. PRINCIPAL BLACK SHALE DEPOSITS/RESOURCES (as of 31 December 2015)

Deposit/district	Country	Resources (tU)	Grade (% U)	Status
Tarfaya Basin	Morocco	6 400 000	0.008	Dormant
Baltoscandia district	Estonia	5 667 000	0.0085	Dormant
Chattanooga Shale	USA	5 000 000	0.006	Dormant
Timahdit Basin	Morocco	2 100 000	0.006	Dormant
MMS Vicken	Sweden	403 000	0.0144	Exploration
Narke	Sweden	257 000	0.0175	Dormant
Ranstad	Sweden	254 000	0.030	Dormant
Haggan	Sweden	243 000	0.0137	Exploration
Lubin-Sierszowice	Poland	144 000	0.006	Dormant
Schmirchau-Reust	Germany	73 410	0.085	Depleted
Buckton Zone	Canada	34 000	0.001	Dormant
Drosen	Germany	29 995	0.085	Depleted
Paitzdorf	Germany	28 750	0.085	Depleted

#### 3.12.14. Geological setting

Within the black shale deposits, two main subtypes are distinguished: (i) stratiform black shale deposits (Ranstad and Chattanooga types), and (ii) stockwork black shale deposits (Ronneburg type).

##### 3.12.14.1. Stratiform black shale deposits

Stratiform black shale deposits are mineralized beds of fairly uniform thickness (a few metres to several hundred metres thick) and of sizeable areal extent (several hundred square kilometres to 10 000 km<sup>2</sup>), and host extremely large quantities of uranium, albeit at low grade (50–150 ppm U). Higher grades are confined to beds (tens of centimetres to metres thick) that are rich in organics,

particularly humic-coaly material. If phosphate nodules are present, they normally contain more uranium than the surrounding shales. The organic matter is derived from marine plankton and land plant (wood spores) debris. Limestone, sand/siltstone and shale strata complete the stratigraphic sequence. On the basis of uranium associated organic substances, Dahlkamp [18] distinguishes two mineralization settings (Fig. 197):

- (a) Uraniferous humic/kolm in alum shale (Ranstad type, Sweden);
- (b) Uraniferous bituminous/sapropelitic black shale (Chattanooga type, USA).

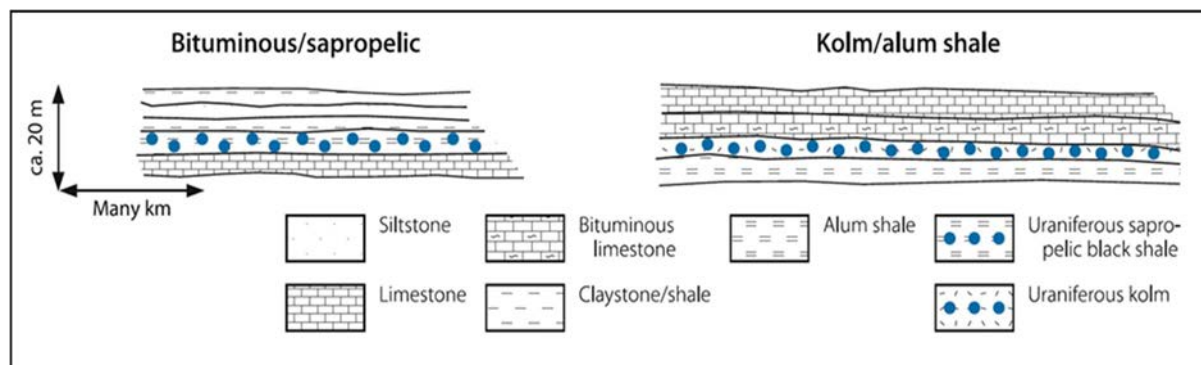


FIG. 197. Uraniferous stratiform black shales deposits [17] (reproduced with permission).

#### 3.12.14.2. Stockwork black shale deposits

Stockwork black shale deposits (Ronneburg type, Germany) consist of stratabound, structure controlled uranium concentrated in stockworks of microfractures or immediately adjacent to carbonaceous, pyritic (black) shale/pelite beds (Fig. 198). Host rocks include argillaceous and siliceous black carbonaceous shale with intercalations of dolomitic and phosphorite nodule-bearing beds. High organic carbon (up to 9% C), sulphide (up to 3.5% S) and anomalous trace elements (U, Mo, Ni, V, As and Sb) are typical for the carbonaceous shales. Mineralization is restricted to segments of intense microfracturing controlled by major faults, thrusts and their intersections. These microfracture systems form stockwork orebodies within the cementation zone [18].

The largest orefield is the Gera-Ronneburg district in Germany, which hosts 17 deposits and resources of more than 200 000 tU. Other mineralized districts are located in Sweden, Uzbekistan and China (Table 39). In China, such deposits are called ‘carbonaceous–carbonate–siliceous–pelite’ type. The resources of individual deposits range from small to large (several hundred tonnes to several tens of thousands of tonnes of uranium), with grades of 0.05–0.20% U.

Black shale occurrences across the world are characterized by elevated concentrations of organic material, which is mostly associated with correspondingly elevated concentrations of metals. In some instances, the concentration of organic material is high enough that the shale can be used commercially, directly as fuel or indirectly as the source for black shale fuel. The metals may be recovered as by-products. Enrichment in metals has drawn scientific interest to the study of black shales and the extraction of metals has been successfully demonstrated. In the case of the Ranstad black shale, about 200 tU were extracted in the 1960s.

The majority of black shale uranium deposits are of Palaeozoic age (Cambrian–Permian), with the exception of the Proterozoic Dieter Lake deposit (Canada). However, hundreds of black shale formations are recorded from Proterozoic up to Cenozoic time.

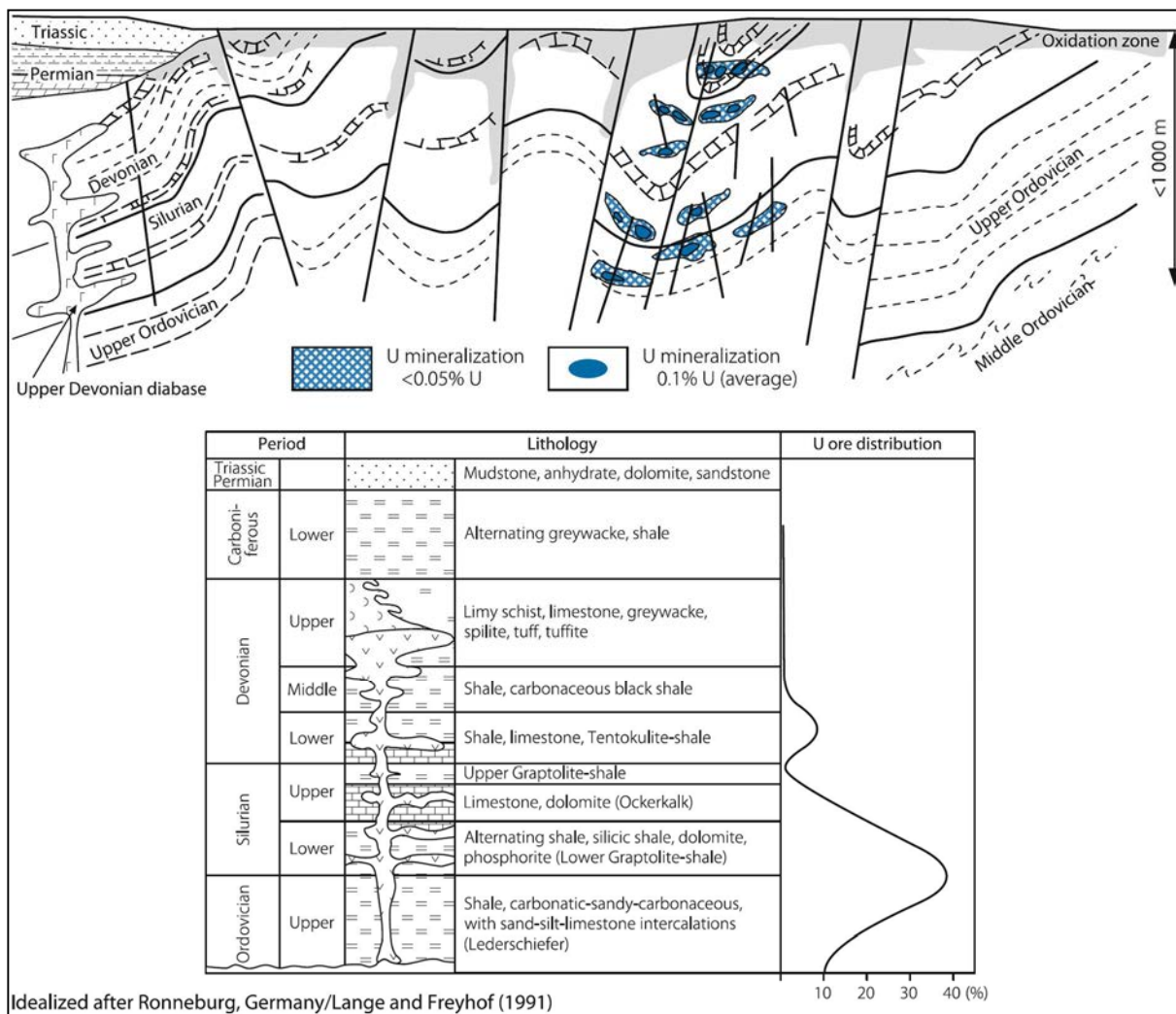


FIG. 198. Uraniferous carbonaceous shale related stockwork deposits (Ronneburg type) [18] (reproduced with permission).

### 3.12.15. Metallogenesis

The pattern of geological distribution of uraniferous and vanadiferous shales indicates that their origin is connected with the rise in sea level during the opening of new ocean basins (Cambrian and Cretaceous deposits) or with major marine transgressions, as in the case of the Devonian Chattanooga Shale or the Permian Phosphoria Formation in the USA. In these periods, the ancient eroded peneplanes became flooded, anoxia was induced as a result of the nutrient supply and eutrofication of the water environment, and metals were supplied from the continent or deeper parts of the ocean [489].

In most black shales, such as the Chattanooga Shale and related shales of the eastern interior USA, increased metal and metalloid contents are generally related to increased organic carbon content, decreased sedimentation rates, organic matter type or position within the basin. In areas where the stratigraphic equivalent of the Chattanooga Shale is deeply buried and the organic material is thermally mature, metal contents are essentially the same as in unheated areas and correlate with organic carbon or sulphur content [490]. However, in the Cambrian Alum Shale Formation of Sweden, increased metal content does not necessarily correlate with organic matter content nor is metal enrichment necessarily related to land derived humic material because the organic matter is all of marine origin. In southern central Sweden, U, Mo, V, Ni, Zn, Cd and Pb are all enriched relative to

average black shales but only U and Mo correlate with the organic matter content. Tectonically disturbed and metamorphosed allochthonous alum shales formations on the Caledonian front in western Sweden have even higher concentrations of some metals (V, Ni, Zn and Ba) relative to the autochthonous shales in this area and to those in southern Sweden [490].

In stratiform black shale deposits, discrete primary uranium minerals are absent. Other metals (Cu, Cr, Mo, Mn, V, P and REE) occur in small quantities. Ore minerals in the carbonaceous shale related stockwork deposits consist of pitchblende and rare coffinite, with subordinate sulphides and arsenides of various metals. They fill and coat joints and cleavage planes and impregnate porous wall rocks. Ore related mineralization is constrained to narrow aureoles of bleaching and haematitization around mineralized structures [18].

The amount of metal contained in metalliferous black shales (MBS) can rival or surpass any other type of metal deposit known. Historically, there has been little consensus as to the source, means of transport or deposition of these metals. The paradigm established over the last twenty years, however, suggests that the abundant metal (and carbon) in MBS reflects oceanographic conditions that enhance organic productivity/preservation and optimize extraction of metals from seawater. Yet, to date, no modern analogues of MBS have been found and, despite intense study, the genetic processes responsible for MBS remain unexplained [491].

MBS are commonly found in sedimentary basins that also host a range of different types of syngenetic metal deposit in correlative strata. The relationship between MBS and hydrothermal synsedimentary exhalative (SEDEX) Zn–Pb–Ag, Ba, Au deposits has previously been ascribed to euxinic ocean conditions enhancing deposition of metal sulphide minerals. Correlative strata commonly contain sedimentary P<sub>2</sub>O<sub>5</sub>, Mn and Fe deposits that have traditionally been explained by upwelling of cold nutrient-rich ocean waters on to continental shelves. Increased nutrients in shallow marine environments are thought to cause, as along modern upwelling coastlines, a surge in bioproductivity and consequent eutrophication, anoxia/dysoxia and sequestration of organic carbon. In this model, metal and phosphate in the shale are sourced from seawater and accumulated through various biogenic and chemical mechanisms [491].

However, mass balance constraints that consider the total mass and recharge of metal to the ocean, ocean circulation and sedimentation rate suggest that typical seawater may be an inadequate source for the amounts of metal present in some MBS. Alternatively, it can be shown that the fluxes of metals delivered to the ocean during SEDEX deposit formation can rival or surpass the modern riverine fluxes into the ocean. Another overlooked aspect of SEDEX systems is that the flux of nutrients (e.g. NH<sub>4</sub><sup>+</sup>, reduced C, trace metals, Ba and Si) can in some cases exceed the modern riverine fluxes. Such an immense nutrient flux into a single sedimentary basin would undoubtedly cause large increases in primary bioproductivity and could potentially trigger eutrophication and basin anoxia/euxinia [491].

Given that the flux of metals and biolimiting nutrients delivered to the ocean by a single SEDEX hydrothermal discharge can rival the entire modern riverine flux, systems of this type are a plausible source for the metals and nutrients required to form MBS. A favourable aspect of the SEDEX trigger model is that it explains the temporal and spatial coincidence of anoxia/euxinia, MBS and various Zn–Pb–Ag, Ba, Au, P<sub>2</sub>O<sub>5</sub>, Mn and Fe deposits at numerous times in Earth history [491].

### **3.12.16. Description of selected deposits**

#### *3.12.16.1. Stratiform disseminated: The MMS Vicken and Häggän deposits (Sweden)*

##### **Introduction**

The MMS Vicken and Häggän deposits are located in Jämtland, near Östersund, in central Sweden, close to the border with Norway (Fig. 199). Both are hosted by Cambrian alum shales, which are comparable to the alum shale deposit of Ranstad.

The term ‘alum shale’ was introduced over three hundred years ago to refer to particular parts of the Late Cambrian black shales from which alum salt ( $KAl(SO_4)_2 \cdot 12H_2O$ ) was extracted. The name Alum Shale Formation is used for the entire lithostratigraphic unit throughout Scandinavia [492].

The area was explored by the Swedish Geological Survey in the 1970s and early 1980s, including core drilling. Owing to the negative results obtained for the Alum Shale project in southern Sweden (Ranstad deposit), no further attention was given to this area. In 2005, two junior companies, Continental Precious Minerals Inc. and Aura Energy obtained leaseholdings in the Östersund region. The MMS (multimetal sediment) Vicken project is operated by Continental Precious Minerals. A NI 43-101 compliant technical report was produced in 2007 and updated in 2008 on the basis of the drilling completed by Continental Precious Minerals. Total uranium resources amount to 447 755 tU with an average grade of 147 ppm U. In addition, substantial low grade concentrations of Mo, Ni and V are included (690 000 t Mo at an average grade of 240 ppm, around 900 000 t Ni at 320 ppm and about 7.5 million t  $V_2O_5$  at 268 ppm). Recovery has been determined to be 85% for  $U_3O_8$ , 90% for  $V_2O_5$  and 85% for Mo. [488]. The project is dormant.

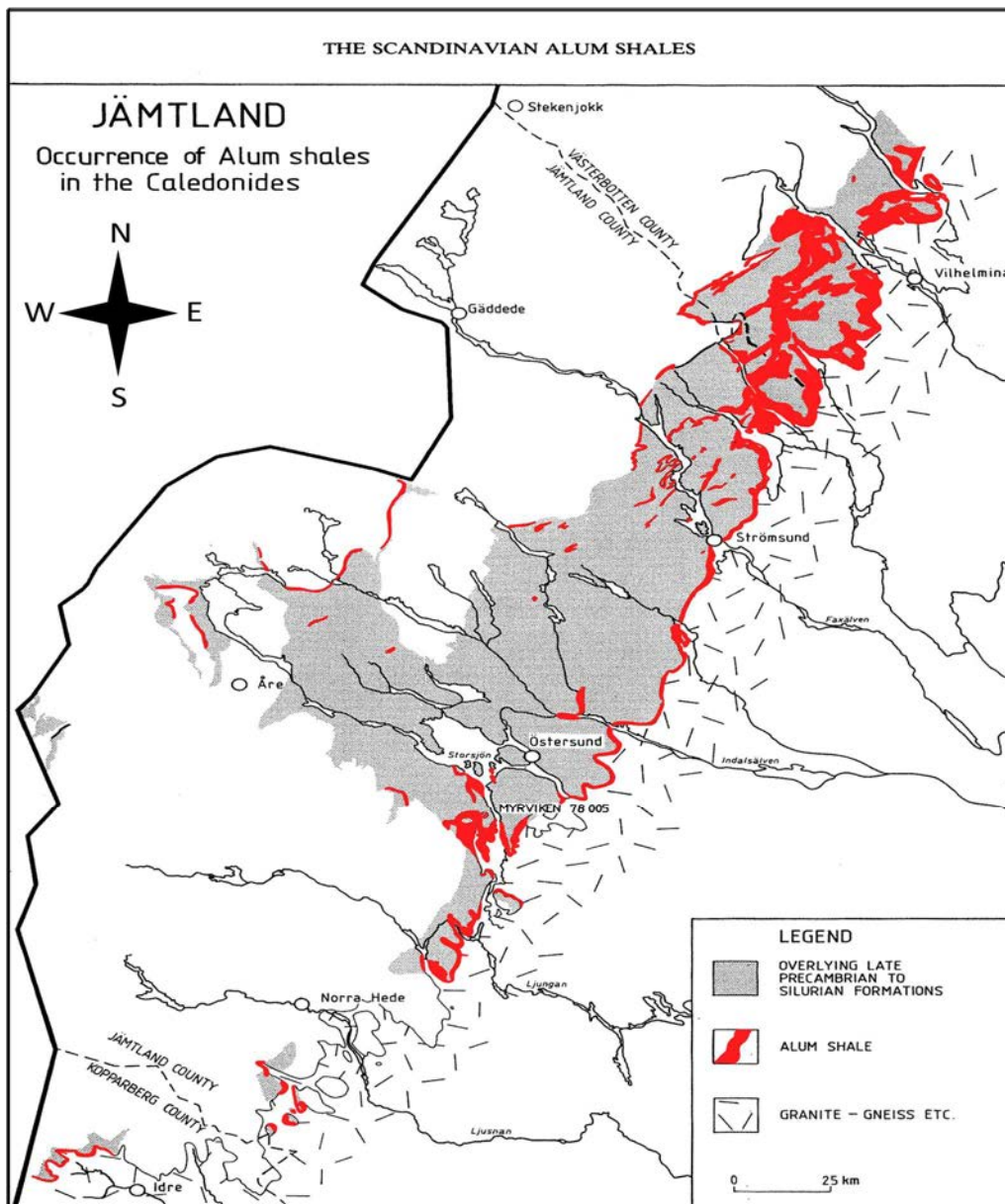


FIG. 199. Distribution of the Alum Shale Formation in western Jämtland, Sweden (adapted from Ref. [487]).

The nearby Häggån and Marby projects are owned by Aura Energy. In 2012, the company announced inferred resources of 308 000 tU at an average grade of 135 ppm U. In addition, large low grade concentrations of Mo (412 000 t at 207 ppm), Ni (630 000 t at 316 ppm), V (3 000 000 t at 1520 ppm) and Zn (860 000 t at 430 ppm) are recorded [489]. As of 2015, the project is dormant.

The considerable thickness and relatively high concentrations of the various elements of the Jämtland Alum Shales imply the presence of a very large reserve of both fossil fuel energy and trace metals. As of 2015, the three projects together host around 730 000 tU in an area covering about 10 km × 3 km and open in every direction (Fig. 200). To the north, the Alum Shale Formation has been traced for at least 300 km (Fig. 199), suggesting that the uranium resources are probably of the order of several million tonnes.

### Geological setting

Black shales of Middle–Late Cambrian and locally of earliest Ordovician age are developed extensively in Scandinavia. Large parts of Sweden are underlain by Precambrian rocks of Archaean and Proterozoic age. At the end of the Proterozoic, marine rift basins were formed (Iapetus Ocean) which filled with classic sediments first, followed during Cambrian time by bituminous shales. These shales, Alum Shales, are found in southern and central Sweden.

The areas for which both Continental Precious Minerals and Aura Energy have leaseholdings relate to their geological setting with respect to the Alum Shale in Västergötland, southern Sweden (Ranstad deposit). The Östersund area is located in the foreland of the Caledonian Mountains (SW–NW Sweden and NE–SE Norway) and has a complicated geological history. At the closure of the Iapetus Ocean during the Silurian, an assemblage of rocks ranging in age from Precambrian to Silurian was thrust eastwards, as an allochthonous Caledonian nappe. Thrusting and folding was responsible for the imbrication of mineralized strata which economically upgraded the area owing to ore zone thickening. The regular thickness of the Alum Shale (20–30 m) is increased by imbrication to 150–200 m (Figs 201 and 202). Metamorphism related to the thrusting and an increase in temperature to 200–300°C partially converted the bituminous material to a semi-anthracitic composition. The Alum Shale exhibits a strong penetrative foliation [492].

Middle and Upper Cambrian black shale is interlayered with subordinate quartzite, limestone and ‘stinkstone’ (bituminous limestone). The black shale is underlain by Proterozoic granite and gneiss thrust over Archaean granitic basement rocks. The licences are situated on the eastern flank of a major NNW trending anticline (the Myrviken Antiform), which is manifested as a broad ridge.

### Mineralization

The mineralization on the properties owned by Continental Precious Minerals and Aura Energy is low grade, syngenetic and stratiform in nature. Uranium, found as minute disseminations of uraninite and organo-metallic compounds, is associated with Mo, Ni, V and Zn, which probably correlate with each other. The element assemblage is typical for black shales (as collectors of metals). Vanadium and molybdenum are thought to be associated with clay minerals and as organo-metallic compounds and perhaps as microscopic mineral disseminations. Chemical analysis data of the regional Jämtland black shale give the following results: organic C (14.2%), S (4.40%), Fe (3.40%), Ti (0.39%), V (0.16%), Mo (0.046%), Ni (0.044%), Zn (0.027%), U (0.0245%), As (0.016%) and Cu (0.138%) [487].

### Metallogenic aspects

Evidence favours the deposition of the Alum Shales on a very stable epicontinental margin. The black shale facies and the fauna clearly indicate a tranquil, marine depositional environment. The shales are parallel laminated. Cross-lamination, grading, scouring and other evidence of current activity have not been recorded. In areas of apparently continuous deposition, maximum thickness of the Upper Cambrian strata is of the order of 45–55 m, suggesting depositional rates of less than 2 m per million

years. The remarkable correlation of shale chemistry with biostratigraphy indicates that the trace element concentrations were essentially syngenetic, occurring in response to small regional changes in the depositional environment [490].

Depth of water is assumed to have been shallow, around 100 m to allow stratification of the water column and formation of a stable, euxinic bottom layer. These anoxic bottom waters caused efficient trapping of metals by reduction and facilitated the preservation of organic matter and associated metals. A low sedimentation rate also enhanced metal contents because of a lack of clastic dilution. As a result, iron is completely sulphidized and all reducible metals are fixed in the sediment as sulphides or associated with organic matter. Excess organic matter and sulphide reductants account for the lack of correlation of most metals because all metals were fixed in the sediments [490].

There is no evidence of contemporaneous volcanic activity in Balto-Scandia during Cambrian time [492]. Secondary redistribution is apparent locally in the Caledonides, where some elements of the Alum Shale are concentrated in zones of high strain. Also, shales on the Caledonian Front have undergone low grade metamorphism and during this process the heated waters appear to have leached metals from the metasedimentary rocks and underlying basement rocks. As a result, metals (V, Ni, Zn, Ba) were epigenetically added to the allochthonous material during the Caledonian Orogeny, about 100 Ma after the shale was deposited. These metals were fixed in the shale by the organic matter, with pyrite (and other sulphides) acting as reductants [490].

In contrast, in most black shales such as the Chattanooga Shale and related shales of the interior USA, increased metal and metalloid contents are generally related to increased organic carbon content, decreased sedimentation rate, organic matter type or position within the basin. In areas where the stratigraphic equivalent of the Chattanooga Shale is deeply buried and the organic material is thermally mature, metal contents are essentially the same as in unheated areas and correlate with organic C and S contents [490].

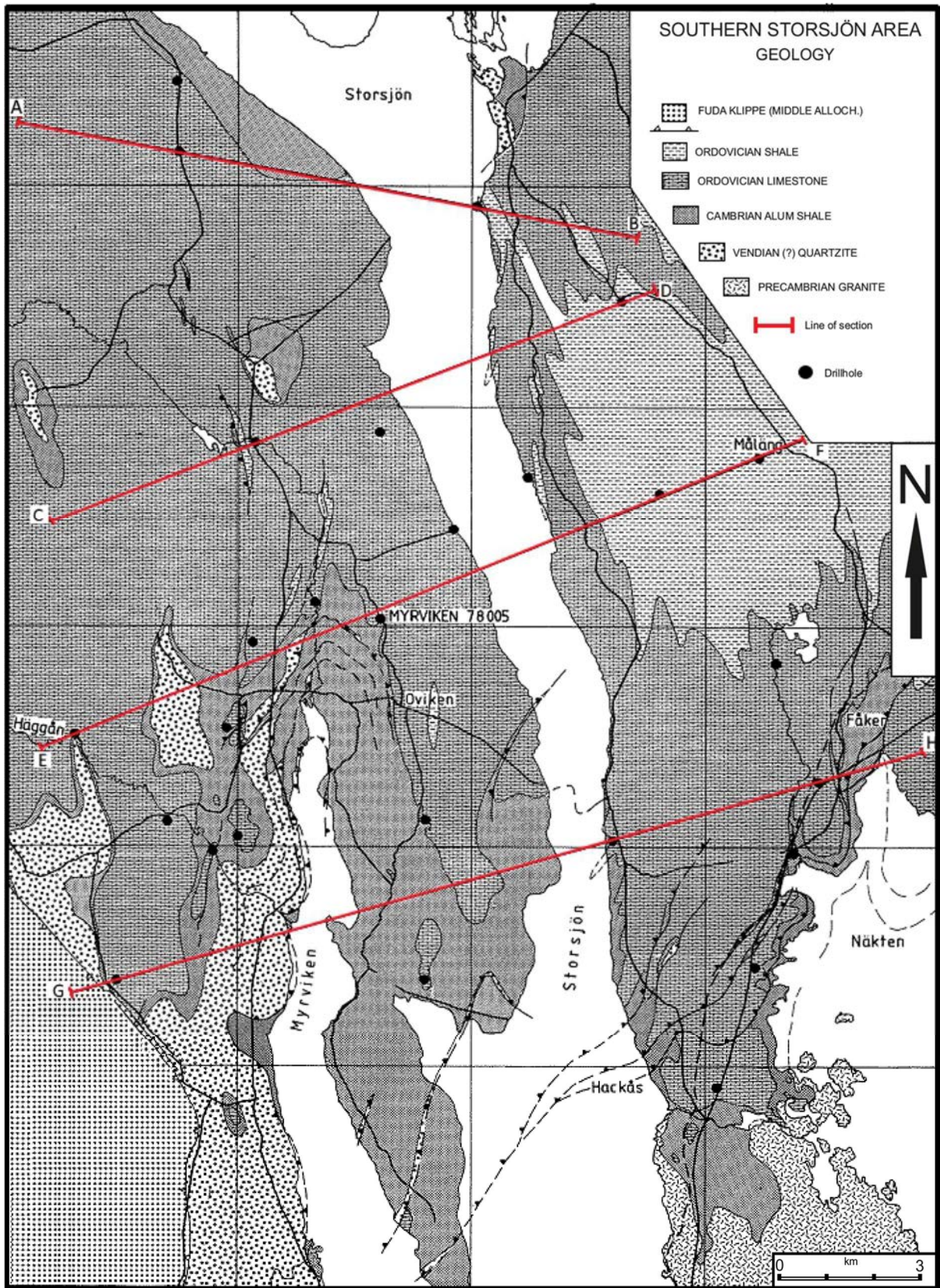


FIG. 200. Bedrock geology of the southern Storsjön area, Jämtland, Sweden (adapted from Ref. [492]).

## SOUTHERN STORSJÖN AREA PROFILES

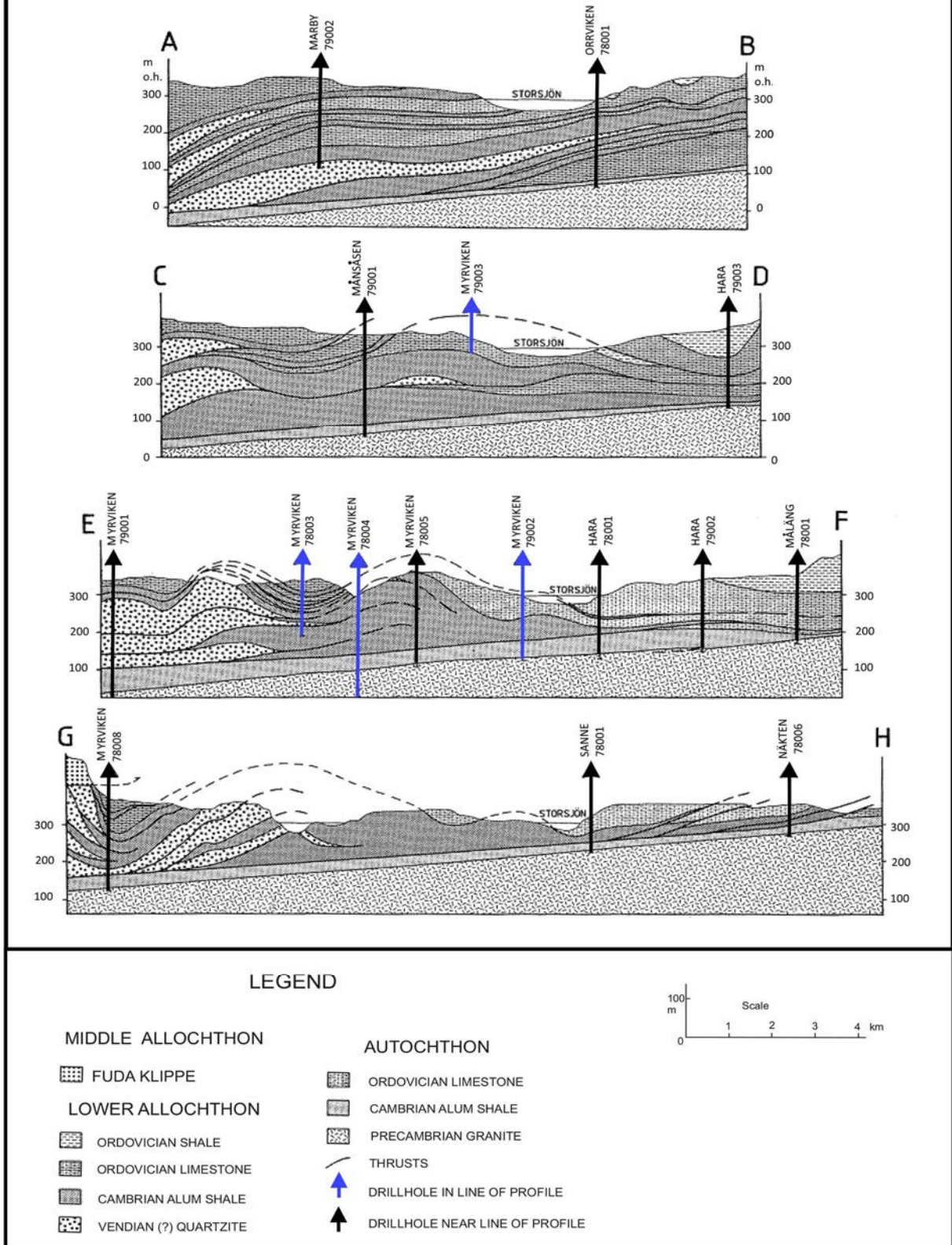
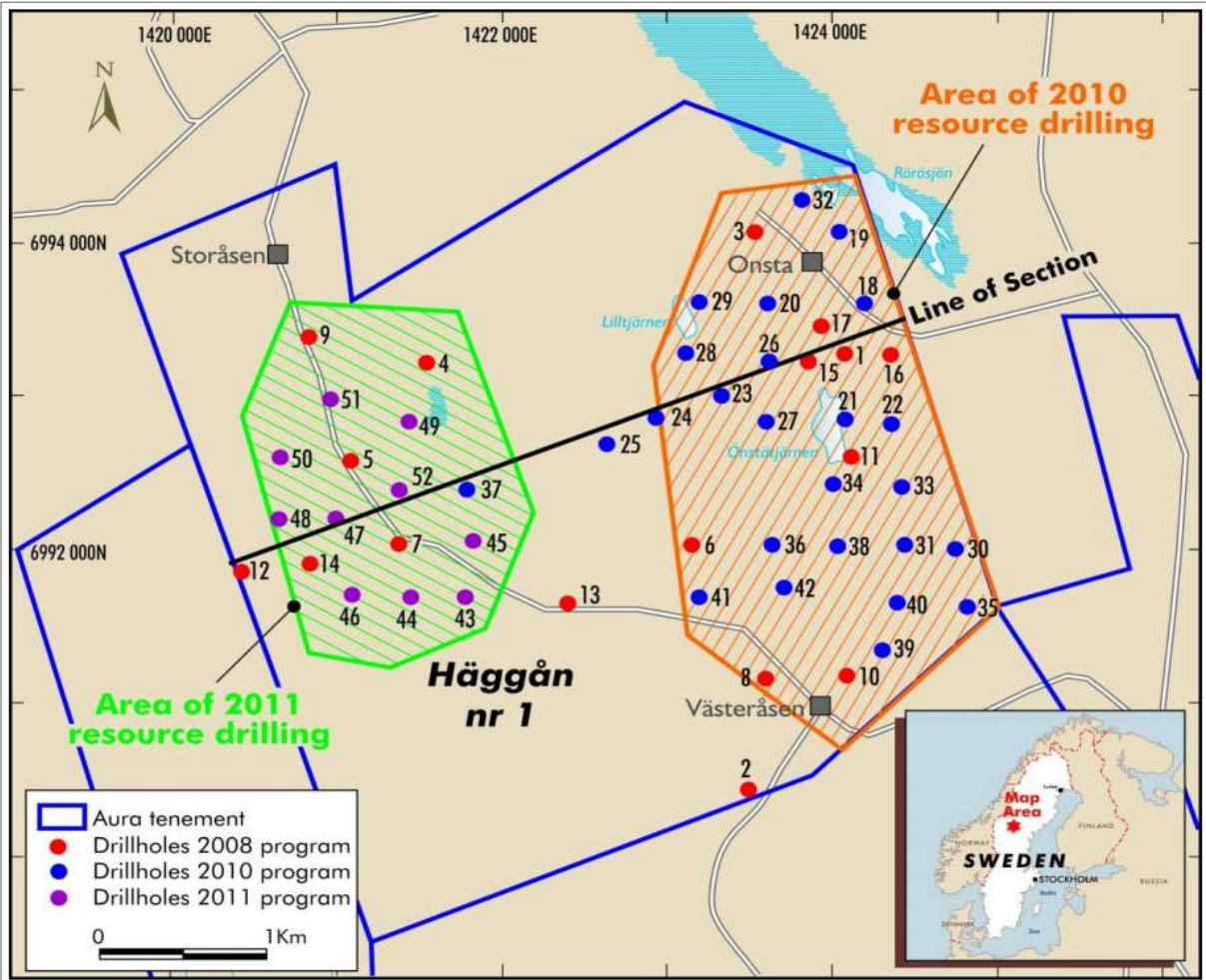
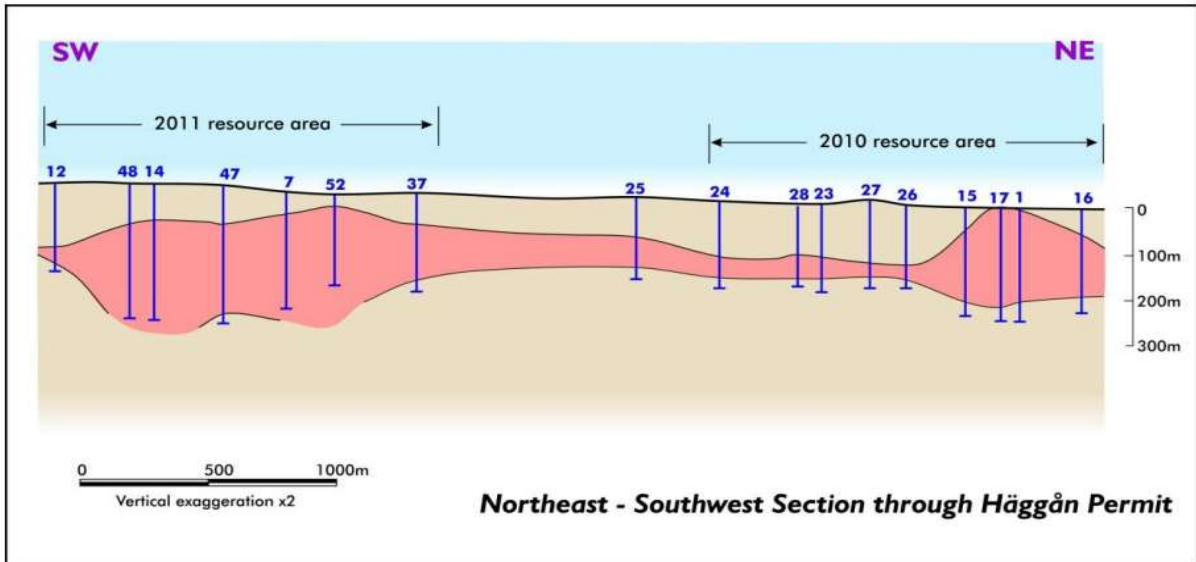


FIG. 201. Sections through the southern Storsjön area, Jämtland, illustrating the thick development of the Alum Shales where they are tectonically repeated (adapted from Ref. [492]).



2010 -11 Haggån drilling



Haggån Drilling Section Highlight

FIG. 202. Haggån prospect: location of Aura Energy drilling and SW-NE cross-section of the deposit [493] (reproduced with permission).

### 3.12.16.2. Fracture-bound or stockwork: The Drosen deposit (Germany)

#### Introduction

The first indications of the presence of uranium came from old reports on radon concentration in spring water at Ronneburg, which had been used for health purposes since the 18th century. Prospecting started after World War II in the region around Ronneburg. Mining took place at the beginning of the 1950s, near the village of Schmirchau. Subsequently, by testing other anomalies, additional deposits were found which permitted extraction by open pit mining, followed by drilling and development of underground mines.

In the Ronneburg area, a number of individual deposits have been found which all share the same characteristics. Therefore, all are considered collectively as 'Ronneburg deposits'.

Mining was carried out in four open pits and six underground mines. The open pit of Lichtenberg was the largest, with a final pit volume of 160 km<sup>3</sup> and a depth of 240 m. A total of 11 000 tU grading 0.094% U were produced from this open pit. The three other open pits (Ronneberg, Stolzenberg, Steinach) were much smaller (only one produced in excess of 100 tU), grading 0.045–0.076% U.

The six underground mines were combined into the following four mining operations:

- |                       |   |
|-----------------------|---|
| (i) Schmirchau/Reust: | 58 800 tu, depth 525 m, average grade 0.082% u; |
| (ii) Paitzdorf :      | 20 300 tu, depth 480 m, average grade 0.085% u; |
| (iii) Beerwalde:      | 7000 tu, depth 600 m, average grade 0.089% u;   |
| (iv) Drosen:          | 3000 tu, depth 780 m, average grade 0.073% u.   |

The Ronneburg orefield produced a total of about 113 000 tU but after deduction of losses, the actual production may have been of the order of 95 000–100 000 tU (exact figures are not known). The Ronneburg orefield was the largest uranium producing area in the former German Democratic Republic and one of the largest producing areas in the world.

The ore was shipped to the nearby processing facility of Seelingstädt. Depending on the chemical composition of ores, acid or alkaline leaching was used. The uranium concentrates were shipped to the former Soviet Union for further treatment.

The remaining resources in the Ronneburg orefield include 51 800 tU in the identified resources category and 39 000 tU as prognosticated resources. The host rocks have been explored for about 150 km<sup>2</sup> and the mining area extended to about 50 km<sup>2</sup>.

Not all the resources are economic and they are no longer accessible as the entire Ronneburg orefield has been remediated. Large parts of the area formerly covered by mining facilities have been transformed into a park-like environment, giving way to a series of gardens.

Nowadays, only a few indications such as the remediated cone-shaped waste rock piles remain as vestiges of the former mining operations. At the time of closure of all WISMUT operations after the reunification of Germany in 1990, an assessment of possible continuation of uranium mining was undertaken. The most favourable area selected was the underground mine at Drosen. However, the potential results of mining could not be economically justified.

#### Geological setting

The Ronneburg area is assigned to the Palaeozoic Saxothuringian metallogenic province (Fig. 203). The sedimentation in the Thuringian Trough started with a 80–100 m thick Lower Ordovician quartzite (Hauptquarzit). Its composition indicates an oxygenated marine environment. By increased subsidence or greater distance to the shore, the marine environment gradually became oxygen-poor in

which shale with organic material was deposited under euxinic to semi-euxinic (sapropelitic) conditions. The shales are at places intercalated with sandy material. Limestone bands are frequent.

The geology of the Ronneburg orefield is shown in Fig. 204. The uranium deposits are hosted by Lower Palaeozoic shale, limestone and mafic intrusions. More specifically, the host units are Upper Ordovician shale (Lederschiefer), which are about 200–250 m thick, Lower Silurian shale (Graptolithenschiefer), which is divided into a lower unit of 30–40 m thickness and an upper bed of 20–30 m thickness, intercalated with a 30–40 m thick bed of limestone (Ockerkalk). A Devonian diabase intrudes the lower part of the Lower Silurian shale and extends into the overlying Lower Devonian limestone package. Intrusions of mafic rocks are frequently observed in similar Silurian–Devonian basins.

Tectonic movements during orogenic phases include thrusting and overturning of strata, which leads to complicated sedimentary sequences. A number of mini-nappes expose the rock sequences in a very intricate way where older strata overlie younger (Fig. 205). As a result of these imbrications, the true thickness is augmented. Compaction and metamorphism to mica schist facies produced a number of metamorphic minerals.

The area belongs to the NE striking East Thuringian Shale Mountains (Östthüringisches Schiefergebirge) and was folded during the Sudetic phase of the Hercynian Orogeny (Carboniferous). The area underwent intense deformation during the Carboniferous, Mesozoic and Cenozoic, resulting in a complicated system of uplifts and depressions with lengths of several kilometres and widths of 200–800 m. Locally, a great number of small faults in zones ranging from a few tens of metres to more than 100 m are observed. These are developed in the area locally known as the ‘ledge of Gera on the uplift of Berga’. The most prominent fault zone is the NW striking Nejdek-Crimmitschau Fault. Along this fault zone, a number of very significant uranium deposits are located near its south-eastern end, including the granite-related uranium deposits of Jachymov, and in its central part, the perigranitic vein style deposits at Schlema and, at its north-western end, the Ronneburg area. To the north and west, the Thuringian Shale area is covered by Permo-Triassic sediments.

#### Mineralization

Genetically, the deposits are of complex nature. They are classified by Dahlkamp [18] as ‘uraniferous carbonaceous shale-related stockwork deposits (Ronneburg type)’ and may be compared to the Chinese ‘carbonaceous–carbonate–siliceous–pelite type’.

About three quarters of the orebodies occur in the Upper Ordovician Lederschiefer, Lower Silurian Graptolithenschiefer and Devonian diabase. The deposits are stratabound and structurally controlled, with mineralization concentrated in stockworks of microfractures within or adjacent to carbonaceous, pyritic black shale/pelite beds. The orebodies are lenticular and are generally found about 300–400 m below the zone of oxidation.

Uranium ore minerals are disseminated pitchblende and occasionally coffinite. Associated gangue and ore phases include carbonates, minor pyrite, Zn and Cu sulphides and occasionally arsenides of Co and Ni [494]. The unweathered shale is rich in organic carbon (up to 9% C), sulphur (up to 3.5% S) and has anomalous values of Mo, V, Ni, As and Sb, thus exhibiting similar features to many other dark shales.

The individual orebodies are of irregular form, variable in size and may contain from 1 tU to more than 1000 tU. The extension of uranium mineralization was followed by drilling to a depth of 1100 m in the northern part of the orefield. Grades vary in the range 0.05–0.3% U, averaging 0.085% U in the mined ore. More than 50% of the ore had grades of 0.07–0.12% U. Grades from underground mines averaged 0.097% U (geological concentration, not production grade).

## Metallogenic aspects

The formation of the orebodies is interpreted by WISMUT [495] as being due to multistage formation. Black shales, exposed at or near the surface, originally containing about 60 ppm U, were oxidized and leached to a depth of about 100 m during Permian weathering (Fig. 206). The presence of sulphides in the shale assisted in the process of leaching during oxidation. Leached uranium was transported downwards along microfaults and fissures and was precipitated at geochemical barriers within the zone of unweathered shale (the cementation zone). Uranium was precipitated in microfaults, fissures and joints. Local conditions were responsible for the complex and irregular distribution of 'ore shoots' (Figs 207–209). Major mineralization events forming the orebodies at different depths occurred around 240 Ma and 90 Ma [495].

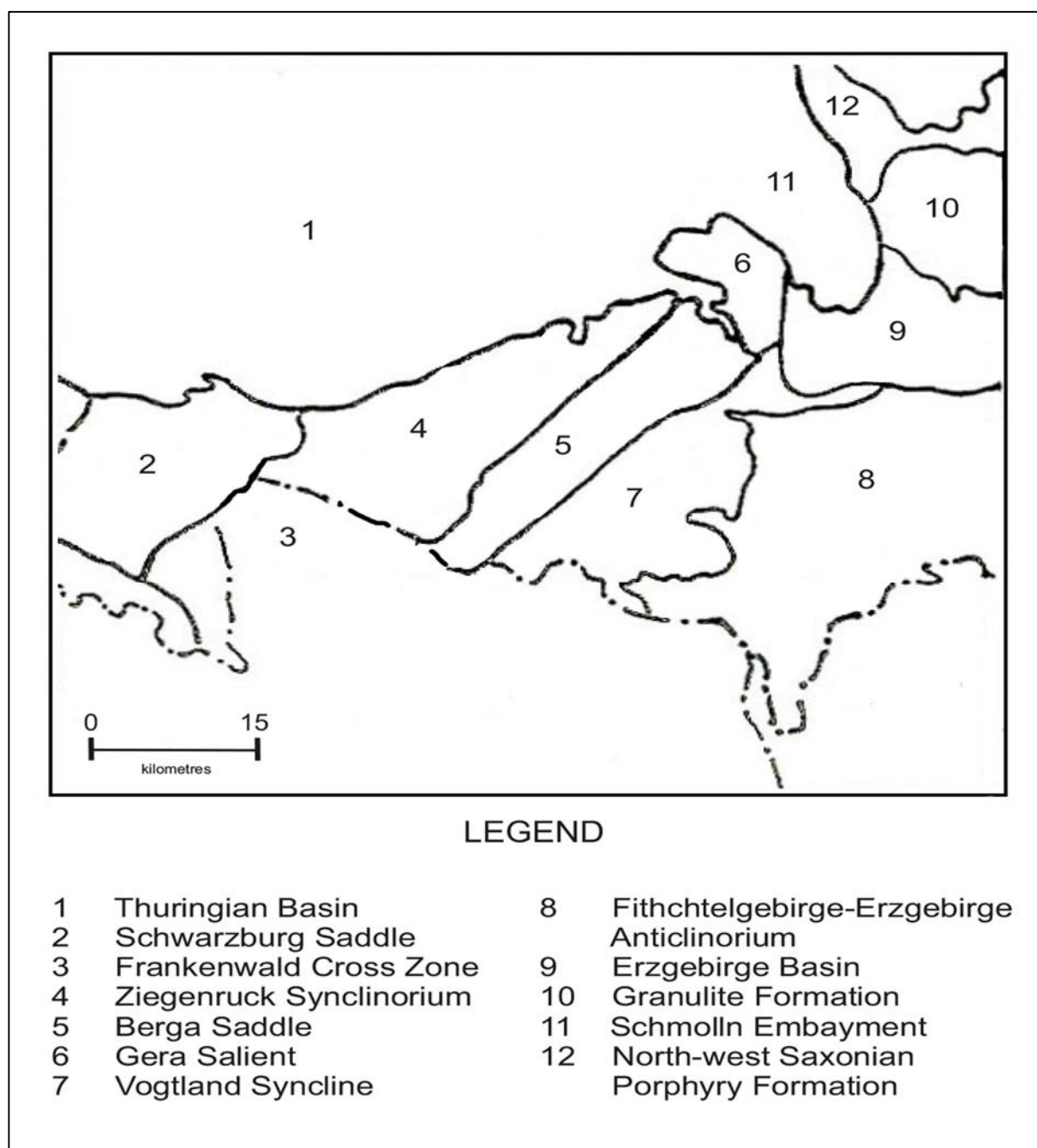


FIG. 203. Schematic geological map of the Thuringian–Vogtland Slate Mountains (adapted from Ref. [494]).

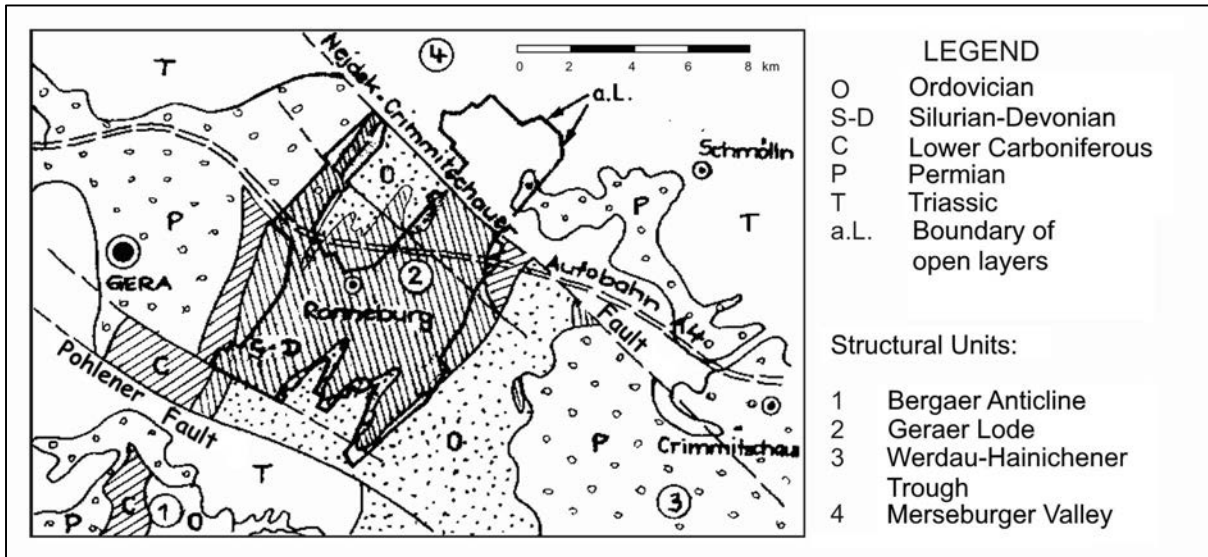


FIG. 204. Schematic geology of the Ronneburg orefield (adapted from Ref. [494]).

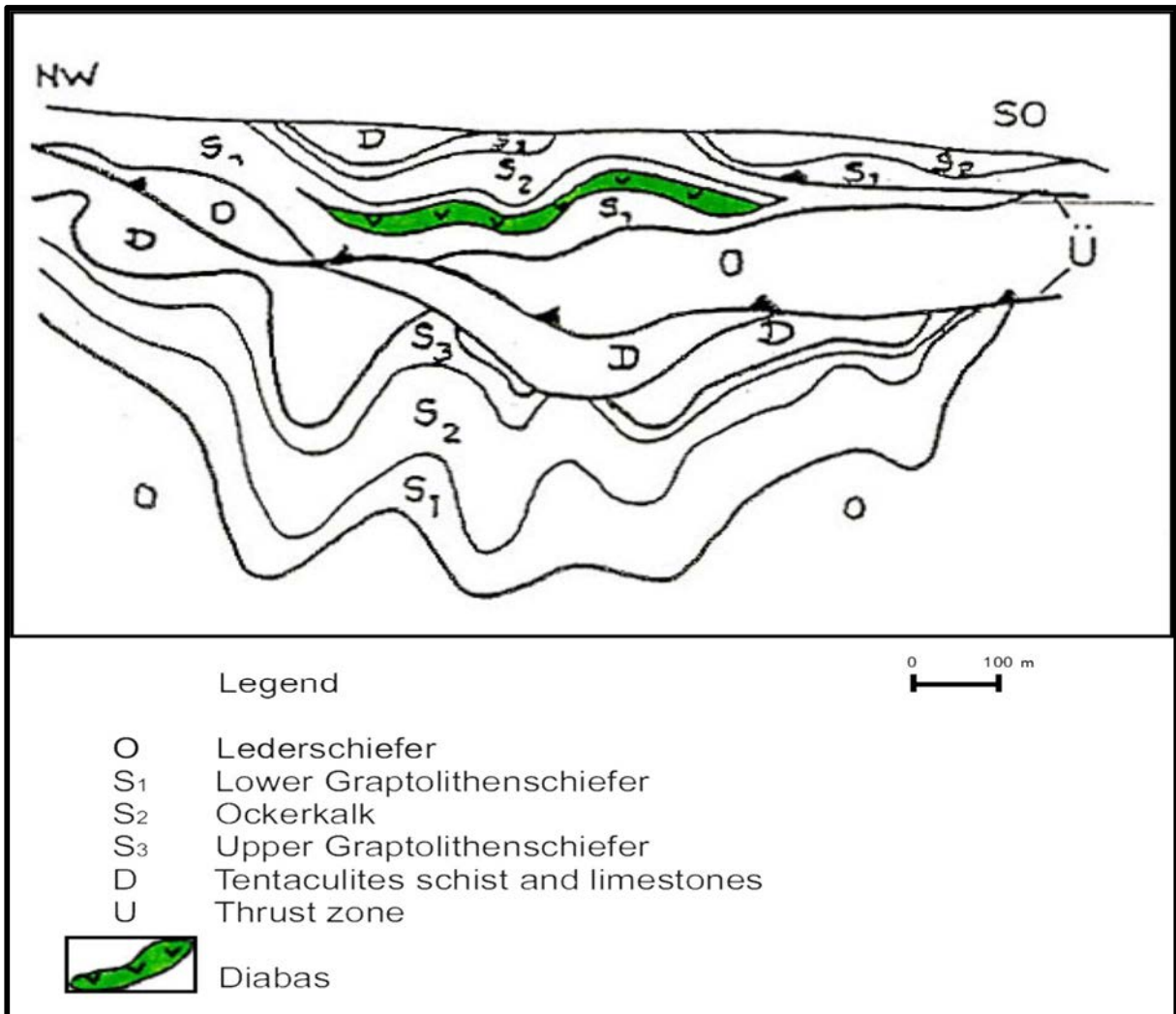


FIG. 205. Geological cross-section showing the thrust tectonics (adapted from Ref. [494]).

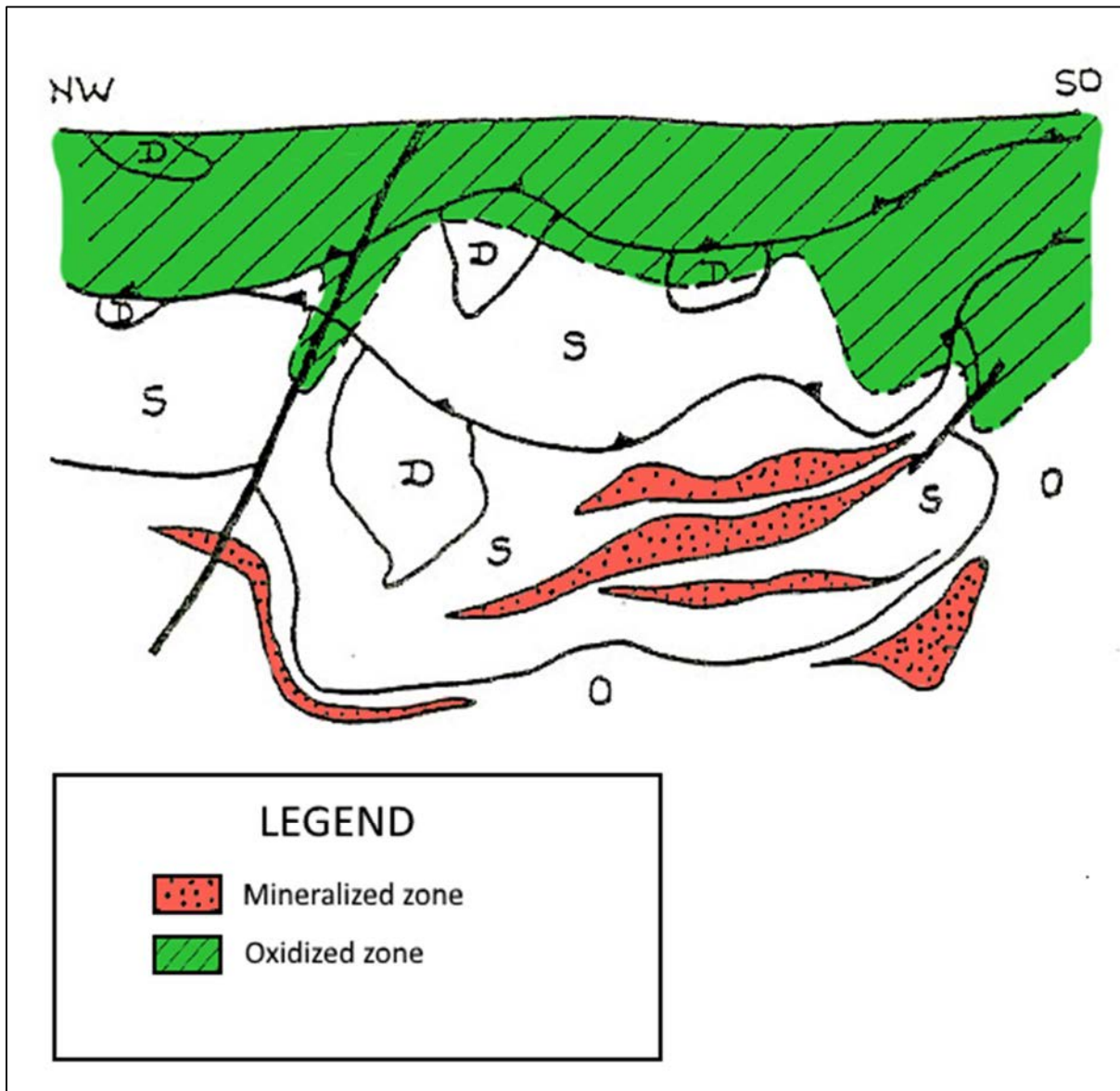


FIG. 206. Geological cross-section showing the oxidation zone (hatched lines) and the mineralized zones (dotted areas) (adapted from Ref. [494]).

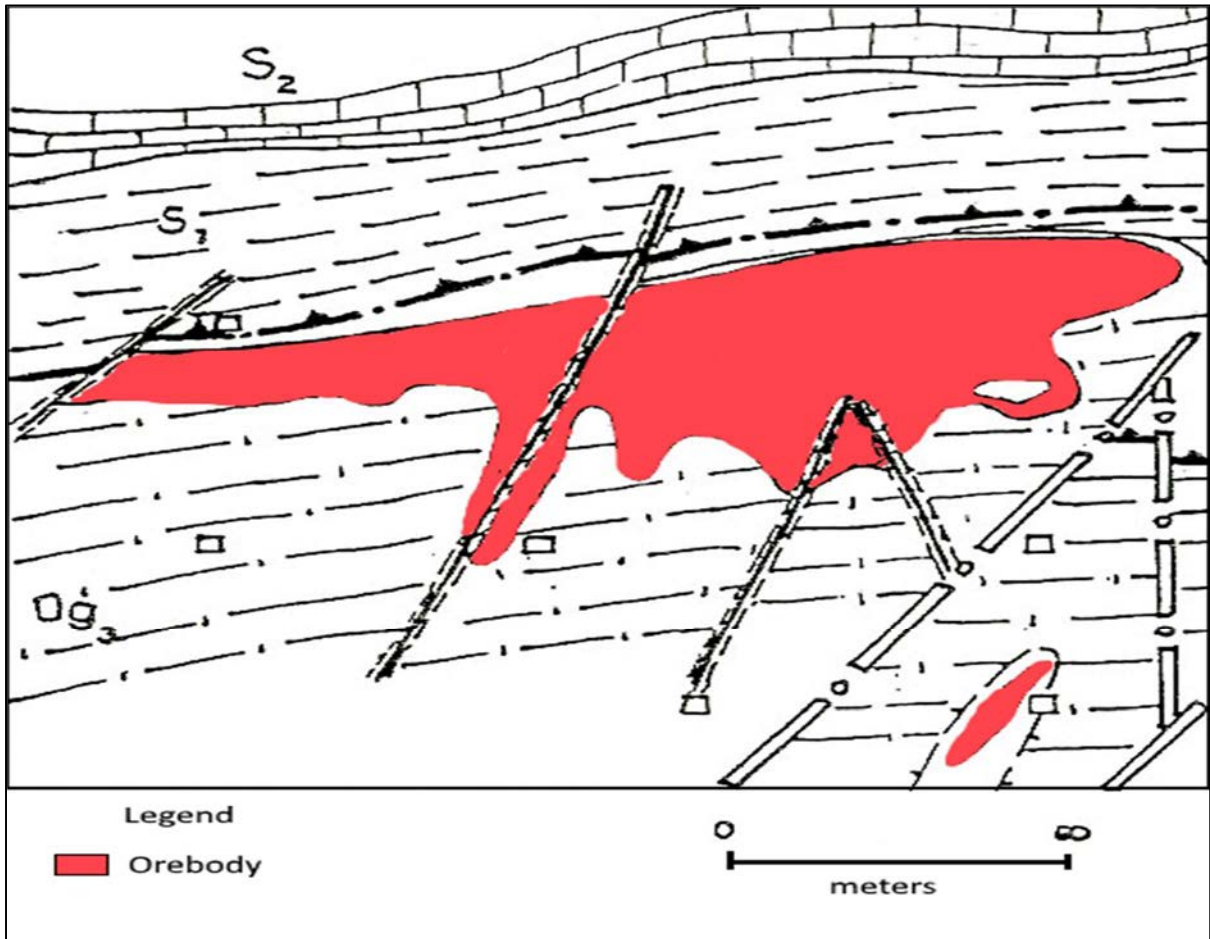


FIG. 207. Cross-section through an orebody (shaded area) (adapted from Ref. [494]).

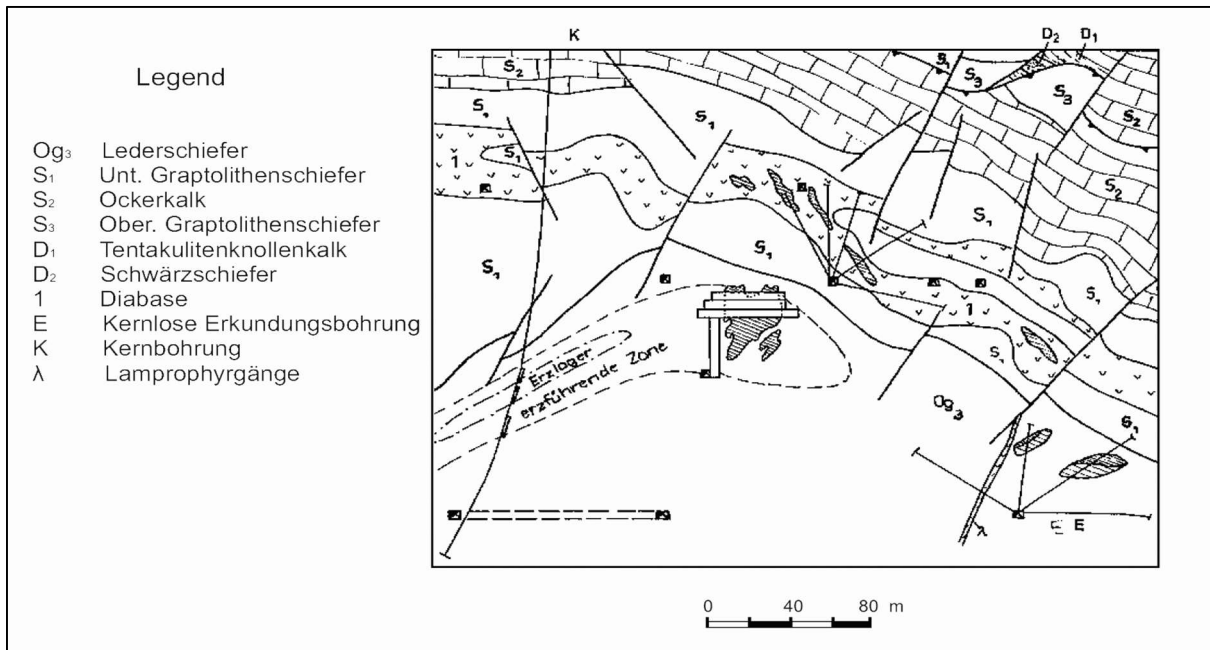
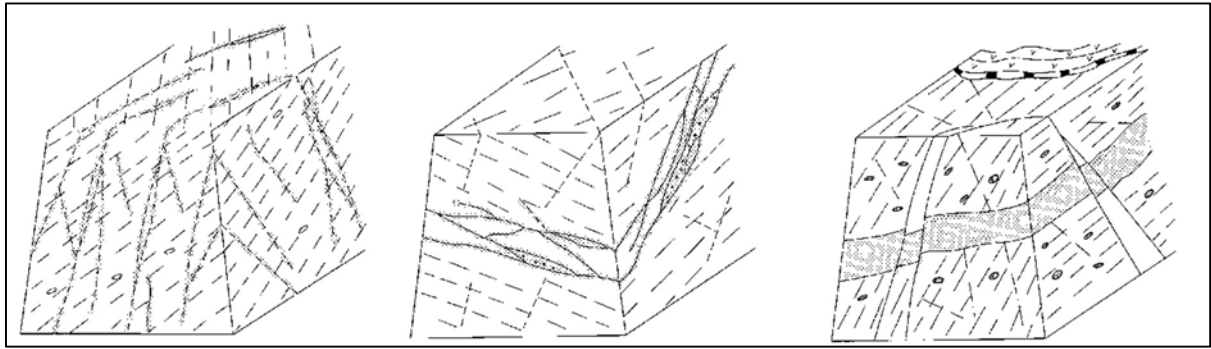


FIG. 208. Ronneburg: geological section illustrating the distribution of orebodies in Ordovician and Silurian strata (adapted from Ref. [494]).



*FIG. 209. Ronneburg, details of cleavage and fracture breccia-hosted uranium mineralization (adapted from Ref. [491]).*

## 4. CONCLUSIONS

After 20 years of low prices, the sharp uranium price rise starting in 2005 produced a dramatic increase in exploration which led to the discovery of numerous new uranium prospects and deposits. Abundant exploration company data became available, considerably expanding the UDEPO database and permitting the improvement of the classification of uranium deposits.

The IAEA saw the necessity for revising the 1993 uranium deposit classification that was used in publications such as the Red Book and based on 582 deposits. In 2010, the IAEA created a working group to review the various existing uranium deposits classifications and to propose a classification which could be internationally used.

This report describes the new geological classification scheme, which is simple and descriptive, but flexible enough to encompass all the recent understanding on the geology and genetic aspects of uranium deposits. Improved type description supported by type examples of well-known deposits for which good data are available are presented, as well as data on deposits with little published information. Along with the descriptive information, new data on uranium resources available for each type is also listed in this report.

On the basis of the 1807 deposits listed in the UDEPO database, 15 types of deposit and more than 40 subtypes/classes are presented in this publication. The actual classification, largely inspired by the work of Dahlkamp, has been used in the 2014 and 2016 editions of the Red Book. In addition, 54 uranium deposits/districts have been described as representative examples of their types/subtypes.

## REFERENCES

- [1] INTERNATIONAL ATOMIC ENERGY AGENCY, World Distribution of Uranium Deposits (UDEPO) with Uranium Deposit Classification, IAEA-TECDOC-1629, IAEA, Vienna (2009).
- [2] BRUNETON, P., CUNEY, M., DAHLKAMP, F.J., ZALUSKI, G., “IAEA geological classification of uranium deposits”, Uranium Raw Material for the Nuclear Fuel Cycle: Exploration, Mining, Production, Supply and Demand, Economics and Environmental Issues, URAM 2014 (Book of Abstracts), Abstract No. 187, IAEA, Vienna (2014).
- [3] BRUNETON, P., CUNEY M., DAHLKAMP, F., ZALUSKI, G., “IAEA geological classification of uranium deposits”, Uranium Raw Material for the Nuclear Fuel Cycle: Exploration, Mining, Production, Supply and Demand, Economics and Environmental Issues, URAM 2014 (Proc. Int. Symp. Vienna, 2014), IAEA, Vienna (in preparation).
- [4] OECD NUCLEAR ENERGY AGENCY, INTERNATIONAL ATOMIC ENERGY AGENCY, Uranium 2014: Resources, Production and Demand, OECD, Paris (2014).
- [5] OECD NUCLEAR ENERGY AGENCY, INTERNATIONAL ATOMIC ENERGY AGENCY, Uranium 2016: Resources, Production and Demand, OECD, Paris (2017).
- [6] UNITED NATIONS, “Géologie de l’uranium et du thorium”, Actes de la conférence internationale sur l’utilisation de l’énergie atomique à des fins pacifiques, Géologie de l’uranium et du thorium, Conference Vol. VI, Geneva (1956).
- [7] ROUBAULT, M., Géologie de l’uranium, Masson et Cie, Editeurs (1958) 463 pp.
- [8] HEINRICH, E.W., Mineralogy and Geology of Radioactive Raw Materials, McGraw Hill, New York, Toronto, London (1958) 654 pp.
- [9] MAUCHER, A., Die Lagerstaetten des Urans. Braunschweig, Vieweg Verlag (1962).
- [10] RUZICKA, V., Geological Comparison between East European and Canadian Uranium Deposits, Department of Energy Mines and Resources, Ottawa (1971) 196 pp.
- [11] ZIEGLER, V., “Essai de classification metallotectique des gisements d’uranium”, Formation of Uranium Ore Deposits (Proc. Int. Conf. Athens, 1974), IAEA, Vienna (1974) 661–677.
- [12] MICKLE, D.G., MATHEWS, G.W., Geologic Characteristics of Environments Favorable for Uranium Deposits, USDOE Rep. GJBX-67 (78) US Department of Energy, Washington (1978).
- [13] MATHEWS, G.W., JONES, C.A., PILCHER, R.C., D’ANDREA, R.F., Jr., Preliminary Recognition Criteria for Uranium Occurrences: A Field Guide, USDOE Rep. GJBX-32 (79), US Department of Energy, Washington (1979).
- [14] NASH, J.T., GRANGER, H.C., ADAMS, S.S., Geology and concepts of genesis of important types of uranium deposits, Econ. Geol. 75th Anniversary Vol. (1981) 63–116.
- [15] BARTHEL, F., DAHLKAMP, F.J., FUCHS, H., GATZWEILER, L., Kernerenergierohstoffe, Angewandte Geowissenschaften (BENDER, F., Ed.) Ferd. Enke Verlag, Stuttgart (1986) 268–298.
- [16] [DAHLKAMP, F.J., Classification of uranium deposits, Mineral. Deposita **13** (1978) 83–104.
- [17] DAHLKAMP, F.J., “Classification scheme of uranium deposits”, Metallogenesis of uranium deposits, IAEA Vienna (1989) 1-31.
- [18] DAHLKAMP, F.J., Uranium Ore Deposits, Springer-Verlag, Berlin (1993) 460.
- [19] DAHLKAMP, F.J., Uranium Deposits of the World: Asia, Springer-Verlag, Berlin and Heidelberg (2009) 493 pp.
- [20] PLANT, J.A., SIMPSON, P.R., SMITH, B., WINDLEY, B.F., Uranium ore deposits: products of the radioactive earth, Reviews in Mineralogy and Geochemistry **38** (1999) 255–319.
- [21] McKAY, A.D., MIEZITIS, Y., Australia’s Uranium Resources, Geology and Development of Deposits, Mineral Resource Report 1, AGSO Geoscience Australia, Canberra (2001) 200 pp.
- [22] KAZANSKY, V.I., LAVEROV, N.P., “Deposits of uranium”, Ore Deposits of the USSR: Vol. II (SMIRNOV, V.I., Ed.), Pitman Publ., London (1977) 349–424.
- [23] BOITSOV, V.E., Geologiya mestorozhdenii urana, NEDRA, Moscow (1989) 302 pp (in Russian).

- [24] BOITSOV, V.E., *Geologiya mestrozhdennii urana: uchebnoe posobie*, MGGA, Moscow (1996) 72 pp (in Russian).
- [25] STOIKOV, H.M., BOJKOV, I.B., *Geology and exploration of uranium deposits*, Spector, Sofia (1991) 148 pp (in Bulgarian).
- [26] PETROV, N.N., YAZIKOV, V.G., AUBAKIROV, H.B., PLEKANOV, V.N., VERSHKOV, A.F., LUKHTIN, V.F., *Uranium deposits of Kazakhstan (exogenous)*, Gylym Almaty (1995) 264 pp (in Russian).
- [27] PETROV, N.N., YAZIKOV, V.G., BERIKBOLOV, B.R., VERSHKOV, A.F., EGOROV, S.A., ZHELNOV, V.P., KARELIN, V.G., KRAVTSOV, E.G., NIKOLAEV, S.L., OSTROKOM, I.M., SHISHKOV, I.A., *Uranium deposits of Kazakhstan (endogenous)*, Gylym Almaty (2000) 523 pp (in Russian).
- [28] MASHKOVTSSEV, G.A., KISLYAKOV, Y.M., MIGUTA, A.K., MODNIKOV, I.S., *Commercial genetic types of uranium deposits*, *Otechestvennaya Geologia* **4** (1998) 37–52 (in Russian).
- [29] TARKHANOV, A.V., POLUARSHINOV, G.P., “Spatio-chronological positions of Precambrian uranium deposits”, *Metallogenesis of Uranium Deposits (Proc. Tech. Mtg Vienna, 1987)*, IAEA, Vienna (1989) 201–210.
- [30] BOITSOV, A., “Basic criteria for U deposits classification”, paper presented at IAEA Tech. Mtg on Classification of World Uranium Deposits with a Focus on Volcanic-related Deposits, Vienna, 2013.
- [31] McMILLAN, R.H., “Metallogenesis of Canadian uranium deposits: A review”, *Geology, Mining and Extracting Processing of Uranium (Proc. Int. Symp. London, 1977)*, Institute of Mining and Metallurgy, London (1977).
- [32] WILPOLT, R.H., SIMOV, S.D., *Uranium deposits in Africa: Geology and exploration (Proc. Regional Adv. Group Mtg Lusaka, 1977)*, IAEA, Vienna (1979) 3–20.
- [33] SULLIVAN, C.J., *Intercratonic basins and ore deposits*, *CIM Bull.* **72** (1979) 812 pp.
- [34] INTERNATIONAL ATOMIC ENERGY AGENCY, *Guidebook to Accompany IAEA Map: World Distribution of Uranium Deposits*, IAEA, Vienna (1996).
- [35] KREUZER, O.P., MARKWITZ, V., PORWAL, A.K., McCUAIG, T.C., *A continent-wide study of Australia’s uranium potential, Part I: GIS-assisted manual prospectivity analysis*, *Ore Geology Reviews* **38** (2010) 334–366.
- [36] INTERNATIONAL ATOMIC ENERGY AGENCY, *Methods of Exploitation of Different Types of Uranium Deposits*, IAEA-TECDOC-1174, IAEA, Vienna (2000).
- [37] CUNEY, M., *Felsic magmatism and uranium deposits*, *Bull. Soc. Géol. France* **185** 2 (2014) 75–92.
- [38] SKIRROW, R.G., JAIRETH, S., HUSTON, D.L., BASTRAKOV, E.N., SCOFIELD, A., van der WIELEN, S.E., BARNICOAT, A.C., *Uranium Mineral Systems: Processes, Exploration Criteria and a New Deposit Framework*, Record 2009/20, Geoscience Australia, Canberra (2009) 49 pp.
- [39] McCUAIG, T.C., BERESFORD, S.W., HRONSKY, J.M.A., *Translating the mineral systems approach into an effective exploration targeting system*, *Ore Geol. Rev.* **38** (2010) 128–138.
- [40] CUNEY, M., *The extreme diversity of uranium deposits*, *Miner. Deposita* **44** (2009) 3–9.
- [41] CUNEY M., “Uranium and thorium: The extreme diversity of the resources of the world’s energy minerals”, *Non-renewable Resource Issues: Geoscientific and Societal Challenges*, Springer-Verlag, Amsterdam (2012) 91–129.
- [42] TURPIN, L., MARUEJOL, P., CUNEY, M., *Comparative U-Pb, Rb-Sr and Sm-Nd chronology of granitic basement, hydrothermal albitites and uranium mineralization (Lagoa Real, South-Bahia, Brasil)*, *Contrib. Mineral. Petrol.* **98** (1988) 139–147.
- [43] INTERNATIONAL ATOMIC ENERGY AGENCY, *World Distribution of Uranium Deposits (UDEPO) 2016 Edition*, IAEA, Vienna (2017).
- [44] BRUNETON, P., CUNEY, M., “Geology of uranium deposits”, *Uranium for Nuclear Power (HORE-LACY, I., Ed.)*, Woodhead Publishing Series in Energy No. 93, Elsevier, Amsterdam (2016) 11–52.

- [45] CUNEY, M., KYSER, K., Recent and not so recent developments in uranium deposits and implications for exploration, Short Course Series, Vol. 39, Mineralogical Association of Canada, Quebec (2008) 272 pp.
- [46] ALEXANDER, R.L., Geology of Madawaska Mines Limited, Bancroft, Ontario, Uranium Deposits of Canada (EVANS, E.L., Ed.), Can. Inst. Min. Metall. **33** (1986) 62–69.
- [47] DAHLKAMP, F.J., Uranium Deposits of the World: USA and Latin America, Springer-Verlag, Berlin and Heidelberg (2010) 517 pp.
- [48] SINGER, D.A., BERGER, V.I., MORING, B.C., Porphyry Copper Deposits of the World: Database, Maps and Grade and Tonnage Models, Open-File Report 2005-1060, US Geological Survey, Reston, VA (2005).
- [49] ORRIS, G.J., GRAUCH, R.I., Rare Earth Element Mines, Deposits and Occurrences, Open-File Report 02-189, US Geological Survey, Reston, VA (2002).
- [50] VERWOERD, W.J., “Mineral deposits associated with carbonatites and alkaline rocks”, Mineral Deposits of South Africa (ANHAEUSSER, C.R., MASKE, S., Eds), Geol. Soc. S. Afr., Johannesburg (1986) 2173–2192.
- [51] BERGER, V.I., SINGER, D.A., ORRIS, G.J., Carbonatites of the World, Explored Deposits of Nb and REE: Database and Grade and Tonnage Models, Open-File Report 2009-1139, US Geological Survey, Reston, VA (2009) 17 pp.
- [52] LENZ, D., U, Mo and REE mineralization in late-tectonic granitic pegmatites, southwestern Grenville Province, Canada, Ore Geol. Rev. **11** (1976) 197–227.
- [53] CUNEY, M., “Processus de concentration de l’uranium et du thorium au cours de la fusion partielle et de la cristallisation des magmas granitiques”, Les méthodes de prospection de l’uranium, OECD, Paris (1982) 277–292.
- [54] REDMOND, P.B., EINAUDI, M.T., The Bingham Canyon Porphyry Cu-Mo-Au Deposit: I. Sequence of Intrusions, Vein Formation, and Sulfide Deposition, Econ. Geol. **105** (2010) 43–68.
- [55] EXTRACT RESOURCES LTD, web site (accessed 2010).
- [56] COFFEY MINING PTY LTD, Husab Project, Namibia, NI 43-101 Technical Report Rossing South – August 2009 Resources Update, prepared by Coffey Mining Pty Ltd on behalf of Extract Resources Ltd (2009) 145 pp.
- [57] SPIVEY, M., PENKETHMAN, A., “Discovery of the granite (alaskite) hosted Rossing South uranium deposit in Namibia: an exploration perspective”, abstract presented at Mineral Exploration Roundup, Vancouver, 2009.
- [58] TRÖGER, W.E., Spezielle Petrographie der Eruptivgesteine: ein Nomenklaturkompendium mit 1 Nachtrag: Eruptivgesteinsnamen, Verlag der Deutschen Mineralogischen Gesellschaft, Stuttgart (1969) 360 + 50.
- [59] EXTRACT RESOURCES LTD, [www.extractresources.com.au](http://www.extractresources.com.au). (accessed 2011).
- [60] [BOWDEN, P., HERD, D., KINNAIRD, A., The significance of uranium and thorium concentrations in pegmatitic leucogranites (alaskites), Rossing mine, Swakopmund, Namibia, Comm. Geol. Surv. Namibia **10** (1995) 44–49.
- [61] CUNEY, M., Comportement de l’uranium et du thorium au cours du métamorphisme: Rôle de l’anatexie dans la genèse des magmas riches en radioéléments, PhD Thesis, Nancy (1981).
- [62] LAFLEUR, J., The North Shore Property, Turgeon, Weegee, Highway, Ponbriand and NE Costebelle Claim Blocks, Province of Quebec, Canada, UFM Ventures Ltd, NI-43-101 Technical Report (2006).
- [63] BOILY, M., LEPAGE, L., The Doran Property, Lower North Shore, Quebec, Canada, NI 43-101 Technical Report and Recommendations, Abbastar Uranium Corporation (2009).
- [64] BRODIE, S., The Double S Zone Deposit on the North Shore of The St. Lawrence Seaway in Eastern Quebec, Canada: Mineralogic, Petrogenetic, and Geochronologic Constraints, BSc. Dissertation (unpublished), University of New Brunswick (2008).
- [65] SRK CONSULTING, Uracon North Shore Property: Double S Zone Technical Report, Quebec, Canada (2010).
- [66] PARRY, W.T., WILSON, P.N., MOSER, D., HEIZLER, M.T., U-Pb dating of zircon and  $40\text{Ar}/39\text{Ar}$  dating of biotite at Bingham, Utah, Econ. Geol. **96** (2001) 1671–1683.

- [67] INTERSTATE TECHNOLOGY AND REGULATORY COUNCIL, Mining Waste Treatment Technology Selection – Bingham Canyon Water Treatment Plant – Kennecott South Zone, [http://www.itrcweb.org/miningwaste-guidance/cs48\\_kennecott\\_south.pdf](http://www.itrcweb.org/miningwaste-guidance/cs48_kennecott_south.pdf)
- [68] TERTIARY MINERALS, <http://www.tertiaryminerals.com/projects/other-projects/ghurayyah> (accessed 2006).
- [69] KUSTER, D., Granitoid-hosted Ta mineralization in the Arabian-Nubian Shield: Ore deposit types, tectono-metallogenic setting and petrogenetic framework, *Ore Geol. Rev.* **35** (2009) 68–86.
- [70] STOESER, D.B., Distribution and tectonic setting of plutonic rocks of the Arabian Shield, *J. African Earth Sci.* **4** (1986) 21–26.
- [71] DRYSDALL, A.L., JACKSON, N.J., RAMSAY, C.R., DOUCH, C.J., HACKETT, D., Rare element mineralization related to Precambrian alkali granites in the Arabian Shield, *Econ. Geol.* **79** (1984) 1366–1377.
- [72] RAMSAY, C.R., DRYSDALL, A.R., CLARK, M.D., Felsic plutonic rocks of the Midyan region, Kingdom of Saudi Arabia: distribution, classification and resource potential, *J. African Earth Sci.* **4** (1986) 63–77.
- [73] LALANDE, P., Final Report on Preliminary Geological and Geophysical Investigation of the Ghurayyah Radioactive Granite, Kingdom of Saudi Arabia, Open File Report DGMR-605, Saudi Arabian Directorate Gen. Mineral Resources, Riyadh (1977).
- [74] JACKSON, N.J., RAMSAY, C.R., Post-orogenic felsic plutonism, mineralization and chemical specialization in the Arabian Shield, *Trans. Inst. Min. Metall.* **B 95** (1986) 83–93.
- [75] GREENLAND MINERALS AND ENERGY LTD, Upgraded Resource Estimate for the Kvanefjeld Multi-Element Project (REEs, U, Zn), press release, March 2011.
- [76] GREENLAND MINERALS AND ENERGY LTD, <http://www.ggg.gl/> (accessed September 2012).
- [77] STEENFELT, A., KUNZENDORF, H., FRIEDRICH, G.H.W., Randboldal: Uranium in stream sediments, soils and water, *J. Geochem. Explor.* **5** (1976) 300–306.
- [78] BOHSE, H., ROSE-HANSEN, J., SORENSEN, H., STEENFELT, A., LOVBORG, L., KUNZENDORF, H., “On the behavior of uranium during crystallization of magma – with special emphasis on alkaline magmas”, *Formation of Uranium Ore Deposits (Proc. Int. Conf. Athens, 1974)*, IAEA, Vienna (1974) 49–60.
- [79] HANSEN, J., A Study of the Radioactive Veins Containing Rare Earth Minerals in the Area Surrounding the Ilimaussaq Alkaline Intrusion in South Greenland: Contributions to the Mineralogy of Ilimaussaq, Issue 12, *Grønlands Geologiske Undersøgelse* (1968) 47 pp.
- [80] STEENFELT, A., BOHSE, H., Variations in the content of uranium of eudialyte in the differentiated alkaline Ilimaussaq intrusion, South Greenland, *Lithos* **8** (1975) 39.
- [81] STEENFELT, A., “Field relations in the roof zone of the Ilimaussaq intrusion with special reference to the position of the alkali acid rocks”, *The Ilimaussaq intrusion, South Greenland: A Progress Report on Geology, Mineralogy, Geochemistry and Economic Geology* (BAILEY, J.C., LARSEN, L.M., SØRENSEN, H., Eds), *Grønlands Geologiske Undersøgelse* **103** (1981) 43–52.
- [82] GREENLAND MINERALS AND ENERGY LTD, Greenland Minerals Extends ‘Zone 2’ Rare Earth–Uranium Deposit with Broad Drill Intercepts, press release, January 2012.
- [83] GREENLAND MINERALS AND ENERGY LTD, “Agpaitic Nepheline Syenites of the Ilimaussaq Complex, Greenland: An Important New Uranium Ore-type”, paper presented at IAEA Meeting on Uranium from Unconventional Resources, Vienna, 2009.
- [84] GREENLAND MINERALS AND ENERGY LTD, Exploration Unearths New Discovery in the Northern Ilimaussaq Complex, press release, July 2010.
- [85] GREENLAND MINERALS AND ENERGY LTD, Agpaitic Nepheline Syenites of the Ilimaussaq Complex, Greenland: An Important New Uranium Ore-Type, company presentation, IAEA – Uranium from Unconventional Resources, November 2009.
- [86] CARVALHO, W.T., VALENÇA, I.R., “A prospecção radiométrica na definição de zonas mineralizadas no complexo alcalino-ultramáfico de Catalão I, GO”, paper presented at XXIX Congr. Bras. Geologia, Belo Horizonte (1976).

- [87] GUIMARAES, H.N., WEISS, A.R., The complexity of the niobium deposits in the alkaline-ultramafic intrusions Catalão I and II, Brazil. *Mineracao Catalao*, Sao Paulo, Brazil (2001).
- [88] RIBEIRO, C.C., *Geologia, Geometalurgia, Controles e Gênese dos Depósitos de Fósforo, Terras Raras e Titânio do Complexo Carbonatítico de Catalão I, GO*, PhD Thesis, Univ. Brasília (2008), <http://repositorio.unb.br/handle/10482/1695>
- [89] NEUMANN, R., *Caracterização Tecnológica dos Potenciais Minérios de Terras-Raras de Catalão I, GO*, PhD Thesis, Univ. São Paulo (1999), <http://www.teses.usp.br/teses/disponiveis/44/44135/tde-08012016-151612/>
- [90] LAPIDO-LOUREIRO, F.E., *Projeto Catalão Sul, Relatório Anual*, NUCLEBRAS/DIGEO (1979).
- [91] BENEDETTO, J.S., *Estudos preliminares de abertura química e separação física em amostras do processamento semi-industrial da METAGO*, NUCLEBRAS-SUEMI-DETM.PD/DEP.EM – Julho/79 (1979).
- [92] SAREYED-DIM, N.A., *Análise e comentários sobre a nota técnica DIGEO*, PM 01/80 (1980).
- [93] SOUZA, A.E., FONSECA, D.S., “Fosfato”, *Economia Mineral do Brasil* (RODRIGUES, A.F.S., Ed.), Departamento Nacional de Produção Mineral, Brasília (2009).
- [94] SOBRAL, L.G.S., SANTOS, R.L.C. e LAPIDO-LOUREIRO, F.E.V., *Estudo de recuperação de alumínio, terras raras, nióbio residual e urânio-tório em escórias da produção de ferro-nióbio standard*, Tech. Rep. No. RT2003-047-00, CETEM, Rio de Janeiro (2003).
- [95] CORDEIRO, P.F.O., *Petrologia e Metalogenia do Depósito Primário de Nióbio do Complexo Carbonatítico-Foscorítico de Catalão I, GO*, M.Sc. Dissertation, Univ. Brasília (2009).
- [96] CORDEIRO, P.F.O., BROD, J.A., SANTO, R.V., DANTAS, E.L., OLIVEIRA, C.G., BARBOSA, E.S.R., Stable (C, O) and radiogenic (Sr, Nd) isotopes of carbonates as indicators of magmatic and post-magmatic processes of phoscorite-series rocks and carbonatites from Catalão I, central Brazil, *Contrib. Mineral. Petrol.* **161** 3 (2011) 451–464.
- [97] CATHELINÉAU, M., Les mécanismes de type “roll-front” dans les granites: un modèle de remobilisation dans les gisements hydrothermaux d’uranium, *Comptes Rendus à l’Académie des Sciences*, 294 (1982) 865–868.
- [98] CUNEY, M., *Geologic environment, mineralogy, and fluid inclusions of the Bois Noirs-Limouzat uranium vein, Forez, France*, *Econ. Geol.* **73** (1978) 1567–1610.
- [99] POTY, B., LEROY, J., CATHELINÉAU, M., CUNEY, M., FRIEDRICH, M., LESPINASSE, M., TURPIN, L., “Uranium deposits spatially related to granites in the French part of the Hercynian Orogen”, *Vein Type Uranium Deposits*, IAEA-TECDOC-361, IAEA, Vienna (1986) 215–246.
- [100] TURPIN, L., CUNEY, M., FRIEDRICH, M., BOUCHEZ, J.L., AUBERTIN, M., *Metaigneous origin of peraluminous granites in NW French Massif Central: Implications for crustal history reconstructions*, *Contrib. Mineral. Petrol.* **104** (1990) 163–172.
- [101] OECD NUCLEAR ENERGY AGENCY, INTERNATIONAL ATOMIC ENERGY AGENCY, *Uranium 1991: Resources, Production and Demand*, OECD, Paris (1992).
- [102] LI TIANGANG, HUANG ZHIZHANG, “Vein uranium deposits in granites of Xiazhuang ore field”, *Vein Type Uranium Deposits*, IAEA-TECDOC-361, IAEA, Vienna (1986) 359–376.
- [103] SHEN FENG, PAN YONGZHENG, GONG ZHIGEN, RONG JIASHU, “Geological features and new development of the Xiashuang uranium ore field in South China”, *New Developments in Uranium Exploration, Resources, Production and Demand*, IAEA-TECDOC-650, IAEA, Vienna (1992) 169–172.
- [104] LESPINASSE, M., *Contexte structural des gisements d’uranium de la Marche occidentale, fracturation, circulations fluides, propagation de l’episyénitisation*, CREGU, *Géologie et Géochimie de l’Uranium*, Mem. **8** (1984).
- [105] STUSSI, J.M., *Granitoid chemistry and associated mineralization in the French Variscan*, *Econ. Geol.* **84** (1989) 1363–1381.
- [106] PATRIER, P., BEAUFORT, D., BRIL, H., BONHOMME, M., FOUILLAC, A.M., AUMAITRE, R., *Alteration mineralization at the Bernardan U deposit (Western Marche, France): The contribution of alteration, petrology and crystal chemistry of secondary phases to a new genetic model*, *Econ. Geol.* **92** (1997) 448–467.

- [107] LESPINASSE, M, PECHER, A, Microfracturing and regional stress field: A study of the preferred orientations of fluid inclusion planes in a granite from the Massif Central, France, *J. Struct. Geol.* **8** (1986) 169–180.
- [108] MICHEL, J.J., Episyénites et concentrations uranifères associées dans le massif de Saint Sulpice les Feuilles (France), PhD Thesis, Institut National Polytechnique de Lorraine (1983).
- [109] LEROY, J., Le gisement uranifère du Bernardan (Marche, France): Un exemple d'épisyénitisation d'un granite à deux micas, *Comptes Rendus à l'Académie des Sciences*, **296** (II) (1982) 75–78.
- [110] LEROY, J., Episyénitisation dans le gisement d'uranium du Bernardan (Marche), comparaison avec des gisements similaires du nord-ouest du Massif Central français, *Miner. Deposita* **19** (1984) 26–35.
- [111] PEINADOR-FERNANDEZ, A., JAMET, P., LE CAIGNEC, R., MOREAU, M., SERRANO, J.R., ZIEGLER, V., Gisements d'uranium dans les schistes péritholitiques (type Ibérique) et dans les leucogranites (type Limousin) (Portugal, Espagne, France), *Livret guide d'excursion, Sciences de la terre* **XXIII** 4 (1977) 1–47.
- [112] GUIOLLARD, P.C., MILVILLE, G., L'uranium de deux 'privés', Editions Pierre-Christian Guiollard (2003).
- [113] DAHLKAMP, F.J., Uranium deposits of the world: Europe, Springer-Verlag, Berlin and Heidelberg (2013).
- [114] FÖRSTER, H.-J., TISCHENDORF, G., TRUMBULL, R.B., GOTTESMANN, B., Late-collisional granites in the Variscan Erzgebirge, Germany, *J. Petrol.* **40** (1999) 1613–1645.
- [115] TICHOMIROVA, M., LEONHARDT, D., New age determinations (Pb/Pb zircon evaporation, Rb/Sr) on the granites from Aue-Schwarzenberg and Eibenstock, Western Erzgebirge, Germany, *Z. Geol. Wiss.* **38** (2010) 99–123
- [116] FÖRSTER, H.-J., The chemical composition of uraninite in Variscan granites of the Erzgebirge, Germany, *Min. Mag.* **63** (1998) 239–252.
- [117] ROMER, R.L., THOMAS, R., STEIN, H.J., RHEDE, D., Dating multiply overprinted Sn-mineralized granites—examples from the Erzgebirge, Germany, *Miner. Deposita* **42** (2007) 337–359.
- [118] FÖRSTER, H.-J., TISCHENDORF, G., RHEDE, D., Mineralogy of the Niederschlema–Alberoda U–Se polymetallic deposit, Erzgebirge, Germany, V – watsinsonite, nevskite, bohdanowiczite and other bismuth minerals, *Can. Miner.* **43** (2005) 899–908.
- [119] WISMUT GmbH, Die Chronik der Wismut (CD-ROM), Chemnitz (1999).
- [120] HARLASS, E.S., SCHUTZEL, H., Zur paragenetischen Stellung der Uranpechblende in den hydrothermalen Lagerstätten des westlichen Erzgebirges, *Z. Angew. Geol.* **11** (1965) 569–582.
- [121] SCHUPPAN, W., BÜDER, W., LANGE, G., “On uranium mineralization in the vein deposits of the western Erzgebirge, Germany”, *Mineral Deposits of the Erzgebirge/Krušné hory (Germany/Czech Republic)* (von GEHLEN, K., KLEMM, D.D., Eds), Gebrüder Bornträger, Berlin and Stuttgart (1994) 191–207.
- [122] FÖRSTER, B., HAACK, U., U/Pb-Datierungen von Pechblenden und die hydrothermale Entwicklung der U-Lagerstätte Aue–Niederschlema (Erzgebirge), *Z. Geol. Wiss.* **23** (1995) 581–588.
- [123] FÖRSTER, H.-J., The late-Variscan granites of the Aue-Schwarzenberg Zone (western Erzgebirge, Germany): Composition of accessory minerals and mineralogical mass balance of the lanthanides and actinides, *Z. Geol. Wiss.* **38** (2010) 125–144
- [124] BARSUKOV, V.L., SOKOLOVA, N.T., IVANITSKII, O.M., Distribution of U, Th, and K in granites of the Aue and Eibenstock massifs, Germany, *Geochem. Int.* **34** (1996) 1041–1056.
- [125] FÖRSTER, A., FÖRSTER, H.-J., Crustal composition and mantle heat flow: Implications from surface heat flow and radiogenic heat production in the Variscan Erzgebirge (Germany), *J. Geophys. Res.* **105** (2000) 917–938.
- [126] NAUMOV, G.B., MIRONOVA, F., Das Verhalten der Kohlensäure in hydrothermalen Lösungen bei der Bildung der Quarz-Nasturan-Kalzit Gänge des Erzgebirges, *Z. Angew. Geol.* **15** (1969).

- [127] NAUMOV, G.B., MOTORINA, Z.M., NAUMOV, V., Conditions of formation of carbonate in veins of the lead-cobalt-nickel-silver-uranium type, *Geochem. Int.* **6** (1971) 590–598.
- [128] KRYLOVA, T.L., VELICHKIN, V.I., POTY, B., CUNEY, M., PIRONON, J., TIMOVEEV, A.V., New data on the composition of ore-forming fluids in veined uranium deposits of Saxonian Erzgebirge, Germany, *Dokl. Earth Sci.* **371A** (2000) 559–561.
- [129] SEIFERT, T., “Giant hydrothermal uranium deposits in the eastern Saxo-Thuringian zone, Germany”, paper presented at symposium on Giant Ore Deposits, Oslo, 2008.
- [130] THOMAS, R., TISCHENDORF, G., Evolution of Variscan magmatic-metallogenetic processes in the Erzgebirge according to thermometric investigations, *Z. Geol. Wiss.* **15** (1987) 25–42.
- [131] CHAKRABARTI, D.J., LAUGHLIN, D.E., The Cu-Se (copper-selenium) system, *Bull. Alloy Phase Diagrams* **2** (1981) 305–315.
- [132] HAYNES, D.W., “Iron oxide copper (–gold) deposits: their position in the ore deposit spectrum and modes of origin”, *Hydrothermal Iron Oxide Copper–Gold & Related Deposits: A Global Perspective* (PORTER, T.M., Ed.), Australian Mineral Foundation, Adelaide (2000) 71–90.
- [133] HITZMAN, M.W., VALENTA, R.K., Uranium in iron oxide-copper-gold (IOCG) systems, *Econ. Geol.* **100** (2005) 1657–1661.
- [134] HITZMAN, M.W., ORESKES, N., ENAUDI, M.T., Geological characteristics and tectonic setting of Proterozoic iron oxide (Cu-U-Au-LREE) deposits, *Precamb. Res.* **58** (1992) 241–287.
- [135] HITZMAN, M.W., “Iron oxide-Cu-Au deposits: What, where, when and why”, *Hydrothermal Iron Oxide Copper–Gold & Related Deposits: A Global Perspective* (PORTER, T.M., Ed.), Australian Mineral Foundation, Adelaide (2000) 9–25.
- [136] POLLARD, P.J., “Evidence of a magmatic fluid and metal source for Fe-Oxide Cu-Au mineralization”, *Hydrothermal Iron Oxide Copper–Gold & Related Deposits: A Global Perspective* (PORTER, T.M., Ed.), Australian Mineral Foundation, Adelaide (2000) 27–42.
- [137] BARTON, M.D., JOHNSON, D.A., “Alternative brine sources for Fe-oxide-(Cu-Au) systems: implications for hydrothermal alteration and metals”, *Hydrothermal Iron Oxide Copper–Gold & Related Deposits: A Global Perspective* (PORTER, T.M., Ed.), Australian Mineral Foundation, Adelaide (2000) 43–60.
- [138] REEVE, J.S., CROSS, K.C., SMITH, R.N., ORESKES, N., Olympic Dam copper-uranium-gold-silver deposit, *Australas. Inst. Min. Metall. Monograph* **14** (1990) 1009–1035.
- [139] REYNOLDS, L.J., “Geology of the Olympic Dam Cu-U-Au-Ag-REE deposit”, *Hydrothermal Iron Oxide Copper–Gold & Related Deposits: A Global Perspective* (PORTER, T.M., Ed.), Australian Mineral Foundation, Adelaide (2000) 93–104.
- [140] WESTERN MINING CORPORATION, ‘Olympic Dam Operations’, *Geology and Mining Technical Handbook: Issue 2*, WMC company brochure (1993).
- [141] CROSS, K.C., DALY, S.J., FLINT, R.B., “Mineralization associated with the GRV and Hiltaba Suite granitoids, Olympic Dam deposit”, *The Geology of South Australia, Vol. 1: The Precambrian* (DREXEL, J.F., PREISS, W.V., PARKER, A.J., Eds), *Geol. Surv. South Australia, Bulletin* **54** (1993).
- [142] ORESKES, N., EINAUDI, N.T., Origin of rare earth element-enriched hematite breccias at the Olympic Dam Cu-U-Au-Ag deposit, Roxby Downs, South Australia, *Econ. Geol.* **85** (1990) 1–28.
- [143] CREASER, R.A., COOPER, J.A., U-Pb geochronology of Middle Proterozoic felsic magmatism surrounding the Olympic Dam Cu-U-Au-Ag and Moonta Cu-Au-Ag deposits, South Australia, *Econ. Geol.* **88** (1993) 186–197.
- [144] JOHNSON, J.P., CROSS, K.C., U-Pb Geochronological constraints on the genesis of the Olympic Dam Cu-U-Au-Ag deposit, South Australia, *Econ. Geol.* **90** (1995) 1046–1063.
- [145] AGODZINSKI, E.A., Compilation of SHRIMP U-Pb data, Olympic Dam Domain, Gawler Craton, South Australia, 2001–2003, Record 2005/20, Geoscience Australia, Canberra (2005).

- [146] BASTRAKOV, E.N., SKIRROW, R.G., BAROVICH, K.M., Towards discriminating Cu-Au mineralized from barren hydrothermal systems using fluids chemistry (FERRIS, G.M., Ed.), Gawler Craton 2002: State of play, Department of Primary Industries and Resources South Australia, Exploration Data Package 10 (2002).
- [147] ROZELLE, J.W., Mineral resource update, Kurišková uranium project, east-central Slovakia, NI 43-101, technical report prepared by Tetra Tech for Tournigan Energy Ltd (2010) 206 pp.
- [148] FERENC, Š., MATO, L., Mineralogical-geochemical and Petrological Evaluations of Samples of the Boreholes KG-J-1, KG-J-1A, KG-J-2 of the U-Mo Jahodná Deposits near Košice, Ludovika Energy, s.r.o., Spišská Nová Ves (2006).
- [149] HYYPPA, R., LAVERTY, T.J., NAUGLE, C.T., NOYES, T.K., Preliminary assessment: Kuriskova uranium project, eastern Slovakia, report prepared by Pincock, Allen and Holt for Tournigan Energy Ltd (2009) 20 pp.
- [150] MORAN, A.V., DAVIESS, F.A., BOWELL, R.J., MORE, S.W., SHARMA, R., BARTALSKY, B., NOVOTNY, L., CISOVSKY, J., POMORSKY, F., NI 43-101 Technical Report on Resources, Kuriskova Uranium Project, Eastern Slovakia, prepared by SRK Consulting for Tournigan Energy Ltd (2008) 127 pp.
- [151] MORAN, A., DAVIESS, F.A., SHARMA, R., Updated NI 43-101 Technical Report on Resources, Kuriskova Uranium Project, Eastern Slovakia, prepared by SRK Consulting for Tournigan Energy Ltd (2009) 141 pp.
- [152] PELHAM, D., WHITE, G., BENNETT, J., BALAKRISHNAN, R., Technical report for Preliminary Assessment of the Jahodna Uranium Project, Slovakia, prepared by A.C.A. Howe International Ltd for Tournigan Gold Corporation (2006) 96 pp.
- [153] ROJKOVIC, I., Uranium mineralization in Slovakia, Monograph Series, Acta Geologica Universitatis Comenianae, Bratislava (1997) 117 pp.
- [154] TOURNIGAN ENERGY LTD, web site (accessed 2009).
- [155] GOLUBEV, V.N., CHEMYSHEV, I.V., AGAPOVA, A.A., Geochronological Study of Uraninite Using Individual grains, in *Mass spektrometriya i izotopnaya geologiya* (Mass Spectrometry and Isotope Geology), Moscow: Nauka, (1983) 74–89.
- [156] CHEMILLAC, R., CUNEY, M., PETROV, V.A., GOLUBEV, V.N., PUJOL, M., “Uranium deposit favorability estimation from pristine rhyolitic magma composition of the Dornot uranium ore field, Mongolia”, paper presented at symposium on Uranium Production and Raw Material for the Nuclear Fuel Cycle – Supply and Demand, Economics, the Environment and Energy Security, Vienna, 2005.
- [157] CHABIRON, A., ALYOSHIN, A.P., CUNEY, M., DELOULE, E., GOLUBEV, V.N., VELITCHKIN, V.I., POTY, B., Geochemistry of the rhyolitic magmas of the Streltsovka Caldera (Transbaikalia, Russia): A magmatic-inclusion study, *Chem. Geol.* **175** (2001) 273–290.
- [158] MIRONOV, Y.B., NAUMOV, S.S., JAMSRANDORJ, G., CHULUUL, O., “The uranium resources of Mongolia”, paper presented at technical meeting on Recent Developments in Uranium Resources and Supply, Vienna, 1995.
- [159] MUELLER, A., HALLBACH, P., The Anderson mine (Arizona): An early diagenetic uranium deposit in Miocene lake sediments, *Econ. Geol.* **78** (1983) 275–292.
- [160] OTTON, J.K., Geology and Genesis of the Anderson Mine: A Carbonaceous Uranium Lacustrine Deposit, Western Arizona — A Summary Report, Open-File Report No. 81-780, US Geol. Surv., Reston, VA (1981).
- [161] SHERBORNE, J.E., Jr., BUCKOVIC, W.A., DEWITT, D.B., HELLINGER, T.S., PAVLAK, S.J., Major uranium discovery in volcanoclastic sediments, basin and range province, Yavapai County, Arizona, *Amer. Ass. Petrol. Geol. Bull.* **63** 4 (1979) 621–646.
- [162] SCARBOROUGH, R.B., Radioactive Occurrences and Uranium Production in Arizona, USDOE Rep. No. GJBX 79-374E, US Department of Energy, Washington, DC (1981) 297 pp.
- [163] OTTON, J.K., Geology of Uraniferous Tertiary Rocks of the Artillery Peak-Date Creek Basin, West Central Arizona, Circ. No. 753, US Geol. Surv., Reston, VA (1977) 35–36.

- [164] KUSHEV, V.G., Alkaline metasomatites of the Precambrian (Shchelochnye metasomaty dokembriia), Nedra, Leningrad (1972) (in Russian).
- [165] CUNEY, M., EMETZ, A., MERCADIER, J., MYKCHAYLOV, V., SHUNKO, V., YUSLENKO, A., Uranium deposits associated with Na-metasomatism from central Ukraine: A review of some of the major deposits and genetic constraints, *Ore Geol. Rev.* **44** (2012) 82–106.
- [166] OECD NUCLEAR ENERGY AGENCY, INTERNATIONAL ATOMIC ENERGY AGENCY, Uranium 2001: Resources, Production and Demand, OECD, Paris (2002).
- [167] GLEVASSKI, E.B., KALAYEV, G.I., Precambrian tectonics of the Ukrainian Shield, *Mineral. J.* **22** (2000) 77–79 (in Russian).
- [168] BELEVTSSEV, Y.N., KOVAL, V.B. (Eds), Genetic Types and Regularities of the Location of Uranium Deposits in Ukraine (Geneticheskie tipy i zakonomernosti razmeshcheniia uranovykh mestorozhenii Ukrainy), Naukova Dumka Publ., Kiev (1995) (in Russian).
- [169] OECD NUCLEAR ENERGY AGENCY, INTERNATIONAL ATOMIC ENERGY AGENCY, Uranium 2009: Resources, Production and Demand, OECD, Paris (2010) 456 pp.
- [170] STAROSTENKO, V.I., KAZANSKY, V.I., POPOV, N.I., DROGITSKAYA, G.M., ZAYATS, V.B., MAKIVCHUK, O.F., TRIPOLSKYI, A.A., CHICHEROV, M.V., From surface structures to the integrated deep model of the Kirovograd ore district (Ukrainian Shield): I, *Geophys J.* **32** 1 (2010) 3–33 (in Russian).
- [171] CUNEY, M., SHCHERBAK, M.P., EMETZ, A.V., PETRYCHENKO, K.V., CINELU, S., Petrological and geochronological peculiarities of the Novoukrainka Massif rocks and age problem of uranium mineralization of the Kirovograd Megablock of the Ukrainian Shield, *Mineral J.* **2** (2008) 5–17.
- [172] SHCHERBAK, N.P., ARTEMENKO, G.V., LESNAYA, I.M., PONOMORENKO, A.N., Geochronology of Early Precambrian of the Ukrainian Shield Proterozoic (Geokhronologiiia rannego dokembriia Ukrainського shchita Proterozoi), Nauk dumka, Kiev (2008) (in Russian).
- [173] MIGUTA, A.K., TARKHANOV, A.V., Mineral types of uranium ores in sodic metasomatites, Ukrainian Shield, *Geol. Rudn. Mestorozhd.* **40** 6 (1998) 483–508 (in Russian).
- [174] BAKARZHIEV, A.Ch., MAKHIVCHUK, O.F., NIZOVSKY, V.N., POPOV, N.I., The Kirovograd uranium ore bearing district, Ukraine, *Otechestvennaya Geologia* **9** (1995) 45–55 (in Russian).
- [175] TARASOV, N.N., Geotectonic position and structure of the Novoukrainsk uranium ore field (Ukrainian Shield), *Geol. Rudn. Mestorozhd.* **40** 4 (2004) 275–291 (in Russian).
- [176] CUNNINGHAM-DUNLOP, I., LEE, C., An update on the exploration activities of Aurora Energy Resources Inc. on the CMB uranium property, Labrador, Canada, during the period January 1, 2007 to December 31, 2007, Part II – CMB mineral resources (2008) 216.
- [177] RYAN, B., Regional Geology of the Central Part of the Central Mineral Belt: Labrador, Department of Mines and Energy, St. John's, NL (1984) 185 pp.
- [178] WILTON, D., Metallogeny of the Central Mineral Belt and Adjacent Archean basement, Labrador, Department of Mines and Energy, St. John's (1996) 178 pp.
- [179] GANDHI, S.S., “Uranium in Early Proterozoic Aillik Group, Labrador”, Uranium Deposits of Canada (EVANS, E.L., Ed.), *Can. Inst. Min. Metall.* **33** (1986) 70–82.
- [180] BARTHEL, F.H., “Uranium occurrences in albitized rocks”, Uranium Mineralization: New Aspects on Geology, Mineralogy, Geochemistry and Exploration Methods (Proc. Symp. Aachen, 1985), Monograph Vol. 27, Gebrüder Bornträger, Berlin and Stuttgart (1987) 1–9.
- [181] MIGUTA, A.K., Composition and mineral assemblages of uranium ore in the Elkon District, Aldan Shield (Russia), *Geol. Ore Dep.* **39** 4 (1997) 275–293.
- [182] BOITSOV, V.E., PILIPENKO, G.N., Gold and uranium in the Mesozoic hydrothermal deposits of the central Aldan region, *Geol. Ore Dep.* **40** 4 (1998) 315–328.
- [183] BOITSOV, A.V., NIKOLSKI, A.L., “Characteristics of uranium districts of the Russian Federation”, Assessment of Uranium Deposit Types and Resources – A Worldwide Perspective, IAEA-TECDOC-1258, IAEA, Vienna (2001) 61–75.

- [184] CONLEY, J.H., HENIKA, W.S., Geology of the Snow Creek, Martinsville East, Price, and Spray Quadrangles, Virginia, Virginia Division of Mineral Resources Report of Investigations No. 33 (1973) 71 pp.
- [185] CONLEY, J.F., Geology of the Southwestern Virginia Piedmont, Virginia Division of Mineral Resources Publication No. 59 (1985) 33.
- [186] WILSON, J.R., U/Pb Ages of Plutons from the Central Appalachians and GIS-based Assessment of Plutons with Comments on their Regional Tectonic Significance, MSc Dissertation, Virginia Polytechnic Institute and State University, Blacksburg, VA (2001) 109 pp.
- [187] TAPPA, M., BODNAR, R.J., AYUSO, R.A., AYLOR, J.G., WOODEN, J.L., VASQUEZ, J.A., Zircon U/Pb geochronology of host rock and mineralization at the Coles Hill uranium deposit, Virginia, *Geol. Soc. Amer.* **42** (2010).
- [188] JERDEN, J.L., Origin of Uranium Mineralization at Coles Hill Virginia (USA) and its Natural Attenuation within an Oxidizing Rock-Soil-Ground Water System, PhD Thesis, Virginia Polytechnic Institute and State University, Blacksburg, VA (2001) 145 pp.
- [189] HALLADAY, C.R., BOWDIDGE, C.R., SINGLETARY, H.M., PARK, I.G., LINEBERGER, H.D., TRUCKLE, D.M., LEE, A.J., GLACKMEYER, K., Geology, mineralogy and geophysics of the Coles Hill uranium deposits, Pittsylvania County, Virginia, company report of Marline Uranium Corporation (1982) 117 pp.
- [190] RANKIN, D.W., The continental margin of eastern North America in the southern Appalachians: The opening and closing of the proto-Atlantic, *Amer. J. Sci.* **275A** (1975) 298–336.
- [191] LUITKUS, C.M., BEARD, J.S., FRASER, N.C., RAGLAND, P.C., Use of fine scale stratigraphy and chemostratigraphy to evaluate conditions of deposition and preservation in a Triassic lagerstätte, south-central Virginia, *J. Paleolim.* **44** (2010) 645–666.
- [192] MAXWELL, R.D., GIBBS, B.L., POOL, T.C., KEIM, K.S., CHRISTOPHER, P.A., Technical report on the Coles Hill uranium property, Pittsylvania County, Virginia, USA, technical report prepared for Virginia Uranium Corporation (2008) 86 pp.
- [193] HIBBARD, J.P., TRACY, R.J., HENIKA, W.S., Smith River allochthon: A southern Appalachian peri-Gondwanan terrane emplaced directly on Laurentia?, *Geology* **31** (2003) 215–218.
- [194] HENIKA, W.S., Geologic map of the Virginia portion of the Danville 30 × 60 minute quadrangle Virginia Division of Mineral Resources Publication No. 166, DGMR, Charlottesville, VA (2002).
- [195] PAN AFRICAN MINING CORPORATION, Latest core drill results from Pan African's Tranomaro uranium project confirm further expansion of the zone: results include 6 m of 0.15% U, press release 18 February 2008.
- [196] PAQUETTE, J.-L., NÉDÉLEC, A., MOINE, B., RAKOTONDRAZAFY, M., U–Pb single zircon Pb-evaporation, and Sm–Nd isotopic study of a granulite domain in SE Madagascar, *J. Geol.* **102** (1994) 523–538.
- [197] NICOLLET, C., MONTEL, J.-M., FORET, S., MARTELAT, J.E., LARDEAUX, J.-M., Microprobe monazite dating of the uplift of the Precambrian in the south of Madagascar, *EUG 8 Strasbourg, Terra Abstract* **7** (1995) 124 pp.
- [198] KRONER, A., WINDLEY, B.F., JAECKELT, P., BREWER, T.S., RAZAKAMANANA, T., New zircon ages and regional significance for the evolution of the Pan-African Orogen in Madagascar, *J. Geol. Soc.* **156** (1999) 1125–1135.
- [199] PILI, E., RICARD, Y., LARDEAUX, J.-M., SHEPPARD, S.M.F., Lithospheric shear zones and mantle–crust connections, *Tectonophysics* **280** (1997) 15–29.
- [200] RAKOTONDRAZAFY, C., Les pyroxénites à urano-thorianite du Sud-Est de Madagascar: Etude pétrographique, minéralogique et géochimique conséquences métallogéniques, PhD Thesis, Université Claude Bernard Lyon I, Villeurbanne (1983) 226 pp.
- [201] MOINE, B., RAKOTONDRAZAFY, C., CUNEY, M., Les pyroxénites à uranothorianite du Sud-Est de Madagascar: Conditions physico-chimiques de la métasomatose, *Bull. Mineral.* **108** (1985) 325–340.

- [202] MARTELAT, J.-E., VIDAL, G., LARDEAUX, J.-M., NICOLLET, C., RAKOTONDRAZAFY, M., Images spatiales et tectoniques profondes des continents: l'exemple du Sud-Ouest de Madagascar, *Comptes Rendus à l'Académie des Sciences* **321** (1995) 325–332.
- [203] MOREAU, M., Le gisement des minéralisations de thorianite à Madagascar, *Ann. Géologiques de Madagascar* **33** (1963) 175–178.
- [204] MOINE, B., RAKOTONDRAZAFY, M., RAMAMBAZAFY, A., RAKOTONDRATSIMA, C., CUNEY, M., “Controls on the urano-thorianite deposits in SE Madagascar”, *Proterozoic Geology of Madagascar* (COX, R., ASHWAL, L.D., Eds), Gondwana Research Group Miscell. Pub. 5, Antananarivo (1997) 55–56.
- [205] ROUBAULT, M., “Madagascar”, *Géologie de l'uranium*, Masson et Cie, Paris (1958) 350–368.
- [206] RAKOTONDRAZAFY, M., MOINE B., CUNEY, M., Mode of formation of hibonite ( $\text{CaAl}_{12}\text{O}_{19}$ ) within the U–Th skarns from the granulites of S-E Madagascar, *Contrib. Mineral. Petrol.* **123** (1996) 190–201.
- [207] ANDRIAMAROFAHATRA, J., DE LA BOISSE, H., NICOLLET, C., Datation U–Pb sur monazites et zircons du dernier épisode tectonométamorphique granulitique majeur dans le Sud-Est de Madagascar, *Comptes Rendus à l'Académie des Sciences* **310** (1990) 1643–1648.
- [208] RAMAMBAZAFY, A., MOINE, B., RAKOTONDRAZAFY, M., CUNEY M., Signification des fluides carboniques dans les granulites et les skarns du Sud-Est de Madagascar. *Comptes Rendus à l'Académie des Sciences* **327** (1998) 743–748.
- [209] TOURET, J.R.L., “LILE-depletion in granulites: myth or reality?”, *Petrology and Geochemistry of Magmatic Suites of Rocks in the Continental and Oceanic Crusts* (DEMAIFFE, D., Ed.), Université Libre de Bruxelles, Royal Museum for Central Africa, Tervuren (1996) 53–72.
- [210] BOULVAIS, P., FOURCADE, S., GRUAU, G., MOINE, B., CUNEY M., Persistence of premetamorphic C and O isotopic signatures in marbles subject to Pan-African granulite-facies metamorphism and U–Th mineralization, Tranomaro, southeast Madagascar, *Chem. Geol.* **150** (1998) 247–262.
- [211] ERIKSSON, S.C., “Phalaborwa: A saga of magmatism, metsomatism and miscibility”, *Carbonatites: Genesis and Evolution* (BELL, K., Ed.) Ottawa-Carleton Geoscience Center, Carleton University, Ottawa (1989) 221–253.
- [212] BARBEY, P., CUNEY, M., K, Rb, Sr, Ba, U and Th geochemistry of the Lapland granulites (Fennoscandia): LILE fractionation controlling factors, *Contrib. Mineral. Petrol.* **81** (1982) 304–316.
- [213] BECK, L., “General geology and uranium deposits of the Beaverlodge district”, *Uranium Deposits of Canada* (EVANS, E.L., Ed.), Can. Inst. Min. Metall. **33** (1986) 85–94.
- [214] PETRASCHECK, W.E., ERKAN, E., SIEGL, W., “Types of uranium deposits in the Austrian Alps”, *Geology, Mining and Extractive Processing of Uranium* (Proc. Int. Symp. London, 1977), Inst. Min. Metall., London (1977) 71–75.
- [215] ERKAN, E., “Facies zones in the Permian in the Eastern Alps”, *The Continental Permian in Central, West and South Europe* (FALK, H., Ed.), (Proceedings of Nato Advanced Study Institute, Mainz, 1975), Reidel, Dordrecht (1976) 137–147.
- [216] DAHLKAMP, F.J., SCIVETTI, N., IUREP/International Uranium Resources Evaluation Project: Austria, OECD, Paris (1981) 87 pp.
- [217] MILLER, A.R., STANTON, R.A., CLUFF, G.R., MALE, M.J., “Uranium deposits and prospects of the Baker Lake Basin and subbasins, central District of Keewatin, Northwest Territories, *Uranium Deposits of Canada* (EVANS, E.L., Ed.), Can. Inst. Min. Metall. **33** (1986) 263–285.
- [218] DUFRESNE, M., Technical Report on the Yathkyed Uranium Project, Kivalliq Region, Nunavut, APEX Geoscience report prepared for Kaminak Gold Corporation and Kivalliq Energy Corporation (2008) 70 pp.

- [219] DUFRESNE, M., SIM, R., DAVIS, B., Technical Report and Resource Update for the Angilak Property, Kivalliq Region, Nunavut, Canada, APEX Geoscience report prepared for Kivalliq Energy Corporation (2013) 174 pp.
- [220] CAMPBELL, D.D., Geology of the Pitchblende Deposits of Port Radium, Great Bear Lake, NWT, PhD Thesis, California Institute of Technology (1955) 323 pp.
- [221] RUZICKA, V., THORPE, R.I., “Arsenide vein uranium-silver”, *Geology of Canadian Mineral Deposit Types: Geology of Canada No. 8* (ECKSTRAND, O.R., SINCLAIR, W.D., THORPE, R.I., Eds), Geological Survey of Canada (1996) 296–304.
- [222] MURSKY, G., Geology of Port Radium Map-Area, District of Mackenzie, Geological Survey of Canada Memoir **374** (1973) 40 pp.
- [223] HILDEBRAND, R.S., “Early Proterozoic Labine Group of Wopmay Orogen: Remnant of a continental volcanic arc developed during oblique convergence”, *Proterozoic Basins of Canada* (CAMPBELL, F.H.A., Ed.), paper 81-10, Geological Survey of Canada (1981) 133–156.
- [224] CAMPBELL, D.D., “Port Radium mine“, In Gilbert, G. Ed. *Structural Geology of Canadian Ore Deposits: Vol. II* (GILBERT, G., Ed.), 6th Commonwealth Mining and Metallurgical Congress (1957) 177–189.
- [225] JORY, L.T., Mineralogical and Isotopic Relations in the Port Radium Pitchblende Deposit, Great Bear Lake, Canada, PhD Thesis, California Institute of Technology (1964) 275 pp.
- [226] ROBINSON, B.W., OHMOTO, H., Mineralogy, fluid inclusions, and stable isotopes of the Echo Bay U-Ni-Ag-Cu deposits, Northwest Territories, Canada, *Econ. Geol.* **68** (1973) 635–656.
- [227] WALLACE, A.R., Alteration and Vein Mineralization, Schwartzwalder Uranium Deposit, Front Range, Colorado, Rep. 83-417, US Geological Survey, Reston, VA (1983) 172 pp.
- [228] WRIGHT, J.H., “Economic geology of the Swartzwalder mine”, *Uranium Resource Technology: Vol. III*, Colorado School of Mines Press, Golden, CO (1980) 73–92.
- [229] LUDWIG, K.R., WALLACE, A.R., SIMMONS, K.R., The Schwartzwalder uranium deposit, II: Age of mineralization and lead isotope constraints on source areas, *Econ. Geol.* **80** (1985) 1858–1871.
- [230] HEYSE, J.V., Mineralogy and Paragenesis of the Schwartzwalder Mine Uranium Ore, Jefferson County, Colorado, Rep. GJO 912-1, US Atomic Energy Commission, Washington, DC (1972) 87 pp.
- [231] NAESER, C.W., Fission Track Dating, Open-File Rep. 76-190, US Geological Survey, Reston, VA (1978) 58 pp.
- [232] MARVIN, R.F., DOBSON, S.W., Radiometric Ages: Compilation B, US Geological Survey, Isochron West no. 25 (1979).
- [233] ALBUQUERQUE, R.O., Alternativa de processos para concentração do minério fósforo-uranífero de Itataia, PhD Thesis, Universidade Federal de Minas Gerais (2010).
- [234] MENDONÇA, J.C.G.S., BRAGA, A.P.G., CAMPOS, M., Considerações sobre a mineralização fósforo-uranífera da jazida de Itataia-CE. In: SBG, Congresso Brasileiro de Geologia, 31. Camboriú – SC, Anais, 4: (1980) 2472-2486.
- [235] ANGEIRAS, A.G., Geology and metallogeny of the northeastern Brazil uranium-phosphorus province emphasizing the Itataia deposit, *Ore Geol. Rev.* **3** (1–3) (1988) 211 pp.
- [236] MENDONÇA, J.C.G.S., CAMPOS, M., BRAGA, A.P., SOUZA, E.M., FAVALI, J.C, LEAL, J.R.L.V., Jazida de Urânio de Itataia-Ceará. In: DNPM. Principais depósitos minerais do Brasil 1: (1985) 121-131.
- [237] SAAD, S., Alguns aspectos do impacto radiológico na indústria de fertilizantes fosfatados: Estudo de um caso – Itataia – CE, MSc Dissertation, IME (1995).
- [238] NETTO, A.M., Contribuição à mineralogia, petrografia e metalogenia da jazida fósforo-uranífera de Itataia-Ceará. In: SBG, Congresso Brasileiro de Geologia, 33. Rio de Janeiro – RJ, Anais, 4 (1984) 1424–1434.
- [239] HADDAD, R.C., LEONARDOS, O.H., Granitos anelares de Taperuaba (Ceará) e processos metassomáticos associados. In: SBG, Congresso Brasileiro de Geologia, 31. Camboriú – SC, Anais, 5: (1980) 2626-2631.

- [240] AZEVEDO, L.F., Quelques aspects de la zone d'altération du gisement à phosphate uranifère d'Itaitaia-Etat du Ceara, Brésil. Rapport CSEVE, Nancy, ENSG-Institut National Polytechnique de Lorraine, (1980) 43 p.
- [241] ANGEIRAS, A.G., NETTO, A.M., CAMPOS, M de, Mineralização fósforo-uranífera, associada a epissienitos sódicos no Precambriano Cearense. In: SBG, Congresso Brasileiro de Geologia, 30. Recife – PE, Anais 1: (1981) 341.
- [242] KING, M., “Exploration for unconformity-style uranium deposits: Geology and mineralization of the Angularli Prospect, Wellington Range Project, West Arnhem Land”, Ages 2012 (Ann. Geosciences Expl. Sem. Alice Springs, 2012), Record of Abstracts, Northern Territory Geological Survey, Darwin (2012) 19–20.
- [243] VERMA, M.B., MAITHANI, P.B., CHAKI, A., RAO, P.N., KUMAR, P., Srisailam sub-basin, an uranium province of unconformity-related deposits in Andhra Pradesh — case study of Chitrial uranium exploration, Nalgonda district, *Curr. Sci.* **96** 4 (2009) 588 pp.
- [244] KRUSE, P.D., SWEET, I.P., STUART-SMITH, P.G., WYGRALAK, A.S., PIETERS, P.E., CRICK, I.H., Katherine SD53-9, 1:250 000 Geological Map Series: Explanatory Notes, Northern Territory Geological Survey, Darwin (1994) 69 pp.
- [245] RAWLINGS, D.J., PAGE R.W., Geology and geochronology and emplacement structures associated with the Jimbu Microgranite, McArthur Basin, Northern Territory, *Precamb. Res.* **94** (1999) 225–250.
- [246] RAMAEKERS, P., JEFFERSON, C.W., YEO, G.M., COLLIER, B., LONG, D.G.F., CATUNEANU, O., BERNIER, S., KUPSCH, B., POST, R., DREVER, G., McHARDY, S., JIRICKA, D., CUTTS, C., WHEATLEY, K., Revised geological map and stratigraphy of the Athabasca Group, Saskatchewan and Alberta, *Geol. Surv. Can. Bull.* **588** (2007) 155–192.
- [247] PAGEL, M., POTY, B., SHEPPARD, S.M.F., “Contributions to some Saskatchewan uranium deposits mainly from fluid inclusion and isotopic data”, *Uranium in the Pine Creek Geosyncline (Proc. Int. Conf. Sydney, 1979)*, IAEA, Vienna (1980) 639–655.
- [248] RAINBIRD, R.H., STERN, R.A., RAYNER, N., JEFFERSON, C.W., Age, provenance and regional correlation of the Athabasca Group, Saskatchewan and Alberta, constrained by igneous and detrital zircon geochronology, *Geol. Surv. Can. Bull.* **588** (2005) 193–211.
- [249] RAINBIRD, R., HADLARI, T., ASPLER, L.B., DONALDSON, J.A., LE CHEMINANT, A.N., PETERSON, T.D., Sequence stratigraphy and evolution of the Paleoproterozoic intracontinental Baker Lake and Thelon basins, western Churchill Province, Nunavut, Canada, *Precamb. Res.* **125** 1–2 (2003) 21–53.
- [250] LUDWIG, K.R., GRAUCH, R.I., NUTT, C.J., NASH, J.T., FRISHMAN, D., SIMMONS, K.R., Age of uranium mineralization at the Jabiluka and Ranger uranium deposits, Northern Territory, Australia: New U-Pb isotope evidence, *Econ. Geol.* **82** (1987) 857–874.
- [251] POLITO, P.A., KYSER, T.K., THOMAS, D., MARLATT, J., DREVER, D., Re-evaluation of the Petrogenesis of the Proterozoic Jabiluka Unconformity-related Uranium Deposit, Northern Territory, Australia, *Miner. Deposita* **40** (2005) 257–288.
- [252] MAAS, R., Nd-Sr isotope constraints on the age and origin of unconformity-type uranium deposits in the Alligator River Uranium Field, Northern Territory, Australia, *Econ. Geol.* **84** (1989) 64–90.
- [253] JEFFERSON, C.W., THOMAS, D.J., GANDHI, S.S., RAMAEKERS, P., DELANEY, J., BRISBIN, D., CUTTS, C., PORTELLA, P., OLSON, R.A., Unconformity-associated uranium deposits of the Athabasca Basin, Saskatchewan and Alberta, *Geol. Surv. Can. Bull.* **588** (2006) 23–68.
- [254] HOEVE, J., SIBBALD, T., On the genesis of Rabbit Lake and other unconformity-type uranium deposits in northern Saskatchewan, Canada, *Econ. Geol.* **73** (1978) 1450–1473.
- [255] HOEVE, J., SIBBALD, T., RAMAEKERS, P., LEWRY, J.F., “Athabasca Basin unconformity-type uranium deposits: a special class of sandstone-type deposits?”, *Uranium in the Pine Creek Geosyncline (Proc. Int. Conf. Sydney, 1979)*, IAEA, Vienna (1980) 565–594.
- [256] KOTZER, T., KYSER, T.K., Fluid history in the Athabasca Basin and its relation to diagenesis, uranium mineralization and paleohydrology, *Chem. Geol.* **120** (1995) 45–89.

- [257] FAYEK, M., KYSER, K., Characterisation of multiple fluid events and rare-earth element mobility associated with formation of unconformity-type uranium deposits in the Athabasca Basin, Saskatchewan, *Can. Mineral.* **35** (1997) 627–658.
- [258] TOURIGNY, G., QUIRT, D.H., WILSON, N., WILSON, S., BRETON, G., PORTELLA, P., Basement geology of the Sue C uranium deposit, McClean Lake area, Saskatchewan, *Geol. Surv. Can. Bull.* **588** (2007) 229–248.
- [259] THOMAS, D.J., MATTHEWS, R.B., SOPUCK, V., “Athabasca Basin (Canada) unconformity-type uranium deposits: Exploration model, current mine developments and exploration directions”, *Geology and Ore Deposits 2000: The Great Basin and Beyond* (Proceedings of Geological Society of Nevada Symposium), *Geol. Soc. Nevada* (2000) 103–126.
- [260] HOEVE, J., QUIRT, D., A stationary redox front as a critical factor in the formation of high-grade unconformity-type uranium ores in the Athabasca Basin, Saskatchewan, Canada, *Bull. Mineralogie* **110** (1987) 157–171.
- [261] DEROME, D., CATHELINÉAU, M., CUNEY, M., FABRE, C., LHOMME, T., BANKS, D.A., Mixing of sodic and calcic brines and uranium deposition at McArthur River, Saskatchewan, Canada: A raman and laser-induced breakdown spectroscopic study of fluid inclusions, *Econ. Geol.* **100** (2005) 1529–1545.
- [262] LE CHEMINANT, A.N., HEAMAN, L.M., McKenzie igneous events, Canada: Middle Proterozoic hotspot magmatism associated with ocean opening, *Earth Planet. Sci. Lett.* **96** (1989) 38–48.
- [263] CUNEY, M., BROUAND, M., CATHELINÉAU, M., DEROME, D., FREIBERGER, R., HECHT, L., KISTER, P., LOBAEV, V., LORILLEUX, G., PEIFFERT, C., BASTOUL, A.M., “What parameters control the high grade-large tonnage of the Proterozoic unconformity-related uranium deposits?” paper presented at Uranium Geochemistry 2003 Int. Conf., Nancy, 2003.
- [264] PAGE, R.W., COMPSTON, W., NEEDHAM, R.S., “Geochronology and evolution of the late-Archean basement and Proterozoic rocks in the Alligator Rivers Uranium Field, Northern Territory, Australia”, *Uranium in the Pine Creek Geosyncline* (Proc. Int. Conf. Sydney, 1979), IAEA, Vienna (1980) 36–68.
- [265] LALLY, J.H., BAJWAH, Z.U., Uranium Deposits of the Northern Territory, Rep. 20, Northern Territory Geological Survey, Darwin (2006) 85 pp.
- [266] POLITO, P.A., KYSER, T.K., SOUTHGATE, P.N., JACKSON, M.J., Sandstone diagenesis and aquifer evolution in the Mt Isa Basin: The isotopic and fluid inclusion history of fluid flow in the Mt Isa Basin, *Econ. Geol.* **101** (2006) 1159–1188.
- [267] POLITO, P.A., KYSER, T.K., JACKSON, M.J., “The role of sandstone diagenesis and aquifer evolution in the formation of uranium and zinc-lead deposits, southern McArthur Basin, Northern Territory, Australia”, *Econ. Geol.* **101** (2006) 1199–1209.
- [268] KYSER, K., HIATT, E., RENAC, C., DUROCHER, K., HOLK, G., DECKART, K., “Diagenetic fluids in Paleo- and Meso-Proterozoic sedimentary basins and their implications for long protracted fluid histories”, *Fluids and Basin Evolution*, Short Course Series No. SC28, Mineralogical Association of Canada, Quebec (2000) 225–262.
- [269] ANNESLEY, I.R., MADORE, C., KWOK, Y.Y., KAMO, S.L., TROY, A., HUGUES, L., “Petrochemistry and U-Pb monazite geochronology of granitic pegmatite from the Ranger U deposit, Australia”, paper presented at 47th Joint Ann. Mtg Geol. Assoc. Canada and Mineral Assoc. Canada, Saskatoon, 2002.
- [270] HEIN, K.A.A., Geology of the Ranger uranium mine, Northern Territory, Australia: Structural constraints on the timing of uranium emplacement, *Ore Geol. Rev.* **20** (2002) 83–108.
- [271] SAVORY, P.J., “Geology and grade control at ERA-Ranger Mine, Northern Territory”, *Australian Mining Looks North: Challenges and Choices* (AusIMM Ann. Conf. Darwin, 1994), Australian Institute of Mining and Metallurgy, Carlton South, VIC (1994) 97–101.
- [272] KENDALL, C.J., “Ranger uranium deposits”, *Geology of the Mineral Deposits of Australia and Papua New Guinea*, Australas. Inst. Min. Metall. Mono. **15** (1990) 799–805.

- [273] POLITO, P.A., KYSER, T.K., MARLATT, J., ALEXANDRE, P., BAJWAH, Z.U., DREVER, D., Significance of alteration assemblages for the origin and evolution of the Proterozoic Nabarlek unconformity-related uranium deposit, Northern Territory, Australia, *Econ. Geol.* **99** (2004) 113–139.
- [274] FISHER, L.A., CLEVERLEY, J.S., POWNCEBY, M., MacRAY, C., 3D representation of geochemical data, the corresponding alteration and associated REE mobility at the Ranger uranium deposit, Northern Territory, Australia, *Miner. Deposita* **48** (2013).
- [275] POLITO, P.A., KYSER, T.K., A report of the significance of alteration assemblages for the origin of the Proterozoic Nabarlek unconformity-related uranium deposit, Northern Territory Australia, Department of Geological Sciences and Geological Engineering, Queens University, Kingston, ON (2002).
- [276] FUCHS, H., HILGER, W., PROSSER, E., “Geology and exploration history of the Lone Gull property”, *Uranium Deposits of Canada* (EVANS, E.L., Ed.), *Can. Inst. Min. Metall.* **33** (1986) 286–292.
- [277] ASHTON, K.E., Further Geological Studies of the ‘Woodburn Lake Group’ Northwest of Tehek Lake, District of Keewatin, paper 82-1A, Geological Survey of Canada, Ottawa (1982) 151–157.
- [278] HENDERSON, J.R., HENDERSON, M.N., PRYER, L.L, CRESSWELL, R.G., Geology of the Whitehills-Tehek area, District of Keewatin, an Archean Supracrustal Belt with Iron-formation-hosted Gold Mineralization in the Central Churchill Province, paper 91-1C, Geological Survey of Canada, Ottawa (1991) 149–156.
- [279] ZALESKI, E., CORRIGAN, D., KJASRGAARD, B.A., JENNER, G.A., KERSWILL, J.A., HENDERSON, J.R., Preliminary Results of Mapping and Structural Interpretation from the Woodburn Project, Western Churchill Province, Northwest Territories, paper 97-C, Geological Survey of Canada, Ottawa (1997) 91–100.
- [280] PEHRSON, S., RAINBIRD, R., JEFFERSON, C., “Correlation of Proterozoic sequences from Greenland to Manitoba: Implications for metallogeny”, paper presented at Western Churchill Metallogeny Project Workshop, Ottawa, 2004.
- [281] YOUNG, G.M., Report on the Geology of the Western Part of the Amer Belt (NTS sheets 66G1, G2, H5, H6 and parts of G8, and H4), Keewatin District, NWT, unpublished report to Western Mines Ltd (1979).
- [282] PATTERSON, J.G., The Amer Belt: Remnant of an Aphebian foreland fold and thrust belt, *Can. J. Earth Sci.* **23** (1986) 2012–2023.
- [283] WOLLENBERG, P., AREVA’s Kiggavik Project: Exploration Update 2010, Nunavut Mining Symposium presentation, <http://2010.nunavutminingsymposium.ca>
- [284] PETERSON, T.D., VAN BREEMEN, O., SANDEMAN, H., COUSENS, B., Proterozoic (1.85-1.75 Ga) igneous suites of the western Churchill Province: Granitoid and ultrapotassic magmatism in a reworked Archean hinterland, *Precamb. Res.* **119** (2002) 73–100.
- [285] VAN BREEMEN, O., PETERSON, T.D., SANDEMAN, H.A., U-Pb zircon geochronology and Nd isotope geochemistry of Proterozoic granitoids in the western Churchill Province: Intrusive age pattern and Archean source domains, *Can. J. Earth Sci.* **42** (2005) 339–377.
- [286] MILLER, A.R., CUMMINGS, G.L., KRSTIC, D., U-Pb, Pb-Pb, and K-Ar isotopic study and petrography of uraniumiferous phosphate-bearing rocks of the Thelon Formation, Dubawnt Group, NWT, Canada, *Can. J. Earth. Sci.* **26** (1989) 867–880.
- [287] REILLY, B., WHEATLEY, K., “AREVA’s Kiggavik-Sissons Project: Nunavut’s largest known uranium deposits”, paper presented at Yellowknife Geoscience Forum, Yellowknife, 2005.
- [288] HASEGAWA, K., DAVIDSON, G.I., WOLLENBERG, P., YOSHIMASA, I., Geophysical exploration for unconformity-related uranium deposits in the northeastern part of the Thelon Basin, Northwest Territories, Canada, *Min. Geol.* **40** 2 (1990) 83–95.
- [289] WEYER, H.J., FRIEDRICH, G., BECHTEL, A., BALLHORN, R.K., “The Lone Gull uranium deposit – new geochemical and petrological data as evidence for the nature of the ore bearing solutions”, *Metallogenesis of Uranium Deposits* (Proc. Tech. Comm. Mtg Vienna, 1987), IAEA, Vienna (1989) 293–306.

- [290] RHYS, D., HORN L., ERIKS, S., Technical Report on the Shea Creek property, Northern Saskatchewan, prepared for UEX Corporation (2009) 157 pp.
- [291] UEX CORPORATION, UEX Reports Increase in Shea Creek Uranium Resource to 67.7 Million Pounds U<sub>3</sub>O<sub>8</sub> in the Indicated Category and 28.2 Million Pounds U<sub>3</sub>O<sub>8</sub> in the Inferred Category, press release 17 April 2013.
- [292] CARROLL, J., ROBBINS J., KONING E., “The Shea Creek deposits, West Athabasca Basin, Saskatchewan”, Uranium: Athabasca Deposits and Analogues (Proc. CIM Field Conf. Saskatoon, 2006), CIM Geological Society, Saskatoon (2006) 33–48.
- [293] YEO, G., COLLIER, B., RAMAEKERS, P., KOENING, P., ROBBINS, E., JIRICKA, D., Stratigraphy of the Athabasca Group in the Southwestern Athabasca Basin, Saskatchewan (NTS 74F and 74K), Summary of Investigations: Vol. 2, Saskatchewan Geological Survey, Regina, SK (2001) 252–265.
- [294] PAGEL, M., SVAB, M., Petrographic and geochemical variations within the Carswell structure metamorphic core and their implications with respect to uranium mineralization, Special Paper 29, Geological Association of Canada, St. John’s, NL (1985) 55–70.
- [295] RAINBIRD, R.H., STERN, R.A., JEFFERSON, C.W., Summary of Detrital Zircon Geochronology of the Athabasca Group, Northern Saskatchewan and Alberta, Summary of Investigations: Vol. 2, paper D-17, Saskatchewan Geological Survey, Regina, SK (2002) 3 pp.
- [296] LORILLEUX, G., JEBRAK, M., CUNEY, M., BEAUDEMONT, D., Polyphase hydrothermal breccias associated with unconformity-type uranium mineralization (Canada): From fractal analysis to structural significance, *J. Struct. Geol.* **24** (2002) 323–338.
- [297] LAVERRET, E., CLAUER, N., FALLICK, A., MERCADIER, J., PATRIER, P., BEAUFORT, D., BRUNETON, P., K-Ar dating and  $\delta^{18}\text{O}$ - $\Delta d$  tracing of illitization within and outside the Shea Creek uranium prospect, Athabasca Basin, Canada, *Appl. Geochem.* **25** (2010) 856–871.
- [298] KISTER, P., Mobilité des éléments géochimiques dans un bassin sédimentaire clastique, du Protérozoïque à nos jours: le bassin Athabasca, Saskatchewan, Canada, PhD Thesis, Institut National Polytechnique de Lorraine, Nancy (2003).
- [299] FAYEK, M., HARRISON, T., EWING, R.C., GROVE, M., COATH, C.D., O and Pb isotope analysis of uranium minerals by ion microprobe and U-Pb ages from the Cigar Lake deposit, *Chem. Geol.* **40** (2002) 205–225.
- [300] LEWRY, J.F., SIBBALD, T.I.I., “A review of pre-Athabasca basement geology in northern Saskatchewan”, Uranium Exploration Techniques (PARSLOW, G.R., Ed.), Saskatchewan Geological Society Special Publication **4** (1978) 19–58.
- [301] SIBBALD, T.I.I., MUNDAY, R.J.C., LEWRY, J.F., “The geological setting of uranium mineralization in northern Saskatchewan”, Uranium in Saskatchewan (DUNN, C.E., Ed.), Saskatchewan Geological Society Special Publication **3** (1976) 51–98.
- [302] SIBBALD, T.I.I., NEA/IAEA Test Area: Basement Geology, Summary of Investigations, Saskatchewan Geological Survey, Regina, SK (1980) 77–85.
- [303] RAMAEKERS, P., Geology of the Athabasca Group (Helikian) in Northern Saskatchewan, Saskatchewan Energy and Mines, Rep. 195, Saskatchewan Geological Survey, Regina, SK (1990) 49 pp.
- [304] RAMAEKERS, P., Hudsonian and Helikian basins of the Athabasca Region, Northern Saskatchewan, paper 81-10, Proterozoic Basins of Canada (CAMPBELL, F.H.A., Ed.), Geological Survey of Canada, Ottawa (1981) 219–233.
- [305] HOEVE, J., SIBBALD, T.I.I., Uranium metallogenesis and its significance to exploration in the Athabasca Basin, Uranium Exploration Techniques (PARSLOW, G.R., Ed.), Saskatchewan Geological Society Special Publication **4** (1978) 161–180.
- [306] MCGILL, B.D., MARLATT, J.L., MATTHEWS, R.B., SOPUCK, V.J., HOMENIUK, L.A., HUBREGSTE, J.J., The P2 North uranium deposit, Saskatchewan, Canada, *Expl. Min. Geol.* **2** (1993) 321–331.
- [307] BAUDEMONT, D., Eastern Tamarack Zone, Unconformity and Perched Mineralization Associated with the Tent Seal Fault, Triple Point Consulting report for Cameco Corporation (2008) 27 pp.

- [308] HIRSEKORN, D., “The geology of Cameco’s Tamarack unconformity-associated deposit, Athabasca Basin, Canada”, paper presented at AusIMM Uranium Conference, Adelaide, 2008.
- [309] RHYS, D., Report on a Structural Geology Study of Drill Core, Collins Creek Zone, Dawn Lake Project, Panterra Geoservices Inc. report for Cameco Corporation (2001) 31 pp.
- [310] CAMECO CORPORATION, 2009 Annual Report (2010) 131 pp.
- [311] JEFFERSON, C.W., THOMAS, D.J., GANDHI, S.S., RAMAEKERS, P., DELANEY, G., BRISBIN, D., CUTTS, C., QUIRT, D., PORTELLA, P., OLSON, R.A., “Unconformity-associated uranium deposits of the Athabasca Basin, Saskatchewan and Alberta”, Mineral Deposits of Canada: A synthesis of Major Deposit-Types, District Metallogeny, the Evolution of Geological Provinces, and Exploration Methods (GOODFELLOW, W.D., Ed.), Geological Association of Canada Special Publication **5** (2007) 273–305.
- [312] NAGARAJA RAO, B., RAJURKAR, S., RAMILIGASWAMY, G., RAVINDRA B., “Stratigraphy, structure and evolution of the Cuddapah Basin”, Purana Basins of Peninsular India, Geol. Soc. Ind. Mem. **6** (1987) 33–86.
- [313] PADMAKURAMI, V.M., DAYAL, A.M., “Geochronological studies of some mafic dykes around the Cuddapah Basin, south India”, Purana Basins of Peninsular India, Geol. Soc. Ind. Mem. **6** (1987) 369–373.
- [314] PANDEY, B.K., GUPTA, J.N., SARMA, K.J., SASTRY, C.A., Sm-Nd, Pb-Pb and Rb-Sr geochronology and petrogenesis of the mafic dyke swarm of Mahbubnagar, South India: Implications for Paleoproterozoic crustal evolution of the Eastern Dharwar Craton, Precamb. Res. **84** (1997) 181–186.
- [315] PANDEY, B.K., PRASAD, R.N., SASTRY, D.V.L.N., KUMAR, B.R.M, SURYANARAYANA RAO, S., GUPTA, J.N., “Rb-Sr whole rock ages for the granites from parts of Andhra Pradesh and Karnataka”, paper presented at Fourth National Symposium on Mass Spectrometry, Bangalore, India, 1988.
- [316] JEYAGOPAL, A.V., PRAKHAR KUMAR, SINHA, R.M., Uranium mineralization in the Palnad Sub-basin, Cuddapah basin, Andhra Pradesh, India, Curr. Sci. **71** 12 (1996) 957–959.
- [317] SINGH, R.V., SINHA, R.M., BISHT, B.S., BANERJEE, D.C., Hydrogeochemical exploration for unconformity-related uranium mineralization: Examples from Palnad sub-basin, Cuddapah Basin, Andhra Pradesh, India, J. Geochem. Expl. **76** (2002) 71–92.
- [318] KONKA, U., ACHAR, K.K., MAITHANI, P.B., Proterozoic Unconformity Related Uranium Mineralization in the Srisailam and Palnad Sub-Basins of Cuddapah Basin, Andhra Pradesh, URAM-2009 Uranium Raw Material for the Nuclear Fuel Cycle: Exploration, Mining, Production, Supply and Demand (Proc. Int. Conf. Vienna, 2009), IAEA, Vienna (2009).
- [319] PANDEY, B.K., Geochronology of the rocks and radioactive minerals in the parts of Andhra Pradesh and Karnataka with special reference to episodes of uranium mineralization during the Proterozoic, AMD special report, December (2004).
- [320] SINHA, R.M., SRIVASTAVA, V.K., SHARMA, G.V.C., PARTHASARATHY, T.N., Geological favorability for unconformity-related uranium deposits in the northern parts of Cuddapah Basin: Evidence from Lambapur uranium occurrence, Andhra Pradesh, India, Expl. Res. Atom. Miner. **8** (1995) 111–126.
- [321] WENRICH, K.J., Mineralization of breccia pipes in northern Arizona, Econ. Geol. **80** (1985), 1722–1735.
- [322] WENRICH, K.J., CHENOWETH, W.L., FINCH, W.I., SCARBOROUGH, R.B., “Uranium in Arizona”, Geologic Evolution of Arizona, Arizona Geol. Soc. Digest **17** (1989) 759–794.
- [323] WENRICH, K.J., VAN GOSEN, B.S., FINCH, W.I., “Solution-collapse breccia pipe U deposits”, Preliminary Compilation of Descriptive Geoenvironmental Mineral Deposit Models, Open-File Report 95-831, US Geological Survey, Reston, VA (1995) 244–251.
- [324] CHENOWETH, W.L., The Orphan Lode Mine, Grand Canyon, Arizona: A Case History of a Mineralized, Collapse-breccia Pipe, Open-File Report 86-510, US Geological Survey, Reston, VA (1986).
- [325] CHENOWETH, W.L., The Production History and Geology of the Hacks, Ridenour, Riverview and Chapel Breccia Pipes, Northwestern Arizona, Open-File Report 88-648, US Geological Survey, Reston, VA (1988) 60 pp.

- [326] OTTON, J.K., VAN GOSEN, B.S., “Uranium resource availability in breccia pipes in northern Arizona”, Hydrological, Geological, and Biological Site Characterization of Breccia Pipe Uranium Deposits in Northern Arizona, Scientific Investigations Rep. 2010-5025, US Geological Survey, Reston, VA (2010) 18–41.
- [327] LUDWIG, K.R., SIMMONS, K.R., U-Pb dating of uranium deposits in collapse breccia pipes of the Grand Canyon region, *Econ. Geol.* **87** (1992) 1747–1765.
- [328] MILLER, D.S., KULP, J.L., Isotopic evidence on the origin of the Colorado Plateau uranium ore, *Geol. Soc. Amer. Bull.* **74** (1963) 609–630.
- [329] KREDWELD, D.A., CARISEY, J.C., Contribution to the geology of uranium mineralized breccia pipes in northern Arizona, *Arizona Geol. Soc. Digest XVI* (1986) 179–186.
- [330] WENRICH, K.J., TITLEY, S.R., “Genesis of uranium-rich, base-metal bearing, solution-collapse breccia pipes, northern Arizona”, paper presented at U2009 Global Uranium Symposium, Keystone, 2009.
- [331] ENERGY FUELS INC., web site (accessed May 2013).
- [332] CASADEVALL, W.P., Exploration geology of Canyon breccia pipe south of Grand Canyon, Arizona, *Am. Assoc. Petrol. Geol. Bull.* **73** 9 (1989) 1150.
- [333] WENRICH, K.J., Breccia pipes in the Red Butte area of Kaibab National Forest, Arizona, Open-File Report 92-219, US Geological Survey, Reston, VA (1992) 13 pp.
- [334] ALPINE, A.E., Hydrological, geological, and biological site characterization of breccia pipe uranium deposits in northern Arizona, Scientific Investigations Rep. 2010-5025, US Geological Survey, Reston, VA (2010) 353 pp.
- [335] INTERNATIONAL ATOMIC ENERGY AGENCY, Geological Environments of Sandstone-Type Uranium Deposits, IAEA-TECDOC-328, IAEA, Vienna (1985).
- [336] GRUTT, E.W., Jr., “Prospecting criteria for sandstone-type uranium deposits”, *Uranium Prospecting Handbook* (BOWIE, S.H.U., DAVIS, M., OSTLE, D., Eds), Institution of Mining and Metallurgy, London (1972) 47–77.
- [337] FINCH, W.I., *Geology of Epigenetic Uranium Deposits in Sandstone in the United States*, Prof. Paper 538, US Geological Survey, Reston, VA (1967) 121 pp.
- [338] HOSTETLER, P.B., GARRELS, R.M., Transportation and precipitation of uranium and vanadium at low temperatures, with special reference to sandstone-type uranium deposits, *Econ. Geol.* **57** (1962) 139–167.
- [339] NAUMOV, S.S., TARKHANOV, A.V., BIRKA, G.I., “Future development of Russian uranium industry” *Developments in Uranium Resources, Production, Demand and the Environment*, IAEA-TECDOC-1425, IAEA, Vienna (2005) 43–49.
- [340] SQUYRES, J.B., “Origin and significance of organic matter in uranium deposits of Morrison Formation, San Juan Basin, New Mexico”, *Geology and Mineral Technology of the Grants Uranium Region*, Memoir 38, New Mexico Bureau of Mines and Mineral Resources, Albuquerque (1980).
- [341] THAMM, J.K., KOVSCHAK, A.A., Jr., ADAMS, S.S., *Geology and Recognition Criteria for Sandstone Uranium Deposits of the Salt Wash Type, Colorado Plateau Province*, Rep. GJBX-6(81), US Department of Energy, Grand Junction, CO (1981).
- [342] GRANGER, H.C., WARREN, C.G., “Genetic implications of the geochemistry of vanadium-uranium deposits in the Colorado Plateau region”, paper presented at Amer. Assoc. Petrol. Geol. Mtg, Albuquerque, 1981.
- [343] CAMPBELL, J., SEXTON, A., ARMITAGE, A., Technical Report on the Amer Lake Property, including Mineral Resource Estimate, Nunavut, Canada, NI 43-101 Tech. Rep. prepared for Uranium North Resources Corporation (2009) 73 pp.
- [344] ARMITAGE, A.E., Technical Report on the Amer Lake Property Nunavut, Canada, Tech. Rep. prepared for Uranium North Resources Corporation (2009) 56 pp.
- [345] MILLER, A.R., Stratabound and Stratiform Sediment-hosted Uranium-Copper Prospects in the Paleoproterozoic Amer Group, Churchill Structural Province, Northwest Territories, *Curr. Res.* 1996-C, Geological Survey of Canada, Ottawa (1996) 49–62.

- [346] YOUNG, G., Geology of the Western Part of the Amer Belt, Keewatin, Westmin Resources Ltd Mineral Exploration Assessment Report 081354, Indian and Northern Affairs Canada, Toronto (1981).
- [347] GANDHI, S.S., An overview of the exploration history and genesis of Proterozoic uranium deposits in the Canadian Shield, *Expl. Res. Atom. Miner.* **8** (1995) 1–47.
- [348] BOWDEN, R.A., SHAW, R.P., The Kayalekera uranium deposit, northern Malawi: Past exploration activities, economic geology and decay series disequilibrium, *Trans. Inst. Min. Metall. Section B* **2** (2007) 55–67.
- [349] PALADIN ENERGY, web site (accessed 2011).
- [350] SCHLUTER, T., *Geology of East Africa*, Gebrüder Bornträger, Berlin and Stuttgart (1997) 484 pp.
- [351] HELLMAN AND SCHOFIELD PTY LTD, Kayelekera Malawi Resource Estimation, Technical Report prepared on behalf of Paladin Resources Pty Ltd (2005) 82 pp.
- [352] HARSHMAN, E.N., ADAMS, S.S., Geology and Recognition Criteria for Roll-type Uranium Deposits in Continental Sandstones, Rep. GJBX-1(81), US Department of Energy, Washington, DC (1981) 185 pp.
- [353] RACKLEY, R.I., Environment of Wyoming Tertiary uranium deposits, *Am. Assoc. Petrol. Geol. Bull.* **56** (1972) 755 pp.
- [354] MIN, M., CHEN, J., WANG, J., WEI, G., FAYEK, M., Mineral paragenesis and textures associated with sandstone-hosted roll-front uranium deposits, NW China, *Ore Geol. Rev.* **26** (2005) 51–69.
- [355] ARTHUR, R.C., IWATSUKI, T., SASAO, E., METCALFE, R., AMANO, K., OTA, K., Chemical constraints on the origin and stability of the Tono uranium deposit, Japan, *Geochem. Expl. Env. Anal.* **6** (2006) 33–48.
- [356] UNITED STATES DEPARTMENT OF ENERGY, Washington, DC, written communication, 2009.
- [357] BOBERG, W.W., The nature and development of the Wyoming uranium province, *Soc. Econ. Geol. Special Pub.* **15** (2010) 653–674.
- [358] McLEMORE, V.T., The Grants Uranium District, New Mexico: Update on source, deposition, and exploration, *The Mountain Geologist* **48** (2011) 23–43.
- [359] ZIELINSKY, R.A., Tuffaceous sediments as source rocks for uranium — a case study of the White River Formation, Wyoming, *J. Geochem. Expl.* **18** (1983) 285–306.
- [360] HARSHMAN, E.N., Geology and Uranium Deposits, Shirley Basin Area, Wyoming, Professional Paper 745, US Geological Survey, Reston, VA (1972) 82 pp.
- [361] STUCKLESS, J.S., MIESCH, A.T., Petrogenetic modeling of a potential uranium source rock, Granite Mountains, Wyoming, Professional Paper 1225, US Geological Survey, Reston, VA (1981) 34 pp.
- [362] STUCKLESS, J.S., NKOMO, I.T., BUTT, K.A., Uranium-thorium-lead Systematics of an Archean Granite from the Owl Creek Mountains, Wyoming, Professional Paper 1388 A-C, US Geological Survey, Reston, VA (1986) 39–48.
- [363] GRUNER, J.W., Concentration of uranium in sediments by multiple migration-accretion, *Econ. Geol.* **51** (1956) 495–520.
- [364] PENINSULA ENERGY LTD, web site, Lance Uranium Project, Wyoming, USA, 2011, [http://www.pel.net.au/projects/lance\\_project\\_wyoming\\_usa.phtml](http://www.pel.net.au/projects/lance_project_wyoming_usa.phtml)
- [365] SMITH, R.B., Report on the Dewey-Burdock Uranium Project, Custer and Fall River Counties, South Dakota, NI 43-101 Technical Report prepared for Denver Uranium and Powertech Industries Inc. (2005) 41 pp ([www.sedar.com](http://www.sedar.com)).
- [366] BUSH, J., Updated NI 43-101 Technical Report on the Dewey-Burdock uranium project, Custer and Fall River Counties, South Dakota, Toronto (2010) ([www.sedar.com](http://www.sedar.com)).
- [367] GOTT, G.B., WOLCOTT, D.E., BOWLES, G.C., Stratigraphy of the Inyan Kara Group and Localization of Uranium Deposits, Southern Black Hills, South Dakota and Wyoming, Professional Paper 763, US Geological Survey, Reston, VA (1974) 57 pp.

- [368] COLLINGS, S.P., CATCHPOLE, G., KIRCHNER, G., “The Crow Butte ISL project: A case history”, *Innovations in Uranium Exploration, Mining and Processing Techniques, and New Exploration Target Areas*, IAEA-TECDOC-868, IAEA, Vienna (1996) 89–117.
- [369] DICKINSON, K.A., *Geological Survey Circular 1069*, US Geological Survey Uranium Workshop (1990), US Geological Survey, Reston, VA (1992) 56 pp.
- [370] SIBRAY, S.S., White River Group paleosols as source rocks for uranium mineralization in western Nebraska, *The Mountain Geologist* **48** (2011) 9–22.
- [371] HANSLEY, P.L., COLLINGS, S.P., BROWNFIELD, I.K., SKIPP, G.L., *Mineralogy of uranium ore from the Crow Butte uranium deposit, Oligocene Chadron Formation, northwestern Nebraska*, Open-File Report 89-225, US Geological Survey, Reston, VA (1989).
- [372] KIRKHAM, R.M., LADWIG, L.R., *Energy resources of the Denver and Cheyenne Basins, Colorado: Resource characteristics, development potential, and environmental problems*, *Environ. Geol.* **12** (1980) 258 pp.
- [373] BONNER, J., Updated NI 43-101 Technical Report on the Centennial Uranium Project, Weld County, Colorado, (2009) 41 pp (<http://www.sedar.com>).
- [374] CLASSEN, D.R., *Mineralogy and Diagenesis of a Uranium Prospect in the Goliad Sandstone, Duval County, Texas*, MSc Dissertation, University of Missouri (1981).
- [375] DEUTSCH, W.J., MARTIN, W.J., EARY, L.E., SERNE, R.J., *Methods of Minimizing Ground-Water Contamination From In-Situ Leach Uranium Mining — Final Report*, NUREG/CR-3709 (PNL-5319R), Nuclear Regulatory Commission, Washington, DC (1985) 88 pp.
- [376] EARGLE, D.H., DICKINSON, K.A., DAVIS, B.O., *South Texas uranium deposits*, *Am. Assoc. Petrol. Geol. Bull.* **59** (1975) 766–779.
- [377] HARSCHMAN, E.N., “Distribution of elements in some roll-type uranium deposits”, *Formation of Uranium Ore Deposits (Proc. Int. Symp. Athens, 1974)*, IAEA, Vienna (1974) 169–183.
- [378] STEWART, C.L., *The Mineralogy of Uranium Rollfront Deposits and Its Significance to In-situ Carbonate Leach Mining: Laramie, WY*, MSc, University of Wyoming (2002).
- [379] CHENEY, E.S., JENSEN, M.L., *Stable isotopic geology of the Gas Hills, Wyoming, uranium district*, *Econ. Geol.* **61** (1966) 44–71.
- [380] GOLDHABER, M.B., REYNOLDS, R.L., RYE, R.O., *Origin of a South Texas roll-type deposit: II: Sulfide petrology and sulfur isotope studies*, *Econ. Geol.* **73** (1978) 1690–1705.
- [381] GALLOWAY, W.E., FINLEY, R.J., HENRY, C.D., “South Texas uranium province — geologic perspective”, *Field Trip Guidebook 18*, *Am. Assoc. Petrol. Geol.* (1979) 81 pp.
- [382] ARREDONDO, A.G., *Geology and Hydrogeology of the Kingsville Dome In-situ Leach Uranium Mine, Kleberg County, Texas*, MSc Dissertation, Texas A&I University (1991).
- [383] CAROTHERS, T.A., NI 43-101 Technical Report for Uranium Energy Corporation’s Goliad Project, In-situ Recovery Uranium Property, Goliad County, Texas, (2008) (<http://www.sedar.com>).
- [384] CAROTHERS, T.A., NI 43-101 Technical Report for Uranium Energy Corporation’s Salvo Project, In-situ Recovery Uranium Property, Bee County, Texas, (2010) (<http://www.sedar.com>).
- [385] REYNOLDS, R.L., GOLDHABER, M.B., BLACKMON, P.D., STARKEY, H.C., FISHMAN, N.S., *Clay Minerals in Two South Texas Roll-type Uranium Deposits*, Open-File Report OF-80-838, US Geological Survey, Reston, VA (1980) 24 pp.
- [386] REYNOLDS, R.L., GOLDHABER, M.B., CARPENTER, D.J., *Biogenic and nonbiogenic ore-forming processes in the south Texas uranium district: Evidence from the Panna Maria deposit*, *Econ. Geol.* **77** (1982) 541–556.
- [387] ADAMS, S.S., SMITH, R.B., *Geology and Recognition Criteria for Sandstone Uranium Deposits in Mixed Fluvial-shallow Marine Sedimentary Sequences, South Texas*, Rep. GJBX-4(81), US Department of Energy, Washington, DC (1981) 145 pp.
- [388] HOEL, H.D., *Goliad Formation of the South Texas Gulf Coastal Plain: Regional Genetic Stratigraphy and Uranium Mineralization*, MSc Dissertation, University of Texas at Austin (1982).

- [389] LUDWIG, K.R., GOLDHABER, M.B., REYNOLDS, R.L., SIMMONS, K.R., Uranium-lead isochron age and preliminary sulfur isotope systematics of the Felder uranium deposit, south Texas, *Econ. Geol.* **77** (1982) 557–563.
- [390] ADLER, H.H., “Concepts of uranium ore formation in reducing environments in sandstones and other sediments”, *Formation of Uranium Ore Deposits (Proc. Int. Conf. Athens, 1974)*, IAEA, Vienna (1974) 141–168.
- [391] GARRIC, J., “L’uranium dans le Carbonifère et le Permien de l’Hérault”, *Les minerais uranifères français: Tome III-2* (1965) 147–265.
- [392] LEBRUN, P., CESBRON, F., LE CLEAC’H, J.-M., LEBOCEY, J., “Minéraux uranifères”, *Minéraux et fossiles, hors série No. 28*, Les Editions du Piat, St. Julien du Pinet (2009) 178 pp.
- [393] MATHIS, V., ROBERT, J.P., SAINT MARTIN, J., Géologie et métallogénie des gisements d’uranium du bassin permien de Lodève (sud du Massif Central français), *Chron. rech. min.* **499** (1990) 31–40
- [394] COMTE, D., BLACHERE, H., VARLET, M., “Geological environment of the uranium deposits in the Permian of Lodève Basin, France”, *Geological Environments of Sandstone Type Uranium Deposits*, IAEA-TECDOC-328, IAEA, Vienna (1985) 69–82.
- [395] CAPUS, G., *Matières organiques et minéralisations uranifères: exemples des bassins carbonifères de l’Aumance (Allier) et de Lodève (Hérault)*, PhD Thesis, Inst. Nat. Polytechnique de Lorraine (1979) 384 pp.
- [396] LAVERSANNE, J., *Sédimentation et minéralisation uranifère du Permien de Lodève (Hérault)*, PhD Thesis, Orsay (1976) 300 pp.
- [397] MENDEZ-SANTIZO, J., *Approche géothermique des remplissages de fractures dans le gisement d’uranium de Lodève*, D.E.A., Univ. de Strasbourg (1986) 38 pp.
- [398] LANCELOT, J.R., DE SAINT ANDRE, B., DE LA BOISSE, H., *Systématique U-Pb et évolution du gisement d’uranium de Lodève*, *Mineral. Deposita* **19** (1984) 44–53.
- [399] BEAUBRON, J.C., DEFAUT, B., DEMANGE, J., MAURY, R.C., *Une coulée sous marine d’âge Jurassique moyen dans les Causses: le basalte alcalin des Vignes (Massif Central Français)*, *Comptes Rendus à l’Académie des Sciences D, Paris* (1978) 225–227.
- [400] BROUAND, M., DELOULE, E., CUNEY, M., *Chemical and isotopic U/Pb ages of uraninite-pitchblende mineralization from South Horn, East Alligator Rivers Uranium Field, Australia*, CREGU, Nancy unpublished report for AREVA (2000) 26 pp.
- [401] POLITO, P.A., KYSER, T.K., RHEINBERGER, G., SOUTHGATE, P.N., *A paragenetic and isotopic study of the Proterozoic Westmoreland uranium deposits, southern McArthur Basin, Northern Territory, Australia*, *Econ. Geol.* **100** (2005) 1243–1260.
- [402] LARAMIDE RESOURCES, web site (accessed 2009).
- [403] PAGE, R.W., JACKSON, M.J., KRASSAY, A.A., *Constraining sequence stratigraphy in the north Australian basins: SHRIMP U-Pb zircon geochronology between Mt Isa and McArthur River*, *Austral. J. Earth Sci.* **47** (2000) 431–459.
- [404] WYGRALAK, A., MERNAGH, T., “Mineral potential of the Murphy inlier and surrounding area”, paper presented at AGES 2008 Annual Geoscience Exploration Sem., Alice Springs, 2008.
- [405] AHMAD, M., WYGRALAK, A.S., *Calvert Hills, Northern Territory, 1:250 000 Metallogenic Map Series, sheet SE53-8: Map and Explanatory Notes*, Northern Territory Geological Survey, Darwin (1989).
- [406] AHMAD, M., WYGRALAK, A.S., “Murphy Inlier and environs: Regional geology and mineralisation”, *Geology of the Mineral Deposits of Australia and Papua New Guinea*, Australas. Inst. Min. Metall., Melbourne (1990) 819–826.
- [407] LARAMIDE RESOURCES LTD, *Laramide announces updated NI 43-101 compliant resource report on Westmoreland*, press release 23 April 2009.
- [408] MERNAGH, T.P., WYGRALAK, A.S., “A fluid inclusion study of uranium and copper mineral systems in the Murphy Inlier, northern Australia”, *Russ. Geol. Geophys.* **52** 11 (2011) 1421–1435.

- [409] RHEINBERGER, G.M., HALLENSTEIN, C., STEGMAN, C.L., “Westmoreland uranium deposits”, *Geology of the Mineral Deposits of Australia and Papua New Guinea*, Australas. Inst. Min. Metall. (1998) 807–814.
- [410] FUCHS, H.D., SCHINDLMAYR, W.E., “The Westmoreland uranium deposit Queensland, Australia”, *Uranium Exploration Case Histories*, IAEA, Vienna, (1981) 59–73.
- [411] COOK, R.B., ROSS, D.A., Technical NI 43-101 Report on the Matoush Uranium Project Central Quebec, Canada, prepared by Scott Wilson Roscoe Postle Associates Inc. for Strateco Resources Inc. (2007) 130 pp.
- [412] STRATECO RESOURCES Inc., web site (<http://www.stratecoinc.com>) (accessed 2012).
- [413] GENEST, S., *Géologie de la Région du Lac Indicateur (Territoire-du-Nouveau-Québec)*. Direction générale de l’Exploration géologique et minérale, ET 86-04, Ministère de l’Energie et des Ressources, Gouvernement du Québec (1987) 21 pp.
- [414] HOHNDORF, A., BIANCONI, F., VON PECHMANN, E., “Geochronology and metallogeny of vein type uranium occurrences in the Otish Basin area, Quebec, Canada”, paper presented at Mtg on Metallogenesis of Uranium Deposits, Vienna, 1989.
- [415] GATZWEILER, R., “Uranium mineralization in the Proterozoic Otish Basin, central Quebec, Canada”, *Uranium Mineralization: New Aspects on Geology, Mineralogy, Geochemistry, and Exploration Methods*, Mineral Deposits Monograph 27, Gebrüder Bornträger, Berlin and Stuttgart (1987) 27–48.
- [416] CHOWN, E.H., CATY, J.L., Stratigraphy, petrography, and paleocurrent analysis of the Aphebian clastic formations of the Mistassini-Otish Basin, Special Paper 12, Geol. Assoc. Can. (1973) 49–71.
- [417] RHYS, D., Matoush Property – Field Visit and Core Evaluation, Strateco Resources Inc. internal report (2007) 18 pp.
- [418] ROBERTSON, J.A., “Huronian geology and the Blind River (Elliot Lake) uranium deposit”, *Uranium Deposits of Canada*, Can. Inst. Min. Metall. **33** (1986).
- [419] BUCK, S.G., MINTER, W.E.L., “Paleocurrent and lithological facies control of uranium and gold mineralisation in the Witwatersrand Carbon Leader placer, Carletonville Goldfield, South Africa”, *Uranium Deposits in Proterozoic Quartz-pebble Conglomerates*, IAEA-TECDOC-427, IAEA, Vienna (1987) 335–353.
- [420] DEPINE, M., FRIMMEL, H.E., EMSBO, P., KOENIG, A.E., KERN, M., Trace element distribution in uraninite from Mesoarchean Witwatersrand conglomerates (South Africa) supports placer model and magmatogenic source, *Miner. Deposita* **48** (2013) 423–435.
- [421] COCHRANE, L.B., HWOZDYK, L.R., Technical NI 43-101 Report on the Elliot Lake Property, Elliot Lake, Ontario, Canada, prepared for Denison Mines Corporation (2007).
- [422] ROSCOE, S.M., CARD, K.D., Early Proterozoic tectonics and metallogeny of the Lake Huron region of the Canadian Shield, *Precamb. Res.* **58** (1992) 99–119.
- [423] THEIS, N.J., Uranium-bearing and associated minerals in their geochemical and sedimentological context, Elliot Lake, Ontario, *Geol. Surv. Can. Bull.* **304** (1979).
- [424] MEDDAUGH, W.S., HOLLAND, H.D., Age and origin of uraninite in the Elliot Lake, Ontario, uranium deposits, *Geol. Soc. Am.* **13** (1981).
- [425] ROBERTSON, D.S., “Basal Proterozoic unit as fossil time markers and their use in uranium prospecting”, *Formation of Uranium Ore Deposits (Proc. Int. Conf. Athens, 1974)*, IAEA, Vienna (1974) 495–512.
- [426] ROBINSON, A.G., SPOONER, E.T.C., Postdepositional modification of uraninite-bearing quartz-pebble conglomerates from the Quirke ore zone, Elliot Lake, Ontario, *Econ. Geol.* **79** (1984) 297–321.
- [427] TOENS, P.D., HAMBLETON-JONES, B.B., “Definition and classification of surficial uranium deposits”, *Surficial Uranium Deposits*, IAEA-TECDOC-322, IAEA, Vienna (1984) 9–14.
- [428] BUTT, C.R.M., MANN, A.W., HORWITZ, R.C., “Regional setting, distribution and genesis of surficial uranium deposits in calcretes and associated sediments in Western Australia”, *Surficial Uranium Deposits*, IAEA-TECDOC-322, IAEA, Vienna (1984) 121–127.

- [429] ROESENER, H., SCHREUDER, C.P., “Uranium”, Mineral Resources of Namibia, Geological Survey of Namibia, Windhoek (1992) 7.1-1–7.1-62.
- [430] HAMBLETON-JONES, B.B., The Geology and Geochemistry of some Epigenetic Uranium Deposits near the Swakop River, South West Africa, Rep. NUCOR PER-78, Nuclear Development Corporation, Pretoria (1983).
- [431] BATULIN, S.G., Regional factors of formation of uranium deposits in calcretes, *Lithol. Miner. Res.* **15** (1980) 437–442.
- [432] SNOWDEN, Technical Report, International Mining Company Invest: Kamushanovskoye Uranium Prospect, Project Review and Resource Estimate (2007) 114 pp, <http://www.imcinvest.com/news/IMCSnowdenKAM.pdf>
- [433] CULBERT, R.R., LEIGHTON, D.G., Young uranium, *Ore Geol. Rev.* **3** (1988) 313–330.
- [434] TIXIER, K., BECKIE, R., Uranium depositional controls at the Prairie Flats surficial uranium deposit, Summerland, British Columbia, *Environ. Geol.* **40** (2001) 1242–1251.
- [435] SHAW, D.R., NASH, J.T., CHENOWETZ, W.L., “Uranium and vanadium deposits”, *The Geology of North America*, Vol. P2, Geological Society of America, Boulder (1991) 103–124.
- [436] PALADIN ENERGY LTD, web site (accessed 2010).
- [437] BRIQUEU, P., LANCELOT, J., VALOIS, J.P., WALGENWITZ, F., Géochronologie U-Pb et genèse d’un type de minéralisation uranifère: les alaskites de Goanikontes (Namibie) et leur encaissant, *Bull. CREP Elf Aquitaine* **4** (1980) 759–811.
- [438] HARTLEB, J.W.O., The Langer Heinrich uranium deposit: Southwest Africa/Namibia, *Ore Geol. Rev.* **3** (1988) 277–287.
- [439] TORO ENERGY LTD, web site (accessed 2013).
- [440] TORO ENERGY LTD, web site (accessed 2011).
- [441] FRENCH, R.R., ALLEN, J.H., “Lake Way uranium deposit, Wiluna, Western Australia”, *Surficial Uranium Deposits*, IAEA-TECDOC-322, IAEA, Vienna (1984) 149–156.
- [442] PACMAG METALS LTD, web site (accessed 2009).
- [443] SEREDIN, V.V., FINKELMAN, R.B., Metalliferous coals: A review of the main genetic and geochemical types, *Int. J. Coal Geol.* **76** (2008) 253–289.
- [444] KISLYAKOV, Y.M., SHCHETOCHKIN, V.N., Hydrogenic Ore Formation, *Geoinformmark*, Moscow (2000) 608 pp (in Russian).
- [445] MAKSIMOVA, M.F., SHMARIOVITCH, E.M., Bedded-infiltrational Ore Formation, *Nedra*, Moscow (1993) 60 pp (in Russian).
- [446] BATULIN, S.G., GRUSHEVOI, G.V., ZELENOVA, O.I., Hydrogenic Uranium Deposits, *Atomizdat*, Moscow (1980) 270 pp (in Russian).
- [447] SHVARTSEV, S.L., Hydrogeochemistry of Supergene Zone, *Nedra*, Moscow (1998) 366 pp (in Russian).
- [448] ARMANDS, G., Geochemical prospecting of a uraniferous bog deposit at Masugnsbyn, northern Sweden, *Geochemical Prospecting in Fennoscandia*, Interscience Publishers, New York (1967) 127–154.
- [449] SOZINOV, N.A., Uranium-germanium ore in Miocene coal-bearing strata, *Materialy koordinatsionnogo soveta*, vol. 2, VIMS, Moscow (1966) 55–59 (in Russian).
- [450] SEREDIN, V.V., ARBUZOV, S.I., ALEKSEEV, V.P., Sc-bearing coals from Yakhlink deposit, western Siberia, *Dokl. Earth Sci.* **409A** (2006) 967–972.
- [451] MASHKOVTSSEV, G.A., KOCHENOV, A.V., KHALDEI, A.E., “On hydrothermal sedimentary formation of stratiform uranium deposits in Phanerozoic depressions”, *Rare-metal–Uranium Ore Formation within Sedimentary Rocks*, Nauka, Moscow (1995) 37–51.
- [452] ENERGY AND MINERALS AUSTRALIA web site (2012).
- [453] DOUGLASS, G.B., BUTT, C.R.M., GRAY, D.J., Geology, geochemistry and mineralogy of the lignite-hosted Ambassador paleochannel uranium and multi-element deposit, Gunbarrel Basin, Western Australia, *Miner. Deposita* **46** (2011) 761–787.
- [454] FULWOOD, K.E., BARWICK, R.E., “Mulga Rock uranium deposits, Officer Basin”, *Geology of the Mineral Deposits of Australia and Papua New Guinea*, Australas. Inst. Min. Metall. (1990) 1621–1623.

- [455] COFFEY MINING PTY LTD, Mulga Rock Project: Ambassador uranium deposit, June 2010 resource estimate, Report for Energy and Minerals Australia (2010) 111 pp.
- [456] JUST, J., Report on Mineralogical Investigation of Samples from Drill Holes CD-795, CD-1101 and CD-1406, prepared for PNC Exploration (Australia) Pty Ltd (1988) (unpublished).
- [457] DOUGLASS, G.B., GRAY, D.J., BUTT, C.R.M., Geochemistry, Mineralogy and Hydrogeochemistry of the Ambassador Multi-element Lignite Deposit, Western Australia, Rep. No. 108, Min. Energy Res. Inst. West Aust., Perth (1993) 85 pp.
- [458] McLEMORE, V.T., CHENOWETH, W.L., “Uranium Resources in the San Juan Basin, New Mexico”, 54th Ann. Fall Field Conf. Guidebook, New Mex. Geol. Soc., Socorro, NM (2003) 163–175.
- [459] FINCH, W.I., McLEMORE, V.T., “Uranium geology and resources of the San Juan Basin”, paper presented at Int. Geol. Cong. on Coal, Uranium and Oil and Gas in Mesozoic Rocks of the San Juan Basin: Anatomy of a Giant Energy-rich Basin, Washington, DC, 1989.
- [460] RAWSON, R.R., “Uranium in Todilto Limestone (Jurassic) of New Mexico – example of a sabkha-like deposit”, Geology and Mineral Technology of the Grants Uranium Region, New Mex. Bur. Mines Miner. Res. Mem. **38** (1981) 304–312.
- [461] NAGARAJA RAO, B., RAJURKAR, S., RAMILIGASWAMY, G., RAVINDRA BABU, “Stratigraphy, structure and evolution of the Cuddapah Basin”, Purana Basins of Peninsular India, Geol. Soc. Ind. Mem. **6** (1987) 33–86.
- [462] RAMAKRISHNAN, M., VAIDHYANATHAN, R., Geology of India, Vol. 1, Geological Society of India, Bangalore (2008) 462 pp.
- [463] RAI, A.K., SHARMA, S.K., UMAMAHESHWAR, K., NAGBHUSHNA, J.C., VASUDEVA RAO, M., “Uranium mineralization in the eastern margin of Cuddapah Basin”, paper presented at Geol. Soc. India Sem. on Cuddapah Basin, Tirupati, 1995.
- [464] VASUDEVA RAO, M., NAGABHUSHANA, J.C., JEYAGOPAL, A.V. Uranium mineralization in the Middle Proterozoic carbonate rocks of the Cuddapah Supergroup, southern Peninsular India, Expl. Res. Atom. Miner. **2** (1989) 29–38.
- [465] ZAKAULLA, S., RAI, A.K., TRIPATHY, B.K., THIRUPATHY, P.V., UMAMAHESHWAR, K., DHANA RAJU, R., Alterations in the basement fracture zones and their bearing on uranium mineralization in southwestern environs of the Cuddapah Basin, Andhra Pradesh, India, Expl. Res. Atom. Miner. **11** (1998) 13–24.
- [466] RAI A.K., ZAKAULLA, S., CHAKI A., “Proterozoic stratabound carbonate rock (dolostone) hosted uranium deposits in Vempalle formation in Cuddapah Basin, India”, paper presented at IAEA Symp. on Uranium Raw Material for the Nuclear Fuel Cycle: Exploration, Mining, Production, Supply and Demand, Economics and Environmental Issues, Vienna, 2009.
- [467] MINATI ROY, DHANA RAJU, R., VASUDEVA RAO, M., VASUDEVA, S.G., (1990) Stromatolitic uraniferous dolostone of the Vempalle formation, Cuddapah Supergroup, Andhra Pradesh, India: Nature and bearing of stromatolites on uranium mineralization, Expl. Res. Atom. Miner. **3** (1990) 103–113.
- [468] THOSTE, V., “Decommissioning of Mailuu-Suu uranium production combinat”, paper presented at Tech. Comm. Mtg on Developments in Uranium Resources, Production, Demand and the Environment, Vienna, 1999.
- [469] ROSLYI, A.I., Concentration of uranium ores in carbonatic rocks, *Litologiya I, Iskokopnaemye*, **1** (1975) 84–97.
- [470] MIN, M., ZHENG, D., SHEN, B., WEN, G., WANG, X., GANDHI, S.S., Genesis of the Sanbaqi deposit: a paleokarst-hosted uranium deposit in China, *Miner. Deposita* **32** 1–2 (1997) 505–519.
- [471] MIN, M.Z., MENG, Z.W., SHENG, G.Y., MIN, Y.S., LIU, X., Organic geochemistry of paleokarst-hosted uranium deposits, South China, *J. Geochem. Expl.* **68** (2000) 211–229.
- [472] CARLOTTA, B., CHERNOFF, ORRIS, G.J., Data Set of World Phosphate Mines, Deposits, and Occurrences: Part A — Geologic Data, Open-File Report 02–156–A, US Geological Survey, Reston, VA (2002) 352 pp.

- [473] US GEOLOGICAL SURVEY, USGS Database of Phosphates, Mineral Commodity Summaries, [http://minerals.usgs.gov/minerals/pubs/commodity/phosphate\\_rock/index.html#mcs](http://minerals.usgs.gov/minerals/pubs/commodity/phosphate_rock/index.html#mcs) (accessed 1 December 2011).
- [474] VAN KAUWENBERG, S., “World phosphate rocks and resources”, paper presented at Fertilizer Outlook and Technology Conf., Savannah, 2010.
- [475] ARMANDS, G., Geochemical studies of uranium, molybdenum and vanadium in a Swedish alum shale, *Stockholm Contr. Geol.* **27** (1972).
- [476] McSWIGGEN, P.L., MOREY, G.B., WEIBLEN, P.W., Uranium in Early Proterozoic phosphate-rich metasedimentary rocks of east-central Minnesota, *Econ. Geol.* **81** (1986) 173–183.
- [477] BATURIN, G.N., DUBINCHUK, V.T., Origin of uranium and rare earth minerals in bone detritus from rare metal deposits, *Dokl. Earth Sci.* **438** 2 (2011) 766–769.
- [478] POOL, T.C., “U.S. uranium production capability, how much and at what price?”, paper presented at Int. Sem. on Uranium Fuel, Williamsburg, 1995.
- [479] CATHCART, J.B., SHELDON, R.P., GULBRANDSEN, N.A., Phosphate rock resources of the United States, *Geol. Surv. Circ.* 888, US Geological Survey, Reston, VA (1984) 53 pp.
- [480] WORLD NUCLEAR ASSOCIATION, Uranium from phosphates, WNA, London (accessed 2012).
- [481] VAN KAUWENBERG, S.J., CATHCART, J.B., McCLELLAN, G.H., Mineralogy and alteration of the phosphate deposits of Florida, *US Geol. Surv. Bull.* **1914** (1990) 56 pp.
- [482] ALTSCHULER, Z.S., CLARKE, R.S., YOUNG, E.J., Geochemistry of uranium in apatite and phosphorite, Prof. Paper 314-D, US Geological Survey, Reston, VA (1958) 45–90.
- [483] RIGGS, S.R., Petrology of the Tertiary phosphate system of Florida, *Econ. Geol.* **74** 2 (1979) 195–220.
- [484] ALTSCHULER, Z.S., CATHCART, J.B., YOUNG, E.J., The geology and geochemistry of the Bone Valley Formation and its phosphate deposits, west central Florida, Fieldtrip 6, Ann. Mtg. Geol. Soc. Am. Guidebook, Geological Society of America, Boulder (1964) 68 pp.
- [485] URCA, Gisement d’uranium de Bakouma. Etude de faisabilité. Volume 1 : généralités, le gisement de Bakouma (1977).
- [486] AMC CONSULTANTS Pty Ltd, Bakouma Resource Technical Report, URAMIN Inc, Bakouma, Central African Republic. AMC Project 207009B (2009) 73 p.
- [487] POIDEVIN, J.L., Sr-isotope stratigraphy and dating of Neoproterozoic carbonates and glacials from the northern and western parts of the Congo Craton, *Comptes Rendus Geoscience* **339** (2007) 259–273.
- [488] MIAUTON, J.P., Bakouma – Genesis and metallogeny of a neoform continental phosphate-uraniferous deposit. Thèse 3<sup>ème</sup> cycle, Nancy (1980) 160 p.
- [489] KRIBEK, B., Metallogeny, structural, lithological and time controls of ore deposition in anoxic environments, *Miner. Deposita* **26** 2 (1991) 122–131.
- [490] LEVENTHAL, J.S., Comparison of organic geochemistry and metal enrichment in two black shales: Cambrian alum shales of Sweden and Devonian Chattanooga shale of the United States, *Miner. Deposita* **26** 2 (1991) 104–112.
- [491] EMSBO, P., Metalliferous organic-rich black shales: Are exhalative hydrothermal processes fundamental to their genesis? International Geological Congress, Abstracts, Resumes, Vol. 33 (2008), <http://iugs.org/33igc/fileshare/PDF/IGC+programme+book.pdf>
- [492] ANDERSSON, A., DAHLMANN, B., GEE, D.G., SNALL, S., The Scandinavian alum shales, *Sver. Geol. Undersokning* **56** (1985) 51 pp.
- [493] AURA ENERGY, Outstanding Haggan uranium resources expands to 800 million pounds, Australian Stock Exchange announcement, 22 August 2012.
- [494] LANGE, G., FREYHOFF, G., Geologie und Bergbau in der Uranlagerstätte Ronneburg/Thüringen, *ERZMETALL* **44** (1991) 264–269.
- [495] BARTHEL, F.H., Die Urangewinnung auf dem Gebiet der ehemaligen DDR von 1945 bis 1990, *Geol. Jb. A* **142** (1993) 335–346.

## CONTRIBUTORS TO DRAFTING AND REVIEW

Aylor, J., Jr.	Consultant, United States of America
Barthel, F.	Consultant, Germany
Basov, V.	Consultant, Russian Federation
Beard, J.	Consultant, United States of America
Biondi, J.C.	Consultant, Brazil
Bodnar, R.	Consultant, United States
Bruneton, P.	Consultant, France
Chaki, A.	AMD, India
Cuney, M.	CNRS, France
Dahlkamp, F.	Consultant, Germany
Fairclough, M.	International Atomic Energy Agency
Hall, S.	USGS, United States of America
Henica, W.	Consultant, United States of America
Jaireth, S.	Geoscience Australia, Australia
Lapido-Loureiro, F.	Consultant, Brazil
Liu, X.	ECUT, China
McKay, A.	Geoscience Australia, Australia
Parihar, P.S.	AMD, India
Poliakovska, K.	International Atomic Energy Agency
Pylypenko, O.	International Atomic Energy Agency
Qing, M.	BRIUG, China
Tulsidas, H.	International Atomic Energy Agency
Van Kalleveen, A.	International Atomic Energy Agency
Zaluski, G.	CAMECO, Canada



**Technical Meeting**

Vienna, Austria: 19–22 February 2013

**Consultants Meetings**

Vienna, Austria: 22–25 November 2011; 2–7 July 2012; 25–28 February 2013





**IAEA**

International Atomic Energy Agency

No. 25

## ORDERING LOCALLY

In the following countries, IAEA priced publications may be purchased from the sources listed below or from major local booksellers.

Orders for unpriced publications should be made directly to the IAEA. The contact details are given at the end of this list.

### CANADA

***Renouf Publishing Co. Ltd***

22-1010 Polytek Street, Ottawa, ON K1J 9J1, CANADA

Telephone: +1 613 745 2665 • Fax: +1 643 745 7660

Email: [order@renoufbooks.com](mailto:order@renoufbooks.com) • Web site: [www.renoufbooks.com](http://www.renoufbooks.com)

***Bernan / Rowman & Littlefield***

15200 NBN Way, Blue Ridge Summit, PA 17214, USA

Tel: +1 800 462 6420 • Fax: +1 800 338 4550

Email: [orders@rowman.com](mailto:orders@rowman.com) Web site: [www.rowman.com/bernan](http://www.rowman.com/bernan)

### CZECH REPUBLIC

***Suweco CZ, s.r.o.***

Sestupná 153/11, 162 00 Prague 6, CZECH REPUBLIC

Telephone: +420 242 459 205 • Fax: +420 284 821 646

Email: [nakup@suweco.cz](mailto:nakup@suweco.cz) • Web site: [www.suweco.cz](http://www.suweco.cz)

### FRANCE

***Form-Edit***

5 rue Janssen, PO Box 25, 75921 Paris CEDEX, FRANCE

Telephone: +33 1 42 01 49 49 • Fax: +33 1 42 01 90 90

Email: [formedit@formedit.fr](mailto:formedit@formedit.fr) • Web site: [www.form-edit.com](http://www.form-edit.com)

### GERMANY

***Goethe Buchhandlung Teubig GmbH***

Schweitzer Fachinformationen

Willstätterstrasse 15, 40549 Düsseldorf, GERMANY

Telephone: +49 (0) 211 49 874 015 • Fax: +49 (0) 211 49 874 28

Email: [kundenbetreuung.goethe@schweitzer-online.de](mailto:kundenbetreuung.goethe@schweitzer-online.de) • Web site: [www.goethebuch.de](http://www.goethebuch.de)

### INDIA

***Allied Publishers***

1st Floor, Dubash House, 15, J.N. Heredi Marg, Ballard Estate, Mumbai 400001, INDIA

Telephone: +91 22 4212 6930/31/69 • Fax: +91 22 2261 7928

Email: [alliedpl@vsnl.com](mailto:alliedpl@vsnl.com) • Web site: [www.alliedpublishers.com](http://www.alliedpublishers.com)

***Bookwell***

3/79 Nirankari, Delhi 110009, INDIA

Telephone: +91 11 2760 1283/4536

Email: [bkwell@nde.vsnl.net.in](mailto:bkwell@nde.vsnl.net.in) • Web site: [www.bookwellindia.com](http://www.bookwellindia.com)

## **ITALY**

### ***Libreria Scientifica "AEIOU"***

Via Vincenzo Maria Coronelli 6, 20146 Milan, ITALY  
Telephone: +39 02 48 95 45 52 • Fax: +39 02 48 95 45 48  
Email: [info@libreriaaeiou.eu](mailto:info@libreriaaeiou.eu) • Web site: [www.libreriaaeiou.eu](http://www.libreriaaeiou.eu)

## **JAPAN**

### ***Maruzen-Yushodo Co., Ltd***

10-10 Yotsuyasakamachi, Shinjuku-ku, Tokyo 160-0002, JAPAN  
Telephone: +81 3 4335 9312 • Fax: +81 3 4335 9364  
Email: [bookimport@maruzen.co.jp](mailto:bookimport@maruzen.co.jp) • Web site: [www.maruzen.co.jp](http://www.maruzen.co.jp)

## **RUSSIAN FEDERATION**

### ***Scientific and Engineering Centre for Nuclear and Radiation Safety***

107140, Moscow, Malaya Krasnoselskaya st. 2/8, bld. 5, RUSSIAN FEDERATION  
Telephone: +7 499 264 00 03 • Fax: +7 499 264 28 59  
Email: [secnrs@secnrs.ru](mailto:secnrs@secnrs.ru) • Web site: [www.secnrs.ru](http://www.secnrs.ru)

## **UNITED STATES OF AMERICA**

### ***Bernan / Rowman & Littlefield***

15200 NBN Way, Blue Ridge Summit, PA 17214, USA  
Tel: +1 800 462 6420 • Fax: +1 800 338 4550  
Email: [orders@rowman.com](mailto:orders@rowman.com) • Web site: [www.rowman.com/bernan](http://www.rowman.com/bernan)

### ***Renouf Publishing Co. Ltd***

812 Proctor Avenue, Ogdensburg, NY 13669-2205, USA  
Telephone: +1 888 551 7470 • Fax: +1 888 551 7471  
Email: [orders@renoufbooks.com](mailto:orders@renoufbooks.com) • Web site: [www.renoufbooks.com](http://www.renoufbooks.com)

## **Orders for both priced and unpriced publications may be addressed directly to:**

Marketing and Sales Unit  
International Atomic Energy Agency  
Vienna International Centre, PO Box 100, 1400 Vienna, Austria  
Telephone: +43 1 2600 22529 or 22530 • Fax: +43 1 2600 29302 or +43 1 26007 22529  
Email: [sales.publications@iaea.org](mailto:sales.publications@iaea.org) • Web site: [www.iaea.org/books](http://www.iaea.org/books)

**International Atomic Energy Agency**  
**Vienna**  
ISBN 978-92-0-101618-8  
ISSN 1011-4289